



Pilidis, Pericles (1983) *Digital simulation of gas turbine performance*.

PhD thesis

<http://theses.gla.ac.uk/3168/>

Copyright and moral rights for this thesis are retained by the author

A copy can be downloaded for personal non-commercial research or study, without prior permission or charge

This thesis cannot be reproduced or quoted extensively from without first obtaining permission in writing from the Author

The content must not be changed in any way or sold commercially in any format or medium without the formal permission of the Author

When referring to this work, full bibliographic details including the author, title, awarding institution and date of the thesis must be given

DIGITAL SIMULATION
OF
GAS TURBINE PERFORMANCE

BY PERICLES PILIDIS

THESIS SUBMITTED FOR THE DEGREE OF Ph.D

DEPARTMENT OF MECHANICAL ENGINEERING
UNIVERSITY OF GLASGOW

NOVEMBER 1983

BEST COPY

AVAILABLE

Variable print quality

CONTENTS

SUMMARY	3
LIST OF SYMBOLS	5
INTRODUCTION	10
1. BACKGROUND	12
1.1 Introduction	12
1.2 Gas Turbine Operation	12
1.3 Previous Work on Gas Turbine Modelling	21
1.4 Choice of Method for Present Work	32
1.5 Choice of Computer	35
2. DESCRIPTION OF GENERAL PREDICTION PROGRAMME	40
2.1 Introduction	40
2.2 The Method	42
2.3 Single Spool Engines	55
2.4 Two Spool Engines	59
2.5 Three Spool Engines	67
3. CALCULATIONS OF CLEARANCES AND THEIR EFFECTS	71
3.1 Introduction	71
3.2 Thermal Effects	73
3.3 Mechanical Effects	77
3.4 Blade Tip Clearance Movements	78
3.5 Simple Method to be included in Programme	81
3.6 Efficiency Loss	84
3.7 Applications	86
3.8 Estimation of Seal Clearance Movements	90

CONTENTS

SUMMARY	3
LIST OF SYMBOLS	5
INTRODUCTION	10
1. BACKGROUND	12
1.1 Introduction	12
1.2 Gas Turbine Operation	12
1.3 Previous Work on Gas Turbine Modelling	21
1.4 Choice of Method for Present Work	32
1.5 Choice of Computer	35
2. DESCRIPTION OF GENERAL PREDICTION PROGRAMME	40
2.1 Introduction	40
2.2 The Method	42
2.3 Single Spool Engines	55
2.4 Two Spool Engines	59
2.5 Three Spool Engines	67
3. CALCULATIONS OF CLEARANCES AND THEIR EFFECTS	71
3.1 Introduction	71
3.2 Thermal Effects	73
3.3 Mechanical Effects	77
3.4 Blade Tip Clearance Movements	78
3.5 Simple Method to be included in Programme	81
3.6 Efficiency Loss	84
3.7 Applications	86
3.8 Estimation of Seal Clearance Movements	90

4. DIRECT HEAT TRANSFER EFFECTS	94
4.1 Introduction	94
4.2 Heat Capacity of the Components	94
4.3 Change in Component Characteristics	99
5. RESULTS AND DISCUSSION	119
5.1 Introduction	119
5.2 Performance of the Components in Transients	119
5.3 Effects of Clearance Movements on Transients	124
5.4 Direct Heat Transfer Effects	127
5.5 Inclusion of all the Effects	130
5.6 Other Effects and Parameters	135
6. DISCUSSION OF THE PREDICTION METHOD	147
6.1 Introduction	147
6.2 Computing Efficiency	147
6.3 The Assumption of Constant Mass Flow	150
7. CONCLUSION	153
REFERENCES	158
FIGURES	166

SUMMARY

A method has been developed to enable the prediction of the steady state and the transient performance of gas turbines. The model is based upon the thermodynamic processes and the performance characteristics of the components of the engines. This method has been incorporated into a computer programme that is suitable for various engine types. All aero-engines currently in service can be simulated with this programme and the computing requirements should be satisfied by a small installation.

Component characteristics were available for four engines of three different configurations. These characteristics were used to predict the behaviour of the respective engines. Once the accuracy of the method was established, the characteristics were suitably modified to study other engine configurations for which characteristics were not available. A total of eleven different engine configurations have thus been simulated. Single-spool, two-spool and three-spool turbojet engines, and one, two or three-spool bypass and turbofan engines with separate or mixed exhausts, of front or aft fan arrangement have been analysed.

All these predictions were made assuming adiabatic conditions hold for both the transient and steady state processes. The next step has been to include the effect of factors which are known to affect the transient behaviour, such as tip clearance changes, heat transfer effects and changes in component chara-

cteristics during the transient. Of these effects, the movement of the characteristics and the effect of the seals not having their steady state clearances produce the largest differences between adiabatic analysis and analysis with heat transfer. Fluid density changes have a small effect on the predicted response, but the thrust achieved at the end of the speed transient is slightly lower. These effects are illustrated on a two-spool bypass engine with mixed exhausts for which the necessary information was available.

In addition several minor effects have been investigated, such as the effect of the extent of mixing in engines of mixed exhausts. Even for the most complex engines, computing time is about five times real time, which indicates that better hardware would enable the achievement of real-time simulation. When the non-adiabatic effects are included, the computing increases to slightly less than double the time needed for the adiabatic model.

List of Symbols

A	Cross sectional or flow area
AVR	Axial velocity ratio
A _l	Altitude
A _r	Aspect ratio
a	Variable exponent of iteration algorithm
B	Bypass ratio
b	Distance of maximum camber from leading edge
C	Clearance
C _d	Drag coefficient
C _l	Lift coefficient
C _p	Specific heat at constant pressure
C _v	Specific heat at constant volume
C ₁ , C ₂ ,...C ₁₂	Constants (not necessarily non-dimensional)
c	Blade chord
D	Diameter
E	Young's modulus
e	Cooling effectiveness
F	Ratio of heat transfer to work transfer
F	Fuel mass flow
f	Denotes any function
f(e)	Error function
Gr	Grashof number
I	Moment of inertia of a rotor
i	angle of incidence of flow
H	Height
L	Axial length of stage
l	Thickness of diaphragm

M	Mach number
m	Mass
\dot{m}	Mass flow rate of working fluid
N	Rotational speed in R.P.M.
Nu	Nusselt number
nc	Polytropic index of expansion (compressors)
nh	Index of expansion with heat transfer
nt	Polytropic index of expansion (turbines)
P	Static pressure
PR	Pressure ratio
PRC	Pressure rise coefficient
Po	Stagnation pressure
Pr	Prandtl number
p	Momentum of fluid
Q	Torque imbalance of a rotor
Q	Rate of heat transfer
R	Gas constant (when unsubscripted)
R	Radius (when subscripted)
Re	Reynolds number
s	Blade pitch
T	Static temperature
TRC	Temperature rise coefficient
To	Stagnation temperature
t	Time
U	Aircraft or blade velocity
V	Volume
v	velocity of fluid
W	Work
X	Any arbitrary variable

α	Air angle
β	Blade angle
γ	Ratio of specific heats C_p/C_v
Δ	Small change or difference
δ	Deviation of air angle from blade angle
ϵ	Deflection of fluid due to blade
η	Efficiency
θ	Camber angle of blade
λ	Non-dimensional clearance C/H_b
ν	Poisson's ratio
ρ	Density
σ	Stress
τ	Time constant
ϕ	Flow coefficient v_a/U
ψ	Blade loading $2 C_p \Delta T/U^2$
ω	Angular velocity

Subscripts

A	Aircraft
a	Axial
act	Actual
ad	Adiabatic
air	Air
an	Annular
b	Blade
bp	Bypass stream
bt	Blade tip
C	Compressor
c	Cooling air
ca	Casing

cg	Core gases
d	Disc
de	Design
e	engine
F	Fan
H	Hoop
HP	H.P. shaft
h	Hub of blade
ht	With heat transfer
IP	I.P. shaft
id	Ideal
i	Inner or inlet
J	Jet
j	j'th section or shaft
L	Longitudinal
LP	L.P. shaft
m	Mean
N	Nozzle
o	Outer or outlet
p	Propeller
pf	Profile
po	Polytropic
pr	Propulsive
r	At a radius r
s	Stage
se	Secondary
sh	Shroud
ss	At the steady state or at a steady state point
T	Turbine

$t, t+dt, t-dt$	At times $t, t+dt, t-dt$
th	Thermal
tr	Transmission
wt	Work transfer

INTRODUCTION

In the year 150 B.C. Hero of Alexandria used an original device to provide movement for some symbolic figures in religious ceremonies. A crude turbine used the flue gases of a furnace to produce the necessary power, in what was one of the first attempts to obtain work from a primitive heat engine. John Barber in 1791 patented the forerunner of gas turbines as they are known today. A few years later, in 1808, the first explosion type of gas turbine was devised. The development of the continuous engine suffered from lack of understanding of the processes involved. In 1905 the first successful centrifugal compressor was designed by Rateau. Later in the same year, Armengaud and Lemale built the first working engine, the efficiency of which was of less than five percent. Further insight and experience were gained with the passage of time, and by the beginning of the Second World War a few industrial gas turbines were in service. This period saw the first development of gas turbines for aircraft propulsion, the main attraction for this particular application being its high power per unit of machinery weight. During the War the main nations developed this type of propulsion, and in the closing years of the conflict both sides had operational squadrons of jet powered aeroplanes.

Since then the gas turbine has become the most important method of aircraft propulsion and is becoming more

widely used in both industrial and marine applications. With the attainment of the required increased powers and efficiencies gas turbines have inevitably become more complex and more expensive to design, test, develop and build. As a result it is highly desirable, if not necessary to be able to predict their performance in both steady state and transient conditions, as early as possible and as accurately as possible. This would reduce development time and cost, and both manufacturers and users would have a better understanding of engine behaviour under different operational conditions. Models have been devised for this purpose. If the models are to be useful they must be accurate and easily adaptable to any modification the engine may undergo during the design period or its operational career. Transient behaviour is of particular interest, because many design aspects are set by events in the transient cycles. Thus, although transient processes account for a small fraction of the engine's working life (minimal in the case of some commercial and marine applications), they must be accurately evaluated. Even more desirable would be to incorporate all the models and methods into one single computer programme. This is a very attractive prospect for both manufacturers designing engines of various configurations and for the users operating them. It is to this end that the present effort has been directed.

CHAPTER I

BACKGROUND

1.1 INTRODUCTION

This chapter starts with a brief outline of the functioning of gas turbines. A fuller description is available in gas turbine text books (Refs. 11, 33). A review of previous work in the field of evaluating gas turbine performance is then given and subsequently the reasons for opting for the method chosen to carry out the present investigation. The information outlined is valid for all gas turbine configurations. The various arrangements analysed are shown in Figs. 1 to 11. For these figures and for the present work the naming of the various configurations is as follows: the name turbojet is meant to describe an engine without bypass flows. A bypass engine is that in which the bypass flow is compressed by a compressor of several stages and in a turbofan the bypass flow is compressed by a single stage fan. Mixed and separate exhausts describe the way in which the bypass flow is returned to the atmosphere, mixed with the core gases or through a second nozzle. The above convention is detailed because it has been noted that the various authors whose subject is gas turbine technology do not all follow the same guidelines when naming the different engine configurations.

1.2 GAS TURBINE OPERATION

The physical processes that occur in a gas turbine are described by the Brayton cycle. In the continuous flow (constant pressure) gas turbine, the working fluid flows without interruption. The processes in the thermodynamic cycle occur in different specialised devices. This cycle is shown in Fig. 12. Referring to this figure, the process starts at point 1 for a stationary engine at ambient conditions, and at points 1A for a moving engine, where the inlet pressure and temperature are higher than the ambient values because of the ram compression occurring at the intake. The compression process within the gas turbine raises the working fluid pressure to that at point 2', this process ideally being isentropic and obeying the law given in equation (1.1).

$$pV^\gamma = C_1 \quad (1.1)$$

Following the compression the fluid will experience an input of heat ideally at constant pressure. This heat input can be either by means of burning fuel in the working fluid in a combustion chamber, or by heat exchange. This heat input will change the fluid conditions to those at point 3' in the cycle. At this point the fluid will start the expansion process which will take it to the conditions corresponding to point 5' in the cycle. The first part of the expansion (to point 4') will occur in the turbine(s) which drive the compressor(s). The expansion will then continue to point 5' of the cycle in the device that produces the work output, either a nozzle or a power turbine. If the cycle is assumed ideal, the compressor work is that represented by the area 1CA2', and the turbine work by area

4'BA3'. In the steady state for an ideal engine, these areas will be the same. For a real engine the turbine work will be larger, to account for losses, mechanical inefficiencies and power for auxiliaries. In the ideal cycle area 5'CB4' represents the useful work output, in the form of shaft work or gas kinetic energy, depending on the application of the engine. Losses cannot be avoided, so some deviations from the ideal cycle have to be accepted. The real cycle is shown by 1235 in Fig. 12. Because of intake losses, the compressor inlet pressure is slightly reduced. The real compression process follows the law

$$pV^{n_c} = C_2 \quad (1.2)$$

the index of compression n_c being a function of the ratio of the specific heats of air and of compressor efficiencies (in the ideal case it is equal to the ratio of specific heats). In the combustion chamber a small pressure loss has to be accepted due to friction and losses associated with the combustion process and its stabilisation. As a result the turbine inlet pressure will be slightly lower than the compressor delivery pressure. In the turbine the aforementioned inefficiencies will result in the expansion obeying the law

$$pV^{n_t} = C_3 \quad (1.3)$$

where the polytropic index n_t is a function of the specific heats of the gases flowing through the turbine, and of turbine efficiency. The working fluid consists of a large proportion

of air (approximately two thirds to three quarters) and a smaller proportion of combustion products. This different composition of the fluid results in indices of expansion slightly different from those of air. Due to all the irreversibilities in the outlet flow, the outlet pressure will be slightly higher than atmospheric (point 5 in the cycle).

It is interesting to notice the effect of component efficiencies in this type of engine. With improved component efficiencies, the work absorbed by the compressor will be of a lesser magnitude, and the turbine will produce work more efficiently. Therefore a larger fraction of the expansion will be available for the production of useful work output. In general, the useful work produced by the engine is of a similar or smaller magnitude than the compression work. Any improvement in component efficiencies will result in a magnified improvement of engine performance, this work output being the difference between two large quantities. The following example will illustrate this magnifying effect. An engine is imagined, where the compressors absorb 30 MW, and 50 MW are available in the expansion process to produce a nett work output of 20 MW. If the efficiencies of the compressors and turbines are improved by one percent, the compressor will absorb 29.7 MW, and in the expansion 50.5 MW will be available, thus producing 20.8 MW of nett power, an improvement of four percent.

A very common way of expressing the performance of a heat engine is the efficiency with which it transforms the energy input (in this case the potential chemical energy of the fuel) into the desired work output. The thermal efficiency

for an ideal Brayton cycle can be shown to be

$$\eta_{th} = 1 - \frac{1}{PR_e^{\frac{\gamma-1}{\gamma}}} \quad (1.4)$$

for an engine with perfect components. From this equation the conclusion is drawn that a higher pressure ratio will result in a more efficient gas turbine. However for real engines other considerations have to be taken into account. Real components do not behave as their ideal counterparts, so some losses have to be accepted. When this occurs, the turbine inlet temperature will also have an effect on the efficiency. The efficiency of such an engine will improve with higher turbine inlet temperature but this effect decreases with increased component efficiency. the limit to turbine inlet temperature is given by metallurgical restrictions, hence the efforts directed towards the production of heat resistant materials. These effects of pressure ratio and turbine inlet temperature are illustrated in Fig. 13, the line of best efficiency representing the engine with ideal components, or equation (1.4). It can be noticed that an engine with real components will have an optimum pressure ratio after which a further increase in this parameter will have a detrimental effect on thermal efficiency. For a gas turbine for power production the thermal efficiency is the overall efficiency.

Up to this point the comments apply to gas turbines in general. For several reasons, not least the availability of suitable information, and the existence of personal contacts with an aircraft engine manufacturer, jet engines are the main subject of the work described in this thesis. Therefore from

this point onwards, gas turbines for aeroplane propulsion are the ones considered. For these engines, the overall efficiency is the product of the thermal and propulsive efficiencies. The propulsive efficiency is defined as the ratio

$$\eta_{pr} = \frac{\text{work on aircraft}}{\text{work output from cycle}} \quad (1.5)$$

and by algebraic manipulation of the various engine and flight parameters it can be shown to be

$$\eta_{pr} = \frac{2U_A}{v_j + U_A} \quad (1.6)$$

For a bypass engine with separate exhausts, Bennet (Ref. 8), suggests that a third factor should be included in the evaluation of the overall efficiency of an aircraft gas turbine installation. This third factor is the transmission efficiency, expressing how efficiently the power of the gas generator is transferred to the cold propulsive jet in a bypass engine. The transmission efficiency is given by the ratio shown in equation (1.7)

$$\eta_{tr} = \frac{\text{actual kinetic energy supplied to bypass air}}{\text{ideal kinetic energy that could be supplied}} \quad (1.7)$$

or in algebraic terms

$$\eta_{tr} = \frac{\frac{1}{2}\dot{m}_{cg}v_{cg}^2 + \frac{1}{2}(\dot{m}_{bp}v_{bp}^2)_{act}}{\frac{1}{2}\dot{m}_{cg}v_{cg}^2 + \frac{1}{2}(\dot{m}_{bp}v_{bp}^2)_{id}} \quad (1.8)$$

where the bypass ratio, B , is defined by equation (1.9)

$$B = \frac{\dot{m}_{bp}}{\dot{m}_{cg}} \quad (1.9)$$

It can be shown that for optimum thrust

$$v_{bp} = v_{cg} \quad (\text{ideal engine}) \quad (1.10)$$

substituting in (1.8) and rearranging the terms,

$$\eta_{tr} = \frac{1 + B\eta_T\eta_F}{1 + B} \quad (\text{real engine}) \quad (1.11)$$

This is the expression proposed by Bennet. This efficiency is a function of the bypass ratio and component efficiencies. A similar type of relationship will apply to bypass engines with mixed exhausts and to turbofans.

The propulsion device is the final nozzle, in which the enthalpy available in the working fluid is to be transformed into the kinetic energy of the propulsive jet. Equation (1.12) is a statement of conservation of energy, where the enthalpy of the fluid and kinetic energy are interchangeable.

$$\dot{m}C_p(T_{0_N} - T_N) = \frac{1}{2}\dot{m}v^2 \quad (1.12)$$

and for a bypass engine

$$\dot{m}C_p(T_{0_N} - T_N) = \frac{1}{2}\dot{m}_{cg}v_{cg}^2 + \frac{1}{2}\dot{m}_{bp}v_{bp}^2 \quad (1.13)$$

In the case of a bypass engine with separate exhausts, the

final nozzle temperature difference includes the fraction of turbine temperature drop needed to deliver the work input to the fan for compression of the bypass stream. An illustration of the benefits of the bypass engine is now given. For simplicity it is assumed that the cold and hot mass flows are similar. For optimum performance the hot and cold stream velocities are also the same at the cold and hot exits. The total mass flow for the bypass engine will be double that of a turbojet engine. Because the gas velocity in the nozzle is to the second power in the equation, it will be reduced by approximately thirty percent in the bypass engine. This will produce a thrust that will be forty percent higher than in the turbojet engine for the same fuel consumption. For a non ideal engine with different bypass ratio and different exit velocities these figures will be modified. Depending on the efficiency of the various components, important gains are possible. The bypass engine designs are an attempt to capitalise on this effect. It must also be noticed that by reducing the velocity of the jets, the propulsive efficiency of the installation is improved. On the other hand, increased bypass ratio means increased engine frontal area with consequent increase in drag and size of landing gear installation. It is also important that the efficiencies of the components in the bypass engine are high, in order to obtain a high transmission efficiency. Because bypass engines have lower outlet jet velocities, their thrust drop with speed is more pronounced than that for turbojet engines. This effect increases with increasing bypass ratios and reduced jet velocities. As a result some aircraft may require larger static installed thrust for safety margin purposes, in particular aircraft with only two engines. All

these problems have been overcome, and satisfactory bypass engine designs have been produced and are in service.

In gas turbine machinery, fuel efficiencies are achieved that are comparable to most other types of heat engine. For industrial and marine applications, the main disadvantage is that this fuel is of a good quality, and therefore more expensive. Attempts are being made to enable the use of lower grade fuels, even coal, but advances have been made only in some industrial applications.

When designing gas turbines intended for aircraft propulsion all these aspects must be balanced against one another. The design must satisfy both the steady state requirements and also the ability to meet the engine operator's need for fast thrust responses to changes in thrust requirement safely and quickly. This ability to meet the changes in thrust requirement which occur in operation is referred to as the transient or dynamic performance of the engine. For this purpose an accurate assessment of the engine's performance is necessary as early as possible for the optimisation process. Extensive work has been carried out for these purposes, both theoretical and experimental. When experimental work is required, it is generally carried out by the manufacturers, frequently with government assistance because of the high costs involved. The transient behaviour in particular is difficult to establish experimentally. Very accurate, fast response apparatus is required, and for the measurement of transient effects such as heat exchange and tip clearance changes, the difficulties are even larger. Because of these experimental difficulties and the high cost of test bed testing, much emphasis has been placed on theoretical work.

1.3 PREVIOUS WORK ON ENGINE PERFORMANCE

When gas turbines were being designed in the mid and late forties, the need to evaluate the performance of these engines in both the steady state and transient aspects become apparent. This would save considerable trial and error experimenting on engines and would provide insight into what was then a novel method of producing power.

The first interest was to predict the performance of the various components and once this was established to evaluate the steady state performance of the whole engine. For the prediction of component performance, reference was made to work with experimental cascade information and aerofoil theory. Typical examples of this work are summarised in Refs. 1, 37, 38, 39, 40. From this information, the component performance was predicted with various techniques such as those proposed by Howell and Bonham, (Ref. 40), Huppert and Benser ^{see} (Ref. 3), Palmer ^{see} (Ref. 3), Doyle and Dixon (Ref. 17), Ainley (Ref. 2). Ballal has tested the accuracy of some compressor stacking techniques in Ref. 3. This work involved the comparison of characteristics predicted with these methods and characteristics of a low speed compressor obtained experimentally. This work is very informative since it provides insight into several methods of axial flow compressor performance prediction.

Once the task of predicting the performance of the components had been completed, the next step was to obtain the steady state engine performance from the predicted characteristics of the components. Typical examples of this type of procedure are described by Mallinson and Lewis (Ref. 60) and Goldstein et al (Ref. 30). Because of the lack of adequate computing facilities at that time, this work usually involved

the evaluation of engine performance by hand calculations. The results were produced in charts where all the necessary parameters were shown. This procedure is adequately described in textbooks such as those by Cohen et al (Ref. 11), Harman (Ref. 33).

Today this type of calculation is carried out with the aid of a digital computer. The digital machine is usually selected because of its accuracy. Palmer and Annand (Refs 70, 71) and Macmillan (Ref. 59) described ways in which this calculation can be carried out. Palmer devised a series of subroutines, which were called "Bricks", to perform various operations on a set of thermodynamic variables. These variables represent the different parameters, such as velocity, temperatures, mass flows, etc. at a given station in the engine. These variables, corresponding to the inlet of any component were fed into the "Bricks", which performed certain operations on these variables. The operations represent the action of the component the brick is meant to model. Some of the bricks represent engine components, others are meant to operate as interfaces between the "component bricks" when the output of one component is the input of another. The task of organising the "Bricks" depends on the desired engine configuration to be analysed and is left to the user who has to produce a "master programme" for this purpose. Such a "master programme" to analyse many configurations of fixed and variable cycle engines has been produced by Macmillan, using the aforementioned "Bricks". This master programme was designed to read the component characteristics and perform Off-Design Point calculations.

The next logical development from these investigations is the prediction of engine performance during the transient phase

In this work the transient or dynamic phase is defined as being that during the controlled acceleration and deceleration of the engine. Originally this work was carried out for control purposes, and possibly for the calculation of maximum stresses, in particular thermal stresses of the turbines. During the early and mid fifties the Lewis Flight Laboratory in Cleveland, Ohio, in the United States, was engaged in this aspect of jet engine performance. In these first studies the engine investigated was a single-spool turbojet with a centrifugal compressor. This engine was assumed to be represented by a linear system. Such was the method proposed by Otto and Taylor (Ref. 66) in 1950. Their analysis was intended to account for any inlet condition and they proposed that the accelerating torque Q was given by equation (1.14)

$$Q = \left(\frac{dQ}{dF}\right)_{ss} \Delta F + \left(\frac{dQ}{dN}\right)_{ss} \Delta N \quad (1.14)$$

The partial derivatives are taken at a steady state point ss . This equation is shown in a simple form, ignoring altitude corrections. From this analysis it followed that the engine's behaviour was adequately described by a first order system where the time constant is given by

$$\tau = \frac{-I}{\left(\frac{dQ}{dN}\right)_{ss}} \quad (1.15)$$

In the discussion of their work, the authors point out that this analysis was satisfactory only for small movements on the performance maps of the engine. When large accelerations were

considered, this method produced only a fair agreement with experimental results. When predicting the performance during decelerations, the results of their analysis differed significantly from the observed results. The authors reached the conclusion that for large scale transients the assumption of the engine behaviour being linear was not so good. Other reasons put forward to account for the discrepancies were the assumption of constant combustion efficiency, and no account having been taken of changes in the component efficiencies.

A similar type of analysis was used by Heidmann (Ref 36) to analyse a similar engine for variation of several parameters, such as efficiencies, flow Mach number, etc. An attempt at scaling the time constant to suit different engine sizes was also carried out. Taylor and Oppenheimer (Ref. 87) extended the analysis to turboprop engines. The expression to obtain the time constant was generalised to include the presence of the propeller.

$$\tau = \frac{C4}{\left(\frac{dQ}{dN}\right)_e + \left(\frac{dQ}{dN}\right)_p} \quad (1.16)$$

where C4 is a constant given by the engine geometry and the design rotational speed. A similar type of analysis was used by Fedor and Hood (Ref. 26) to study the effect of afterburning.

In 1952 Delio examined three methods of calculating the engine behaviour in the transient phase following step and oscillatory movements of fuel flow and final nozzle area. Each method was a compromise between accuracy and complexity. Delio proposed that depending on the needs of the user, a different method would be suitable for a certain set of circumstances.

It must be stressed that the year was 1952 and that digital computing was virtually non-existent. All the work described so far was aimed at control systems analysis. The objective was to achieve a better understanding of the engine and to produce work such as that of Dandois and Novik (Ref. 14) where a control system is proposed, or Otto et al (Ref. 67) who designed fuel controls.

This early research paved the way for Ketchum and Craig (Ref. 43) and Pack and Phillips (Ref. 69). In these exercises an analogue computer was used to simulate the engine behaviour. The engines were still being represented by linear systems. The analogue computer was used to obtain real time engine simulation and to allow the coupling of the control device to the computer rather than to the engine.

The need for more accurate modelling started to be felt when more complex engines were envisaged and designed. Novik (Ref. 64) still proposed a linear system analysis for a two-spool turbojet, but he recognised the need to use a second order system for such a complex configuration.

This was the time when the N.A.C.A. became the N.A.S.A. and work on this field became less intensive, taking second place to the requirements of the space programme.

The simplicity and shortcomings of the simulations so far described were becoming apparent, and the need to analyse the engine as a non-linear system was realised. Filippi and Dugan (Ref. 29) investigated the effects on accelerations of three compressor arrangements of two-spool engines. These calculations were carried out manually, and some simplifying assumptions were made, but the engine was treated as a non-linear system. From the component mass flow characteristics,

component efficiencies being assumed constant, charts of constant mass flow were drawn where the various engine variables were plotted. From these charts, assuming instantaneous turbine inlet temperature rise, the accelerating torques for the shafts were obtained. This process was repeated for a continuing series of time intervals until the steady state was attained. This procedure is a typical example of how a hand calculation would be carried out. Larrowe et al (Ref.47) investigated the possibility of using map reading to provide the engine characteristics. This investigation was the first time the method of constant mass flow was used on a computer. When an analogue computer is used to simulate the engine, the circuits of the machine will automatically satisfy the requirement of continuity of flow, thus no iteration technique is necessary. Durand (Ref. 18) describes the use of digital computer systems to simulate engine performance, using this method. Time lags on combustion, fuel input and increase of mass flow were used to obtain good agreement between predicted and observed transient parameters.

In the early 1960's, Saravanamutto pursued a similar approach using an analogue computer to analyse a small shaft power engine. These analogue computer techniques are described in Ref. 77, and in Ref. 78. At this time Saravannamutto started work on his Doctorate Thesis which was based on this approach to transient behaviour simulation. In this thesis (Ref. 79) a single-spool turbojet and a two-spool turbojet with reheat were analysed. While this work was being conducted, Fawke started work on his own Doctorate Thesis. This ersearch was directed towards the production of a digital computer method for the transient performance. The method adopted was that of

intercomponent volumes, where allowance for the storage of mass in the engine is included. Ref. 21 described this work in which five engines of four different configurations were analysed. This work was continued in a fruitful collaboration with Saravanamuttoo in which both the constant mass flow method, and the intercomponent volume method were used. The calculations are performed with the three types of computer, digital, analogue and hybrid. This work is outlined in Refs. 22, 23, 24, 25, 80. The discussion to Ref. 25 prompted some rethinking of some of the techniques used, but it was recognised that the method of intercomponent volumes had been thoroughly analysed. Additional work was produced by Saravanamuttoo and MacIsaac in which the method developed by Fawke was used for analysing different engines for a range of purposes (Refs. 58, 81, 82). In Ref. 57, a comparison was made between the three types of computer used for engine simulation. Since that time the digital computer has been intensively developed, the result of this progress being the feasibility of real time digital engine simulation.

With regard to other types of gas turbine engines, Bammert and Krey (Ref. 4) have analysed the transient behaviour of a closed cycle machine. This gas turbine uses helium as its working fluid, the machine being a nuclear heated closed cycle gas turbine. In this engine, a large amount of intercomponent ducting existed, dictated by the use of intercoolers in the design. Account had to be taken of steady state heat transfer and mass storage in the plant. No account was taken of transient heat transfer, although the need for this was recognised. This investigation shows how different the requirements of gas

turbines for various applications can be.

Returning to aero gas turbines the N.A.S.A. has produced two general simulation programmes designed to model several engine configurations. This is the only attempt known to produce a general transient programme in which no reprogramming is necessary if different gas turbines are to be simulated. The only parameters to be changed are the control variables defining the engine geometry. One of the programmes is known by the acronym HYDES, described by Szuch and described in Ref. 85. This programme was developed for hybrid computer facilities. It can analyse eight engine configurations, although it cannot model three-spool engines. DYNGEN, designed by Sellers and Daniele (Ref. 83), can analyse eleven engine types, three of which are three-spool configurations. DYNGEN has been programmed for digital computers. These two programmes, which were produced in the mid 1970's, are both based on the method of intercomponent volumes. A disadvantage of HYDES is that if a compressor is designed with air bleeds the programme allows these flows to be extracted only between two components. It would be possible to treat a compressor as two separate components, one before the point from where the bleed flow has been removed, and one after this point, but it is not clear if the programme has such a capability. If it does, it would need longer computing times, and more extensive data inputs and data manipulation. From the report on DYNGEN it is not very clear if bleeds can be removed from any point along the length of a component.

At about the same time as the N.A.S.A., work was being carried out, Itoh et al (Ref. 41) used analogue techniques to

analyse a two-spool turbofan. This work is very similar to the early work carried out by Saravanamuttoo (Refs. 77, 78, 79), but the more advanced computer enabled the presentation of more information.

Investigations of the types described above are still being made for control purposes. The insight obtained by non-linear engine simulation has helped the research carried out in this field such as that of Ushiyama (Ref. 89) and that of Fett (Ref 27). Ushiyama investigated engine performance modifications due to changes in the prevailing atmospheric conditions. Fett studied the effect of various other disturbances such as the effect of the asymmetry of the bleeds.

In virtually all the models described so far, it had been assumed that the flow in the components such as compressors and turbines, was adiabatic. It was further assumed that the characteristics obtained from steady state running tests could be applied during the transient. The weakness inherent in this approach was uncovered in the early 1960's, when a very accurate transient analysis was required for a German helicopter turbo-shaft engine. This theoretical work was carried out in parallel with the experimental development of the engine. It was soon realised that consistent discrepancies existed between the predicted and the observed results, the predicted performance erring on the optimistic side. Bauerfeind (Refs. 5, 6, 7) reported on these observations, and attributed these differences to three factors:

Effects of heat storage in the engine

Effects of mass storage in the engine

Effects of combustion inefficiencies.

This work formed the basis of his Doctorate Thesis. Thomson,

(Ref. 88) continued to investigate these effects and he suggested that blade tip clearances are another factor to be considered. Thomson's predictions showed a good agreement with those of Bauerfeind.

In Britain a few years later, Maccallum started to investigate these effects. Ref. 50 of 1969 described experimental work in a single-spool turbojet. In this work it was observed that the thermodynamic variables of the engine immediately after the end of a speed transient were not the same as those three minutes after the end of this transient. These modifications in performance were attributed to the fact that the engine materials need some time to attain their equilibrium temperatures. These non equilibrium temperatures result in modifications of component characteristics, non design blade tip and seal clearances, non-adiabatic work transfers, density changes of the fluid, etc. caused by heat transfer. Some of the effects of heat transfer on the boundary layer of aerofoils and how this affected compressor performance were studied by Maccallum and Grant (Refs. 51, 56), who also studied the effect of density changes of the working fluid due to heat exchange between this fluid and the engine materials. In subsequent work (Refs. 53, 54) these effects were incorporated in the engine transient investigations, particular attention being paid to the changes in compressor performance due to this heat exchange. For the evaluation of these effects a transient programme based on a modified version of the constant mass flow method was used. The component performance charts were considerably simplified to save computer storage space and running time. These simplifications were justified because the aim of this work was to evaluate the magnitude of the effects, rather than

to produce an accurate simulation of the engine performance.

Other more recent attempts to include these effects are described in the work of Onions and Foss (Ref. 65) of the N.G.T.E. They proposed simple techniques, such as scaling up the values of the rotor inertia to obtain good agreement with test bed information. Some more realistic methods are proposed by Rick and Mugli (Ref. 74) and Larjola (Ref. 48), the latter suggesting very detailed analysis of the heat transfer effects. The aim of these investigations has been to minimise the type of work carried out by Rubis (Ref. 76) who investigated experimentally the transient performance of an aero-derived marine gas turbine. Experimental engine test bed running is essential, but due to the high costs involved it should be minimised.

Summarising the above, two methods are currently in use for predicting transient performance. These methods are the method of intercomponent volumes and the method of constant mass flow. The N.A.S.A., Saravanamuttoo and Fawke and subsequent co-workers have used principally the method of intercomponent volumes. Bauerfeind and Maccallum have carried out their simulations using the method of constant mass flow. Bauerfeind has incorporated an algorithm to account for heat storage and mass storage. Maccallum has included a detailed analysis of heat transfer effects. There is no doubt that engine manufacturers have produced their own engine analysis programmes, probably using both methods and making some allowances for heat transfer effects. Unfortunately it is difficult to gain access to this work because of commercial or military security reasons. There may be additional work which has been carried out and is not subject to security restrictions, but the author is not aware of its existence.

1.4 CHOICE OF METHODS FOR PRESENT WORK

As previously discussed, the first attempts to establish the transient behaviour of an engine were of an empirical nature and they were based on the test bed analysis of the machines. The first theoretical methods of calculation of transient behaviour involved the calculation of an engine time constant. This time constant governed the rate of acceleration or deceleration of the engine. In the first attempts to predict the transient performance of a gas turbine, it was realised that the use of the engine's component characteristics was the best means of carrying out this analysis. Component characteristics are unique to each engine model. Any theoretical model not using them has to evaluate them, or some equivalent parameter from the engine's geometry with consequent increase in computing cost. Alternatively, assumptions are made sacrificing the accuracy of the model. Current techniques recognise the importance of using steady state component characteristics, and two distinct methods based on these characteristics are employed, these being:

The mass flow method, which assumes mass continuity at all times and points in which the engine is operating.

The intercomponent volumes method, which for the calculation of the engine's pressure dynamics uses mass flow imbalances between the engine's components.

In the constant mass flow method, the inlet parameters of a component and its rotational speed are known, or have been assumed. From these conditions and the component's characteristics

the outlet thermodynamic variables can be evaluated. This is carried out for all the components in the engine and the mass flows are noted. In general the mass flows will not satisfy the principle of continuity. To satisfy this principle the initial parameters of some components are modified and the process is repeated until the mass flows are compatible. The work produced or absorbed by each component is then calculated and acceleration or deceleration rates evaluated for the shaft(s).

In the method of intercomponent volumes, mass flow imbalances are allowed to occur. Volumes are introduced between the various components and all flow imbalances are assumed to occur in these volumes. The mass flow through each individual component is assumed to be constant. These mass imbalances are used to evaluate the rate of pressure increase to the engine. For the combustion chamber, the energy equation can be used, alternatively, this component can be separated into two sections, the energy input occurring in the plane where they are separated. Once all the components have been analysed in this fashion, the power delivered or absorbed by the components is evaluated and subsequently the rotor torques and accelerations are determined. In both methods the process is repeated for the next time interval until a limiting time is reached.

The method of intercomponent volumes has been thoroughly analysed by Fawke and Saravanamuttoo and the N.A.S.A. using both digital and analogue computers. The method of constant mass flows has also been used, but has not been analysed so thoroughly. So far no work employing the method of constant mass flow has been published where very complex engines, in particular with split compressors, are analysed. Obviously each method has its own merits and demerits. The method of

intercomponent volumes is more realistic from the point of view that flow imbalances do occur during transient operation. As mentioned, this method involves a straight-through calculation on the engine, without the need for iterative loops, to obtain an appropriate operating point of the various components. The engine is treated one component at a time, starting with the intakes and compressors, and the analysis progresses with the knowledge of parameters from the previous time interval, until the final nozzle of the engine is reached.

In the constant mass flow method, particular attention needs to be paid to the convergence process. Fawke (Ref. 21) found that convergence could not be obtained when he tried to analyse a two-spool bypass engine. The reason why convergence was not achieved must have been a convergence routine which was not efficient. Durand also reported problems in obtaining convergence for such a configuration, although in his case the difficulties were overcome. If in the mass flow method, convergence is efficient, a potential saving of computing time can be realised. The assumption of constant mass flow on any engine is not unrealistic because the mass flow imbalances are small when compared to the engine mass flows. If the chosen time intervals are sufficiently long, pressure dynamics may be assumed to have taken place between two time steps. Fawke (Ref. 21) using the method of intercomponent volumes, quotes that for the engines he analysed, the choice of the size of the volumes to be included between the components has little effect on the prediction of the transient. Indeed, halving the volumes produced no difference in the calculations. This would lead to the conclusion that mass flow imbalances are not so large. This fact is confirmed by Rick and Mugli (Ref. 74) who found

out that mass storage effects are significantly smaller than heat storage effects, and the former could be neglected in most cases.

It is also important to notice that when an engine moves from idle to design conditions, a large increase in engine mass flow occurs, but the increase in the mass of the fluid stored in the engine is less marked. This increased mass flow is proportional to the product of the increased fluid density in the engine and the higher velocity of the fluid at this characteristic position. In the engine investigated in chapters three, four and five, the core mass flow increases by a factor of five, but the density increases only by a factor of three, the fluid density being the parameter that determines the amount of fluid mass present in the engine at any instant. When the bypass duct was examined, the influence of velocity change was even more noticeable, mass flow increased by a factor of 2.5, while density increased only by a factor of 1.6.

In the present work an investigation of this effect was carried out to confirm these facts and is detailed in Chapter V.

When comparing the predictions of the intercomponent volumes and constant mass flow methods, a small difference can be observed on the initial section of the predicted paths on the compressor performance maps. This difference is apparent only for a few time intervals following a sudden change in the fuel flow (Ref.21). The constant mass flow method will predict an instantaneous pressure rise or drop on the non-dimensional speed line. During an acceleration, for example, a small initial reduction in the mass flow of the engine will be caused by the sudden increase in the temperature of the fluid in the

hot section of the engine. This fact is supported by the investigation detailed in Chapter VI. The resulting path of the compressor characteristics will have an angular shape. The method of intercomponent volumes will predict a more rounded shape for the path of the characteristics. The pressure dynamics included in the model will produce a more gradual change in the fluid's variables.

To summarise, the method of constant mass flow was adopted in this work because of the following reasons:

- 1). The method provides a realistic representation of the events occurring in the engine during a transient, mass flow imbalances being small.
- 2). Development of the method seems to have stopped when the converging processes became difficult for complex engine configurations.
- 3). A potential for saving computing time exists if a suitable algorithm to ensure efficient convergence is designed.
- 4). An engine should always converge to a given mass flow if the components are compatible.
- 5). The time interval to be used is larger than the critical time interval.

1.5 CHOICE OF COMPUTER

An extensive amount of numerical handling and storing results from the mathematical modelling of gas turbine engines. To obtain results quickly, and to allow the models to have some degree of sophistication, the use of a computer is indispensable. Three kinds of computer are available to perform these calculations:

the analogue, the digital and the hybrid computers. If the modelling is to be carried out with an analogue computer, electrical circuits are set up to represent the engine components and their performance characteristics. This machine has the great advantage of allowing the different component parameters to be evaluated simultaneously, thus enabling what is termed "real time" simulation. The term real time simulation denotes the capability of carrying out the simulation in the time the real engine performs the transient. This feature makes the analogue computer ideal for the design and testing of control devices, where the device is connected to the computer rather than the real engine. This capability of doing several component simulations simultaneously is termed "parallel calculation" capacity. The result of the analysis is in the form of voltages which represent the thermodynamic variables. Saravanamuttoo in his Doctorate Thesis (Ref. 79) gives a very good description of such a system. The analogue computer allows the circuits representing engine components to operate simultaneously, thus algebraic loops to achieve some parameters, such as the mass flow to satisfy continuity, are not required. For modern high precision analogue computers, reliability and repeatability do not present any major problem. However, when complex engines are analysed, the simulation will be less accurate due to the large number of components involved. The most important drawback of the analogue computer is the difficulty of programming. The user needs more experience and expertise to set up the analogue circuits than the user of a digital computer would require to programme his machine. On the other hand, the programming of an analogue computer will be made easier because the differential equations describing the thermodynamic processes are performed continuously, without need of numerical techniques

to solve these equations. These techniques are essential when a digital machine is employed, and one typical result is the need to divide the processes into a series of time intervals.

One feature of the digital computer is repeatability and accuracy. Its main disadvantage used to be its slower speed of computation. The digital computer with a single processor performs only one operation at a time. Some more modern machines have more than one processor and more than one operation can be carried out at any time. Their speed of computation is increasing with continuous development. At the present date there is no doubt that some digital machines have the capacity to operate in real time. With continuous progress this capacity will increase. Digital computers are also superior when large amounts of data are to be stored and handled. If a different engine is to be simulated, a digital computer would only require modifications in the data supplied. An analogue computer would need substantial modifications in the function generators representing engine components. If a new engine of a different configuration is to be analysed, a new electrical set-up will be required.

The hybrid computer was designed to combine the advantages of both machines. An analogue computer is used for the integration processes, and a digital machine stores the data and performs the numerical manipulations. This machine is the most powerful, but the most complex, in particular at the digital-analogue interface. This interface provides for the interchange of both logical and variable signals between the two component machines.

With the development and improvement of high-speed digital computers, the digital machine has become the most favoured for engine analysis. From the commercial point of

view, it is easier to justify the purchase and maintenance of a digital machine because of its extreme versatility. An analogue computer would only be useful for the purpose for which it has been set up.

The present work was carried out on a digital computer primarily because of the availability of adequate digital computer facilities in the University of Glasgow. The machine was an I.C.L. 2976 and in the last months of the work an I.C.L. 2988. The simulations in these machines were achieved in about one and a half to five times the real time, depending on the complexity of the engine configuration, and the effects included in the simulation.

CHAPTER II

DESCRIPTION OF GENERAL TRANSIENT PROGRAMME

2.1 INTRODUCTION

When the representation of a system is desired, a model is devised, and the behaviour of this model is compared to that of the system. If the agreement is close enough, the model is said to represent the system.

In the particular case of a gas turbine, the model is physical or mathematical. A physical model requires experimental work on a scaled version of the engine or its components. A mathematical model invariably involves computer programming, because of the lengthy calculations involved, particularly for the more complex engines. Some early attempts (Ref. 29) employing hand calculations were carried out, and although successful, they were lengthy and tedious, and only the simplest of systems were analysed. In addition, some unrealistic assumptions had to be made to make the simulation feasible.

The simplest modelling of the engines is by assuming a linear system to represent them. This is a good assumption for small changes from a given operating point and is the type of model used for engine control, and when studying the influence of different disturbances at some critical or important points of performance range. Manufacturers have what is called the "Small Change Matrix" of an engine for a given operating point

or points. These models are not useful for large scale transients nor for the determination of the operating line and therefore they are of limited usefulness in the present work.

Another possible approach is the fundamental one, in other words, working from first principles. In this type of model, many engine parameters, in particular the performance of each component, have to be calculated from the engine's geometry. This approach suffers from the disadvantage of lengthy calculations and frequently the predictions are not of satisfactory accuracy.

A more convenient approach is to divide the above procedure into two steps. The first step is to predict the performance of the components, working from the engine's geometry. Once this has been accomplished the predicted characteristics are used for the calculation of the complete engine's steady state and transient performance. As the development proceeds and experimentally observed performance of the components becomes available, only the component performance maps need to be modified for continuing investigations. This type of procedure has many advantages. Component characteristics are frequently readily available and in particular for older engines they are very easy to obtain. If the characteristics for the components of a given engine configuration are not available it is not very difficult to generate them from those of other engines. Thus 'imaginary' engines can be simulated, as in the case of the single-spool turbofan analysis described later in this chapter, in section 2.3. The programme will remain unchanged, only the information required will be modified.

A word of caution must be expressed at this point on the use of steady running characteristics for the prediction

of transient performance. Most of the transient programmes that have been described and are currently employed, use steady running characteristics. However it is generally accepted (Refs. 45, 56) that the characteristics of the components at a particular instant during a transient will differ from the characteristics observed in the steady state at the same non-dimensional speed. These changes in component performance, due to tip clearance changes, and heat transfer effects are described in chapters III and IV. In the performance prediction programme developed in the present work, allowance is made for these changes in component performance. Typical results are given in chapter V.

2.2 THE METHOD

The present method is designed using the component characteristics (initially the steady running characteristics) as a basis to carry out the performance analysis. The objective of the programme is to calculate the acceleration that the engine will experience under various circumstances. The acceleration is a function of various parameters

$$\frac{dw}{dt} = f(N_j, F, A_l, M) \quad (2.1)$$

It is evident that this acceleration will be a function of several other variables, such as component pressure ratios, temperature ratios, efficiencies etc. These parameters are also dependent on the rotational speed and the fuel flow and for this reason they are omitted from the above expression. Once the acceleration is evaluated, there are several methods of treating this parameter to obtain the rotational speed for the next time interval. Numerical techniques of various orders

and varying complexity can be used for this purpose. The simplest of all these techniques, and the one used in this programme is Euler's method, where it is assumed that the acceleration will remain unchanged during the time interval for which it has been calculated (equation (2.2)).

$$w_{t+dt} = w_t + \left(\frac{dw}{dt}\right)_t \Delta t \quad (2.2)$$

The first step is to evaluate the fluid properties at the principal sections in the engine. For this purpose the principle of mass continuity is assumed to hold under all engine operating conditions. If certain parameters of an engine are fixed, then the state of the engine is defined. This number of parameters is a function of the complexity of the engine.

For example if a single-spool turbojet is operating at a given altitude and forward speed, the external parameters of inlet pressure, inlet temperature and flight Mach number are defined. If for this engine of a given geometric configuration, the rotational speed and the fuel flow are fixed, there is only one value of engine pressure ratio that will satisfy the the criterion of mass continuity. In this case the state of the engine is defined. The procedure for obtaining the values of the parameters which define the engine state is now outlined. An iterative procedure, starting with an arbitrary value for the compressor pressure ratio is devised. From the compressor characteristics, the non-dimensional mass flow and the isentropic efficiency are obtained. With the evaluation of these parameters, and the knowledge of the externally defined parameters, the compressor delivery pressure, compressor outlet temperature and mass flow are calculated.

The fuel flow into the combustion chamber, and the air mass flow into this component will define the combustion temperature rise. If the combustion chamber inefficiencies are known, allowance is made for them. Thus the non-dimensional mass flow at the entry to the turbine is calculated. When the turbine is unchoked, the turbine pressure ratio is then defined, if the turbine is choked, an arbitrary pressure ratio is chosen. From the turbine characteristics, the isentropic efficiency is found, and hence the turbine outlet temperature. Knowledge of these parameters enables the calculation of a required nozzle area to discharge the flow (the programme has been extended to incorporate reheat systems, if required). In general, mass continuity (equation 2.3) will not be satisfied.

$$\frac{dA}{A} + \frac{dv}{v} + \frac{dp}{p} = 0 \quad (2.3)$$

Conditions which will satisfy mass continuity are then obtained by first comparing the nozzle area required to discharge the flow and the actual geometric nozzle area (the latter corrected by a coefficient of discharge if appropriate). A variable, X, to be modified is then selected and the relationship (2.4) is then established.

$$\frac{dX}{X} = f\left(\frac{dA}{A}\right) \quad (2.4)$$

In equation (2.4) A is the geometric area available to discharge the flow, and dA the error in the area produced by choosing the given state parameters for the current iteration. In this particular example, if the turbine is ~~unchoked~~, the variable to be modified is the compressor pressure ratio. If the turbine is choked, the variable to be modified is the pressure ratio of the choked turbine, a previous iteration sequence will have

adjusted the compressor ratio to meet the capacity of the choked turbine. This variable X , is then adjusted to bring the required nozzle area into agreement with the geometric nozzle area. Since the system is not linear, and the desired function $f(dX/X)$ will change along the different running conditions of the engine, an iterative procedure is devised to obtain the equality between the required and geometric nozzle areas. The desired function is assumed to be of the form shown in equation (2.5)

$$f\left(\frac{dA}{A}\right) = \left(1 + \frac{dA}{A}\right)^a \quad (2.5)$$

where the exponent a is a variable exponent which is continuously modified as will be outlined later.

The above description illustrates the mathematical procedure for the simplest gas turbine. More complex engines require more elaborate procedures. A summary of the general approach is now given. For turbojets and for engines with separate exhausts, the variable to be modified is chosen according to engine configuration, the shape of the curves in the compressor characteristics and the state of the turbines. If a turbine is choked, the compressor pressure ratio is modified until the required value of the turbine capacity is obtained. Once this has been achieved the variable adjusted to satisfy mass continuity at the final nozzle is the pressure ratio of the choked turbine nearest to this nozzle. The fluid velocity at this turbine is the fluid's sonic velocity, and any pressure signals cannot be transmitted upstream of this point. Once the chosen parameter is modified the process is repeated until the desired equality between required and geometric final nozzle areas is achieved. With the principle of mass

continuity satisfied along the engine, the next step is to evaluate the torque imbalance of the shaft(s). This torque imbalance then determines the instantaneous acceleration, which as previously stated is assumed to be constant for the given time step. This acceleration is then integrated over the time interval to find the rotational speed of the shaft at the next time step. The process is then repeated until a limiting time is reached.

For engines with mixed exhausts there is an additional requirement. The principle of momentum conservation, equation (2.6) must be satisfied by the fraction

$$\rho A v dv + A dp = 0 \quad (2.6)$$

of core gas and the fraction of bypass air to be mixed. For this purpose an infinitely thin control volume is set up in which all the mixing is assumed to occur. At entry to this control volume, the static pressures of the hot and cold streams are equal. To obtain this equality in static pressure, an iteration loop similar to the one devised for the continuity principle has been implemented. No dissipation is assumed in mixing process. If required, losses can be represented by means of a small pressure loss occurring at the final nozzle. Integrating equation (2.6) takes the form of (2.7), in which momentum conservation is expressed as the impulse function being constant.

$$\rho A (1 + \gamma M^2) = C5 \quad (2.7)$$

Integrating the equation of continuity of mass flow, substituting the static temperature and pressures by stagnation or total temperature and pressures, and expressing the velocity as a function of Mach number and the sonic velocity, equation (2.8)

is obtained by rearranging the terms.

$$P_{o_o} = \frac{\dot{m}}{A} \left(\frac{R T_o}{\delta} \right)^{\frac{1}{2}} \frac{\left(1 + \frac{\delta-1}{2} M_o^2 \right)^{\frac{1}{2} \left(\frac{\delta+1}{\delta-1} \right)}}{M_o} \quad (2.8)$$

Rearranging the equation (2.7), which describes momentum conservation, and substituting to obtain the stagnation pressure, equation (2.9) is obtained

$$P_{o_o} = \frac{\sum p_i}{A} \frac{\left(1 + \frac{\delta-1}{2} M_o^2 \right)^{\frac{\delta}{\delta-1}}}{1 + M_o^2} \quad (2.9)$$

The solution to these two equations (2.8 and 2.9) will yield the mixed flow Mach number, and the stagnation pressure of this flow. The stagnation temperature of the mixed flow has been evaluated by means of (2.10) which is a form of expressing energy conservation.

$$T_{o_o} = \frac{\dot{m}_{cg} C_{p_{cg}} T_{o_{cg}} + \dot{m}_{bp} C_{p_{bp}} T_{o_{bp}}}{\dot{m}_{cg} C_{p_{cg}} + \dot{m}_{bp} C_{p_{bp}}} \quad (2.10)$$

The two equations obtained from mass continuity and momentum conservation, are to be solved by an iteration process. Analytical solution is not possible.

A comment should be made on the choice of the time interval used in this procedure. If the time interval is too large the assumption of constant acceleration is not valid, and this will lead to unrealistic modelling, and could lead to instabilities in the calculations. If too small it will lead to computation times which will be longer than necessary.

2.2.1 Iteration Requirements of Various Configurations

The convergence process follows the nested loop approach. Before proceeding to the next component, all tests on the previous components have to be satisfied. If not, the inlet

parameters of the nearest upstream "free component" are modified until a satisfactory operating point is obtained for the component in question. The term "free component" describes a component on which the thermodynamic variables for the operations of the components downstream are generated. Three types of components can be "free components": the first compressor, the first compressor of the core section in a bypass or turbofan engine with mixed exhausts, or a choked turbine.

A choice is available on the set of inlet variables for the first compressor. This is necessary because many fans and L.P. compressors exist whose characteristics are very flat, even double valued. In this case it is desirable to start the iteration process by using the mass flow rather than the pressure ratio as initial input. For single valued characteristics which are not very flat, the choice of inlet variable is irrelevant. The downstream compressors have pressure characteristics which are fairly steep, nearly vertical in some cases. For these compressors, the inlet parameter is the non-dimensional mass flow, which is defined from the outlet parameters of the previous compressor. It is only when a "free component" is encountered that an arbitrary pressure ratio is chosen as the input variable.

When a mixer is present, the engine is less sensitive to instabilities of the convergence process. To obtain the correct engine mass flow the iterations are not started from the first compressor, but from the first core compressor, thus reducing the number of components within the iteration loops. When an engine with mixed exhausts is analysed, the principles of mass conservation and momentum conservation at the entry to the mixer nozzle must be satisfied, in addition to the already described mass continuity at the final nozzle. Because of the

additional iterations imposed by these requirements, the convergence process takes longer to be completed.

Turbojet engines, and engines with separate exhausts have exactly the same convergence procedure. For the analysis of these engines, the inlet parameters of any compressor are defined by the outlet parameters of the previous compressor. The mass flow through the cold nozzle of an engine with separate exhausts is calculated from the pressure ratio across this nozzle, the fluid density and the flow area. The flow exhausted is subtracted from the total flow to obtain the flow through the core components. In a turbojet engine the flows are basically constant, only bleeds being removed from the engine flow.

In Fig. 14 a block diagram of above described iterative procedure is illustrated. This procedure is general and can be applied to engines having any number of spools, and to turbojets and engines having any bypass arrangement. The engines may incorporate reheat. All bleed flow calculations, cold exhausts and individual tests have been omitted for reasons of clarity. The remainder of the procedure, torque calculations and transient effects are not illustrated because they are straightforward.

2.2.2 Convergence Algorithm

The previous sections describe the procedure employed to satisfy the requirement of continuity of flow in any engine configuration. When this procedure was first applied to a single-spool turbojet engine, convergence was achieved in five or six iterations. With the adaptation of the programme to more complex configurations, the total number of iterations increased greatly due to more complex algebraic loops and more nested loops. The iterating technique had to be improved to economise in

computing time. One method of improving the convergence is for the index which modifies the parameter X , to be a variable (equation 2.5). This exponent should be variable because indirectly it is a function of the slope of the compressor characteristics for unchoked turbine conditions, and of $(dA/A)/(dP/P)$ for choked turbine conditions. It is realised that such a facility would be particularly important in the more complex engines, where the convergence procedure is critical. In these engines a small change in the initial set of chosen parameters will produce a large change in the calculated variables at the hot end of the engine.

A procedure for continuously adjusting the index (symbol a) has been developed. Initially, " a " is arbitrarily set at a low figure (to avoid instability) and the new parameter for the next iteration is modified as a function of the error the previous input had produced.

$$X_{t+dt} = X_t \left(1 + \frac{dA}{A}\right)^a \quad (2.11)$$

The error emerging at the end of the new iteration is compared with the previous error and the index " a " is revised as follows:

$$a_{t+dt} = a_t \left(\frac{C6}{1 - f(e)}\right)^{C7} \quad (2.12)$$

where

$$f(e) = \frac{(dA/A)_t}{(dA/A)_{t-dt}} \quad (2.13)$$

The effects of using a range of values for $C6$ and $C7$ have been examined. It was found that near optimum convergences were generally obtained if $C6$ was given the value 0.7 and $C7$ the value 0.6. This choice was satisfactory for most engine types,

although in the case of a two-shaft turbofan with separate exhausts, calculations moved outside the allowable non-dimensional speed of a component. This difficulty was avoided by lowering C_7 to 0.4.

The original intention was to apply the method of convergence using the variable exponent to the two external loops, these being the loop dictated by the mass continuity equation, and the loop dictated by the requirement of similar pressure ratios at the entry to the mixer nozzle. When the analysis was extended to the internal loops of the various components, a significant amount of computing time was saved by optimising the exponents of the convergence loops corresponding to these components. The time saved was of the order of ten to fifteen percent, depending on the engine type.

The variation of the exponent achieved in the above procedure ensured that the convergence was not too fast and prone to instability, nor too slow resulting in long computing times.

2.2.3 Handling of Engine Variables

The characteristics of the compressors and turbines are loaded as constant non-dimensional speed lines with as many points as desired. Characteristics for both types of components are fed in tabular form, where the pressure ratio, efficiency and non-dimensional mass flow are loaded for several points of many speed lines.

An examination of the method of interpolating between speed lines was carried out. The original intention had been to load only a few speed lines, and use Lagrangian interpolation to obtain the desired speed lines. Although this proved success-

ful for some components of some engines it was not so for all cases. Trials of the interpolation process were carried out with several sets of characteristics for which the information for about thirty speed lines was available. Five non-dimensional speed lines were loaded and interpolations were carried out at intermediate values of the non-dimensional speed where the performance was known. Turbine mass flow characteristics were always accurately interpolated. However interpolations of compressor characteristics of pressure ratio and efficiency (for a given mass flow) were not so satisfactory. There was only one instance with compressors in which the interpolations were accurate, within one percent, this being the L.P. Compressor of an older version of the two-spool bypass engine with mixed exhausts. In the general case, no improvement was made when the order of the interpolating polynomials was reduced to parabolic. It was also observed when using Lagrangian interpolation that the computing time was thirty percent longer than that observed by loading all thirty one speed lines and interpolating linearly between the much shorter intervals. For these reasons it was therefore decided to use as many speed lines as possible and interpolate linearly across the small intervals. If there were not many speed lines available then the interpolation procedure reverted to the method of Lagrange.

A facility has been introduced for scaling component characteristics. When the programme was being developed, it was evident that the characteristics of many configurations would not be available. It would be desirable to factor up and down the performance maps of other engines to suit the engine configuration being investigated. Thus it is possible to scale the non-dimensional mass flow, pressure ratio, and the efficiency.

In addition, a constant loss or gain can be incorporated to the efficiency characteristics of any component, to study such an effect if desired. Another reason for introducing these scaling facilities is the fact that, normally, the observed steady running performance in the engine will not necessarily be the same as the one observed in the component rig. The reason for this is that when the components are assembled to form the engine, inter-component effects modify the performance. Pressure losses occur in the intercomponent ducts, some clearances, in particular seal clearances will not be as at the design conditions, and bleeds are removed from some components for cooling purposes. This observation is confirmed by Onions and Foss (Ref. 65).

Compressor bleed valve openings are scheduled as a function of the non-dimensional speed of the rotor in question. Provision has been made to remove bleeds from any point in the compressors, and they can be returned anywhere in the engine, to the bypass ducts or discharged overboard. Cooling flows are similarly treated. It should be noted that the magnitudes of these cooling flows are influenced by the clearance of the seals controlling them. These clearances are treated in Chapter III.

When the throttle of an aeroplane is moved to a different control setting, the fuel flow does not change instantaneously to the new final fuel flow demanded by the lever angle. If this occurred, the transient could endanger the engine. The fuel flow is controlled by a device which senses one or several engine parameters. The controller allows a given fuel to be fed to the engine according to a predetermined schedule which is a function of these engine parameters. Gas turbines must avoid operation beyond two limits, and the function of the fuel controller is to ensure operation within these limits. One

of the limits is compressor surge. This occurs when the air flow in a compressor breaks down because of aerodynamic reasons, and the air, or part of the air flows backwards. The other limit is the maximum allowable turbine entry temperature. This temperature is given by metallurgical considerations, and exceeding it may produce considerable damage to the engine. These two limits will not allow fuel schedules that would produce too fast a change of state of the engine. In general at low speeds, the limit will be given by the surge of the compressor(s), and at this range the transient is said to be "surge limited". At higher speeds the turbine inlet temperature can be reached before compressor surge will occur. Thus transients at the high speed section of the performance range would be temperature limited. The controllers are designed to ensure engine safety by not allowing fuel flows that could result in component operation beyond these limits. Several such fuel mass flow schedules have been introduced. One possibility is for the fuel to be scheduled as a function of the rotational speed of any one of the shafts as shown in equation (2.14).

$$\dot{F} = f(N_j) \quad (2.14)$$

This is acceptable practice only for one altitude and Mach number. When the engine changes altitudes, if the same fuel flow function is employed, the desired transient will not be obtained. The solution is to introduce a non-dimensional fuel flow schedule such as the one given in expression (2.15).

$$\left(\frac{\dot{F}}{N P_i} \right)_{HP} = f(PR_c) \quad (2.15)$$

All the parameters shown relate to the H.P. Spool in this case. This particular method of scheduling the fuel flow is suitable for all altitudes. The parameters included in the left hand side of (2.15) show a way of obtaining the fuel flow in a non-dimensional form. In Chapter V fuel schedules are further discussed.

Several other minor effects have also been taken into account, for example bypass duct pressure loss, combustion chamber pressure loss, combustion efficiency, etc. There is some difficulty in obtaining much of the information required for a credible evaluation of these factors, so a simple but realistic approach was adopted. All these variables are scheduled as a function of the H.P. shaft rotational speed. It is desirable to introduce these factors in this convenient way because their effects are relatively small and their exact evaluation does not merit particular attention.

A provision has been introduced for altering the final nozzle area, reheat fuel flow, and reheat duct pressure loss, again all loaded as schedules which vary with the high pressure shaft rotational speed.

2.3 SINGLE-SPOOL ENGINES

When the present work was carried out, the only type of single-spool engine in existence was the single-spool turbo-jet, the simplest of all gas turbine systems. This was the first engine to be studied and most techniques were tried with this particular engine type. Subsequently the method was developed for more complex configurations, including the single-spool turbofans, one with mixed exhausts and the other with

separate exhausts.

2.3.1 The Single-Spool Turbojet

This engine is one of the real gas turbines analysed. Enough information was available for realistic simulations. The components of this engine are a sixteen stage axial compressor and a three stage turbine to drive this compressor. The engine is in service in both civil and military applications, although is being gradually phased out.

Fig. 15 illustrates the acceleration, steady state and deceleration paths on the compressor characteristic map. A fuel schedule based on the rotational speed of the shaft was used in both transients. The paths on the compressor characteristics are as would be expected from such a configuration. The running line of the acceleration is above the steady running line, closer to surge, and the deceleration line is below. Noticeable are two steps in these paths, they are caused by the sudden closing or opening of the bleed valves (two in this engine). Figs. 16 and 17 illustrate the variation of other parameters during the transient and the steady state phases. For the transient phase, the shaft rotational speed, the thrust developed, the engine pressure ratio and the specific fuel consumption are plotted with time the independent variable. Also shown are the same parameters as functions of fuel flow, to show the steady state performance and the departures from this state during the transient. The high specific fuel consumption is typical of turbojet engines. This parameter does not have much meaning during a transient because of the short duration of the transient, but it is shown to illustrate the large departures from the steady state values.

2.3.2 The Single-Spool Turbofan with Mixed Exhausts

An improvement in specific fuel consumption can be obtained by allowing some of the air to bypass the combustion chamber and turbine. The resulting cold stream can emerge from a separate nozzle or can be mixed with the core gases after these have passed the turbine. This potential benefit was realised very early in the development of gas turbine engines. The theoretical principles on which these gains are based have been described in Chapter 1. As early as 1943 a bypass engine was developed on these principles. Although this particular engine never went into production it is an example of a ducted fan system. It consisted of a ten stage axial compressor driven by a two stage axial flow turbine. Downstream of the compressor turbine were two power turbines, which drove fan blades mounted at their tips. This was an example of an aft fan gas turbine configuration. The main problem encountered was that of severe thermal stresses on the fan blades due to the very high temperature differences between the core flow and the bypass flow which produced very high temperature gradients in the materials.

In the late fifties another turbofan was designed in France. This engine was a single-spool turbofan with mixed exhausts. It was a small engine and consisted of a core section with a single sided centrifugal compressor and a two stage axial flow turbine. Coupled to this assembly by means of a gearbox was a single stage axial flow fan. A proportion of the air compressed by the fan went to the compressor and the core components of the engine, and the remainder was directed to a bypass duct. The core and bypass streams emerged from the engine after being mixed in a common nozzle.

It was decided to build in this programme the capability of modelling such an engine. This configuration is an inter-

mediate step between the jet engine and the turboprop engine. If such an engine was developed it could prove inexpensive to build, with better performance than the single-spool turbojet and without involving the complexity of the two-spool engines. The analysis of these engines when compared to the performance of a single-spool turbojet, reveals a marked improvement of the thrust produced by the bypass arrangement. This illustrates the point made in Chapter one, where by increasing the mass flow and reducing the the flow velocity, an increased thrust is obtained. These gains are very realistic because the engines were analysed with real losses. The bypass ratio at the maximum fuel flow is approximately 1.25:1. The engines analysed have the fan directly coupled to the compressor-turbine assembly. A provision for including gearboxes is included although it was not used. The performance of this engine during transients and the steady state is shown in Figs. 18, 19, 20 and 21.

2.3.3 The Single-Spool Turbofan With Separate Exhausts

Another possible single-spool turbofan design is that with a sparate nozzle for the cold air flow. This configuration can be studied with the present programme, and it's predicted behaviour proved to be very similar to that of the single-spool turbofan with mixed exhausts. Paths on the compressor characteristics are illustrated in Figs. 22 and 23, and the engine performance in the next two figures 24 and 25. Both single-spool turbofan engines present peculiarities in the acceleration, deceleration and running paths in the compressor map. This is attributed to the mismatch of the characteristics of the fan and the compressor. No attempt was made to eliminate these irregularities because the aim pursued was to establish the capability of modelling these engines, not to design one. The most imporatant

point of this analysis is adequately illustrated. Important gains in performance are possible, although these gains will be less important at altitude. When in flight the thrust produced is also a function of the forward speed of the aircraft, which will reduce substantially the thrust obtained from the cold stream.

2.4 TWO-SPOOL ENGINES

It has been shown that the thermal efficiency of a gas turbine installation will improve with increased engine pressure ratio. It is natural therefore to pursue the development of higher pressure ratio engines. When higher pressure ratio one-spool engines were being designed certain difficulties became apparent in the compression process. When axial compressors operate at non-design conditions, instability is likely to occur. When operating at low rotational speeds, the fluid density at the high pressure end of the compressor is low, and the axial velocity becomes high. The rear stages then are operating near choking conditions. At the front end the axial velocity is low, producing high angles of attack which results in stall because of the incorrect angle of incidence of the flow on the blades. At high rotational speeds, stall is likely to occur in the rear stages. The axial velocity is low because of the high density of the fluid, and again a high angle of attack of the blades on the flow is the result. This mismatch tends to occur when pressure ratios over eight or nine are to be obtained from the compressor. This problem is severe. A solution to this problem is to design the engine with two compressors and two turbines with mechanically independent shafts. This gave rise to the two-spool engine design. Engines of this

type easily achieve pressure ratios of over twenty. The two-spool layout is now the most common, in the turbojet, and in various bypass configurations.

2.4.1 The Two-Spool Turbojet

This system is the simplest of the two-spool engines, and it has many applications in the present day. Although no component characteristics were available for this type of engine, it was considered essential that the modelling capability should be provided. Characteristics from a two-spool bypass engine were appropriately modified and these characteristics loaded into the computer. As in the case of the single-spool turbofans the paths on the compressor maps indicates incorrectly matched design, for example the high non-dimensional speed range of the H.P. Compressor is not entered. Again it was not deemed necessary to correct these irregularities because the aim of incorporating the modelling capability in the programme was achieved.

Figures 26, 27, 28 and 29 show the paths on the characteristic carpets, the performance during an acceleration and a deceleration, and the variation of several parameters with fuel flow. Interesting to notice in the transient paths of this engine is the movement of the running lines of the L.P. Compressor. This component's trajectories move closer to surge during a deceleration and further away from surge during an acceleration, these movements of the running lines being opposite to those of the H.P. Compressor.

2.4.2 The Bypass Engine With Mixed Exhausts

This is another of the real engines simulated. This

gas turbine is very widely used in various commercial and military versions. It consists of a four or five stage L.P. compressor (depending on the model) which delivers approximately half of its flow to a bypass duct, the other half is absorbed by a twelve stage H.P. Compressor. Both compressors are driven by two stage turbines. The hot and cold streams are mixed before being exhausted through the final nozzle. A large amount of information was available for the latest model of this engine. Test bed steady running performance has been obtained from the manufacturers and is used to compare the performance of the engine with that predicted by the programme. In addition, information of many structural details was available. Knowledge of these details enabled the inclusion of heat transfer effects. The investigation of these effects on the predicted performance is described in the last three chapters of this work.

The convergence procedure for this engine consists of the continuous modification of the pressure ratios of both compressors to satisfy the requirements of the turbines, the mixing process and the final nozzle.

Figures 30 and 31 show trajectories on the characteristics for the most recent version of these engines, and in figures 32 and 33, several other parameters are shown. These results are discussed in more detail in Chapter V, where comparisons are made between the adiabatic model and the non-adiabatic model which is described in Chapters III and IV. However it is necessary to mention that both compressors of this engine behave in a similar way, their trajectories move nearer to surge during an acceleration, and away from surge during decelerations. This behaviour is the opposite of that observed in the two-spool turbojet.

The agreement between the predicted and the test bed steady state performance is good because some small adjustments have been made to the characteristics to account for inter-component effects. These adjustments consisted of scaling the characteristics with factors recommended by the manufacturers. In addition, an additional scaling factor of 1.02 was introduced in the H.P. Turbine mass flow characteristics to produce a satisfactory agreement. Agreement of fuel flow when compared to other engine parameters, such as rotational speed, engine pressure ratio, turbine temperatures etc. was also satisfactory after these modifications were introduced.

2.4.3 The Bypass Engine With Separate Exhausts

This type of engine is also very common today, so it is considered essential to include it in the modelling capability of the programme. The characteristics are exactly the same as those of the engine analysed in section 2.4.2. Only the exhaust arrangement was modified so the hot and cold streams would emerge from separate nozzles. This engine was also analysed with heat transfer effects in Chapter V. The component dimensions and other parameters are taken to be the same as those of the engine with mixed exhausts. The purpose of this investigation was to determine if the heat transfer effects produce different modifications in engines of various configurations.

Transient paths and various parameters for this engine are shown in figures 34, 35, 36 and 37. The paths on the compressors of this engine are similar to those of the two-spool turbojet, although the movements of the L.P. Compressor are significantly smaller.

There is a small difference in the steady state performance between this engine and the engine with mixed exhausts. The observed thrust of this engine is slightly lower because the two streams emerge through separate nozzles. If the two bypass engines are compared to the turbojet, important gains in thrust are observed for the same fuel flows. This confirms the theoretical advantage of bypass engines over turbojets.

2.4.4 The Two-Spool Turbofan With Mixed Exhausts

This type of engine and the one described in the next section have been developed to improve the performance of a two-spool engine without going to the more complex three-spool configuration. Abundant data was available for this engine configuration, but not many structural details. This engine is in the early stages of its development, and is a derivative of the engine of section 2.4.2. The H.P. Shaft components of this engine are used without modifications. The L.P. Shaft consists of a single stage fan delivering a high fraction of its flow into the bypass duct, and a three stage I.P. Compressor. This assembly is driven by a three stage turbine. Both streams are mixed before being exhausted into the atmosphere.

For this type of engine two possible methods of presentation of characteristics are possible. The fan can be analysed as one compressor with one set of characteristics, or two sets of characteristics can be provided: one for the core section and one for the outer annulus. For engines of large bypass ratio the latter approach should be used, because of the large diameter of the fans, the varying blade angles along the blade height and the suction effect of the core

annulus result in non-uniform flow. The engine under consideration has very flat characteristics for the core section of the fan. This means that the converging process has to start by using the compressor mass flow rather than the pressure ratio. The remainder of the procedure is basically similar to that of the two-spool bypass engine with mixed exhausts.

Figs. 38, 39, 40 and 41 show the paths on the characteristic carpets. These illustrations also show how flat are some of the curves of fan characteristics. The performance of this engine is shown in Figs 42 and 43. The agreement of steady running performance between the manufacturer's predictions and the predicted results of the present programme is reasonable. No refinements, such as scaling factors, were introduced to make the agreement more exact, as the aim was simply to illustrate how the model would analyse an engine in a first attempt.

Figs. 44, 45, 46, 47 and 48 show the performance of an engine of a similar configuration, but with the fan analysed as a single component. The mass flow characteristics of the fan's outer annulus were scaled up by a factor of 1.3 to produce similar mass flows to those obtained when the fan characteristics were fed for the inner and outer annulus. If the steady state performance of these engines is compared, it can be observed that the predictions of both methods show a close agreement. A slightly better thrust is predicted for the two-component-fan analysis. However the predicted steady state running line of the H.P. Compressor is slightly nearer to the surge line in the single-component-fan analysis. An interesting apparent difference is observed when comparing the transient responses obtained with the alternative models

for the fan. Although the same fuel schedule was used in both cases, and the paths in the I.P. Compressor and the H.P. Compressor are of similar shape, the single fan analysis predicted an acceleration which is faster by one second. A similar but reduced effect has been observed for the deceleration. These effects are probably due to the incorrect scaling of the fan. The scaling factor of the single fan analysis had been introduced to produce similar engine mass flows.

If the trajectories of the two core compressors are compared, it can be observed that the engine with the fan analysed as a single component exhibits smaller departures from the steady running lines, despite experiencing the faster transients. This effect is more evident in the I.P. Compressor characteristic maps, less so in the characteristics of the H.P. Compressor. Both types of analysis predict that in this engine, the movements of the transient running lines on the compressor maps of the I.P. and the H.P. Compressors are in opposite directions during the transients. The H.P. Compressor running line moves nearer to surge in an acceleration, while the I.P. line does so during a deceleration.

2.4.5 The Two-Spool Turbofan With Separate Exhausts

It is desirable to be able to analyse the engine with separate exhausts because several engines of this configuration are currently in service. The component characteristics of the engine described in the previous section were used unchanged for the analysis of this type of engine. This engine was analysed in two ways, as the turbofan of the previous section, one treating the fan as an inner and an outer component, and the other analysing the fan as a single L.P. Compressor. The

transient performance of the first arrangement is shown in Figs. 49, 50, 51, 52, 53 and 54, the behaviour of the second arrangement in the next five figures, 55 to 59. The fuel schedule used is the same as that for the two-spool turbofan with mixed exhausts. The running line movements of this engine follow closely the pattern predicted for the previous engine, although in this case the single-component-fan analysis shows a better agreement with the results of the alternative analysis. In this case the difference between the acceleration times is very small, but still the engine with the fan analysed as a single component accelerates slightly faster. The paths on the compressor characteristics show that this engine would experience surge with these fuel schedules in the I.P. Compressor during a deceleration and in the H.P. Compressor during an acceleration. The paths of the two-component-fan analysis in the I.P. Compressor exhibit larger departures from the steady running values than those of the alternative analysis. The paths on the H.P. Compressor characteristics are essentially the same. In the analysis of both this engine and the turbofan with mixed exhausts, very noticeable is the excursion of the H.P. Compressor to the high speed end of the performance map during an acceleration. This is caused by the low inertia of the H.P. Shaft which has an inertia a quarter that of the L.P. Shaft. When accelerating the high inertia L.P. Shaft tends to lag, and the H.P. Shaft tends to overspeed. The speed overshoot in this particular transient is not as large as the path on the compressor characteristic maps, which are illustrated in Figs. 41, 46, 52 would indicate. The slower than normal speed of the L.P. Shaft will result in lower delivery pressures and thus lower delivery temperatures to the H.P. Compressor, which in turn produce a

larger increase of the non-dimensional speed than due to the rotational speed alone.

The same comments made for the engine of the previous section apply for this turbofan. Only small discrepancies can be observed between the predicted performance when using the two different methods of analysing the fan. Naturally great care must be taken when condensing the two sets of characteristics into one. This is better accomplished directly, either from rig tests or from detailed analysis of the blade geometry. The simple method chosen to condense these characteristics is adequate for the required simulation of an imaginary engine.

2.5 THREE-SPOOL ENGINES

The same problem that gave rise to the design of the two-spool engine, became apparent when pressure ratios of over twenty were to be attained to obtain better efficiencies. The solution to this problem was to add a third shaft to the gas turbine engine. This type of engine is now established in both commercial and military applications. All current engines of this kind are of the bypass configuration, either with mixed or with separate exhausts.

No engine with more shafts is envisaged. The reason for this is the increasing mechanical complexity that each shaft has brought about. From the aerodynamic point of view the performance of the engine will improve with increased number of shafts because the different stages operate nearer their optimum points. No three-spool engine with split compressors is in operation or envisaged. If a more complex configuration is required, the next development of a three-spool engine would

be an engine with split compressors, and possibly two bypass streams, one emerging through a cold nozzle, and another through a mixer

2.5.1 The Three-Spool Turbojet

No engine of this type is currently in service or envisaged. However it is worthwhile modelling it as a theoretical exercise. The characteristics for this engine were obtained by modifying the characteristics of the three-spool engine with separate exhausts. In Figs. 60, 61 and 62 steady state and transient paths on the compressor maps are illustrated. The L.P. Compressor transient running line movements of this engine are in the opposite direction to those of the H.P. Compressor. The I.P. Compressor line movements do not follow a set pattern because these components have to behave in such a way as to satisfy the requirements of the other two compressors. The awkward shapes of the artificially generated characteristics are evident in this engine and the other two described in this section. However their shapes do not detract from the merit of the programme of having the modelling capability for these configurations. If the performance of this engine is studied, (Figs. 63 and 64) it is seen that the specific fuel consumption of this engine is very high partly because of the way the characteristics were modified to obtain reasonable paths on the performance maps and partly because of the high jet velocity inherent in a turbojet engine. No attention was devoted to these details once the modelling capability of this configuration was established.

2.5.2 The Three-Spool Turbofan With Separate Exhausts

This engine is used by many commercial operators. It is a high bypass ratio engine which went into service in the early seventies. No component characteristics of this engine were available so a set had to be generated. The manufacturers had provided comprehensive data for three steady state points, and for the idle condition. From this information fictitious characteristics were generated, which although inaccurate, enable the performance prediction of an engine of this type. The fan of this engine was treated as a single component, rather than as an inner and outer fan as was the case of the two-spool turbofans. This engine, if so desired, can be modelled with two sets of component characteristics for the fan. For an engine with such a high bypass ratio, this would be the correct approach.

The predicted performance of the three-spool turbofan with separate exhausts is illustrated in Figs. 65 and 69. No comparison is attempted with the engine of section 2.5.1 because of the simple way in which the characteristics had been obtained for that turbojet. The fan running line of this engine moves only very slightly during the transients, while the I.P. and H.P. Compressors both move towards surge in an acceleration and vice-versa in a deceleration.

2.5.3 The Three-Spool Turbofan With Mixed Exhausts

This engine type has both military and commercial applications. The commercial version is a development of the engine with separate exhausts and it is a high bypass ratio configuration. The military application is a medium bypass ratio gas turbine. The results of the analysis of the high

bypass ratio engine are shown in Figs. 70 to 74. The predicted behaviour is very similar to that of the engine with separate exhausts. The movements of the fan running line are very small, but if they are closely observed it can be noticed that they are in the same direction as those of the I.P. , and H.P.

Compressor movements. This influence of the exhaust system on the transient running lines is the same as had been in the two-spool bypass engines.

The two three-spool turbofans of high bypass ratio analysed operate with the I.P. Turbine unchoked. When the performance of this engine was simulated using the simple set of characteristics generated, this phenomenon was predicted. This would indicate that the characteristics generated, although inaccurate were reasonably realistic.

All the turbofan engines analysed are of the frontal fan arrangement. With this programme it is possible to simulate an aft fan configuration by careful choice of the control variables defining the engine geometry. The paths on the component performance maps would be similar to those shown for the front fan engines. The aft fan could be mounted on any of the shafts or could be an additional shaft with its own power turbine.

CHAPTER III

CALCULATION OF CLEARANCE EFFECTS IN TRANSIENTS

2.1 INTRODUCTION

In the previous chapter a method that enables the prediction of gas turbine performance has been described. As it stands the method is suitable for the calculation of the steady state performance. For the transient performance there are some other effects to be taken into account. Neglecting these effects will result in important discrepancies between the programme results and test bed data (Ref. 88). Typically the time required to accomplish an acceleration will be under-predicted by twenty or thirty percent. These discrepancies between experimental and predicted performance during transients has been attributed in the past to the following reasons:

- 1) Heat being exchanged between the engine metals and working fluid.
- 2) Modifications in the steady state component characteristics, mainly in the compressors, due to the aforementioned heat exchanges.
- 3) Incorrect blade tip clearances resulting from the differential expansions of the components produce changes in efficiencies.

- 4) Incorrect seal clearances result in incorrect mass flows.

The direct heat transfer effects 1 and 2 are discussed in the next chapter. The present chapter describes a study of tip clearance and seal clearance effects.

Gas turbines are subjected to varying thermal and mechanical loading which produce small changes in the dimension of the various components of the engine in both the radial and the axial direction. These changes of dimension occur during transient operation. They result in relative movements between rotating and stationary components, thus causing varying tip clearances and off-design mass flows. In the present work only radial clearances have been treated. The H.P. Compressor of a typical two-spool bypass engine has been selected to demonstrate how the representation of a multi-stage turbomachine can be simplified, still retaining reasonable accuracy. In this chapter a model for the calculation of blade tip and seal clearances is proposed, and a simplified version of this model is included in the engine performance programme. All the necessary information was available for this engine, hence it's selection to illustrate how the predicted performance is affected by allowing for these transient phenomena.

Investigations have been carried out in predicting the actual clearance movements of blade tips and seals (Refs. 49 and 52) and extensive studies have been carried out by Lakshminarayana on the flow and losses occurring in these regions (e.g. Refs. 46 and 72). Unfortunately no work in which an attempt to link these two aspects of performance has been encountered, other than commercially classified information based on experimental results. The experimental

verification of blade tip clearances is very difficult during the transient phase. Therefore much weight should be placed on the theoretical investigation of these effects.

3.2 THERMAL EFFECTS

During transients the components of an engine expand at different rates because some sections absorb heat faster than others. It has been found that a convenient subdivision of a disc is possible. For this purpose the finite element programme for transient heat conduction of Ref. 63 was modified to analyse the thermal response of the disc components of a rotor. This work indicated that the complex shape of the disc can be broken down into three components: a thick hub portion, a thin diaphragm, and an outer section or rim (Fig. 75). The different patterns of expansion arise from the different shapes of the sections and the different rates of heat transfer. The various rates of heat transfer are a consequence of the different flow regimes experienced by each section. Some faces are rotating adjacent to stationary faces, while others form walls of what are effectively rotating chambers. For rotating faces adjacent to stationary faces, the correlation used is (Ref. 52)

$$Nu = 0.0253 Re^{0.8} \quad (3.1)$$

For rotating faces which form the walls of rotating chambers the heat transfer mechanism is effectively natural convection in a high gravity field, the value of the local acceleration (gravitational) being a function of both the local radius and the rotational speed. The correlation is (Ref. 52)

$$Nu = 0.12 Gr^{\frac{1}{3}} Pr^{\frac{1}{3}} \quad (3.2)$$

For heat transfer to turbine blades, a suitable correlation is that given by Halls (Ref. 32).

$$Nu = 0.235 Re^{0.64} \quad (3.3)$$

For compressor blades one approach has been to adopt a weighted average between laminar and turbulent boundary layers developing on flat plates (Ref. 52). The results of this method have been found to be within five percent of the results obtained by applying Halls' turbine correlation to the compressor blades. Therefore for convenience in the present work, which is intended to produce a model applicable to both compressor and turbine tip movements, Halls' correlation is used for all blades.

It is common practice for turbine blades to be cooled to allow gas of higher temperature to flow past the blades to obtain higher efficiencies. It is therefore, desirable to include the capability of simulating this feature in the model. This effect has been analysed in a very simple form. The cooling effectiveness of a flow is defined by equation (3.4)

$$e = \frac{T_{cg} - T_b}{T_{cg} - T_c} \quad (3.4)$$

Defining the effectiveness of the cooling flow determines the final metal temperature. This temperature is used as the temperature producing the transfer of heat, rather than the fluid temperature. When this effectiveness is zero, the temperature driving the transfer of heat is the fluid temperature, this means the blade is not cooled. A typical value used for this

effectiveness for a cooled blade is 0.6, and this is the value that has been adopted, when cooling capability simulation was desired.

The casing structure of the H.P. Compressor is subjected to internal pressure from the core air and to external pressure from the bypass air. It also exchanges heat with these two air flows. In order to estimate the heat transfer coefficient at the internal surface of the casing, one approach is to regard this as a cylinder in which a smaller cylindrical shape is rotating. The heat transfer coefficient in this case is given by the correlation (3.5) of Ref. 86. This equation is shown with the subscripts of the locations corresponding to the engine, in which form it is used in the present programme.

$$Nu = 0.015(1+2.3(\frac{D_{ca}+D_h}{L})(\frac{D_{ca}}{D_h})^{0.45} Re^{0.8} Pr^{0.33} \quad (3.5)$$

In applying the above equation to the present work, the linear dimension L used was the axial length of the blade pair, it being assumed that the end wall boundary layer is effectively restarted at each blade pair. For the outer surface of the casing, the expression for a developing turbulent boundary layer on a flat plate was used.

Extensive work has been published on the evaluation of heat transfer coefficients by many investigators, so there is a wide choice of relevant work on this field. Owen for example has carried out important work on the evaluation of heat transfer coefficients applicable to turbomachinery (e.g. Refs. 34 and 68). This wide choice of methods required examination, so some investigations were carried out on the

choice and magnitudes of the heat transfer coefficients. By introducing modifying factors on the various heat transfer coefficients it was established that the system is not very sensitive to small alterations of the coefficient. The changes in linear dimension of the platforms, blades and casings are quite insensitive. This is due to their larger surface area to volume ratios, and to their smaller radial dimension. The large blades of the L.P. Compressor which are very long have to endure milder temperature and rotational speed modifications. Disc hubs and diaphragms on the other hand are more sensitive, in particular the former, but this sensitivity is only apparent when very long term transients are analysed. For the purposes of the analysis of the speed transient, and the medium term transients, the effect is not noticeable. Some investigations were also carried out on the choice of heat transfer coefficients for the hub, the casing and the blades. The casing expansion has been found (Refs. 62, 75) to occur immediately after the end of the speed transient. It has been found that the only relevant work that gave coefficients high enough for this purpose is the work of Tachibana and Fukui. Since the coefficients proposed in their work gave good agreement with Ref. 75 their method was adopted for this work. As far as the blades are concerned both methods analysed gave equally satisfactory results. The disc hub experiences a very low rate of heat transfer, when compared to the other components of the disc. A correlation that yields a coefficient of the required magnitude is that shown in equation (3.2). Another approach to the heat transfer occurring in the hub is to use the correlation obtained by Owen and Onur (Ref. 68) shown in expression (3.6).

$$Nu = 0.267 Gr^{0.286} \quad (3.6)$$

This is an alternative expression for natural convection. This expression is valid for Grashof numbers of up to $1.3 \cdot 10^{12}$, in practice with this engine, the Grashof number is approximately 10^{14} . For this value of Grashof number, the Nusselt number obtained with this equation is about forty percent lower than that obtained with equation (3.2). When used for the intended Grashof number of 10^{12} , the discrepancy is reduced to about fifteen percent. The compared clearance paths do not show a large difference when changing from one method to the other. However equation (3.2) was preferred because of a slightly better agreement with alternative analyses of clearances of a three-spool engine (Ref. 75).

3.3 MECHANICAL EFFECTS

When a gas turbine changes state, the modified rotational speed results in changes of the stresses experienced by the components. These mechanical effects cause centrifugal growth due to changes in the angular velocity of the rotor, changes in the 'pull' of the blades on the disc resulting from the alteration in angular velocity and changes in pressure difference across the section.

For the calculation of mechanical effects the same subdivision of the rotor was used as for the calculation of thermal effects.

Each disc is assumed to be represented by the same three rings used for the thermal model. To make the overall growth line up with the growth calculated by means of finite

elements a multiplying factor of 1.3 was introduced.

Disc distortion in the tangential direction during a transient was calculated, and the resulting radial movement was found to be negligible. So no account is taken of this effect.

The combined thermal and mechanical effects result in a change in dimensions in each of the three rings. Once these movements are calculated, they are combined ensuring continuity of radial dimensions at the interfaces. Thus the overall changes in disc dimension are calculated.

The blades are assumed to be rods of uniform cross sectional area with or without a shroud at the blade tip. By means of integral calculus blade elongations can be calculated as a function of geometry, material properties and rotational speed. The elongations obtained using this procedure were in good agreement with those obtained using the finite element methods of Ref. 84.

With regard to the casing, the only relevant mechanical loading considered is the pressure change during the transient and it's effect is found to be very small, about one percent of the total movement of the rotor due to mechanical effects.

3.4 BLADE TIP CLEARANCE MOVEMENTS

Once all the effects on the dimension of the rotor stage or component are calculated, they are added to obtain the resulting change in the clearance.

All material, gas and air properties are calculated as functions of the temperature of the metal or fluid. In

the prediction procedure it is of course possible to change the materials in any section very easily. In Fig. 76 the predictions of blade tip clearances obtained with the present model are compared to clearance predicted by the manufacturer of the three-spool engine first investigated. The results are tested with this engine because some structural information was available and also the predictions with alternative methods. The clearances are shown normalised with the steady state clearance because of commercial security considerations. The results shown are for two stages of the H.P. Compressor during an acceleration and for one stage during a deceleration.

The methods described in the preceding sections have been used to predict the tip clearance movements during and following an acceleration for each of the twelve stages of a two-spool bypass engine H.P. Compressor. The engine was stationary, at sea level and the speed transient was completed in four seconds (as compared to six seconds in Ref. 73). The predicted results for stages 1, 6, and 11 are shown in Fig. 77. Looking at the clearance paths at the beginning of the transient there is a sharp decrease in tip clearance due to mechanical effects and the fast thermal response of the blades. The thermal growth of the casing is slower than that of the blades. Much of this takes place after the speed transient is completed, producing the increased tip clearances observed soon after the end of the said transient. The disc has the slowest response and the final slow decrease in tip clearance is due to the slow expansion of the disc, which can take over five minutes. It is interesting to notice that for stage 1 the clearance at the end of the thermal transient is smaller than that at the end of the speed transient, for stage 6 they are similar, while for stage 11 the opposite to

stage 1 is the case. This is due to the effect of the air inside the shaft. In this engine the cooling air is drawn from between the fifth and sixth stages of the H.P. Compressor. Therefore the air inside the shaft is hotter than the core air for stage 1. The two air streams have similar temperatures at stage 6 and the core air is hotter than the shaft cooling air at stage 11. The cooling air dominates the expansion of the disc, whereas the core air dominates the expansion of the blades and the casing. This explains the different end points of the clearance paths as compared to the clearance at the end of the speed transient.

To indicate the relative rates of thermal response of the various sections, the time constants for the major components of stage five are shown in tables 1 and 2 at three instants during an acceleration and three instants during a deceleration. The heat transfer coefficient is the only parameter affecting this constant, since for a given configuration, the geometry is fixed and the material property changes due to variations in temperature are small. It is worth noticing that the changes in the time constants of the disc hub and the diaphragm follow a similar pattern. The very small difference in the pattern of time constant variations is due to the slightly different shapes of these sections. In this analysis, the diaphragm consists of two surfaces perpendicular to the axis of rotation, while the hub has an additional surface parallel to the axis of rotation. The latter surface affects the average magnitude of the heat transfer coefficient for this section. Another different pattern can be observed in the time constants for the disc outer section and the blades. This is a result of the two sections in each case being subjected to the same fluid flow. When analysing the blades and the disc outer section it was found that although

different correlations were used to evaluate the heat transfer coefficients, these were of similar magnitudes. This explains the similar behaviour of the two sections. The casing on the other hand is influenced by two fluid flows and so it exhibits a pattern peculiar to itself.

Time in transient	2s	6s	10s
Disc Hub	108s	66s	37s
Disc Diaphragm	38s	17.8s	9.6s
Disc Outer Section	12.7s	9.0s	5.5s
Blades	2.3s	1.6s	1.0s
Casing	10.4s	7.6s	4.8s

Table 1. Stage 5, Two-Spool engine H.P. Compressor.

Time constants during an acceleration at sea level, static

Time in transient	3s	6s	10s
Disc Hub	60s	55s	62s
Disc Diaphragm	21s	20s	23s
Disc Outer Section	13.1s	15.0s	26.0s
Blades	2.0s	2.3s	3.5s
Casing	6.1s	4.9s	12.5s

Table 2. Stage 5, Two-Spool engine H.P. Compressor.

Time constants during a deceleration at sea level, static

3.5 SIMPLIFIED METHOD TO BE INCLUDED IN PROGRAMME

IT would be excessively cumbersome to include each individual blade row of each compressor and turbine into the transient programme for the engine. The use of single 'equivalent' stages instead of complete components would be

highly desirable. A single equivalent stage can give satisfactory heat transfer rates (Ref. 53). A single equivalent stage has therefore been developed based on averaged dimensions of the twelve stages and using averaged properties of specific heat, thermal expansion coefficient, Youngs modulus and material density to represent tip clearance and associated efficiency changes. The following simplifications have been carried out to reduce computer storage and running times.

The subdivision of the equivalent disc as described in section 3.2 is retained for the calculation of thermal effects. As in the previous more complex model, the various rotor sections are assumed to have infinite thermal conductivity, material properties are assumed to be constant throughout the relevant temperature range, although air and gas properties are still calculated as a function of temperature. The process ensuring the continuity of the radial dimension of the disc interfaces is eliminated. Instead an average disc temperature is calculated by using equation (3.7) and hence the thermal expansion of the disc is obtained.

$$T_m = \frac{\sum V_i T_i}{\sum V_j} \quad (3.7)$$

It will be shown later that this approximation provides adequate accuracy. The method of calculating the thermal growth of the blades and the casing of the previous section is retained.

The centrifugal growth is simplified for this model by calculating the expansion of a disc of the same inner and outer radii and an uniform thickness equal to the minimum diaphragm thickness. For such a system the hoop and radial stresses are given by the Lamé equations (Ref. 35).

$$\sigma_H = C8 + \frac{C9}{R_r^2} \quad (3.8)$$

$$\sigma_R = C8 - \frac{C9}{R_r^2} \quad (3.9)$$

Where C8 and C9 are constants and R_r is the radius for which the stresses are to be evaluated. The constants C8 and C9 are found from the material properties of the system, the disc geometry and the boundary conditions to which the disc is subjected. Once the constants are evaluated, the strains will be related to the stresses by equation (3.10) and the displacement will be evaluated.

$$\frac{\Delta R}{R} = \frac{1}{E_d}(\sigma_H - \sigma_R - \sigma_L) \quad (3.10)$$

The expression for the displacement (3.11 and 3.12) has been localised to represent the displacement occurring at the outer rim due to the centrifugal stresses. Since the stresses due to rotation are much larger than those due to the pressure of the fluid, the longitudinal stresses of equation (3.10) will be small and can therefore be neglected. To check the validity of these assumptions, growths were compared to those obtained with finite element analysis. It was found that the introduction of the same factor of 1.3 as in section 3.3 gave satisfactory agreement. The resulting expression for centrifugal growth of the disc is given next, where equation (3.11) represents the expansion due to the attachment of external masses to the disc rim (shrouded or unshrouded blade). Equation (3.12) represents the growth of the disc due to centrifugal stresses of the disc itself.

$$\Delta R_d = \frac{\omega^2 ((R_h + R_{bt}) \sum m_b + 2 R_h \sum m_{sh})}{E_d^4} \left[\frac{R_h^2 + R_i^2}{R_h^2 - R_i^2} - \nu \right] \quad (3.11)$$

$$\Delta R_d = \frac{R_h \rho_d \omega^2}{4 E_d} ((1 - \nu) R_h^2 + (3 + \nu) R_i^2) \quad (3.12)$$

Once the deflection due to each one of these causes is evaluated, they are added to obtain the total disc expansion. In section 3.3 pressure effects were found to be very small, so they are ignored in this simplified analysis.

The centrifugal growth of the blades is calculated as described in section 3.3. Hence equation (3.13) is obtained from integral calculus. The first term inside the square brackets represents the expansion of the blades due to the centrifugal stresses. The second term represents the elongation due to the mass of the shroud.

$$\Delta H_b = \frac{\omega^2}{E_b} \left[\rho_b \left(\frac{R_{bt}^3}{3} + \frac{R_h^3}{6} - \frac{R_{bt}^2 R_h}{2} \right) + \frac{R_{bt} (R_{bt} - R_h)}{A_b} \right] \quad (3.13)$$

3.6 EFFICIENCY LOSS

The most important effect of non-design blade tip clearance is that of efficiency changes of the compressors and turbines. The component being considered is simplified to a one stage equivalent compressor or turbine with the methods described in the previous sections. The tip clearance at that condition is estimated as indicated above and the efficiency reduction relative to zero tip clearance is obtained from the relation (3.14) from Ref. 46.

$$\Delta \eta = \frac{0.7 \lambda \psi}{\cos \alpha_m} \left(1 + 10 \left(\frac{\phi \lambda A_r}{\cos \alpha_m} \right)^{\frac{1}{2}} \right) \quad (3.14)$$

This expression has given good agreement with experiments carried out by several investigators. It depends directly on the clearance and the blade loading, while the square root term accounts for losses in the spanwise motion in the blade boundary layer. In this work (Ref. 46) it is quoted that a drop of two percent in efficiency can occur when the tip clearance is doubled.

As an illustration, the efficiency changes in the H.P. Compressor of the two-spool bypass engine, relative to zero tip clearance, have been calculated during a sea level acceleration transient using the simplified procedure outlined above. The results, labelled "simplified" are shown in Fig. 78. For comparison, the predictions of the single equivalent stage model using the more accurately calculated disc expansion as described in sections 3.3 and 3.4 are shown alongside, marked "one stage". The efficiency changes that are predicted by treating all twelve stages individually are also given, labelled "engine". It can be seen that the results of the two simplified methods are in close agreement with the results obtained from the stage by stage analysis, discrepancies not exceeding 0.5 percent of efficiency. The "simplified" procedure has therefore been adopted for use in the performance prediction programme because it is a satisfactory representation of the more complex model.

The next step in this analysis is the calculation of the efficiency loss compared to the stabilised value of clearance at that particular speed and inlet conditions. Stabilised clearances at the desired conditions are evaluated using the same methods and hence stabilised value of efficiency loss due to clearance openings are obtained. The difference in efficiency

is calculated by subtracting the stabilised efficiency loss from the transient efficiency loss and the efficiency of the component obtained from the characteristics can then be modified accordingly. This difference is shown in Fig. 78. In this particular compressor, the efficiency changes are very small.

3.7 APPLICATIONS

The model described in the previous sections was developed with engine performance in mind. It is satisfactory for the purpose for which it is intended and it can be useful by itself. In addition to efficiency losses, there are other considerations which may be of interest to the gas turbine designer.

3.7.1 Compressors

The performance prediction programme was designed to include the model described. The H.P. Compressor is analysed as a single stage equivalent compressor and by means of the simplified model the clearance is calculated at each time step both in the transient and for steady running at that non-dimensional speed and pressure ratio. The modification of compressor efficiency is then used when calculating the next incremental acceleration in the transient. A similar approach is used for the L.P. Compressor of this engine. This compressor will be subjected to milder ranges of temperature and rotational speed, because of the design of the engine. A typical example of the application of the model is shown in Fig. 79. In this case, the cooling arrangement in the H.P. Compressor of a three-spool turbofan has been modified so that a reduction in clearance

will occur, without changing the cold built clearance. The resulting reduction in clearance will increase the efficiency of the component by about two percent. It would be possible to reduce the cold built clearance to obtain the same result, but this approach provides another choice for the designer. This work was carried out employing the more complex model in which the continuity at radial interfaces is ensured. As described in section 3.5 the simplified method was included in the prediction programme. This method is satisfactory in that, despite the simplifications made, it predicts movements which are very similar to those of the more complex method. This agreement is illustrated in Fig. 80 where the clearances of the equivalent single stage H.P. Compressor of the two-spool bypass engine with mixed exhausts are shown.

3.7.2 Turbines

Predicted tip clearances of the H.P. Turbine during a sea level acceleration are shown in Fig. 80. The models for the disc and blade can accommodate both shrouded and unshrouded blades. In the former case the centrifugal expansions are greater due to the weight of the shroud. Also the thermal model for the blades incorporates the cooling arrangement. In Fig. 80 two blading arrangements are considered. In one of these arrangements, the blades are unshrouded and uncooled (labelled 'simple'), in the other, the blades are both shrouded and cooled (labelled 'S & C'). Both arrangements start with the same cold clearances. In this case the additional expansion produced by the shroud is approximately balanced by the reduction in thermal expansion that results from cooling the blades. In the real engine the blades and nozzle guide vanes are shrouded and the

early rows are cooled. For this scheme the tip clearance movements are determined for each row. These movements were transformed into efficiency changes using the correlation of equation (3.14) with the suggested modification (Ref. 9) of reducing the efficiency changes by 80 percent for shrouded nozzle guide vanes. It is estimated that a smaller reduction, for example 50 percent should be applied to shrouded rotor blades. As for the compressors, the efficiency changes are obtained by comparing the steady state value of the clearance with the transient value and the efficiency change obtained by comparing the efficiency loss of each case compared to that at zero clearance. These efficiency changes are found to be small, and during an acceleration, beneficial.

Turbine tip clearances are a very important factor to be studied. The sensitivity of the engine to turbine efficiency is illustrated in Chapter V where a one percent reduction in H.P. Turbine efficiency slows down the acceleration by nearly ten percent. The effect of clearances on turbine efficiency is large due to their high blade loading. Turbines are also very sensitive to axial displacements of the shaft. These axial movements are a result of differential thermal expansions, various thrust loadings, and pressure effects. At some points of the engine, expansion joints are placed to accommodate the expansion resulting from a wide range of temperatures on a given cross section, such as the combustion chamber. As opposed to seal and compressor stages, large density changes occur in the turbine in a small axial distance. This is reflected in the high tapering of the blade tips of rotors and stators and of the end walls. This tapering makes the clearances very sensitive to axial movements of the rotor. Axial deflections will result in changes in the tip

clearances, and stepping of the walls. Compressor stages and seals do not experience these large fluid density changes, so their sides and end walls have a less pronounced tapering. It must be mentioned that some compressors exist in which the radius of both endwalls decreases as the high pressure end of the compressor is approached. This design can be very sensitive to axial deflections.

Neal (Ref. 62), examined a turbine and illustrated these movements in both radial and axial directions. The component he investigated is the H.P. Turbine of a three-spool engine. This particular component was not analysed in the present work, but the trends observed in Neal's analysis have been reproduced with the present model.

3.7.3 Decelerations of Compressors and Turbines

In a deceleration, the opposite processes to those occurring in an acceleration are observed, but the time scale is considerably longer. First there is a sudden increase in the tip clearance. This is due to the contraction of the rotor components resulting from the reduced centrifugal stressing of the materials and from the very fast thermal response of the blades. Soon after the end of the speed transient, the clearance starts closing when the comparatively fast thermal contraction of the casing occurs. Following this reduction in clearance there is a slow increase in the tip clearance due to the slower response of the disc. During a deceleration the engine reaches the equilibrium condition after a longer period of time because the 'heat soak' period is considerably lengthened by the reduced mass flows and rotational speeds. These reduced speeds and mass flows result in much lower values of the heat transfer coefficient.

All the components were studied in both accelerations and decelerations, and no rubs were predicted. The prediction of undesirable clearance openings is another possible application of the model developed. If a rub is predicted with this simple method, the user realises that this fact is possible with a given design. A more detailed analysis of the component would then be required to establish if any modifications of the design would be necessary.

3.8 ESTIMATION OF SEAL CLEARANCE MOVEMENTS

The methods and model used for tip clearance can be adapted for making estimates of seal clearance movements during transients. The clearance of a seal controls the amount of fluid leaking through it. These seals are placed at several positions of the engine to allow controlled amounts of air to reach and cool the hot section of the engine. It is the clearance of these seals that controls the flow escaping from the core, and if this clearance is not as designed the incorrect amount of flow will escape from the core. If this amount is too large, the gas turbine will experience a deterioration in performance, if too small, the hottest parts of the engine, in particular the turbine blades, are endangered. This section describes a simple investigation to gain some insight into these effects. In the two-spool bypass engine two important seals are the H.P. Compressor 12th stage outer seal and the H.P. cooling air seal on the H.P. 1 Turbine disc.

3.8.1 H.P. Compressor 12th Stage Outer Seal

This seal is placed on a small disc of its own at the upstream end of the H.P. Compressor, controlling the flow that is bled to the bypass duct from the H.P. Compressor delivery. Its movements have been studied previously by Lim (Ref. 49) using finite difference methods. The predictions of Lim and of the present method are compared in Fig. 81. The agreement is sufficiently close to allow the present models to be used for seal clearance predictions during transients. It is seen that during most of the acceleration speed transient, the clearances of this seal exceed the maximum speed stabilised values by more than 30 percent.

3.8.2 H.P. Cooling Air Seal on H.P. 1 Turbine disc

This seal is mounted on the H.P. 1 Turbine disc. It controls approximately one quarter of the flow bled from the H.P. Compressor delivery for the purpose of cooling the H.P. Turbine discs of the two-spool bypass engine. The movements of this seal have been studied previously by finite difference methods (Ref. 52). The seal clearances during the acceleration speed transient exceed the maximum speed stabilised clearance by about 100 percent. The results of Ref. 52 are compared to the present methods in Fig. 81. The agreement is regarded as satisfactory.

3.8.3 Seal Clearance Effects in Transients

In the early programmes for predicting the acceleration or deceleration rates of gas turbines it would probably be assumed that cooling and bleed air flows remained a constant fraction of the core air flow during the transient. However

it has been illustrated that seal clearances during the speed transient can be very much higher than the maximum speed design clearances. Consequently these cooling and bleed flows expressed as fractions will exceed the design fractions. Wittig et al (Ref. 92) have carried out experimental investigations of seal clearance flows. Their work consisted of choosing a standard clearance and by scaling it up investigate the mass flow through the seal. Their findings suggest a simple relationship between seal opening and flow. For a set of given engine conditions, a nearly linear relationship existed between the value of mass flow allowed through the seal, and the clearance between the labyrinth seal walls. The tests they carried out, were on labyrinths of up to five indentations. In the present work the seals investigated have four indentations (H.P. Turbine seal) and six indentations (H.P. Compressor seal). The scale of the experiment was the same as that normally encountered in gas turbine operation, so the results are directly applicable. Meyer (Ref. 61) has published work that is applicable to several types of seal, but this work does not include a scaling effect, which is the one desired in the present investigation. Kearton and Keh (Ref. 42) propose a semi empirical method for staggered type labyrinth seals. These seals have indentations that interleave, so they are not used in gas turbine practice because the margin of axial deflection allowed by these seals is too small for the deflections encountered in practice. In addition information is required which is not readily available. Vermes (Ref. 91) also investigated several sealing arrangements, and his work produced methods that could be an alternative for the methods employed in this section. Vermes' work is intended to evaluate

the flow of steam for steam turbine seals, and his semi empirical correlations were obtained from experiments with steam machinery. Unfortunately no additional work has been encountered for other types of gas turbine seals. It was therefore decided in view of the validation by the experiment of Wittig et al. to use the simple proportional relationship proposed.

CHAPTER IV

DIRECT HEAT TRANSFER EFFECTS

4.1 INTRODUCTION

In the previous chapter a method to enable the prediction of the effects of the occurrence of non-design seal and blade tip clearances on the predicted engine performance has been proposed. In this chapter some direct effects of heat transfer are evaluated, and simplified methods to include in the transient programme are proposed.

4.2 HEAT CAPACITY OF THE COMPONENTS

When a gas turbine experiences a change of state, the engine metal will exchange heat with the working fluid because of the temperature changes of the latter. Thus the various parameters that influence the transient processes will be influenced by this transfer of heat. These effects have been extensively analysed by Maccallum (Refs. 50, 51), Bauerfeind (Refs. 5, 6 and 7) and Thomson (Ref. 88). The latter propose a model in which the engine is treated as an equivalent heated up mass, where all the heat absorption occurs in a lump of mass placed in the combustion chamber. This mass absorbs heat, and the heat absorbed at each time interval is transformed into a fuel equivalent which is subtracted from the engine fuel flow. In this way the accelerating fuel flow is reduced, slowing an

acceleration. In a deceleration the opposite is the case, the fuel flow is increased by an amount proportional to heat released by the engine materials, also lengthening the time for the transient to take place. Account of the modified temperatures in the working fluid is accounted by means of modifying the component isentropic efficiencies.

Maccallum (Ref. 51) proposes a more elaborate method of assigning a thermal storage capacity to each component of the engine, and heat is transferred to and from this component during the transients. Thus the expansion and compression paths are modified altering the work transfer. This method is also used by Larjola (Ref. 48) whose interest was with industrial gas turbines. In these machines the presence of heat exchangers dictates the need for the calculation of steady state and transient heat transfer effects. This method is a very good representation of the heat transfer processes occurring in the engine.

In the present work a procedure that follows closely Maccallum's technique is adopted. Some modifications to this method have been introduced to enable the various heat transfer modes of the different sections to be represented. In the present model, the heat transferred to the blades, the casing and the blade platform is calculated separately, enabling a more detailed analysis.

The following mathematical procedure explains the basis of the method employed for these calculations. In this analysis, the ratio F denotes the ratio of heat transfer to the working fluid to the work transfer from the working fluid in an element of the compressor.

Considering a small change in an isentropic compression

$$\frac{T_2}{T_1} = \left(\frac{P_2}{P_1}\right)^{\frac{\gamma-1}{\gamma}} \quad (4.1)$$

or

$$1 + \frac{dT'}{T} = \left(1 + \frac{dP}{P}\right)^{\frac{\gamma-1}{\gamma}} \quad (4.2)$$

using the binomial expansion and ignoring the second order terms

$$1 + \frac{dT'}{T} = 1 + \left(\frac{dP}{P}\right)^{\frac{\gamma-1}{\gamma}} \quad (4.3)$$

or

$$\frac{dT'}{T} = \frac{\gamma-1}{\gamma} \left(\frac{dP}{P}\right) \quad (4.4)$$

for a real adiabatic compression with index n_c a similar manipulation would yield equation (4.5).

$$\frac{dT}{T} = \frac{n_c-1}{n_c} \left(\frac{dP}{P}\right) \quad (4.5)$$

For a compression process equation (4.6) relates isentropic and real temperature changes.

$$dT = \frac{dT'}{\eta_{po}} \quad (4.6)$$

Therefore substituting in equation (4.5) and using equation

(4.4)

$$\frac{n_c - 1}{n_c} = \frac{\gamma - 1}{\gamma} \left(\frac{1}{\eta_{po}} \right) \quad (4.7)$$

For a process with heat transfer, where the index of compression is n_h , equation (4.8) can be derived.

$$\left(\frac{dT}{T} \right)_{act} = \frac{n_h - 1}{n_h} \left(\frac{dP}{P} \right) \quad (4.8)$$

where

$$dT_{act} = dT_{wt} - dT_{ht} = (1-F)dT_{wt} \quad (4.9)$$

or

$$dT_{ht} = \frac{(1-F) dT'}{\eta_{po}} \quad (4.10)$$

therefore

$$\frac{(1-F) dT'}{\eta_{po} T} = \frac{n_h - 1}{n_h} \left(\frac{dP}{P} \right) \quad (4.11)$$

and

$$\frac{n_h - 1}{n_h} = \frac{(1-F)}{\eta_{po}} \frac{\gamma - 1}{\gamma} \quad (4.12)$$

for the turbine a similar analysis will yield equation (4.13)

$$\frac{n_h - 1}{n_h} = (1-F) \eta_{po} \frac{\gamma - 1}{\gamma} \quad (4.13)$$

The same correlations that have been used for the evaluation of the heat transfer coefficients in the calculation of the thermal expansion of the discs for clearance purposes, are also used to find the magnitude of the heat transfer effects being considered here. All these effects are evaluated once and once only in a subroutine developed for this specific purpose. Thus the factor F is calculated once at the end of each time interval, for each component. This value is then used at the next time interval. This approximation is realistic, and it saves considerable computing time, since the quantity needed for the calculations of the index of compression is not F , but $(1-F)$. In the compressor, the ratio F in the first few time intervals changes substantially its magnitude because it is a very small number, but the quantity $(1-F)$ seldom changes by more than one percent from one time step to the next. This inaccuracy is small, and considered acceptable, in particular if compared to the uncertainties involving the determination of the heat transfer coefficients. For the turbine, the same trend is observed throughout the transient, with the exception of the first time interval. At this point a sudden temperature rise is experienced by the turbine(s) due to the step change of fuel flowing into the combustion chamber. To account for this effect, the second step in the transient is executed twice if the heat transfer effects are to be included, once adiabatically to obtain an estimate of the thermodynamic variables of the engine, and the magnitude of the correcting parameters, and then a second time where the correcting parameters are included in the computation. The difference between the first and second computation of this time step, yields very small differences, which have little effect. In any case the method has been retained,

because the additional computing time required is a very small fraction of the total.

The effects of heat transfer in the combustion chamber have not been included, because a fuel controller could sense a slightly reduced turbine entry temperature, and the fuel flow would be slightly increased. Since the sensor devices are usually placed in the outlet of the last turbine, the heat absorbed by any of these components will also influence the degree of overfuelling. Also neglected are the heat transfer effects into the propulsion nozzle material. Two conflicting effects are experienced by this component. Taking an acceleration as an example, the nozzle will be colder than in the equilibrium conditions, thus a slightly smaller outlet area will be discharging the flow. The other effect is that due to heat being transferred from the fluid into the nozzle material, the boundary layer will be thinner than in the steady state situation, thus providing an increased effective area. Also due to the removal of heat from the fluid, its density will be slightly increased. According to MacCallum (Ref. 50), there are experimental observations which indicate that these effects approximately cancel each other. In view of this evidence these effects have not been included in the present calculation. When analysing a deceleration, it is safe to assume that the opposite processes are happening, again nearly cancelling each other.

4.3 CHANGES IN COMPONENT CHARACTERISTICS

The heat exchange occurring between engine materials

and working fluid produces changes in the component characteristics. These changes are due to the density changes of the fluid, affecting the axial velocity, and changes in the aerofoil performance, which produce changes in the magnitude of the deflection experienced by the fluid.

4.3.1 Compressor Performance and it's Prediction

To enable the prediction of characteristic movements, some insight is required into the methods available for the evaluation of component performance maps from a given blade configuration and inlet flow parameters. To illustrate these calculations, an ideal stage is to be considered, with a perfect gas. In this case, the stage is assumed to consist of a stator and a rotor, in this order. This arrangement is arbitrary and the opposite arrangement can be used equally well for illustration purposes.

The fluid enters the set of stators of this hypothetical blade pair at S1 (Fig. 82) where it is restricted to flow through an area defined by the blade pitch and the air angle, entering at an angle α_1 to the engine axis. This angle is determined by the inlet guide vanes, or the previous blade pair. The blading will deflect the flow to an angle α_2 . This angle α_2 also defines the throat area through which the flow will emerge from the stators. Compressor blading is designed in such a way that the inlet area of the blade row is smaller than the outlet area, acting as a diffuser. From the equation of continuity

$$\frac{dV}{V} + \frac{dp}{p} + \frac{dA}{A} = 0 \quad (2.3)$$

the conservation of energy equation,

$$T_o = T + \frac{v^2}{2C_p} \quad (4.13)$$

and isentropic compression

$$\left(\frac{P_2}{P_1}\right) = \left(\frac{T_2}{T_1}\right)^{\frac{\gamma}{\gamma-1}} \quad (4.1)$$

the relationship between the stagnation parameters and the flow velocities, or Mach numbers can be obtained at any point. Equation (4.14) which is an alternative form of equation (2.8) is obtained.

$$\frac{P_o A}{m} \sqrt{\frac{\gamma}{R T_o}} = \frac{(1 + \frac{\gamma-1}{2} M^2)^{\frac{1}{2}(\frac{\gamma+1}{\gamma-1})}}{M} \quad (4.14)$$

The knowledge of the Mach number at outlet enables the calculation of pressure, velocity, and temperature at the outlet from the stator blades. As stated the blades form a diffuser, which produces an increase of static pressure and temperature and a reduction of the velocity of the fluid. The flow will then enter the rotor blades which are usually designed to act as diffusers. These blades are moving with a peripheral velocity U perpendicular to the axis of the machine. This will result in a high relative velocity between the fluid and the blading at the entrance of the latter. The relative velocity at entry to the rotor is the vector subtraction of the absolute velocity of the fluid and the peripheral velocity U of the rotors. These parameters are illustrated by means of the well known velocity diagrams to be found in gas turbine textbooks. These relative velocities

again result in air angles and flow areas which define the diffusion process. Knowledge of these parameters will enable a calculation similar to the one performed for the stators, and the calculation of the various fluid parameters will follow. The flow will then enter the next set of stators and the process is repeated. If the velocity triangle at rotor exit is examined, it is evident that the flow has been decelerated with respect to the rotor and accelerated with respect to the stator. The stagnation temperature rise can be evaluated from these parameters, and from isentropic relations the pressure rise. The work input to the fluid is given by equation (4.15).

$$\dot{W} = \dot{m}C_p (T_{0_3} - T_{0_1}) \quad (4.15)$$

In most compressors the inlet and outlet area ratio will not be given by the ratio of the air angles because the blade height will not be constant along the chord. In general axial turbomachines are designed on the basis of constant axial velocity, and the flow path annulus is tapered with a reduction in flow area as the high pressure end of the turbomachine is approached. Thus increased density fluid passages have smaller flow areas. Although axial velocity is constant at the design condition, it will vary along the length of the compressor during off-design operation. In Refs. 37, 38, and 40 the analysis is carried out assuming constant axial velocities and incompressible flow, so the familiar relationships from the blade triangles are produced. It is general practice to make these simplifications, the reason being historical. When the first gas turbines with axial compressors were designed, these compressors had a low working pressure ratio. Conse-

quently the pressure rise per stage was small and so were the density changes. So incompressible flow was a realistic assumption. The above example is useful in illustrating how the compressor blades behave to produce a pressure rise in the fluid. This is the ideal which compressor designers try to achieve. From these procedures, a performance map for a given turbomachine can be evaluated. The pressure ratio of the compressor is obtained from the inlet and outlet values of the stagnation pressure, the non-dimensional mass flow from the amount of air and the inlet temperature and pressure. In this manner one point is evaluated on a constant speed line. The process is then repeated for several values of the mass flow to determine the complete speed line. Repeating this calculation for several speed lines will produce the familiar maps of component characteristics.

So far the process has been assumed to be reversible so the isentropic efficiency is unity. In the real case, an estimate can be made of the various losses as a function of blade geometries and flow parameters to produce a predicted map of efficiency characteristics, as will be shown later.

It is general practice to obtain the ratio of enthalpy rise across the rotor to enthalpy rise across the blade pair. This is defined as the degree of reaction. The desired degree of reaction at one fixed value of the blade height will determine the blade angles. If the degree of reaction is zero, the blade pair is termed an impulse stage, in which all the energy interchange in the rotors is obtained by redirecting the flow. In such a case the inlet and outlet relative velocities of the rotor are the same, and all the diffusion would occur in the

stators. In the case where the degree of reaction is not zero, some diffusion will occur in the rotors and some in the stators. Many turbomachines are designed with a fifty percent degree of reaction at the design blade height. Once the degree of reaction at the mean blade height has been established, there are several options to determine the blade angles at each value of the blade height, such as free vortex design, or constant reaction blading.

In the previous illustration it is important to know the air angles α_1 , α_2 , α_3 . Howell (Ref. 37) conducted extensive experimental work to establish axial compressor performance predictions from theory and tests on cascades. Part of this experimental work was directed towards establishing the fluid deflection that would result from various blade geometries and flow arrangements. It was suggested that a blade would be designed for a given deflection, given by various air and geometric parameters.

$$\delta_{de} = C10 \theta \left(\frac{s}{c}\right)^{\frac{1}{2}} \quad (4.16)$$

where

$$\alpha_2 = \beta_2 + \delta \quad (4.17)$$

and

$$C10 = 0.23 \left(\frac{2b}{c}\right)^2 + 0.1 \frac{\alpha_2}{50} \quad (4.18)$$

$$\theta = \beta_2 - \beta_1 \quad (4.19)$$

$$\epsilon = \alpha_2 - \alpha_1 \quad (4.20)$$

In this work the design condition was arbitrarily defined as a function of the stalling deflection.

$$\epsilon = 0.8 \epsilon_{st} \quad (4.21)$$

Where ϵ_{st} is the stalling deflection, which is defined to occur when the pressure loss is double its minimum value (see Fig. 4 of Ref. 37). It is improbable that the blade pair will be operating at its design condition, so it is important to evaluate the blade performance at conditions other than the design conditions. In Ref. 37 a set of curves has been produced where deflection is plotted as a function of the non-dimensional incidence $(i - i_{de})/\epsilon_{de}$. These curves are an approximate mean of the results deduced from tunnel cascades and worked back from compressor tests.

It is extremely important to evaluate the losses arising due to the physical presence of the aerofoils and the walls. The same author, in the method described above, also proposes a method to calculate the efficiency of the blading, by accounting for these losses. It would be possible to employ methods such as those of Koch and Smith (Ref. 44), which are based on more recent experimental information taken from turbomachines of current technology, but to use a single method throughout and because of its simplicity, Howell's method was adopted as a basis on which to develop an alternative model.

Howell further suggested that drag is caused by three reasons, annulus drag which is the drag due to the end walls of the stage, profile drag, due to the shape of the blade, and drag caused by secondary effects, such as tip vortices and

leakages due to tip clearances. So the total drag coefficient will be given by the addition of these coefficients for the three losses, equation (4.22).

$$C_d = C_{d_{pf}} + C_{d_{an}} + C_{d_{se}} \quad (4.22)$$

The profile drag coefficient is obtained from the same figure from which the fluid deflections are obtained, Fig 4 of Ref. 37. The coefficient of profile drag is a function of the non-dimensional incidence of the fluid on the blade.

$$C_{d_{pf}} = f\left(\frac{i - i_{de}}{e_{de}}\right) \quad (4.23)$$

The annulus drag coefficient is given by equation (4.24)

$$C_{d_{an}} = 0.02 \frac{s}{H_b} \quad (4.24)$$

while the drag coefficient for secondary losses is given by equation (4.25),

$$C_{d_{se}} = 0.018 C_l^2 \quad (4.25)$$

where

$$C_l = 2 \frac{s}{c} (\tan \alpha_1 - \tan \alpha_2) \cos \alpha_m - C_d \tan \alpha_m \quad (4.26)$$

Once the drag coefficients have been evaluated, the total drag coefficient is found from equation (4.22). The pressure loss due to irreversibilities, dP , is related to the drag coefficient by the expression

$$C_d = \frac{s}{c} \left(\frac{dP}{\frac{1}{2} \rho v_1^2} \right) \frac{\cos^3 \alpha_2}{\cos^2 \alpha_1} \quad (4.27)$$

The theoretical static pressure rise is evaluated from

$$\frac{\Delta P}{\frac{1}{2} \rho v_1^2} = 1 - \frac{\cos^2 \alpha_1}{\cos^2 \alpha_2} \quad (4.28)$$

this expression arising from the velocity triangles and incompressible flow. If desired, this expression can be modified to account for variations in the axial velocity, by modifying the second term of the right hand side of equation (4.28) to obtain equation (4.29).

$$\frac{\Delta P}{\frac{1}{2} \rho v_1^2} = 1 - \frac{\cos^2 \alpha_1}{\cos^2 \alpha_2} AVR^2 \quad (4.29)$$

The efficiency is then given by

$$\eta_s = 1 - \frac{dP}{\Delta P} \quad (4.30)$$

With the knowledge of these parameters, the temperature rise coefficient, equation (4.31), is evaluated,

$$TRC = \frac{C_p \Delta T_s}{\frac{1}{2} v^2} \quad (4.31)$$

and the pressure rise coefficient, given by

$$PRC = \frac{\Delta P_s}{\frac{1}{2} \rho v^2} \quad (4.32)$$

is obtained by multiplying the temperature rise coefficient by the stage efficiency as shown in equation (4.33)

$$PRC = TRC \eta_s \quad (4.33)$$

This is one of the classical methods of stage performance prediction. It has been mentioned that in this method no account has been taken of changes in the density of the fluid and the early workers assumed that the axial velocity was constant. These approximations are valid in Howell's work because it was carried out in the very early periods of gas turbine development, when compressor pressure ratios were not too high, and the density change across a stage was small. To account for these departures from these approximations, a method is proposed with some slight modifications, but based on Howell's method. In this modified calculation, the air angles and the drag coefficients are calculated as described in Howell's method. The drag coefficient is then used to evaluate the pressure loss for the blade row. This pressure loss is assumed to be a static pressure loss. The drag coefficient is then used to evaluate the efficiency as in Howell's method. This efficiency has a very similar magnitude to the isentropic efficiency of a small stage. So it is assumed that this efficiency is the isentropic efficiency of the blade row. Then with the knowledge of static pressures at inlet and outlet, the inlet static temperature and the isentropic efficiency, the static temperature at outlet is evaluated. The fluid velocity is then calculated from continuity (2.3) and the stagnation pressure at outlet can be calculated. The process is then repeated for the rotor. Throughout this process the air angles are assumed to be as evaluated at the beginning by using Howell's method. At this point all the stage outlet parameters have been evaluated. The next step is to repeat the procedure for the

next stage. The outlet parameters of a stage will be the inlet parameters for the next one. This process is continued until the last blade pair of the component is reached. The process is then repeated for different values of the mass flow to evaluate the performance in a non-dimensional speed line. These different values of the mass flow result in different magnitudes of the axial velocity. Once the calculation has been repeated for several non-dimensional speed lines, the compressor performance map will be obtained. The method described above is complete, and provides a basis on which the compressor performance maps can be evaluated. The next step is to establish the accuracy of the method by comparing the results to those of rig tests of the component studied. As stall is approached, the predicted performance will differ from the observed performance. The reason for this is the difficulty of the quantitative analysis of the stall and surge phenomena. It is evident that although the basic calculation of compressor performance is based on 'passage' theory, where isentropic flow is the ideal against which design is attempted, the losses and limitations of compressor performance are those encountered in aerofoil work. The described analysis consists basically of one-dimensional flow equations and information derived from cascade data. In a turbomachine the pitch is not constant along the blade height, and three-dimensional effects are always present. The above analysis will therefore be fairly good for high hub to tip ratio turbomachines, typically over 0.6. In the High Pressure Compressor of the present engine, the hub to tip ratio of the various stages lies between 0.61 and 0.9, so this analysis is applicable to this component. The

L.P. Compressor on the other hand falls below this value, the hub to tip ratio of the first stage of this component being 0.35. As it will be shown later, the effects of characteristic movements of this compressor on the transient phase, are very small, even when fuel is scheduled on the L.P. Shaft rotational speed. This is the reason why the above analysis has been extended to this compressor. However some doubts arise when predicting surge line movements of this component at the end of decelerations.

Work can be pursued along these lines to obtain better compressor performance prediction methods. Better accuracy could be obtained by a radial integration on each blade row, and then stacking along the length of the compressor. The present method is adequate for the present analysis because what is required is a simple method to carry out component performance calculations. This process will be repeated introducing some modifications in the variables due to the heat exchange between metal and fluid, and the results compared to those of the standard method which represent the adiabatic process. Thus what is desired is to obtain the relative movements of the non-dimensional speed lines due to the heat transfer effects.

When heat transfer is present, the blades will not deflect the flow as they do under adiabatic conditions. The result will be a modification of the performance of the component in question. Two reasons are suggested for the modification of the characteristics during a transient.

Fluid density changes

Alterations in the aerofoil boundary layer

4.3.2 Fluid Density Changes

When heat is exchanged between the fluid and the engine materials, a change in the fluid's temperature occurs. This modification will result in a modification of the fluid density, pressure being assumed constant. This in turn will modify the ratio of axial fluid velocity to blade speed, thus altering the working point of the blade pair. Maccallum (Refs. 55 and 56) has investigated this effect, and analysing the machine stage by stage with the non-adiabatic fluid conditions has obtained a linear relationship to predict this modification in the non-dimensional speed line. In this case all the heat transferred is allowed to occur at a plane between two consecutive stages. Thus the calculation proceeds normally for the next blade pair, but with a reduced inlet temperature (during an acceleration) because some heat has been removed after the exit from the previous blade pair. The amount of heat removed is the heat transferred to the material. This loss of heat will alter the density of the fluid, for which the pressure is assumed to be constant. As a result the velocities will change. The fluid will be entering the next stage with properties that are not those that would be in the adiabatic case.

As stated, during the heat transfer process the stagnation pressure is assumed to be constant. This is a realistic assumption. This fact was verified by assuming a frictionless flow with heat transfer (Rayleigh flow). The level of heat transfer was set by assigning a very large value to the ratio F , of 0.6 (this was the largest value obtained during a deceleration in the L.P. Compressor). The results of this investigation pointed out that at this level of heat transfer,

the change of stagnation pressure is of the order of 0.2 per-cent for each blade pair. This pressure change is in the opposite direction of the temperature change due to the heat transfer, so in an acceleration it will be beneficial. This error is acceptable because there are other uncertainties in the method which would produce larger errors, typically the definition of the air angles.

This process of modification of the fluid density has been carried out for several non-dimensional speed lines during various transients, accelerations and decelerations at both sea level and altitude conditions. An approximate expression describing the behaviour of the modified non-dimensional speed line is given in equation (4.34). In this expression, the constant coefficient C_{10} is valid for several transients in various situations, but for only one compressor. If another compressor is to be analysed, the process has to be repeated to evaluate this coefficient for this other component.

$$\frac{\Delta N}{N} = C_{11} \frac{\dot{Q}}{\dot{m} T_m} \quad (4.34)$$

The engine studied in Ref. 54 is the same as the one currently analysed, so the constants defining this quantity for the two compressors are -0.15 and -0.1.

4.3.3 Aerofoil Boundary Layers

Heat transfer from a wall to a fluid will increase the rate at which the fluid boundary layer develops. In the case of the compressor the problem is accentuated by the fluid moving against the pressure gradient. If the boundary layer

is to separate, the transfer of heat to the fluid will generally accelerate the process and induce it to occur further upstream. These boundary layer phenomena have been studied by Maccallum and Grant (Refs. 55,56). This investigation has shown that heat transfer will generally result in an increase in the displacement thickness of the boundary layer on the suction side of the blade. This effect will result in an incorrect deflection of the working fluid, in an increase of the profile drag of the blade, and in a wider wake at the trailing edge. The changed deflection will produce changes in profile drag and blade performance. From Ref. 56 the change in deflection was found to be approximately described by equation (4.35).

$$\frac{\Delta \alpha}{e_{de}} = \frac{\Delta T}{1000} (0.5 + 0.84 \frac{i - i_{de}}{e_{de}}) \quad (4.35)$$

The next step then was to find a 'pseudo' inlet angle, that will produce the same outlet angle under adiabatic conditions. The purpose of this procedure was to evaluate the drag coefficients to obtain the stage efficiency. An iterative process was necessary at this point, because the analytical solution of this problem was not possible. This iterative loop used the information obtained from Fig. 4 of Ref. 37. The rest of the calculation continued as described above, with the modified angles and drag coefficients. From repeated analyses of this type of equation (4.36) has been obtained. This equation gives a fairly satisfactory approximation to the behaviour of the engine (Ref. 55). As in the previous section regarding density changes due to heat transfer, the constant coefficient C12 in equation (4.36) is valid for all conditions

but only for the component being investigated. It must be mentioned that this approach is very approximate, and that more investigation is required in this topic. The value of C_{12} is -0.15 for the H.P. Compressor and -0.10 for the L.P. Compressor of this engine. These values have been obtained from Ref. 54.

$$\frac{\Delta N}{N} = C_{12} \frac{T_b - T_{air}}{T_{air}} \quad (4.36)$$

These relationships are adequate when they result only in small changes in the characteristics. Although small, their effect in a transient is not negligible. Some reservations must be made when the magnitude of the F value is very large, as is the case of the L.P. Compressor during a deceleration.

4.3.4 Movements of the Surge Line

The above methods are representative of the processes occurring during the transient phase of engine behaviour. After investigating these effects, simplified correlations that are sufficiently economical to be included in the transient programme have been devised. A similar procedure has been followed in the investigation of surge line movements. From the same methods, a simplified correlation has been obtained to represent the movements of the surge line. As previously discussed, one of the limiting aspects in an engine transient is the occurrence of surge in any of the compressors. It is generally accepted that surge involves the stalling of a few stages. It is therefore important to determine the occurrence of this phenomena. A choice exists of several such methods (Refs. 13, 15, 31). However a method to predict surge or stall

that is entirely satisfactory has not been developed so far, other than experimental procedures. It is generally accepted that surge is associated with local stalling at various stages. At reduced speeds, the low density of the fluid, in particular at the rear stages, will result in higher velocities, and the rear stages will be approaching choking conditions. At these conditions the low velocities at the inlet will result in high angles of attack, thus the probability of stall will be high. At high speeds, the compressor will surge because of stall occurring in the higher pressure stages. The fluid is of a high density, and the resulting axial velocities are low, again resulting in high angles of incidence. The easiest approach for the determination of surge is to arbitrarily choose the peak of the non-dimensional speed line as the point at which surge occurs. This procedure is not entirely satisfactory because many sets of characteristics, fan characteristics in particular, have been encountered where the engine will operate satisfactorily with one of the compressors working on a positive slope section of one of the non-dimensional speed lines. An alternative approach is to define the stalling point, as that at which the coefficient of profile drag will be twice its minimum value. This is when the non-dimensional incidence is equal to 0.4.

The characteristic prediction performance was then carried out, and adjusting factors introduced, to bring the adiabatic prediction into fair agreement with the characteristics supplied by the engine manufacturer. The various heat transfer effects are then introduced, and the points where surge is predicted to occur are noted. Despite its shortcomings, the method of assuming that surge occurs at the peak

of the non-dimensional speed line has been adopted. What is sought are the relative movements of the curves, rather than accurate predictions of the speed lines, so this simplification is justified. The aim of these calculations is to produce a simple correlation between the surge line movements and the rate of heat transfer. Plots of surge line rise were plotted in two forms as a function of F (the heat transfer to work transfer ratio). In one form the pressure ratio is divided by the adiabatic pressure ratio

$$\frac{PR_{ht}}{PR_{ad}} = f(F) \quad (4.37)$$

The correlation of this form that has been obtained is given in equation (4.38).

$$f(F) = 1 + 0.357 F \quad (4.38)$$

The other expression, and the one currently used is of the form

$$\frac{PR_{ht} - 1}{PR_{ad} - 1} = f(F) \quad (4.39)$$

This alternative analysis yielded equation (4.40)

$$f(F) = 1 + 0.541 F \quad (4.40)$$

This procedure was carried out for two non-dimensional speed lines for two decelerations and three accelerations, some at sea level static, and the others at altitude 9150 m and flight

Mach number 0.6 (Fig. 83). This analysis reveals a moderate scatter in the results. For the purpose of the model, a linear relationship has been assumed between F , the ratio of heat transfer to work transfer, and the surge line movement (Fig. 84). These coefficients have been adjusted in the evidence of further investigation, including the effects of end-wall boundary layer development, carried out by MacCallum (Ref. 55) where a more elaborate method predicted smaller movements than the ones resulting from the above method. This reduction is accomplished by introducing a multiplying factor of 0.67. Provision for these effects has also been made for the L.P. Compressor, despite the small departures of the transient running lines from the steady running lines. The coefficients of equations (4.38) and (4.40) have been reduced by one third because the same proportionality was observed between the coefficients that simulate the effects of the characteristic movements on the two compressors.

As previously stated, these methods have been treating the compressor stage as a passage. In practice, the blades act more as aerofoils, this point being strikingly illustrated by Epstein (Ref. 20). This work reveals how complex the flow in the compressor is. The present calculations are justified in that no accurate compressor performance is required, simply the relative movements due to the various heat transfer effects.

4.3.5 Turbines

Turbines also exchange heat with the working fluid during transients. In the turbines, the performance characteristics are dependent on the inlet guide vane area. During an acceleration where heat is transferred from the fluid to

the metal, a smaller displacement thickness of the boundary layer would be expected, thus reducing the drag and the blockage. However a smaller geometric cross sectional area would be available for the flow due to the material temperature being less than that of the steady state conditions. These processes resemble very much those occurring at the final nozzle of the engine. It should also be mentioned that the effects of non-design gas angle in the turbine blading will result in far smaller effects than those affecting the compressors. There are three important reasons for this fact. Firstly, the turbine blading produces much larger deflections on the gas flow than those produced by the compressor, therefore any non-design deflections due to modified boundary layers will have a smaller relative effect. Also since the flow is experiencing a favourable pressure gradient and accelerating, no danger of separation which could result in a phenomenon such as stall, exists as in the compressor. The third reason is that a turbine consists of very few stages, typically three or less, so the effects will not be affecting many subsequent stages as happens in the compressors, compressors of over ten stages being very common. These considerations led to the conclusion that heat transfer effects on turbine performance characteristics would not be as important a factor as the effects on compressor characteristics. Therefore the penalty in accuracy for not including them is acceptable.

CHAPTER V

RESULTS AND DISCUSSION

5.1 INTRODUCTION

In the previous chapters methods have been described which enable the evaluation of the performance of a gas turbine engine. In the procedures described in Chapters III and IV, provision has been made for the inclusion of important factors that can effect the predicted performance of an engine during a transient. In this chapter these factors are included in the prediction methods and the results obtained are compared to those obtained using the adiabatic models of Chapter II. The predicted performance of an engine can be modified in both the steady state and the transient phases by several other variables, and some of these possibilities are also studied in this chapter. A two-spool bypass engine with mixed exhausts, for which adequate structural information was available, has been selected to illustrate these effects.

5.2 PERFORMANCE OF THE COMPONENTS DURING A TRANSIENT

The first step in this investigation was a study of the sensitivity of the selected engine configuration to component inefficiencies. The results are shown in Fig. 85. By far the most important effect is that of H.P. Turbine efficiency. A deterioration of turbine efficiency of only one percent will

produce a retardation of nearly ten percent of the time needed to accomplish the transient. This deterioration of the efficiency will also have a detrimental effect on the performance level at the end of the transient. The inefficiencies of other components produce much smaller effects. For this demonstration the H.P. Compressor efficiency has been reduced by two percent, a one percent deterioration produced too small a change to be illustrated. The efficiencies of the L.P. Shaft, which are also changed by two percent, have very small effects on the engine's response. Inefficiencies of the latter three components have a smaller effect on the final value of the performance. The efficiencies of the L.P. Shaft have been improved so that the illustration is clearer. It has been observed that the magnitude of the effect on the performance is the same whether the efficiencies are increased or decreased, the effect always being in the same direction as the deterioration, i.e. a decrease in component efficiency always produces a slower acceleration.

In Figs 86 to 100, the performance of the various components during three transients is illustrated. These transients are at sea level static acceleration (Figs. 86 to 90), an acceleration at simulated altitude conditions of 9150m and a flight Mach Number of 0.8 (Figs. 91 to 95), and a deceleration at sea level static conditions (Figs. 96 to 100). During the sea level acceleration, the clearance path of the L.P. Compressor (Fig. 86) follows very closely the path the stabilised clearances would take. The clearance of this component is dominated by the centrifugal stresses of the disc because the temperature changes experienced by the L.P. Compressor are modest, the high pressure end of the component experiencing a temperature rise of only 80K. The small departures from the design clearances result in

extremely small efficiency losses. The factor F relating heat transfer to work transfer peaks at a value of about 0.1, and falls off fairly quickly with the engine stabilising. It must be borne in mind that this component handles a fluid mass flow which is about twice that flowing through the core components, so heat transfer rates are comparable to those of the other components which experience much larger temperature changes. The lowest frame of Fig. 86 illustrates the movement of the compressor characteristics. These movements reach a maximum of about one percent of the non-dimensional speed. The shape of the curve of modification of the characteristics resembles very much the curve of the factor F , as would be expected.

The H.P. Compressor clearances present a larger deviation from the steady state values. The reason for this is the larger range of temperatures which the metal has to undergo (Fig. 87). The efficiency changes are larger than those of the L.P. Compressor, but still too small to have an influence on the transient. The factor F peaks at about 0.14 and the modifications of the characteristics peak at about four percent. The H.P. Compressor heat transfer effects peak at higher values than those of the L.P. Compressor but also move faster towards stabilisation due to the larger magnitudes of the heat transfer coefficients and the smaller masses to be heated.

The effects on L.P. and H.P. Turbine due to heat transfer are shown in Figs 88 and 89 respectively. The effects of heat transfer on both turbines follow the same pattern. The sudden increase in inlet temperature at the beginning of the transient will produce clearances that are lower than those at the same conditions at the steady state. The casing does not have time to expand and open the clearance, while the disc will not expand

so much due to more effective cooling. The result is an improvement in efficiency which can be important in the case of the H.P. Turbine. The reason for this is that, compared to the L.P. Turbine the blade loading is much higher and the blades are shorter resulting in a higher value of the non-dimensional clearance. The factor F rises suddenly to a value of about 0.4 in the L.P. Turbine, and about 0.16 in the H.P. Turbine. In both cases the large magnitude of these effects falls off quite quickly. The second smaller peak that appears in these curves is due to the bleed valves closing, and at this point the acceleration proceeds substantially faster.

For the two compressors, the heat transfer effects change magnitude in a fairly smooth fashion during the transient. Turbines on the other hand experience a sudden change of state during the first time interval. This is the result of the sudden increase of fuel flow in the combustion chamber, effectively a step change of fuel flow and of turbine inlet temperature. This is reflected in the sudden change of the magnitude of the heat transfer effects at the beginning of the transient.

Seal openings during a sea level acceleration are shown in Fig. 90, compared to the steady state value at those running conditions. The seal openings throughout the transient are significantly larger than the design speed steady state values, thus allowing excessive amounts of coolant to escape from the compressors.

During this acceleration, all the components exhibit large changes in these transient effects when the time is about three seconds. After three seconds, the bleed valves close when the H.P. Shaft reaches the required non-dimensional speed, and the engine accelerates very quickly. The behaviour

of the seals as predicted by the simplified models used here in the engine transient programme follows closely the paths discussed in Chapter III.

When an acceleration at altitude is examined (Figs 91 to 95), the same patterns for all the components can be observed but two differences are evident. In general the curves are flatter, and the magnitude of the effects is smaller. The acceleration takes longer to be accomplished at altitude. This is because the magnitude of the mass flow of the engine is much smaller than that at sea level, while the temperatures are only slightly reduced due to the colder environment. As a result the torques produced by each component will be reduced. A slower acceleration will result in diminished magnitudes of heat transfer effects. Also the reduced range of the transient results in smaller amounts of heat to be transferred between the equilibrium values corresponding to the initial and final points of the transient. Therefore the "peakiness" of the effects is not so evident at altitude because the acceleration takes longer to be accomplished, and the heat is transferred more evenly over the relevant period of time.

During a deceleration (Figs. 96 to 100), the clearance of all the components increases because the centrifugal contraction is fast while the heat transfer effects take longer to be accomplished. However the resulting efficiency changes at the end of the transient are smaller than in the acceleration because of the reduced blade loading of the various components. The magnitude of the F factors for all the components are large at the end of the transient because of the lower value of the work input or output. Naturally the signs of all effects are reversed because the transfer of heat is from metal to fluid

in these circumstances. As mentioned previously the effects of heat transfer take longer to disappear in the deceleration because the reduced mass flows and rotational speeds produce lower heat transfer coefficients. For the same reason these effects retain their higher value for a longer period of time. During the altitude transient and the deceleration, the seals have non-design openings. During the deceleration the seal clearances are not substantially larger than those of the design point because the swift thermal response of the casing counteracts the contraction due to reduced centrifugal stresses. When a deceleration is occurring the heat transfer effects tend to improve the performance of the components thus retarding the transient.

5.3 EFFECTS OF CLEARANCE MOVEMENTS ON TRANSIENTS

5.3.1 Blade Tip Clearances

As shown in section 5.2, the tip clearances of both compressors and turbines are tighter at most points of the acceleration speed transient than they would be at the same engine conditions at the steady state. The reason for this is that centrifugal growth and thermal growth of the blades are the closing parameters which respond fastest, while the parameter that opens the clearance, the casing thermal expansion starts being felt very soon after the end of the speed transient. The casing expansion is larger than the disc expansion which will bring the clearance to the equilibrium value. The reason for this is that the disc is cooled much more effectively than the casing, thus its final temperature change is substantially

lower. This transient clearance reduction will result in a small beneficial effect on the engine's behaviour. However, during the last stages of the speed transient and the period of time immediately following this transient the clearances start increasing with the casing reaching its final temperature, before the discs. The resulting openings are larger than those at the steady running condition and they will produce a deterioration in efficiency.

In Fig. 101 the effect of efficiency changes due to modifications in the clearances is illustrated. The only component clearance that produced any effect on the predicted response of the engine is the H.P. Turbine clearance. A small improvement in the predicted performance is the result of the inclusion of this effect on the analysis. The effect of the other components is small, and whether their effect is included or not will produce no noticeable difference in the engine response.

5.3.2 Seal Clearances

When an engine is designed a specified cooling flow is bled from the compressor to several engine components, blades, discs, casings, etc. The seal opening is designed so that at a given operating point, in general cruise, a predetermined amount of air will be removed from the core flow. This has effect on the performance (Fig. 102), the cooling flow is allowed to leave the compressor core flow through what is called a source seal (the H.P. Compressor seal investigated here is such a seal), and is allowed back into the core gases through what is termed a sink seal (such as the H.P. Turbine disc seal) after they have performed their cooling function. Some flows can be thrown overboard (usually for other uses within the aeroplane). It

is general practice to have many sinks to one source. The flow bled through the H.P. Compressor seal in this case is sent to the bypass duct. The H.P. Turbine seal controls approximately one quarter of the cooling flow extracted from the compressor delivery of this engine. Both these seals have throughout the transient openings that exceed substantially, the design values. In such cases the danger exists of sink sources allowing too much flow back into the core gases, and if the compressor air supply is not adequate, some of these sinks will become sources, allowing hot turbine gases inside the discs. Serious engine damage can be the result of such an event. No attempt was made to analyse this possibility, in this case, all flows are assumed to follow their designed direction. The engine behaviour is very critically dependent on the amount of overfuelling at the end of the speed transient. If the fuel schedule is very near the equilibrium value the transient will last substantially longer than if the opposite is happening. The amount of overfuelling on the other hand is limited by the amount of surge margin available.

As Fig. 102 shows, the engine is very sensitive to the seal flows being larger than designed. In this case the H.P. Turbine seal has the largest effect on the transient because the ratio of maximum seal opening to stabilised seal opening is larger than that for the H.P. Compressor seal. The main reason for this situation is the larger design opening of the compressor seal. The movements of both seals are approximately of the same magnitude, but the turbine seal has a design opening which is nearly half that of the compressor seal. Thus the ratio will be double for the former seal. Also to be noticed, is that the increased seal openings do not produce a significant

change in the final performance of the engine. Their effect is limited to a slower dynamic response to the fuel schedule. The seal clearance effects were also examined in the steady state mode to determine whether seals are responsible for modifications in steady state performance. The influence of non-design seal openings is minimal in the steady state performance.

The effects on the acceleration rates shown here are more noticeable than those shown in an earlier published paper (Ref. 73) because different acceleration schedules have been used.

5.4 DIRECT HEAT TRANSFER EFFECTS

5.4.1 Effects of Component Heat Capacities

The influence of the heat capacity of the components on the predicted response of the engine during a transient is illustrated in Figs. 103 and 104. L.P. Compressor and L.P. Turbine influences are very small and their inclusion in the prediction method produces no distinguishable changes in the results obtained with the adiabatic model. This is despite the fact that the L.P. Turbine experiences at some points a heat transfer rate that is nearly forty percent of the work transfer rate. The inclusion of the H.P. Compressor heat capacity in the method results in an improved predicted response (Fig. 103), while the effect of the inclusion of the H.P. Turbine heat capacity deteriorates the predicted acceleration rate. When all heat capacities are allowed for simultaneously, a small deterioration in performance is observed. Noticeable is that apart from the slightly slower response when accelerating, the effect of including these heat capacities is a significant

reduction in the thrust developed at the end of the speed transients. This effect occurs when the heat capacities of any one of the components is included, the reduction in the predicted thrust when analysing the transient with all the components having heat capacity being an addition of the deteriorations due to each one of them. This reduction in thrust is experienced while the components are absorbing heat, and gradually the steady state thrust value is attained when the components have reached their equilibrium temperatures. No such modification is observed in the engine pressure ratio or the rotational speeds. These processes were studied using three methods of scheduling the fuel flow into the combustion chamber. In the first method, the fuel flow has been scheduled as a non-dimensional function of H.P. Compressor pressure ratio. The other alternatives introduced are scheduling fuel flow as a function of H.P. Spool rotational speed or as a function of L.P. Spool rotational speed. The results are very similar whichever of the fuel schedules is used.

The influence of the inclusion of the heat capacities of the components of the L.P. Shaft on the prediction of the response is very small. This is so because of the smaller amount of work produced in the shaft, which amounts to approximately one half of the work produced in the H.P. Shaft. Another reason for the small magnitude of these effects is the reduced temperature rise experienced by these components, in particular the compressor.

5.4.2 Changes in Compressor Characteristics

As described in the previous chapter, when heat is exchanged between the engine metal and the working fluid, a

modification of the component characteristics is observed. As in the case of heat capacities and for the same reasons, the effect of changes in the characteristics of the L.P. Compressor has a very small effect on the transient. The effect of the H.P. Compressor characteristics movements is very large. This effect is one of the most important reasons why the adiabatic analysis and the predictions with heat transfer effects show large discrepancies when the results are compared.

When the engine is analysed only with changes in the compressor characteristics, three trends are immediately noticed in the results obtained when comparing them to the adiabatic calculations. The first and most evident of the effects is the considerable retardation of engine response due to the changed characteristics of the H.P. Compressor. The second observation to be made is that the thrust and engine pressure ratio obtained at the end of the speed transient are the same as if the engine was analysed in the adiabatic mode. Thirdly, the rotational speed at the end of the speed transient is slightly lower than that predicted in the adiabatic case. This is because although the speed is lower than in the equilibrium conditions, the "effective speed" due to heat transfer is that corresponding to the final steady state point. It was explained in Chapter IV that characteristic changes need not be included in the turbine performance maps, therefore the power delivered by the turbine is the same as in the steady state. Consequently the compressor delivers the fluid at equilibrium conditions but at non equilibrium rotational speeds, due to the modifications in the characteristics. The rotational speed will gradually reach its equilibrium value when the engine approaches its equilibrium condition.

5.4.3 Movements of the Surge Line

The models to calculate the movement of the surge line have been included in the prediction programme. As can be observed in Figs. 106 and 107, the heat transfer effects produce an upwards movement of the surge line in an acceleration. In a deceleration the surge line is lowered. In most engines this is not of great concern because the deceleration is the least demanding transient. However it has been illustrated in Chapter II that the movement of the deceleration running line can be towards the surge line. The components that show this effect are compressors delivering their complete mass flow to the last compressor before the combustion chamber, such as the I.P. Compressor of the turbofans, or the L.P. Compressor of the two-spool turbojet. There is also another case in which this lowering of the surge line can be of interest. For several reasons an acceleration may be required immediately after a deceleration. When this is the case the initial fraction of the acceleration will be carried out with a smaller surge margin due to the lower position of the surge line. A fuller description of this transient is given in the next section of this chapter.

5.5 INCLUSION OF ALL THE EFFECTS

The inclusion of all these effects results in a marked increase in the predicted time required for an engine to attain its desired state, when compared to the adiabatic prediction. In particular the last four or five percent of the thrust will take much longer to be attained. This deterioration is influenced by the type of fuel schedule used. If the fuel flow

is scheduled as a non dimensional parameter which is a function of H.P. Compressor ratio, (Fig. 108) the predicted response is slowed by about one second. If the fuel flow is scheduled on the H.P. Shaft rotational speed (Fig. 109) the speed response is slowed by about two seconds. Scheduling the fuel as a function of the L.P. Shaft rotational speed (Fig. 110) the predicted acceleration time is slowed by about one second. These fuel flow schedules had been devised to achieve similar accelerations with all three when the engine was analysed as an adiabatic system.

The effects that appear to have the most important influence on the engine dynamic response are the non-design seal clearances and the movement of the characteristics of the H.P. Compressor. It is interesting to notice that both these effects are "capacity" effects, in which the compressor capacity is altered. These effects alter the predicted response of the engine during the transient, but seem to have a small effect on the final value of the thrust that is attained. The changes of fluid density resulting from the heat exchange are of smaller magnitude. The latter seems to have a large effect on each of the components of the H.P. Shaft, but the effects act against each other, and the resulting influence is a small slowing in the response. The way in which the heat capacities do modify the engine performance is the lower thrust that results at the end of the speed transient. This reduction will gradually disappear as the components slowly attain their equilibrium temperature.

Investigations to establish the effect on engine performance during a deceleration (Fig. 111) have established that the engine will take substantially longer to slow down

if analysed with heat transfer effects. The heat transfer effects will have a larger effect in a deceleration because the engine mass flows are much lower at the end of the transient. So the effects will be a larger proportion of the useful work produced in the various components. These effects also persist longer because the heat stored in the engine material is transmitted to the air at a reduced rate due to the reduced heat transfer coefficients resulting from reduced fluid mass flows and rotational speeds.

These effects were also investigated at altitude (Fig. 112), where due to the reduced mass flows through the engine, the effects are a larger proportion of the work transfer. So as it would be expected, the effects on the engine performance are more important. The engine was simulated at an altitude of 9150m and the flight Mach Number assumed to be of 0.8.

A transient simulation was also carried out on the two-spool engine with separate exhausts, to establish if the engine configuration in combination with the heat transfer effects could have an effect on the retarded response during a transient. For this purpose the component dimensions and parameters of the two-spool bypass engine with mixed exhausts were used, thus making the engines identical but with a different exhaust system. The results of this investigation are shown in Fig. 113. it can be seen that the inclusion of heat transfer effects in the configuration produces approximately the same changes in predicted transient performance as in the mixed exhaust arrangement.

Fig. 114 shows a middle term transient of the bypass engine with mixed exhausts. In this case, of interest are the movements of the H.P. Turbine inlet temperature. When an engine is accelerated, it has been shown that the rotational speed of

the engine at the end of the speed transient will be slightly reduced due to the heat transfer effects (Fig. 111,114). The engine operator observes that the rotational speed has not reached its desired value, so he will overfuel the engine slightly. As the thermal stabilisation of the engine proceeds, a combination of effects will force the operator to reduce the fuel flow. At the final stages of the speed transient, and during the period of time immediately following, the blade tip clearances are larger than what the equilibrium values would be. This increase in the clearance opening coincides with the largest seal opening during the transient. The deterioration in compressor efficiency will result in a higher compressor delivery temperature. The larger seal opening will allow a larger amount of air to leave the core flow for cooling purposes, reducing the flow of air in the combustion chamber. These two effects result in a higher gas temperature at the turbine entry, which when sensed by the temperature control device, will command a reduction in the fuel flow. The end result is a reduction of thrust soon after the end of the speed transient. This could mean at or near the point of take-off. This phenomenon has been observed by several airline pilots. The deterioration of component efficiencies due to larger values of the tip clearance, and due to the large seal openings manifests itself in a gradual increase of the turbine inlet temperature of approximately 50 K. This temperature rise occurs after the end of the speed transient. Also noticeable is the gradual increase of the thrust to the steady state value.

In Figs. 115 and 116 a comparison of the paths during an acceleration is shown. One of the paths was obtained analysing the engine as an adiabatic system, while heat transfer

effects were allowed for in the second prediction. It can be noticed that the acceleration including the heat transfer effects results in a path further away from the surge line than the path predicted with the adiabatic model. Also the surge line has moved away from the running line so there is an increase in the surge margin. This movement of the surge line leads to the investigation of the events occurring in a "Bodie" transient. This transient consists of allowing the engine to reach thermal equilibrium at maximum speed, the decelerating, and before the components have cooled to their new equilibrium values, accelerating again to maximum speed. This transient is illustrated in Figs. 117 and 118 where an acceleration is performed, and the engine is allowed to attain the equilibrium temperatures. After stabilising the engine, a deceleration followed by another acceleration is carried out, before the engine cools down after the deceleration. At this point the surge margin has been reduced due to the heat transfer effects, and the engine, because of these effects will follow a path nearer to the surge line. A short period of time will elapse before the heat transfer effects will raise the surge line to its adiabatic position. Beyond this point the surge line is higher than the adiabatic value, but always lower than the surge line position during a cold acceleration. Fig. 119 illustrates the engine performance during this transient. In this illustration an adiabatic, a cold and a hot acceleration are compared. It is interesting to notice that the hot acceleration is the fastest of the three. It is also the acceleration with the smallest surge margins. However after the end of the speed transient, the thrust is not as high as that of an adiabatic system, despite being slightly better than that of the cold

acceleration.

5.6 OTHER EFFECTS AND PARAMETERS

In addition to the heat transfer effects discussed above, there are some other influences which can affect the performance of gas turbines. Some of the effects which have to be investigated are the effects of the extent of mixing, the effect of pressure on the value of specific heat, the incorporation of reheat and the choices available for scheduling the engine fuel flow.

5.6.1 Mixing

When investigating an engine where the core exhaust gases and the bypass flow are mixed, an uncertainty arises as to the degree to which the cold and hot streams are mixed. If the flows are of similar magnitudes, a significant change in performance can result from different degrees of mixing of the flows. In the engine analysed, these flows are approximately of the same magnitude. In the programme a capability has been introduced to mix any fraction of the core flow with any fraction of the bypass flow. Thus it is assumed that at the exit of the nozzle, a minimum of one, and a maximum of three gas flows are discharged. These flows are a mixed flow, a cold one and a hot core gas flow, the fraction of the total each accounts for depending on the degree of mixing chosen. The results of analysing the engine, assuming complete mixing in one case, and no mixing in the other, are shown in Fig. 120 for the sea level case. When intermediate degrees of mixing are assumed, the predicted performance of the engine will lie between the

two extremes. The most noticeable features are the effect on the thrust and on the speed of the L.P. Shaft at the higher fuel flow ranges. When complete mixing occurs the thrust is raised by about four percent and the L.P. Shaft speed is lowered by about five hundred R.P.M., compared to the case when mixing is not allowed to occur. This implies a better specific fuel consumption of about four percent. The effects at medium and lower fuel flows are of a smaller magnitude. The effect on engine pressure ratio is not illustrated because it is small.

The different approach to mixing in the mixer duct produces no difference in the time that the engine takes to accelerate or decelerate. This investigation was also carried out at a simulated altitude of 9150m and flight Mach Number of 0.8. The results are shown in Fig. 121. At altitude the effect of the degree of mixing is larger. The improvement on specific fuel consumption is of the order of eight percent. In this situation the L.P. Shaft speed change is even more significant than at sea level, about eight hundred R.P.M. The effect on overall pressure ratio is very small. If the ram compression due to the forward speed of the aeroplane is included, the maximum overall engine pressure ratio is about 25. In general when an engine with a mixing duct is analysed as if no mixing occurred, the performance of this engine is not distinguishable from an engine with separate exhausts, despite the fact that for the engine with mixed exhausts, the requirement of similar static pressure ratio at the mixing control volume must be satisfied.

Another, simpler method of analysing the mixing process, although not physically correct, but that provides a very

good approximation is to assume that the fluid static pressure during the mixing process remains unchanged. This method gives the same answers as the previously described method. It was adopted as a trial, and it saved a small amount of computing time (about one to two percent) in the simpler engines, but less in the more complex engines. For this reason the correct method, previously described, is the one adopted in the prediction procedure.

Cullom and Johnsen (Ref. 12) carried out experimental work on a two spool turbofan, and they found improvements in thrust similar to those predicted above. Their experiments were carried out in a two-spool turbofan with bypass ratio of unity and an overall compressor pressure ratio of 17. Their engine had a variable length tailpipe, and a demountable mixer chute which was the key to the experiment. The pressure loss reported due to the inclusion of this device was small. Unfortunately their work was limited only to the high end of the performance spectrum of the engine. Tests were conducted for simulated altitude conditions for both subsonic and supersonic flight. Gains of similar magnitude are claimed for a version of a commercial three-spool turbofan, when a version of the engine with separate exhausts was to be modified to a mixed exhaust configuration (Ref. 90).

In addition there are other locations where mixing of the flows can occur. All engines have some cooling flows removed from the compressors, and returned to the core flows at some point in the engine. These flows are small and the method of returning them to the core flow will not produce a significant change in performance.

5.6.2 Effect of Pressure on Specific Heat Capacity of Air

A very important parameter in the evaluation of gas turbine performance is the value of the specific heat of the gases used in the thermodynamic calculations. The specific heat at constant pressure of air at temperatures near ambient is slightly affected by pressure. At higher temperature this dependence becomes very small (Ref. 19). In the programme this specific heat at a pressure of one atmosphere is calculated with a fourth order polynomial fit as a function of temperature. The specific heat at constant volume is then calculated at atmospheric pressure by subtracting the air gas constant which remains nearly constant for all the relevant temperature ranges (again at atmospheric pressure). The specific heat at constant volume at temperatures above 280 K is insensitive to pressure. At lower temperatures the effect is very small, so a satisfactory approximation is to assume that on the working range the specific heat at constant volume is independent of pressure. Once the two specific heat values are determined, the specific heat at constant pressure is adjusted for pressure according to information given in Ref. 19. The new value of specific heat at constant pressure is then used to evaluate the ratio of specific heats. For the turbines, a correction factor is applied to the specific heat of air to account for the presence of combustion products. This correction factor is a function of temperature and of air to fuel ratio. For this purpose it must be assumed that air and combustion gases have the same molecular weight so the gas constant R is the same for both. The agreement of the values of specific heat and ratio of specific heats with those published in Ref. 28 is good. This method is accurate to within one percent on the value of specific heats and to within 0.3

Parameter	Fuel	Standard From min	Standard From max	With Effect
	0.10	1.1161	1.1161	1.1161
L.P.C. Po/Pi	0.50	1.9245	1.9334	1.8787
	0.95	2.4177	2.4179	2.4187
	0.10	2808.6	2808.7	2807.4
L.P.C. R.P.M.	0.50	6986.9	6987.0	6860.1
	0.95	8311.0	8313.1	8273.9
	0.10	2.5684	2.5684	2.5674
H.P.C. Po/Pi	0.50	6.7668	6.7881	6.6820
	0.95	7.6195	7.6331	7.5854
	0.10	6906.3	6906.0	6903.1
H.P.C. R.P.M.	0.50	10415.1	10412.7	10267.8
	0.95	11474.8	11470.1	11383.7
	0.10	752.8	752.7	753.6
Turb. I.T.	0.50	1125.6	1125.3	1100.6
	0.95	1390.9	1392.2	1368.7
	0.10	3635.7	3635.6	3635.0
Thrust	0.50	36974.6	36976.8	36690.3
	0.95	55710.9	55713.0	54988.9

Table 4.

Effect of pressure on specific heat

percent for the ratio of the specific heats when compared to the values of Ref. 28. The effect of pressure on the value of specific heat on a standard day is too small to be observed, so a very cold day (248 K) and a very high ambient pressure (105.3 kPa) have been chosen. The effects of these calculations is too small to be shown graphically, so it is presented in tabular form in table 4. In some cases the effects are smaller than the errors due to tolerances. The effect is most significant at a medium speed, where temperatures are not so high as to reach the point where the effect is negligible, yet pressure are high enough for the effect to be noticed. If the test were conducted at altitude, the absolute pressures would be too low for this effect to be felt. The most important effect is a reduction of about 25 K in the predicted turbine inlet temperature. No effect whatsoever was detected on the transient behaviour of the engine.

5.6.3 Altitude Operation

The performance of an engine is different at altitude from that at sea level. Figs. 122 to 125 show the altitude performance, both steady state and transient, of the two-spool bypass engine. These figures show that for a given fuel flow the engine R.P.M., are much higher at altitude than at sea level. This is of course due to the much lower air mass flow passing through the engine. The thrust is lower for the same reason and also because of the forward speed of the aeroplane.

5.6.4 Fuel and Fuel Scheduling

The calorific value of the fuel used in this work is 43.15 MJ/Kg but any other kind of fuel can be used instead.

As previously stated, three types of fuel schedules have been introduced. In the first the fuel flow is scheduled with the H.P. Shaft rotational speed, in the second the fuel is scheduled with the L.P. Shaft rotational speed, and the third schedules the non-dimensional fuel mass flow on the function of the H.P. Compressor pressure ratio. This last schedule is the kind used in practice. These schedules have also been described in Chapter II. These are loaded as polynomial fits of up to the third power.

This method of loading the fuel function is to be used only when a known fuel schedule is to be employed. Fuel flow functions may not be known at the design stage, so it is necessary to optimise this parameter as well. For this reason, a second way of loading the fuel function is possible. The fuel schedule variable, and the parameter against which it is scheduled can be loaded point by point, and interpolation between them carried out. In this way, if the performance of the engine at a given point is not considered satisfactory, the fuel schedule is changed only at the point being considered.

When the data of an engine are loaded to the computer, two fuel schedules are loaded. One for an acceleration and one for a deceleration. The fuel schedules must be of the same type, a function of the same variable. One of the data parameters is a control variable that defines the combination of transients to be studied. Eight such different combinations are possible - combinations of acceleration, deceleration and steady state runs.

Another factor that can have a small effect on the transient performance of a gas turbine is the type of burner employed in the combustion chamber. When Fawke (Ref. 21) was

investigating engine test data he discovered that there was a "dead time" before the engine started to respond to the increased fuel flow. It was observed that the "dead time" was different for engines with vapourising burners, when compared to those with atomising burners. The reason for this dead time is the following. When the fuel controlling valve allows more fuel into the combustion chamber, some time will elapse until this increased flow reaches the combustion chamber. When the combustion chamber is reached, there is a further delay in the rise of the flame temperature. Before being burnt, the droplets have to be vapourised, and for this, energy has to be extracted from the combustion chamber environment. When the increased fuel flow reaches the chamber, there is an increased amount of energy absorbed for vapourising fuel, so there will be a small decrease in the combustion chamber temperature. This is the reason for the initial "dead time". During the transient a similar effect must be present. Since the fuel flow is constantly increasing, the energy absorption for vapourisation will be provided by a smaller quantity of fuel than in the steady state. This is the case until a steady fuel flow is reached. No attempt has been made to quantify this effect; because apart from an initial "dead time", the effect is small when compared to heat exchanges between engine material and working fluid. Gas turbines are designed with one of the two types of burner previously stated. The atomising burner, delivers a spray of small fuel droplets into the flame. The vapourising burner feeds the fuel in vapour form. Thomson, (Ref. 88) quotes that the time lag associated with an atomising burner is about twenty milliseconds. The time lag for the vapourising burner is between fifty and eighty milliseconds.

The difference may be due to the thermal capacity of the vapourising coil.

Returning to the methods employed in the present work, the engine's response to a step increase in fuel flow was investigated to check whether the various numerical approximations were valid. The results of this test are shown in Fig. 126. The variables shown are the shaft rotational speeds, the thrust and the engine's pressure ratio. This test was conducted at sea level, static conditions. The increase in fuel flow was from 0.5kg/s to 0.55kg/s, and the decrease in fuel flow taken was from 0.50kg/s to 0.45kg/s. This intermediate level of fuel flow was chosen with the intention of operating the engine far from the idle conditions, where the step increase could be a large proportion of the total fuel flow, but not too near the design point where the engine is supposed to operate under its optimum conditions. It can be observed from Fig 126, that the engine's behaviour following the decrease in fuel flow is the reverse of that following the increase in fuel flow, all curves being nearly symmetric about the starting steady state point condition. This indicates that the rates of change of the various parameters are the same at a point whether an acceleration or a deceleration is considered. The consistency is very good for engineering purposes. This test was repeated for the same altitude conditions as for the other tests. In this case the step change in fuel flow was of 0.03 kg/s upwards or downwards from a fuel flow of 0.3kg/s. The results of this test are shown in Fig. 127. Again the results show the same trends as those noted in the sea level static case, although there are noticeable differences. One difference is the longer time that the engine takes to reach the new steady

state condition. This effect has been observed in tests, and has been predicted from the early fifties (Ref. 66). The other difference is that the curves obtained for the L.P. Shaft rotational speed are not quite symmetrical. The significant section of the graph, that immediately following the step increase in fuel flow, is symmetrical as desired.

The above tests have shown that the procedure of using as many non dimensional rotational speed lines as possible, and interpolating between them, will produce realistic results. It has been suggested that interpolating with higher order routines will give better accuracy. The problem with this procedure, is that irregularities that may be present at some points of the characteristics, such as kinks, or bleed valves being opened or closed, will have an effect on the non dimensional speed line that is to be interpolated. Depending on the order of the interpolating routine, the effect of these discontinuities will be felt at points distant from the irregularitie(s). This effect is undesirable, and is minimised by linear interpolation. The basic disadvantage of linear interpolation is inaccuracy, but this is satisfactorily remedied by the provision of information at as many non dimensional speed lines as possible.

5.6.5 Reheat

This feature is a standard accessory for all supersonic aircraft. It augments thrust significantly without the need to install heavier engines on an aeroplane that will require a large thrust only sporadically in its flight programme. In essence it is the addition of fuel before the core gas is discharged to the atmosphere. In the programme it is simulated

as such with a pressure loss due to the extended length of the final duct. The reheat fuel flow can be switched off if it is desired to simulate such an engine operating in the "dry" mode. The aircraft operating this type of engine have final nozzles of variable area to accommodate the flow of gas of reduced density because of the higher temperature. All the reheat parameters, fuel flow, pressure loss and nozzle area schedule are loaded as a function of the H.P. Shaft rotational speed. When an engine is designed with afterburning capability, the design criterion used is to schedule the nozzle area in such a way that the gas generator working points will be the same as for the design condition when used in the "dry mode", with the aim of obtaining the best efficiency from the engine components. The mode of operation when in a transient, is to perform the transient with no reheat in the tailpipe, and once the desired engine state is achieved, to light the after - burner.

The steady state performance of the two-spool bypass engine is shown in Fig. 128. The engine works in the "dry" mode up to the point where fuel flow into the combustion chamber reaches the maximum value of 0.85kg/s after which the reheat is lit. From these figures it can be observed how the engine state has remained unchanged by altering the final nozzle area. The engine outlet flow has been assumed to be fully mixed. The fuel flow at the reheat chamber reaches a maximum of 2.05 kg/s. This is a total fuel flow of 2.90kg/s or approximately three and a half times the maximum fuel flow in the combustion chamber. The increase in thrust has been of the order of fifty percent. This illustrates that reheat is an inefficient way of providing additional thrust. This is why it is used in

aircraft that would only sporadically use the increased thrust, relying for a large part of their operational life on the "dry" thrust. This avoids the need of carrying a larger engine that would not be used at its full power very frequently. At altitude the specific fuel consumption will be better when the reheat is lit, when compared to the ground static case, but still not as good as the engine operating in the "dry" mode. The reason for the specific fuel consumption in flight deteriorating at a lower rate than that at sea level is because the ratio of the pressure in the reheat chamber to ambient pressure is greater in flight than when static. The heat addition is therefore more efficient thermodynamically.

In the reheat mode, the final nozzle area was increased by approximately fifty percent to discharge the lower density exhaust without changing the operating point of the gas generator.

CHAPTER VI

DISCUSSION OF THE PREDICTION METHOD

6.1 INTRODUCTION

In Chapter II a method has been proposed to produce more efficient convergence. It is due to this procedure that the computation of engine performance is efficient. In the same chapter the method of constant mass flow has been selected to carry out this investigation. This model assumes that the engine mass flow is constant at any instant at all operating conditions. In this section these assumptions are examined.

6.2 Computing Efficiency

As shown in Fig. 130, the time required for the mass flow continuity equation to be solved, by means of the convergence method previously described, increases proportionately with the number of components constituting the engine. In general, engines with mixed exhausts take slightly longer to converge, when compared to either turbojet engines or to engines with separate exhausts. The reason for this is the additional convergence requirement at the mixing duct. If an engine is to be analysed with the inclusion of heat transfer effects, a certain fixed time is required per disc analysed. The programme is built in such a way that all the heat transfer effects are calculated simultaneously, and they are included in

the analysis by setting control variables as required. In the case of the two-spool bypass engine, six discs were analysed. The additional computing time for these six discs is approximately eighty percent. Another aspect of the programme that was looked at is the effect of tolerances on the results produced by the computer. The programme has to converge at various points to a desired value, depending on the engine configuration and on the operating point. A minimum of one, and a maximum of two plus the number of choked turbines will be the maximum number of occasions, where the procedure has to converge to a required value. The minimum of one is for the mass balance at the final nozzle. If an engine has mixed exhausts, another convergence procedure is introduced, when calculating the static pressures of the flows before mixing. Further if any turbines are choked this will involve another convergence procedure to obtain a value for the mass flow function at entry to the choked turbine. The effect of the tolerances at these tests has been investigated to establish their effect on engine calculations. From the outset the tolerances of the final nozzle and the mixing duct were set very tight, and when increased or decreased by a factor of two they produced no effect on the calculated performance of the engine. The tolerance of the turbine choking band has to be set at a value of less than 0.0025 of the maximum value of the mass flow function of the particular non-dimensional speed line. If the value is larger, the engine will converge at points that can result in slightly different performance levels depending on the history of the previous calculations. These investigations were carried out in the steady state, and the effect of increased tolerances revealed itself in fluctuations

of the predicted performance about some point. The larger the tolerance, the larger the fluctuations would be. When the value of the tolerance was set at about one percent, the fluctuations would be of up to 200 R.P.M., halving the tolerance to half the previous value, the fluctuations would be reduced to about 50 R.P.M., and when the tolerances were reduced to their final value, the fluctuations were of about 10 R.P.M., this being about 0.1 percent of the design rotational speed. The fluctuations in the values obtained for the thrust were of a similar order. The smaller fluctuations do not occur from one interval to the other, but take a few time intervals. For this purpose a very small time interval was set to minimise the influence of nonlinearity of the acceleration. All these tests were carried out with double precision, that is to sixteen significant figures, to minimise the effect of the rounding off error in the computer. The programme will give satisfactory accuracy in single precision, this being eight significant figures for the calculations.

An examination was made of the effect of changing the time interval. At sea level all engines were found to be adequately simulated with time steps of 0.05 seconds (adequate simulation means that a reduction of the time interval by one half produced no significant alteration in the predictions). When analysing the engine at altitude it was found necessary to reduce the time step to one half the sea level optimum, that is to 0.025 seconds to obtain a reasonable engine simulation.

Throughout this work, the time step has always been larger than the critical time interval. This time interval is given by the time a pressure wave will take to traverse the length of the engine. In gas turbine practice this critical

time interval in very rare circumstances will exceed 0.01 seconds. If shorter time intervals were required, the method will still be satisfactory, only the calculation of the first time step during a transient will not be accurate.

6.3 VALIDITY OF THE ASSUMPTION OF CONSTANT MASS FLOW

An investigation to confirm the validity of the assumption of constant mass flow was considered necessary. This assumption is probably the weakest aspect of the present method. If the engine gases are assumed to be perfect, the perfect gas equation (6.1) will hold. This principle is shown with the mass as the subject of the expression.

$$m = \frac{P V}{R T} \quad (6.1)$$

The partial derivatives with respect to time, the volume being constant, are then given by equation (6.2).

$$\frac{dm}{dt} = \frac{V}{RT} \frac{dP}{dt} - \frac{PV}{RT^2} \frac{dT}{dt} \quad (6.2)$$

If it is assumed that the time interval is small enough to allow the equation to be linearised, the above expression becomes equation (6.3).

$$\frac{\Delta m}{\Delta t} = \frac{V}{RT} \frac{\Delta P}{\Delta t} - \frac{PV}{RT^2} \frac{\Delta T}{\Delta t} \quad (6.3)$$

This analysis was carried out during several instants during an acceleration of the two-spool bypass engine. A typical

volume was chosen for this investigation. The volume chosen was the duct leading the core gases from the L.P. Turbine outlet to the mixer nozzle. This particular volume was chosen for two important reasons. Firstly, it is a volume of considerable size, and from equation (6.3) the size of the volume has an influence on the mass flow imbalance. The second reason that led to the choice of this volume is that it is downstream of the combustion chamber, thus any temperature changes due to increased fuel flow would be reflected in this volume. This was the reason why the bypass duct was not selected. This duct, although of larger volume, would not reflect the drastic temperature changes due to sudden increases in fuel flows. From these calculations it was established that the two terms are of similar magnitude throughout the transient, as a result they cancel out. Only when the step fuel flow increase was introduced, was the difference substantial—about three percent of the core mass flow. As would be expected, in this case the temperature term dominated. The mass flow storage thus indicated was of a negative sign. In this first instant, the mass flow imbalance was slightly over three percent of the core flow, and about one percent of the total mass flow. From the next time interval onwards, where the fuel flow was increased by a smooth schedule, with no discontinuities, the two terms were of similar size, and the resulting mass storage was always less than 0.4 percent of the core flow. In this case the time interval chosen was of 0.05 seconds. This time interval is seven times larger than the time necessary for a pressure wave to traverse the length of the engine. If the time interval is reduced below this critical time interval it

would be necessary to include the effects of the pressure dynamics. This is the reason why this effect shows up only in the first time interval.

CHAPTER VII

CONCLUSION

A method to evaluate the steady state and transient performance of gas turbine engines has been developed. This method has been incorporated into a computer programme that can analyse any gas turbine configuration in existence or likely to be designed in the near future.

The programme uses the method of constant mass flow as the basis for the evaluation of gas turbine performance. The greatest difficulty that has been encountered hitherto in this method is the achievement of efficient convergence to the required value of the mass flow. This problem was overcome in the present work by designing a routine that incorporates a self-adjusting variable exponent in the function that governs the iteration processes. This method proved most satisfactory even when the most complex engines presently in service were analysed. It can be said that if the characteristics of the components are compatible, convergence should be obtained.

Once confidence in the method was acquired, the programme was extended to analyse eleven different configurations of single or multi-shaft engines and of any bypass arrangement. Characteristics for most of these engines were not available, so they had to be generated. This was done by introducing scale factors on the characteristics of known engines (four in total)

or they were generated from steady state information.

The accuracy of the method has been established by comparing the predicted steady state performance of a two-spool bypass engine with mixed exhausts with the observed performance of this gas turbine on the test beds. Unfortunately no such comparison could be made with the transient performance of any engine because no such information was available. Another engine was analysed for which the steady state performance from an alternative simulation was known. The results obtained in this case were very close without any adjusting factors being introduced, which indicates that the methods used are quite accurate.

The general transient procedure has been developed by incorporating estimates of several effects due to the heat exchange between engine metal and fluid. This heat exchange produces non-design blade tip and seal clearances, movements of the compressor characteristics and modifications of the processes of compression and expansion of the gases in the engine. It has been found that these effects produce significant departures from the adiabatic behaviour of the engine.

Particular attention has been paid to the development of models for the calculation of tip clearances. No previous work in this area was encountered, so the method employed in this programme had to be developed. It has been illustrated that this model is useful by itself, but the emphasis of this work is on engine transient performance, and another model, much simpler had to be devised to be included in the general programme, without significant sacrifice in accuracy.

Additional work is required in the sense that axial movements between rotating and stationary parts have not yet been treated.

Work on the evaluation of direct heat transfer effects

was available and procedures that have already been tried were modified and included in the programme. A model to calculate movement of characteristics during transients has been shown, and simplified versions of this model were used to calculate movements of the characteristics and the surge line.

It has been found that the compressor and turbine clearance movements result in small beneficial effects during an acceleration. Of the blade tip clearance effects the most important one is that in the H.P. Turbine. Seal clearances have an important retarding effect during an acceleration. Of the two seals investigated, the H.P. Turbine seal has the most important effect. During an acceleration these seal effects in conjunction with the characteristic movements of the compressors account for most of the differences between adiabatic and non-adiabatic modelling. Another factor to be considered is the effect of heat capacities, which although having no significant effect on the transient response, produce an important deterioration of the thrust developed by the engine at the end of the speed transient. It has been found that if the heat transfer effects of the L.P. Shaft components are neglected, there will be no modification in the predicted engine performance during transients.

Another interesting aspect of performance that has been investigated is the period of time immediately following the end of the speed transient. During this period of time, important changes of performance have been predicted due to the gradual thermal stabilisation of the engine.

The usefulness of this programme as a tool has been illustrated in Chapters II and V. In Chapter II eleven engine configurations have been analysed, and a provision for two

alternative methods of analysing fans of bypass engines and turbofans have been demonstrated. In Chapter V various effects have been analysed in addition to the heat transfer effects. These effects are the incorporation of reheat, the importance of the degree of mixing in an engine with mixed exhausts and the effect of pressure on the value of the specific heat of air. The programme can simulate engines with reheat, one of its possible uses being the development of nozzle area schedules. It has been shown that important gains in performance are possible if it is ensured that the two flows in a bypass engine are fully mixed, and that the effect of pressure on specific heat can safely be ignored. Another useful use of the programme is that of designing fuel schedules to study different transients.

The present programme from the point of view of computing time is not very far from real time simulation. A single spool turbojet was analysed in approximately one and a half real time and the most complex configurations in about four to five times real time. This is due to the efficient convergence procedures designed and to the availability of modern computers. Typically an engine if analysed as a non-adiabatic system will require an increase of eighty percent of computing time on the time required for the adiabatic model. It is considered that this penalty is acceptable, because of the large number of the additional effects calculated, and their effect on the transient. It has been shown that some transients such as the 'Bodie' transient, produce such different results when analysed with or without heat transfer effects, that a non-adiabatic system is necessary.

The present method is a natural development of the

long list of procedures available for the simulation of gas turbine performance. The main difference from previous work is the inclusion in the programme of models representing the non-adiabatic effects. These models are in a simplified form, but reasonably accurate. The simplifications are necessary to produce a manageable computer programme the scope of which is a general and realistic simulation of gas turbine performance.

REFERENCES

1. Abbot, I.H., Von Doenhoff, A.E., Stivers, L.S.,
Summary of Airfoil Data.
N.A.C.A. Report 824, 1945
2. Ainley, D.G.,
Performance of Axial Flow Turbines.
Proc. I. Mech. Eng., Vol 158, 1948
3. Ballal, D.R.,
Axial Flow Compressor Stacking Techniques.
Ph.D. Thesis, Cranfield College of Technology, 1968
4. Bammert, K., Krey, G.,
Dynamic Behaviour and Control of Closed Cycle Single
Shaft Gas Turbines.
A.S.M.E. Paper 71 GT 16, 1971
5. Bauerfeind, K.,
Transient Performance of Jet Engines.
M.A.N. Report 33878, 1967
6. Bauerfeind, K.,
A New Method for the Determination of Transient Jet
Engine Performance Based on the Nonstationary
Characteristics of the Components.
AGARD CP 34, 1968
7. Bauerfeind, K.,
Aircraft Gas Turbine Cycle Programmes. Requirements
for Compressor and Turbine Performance Predictions.
AGARD, 1976
8. Bennet, H.W.,
Aero Engine Development of the Future.
Proc. I. Mech. Eng., Vol 197, 1983
9. Breugelmans, F.A.E.,
Industrial Compressors, Aerodynamic and Mechanical
Factors Affecting the Surge Line. Tip Clearance
Effects in Axial Flow Compressors.
Lecture Series 91, Von Karman Institute, 1976
10. Brown, L.E.,
Axial Flow Compressor and Turbine Loss Coefficients.
A Comparison of Several Parameters.
A.S.M.E. Journal of Engineering for Power, July 1972
11. Cohen, H., Rogers, G.F.C., Saravanamuttoo, H.I.H.,
Gas Turbine Theory.
2nd Edition, Longman 1972
12. Cullom, R.R., Johnsen, R.L.,
Altitude Engine Test of a Turbofan Exhaust Gas Mixer
to Conserve Fuel.
A.S.M.E. Journal of Engineering for Power, October 1977

13. Cumpsty, N.A., Greitzer, E.M.,
A Simple Model for Compressor Stall Cell Propagation.
A.S.M.E. Paper 81 GT 73, 1981
14. Dandois, M., Novik, D.,
Application of Linear Analysis to an Experimental
Investigation of a Turbojet Engine With Proportional
Speed Control.
N.A.C.A. TN 2642, 1952
15. Day, I.J., Greitzer, E.M., Cumpsty, N.A.,
Prediction of Compressor Performance in Rotating Stall.
A.S.M.E. Paper 77 GT 10, 1977
16. Delio, G.J.,
Evaluation of Three Methods for Determining the Dynamic
Characteristics of a Turbojet Engine.
N.A.C.A. TN 2634, 1952
17. Doyle, M.D.C., Dixon, S.L.,
The Stacking of Compressor Stage Characteristics to
Give an Overall Performance Map.
The Aeronautical Quarterly, Vol 13, November 1962
18. Durand, H.P.,
Simulation of Jet Engine Transient Performance.
A.S.M.E. Paper 65 WA/MD 16, 1965
19. Ellenwood, F.O., Kulik, N., Gay, N.R.,
The Specific Heats of Certain Gases over Wide Ranges
of Pressures and Temperatures.
Cornell Univ. Eng. Experimental Stn. Bull., 1942
20. Epstein, A.H.,
Quantitative Density Visualisation in a Transonic
Compressor Rotor.
A.S.M.E. Journal of Engineering for Power, July 1977
21. Fawke, A.J.,
Digital Computer Simulation of Gas Turbine Dynamic
Behaviour.
Ph.D. Thesis, University of Bristol, 1970
22. Fawke, A.J., Saravanamuttoo, H.I.H.,
Experimental Investigation of Methods for Improving
the Dynamic Performance of a Twin Spool Turbojet
Engine.
A.S.M.E. Paper 71 GT 14, 1971
23. Fawke, A.J., Saravanamuttoo, H.I.H.,
Digital Computer Methods for Prediction of Gas Turbine
Dynamic Response.
SAE Paper 710550, 1971
24. Fawke, A.J., Saravanamuttoo, H.I.H.,
Experimental Verification of a Digital Computer
Simulation Method for Predicting Gas Turbine
Dynamic Behaviour.
Proc. I. Mech. Eng., Vol 186, 1972

25. Fawke, A.J., Saravanamuttoo, H.I.H.,
Digital Computer Simulation of the Dynamic Response
of a Twin Spool Turbofan with Mixed Exhausts.
Aeronautical Journal, Vol 24, Sept 1983
26. Fedor, M.S., Hood, R.,
Analysis for Control Application of Dynamic
Characteristics of Turbojet Engines with Tail
Pipe Burning.
N.A.C.A. TN 2183, 1950
27. Fett, F.,
The Dynamic Behaviour of Jet Engines Under Internal
and External Action.
AGARD CP 34, 1968
28. Fielding, D., Topps, J.E.C.,
Thermodynamic Data for the Calculation of Gas
Turbine Performance.
A.R.C. R&M 3099, 1959
29. Filippi, R.E., Dugan, J.F.,
Effect of Overall Compressor Pressure Ratio
Division on Acceleration Characteristics of Three
Hypothetical Two Spool Turbojet Engines.
N.A.C.A. RM E56 D13, 1956
30. Goldstein, A.W., Alpert, S., Bede, W., Kovack, K.,
Analysis of Performance of Jet Engine Characteristics
of Components, Part II, Interaction of Components as
Determined from Engine Operation.
N.A.C.A. Report 928, 1948
31. Greitzer, E.M.,
Surge and Rotating Stall in Axial Flow Compressors.
A.S.M.E. Journal of Engineering for Power, April 1976
32. Halls, G.A.,
Air Cooling of Turbine Blades and Vanes.
Lecture to AGARD, Varenna, Italy, 1967
33. Harman, R.T.C.,
Gas Turbine Engineering.
Macmillan Press, 1981
34. Haynes, C.M., Owen, J.M.,
Heat Transfer From a Shrouded Disk System With a
Radial Outflow of Coolant.
A.S.M.E. Journal of Engineering for Power, January 1975
35. Hearn, E.M.,
Mechanics of Materials.
Pergamon Press, 1977
36. Heidmann, M.F.,
Analysis of the Effect of Variations in Primary
Variables on Time Constant, and Turbine Inlet
Temperature Overshoot of Turbojet Engines.
N.A.C.A. TN 2182, 1950

37. Howell, A.R.,
The Present Basis of Axial Flow Compressor Design.
Part I, Cascade Theory and Performance.
A.R.C. R&M 2095, 1942
38. Howell, A.R.,
Fluid Dynamics of Axial Compressors.
Proc. I. Mech. Eng., Vol 156, 1946
39. Howell, A.R.,
Design of Axial Compressors.
Proc. I. Mech. Eng., Vol 156, 1946
40. Howell, A.R., Bonham, R.,
Overall and Stage Characteristics of an Axial Flow
Compressor.
Proc. I. Mech. Eng., Vol 163, 1950
41. Itoh, M., Ishigaki, T., Sagiya, Y.,
Simulation Study of Transient Performance Matching
of a Turbofan Engine Using an Analogue Computer to
Evaluate its Usefulness as a Design Tool.
A.S.M.E. Journal of Engineering for Power, July 1975
42. Kearton, W., Keh, T.H.,
Leakage of Air Through Labyrinths of Staggered Type.
Proc. I. Mech. Eng., Vol 166, 1952
43. Ketchum, J.R., Craig, R.T.,
Simulation of Linearised Dynamics of Gas Turbine
Engines.
N.A.C.A. TN 2826, 1952
44. Koch, C.C., Smith, L.H.,
Loss Sources and Magnitudes in Axial Flow Compressors.
A.S.M.E. Journal of Engineering for Power, July 1976
45. Koff, B.L.,
Designing for Fighter Engine Transients.
AGARD CP 324, 1982
46. Lakshminarayana, B.,
Methods of Predicting the Tip Clearance Effects in
Axial Flow Turbomachinery.
A.S.M.E. Journal of Basic Engineering, September 1970
47. Larrowe, V.L., Spencer, M.M., Tribus, M.,
A Dynamic Performance Computer for Gas Turbine Engines.
Transactions A.S.M.E. October 1957
48. Larjola, J.,
Transient Simulation of Gas Turbines Including the
Effects of Heat Capacity of the Solid Parts.
Ph.D. Thesis, Helsinki University of Technology, 1982
49. Lim, T.C.,
An Investigation into the Seal Clearance and Temperature
Response During Transient of the Stage 12th H.P.
Compressor of a Twin-Spool Bypass Jet Engine.
Final Year Project, University of Glasgow, 1980

50. Maccallum, N.R.L.,
The Performance of Turbojet Engines During the
Thermal Soak Transient.
Proc. I. Mech. Eng., Vol 184, 1969
51. Maccallum, N.R.L.,
Effect of Bulk Heat Transfer in Aircraft Gas Turbines
on Compressor Surge Margins.
Heat and Fluid Flow in Steam and Gas Turbine Plant.
I. Mech. Eng., London, 1974
52. Maccallum, N.R.L.,
Transient Expansion Of the Components of an Air Seal
on a Gas Turbine Disc.
SAE Paper 770974, 1977
53. Maccallum, N.R.L.,
Thermal Influences in Gas Turbine Transients, Effects
of Changes in Compressor Characteristics.
A.S.M.E. Paper 79 GT 143, 1979
54. Maccallum, N.R.L.,
Further Studies of the Influence of Thermal Effects
on the Predicted Accelerations of Gas Turbines.
A.S.M.E. Paper 81 GT 21, 1981
55. Maccallum, N.R.L.,
Axial Compressor Characteristics During Transients.
AGARD CP 324, 1982
56. Maccallum, N.R.L., Grant, A.D.,
Effect of Boundary Layer Changes due to Transient Heat
Transfer on the Performance of Axial Flow Compressors.
Paper 770284, SAE Conference, Detroit, March 1977
57. MacIsaac, B.D., Saravanamuttoo, H.I.H.,
The Comparison of Analog, Digital and Hybrid Computers
in the Optimisation of Control Parameters.
A.S.M.E. Paper 73 GT 13, 1973
58. MacIsaac, B.D., Saravanamuttoo, H.I.H.,
Aerothermodynamic Factors Governing the Response
Rate of Gas Turbines.
AGARD CP 324, 1982
59. Macmillan, W.L.,
Development of a Modular Type Computer Programme for
the Calculation of Gas Turbine Off-Design Performance.
Ph.D Thesis, Cranfield Institute of Technology, 1974
60. Mallinson, D.H., Lewis, W.G.E.,
The Part Load Performance of Various Gas Turbine Engine
Schemes.
Proc. I. Mech. Eng., Vol 158, 1948

61. Meyer, C.A.
The Leakage Thru Straight and Slant Labyrinths and Honeycomb Seals.
A.S.M.E. Journal of Engineering for Power, October 1975
62. Neal, P.F.,
Mechanical and Thermal Effects on Transient and Steady State Component Performance of Gas Turbines.
AGARD CP 324, 1982
63. Neilson, W.,
The Finite Element Method in Transient Heat Conduction.
Final Year Project, University of Glasgow, 1973
64. Novik, D.,
Some Linear Dynamics of Two-Spool Turbojet Engines.
N.A.C.A. TN 3274, 1956
65. Onions, R.A., Foss, A.M.,
Improvements in Dynamic Simulations of Gas Turbines.
AGARD CP 324, 1982
66. Otto, E.W., Taylor, B.L.,
Dynamics of a Turbojet Engine Considered as a Quasi-Static System.
N.A.C.A. TN 2091, 1950
67. Otto, E.W., Gold, H., Hiller, K.W.,
Design and Performance of Throttle Type Fuel Controls for Engine Dynamic Studies.
N.A.C.A. TN 3445, 1955
68. Owen, J.M., Onur, H.S.,
Convective Heat Transfer in a Rotating Cylindrical Cavity.
A.S.M.E. Journal of Engineering for Power, April 1983
69. Pack, G.J., Phillips, W.E.,
Analog Study of Interacting and Non-Interacting Multiple Loop Control Systems for Turbojet Engines.
N.A.C.A. TN 3112, 1954
70. Palmer, J.R.,
The TURBOCODE Scheme for the Programming of Thermodynamic Cycle Calculations on an Electronic Digital Computer.
CoA Report Aero 198, Cranfield, 1967
71. Palmer, J.R., Annand, K.P.,
Description of the Algol Version of the TURBOCODE Scheme for the Programming of Thermodynamic Cycle Calculations on an Electronic Digital Computer.
CoA Report Aero 203, Cranfield, 1968
72. Pandya, A., Lakshminarayana, B.,
Investigation of the Tip Clearance Flow Inside and at the Exit of a Compressor Rotor Passage.
A.S.M.E. Journal of Engineering for Power, January 1983

73. Pilidis, P., Maccallum, N.R.L.,
Models for Predicting Tip Clearance Changes in Gas
Turbines.
AGARD CP 324, 1982
74. Rick, H., Mugli, W.,
Generalised Digital Simulation Technique With
Variable Engine Parameter Input for Steady State
and Transient Behaviour of Gas Turbines.
AGARD CP 324, 1982
75. Rolls-Royce
Private Communications, 1982
76. Rubis, C.,
Transient Response of a 25000 HP Marine Gas Turbine
Engine.
A.S.M.E. Paper 71 GT 61, 1971
77. Saravanamuttoo, H.I.H.,
Analogue Computer Study of the Transient Performance
of the Orenda 600 HP Regenerative Gas Turbine Engine.
A.S.M.E. Paper 63 AH/GT 38, 1963
78. Saravanamuttoo, H.I.H.,
Use of an Analog Computer in the Design and Develop-
ment of an Advanced Regenerative Gas Turbine.
4th International Analogue Computer Meeting, 1964
79. Saravanamuttoo, H.I.H.,
Analogue Computer Simulation of Gas Turbine Dynamic
Performance.
Ph.D. Thesis, University of Bristol, 1968
80. Saravanamuttoo, H.I.H., Fawke, A.J.,
Simulation of Gas Turbine Dynamic Performance.
A.S.M.E. Paper 70 GT 23, 1970
81. Saravanamuttoo, H.I.H., MacIsaac, B.D.,
The Use of a Hybrid Computer in the Optimisation of
Gas Turbine Control Parameters.
A.S.M.E. Paper 73 GT 13, 1973
82. Saravanamuttoo, H.I.H., MacIsaac, B.D.,
An Overview of Engine Dynamic Response and
Mathematical Modelling Concepts.
AGARD CP 324, 1982
83. Sellers, J.F., Daniele, C.J.,
DYNGEN. A Program for Calculating Steady State and
Transient Performance of Turbojet and Turbofan Engines.
N.A.S.A. TN D 7901, 1975
84. Sham, T.L.,
The Development and Application of a Finite Element
Programme in Solid Mechanics.
Final Year Project, University of Glasgow, 1977

85. Szuch, J.R.,
HYDES. A Generalized Hybrid Computer Program
for Studying Turbojet or Turbofan Engine Dynamics.
N.A.S.A. TM X 3014, 1974
86. Tachibana, F., Fukui, S.,
Convective Heat Transfer of the Rotational and
Axial Flow Between Concentric Cylinders.
Bull. of Japanese Soc. of Mech. Eng., Vol 7, 1964
87. Taylor, B.L., Oppenheimer, F.L.,
Investigation of Frequency Response Characteristics
of Engine Speed for a Typical Turbopropeller Engine.
N.A.C.A. TN 2184, 1950
88. Thomson, B.,
Basic Transient Effects of Aero Gas Turbines.
AGARD CP 151, 1975
89. Ushiyama, I.,
Theoretically Estimating the Performance of Gas
Turbines Under Varying Atmospheric Conditions.
A.S.M.E. Paper 75 GT 115, 1975
90. Velupillai, D.,
Rolls-Royce Better RB 211 535.
Flight International, 14 February 1981
91. Vermes, G.,
A Fluid Mechanics Approach to the Labyrinth Seal
Leakage Problem.
A.S.M.E. Journal of Engineering for Power, April 1961
92. Wittig, S.L.K., Dorr, L., Kim, S.,
Scaling Effects on Clearance Losses in Labyrinth Seals.
A.S.M.E. Journal of Engineering for Power, April 1983

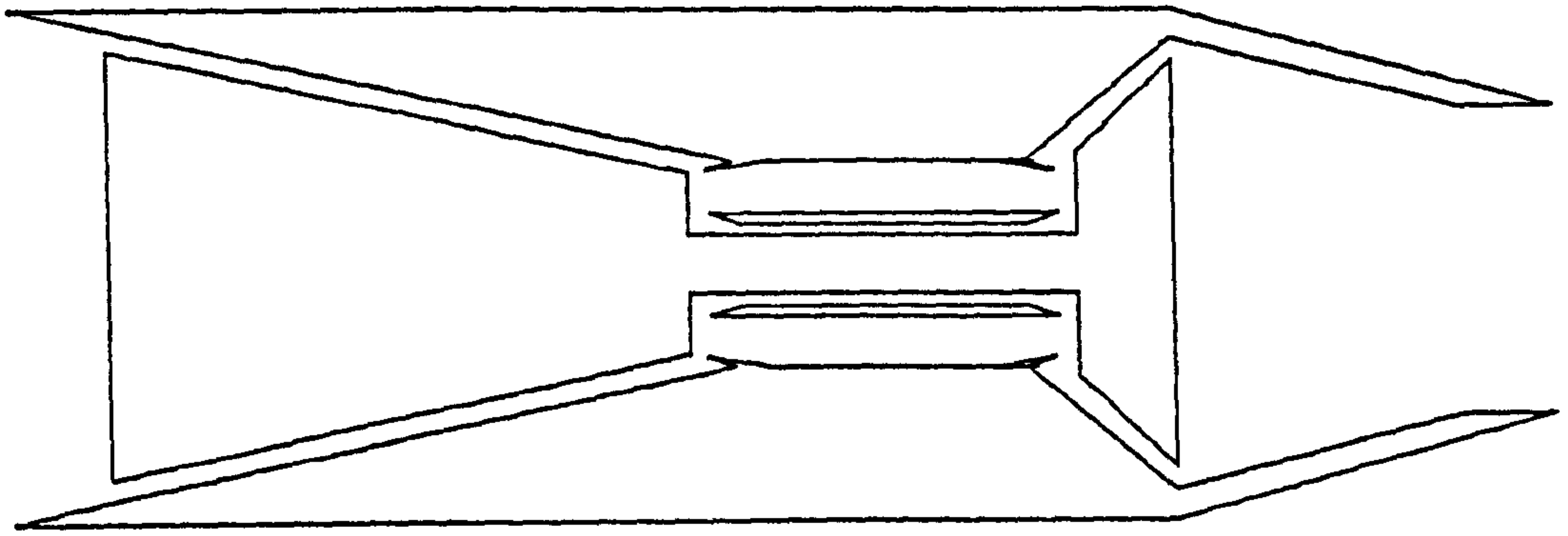


FIG. 1
SINGLE SPOOL TURBOJET

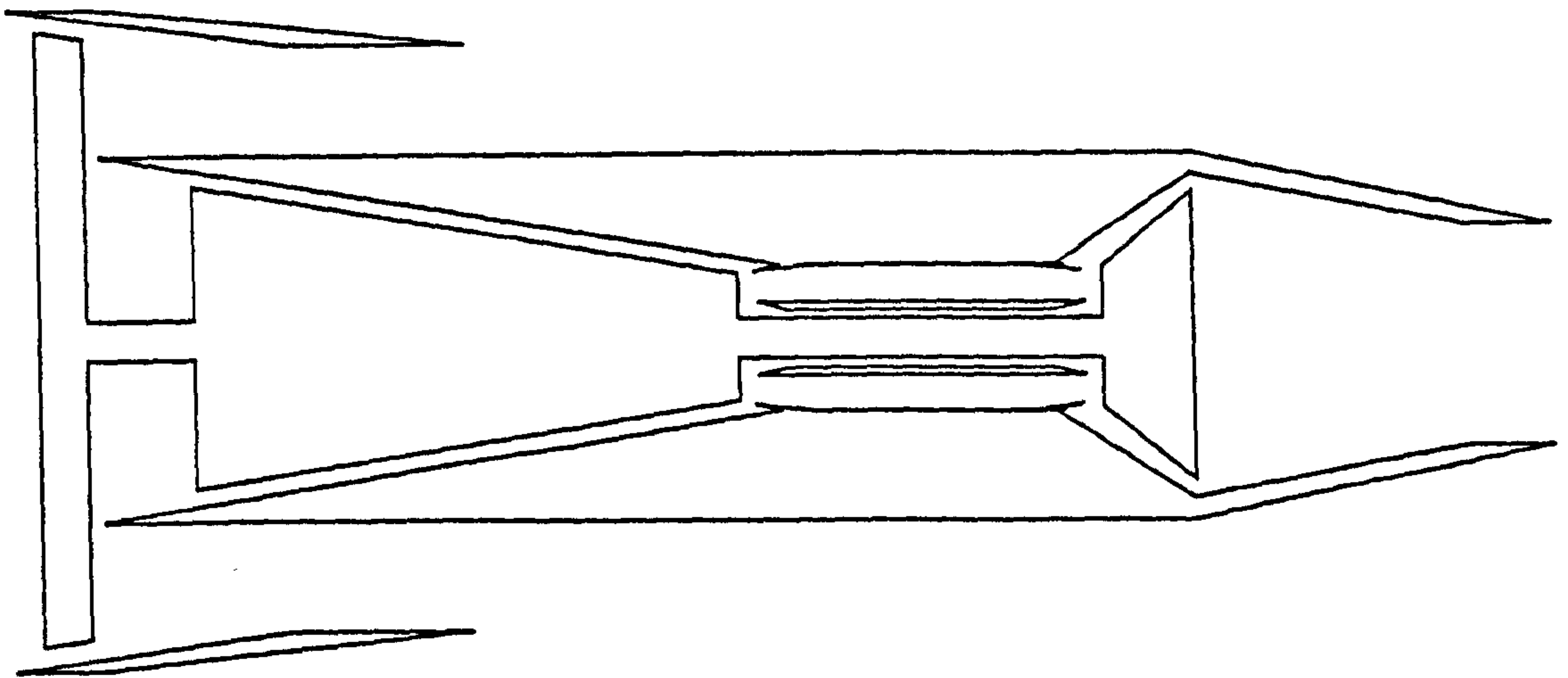


FIG. 2
SINGLE SPOOL TURBOFAN WITH SEPARATE EXHAUSTS

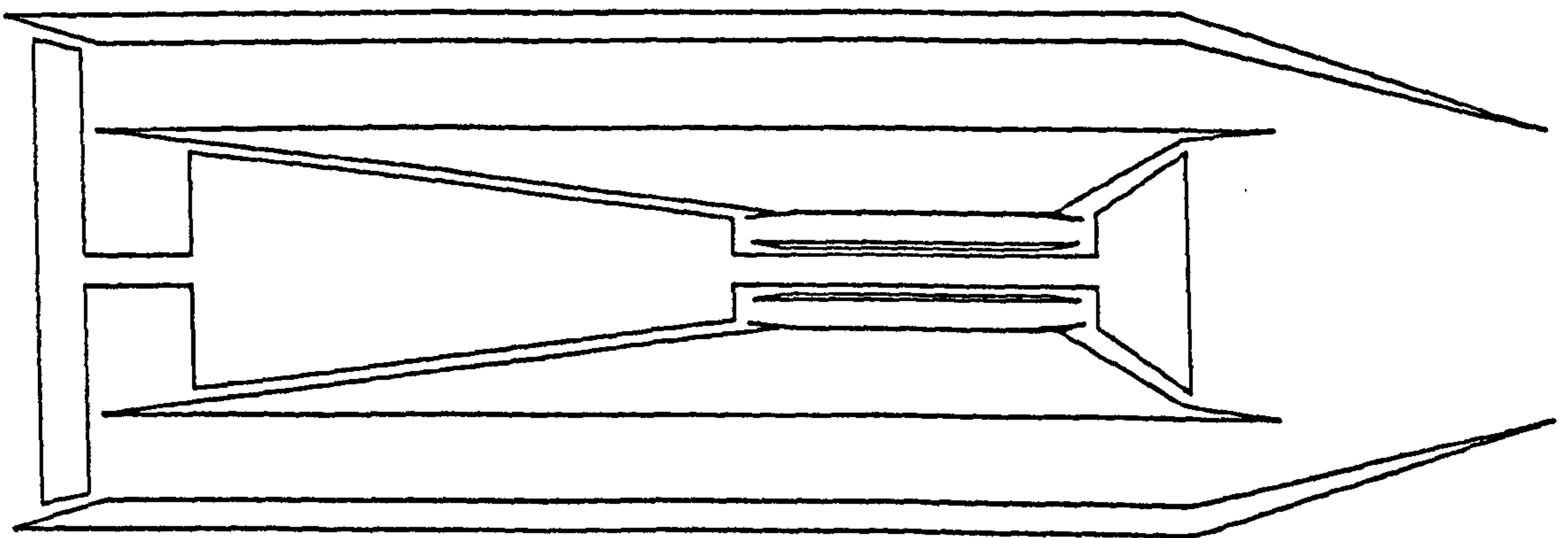


FIG. 3
SINGLE SPOOL TURBOFAN WITH MIXED EXHAUSTS

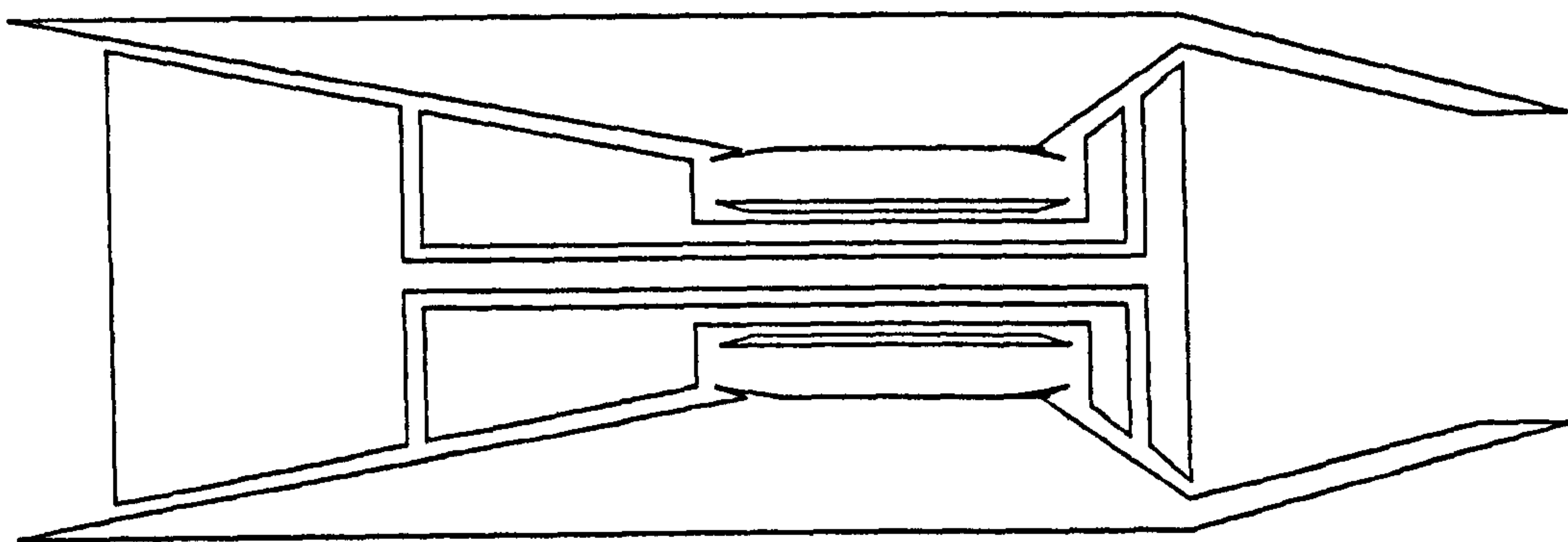


FIG. 4
TWO SPOOL TURBOJET

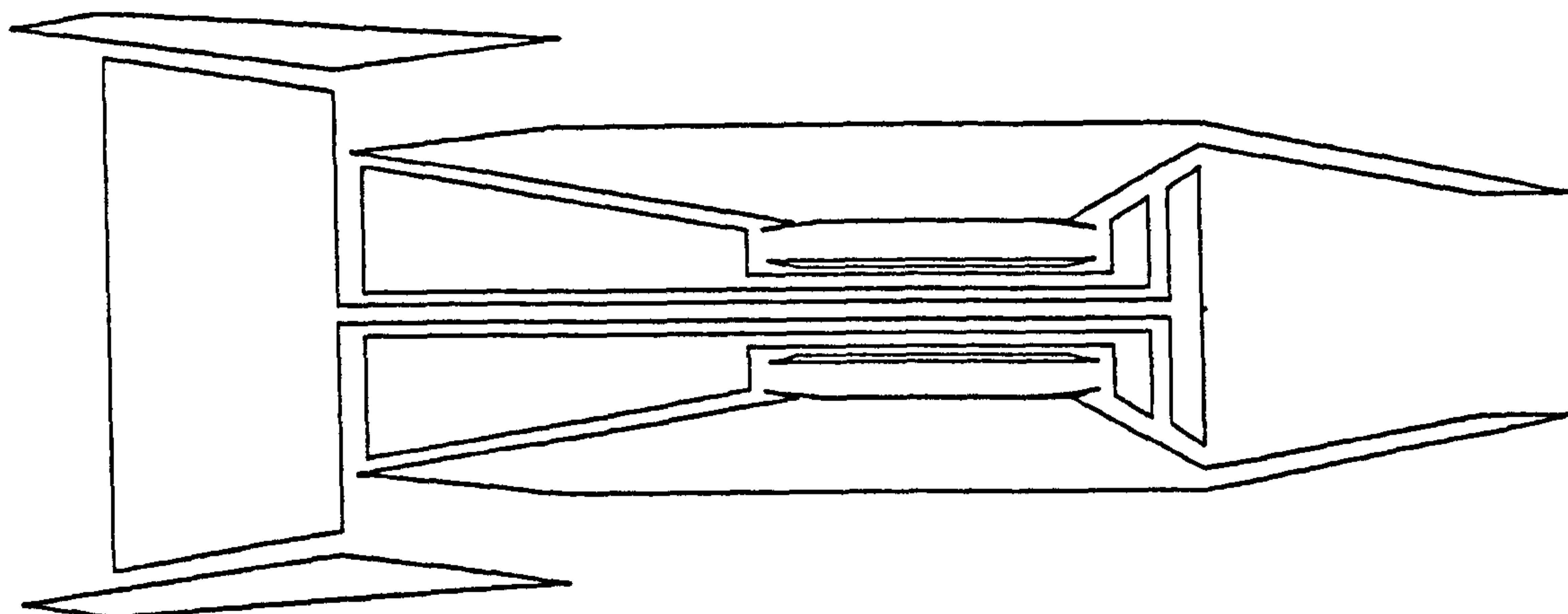


FIG. 5
TWO SPOOL BYPASS ENGINE WITH SEPARATE EXHAUSTS

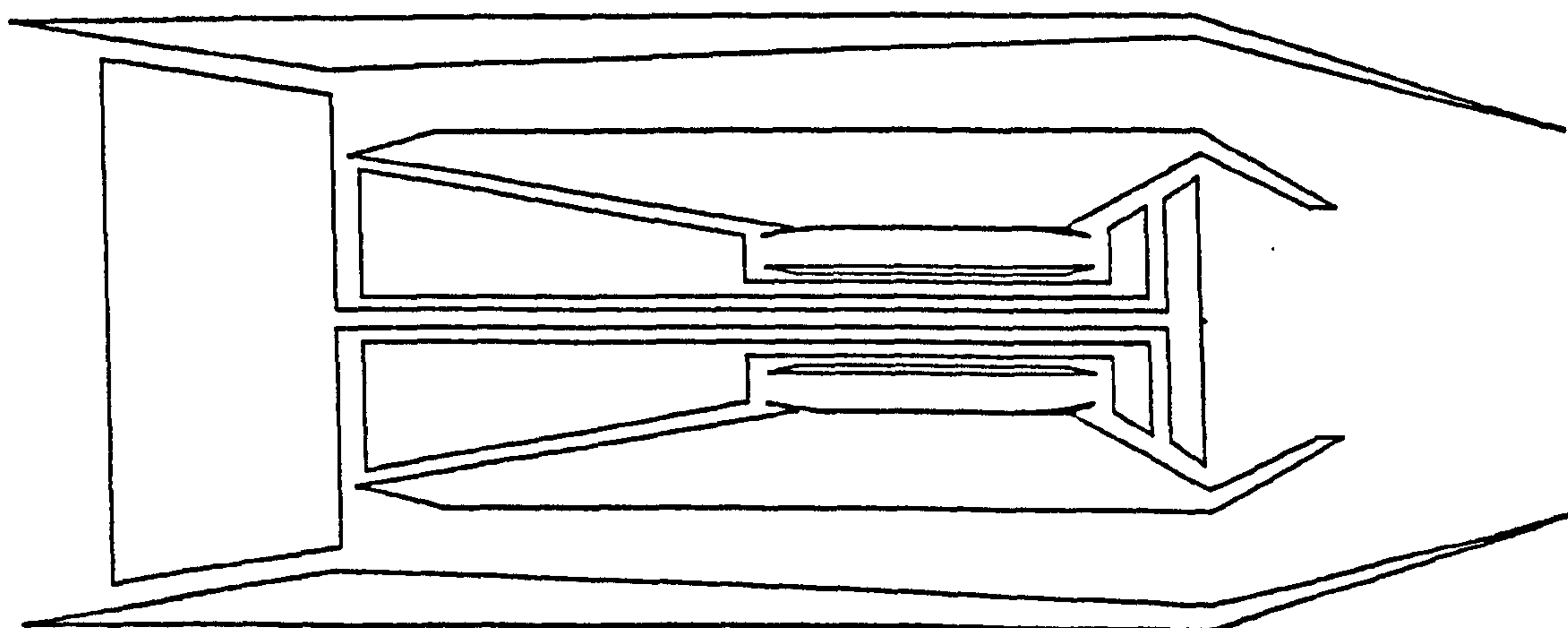


FIG. 6
TWO SPOOL BYPASS ENGINE WITYH MIXED EXHAUSTS

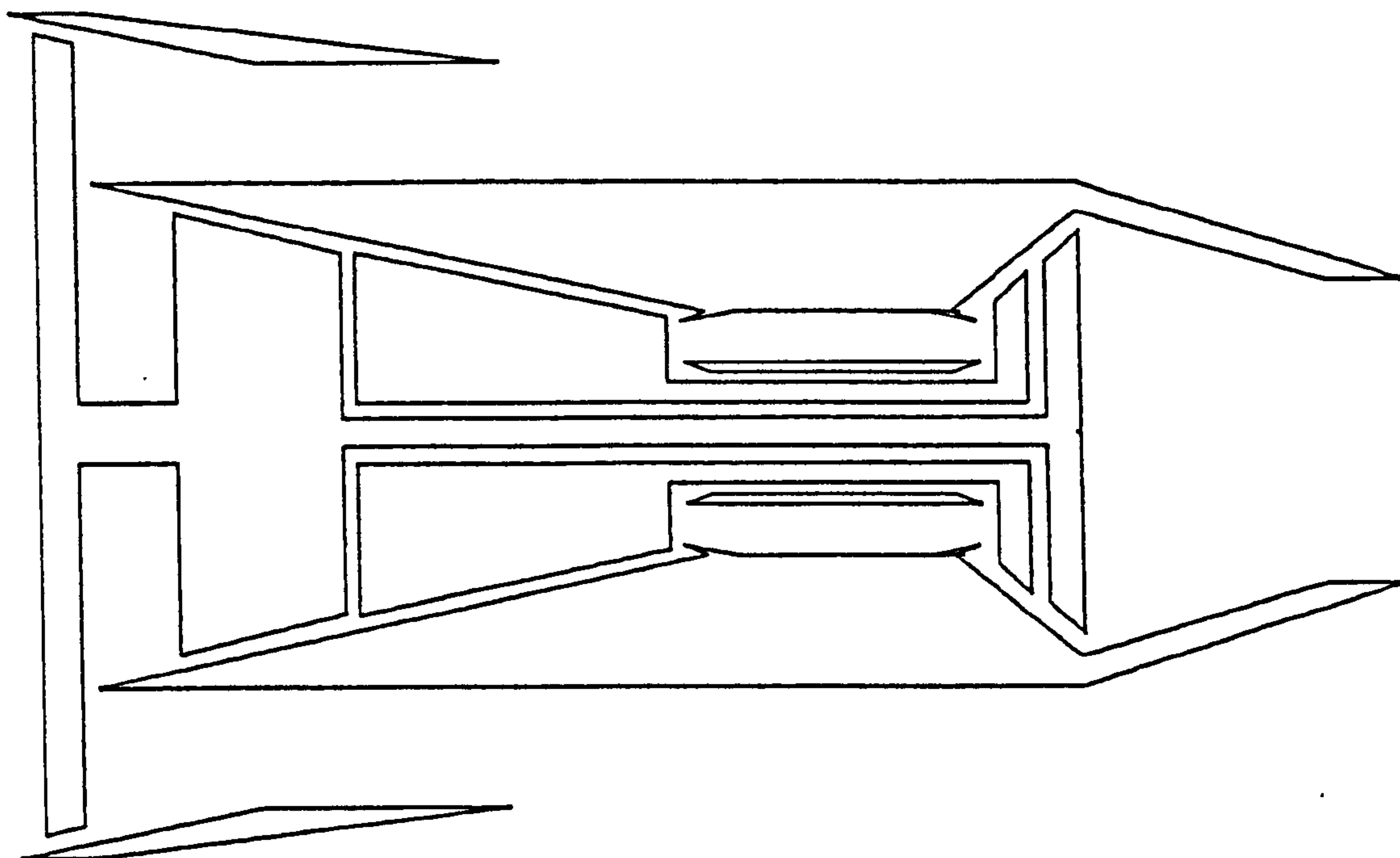


FIG. 7
TWO SPOOL TURBOFAN WITH SEPARATE EXHAUSTS

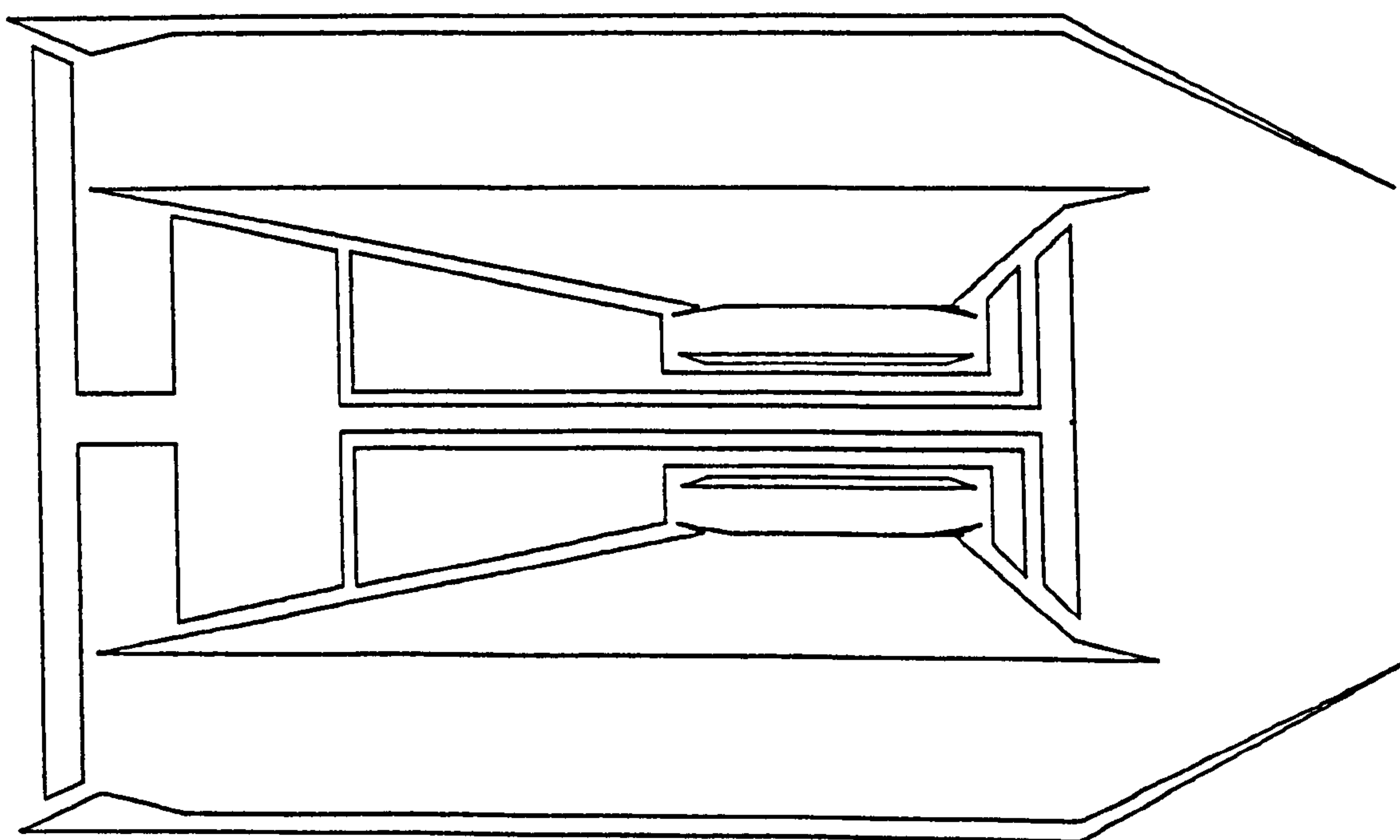


FIG. 8
TWO SPOOL TURBOFAN WITH MIXED EXHAUSTS

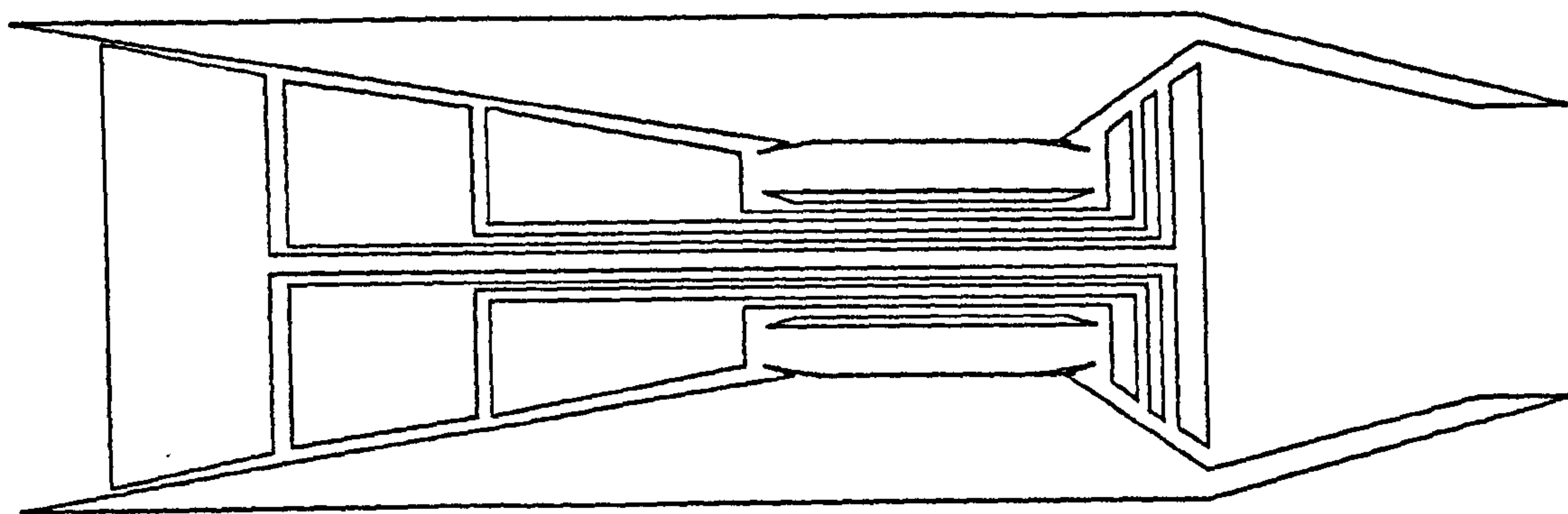


FIG. 9
THREE SPOOL TURBOJET

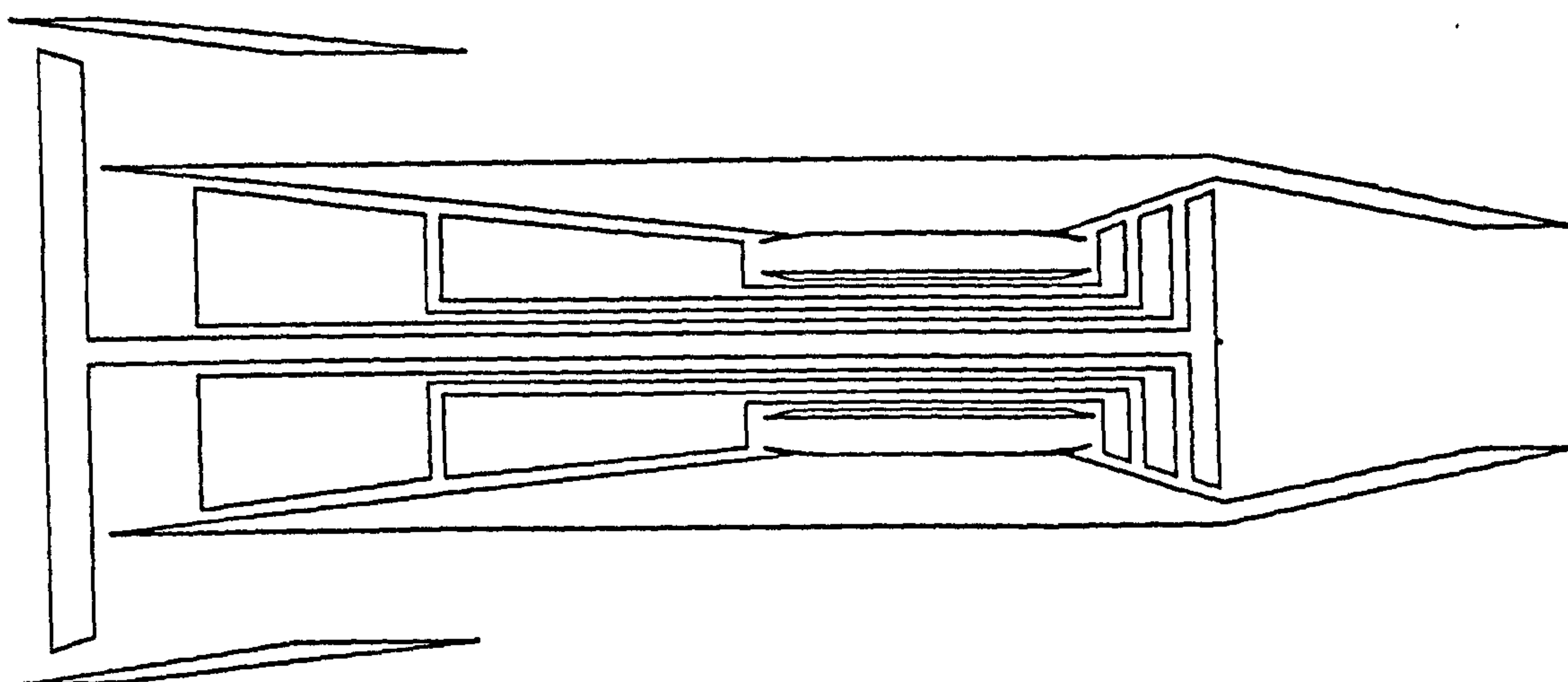


FIG. 10
THREE SPOOL TURBOFAN WITH SEPARATE EXHAUSTS

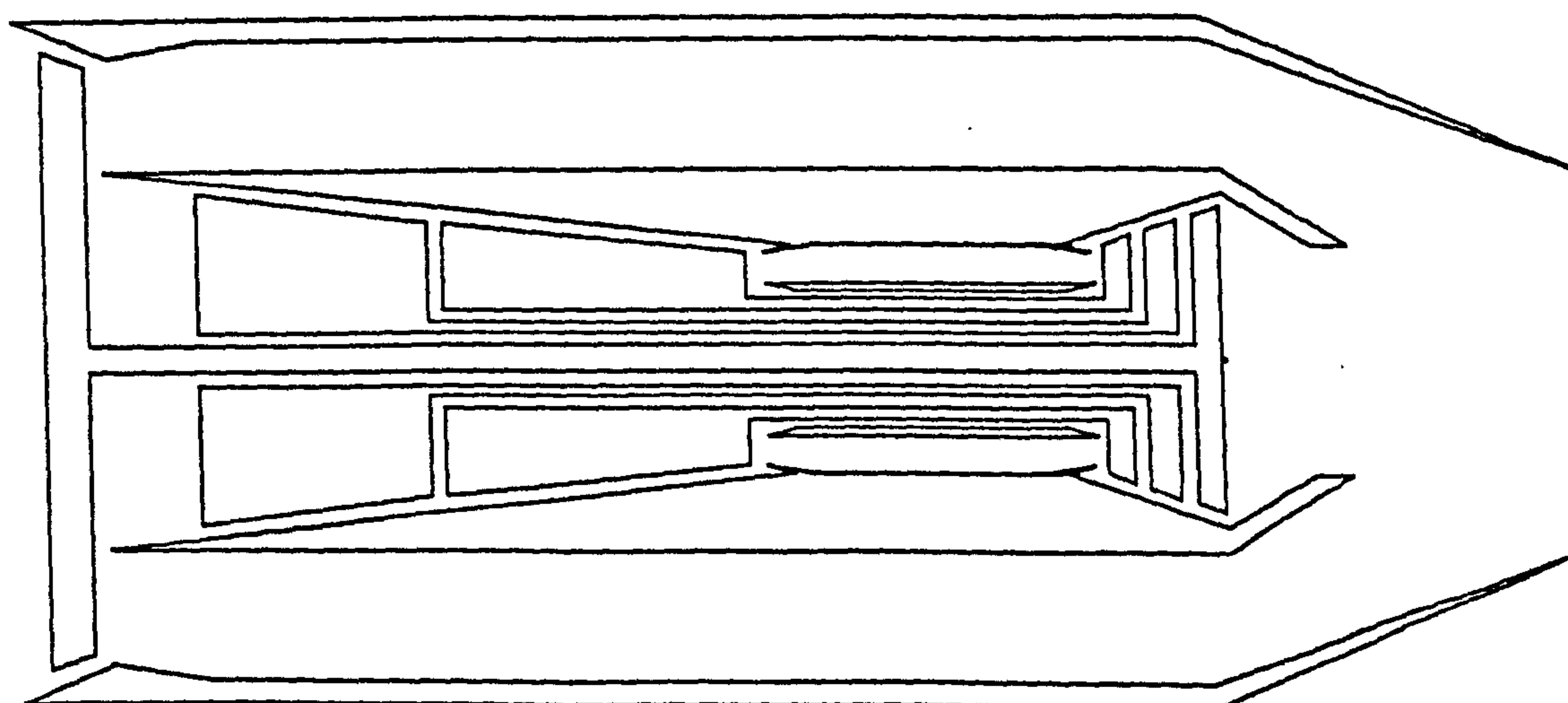


FIG. 11
THREE SPOOL TURBOFAN WITH MIXED EXHAUSTS

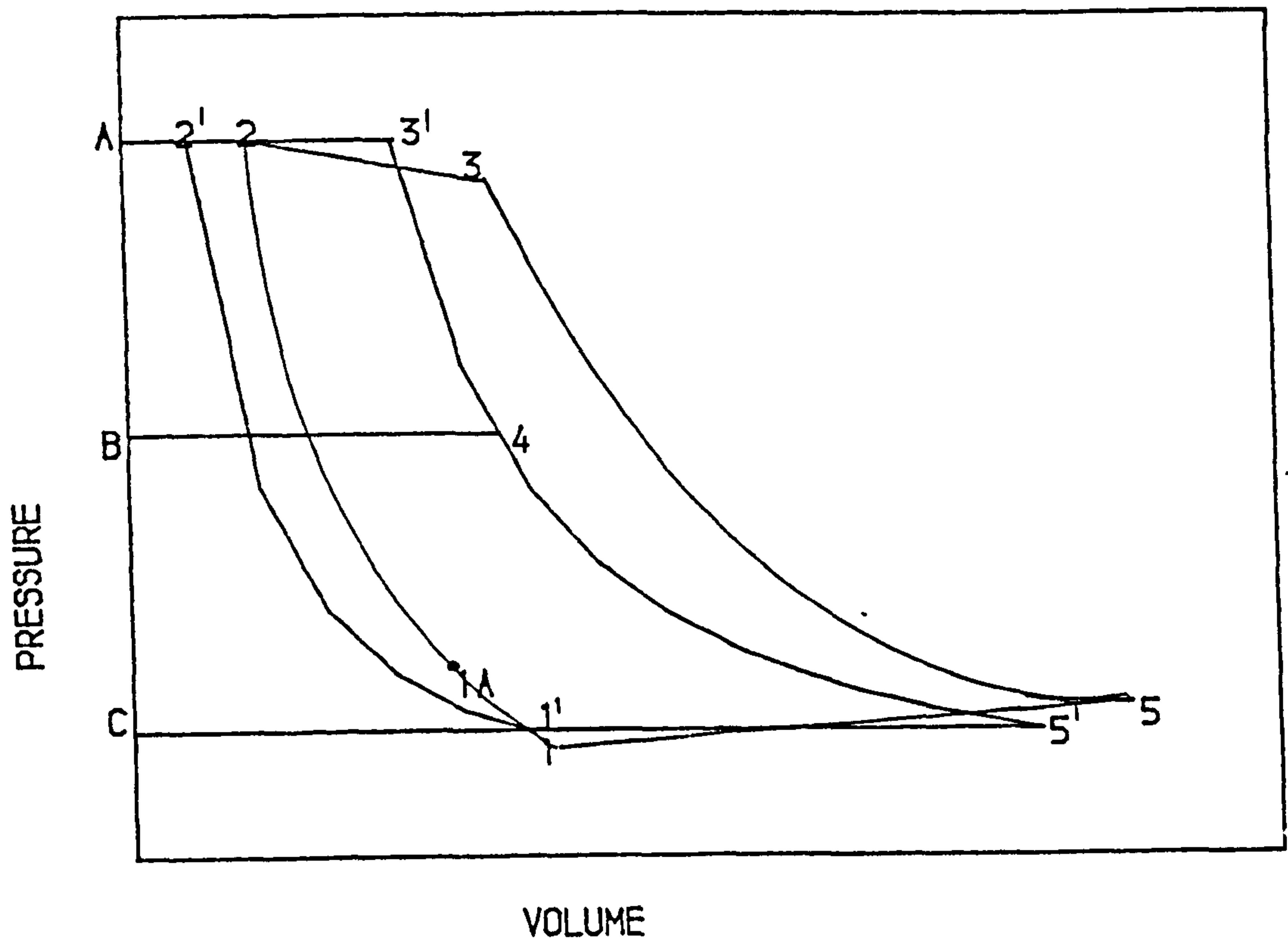


FIG. 12
BRAYTON CYCLE DIAGRAM
12'3'5' IDEAL, 1235 REAL

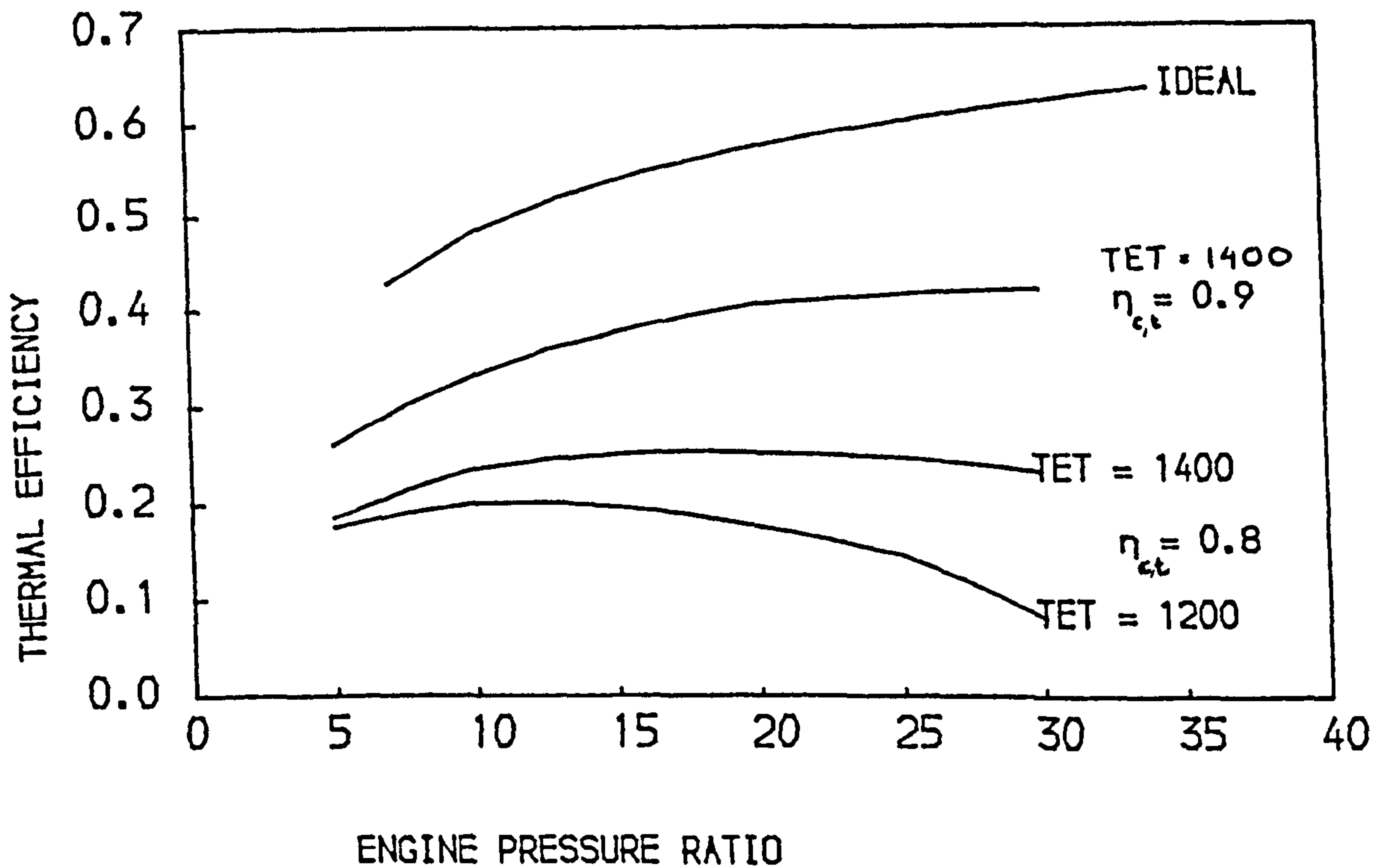


FIG. 13
EFFECT OF PRESSURE RATIO AND TURBINE INLET TEMPERATURE
ON THERMAL EFFICIENCY

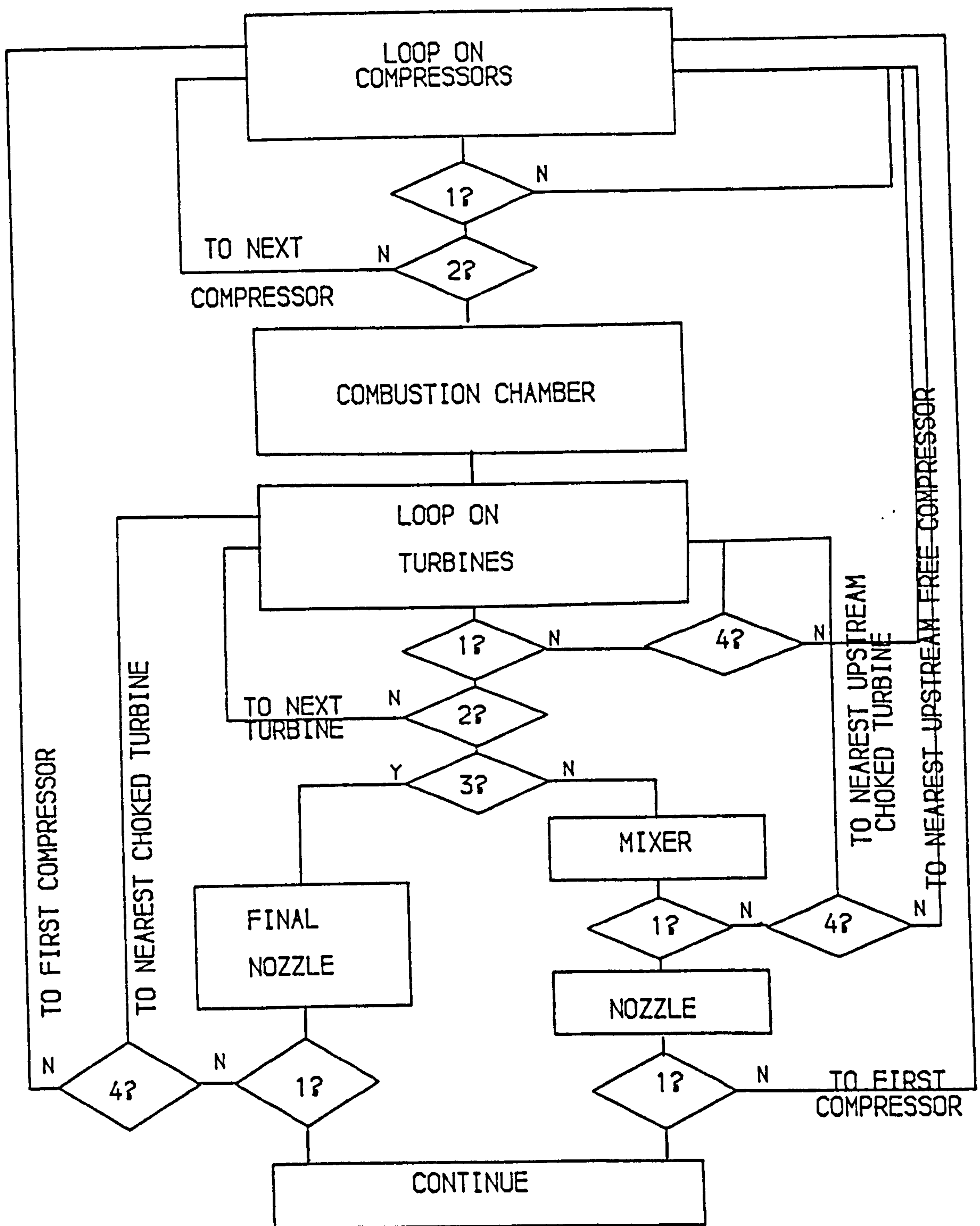


FIG. 14

BLOCK DIAGRAM OF THE MASS FLOW EVALUATION PROCEDURE
 1? IS COMPONENT TEST SATISFIED?
 2? IS THIS THE LAST COMPONENT OF THIS KIND?
 3? DOES THE ENGINE ANALYSED HAVE A MIXER DUCT?
 4? IS ANY TURBINE CHOKED?
 Y = YES, N = NO

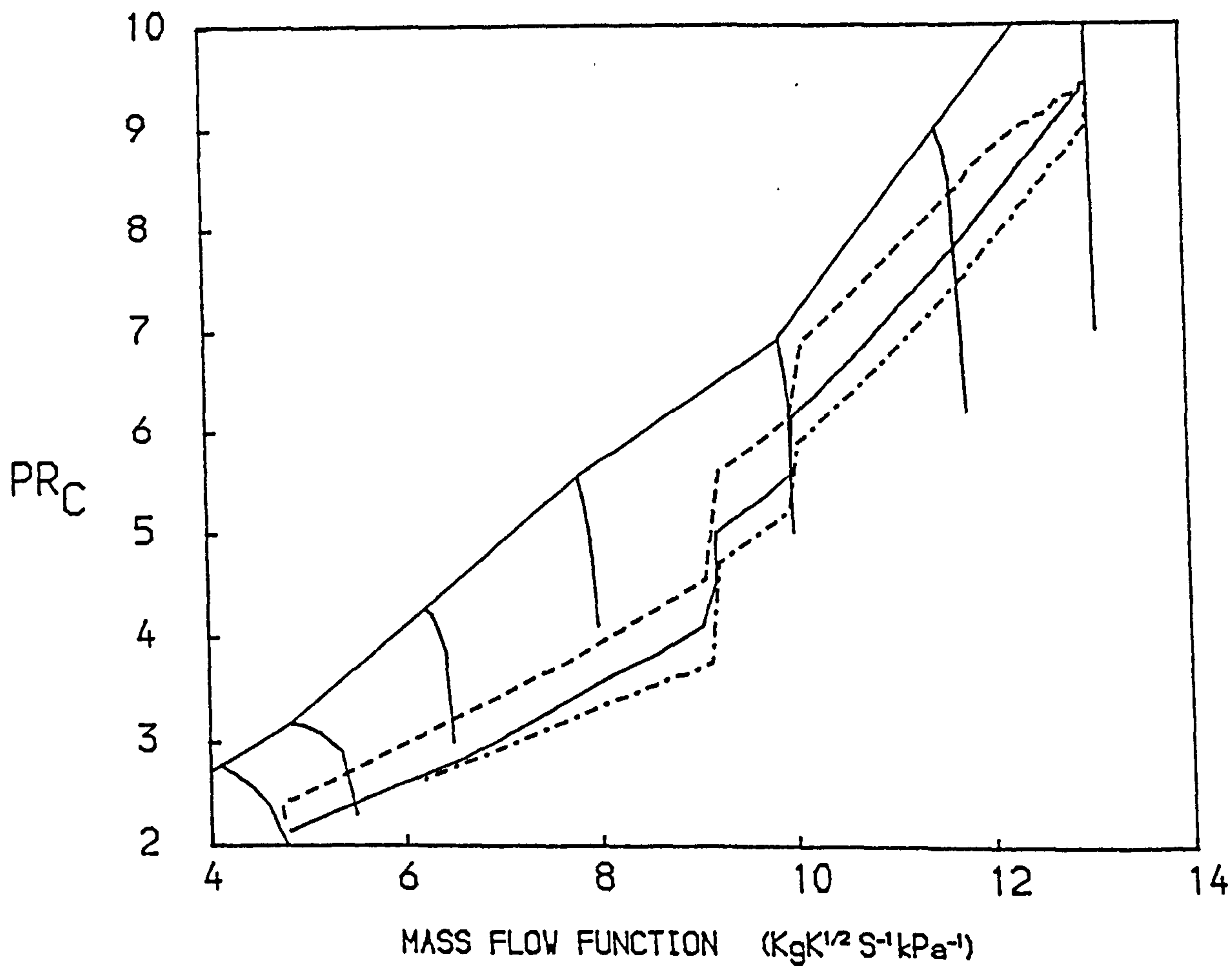
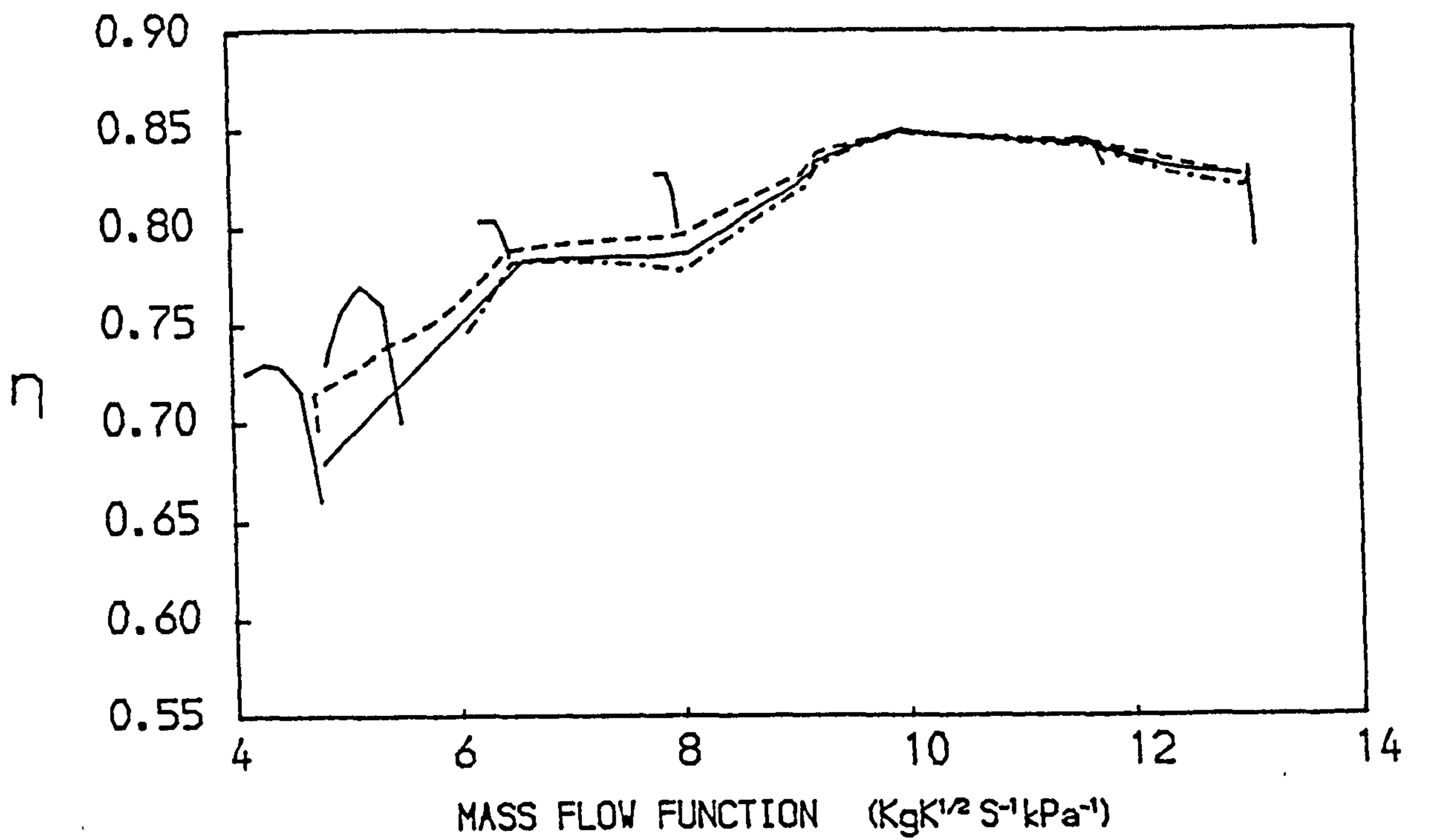


FIG. 15
 PATHS ON THE CHARACTERISTIC MAPS OF THE COMPRESSOR OF A
 SINGLE SPOOL TURBOJET
 -- ACCELERATION — STEADY RUNNING --- DECELERATION

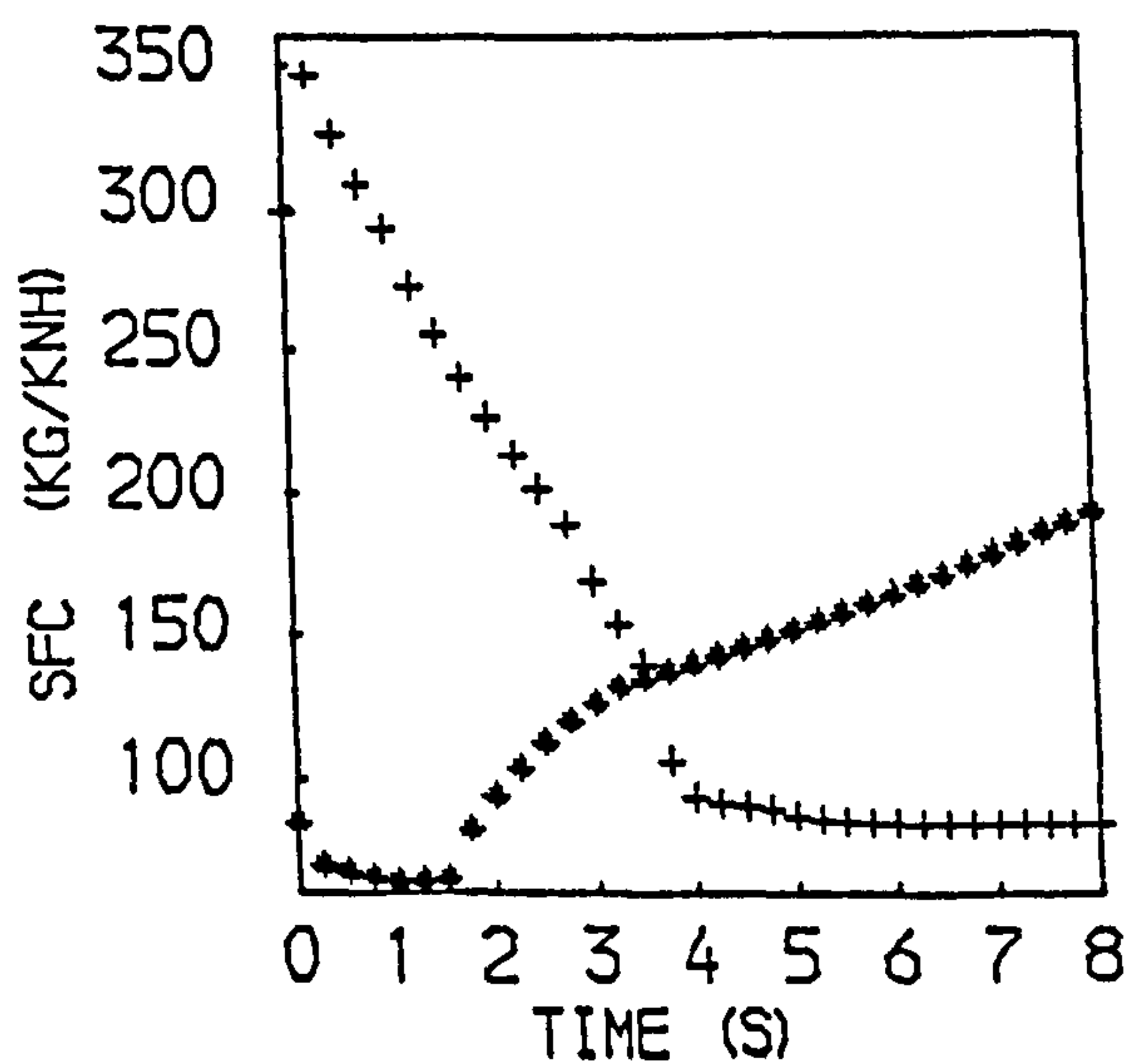
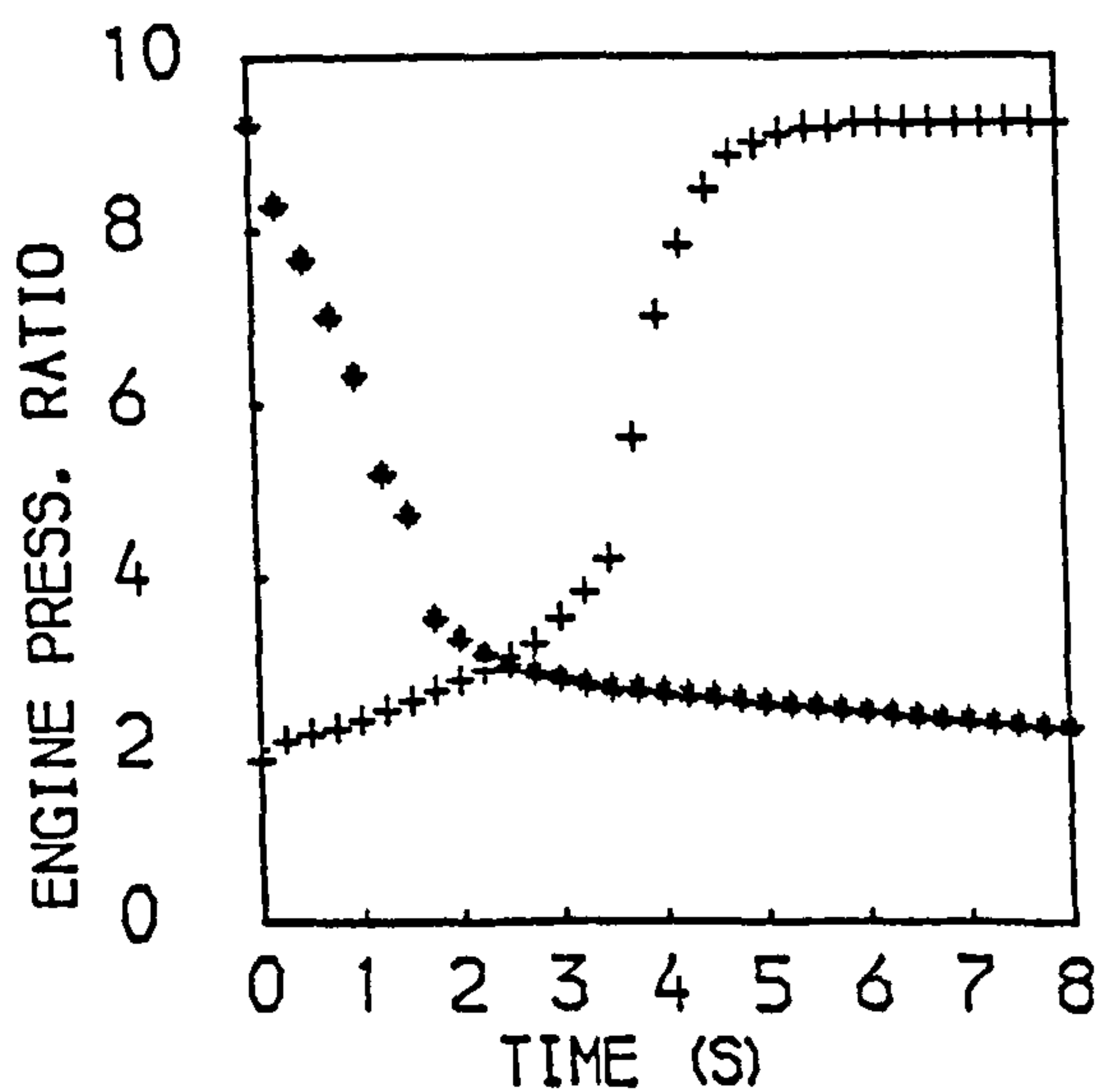
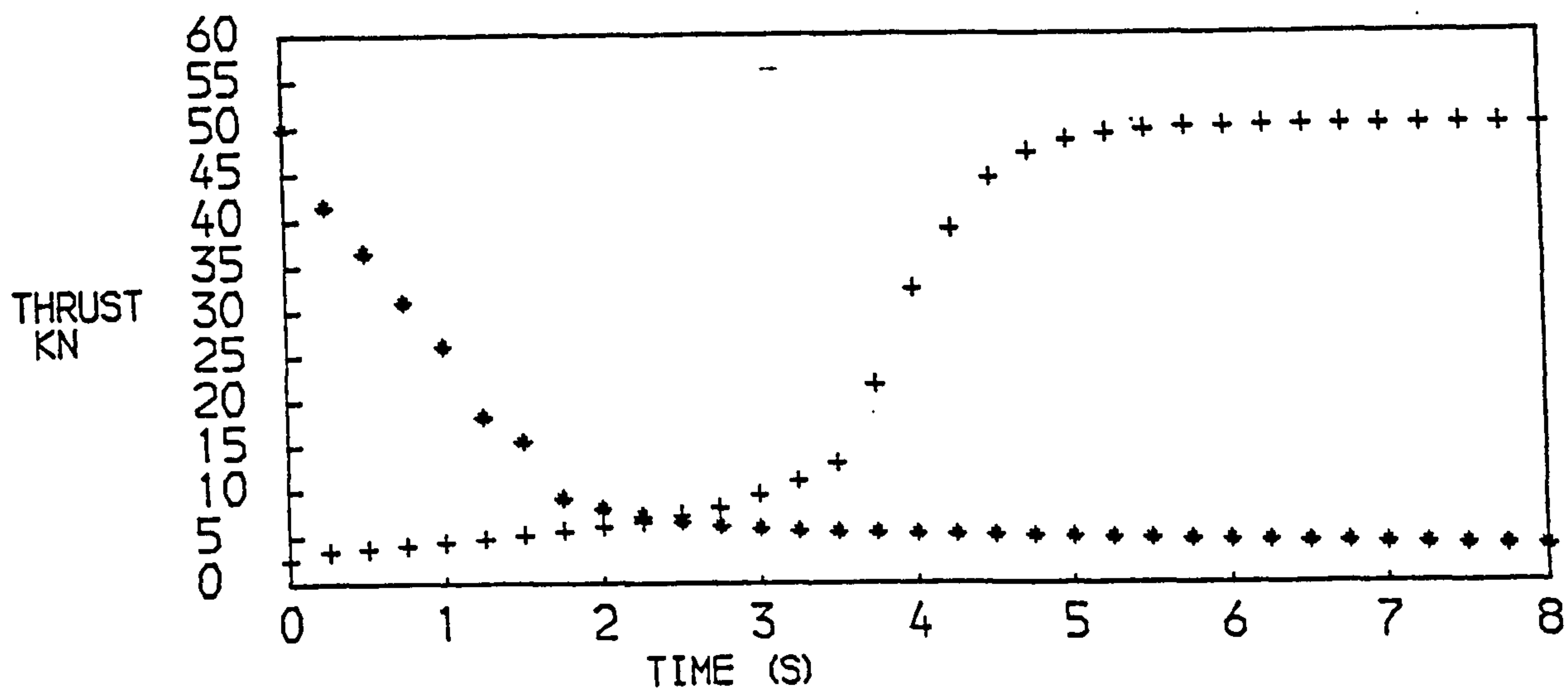
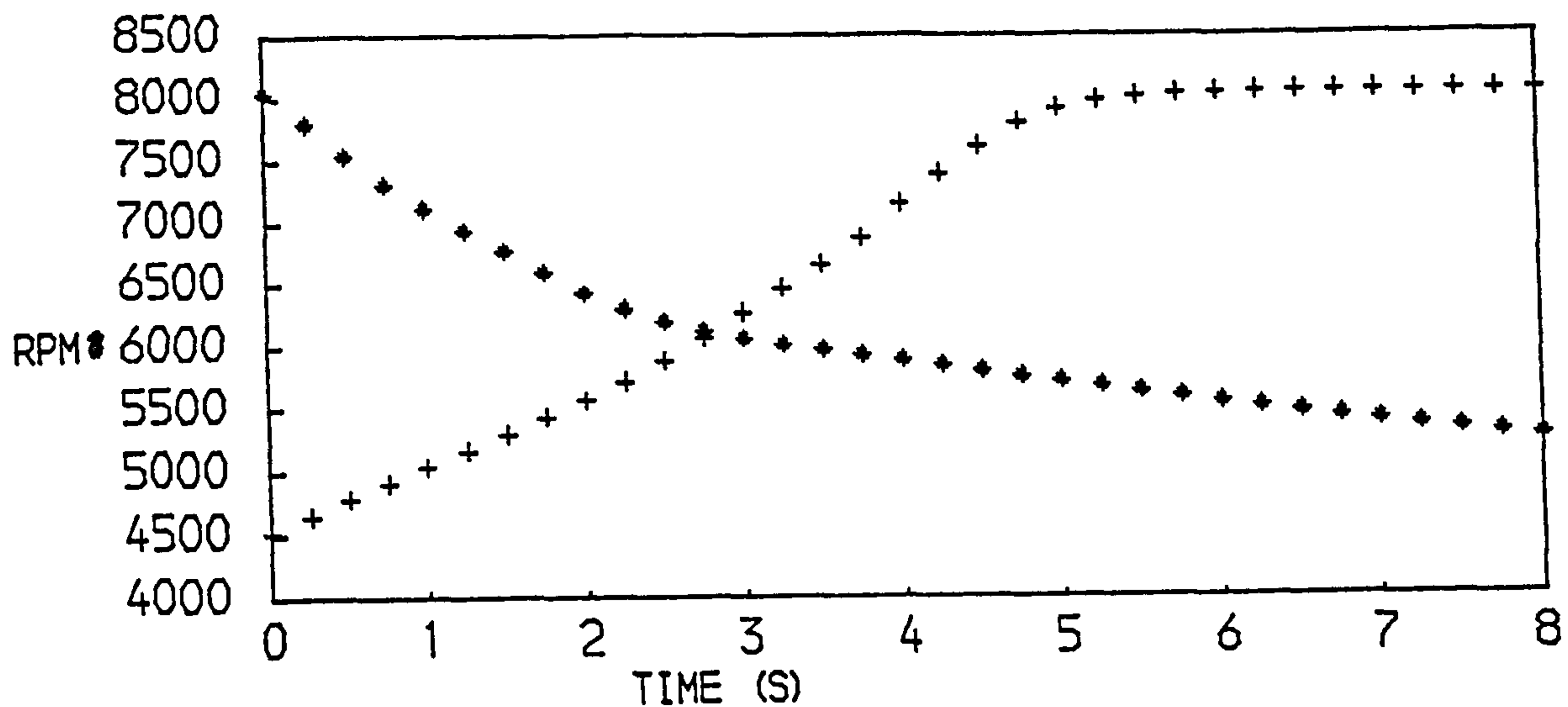


FIG. 16
PERFORMANCE OF A SINGLE SPOOL TURBOJET ENGINE
+ACCELERATION * DECELERATION

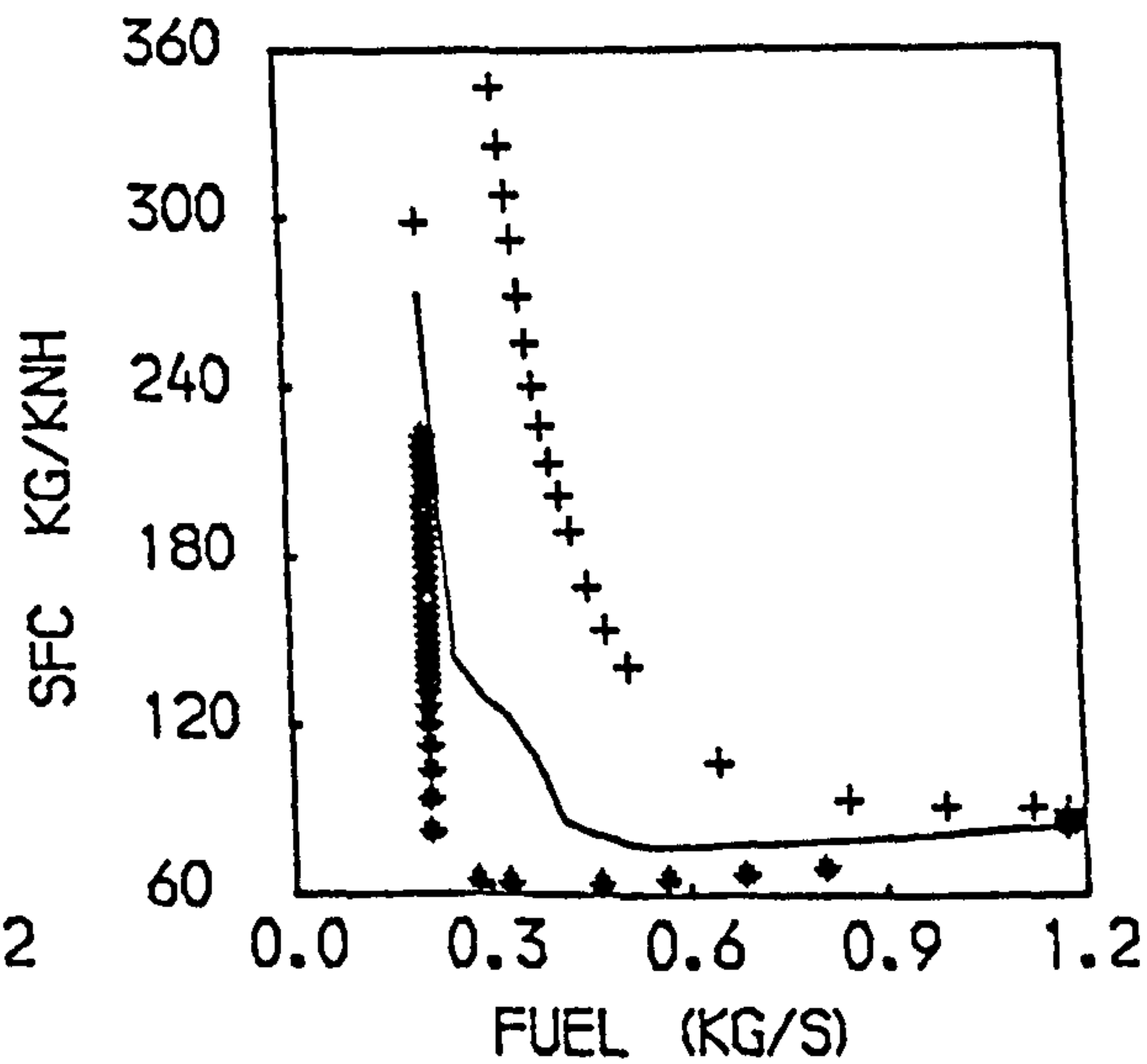
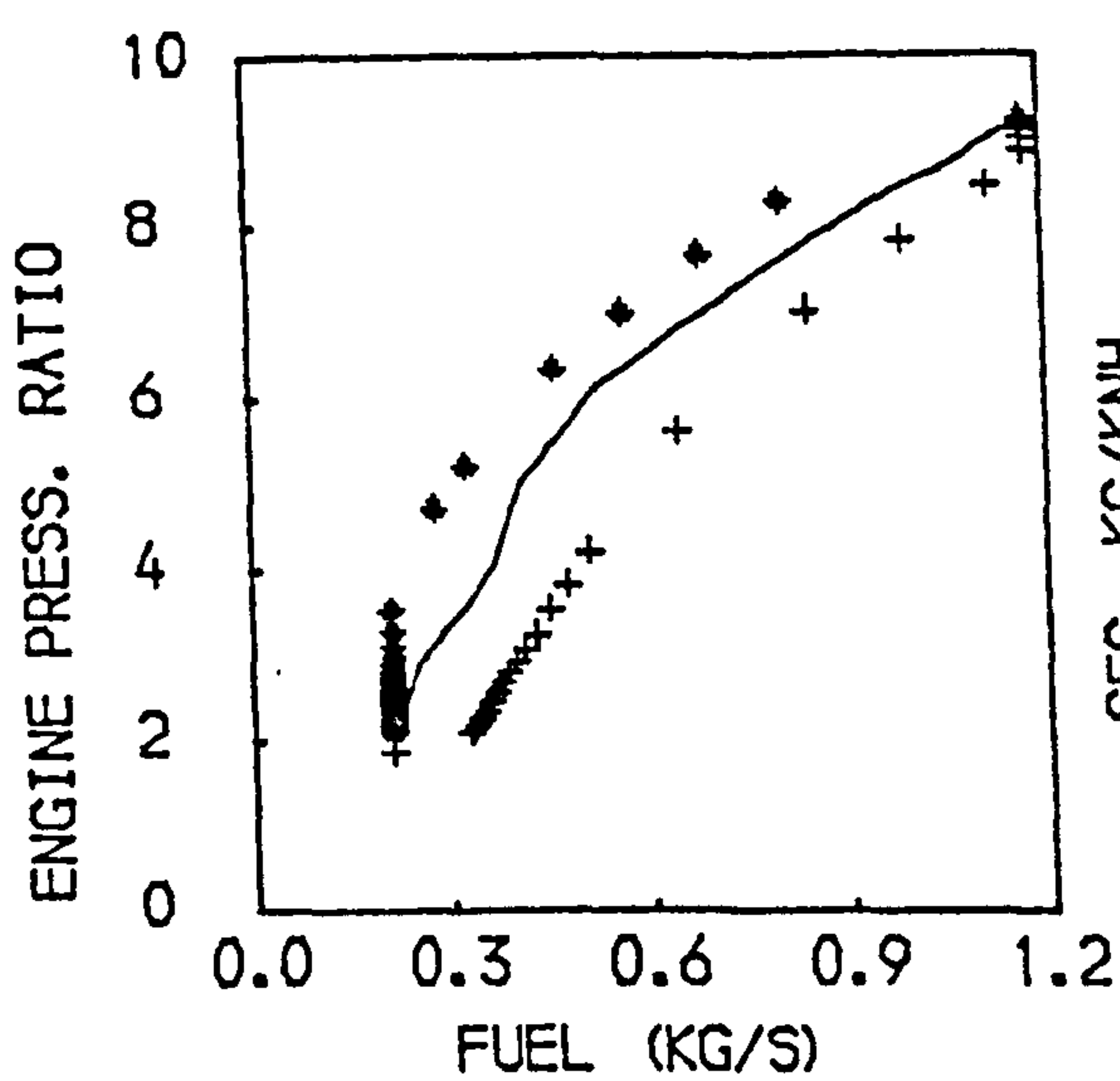
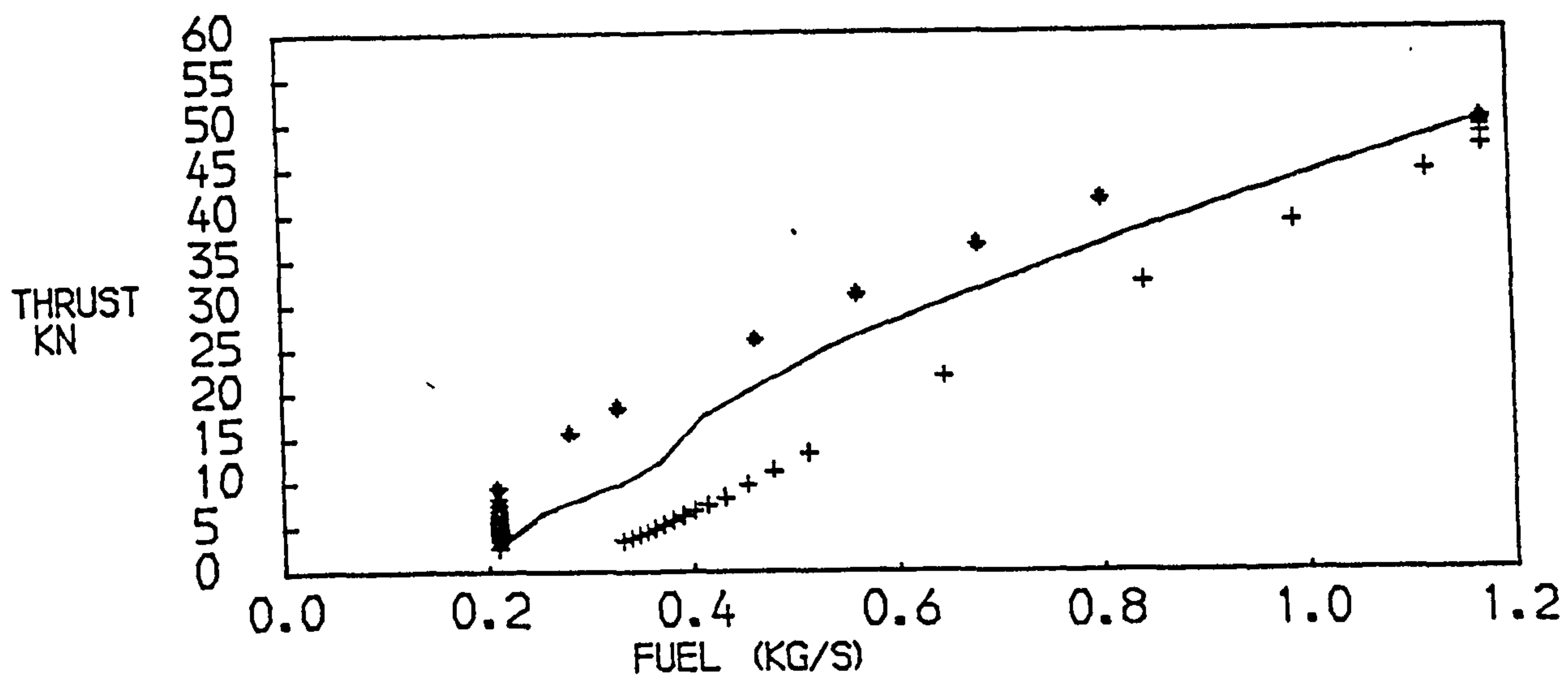
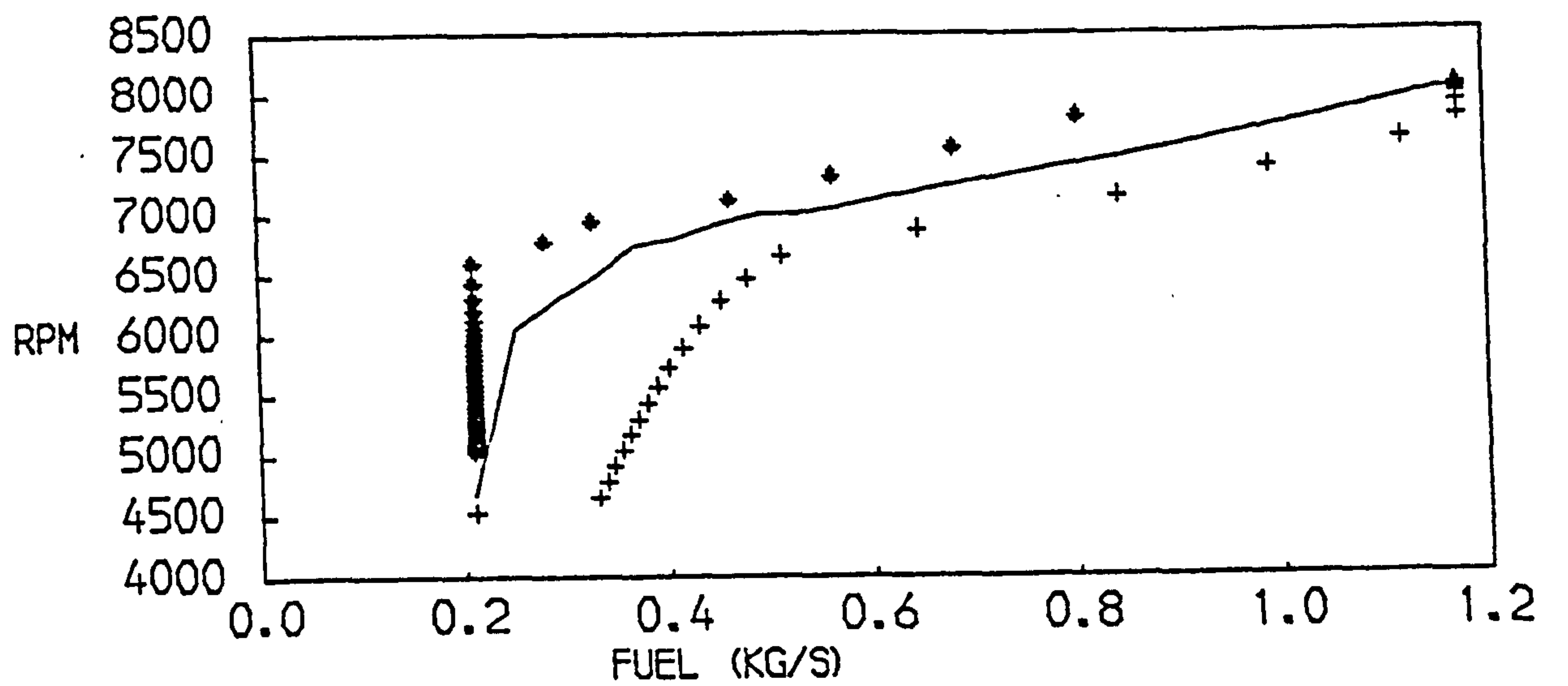


FIG. 17
PERFORMANCE OF A SINGLE SPOOL TURBOJET
+ACCELERATION * DECELERATION —STEADY RUNNING

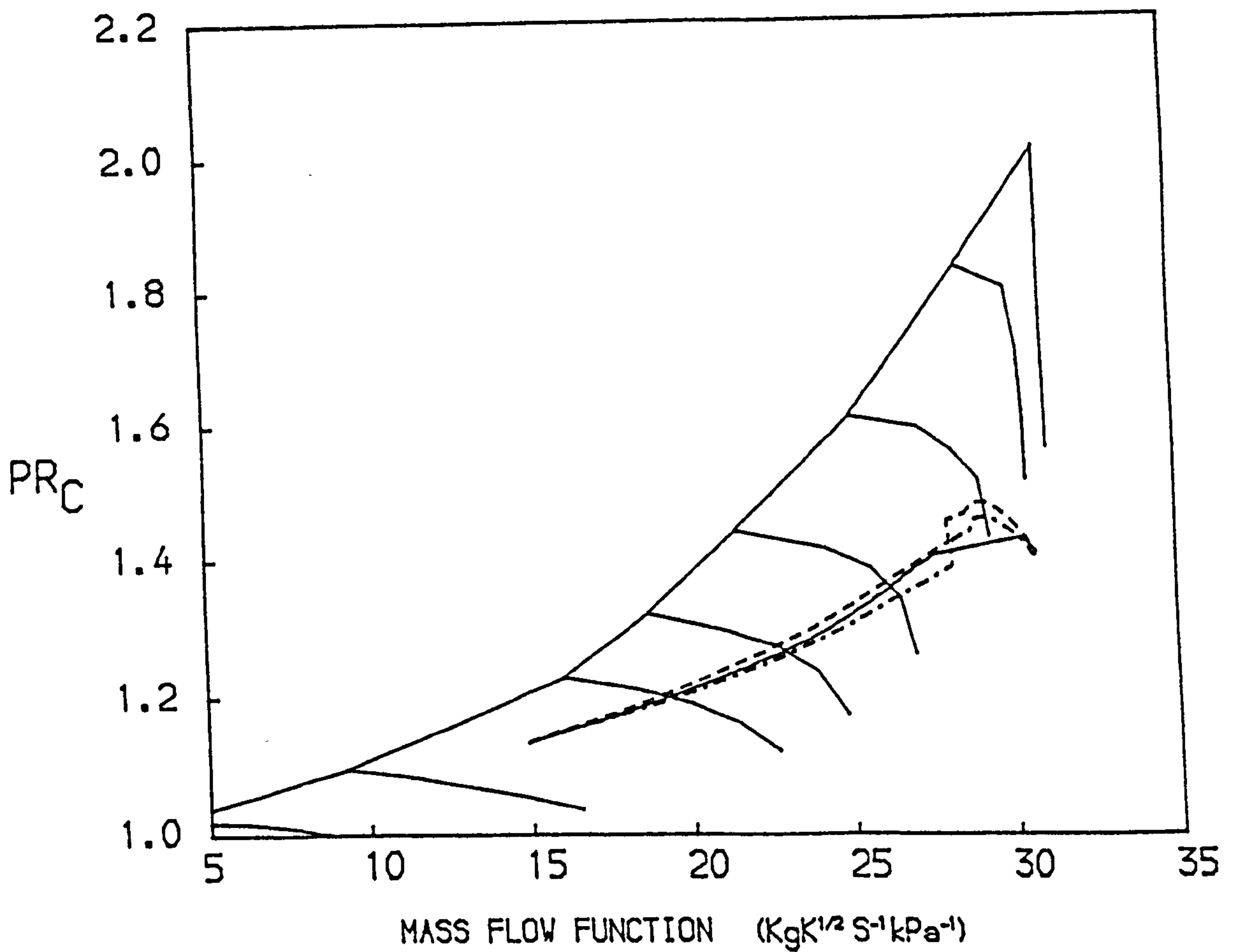
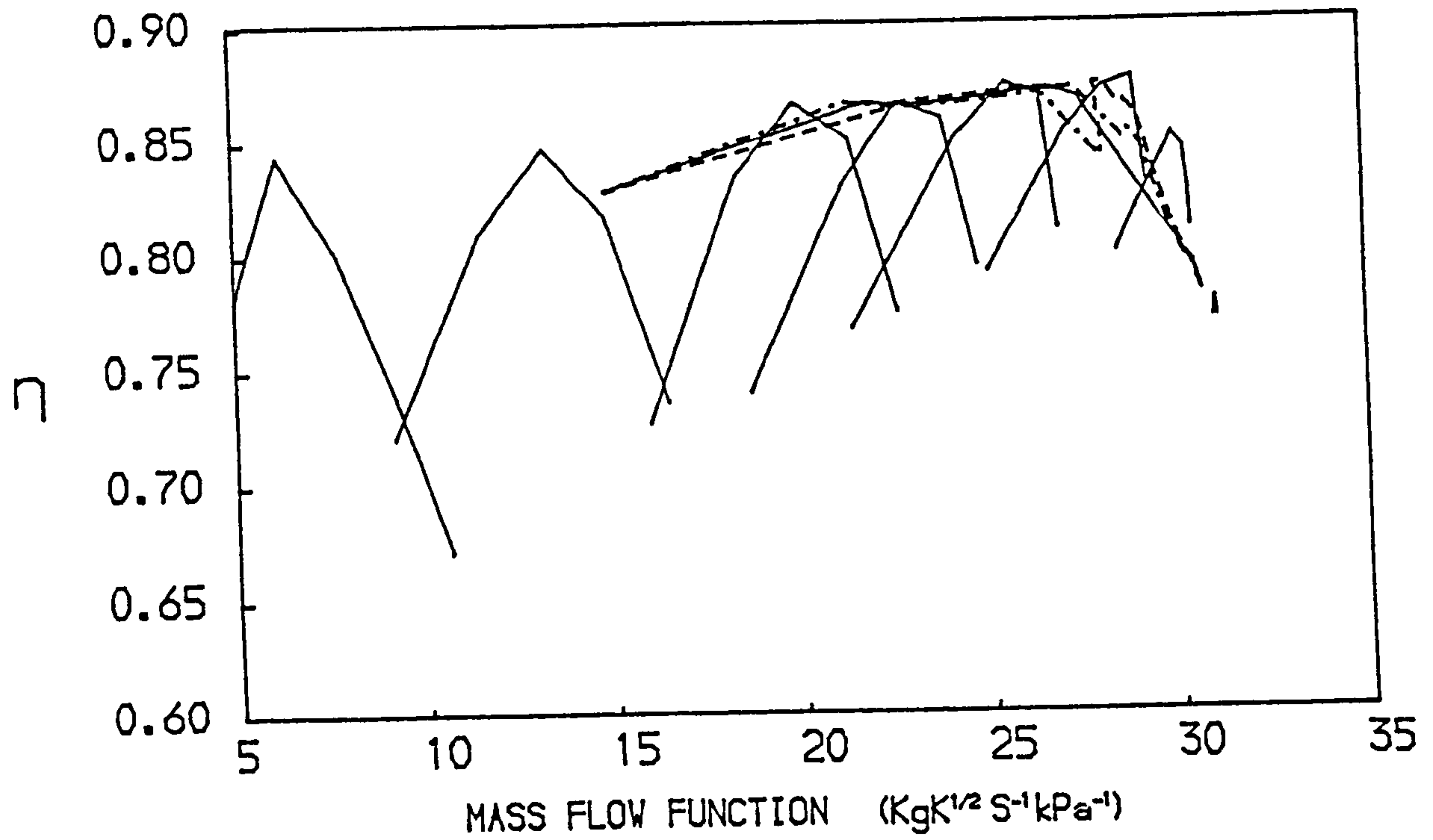


FIG. 18
 PATHS ON THE CHARACTERISTIC MAPS OF THE FAN OF A
 SINGLE SPOOL TURBOFAN WITH MIXED EXHAUSTS
 -- ACCELERATION — STEADY RUNNING --- DECELERATION

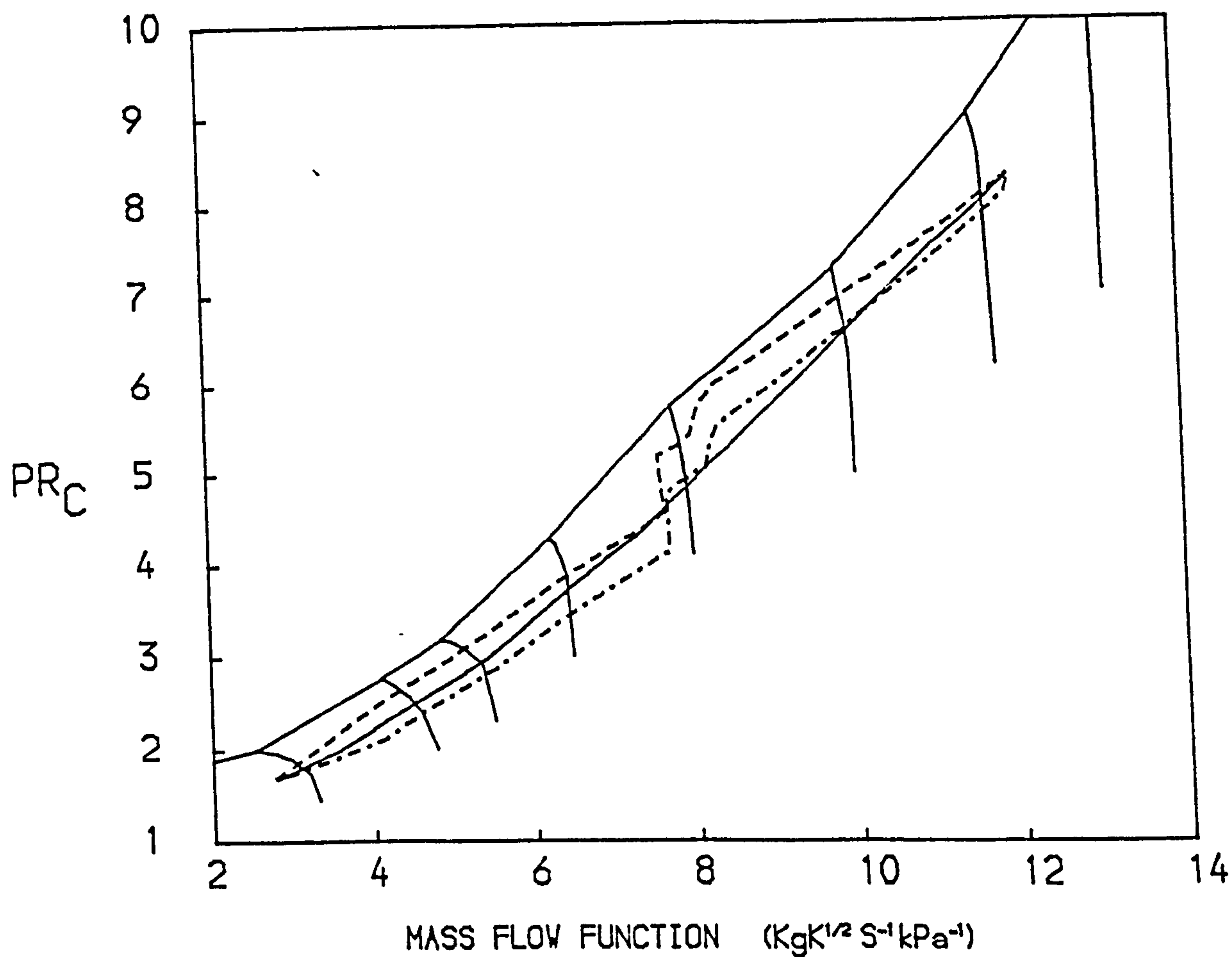
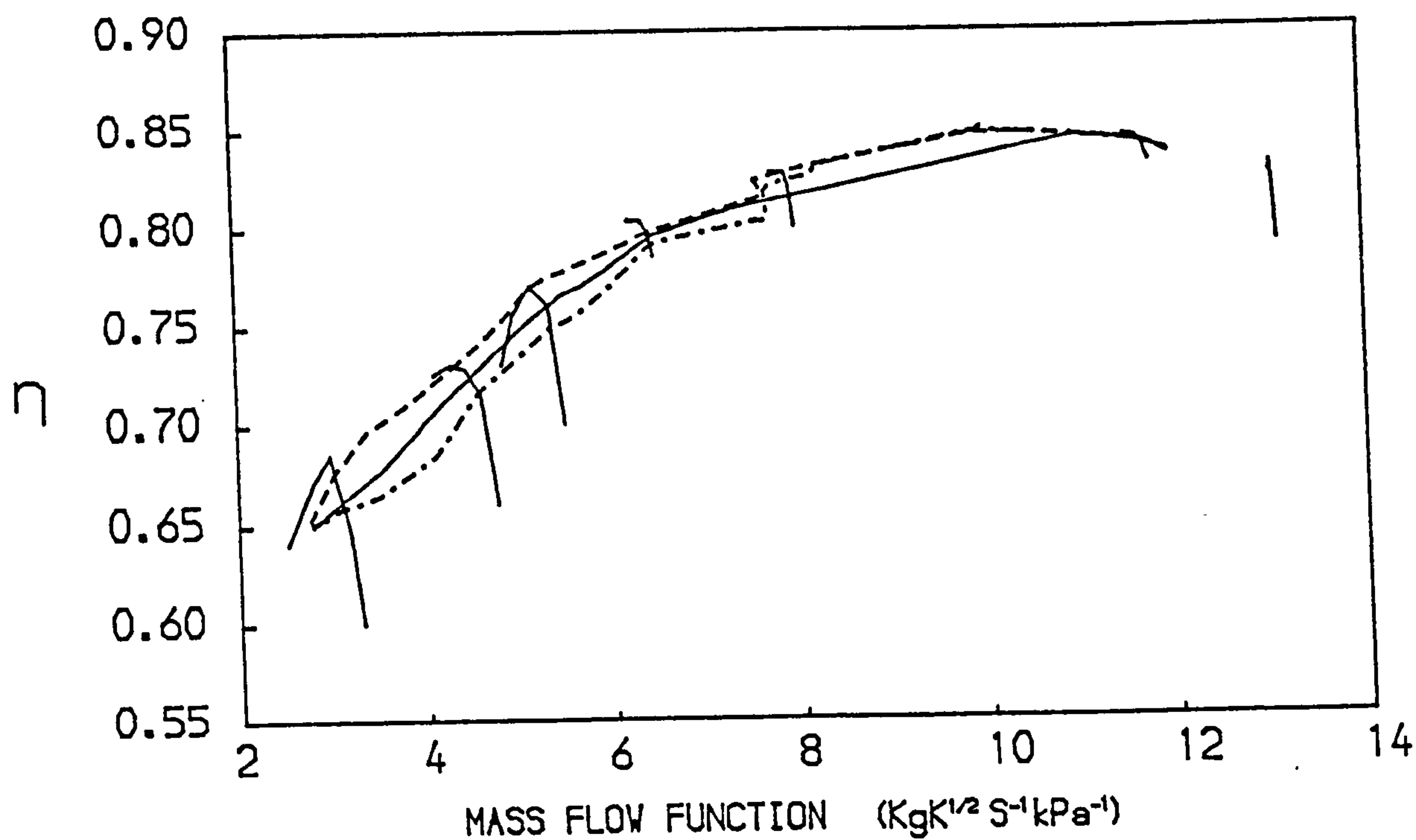


FIG. 19
 PATHS ON THE CHARACTERISTIC MAPS OF THE COMPRESSOR OF A
 SINGLE SPOOL TURBOFAN WITH MIXED EXHAUSTS
 -- ACCELERATION — STEADY RUNNING --- DECELERATION

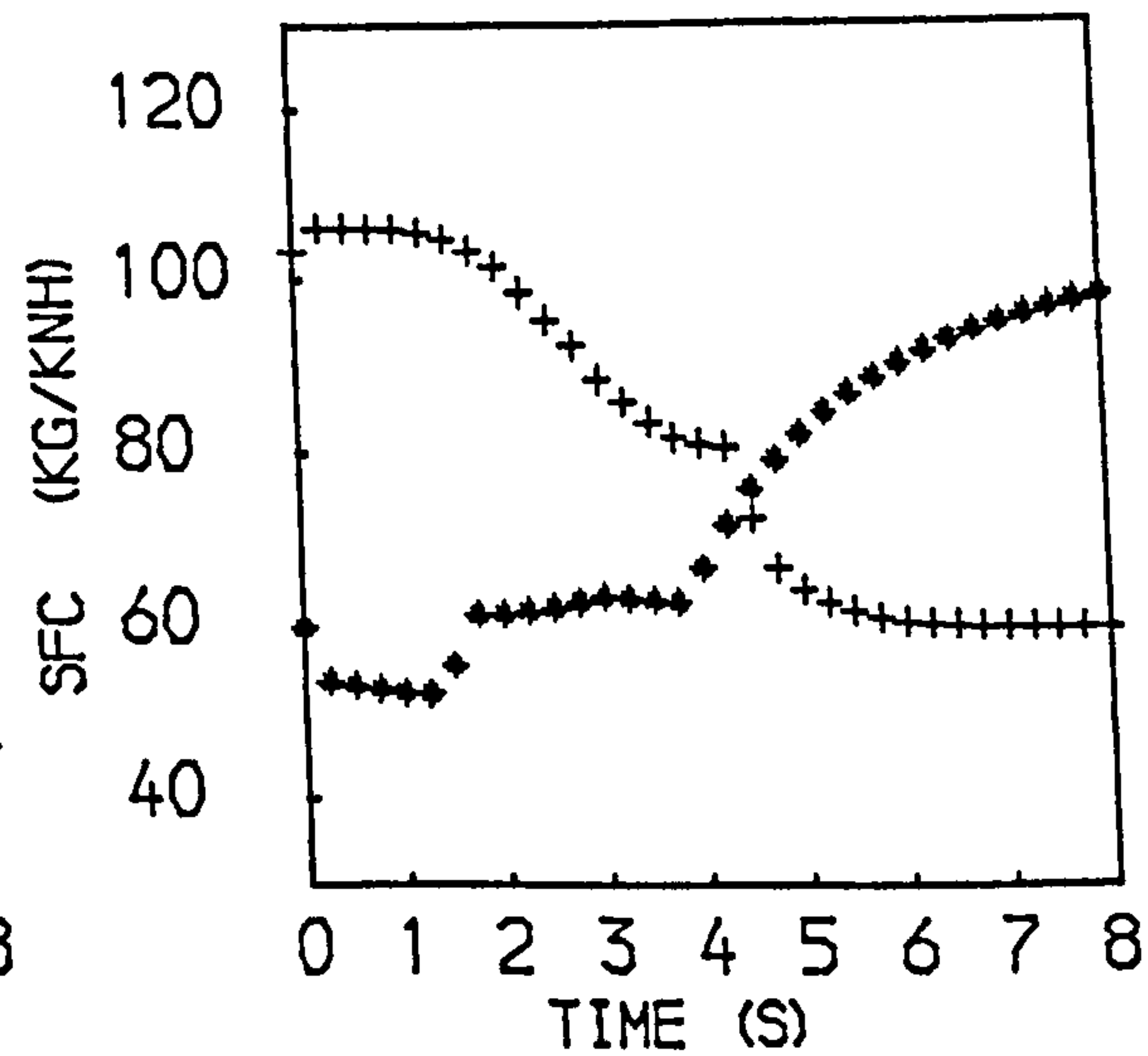
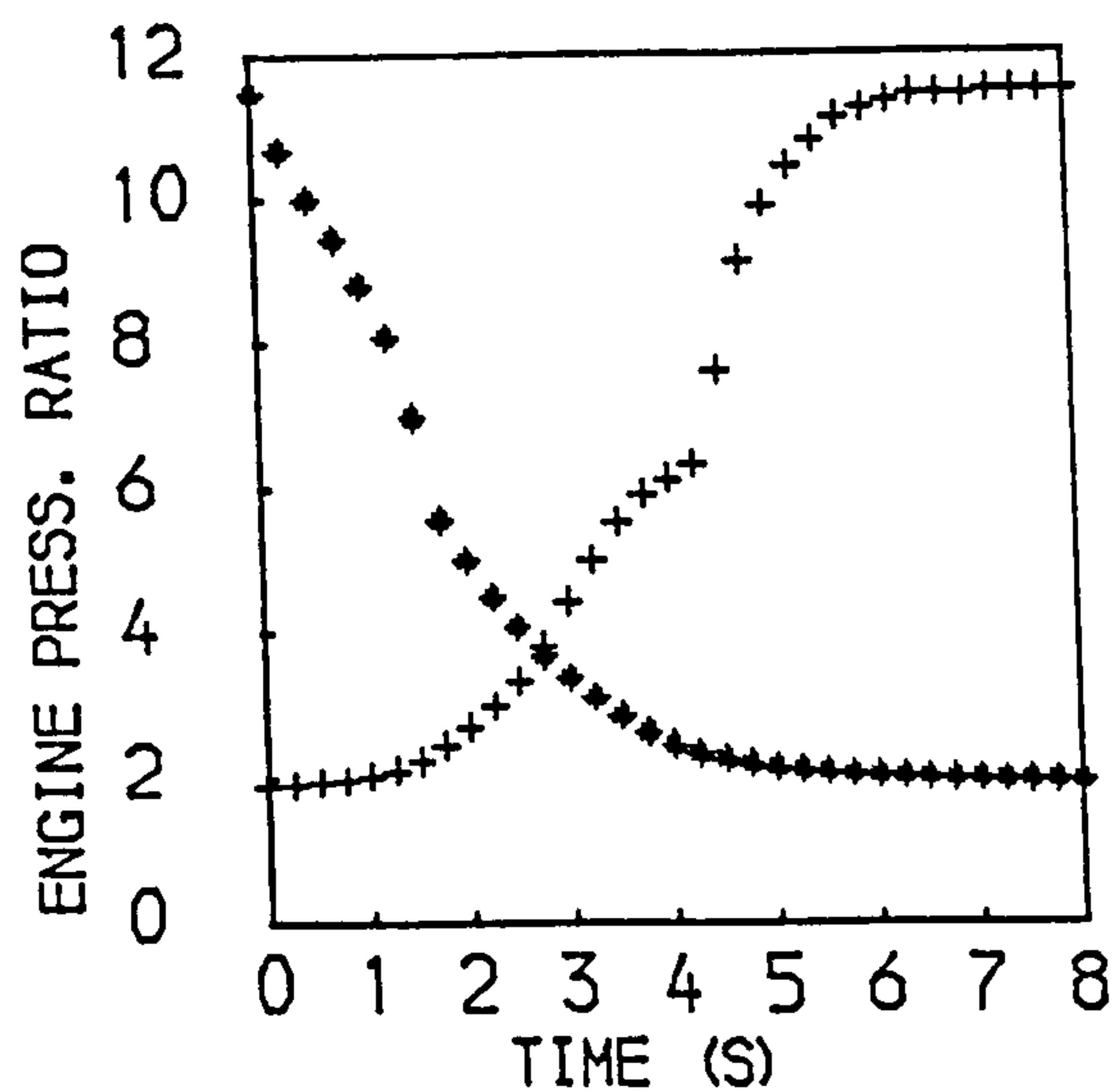
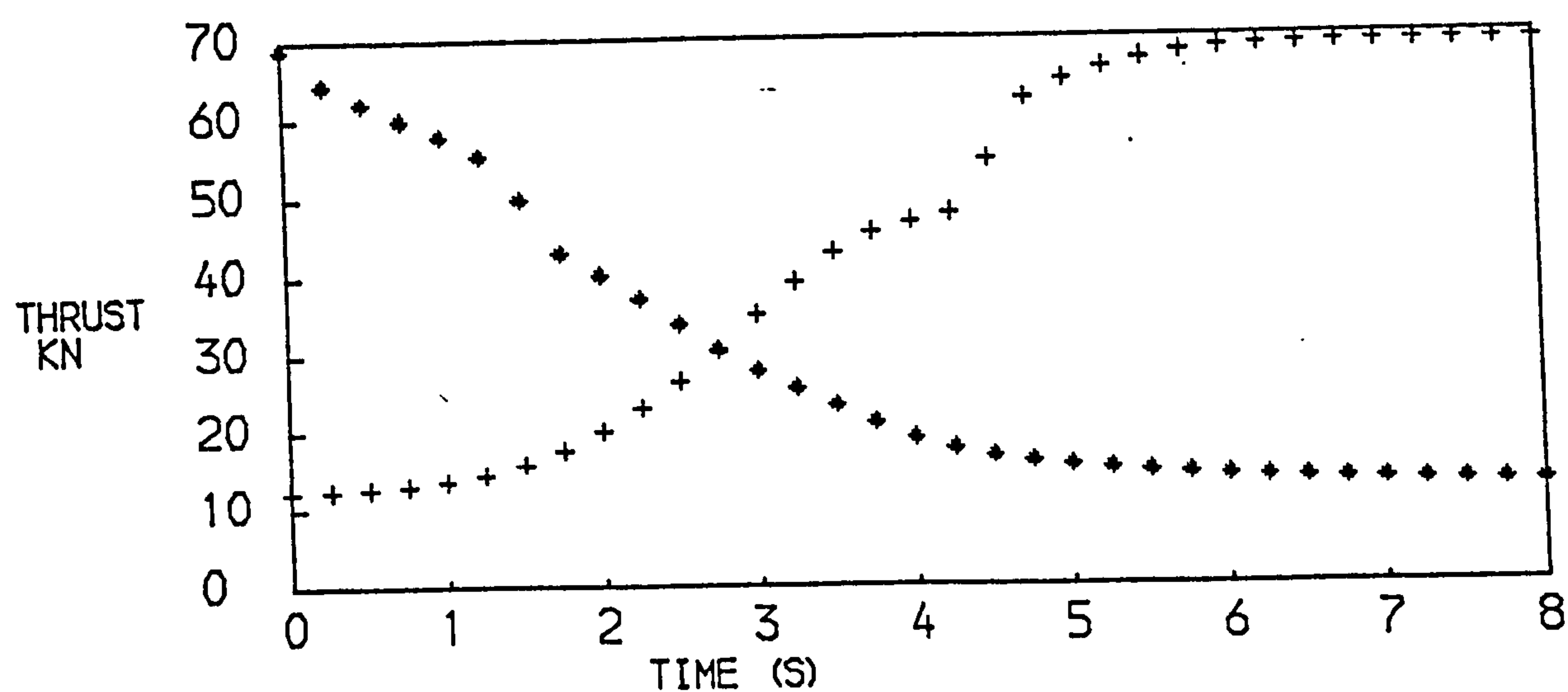
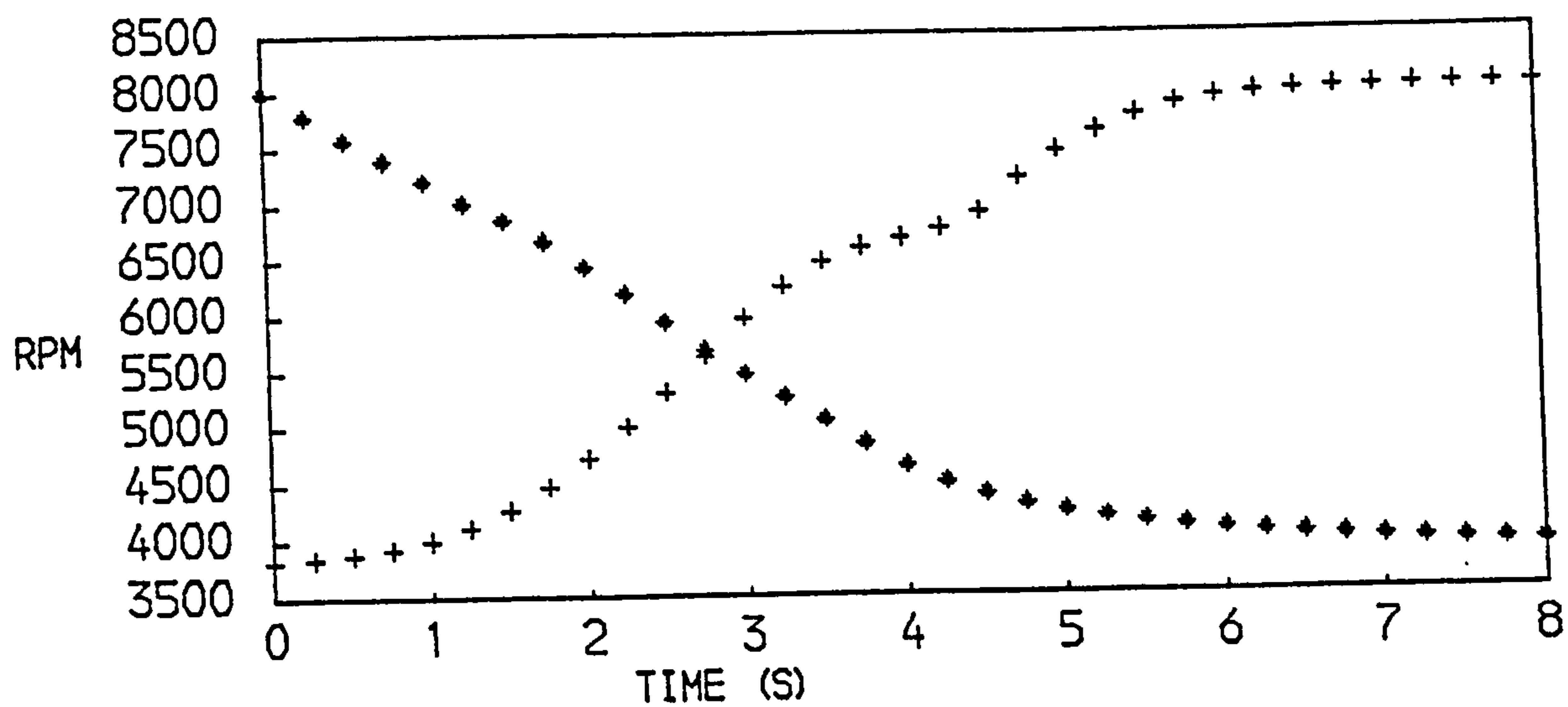


FIG. 20
PERFORMANCE OF A SINGLE SPOOL TURBOFAN WITH MIXED EXHAUSTS
+ACCELERATION * DECELERATION

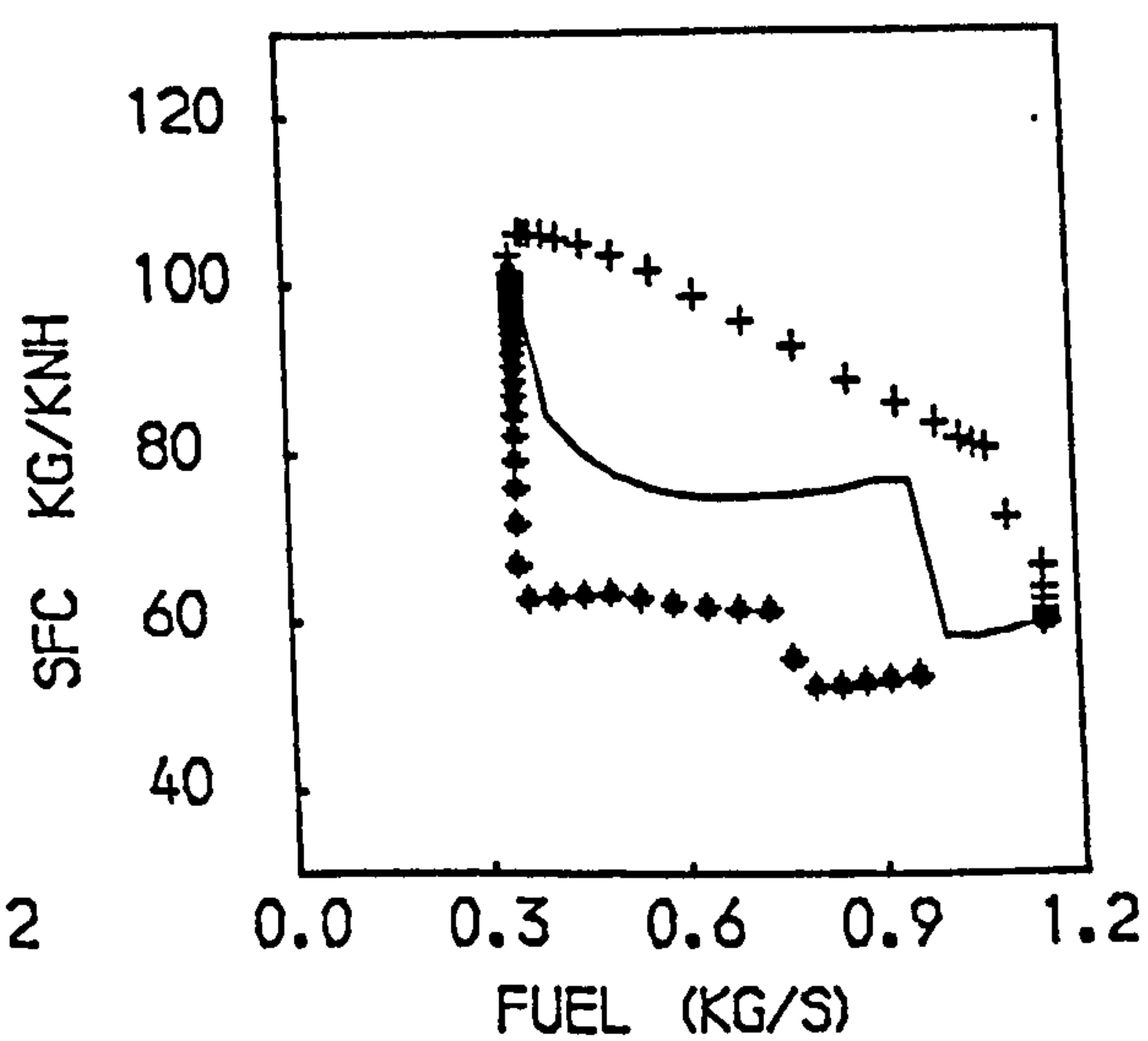
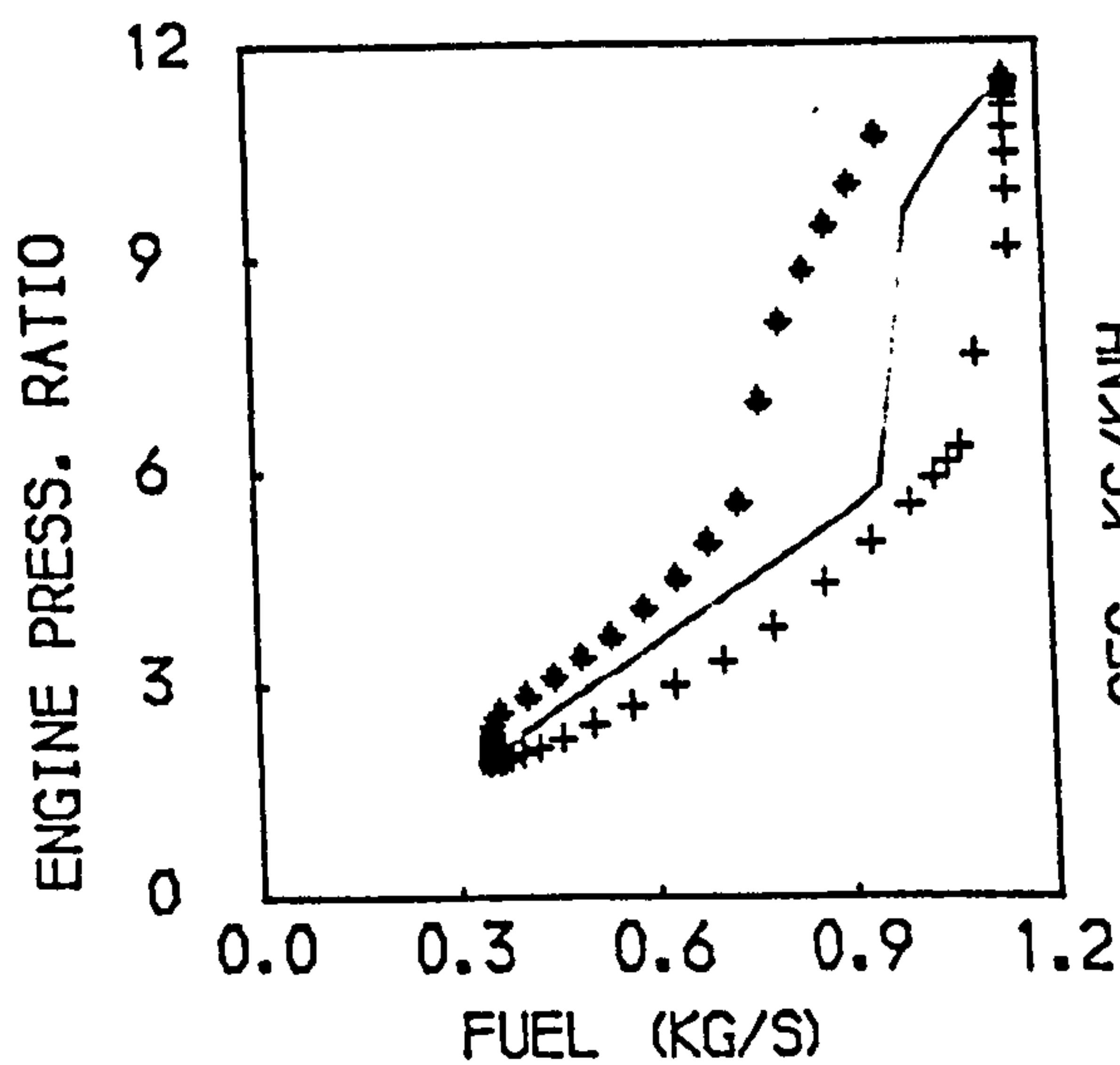
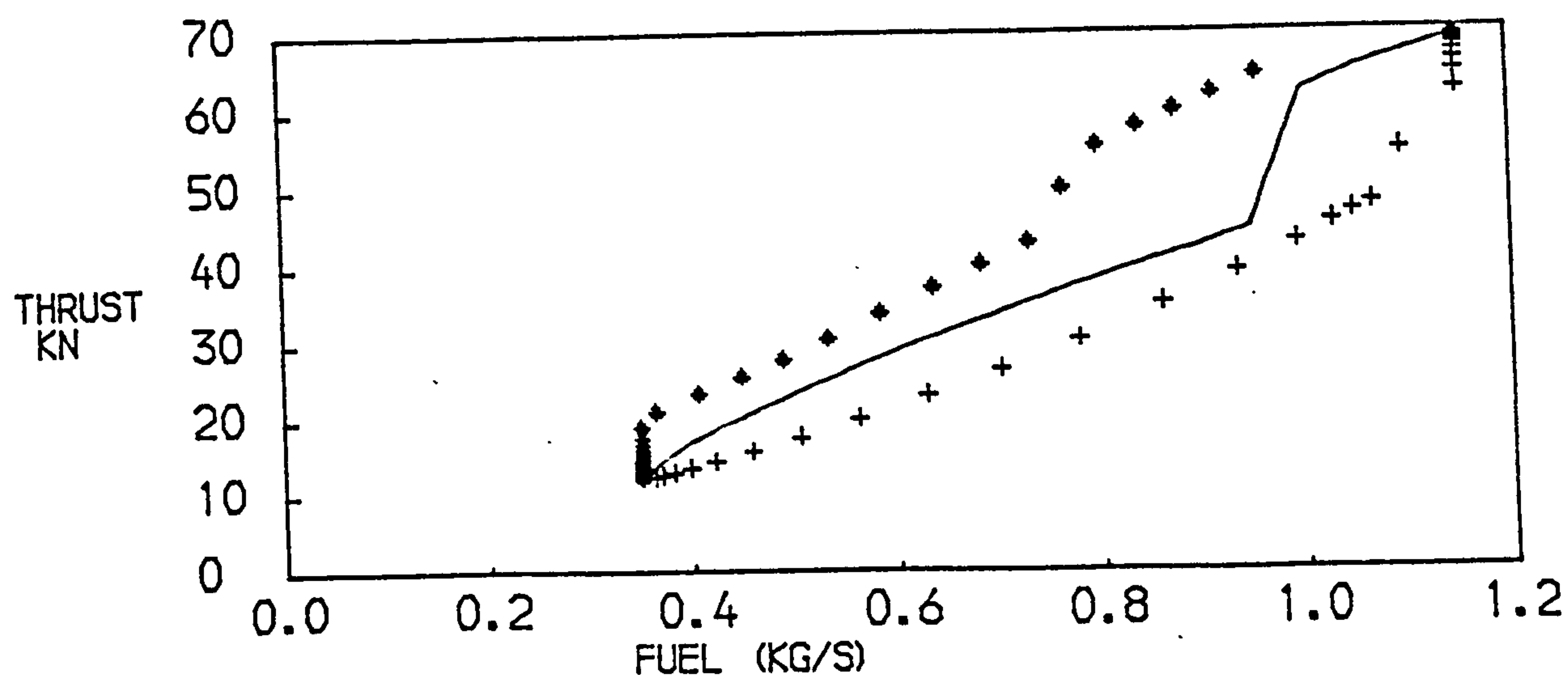
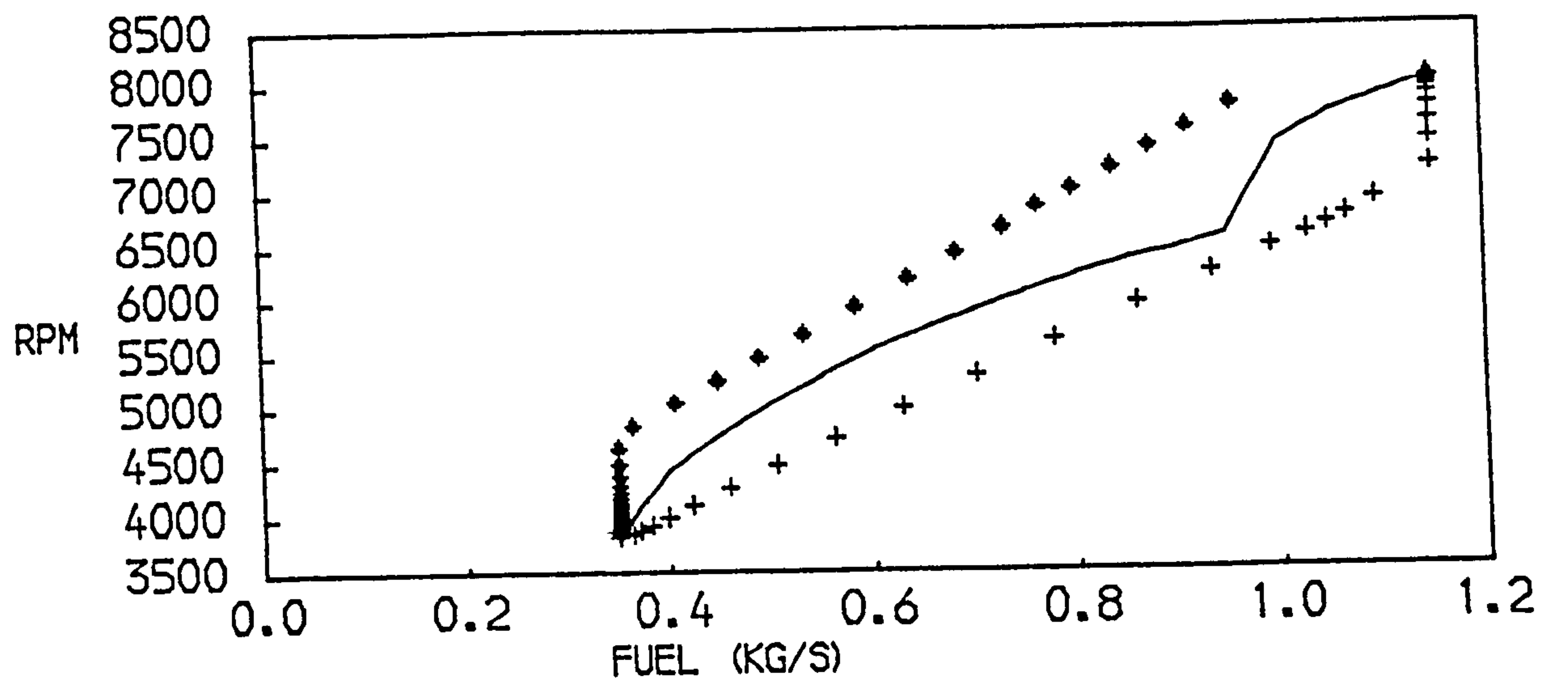


FIG. 21
PERFORMANCE OF A SINGLE SPOOL TURBOFAN WITH MIXED EXHAUSTS
+ACCELERATION x DECELERATION —STEADY RUNNING

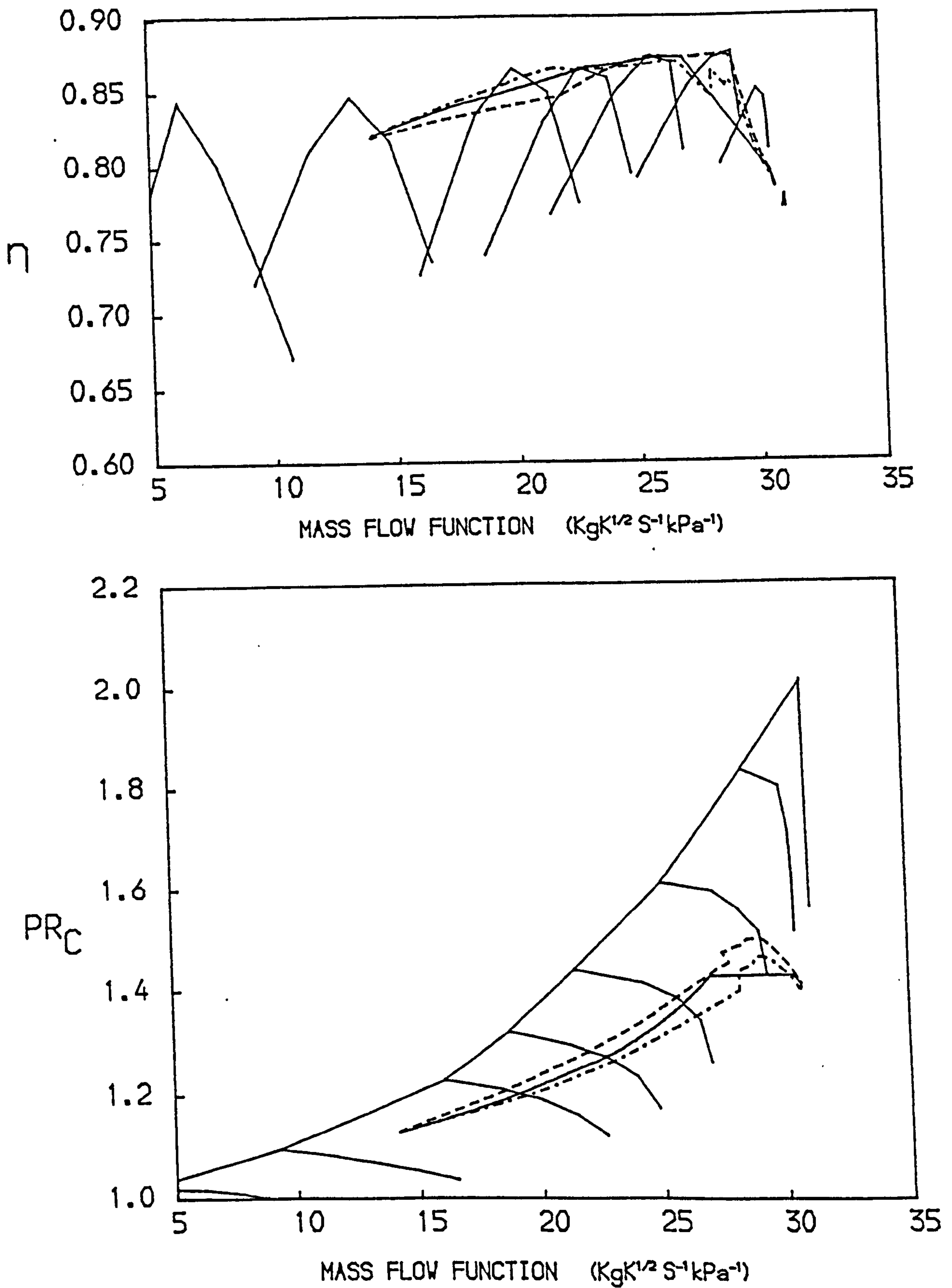


FIG. 22
 PATHS ON THE CHARACTERISTIC MAPS OF THE FAN OF A
 SINGLE SPOOL TURBOFAN WITH SEPARATE EXHAUSTS
 -- ACCELERATION — STEADY RUNNING --- DECELERATION

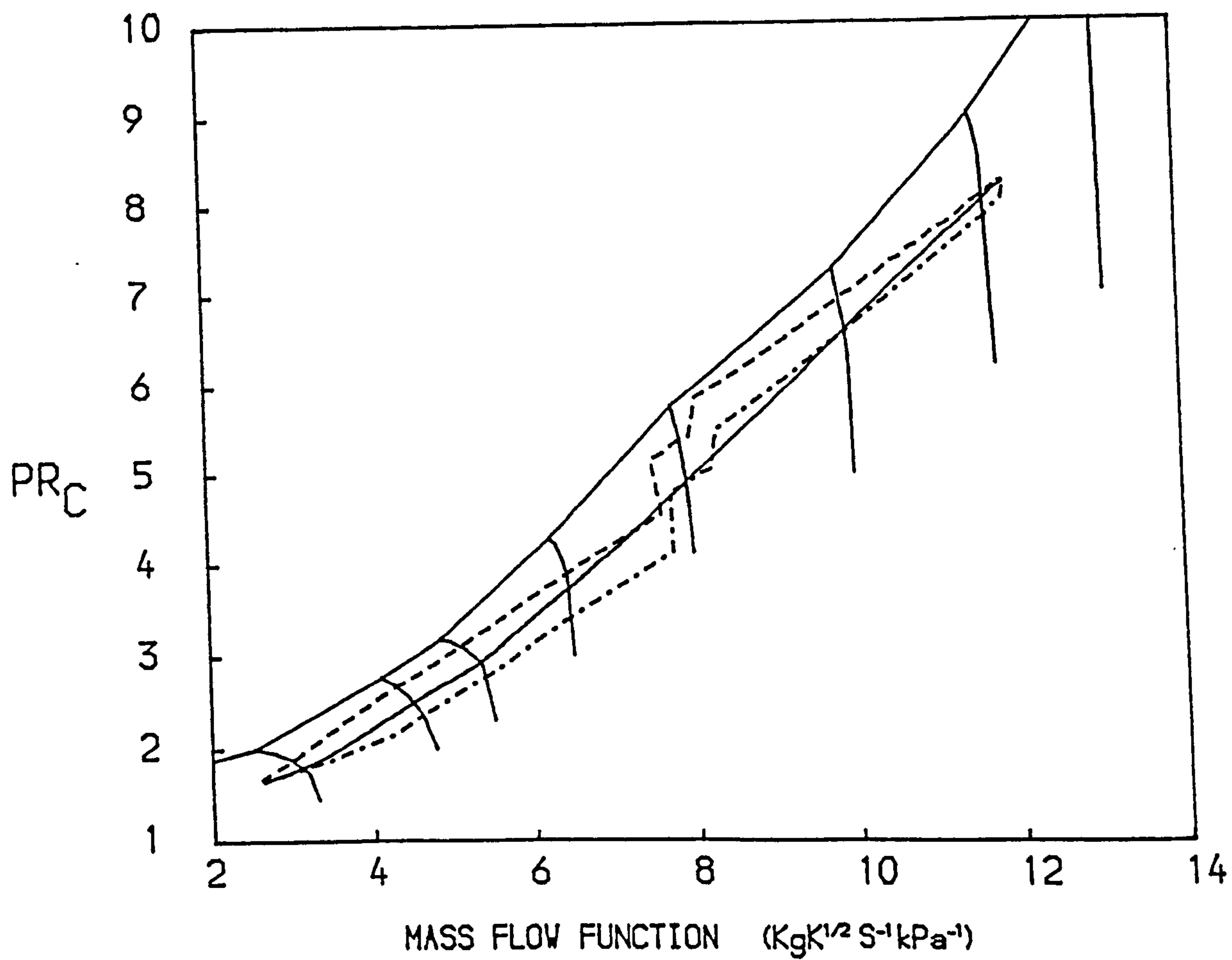
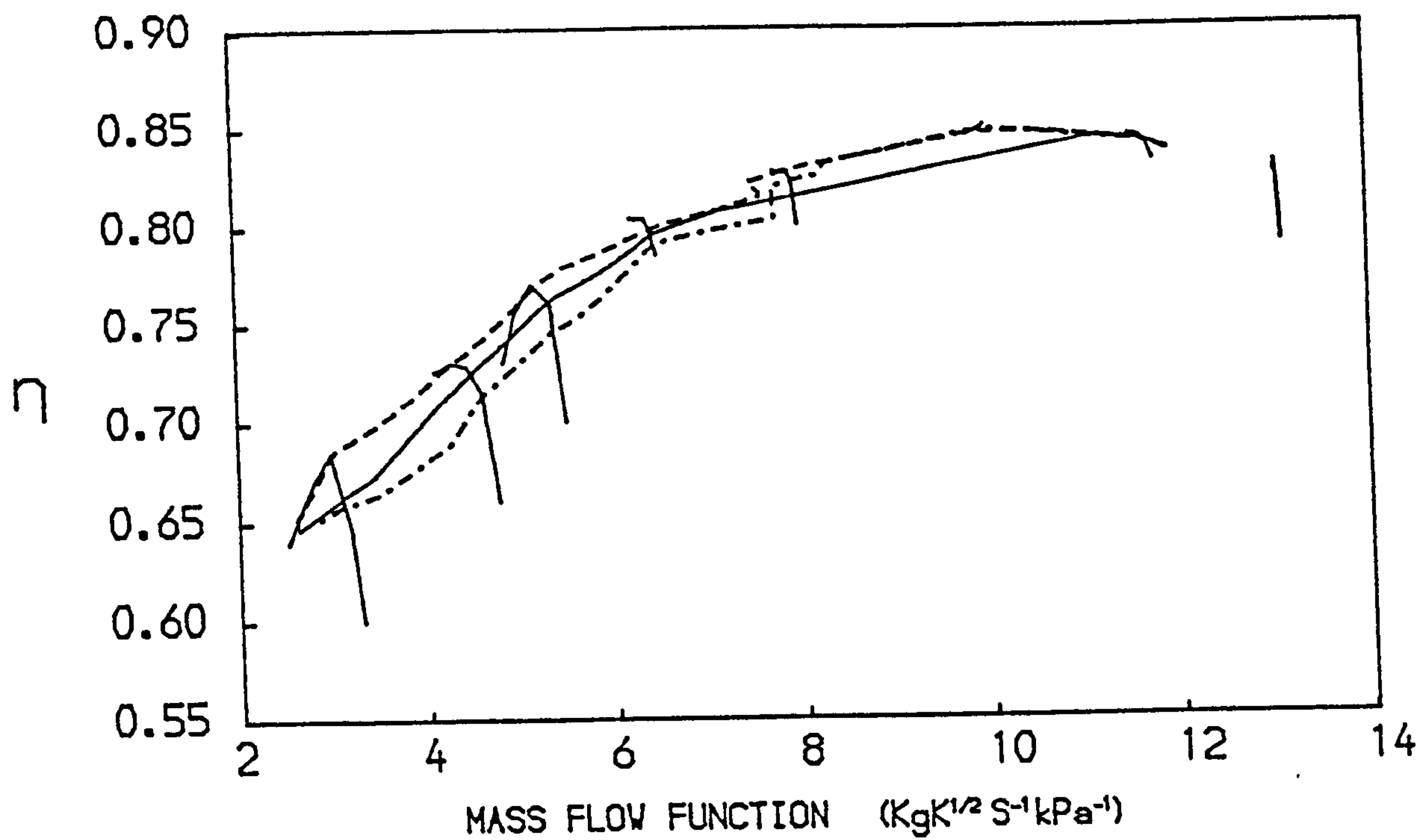


FIG. 23
 PATHS ON THE CHARACTERISTIC MAPS OF THE COMPRESSOR OF A
 SINGLE SPOOL TURBOFAN WITH SEPARATE EXHAUSTS
 -- ACCELERATION — STEADY RUNNING --- DECELERATION

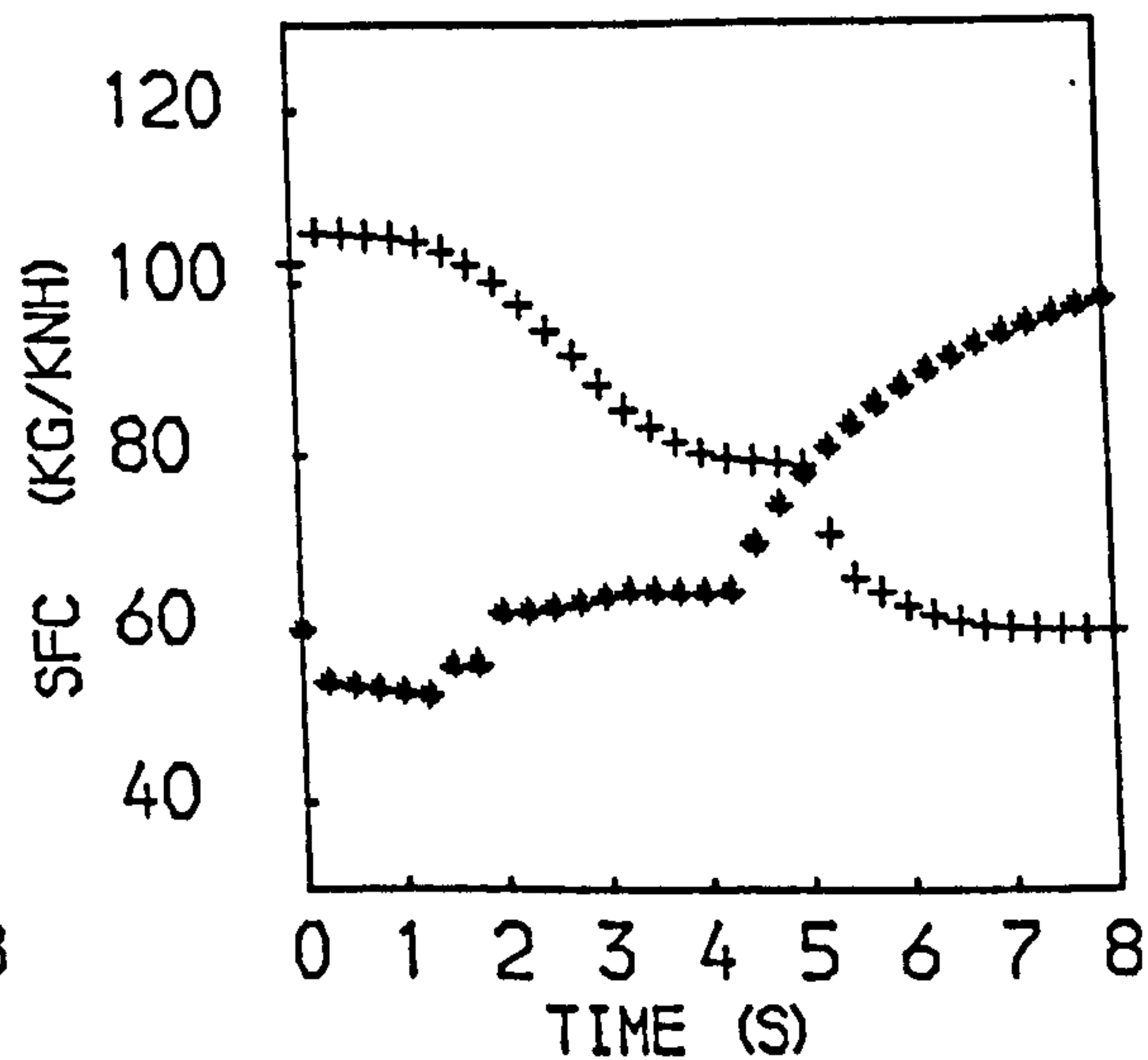
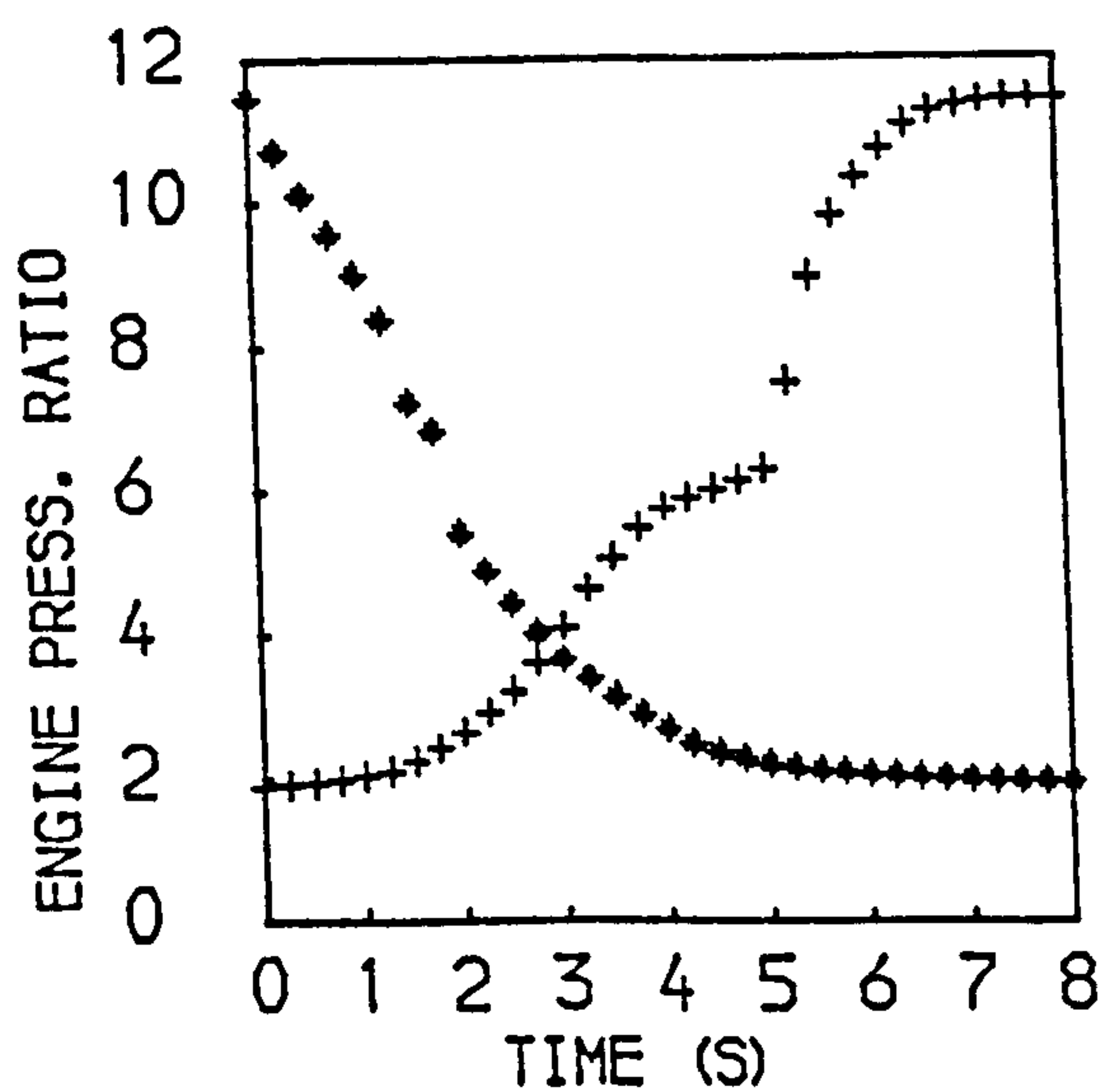
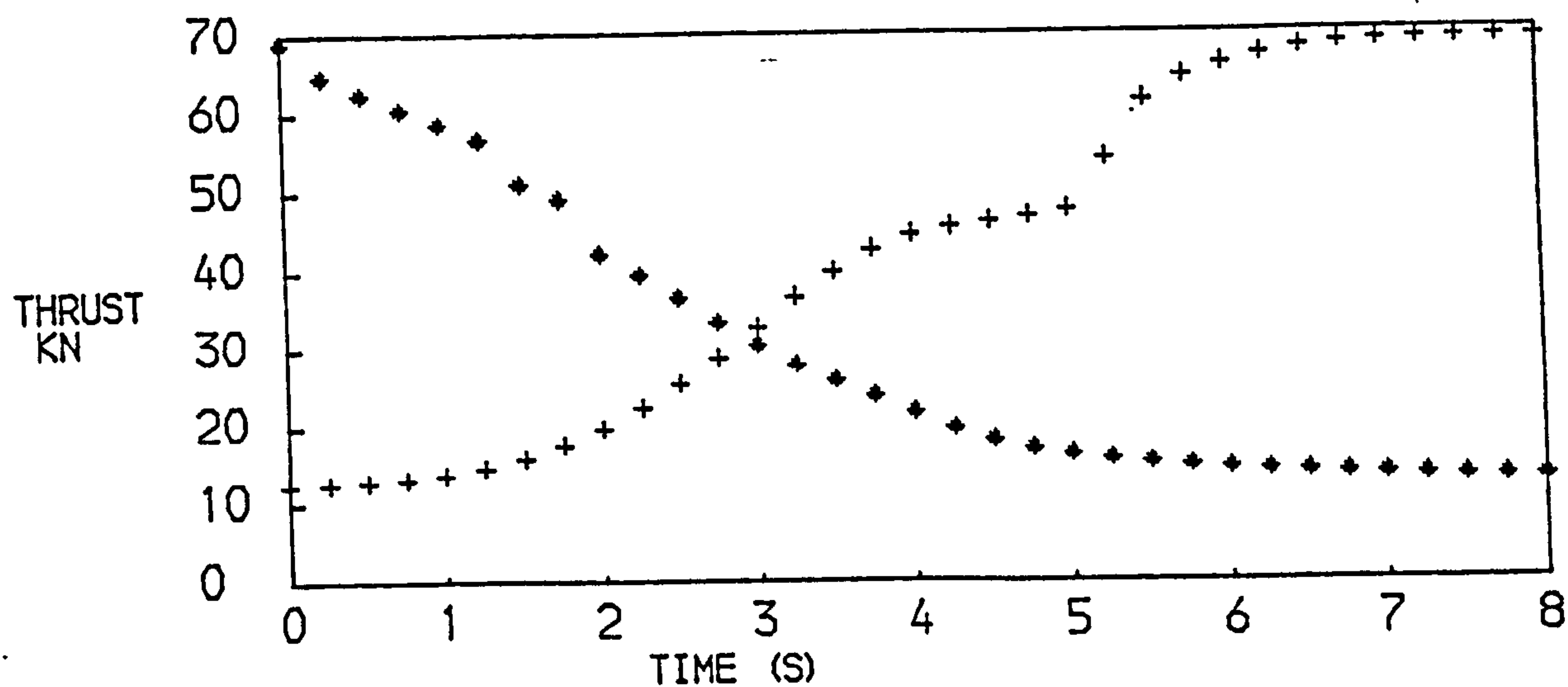
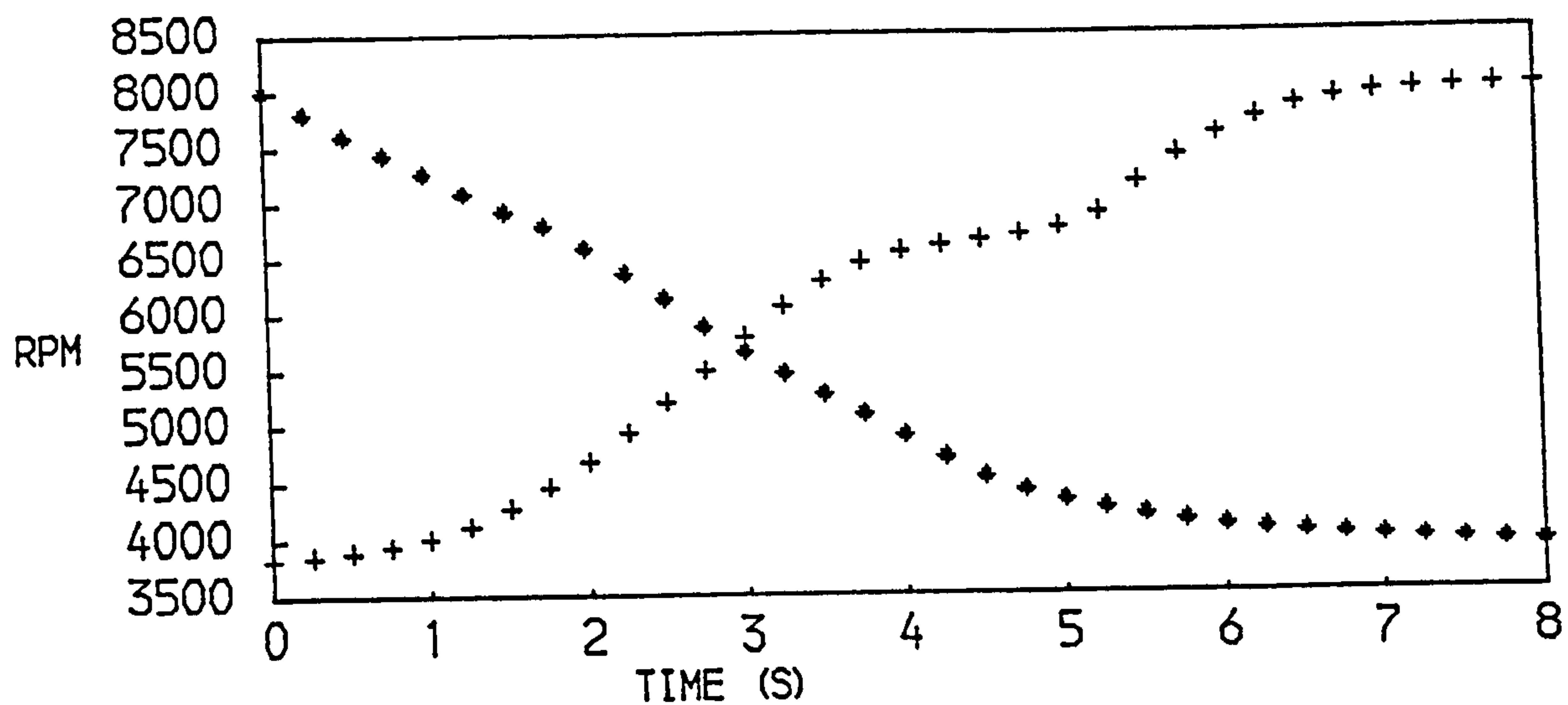


FIG. 24
PERFORMANCE OF A SINGLE SPOOL TURBOFAN WITH SEPARATE EXHAUSTS
+ACCELERATION * DECELERATION

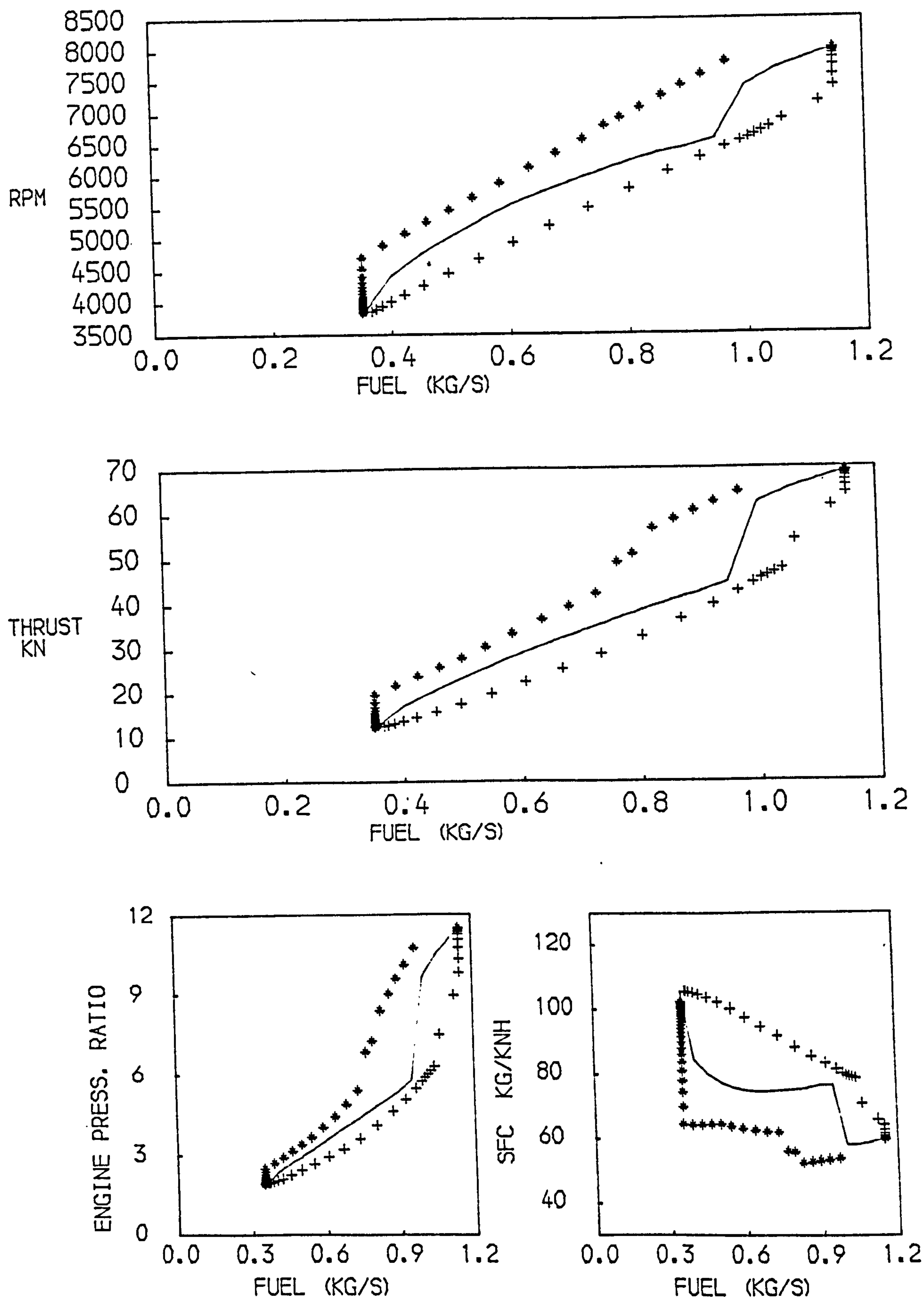


FIG. 25
 PERFORMANCE OF A SINGLE SPOOL TURBOFAN WITH SEPARATE EXHAUSTS
 +ACCELERATION * DECELERATION —STEADY RUNNING

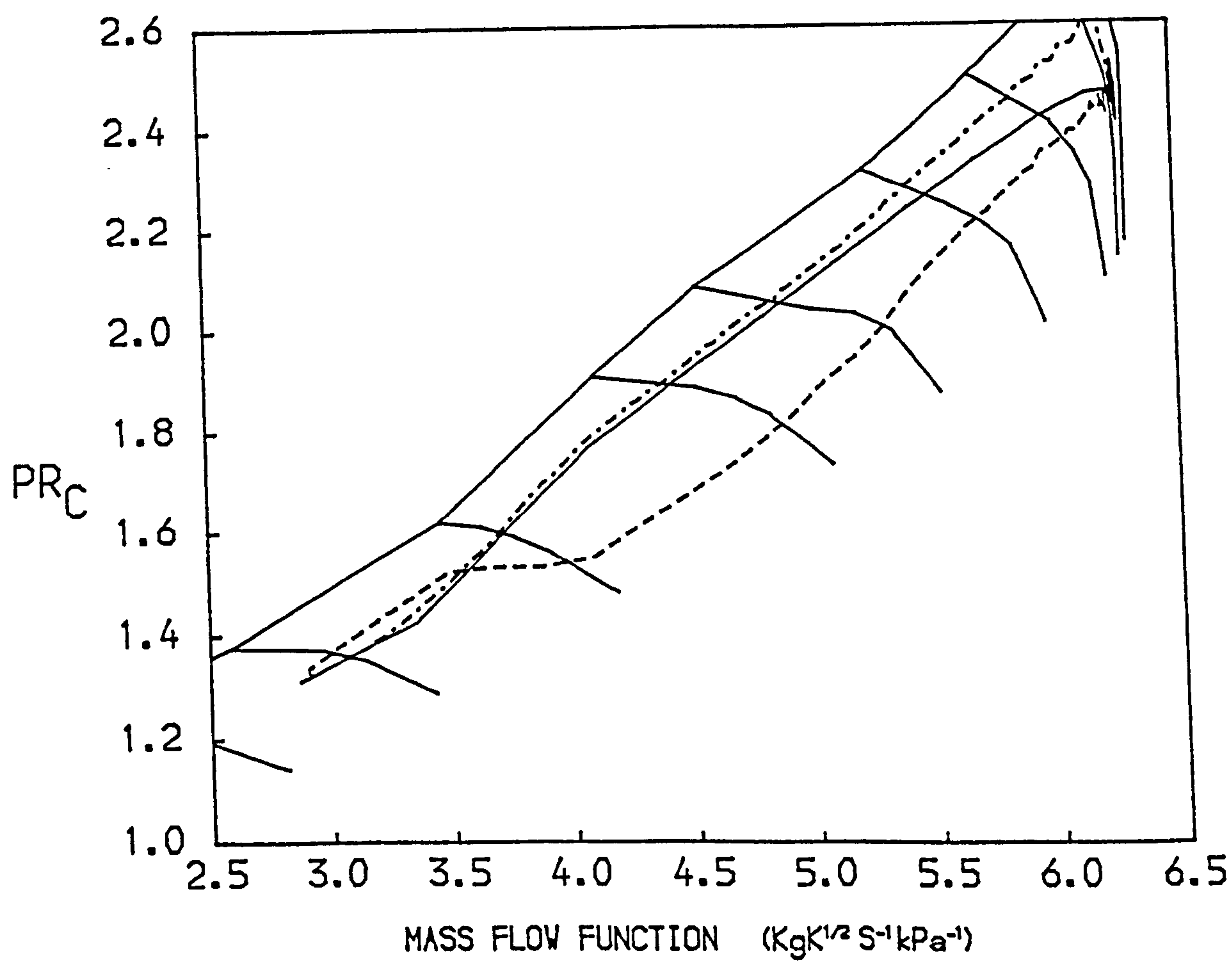
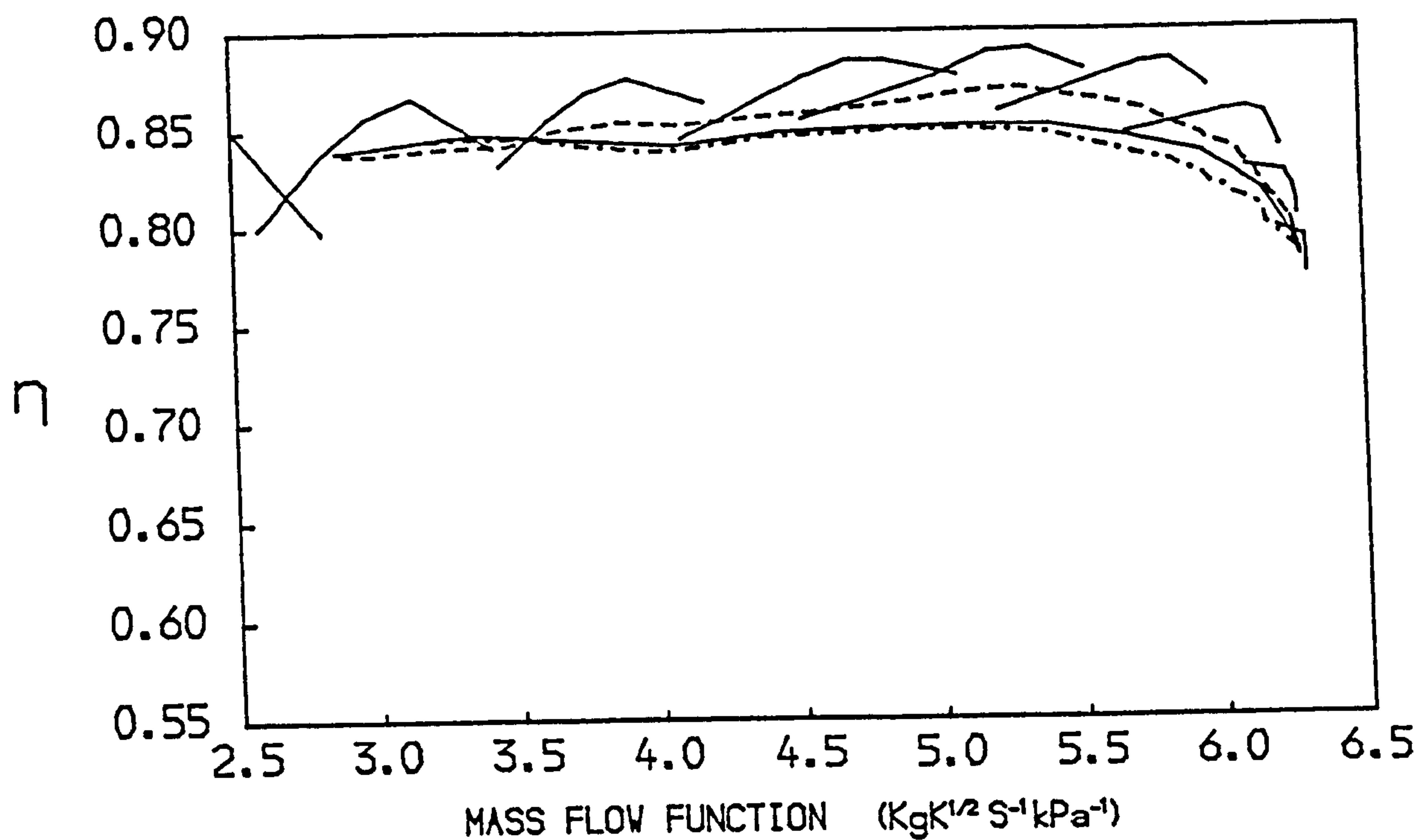


FIG. 26
 PATHS ON THE CHARACTERISTIC MAPS OF THE L.P. COMPRESSOR OF A
 TWO SPOOL TURBOJET
 -- ACCELERATION — STEADY RUNNING --- DECELERATION

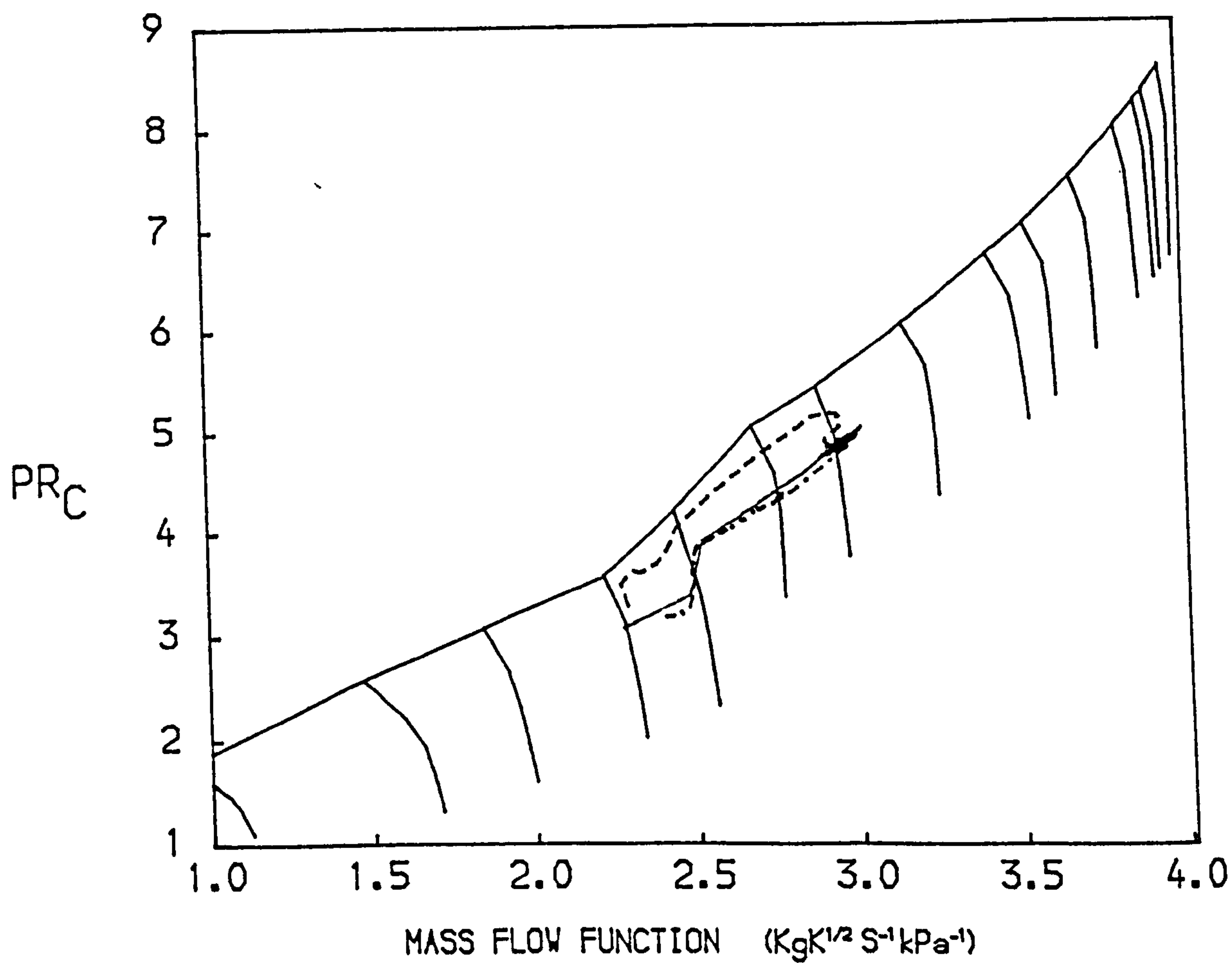
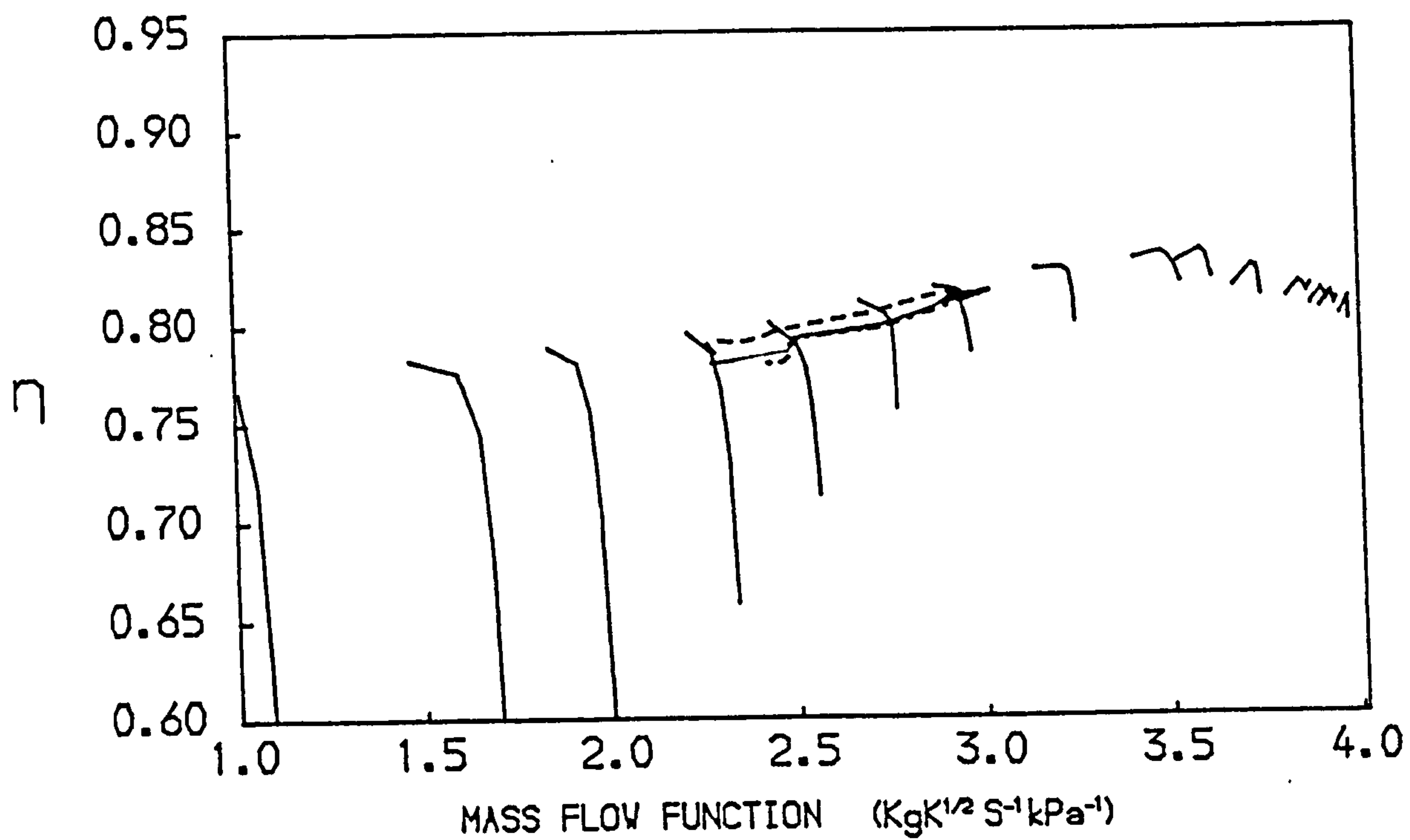


FIG. 27
 PATHS ON THE CHARACTERISTIC MAPS OF THE H.P. COMPRESSOR OF A
 TWO SPOOL TURBOJET
 -- ACCELERATION — STEADY RUNNING --- DECELERATION

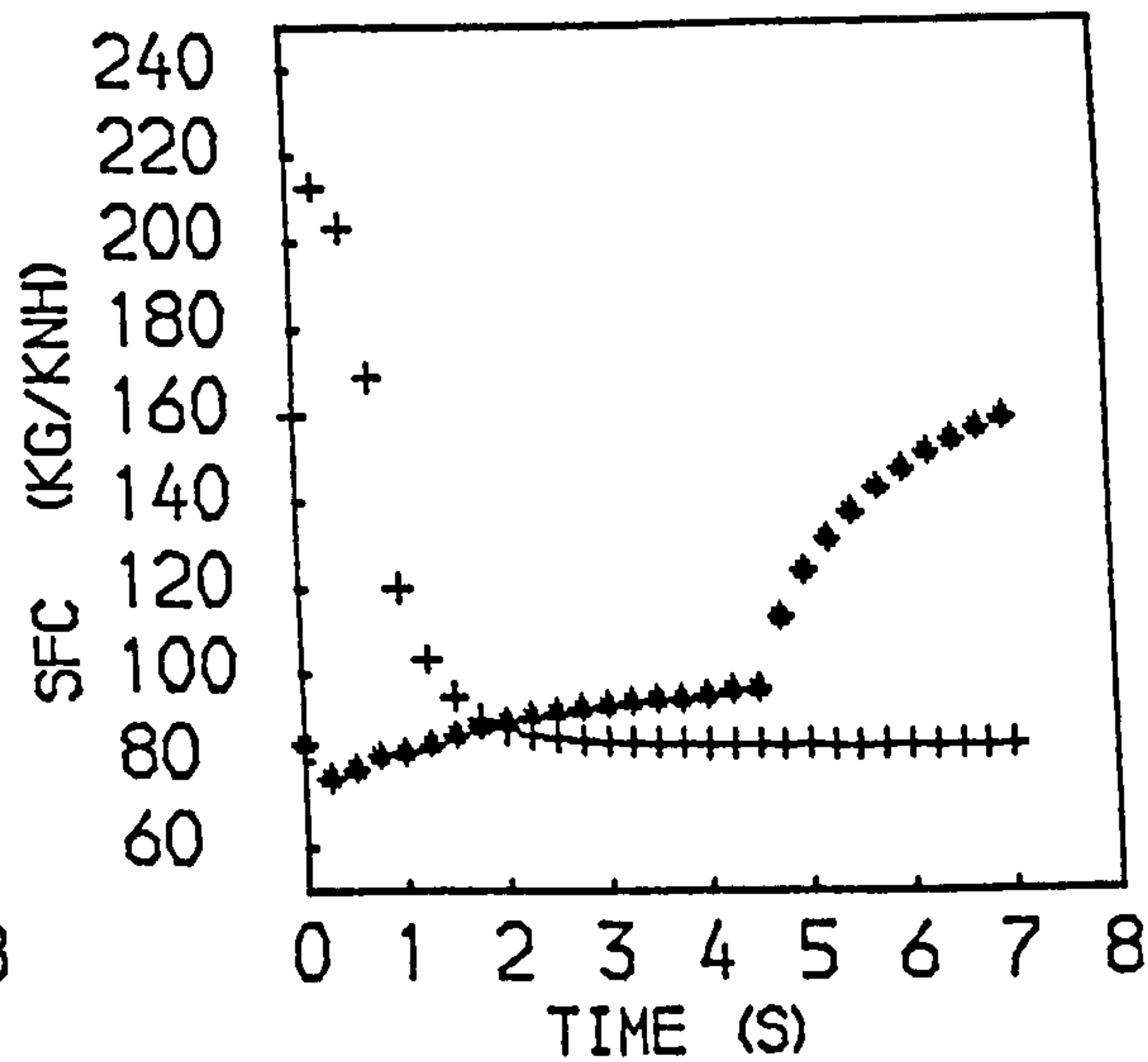
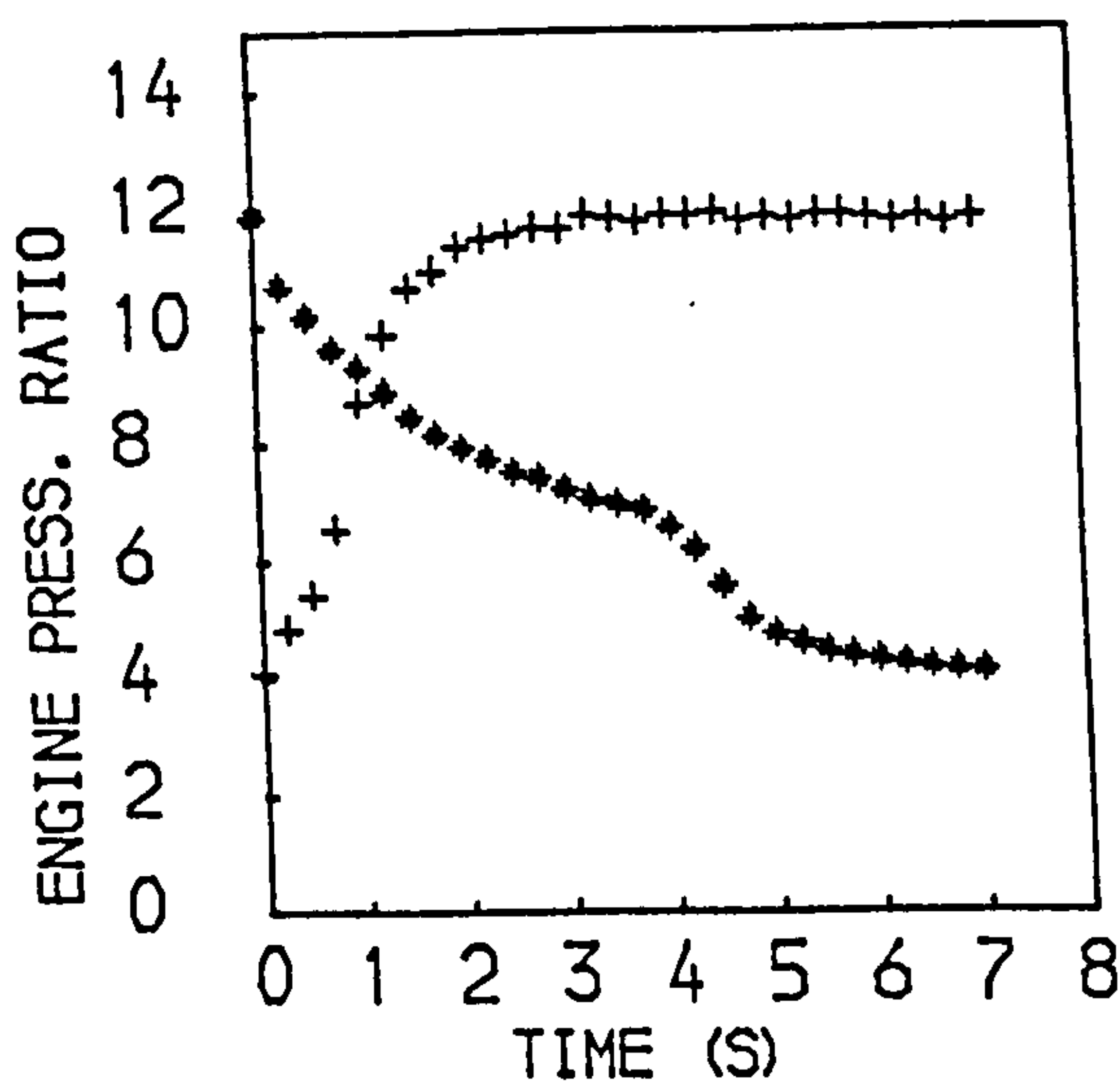
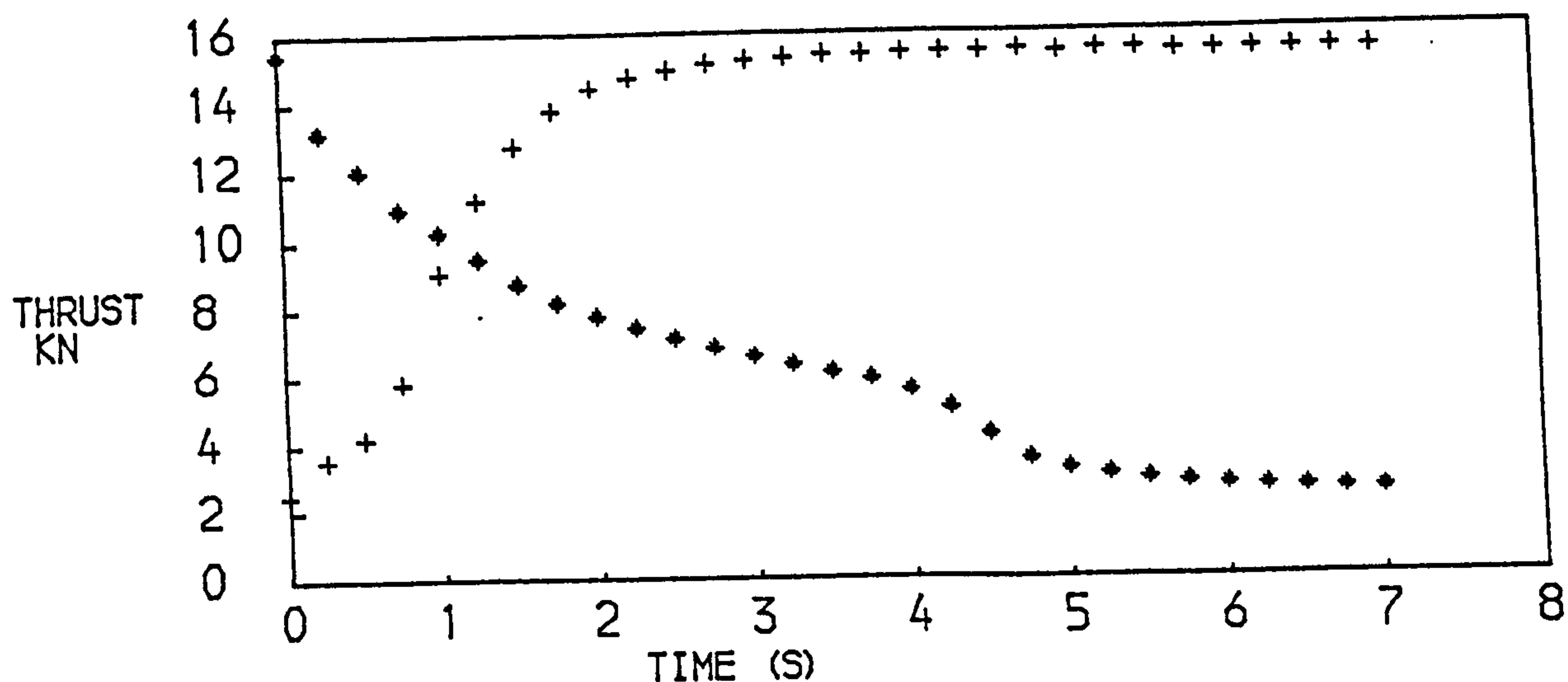
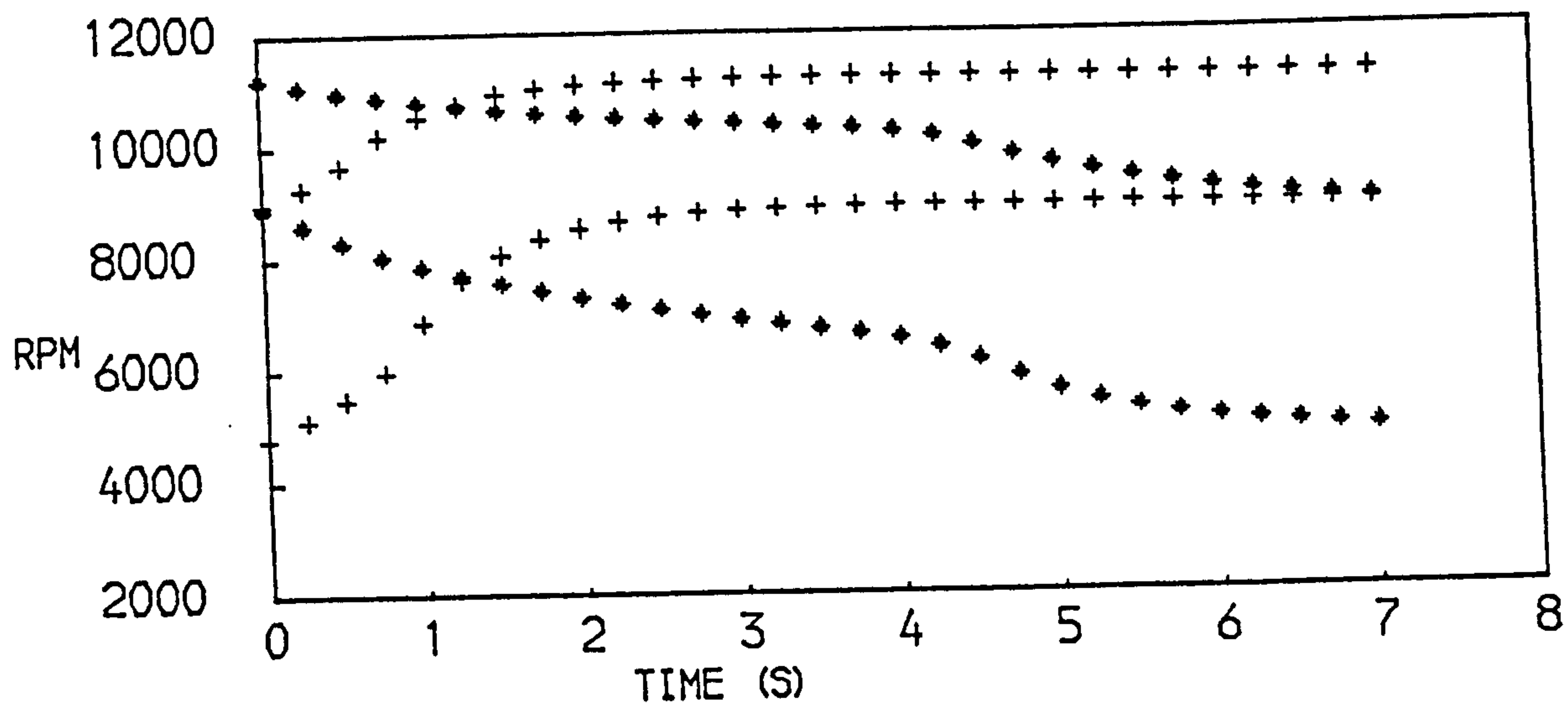


FIG. 28
PERFORMANCE OF A TWO SPOOL TURBOJET ENGINE
+ACCELERATION * DECELERATION

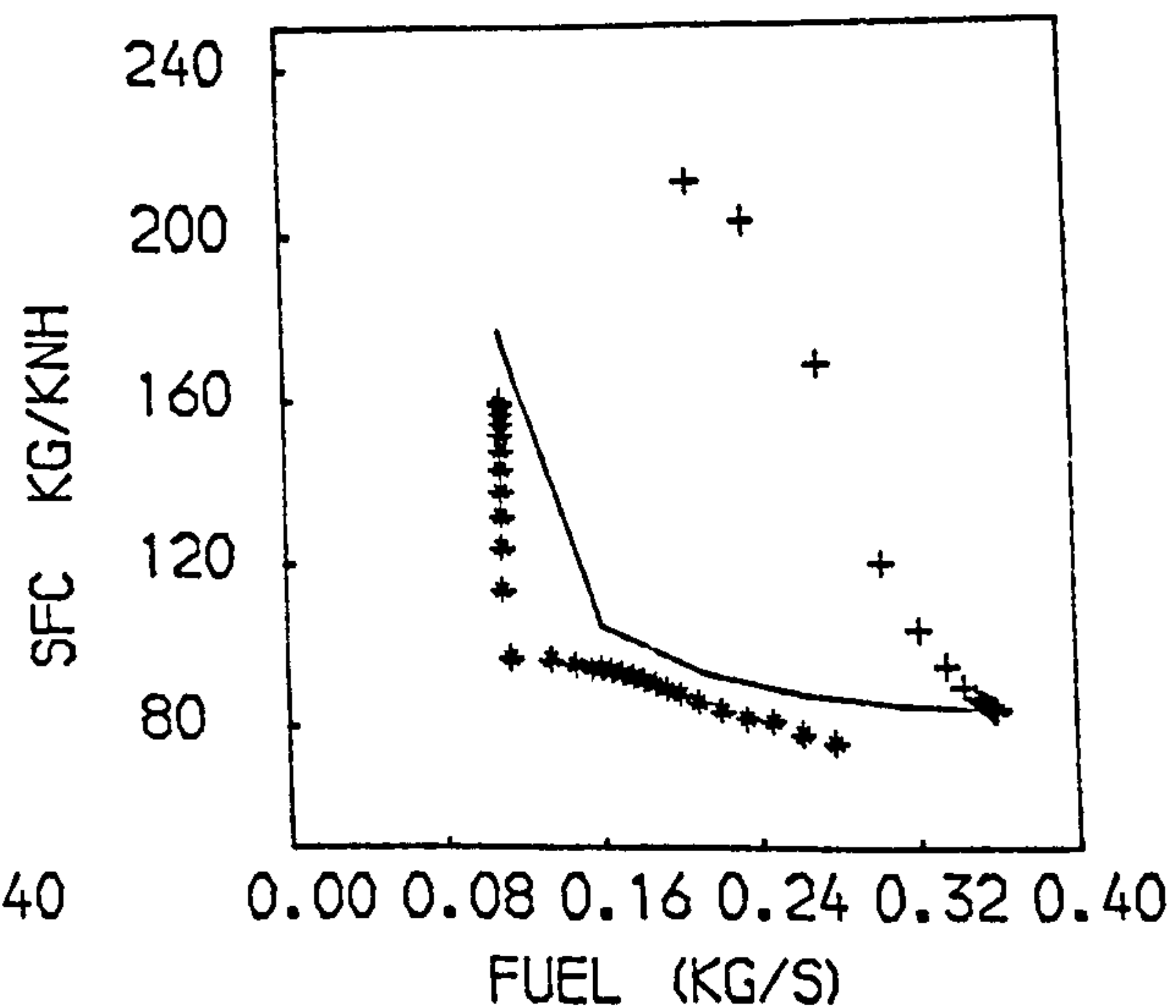
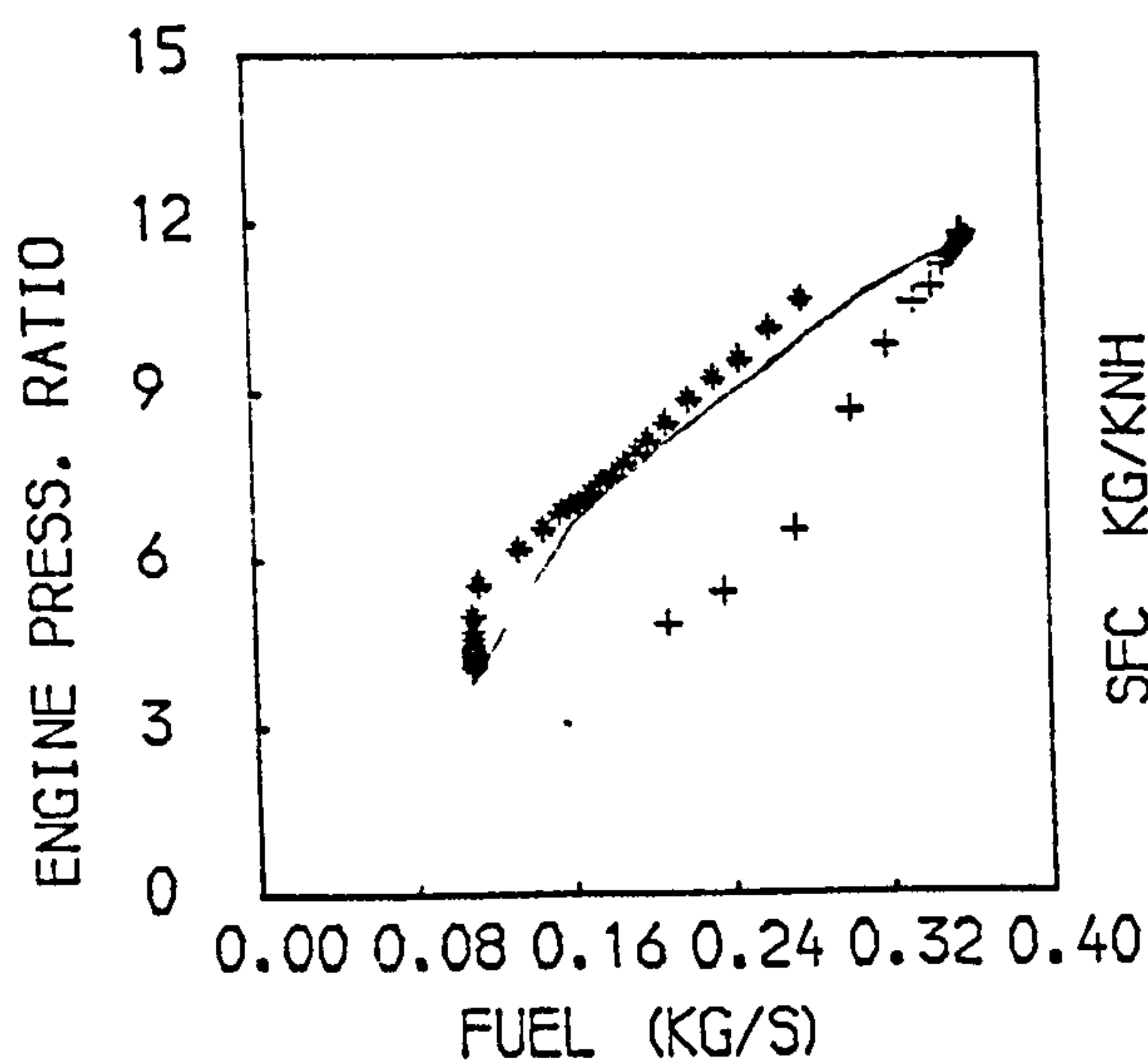
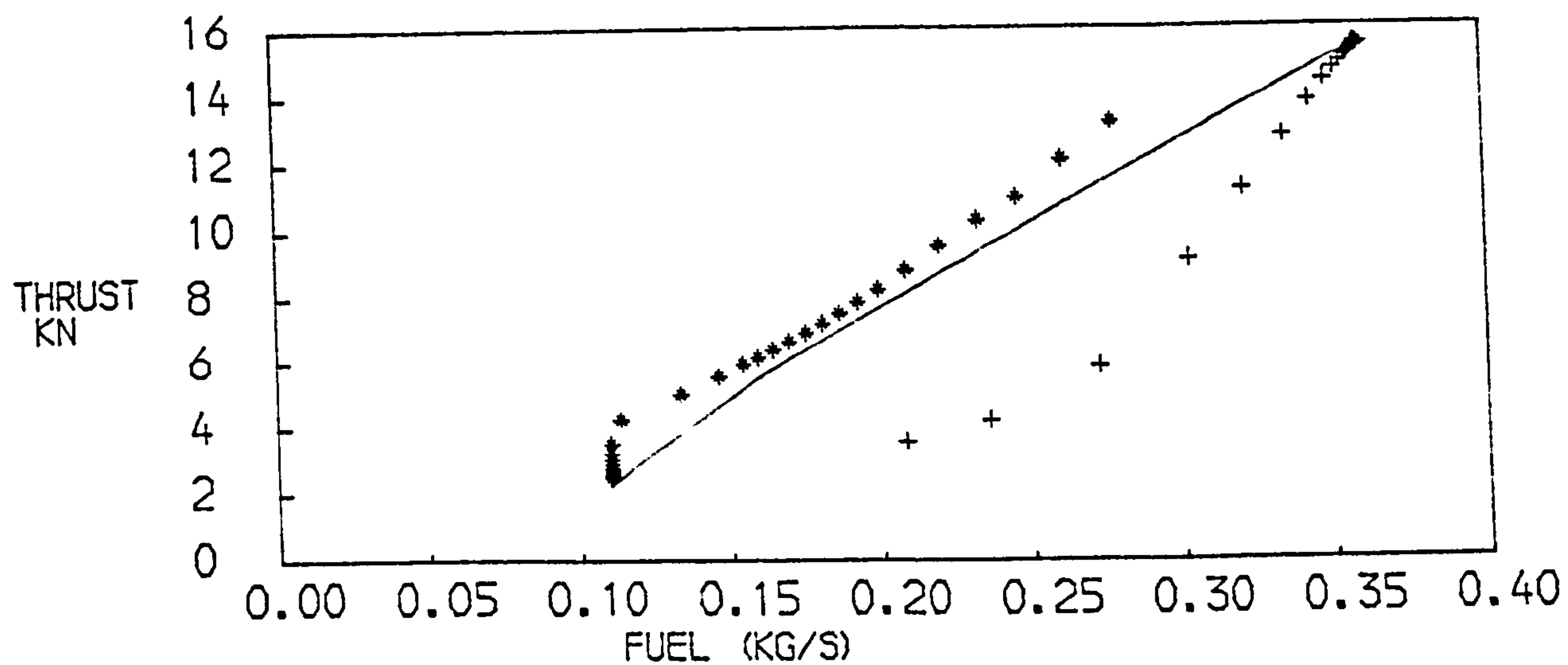
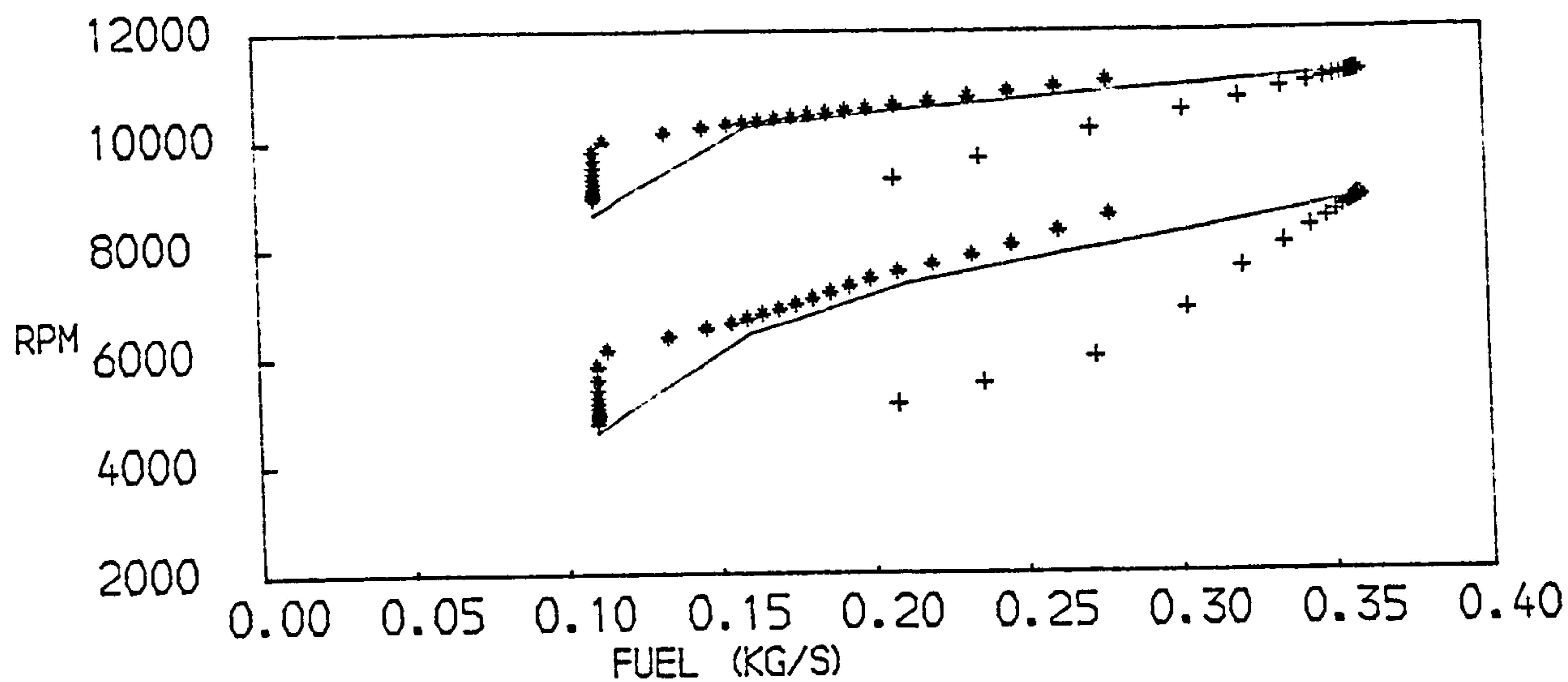


FIG. 29
PERFORMANCE OF A TWO SPOOL TURBOJET
+ACCELERATION * DECELERATION —STEADY RUNNING

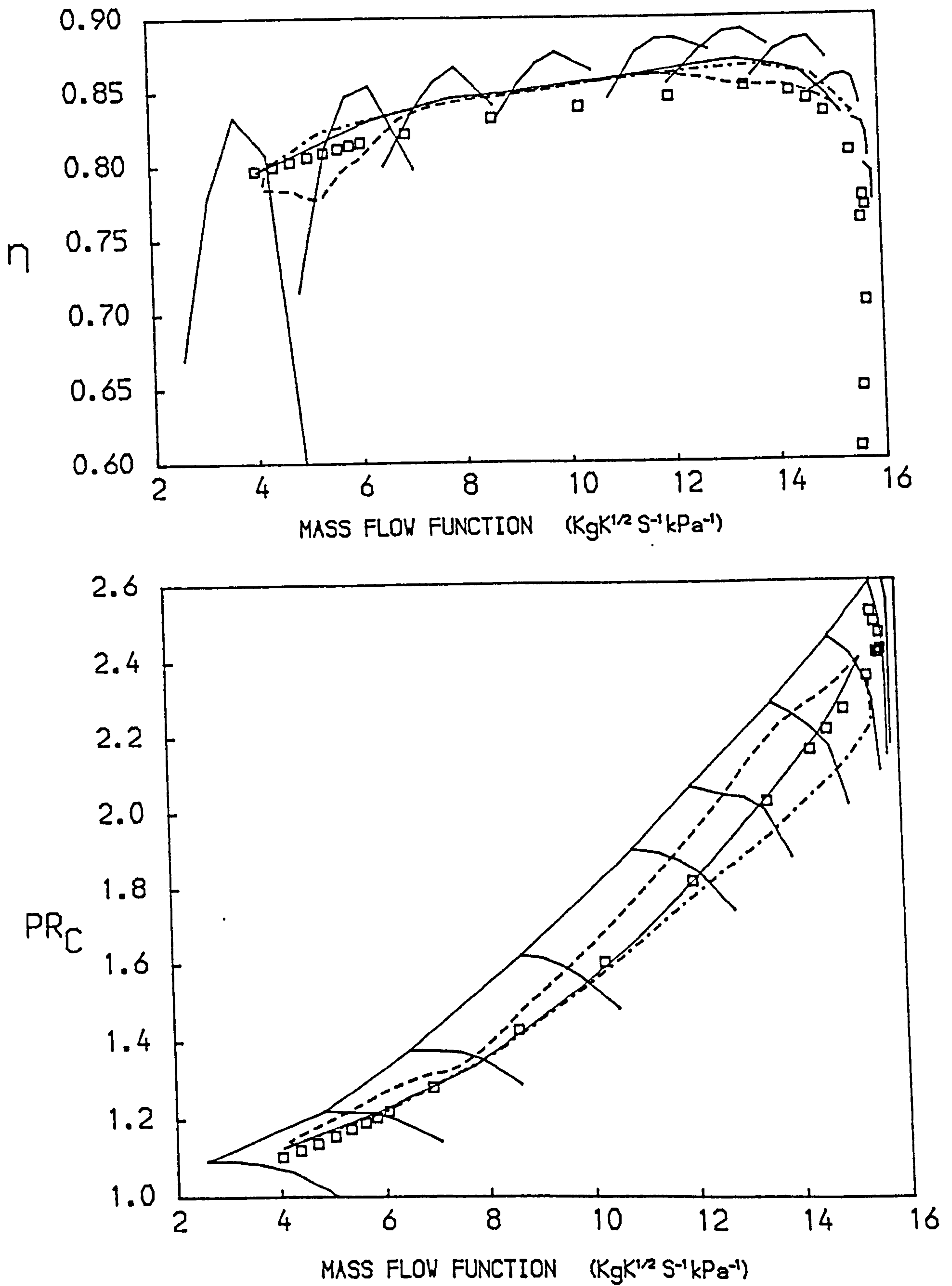


FIG. 30
 PATHS ON THE CHARACTERISTIC MAPS OF THE L.P. COMPRESSOR OF A
 TWO SPOOL BYPASS ENGINE WITH MIXED EXHAUSTS
 -- ACCELERATION — STEADY RUNNING --- DECELERATION
 □ STEADY RUNNING TEST BED DATA

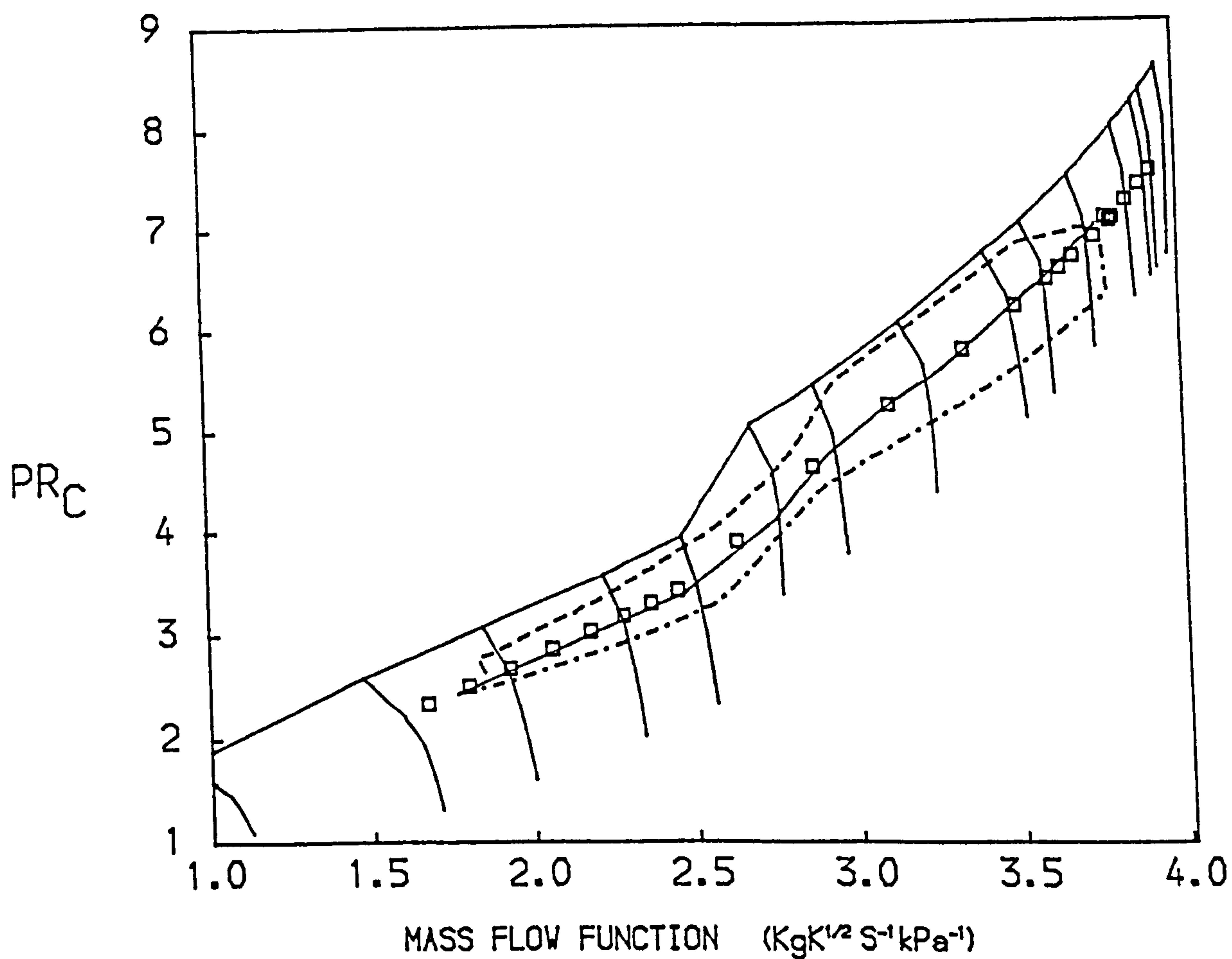
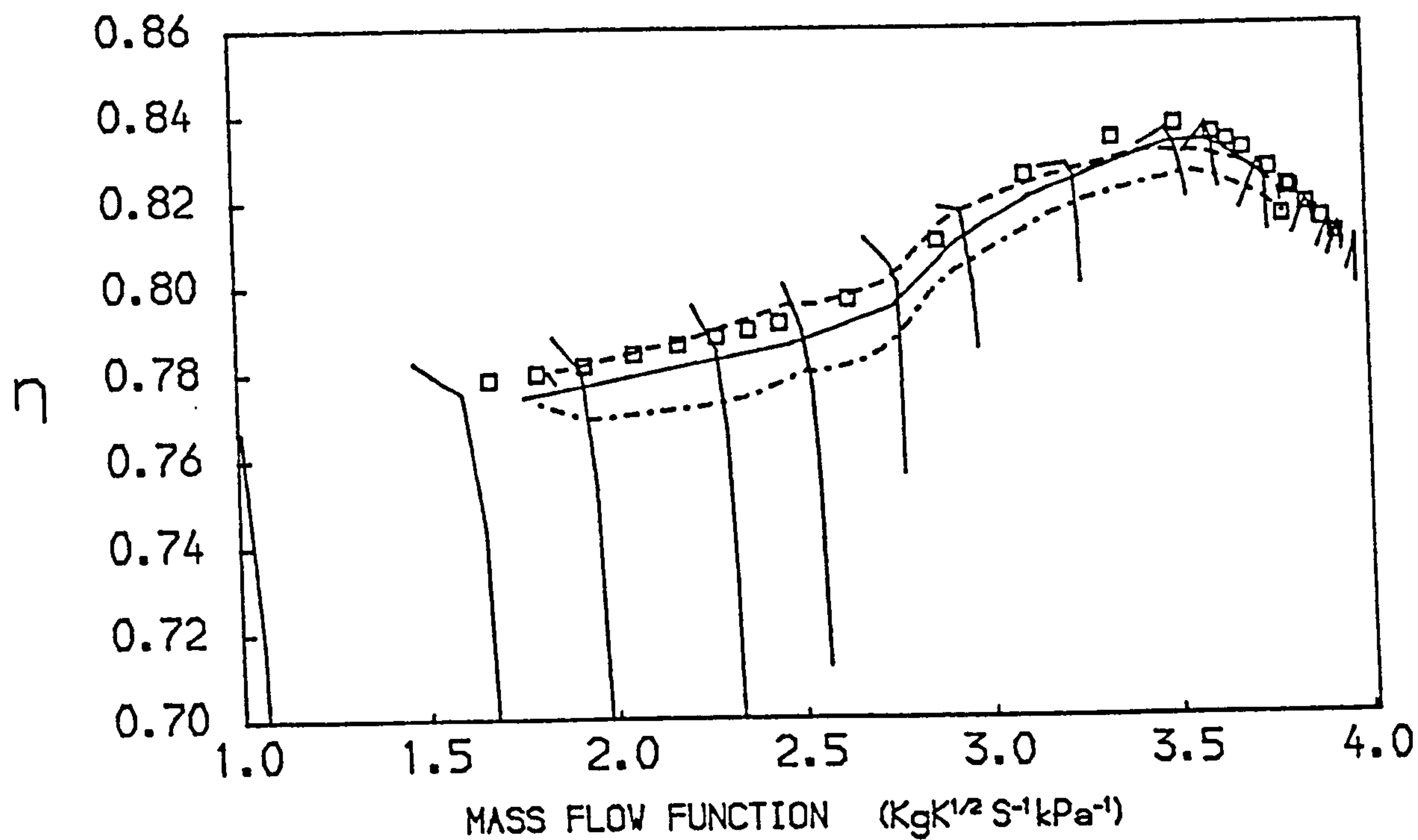


FIG. 31
 PATHS ON THE CHARACTERISTIC MAPS OF THE H.P. COMPRESSOR OF A
 TWO SPOOL BYPASS ENGINE WITH MIXED EXHAUSTS
 -- ACCELERATION — STEADY RUNNING --- DECELERATION
 □ STEADY RUNNING TEST BED DATA

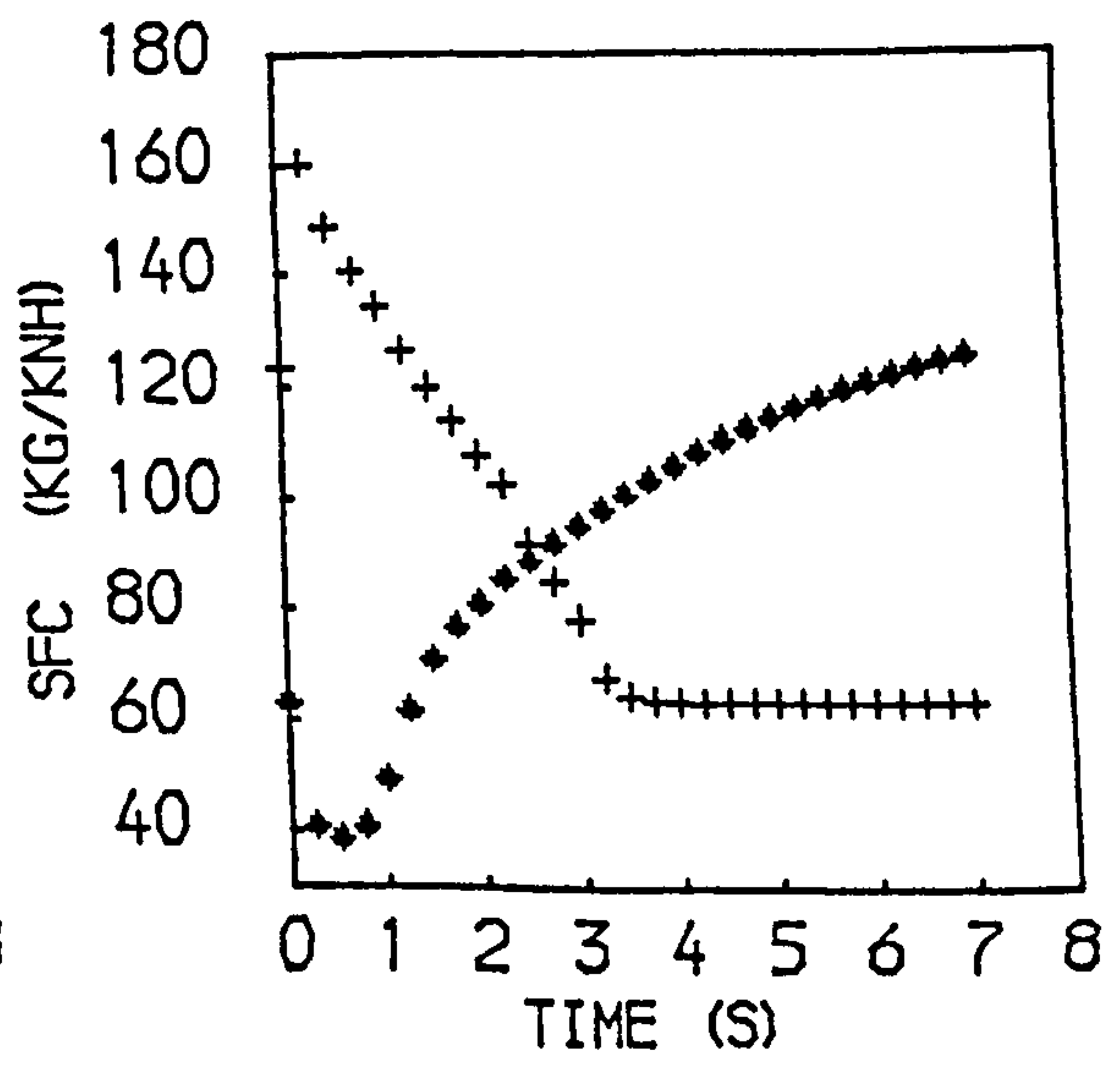
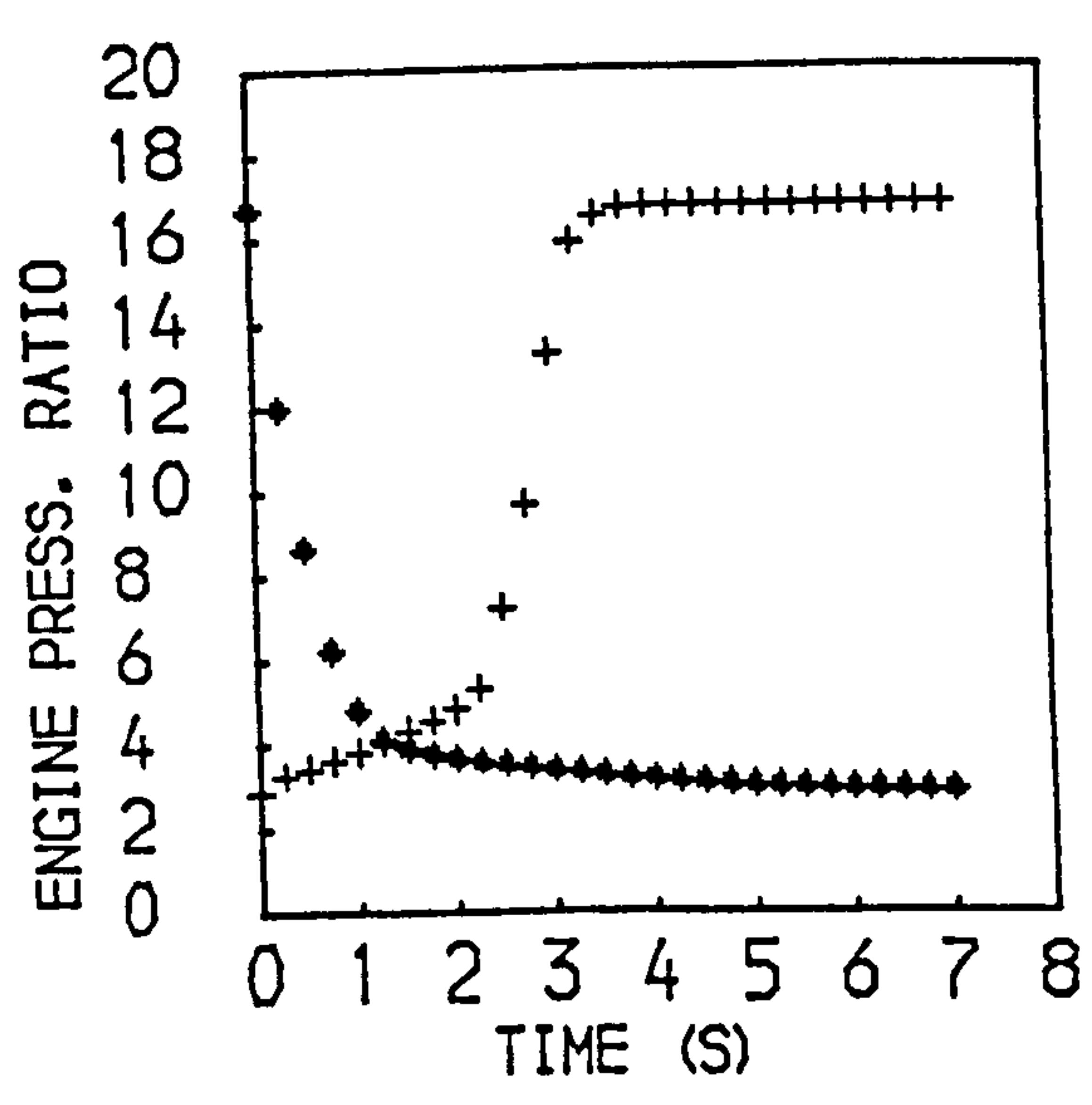
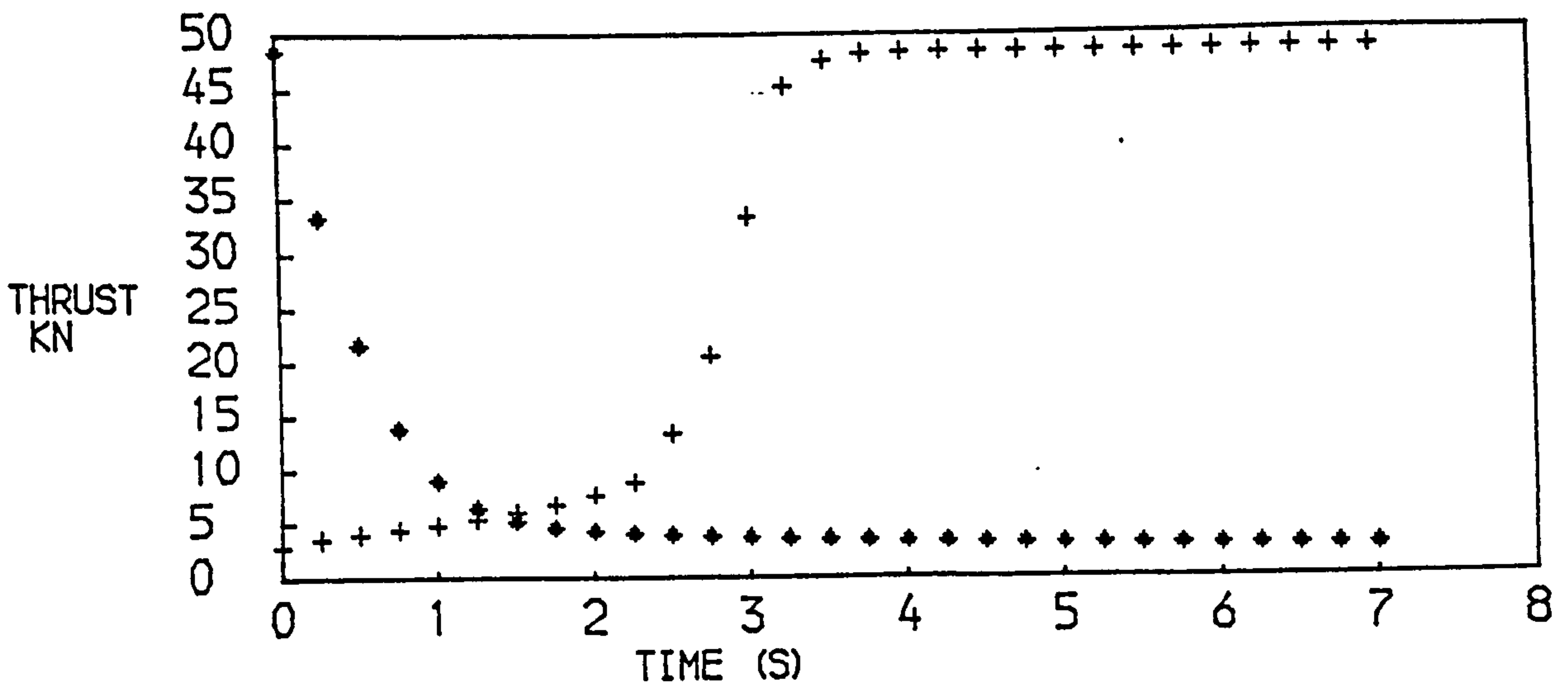
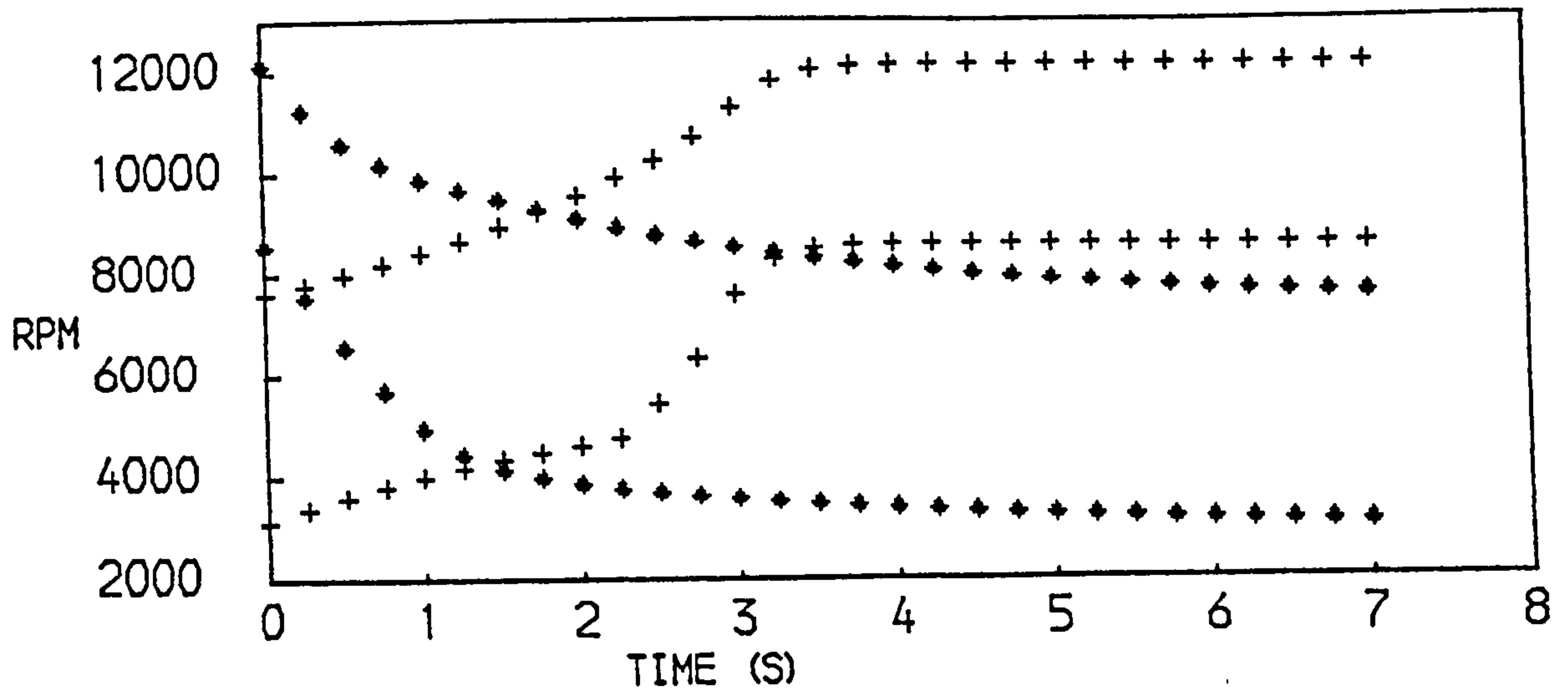


FIG. 32
PERFORMANCE OF A TWO SPOOL BYPASS ENGINE WITH MIXED EXHAUSTS
+ACCELERATION ♦ DECELERATION

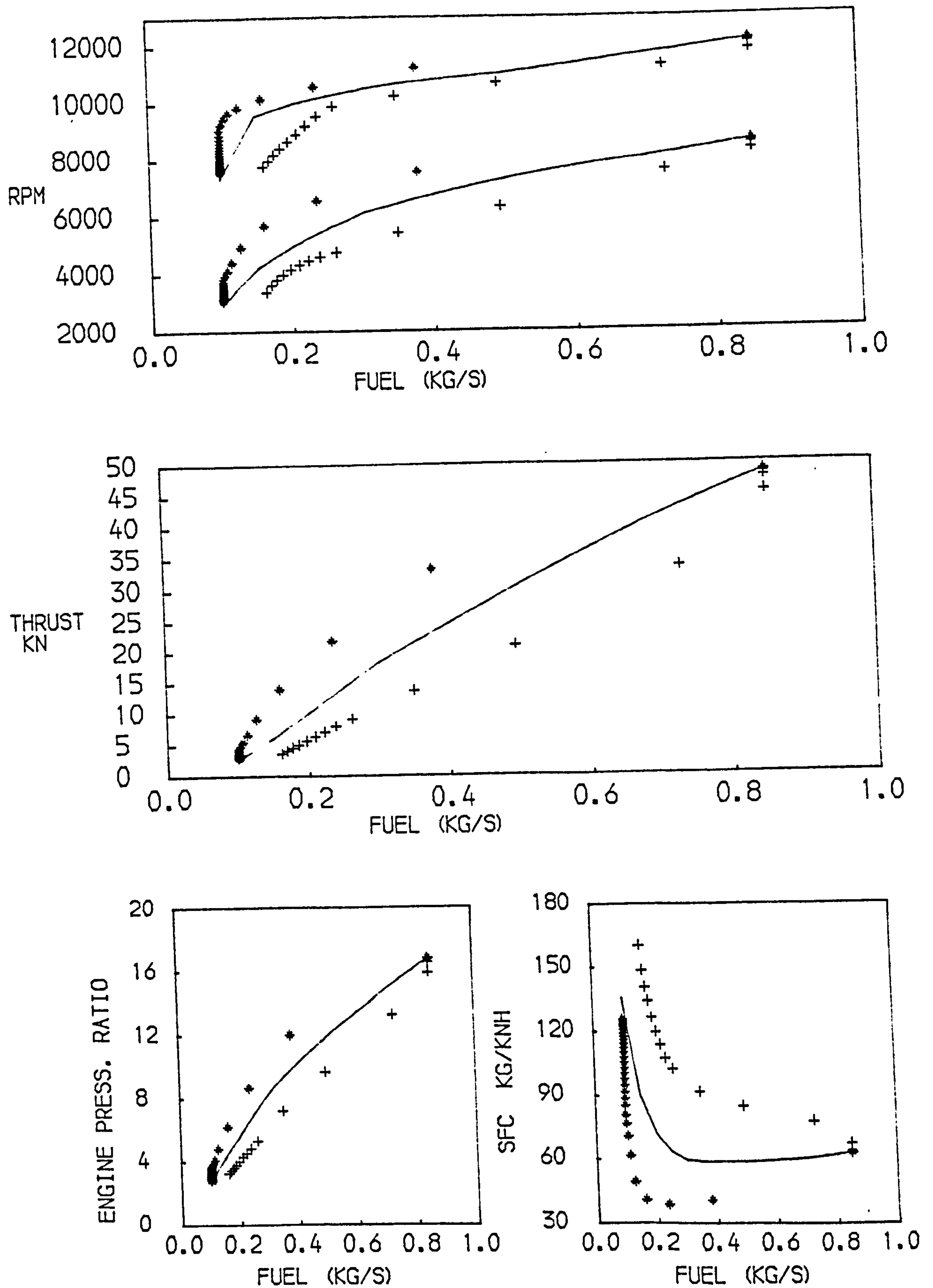


FIG. 33
 PERFORMANCE OF A TWO SPOOL BYPASS ENGINE WITH MIXED EXHAUSTS
 +ACCELERATION * DECELERATION —STEADY RUNNING

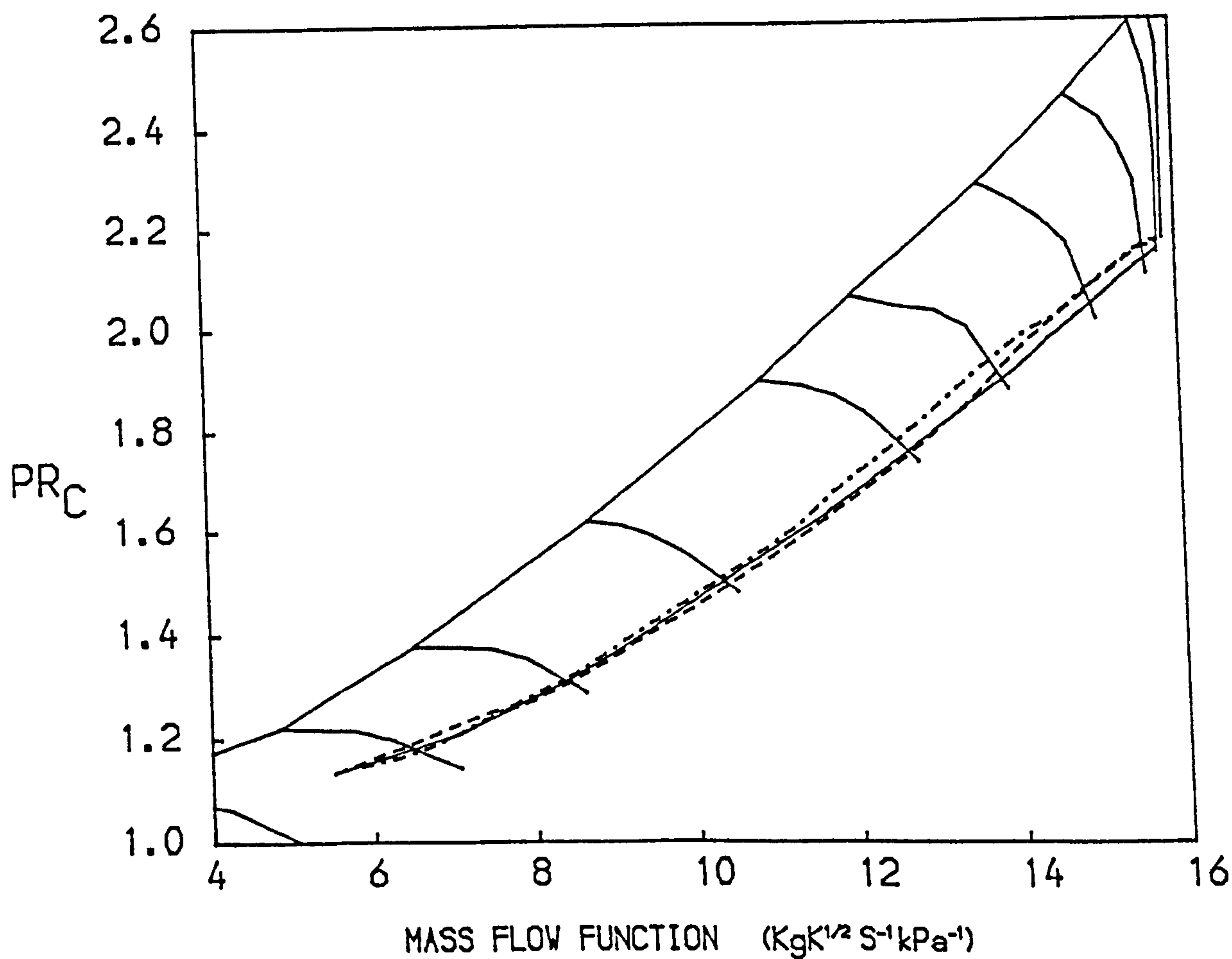
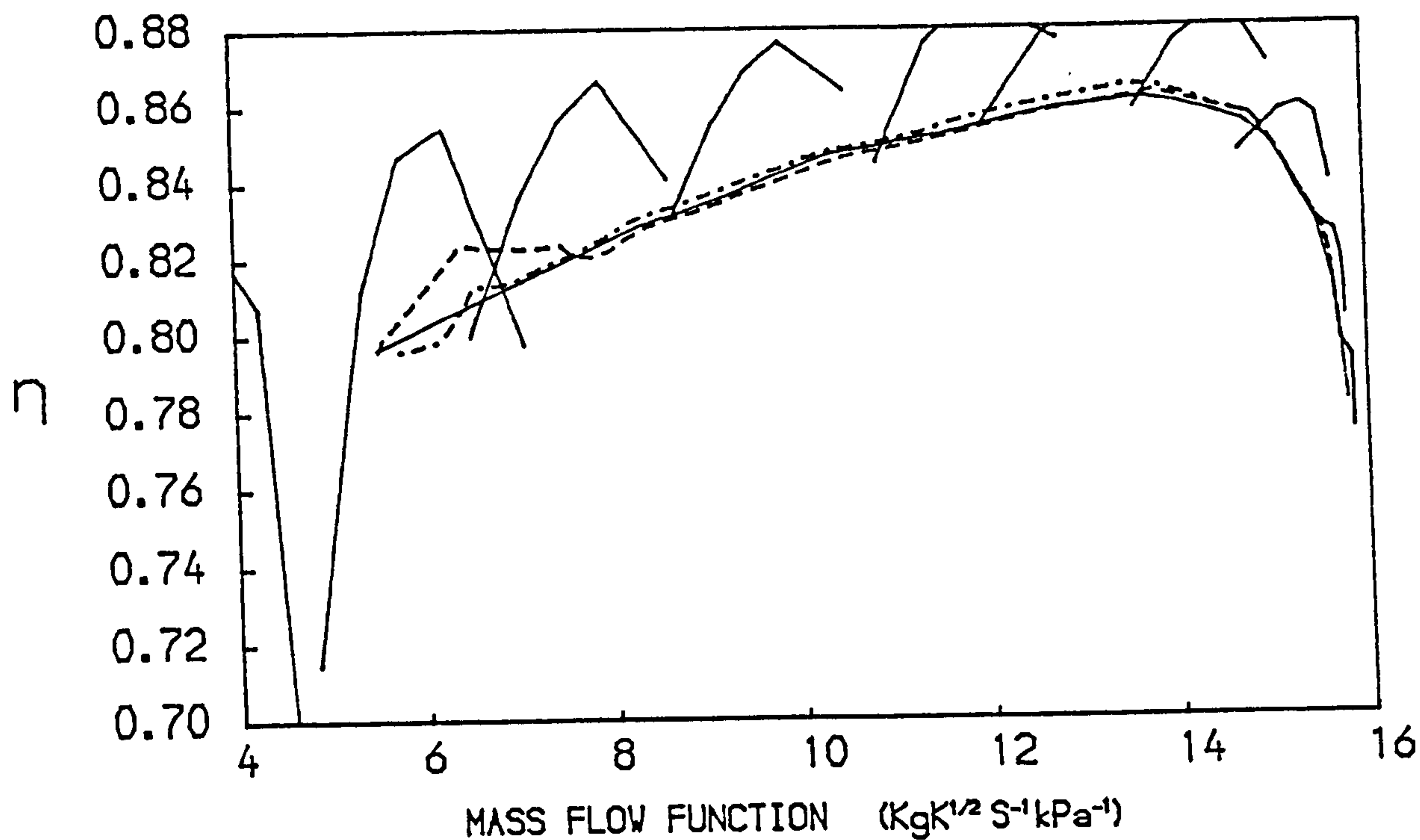


FIG. 34
 PATHS ON THE CHARACTERISTIC MAPS OF THE L.P. COMPRESSOR OF A
 TWO SPOOL BYPASS ENGINE WITH SEPARATE EXHAUSTS
 -- ACCELERATION — STEADY RUNNING --- DECELERATION

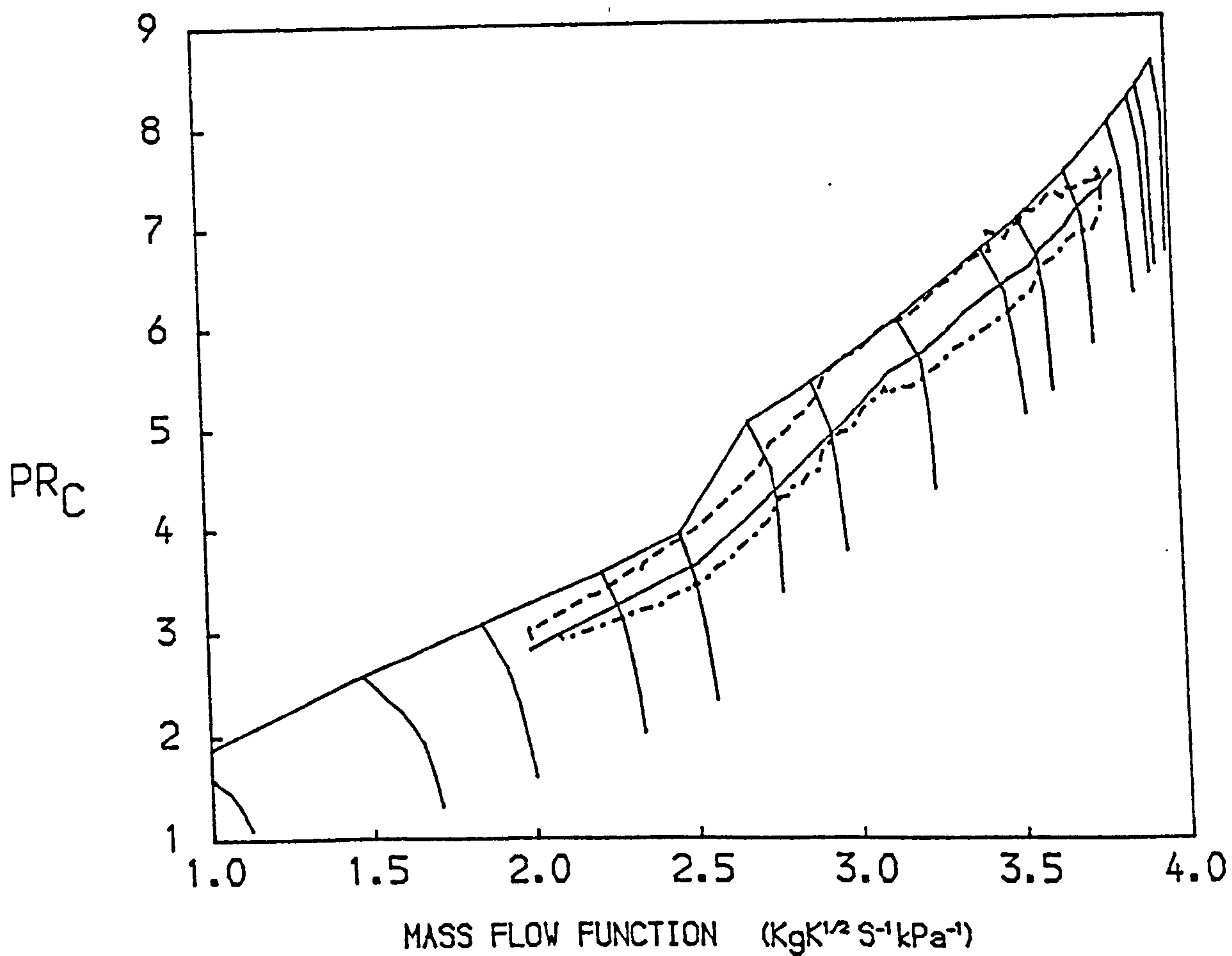
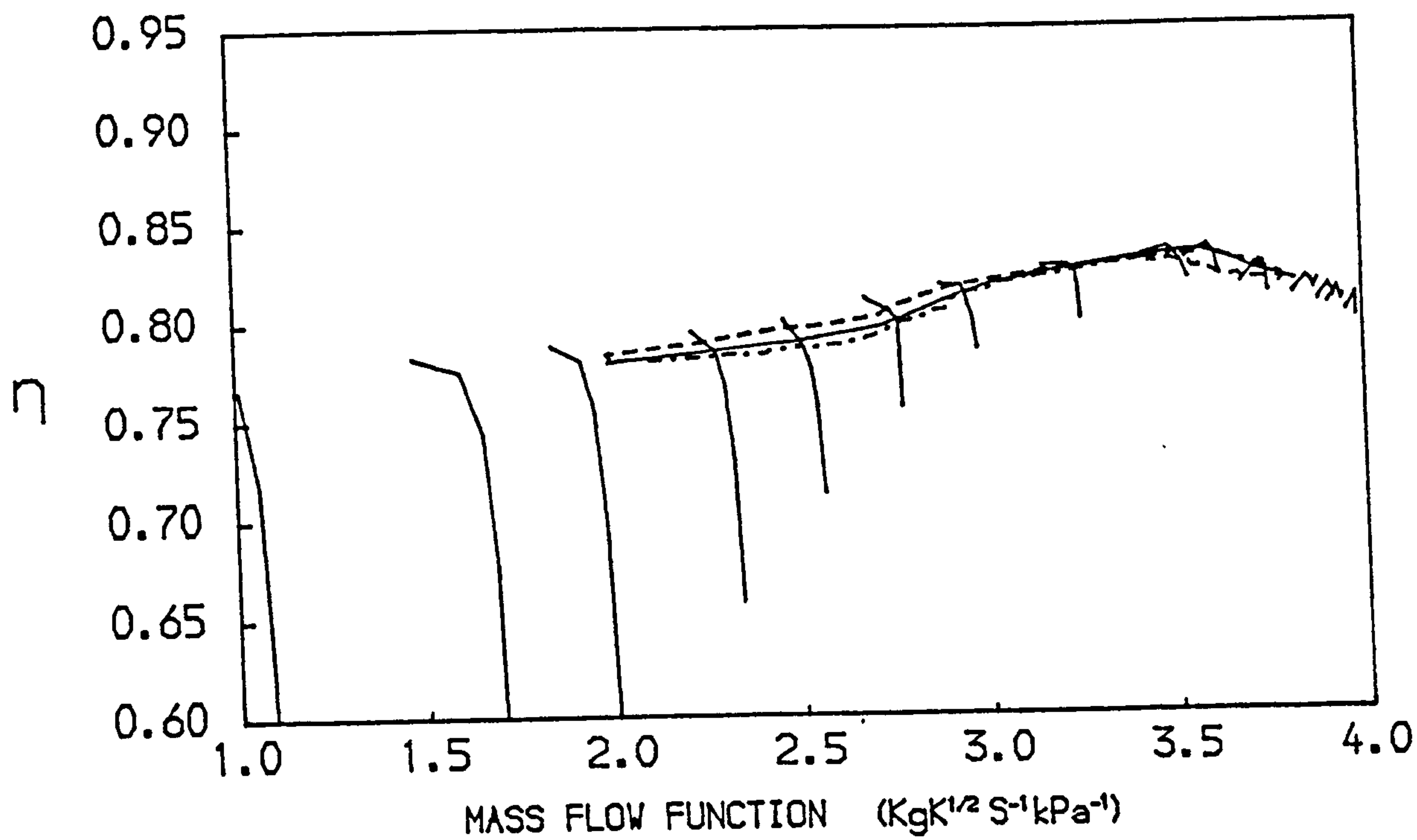


FIG. 35
 PATHS ON THE CHARACTERISTIC MAPS OF THE H.P. COMPRESSOR OF A
 TWO SPOOL BYPASS ENGINE WITH SEPARATE EXHAUSTS
 -- ACCELERATION — STEADY RUNNING ... DECELERATION

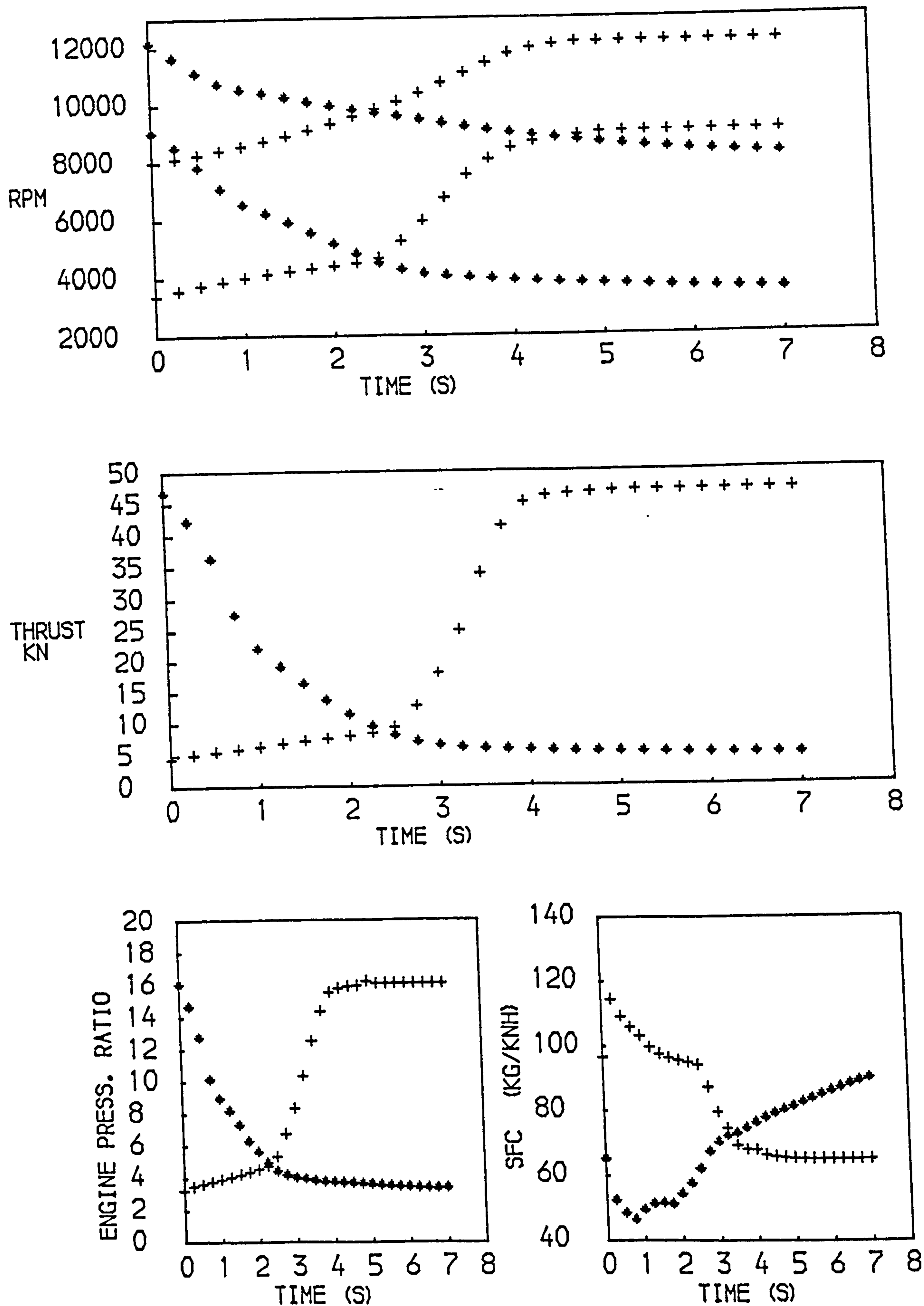


FIG. 36
PERFORMANCE OF A TWO SPOOL BYPASS ENGINE WITH SEPARATE EXHAUSTS
+ACCELERATION • DECELERATION

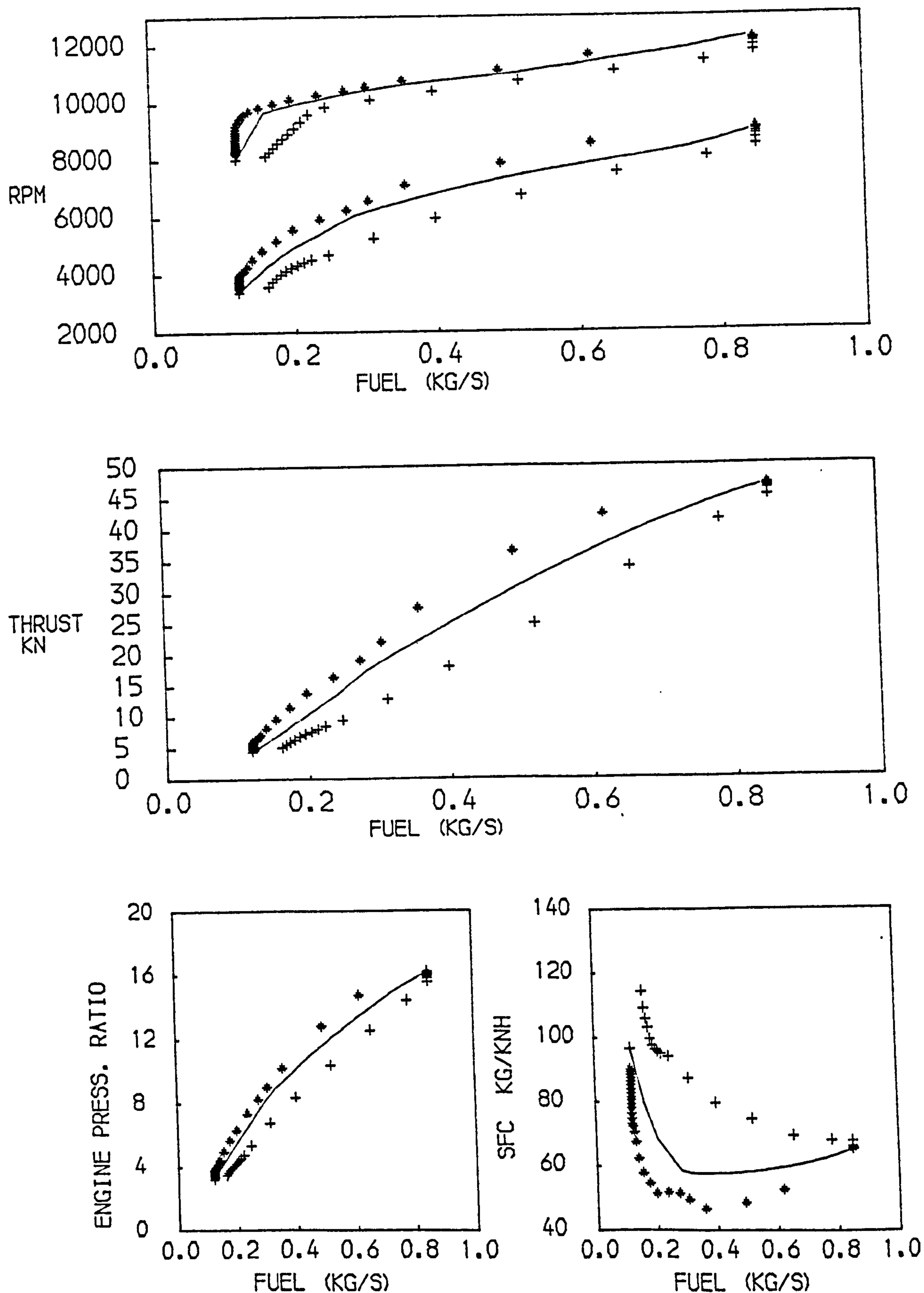


FIG. 37
 PERFORMANCE OF A TWO SPOOL BYPASS ENGINE WITH SEPARATE EXHAUSTS
 +ACCELERATION * DECELERATION —STEADY RUNNING

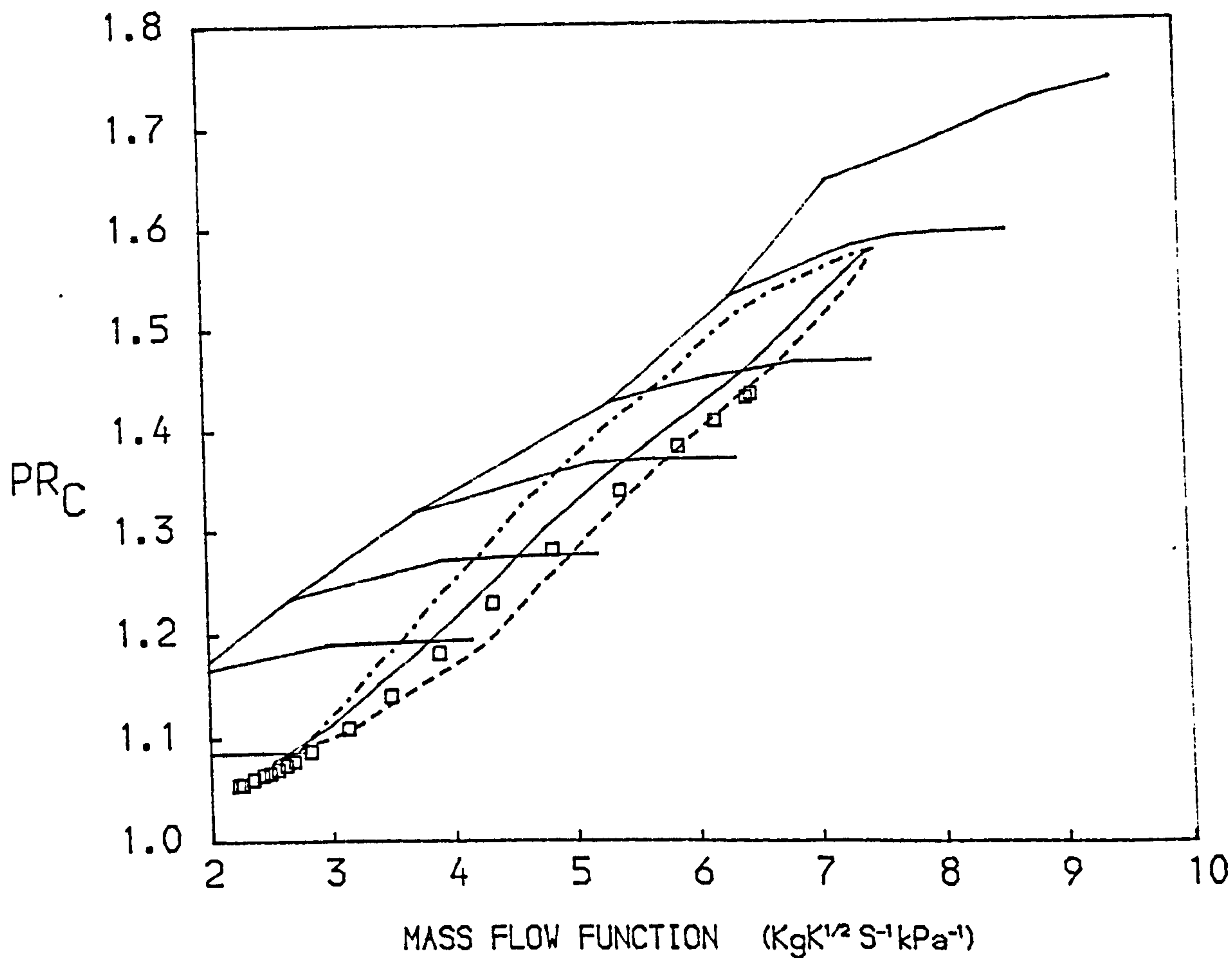
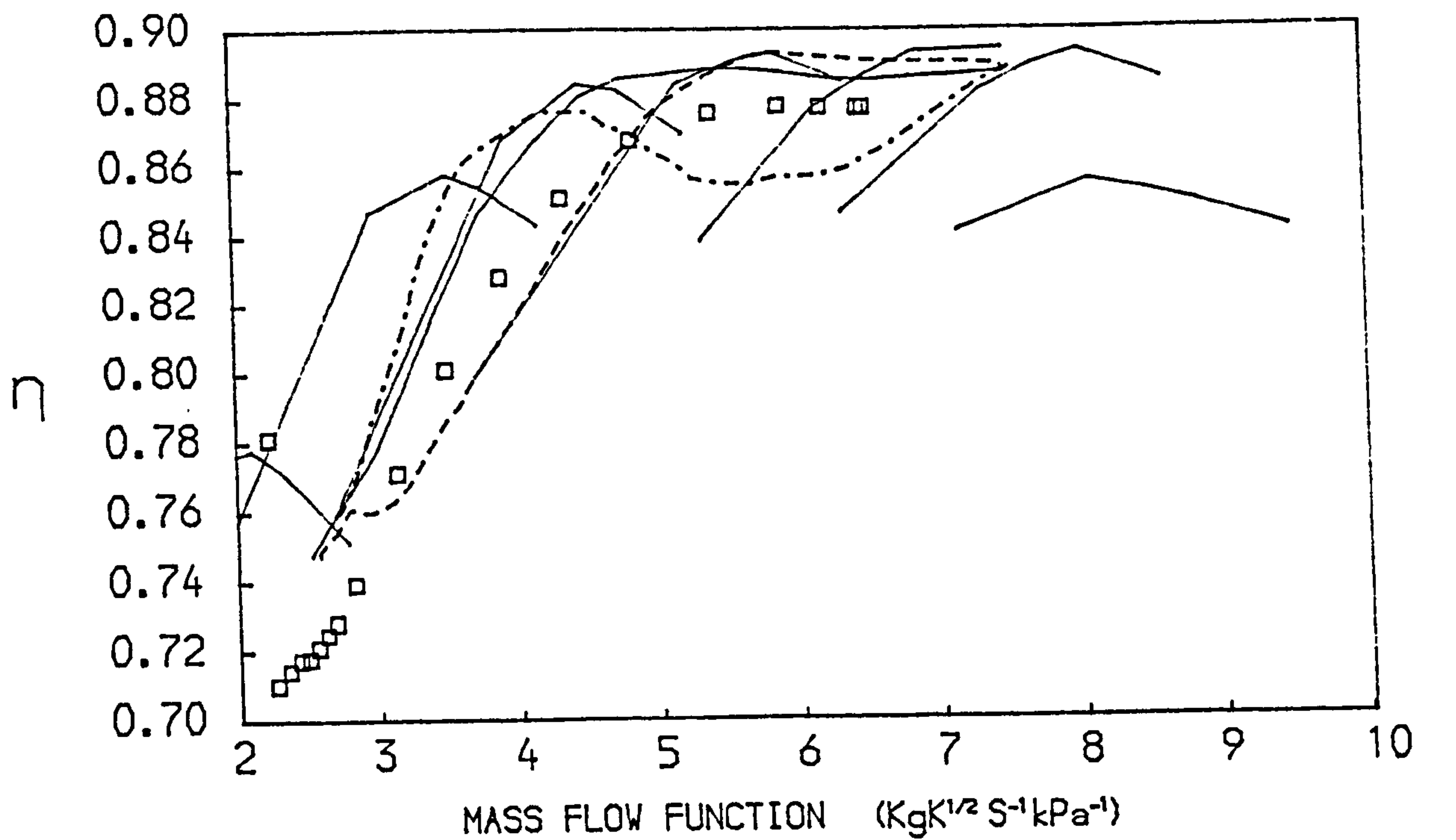


FIG. 38
 PATHS ON THE CHARACTERISTIC MAPS OF THE INNER FAN OF A
 TWO SPOOL TURBOFAN WITH MIXED EXHAUSTS
 -- ACCELERATION — STEADY RUNNING --- DECELERATION
 \square STEADY RUNNING RESULTS FROM REF. 75 AT SEA LEVEL

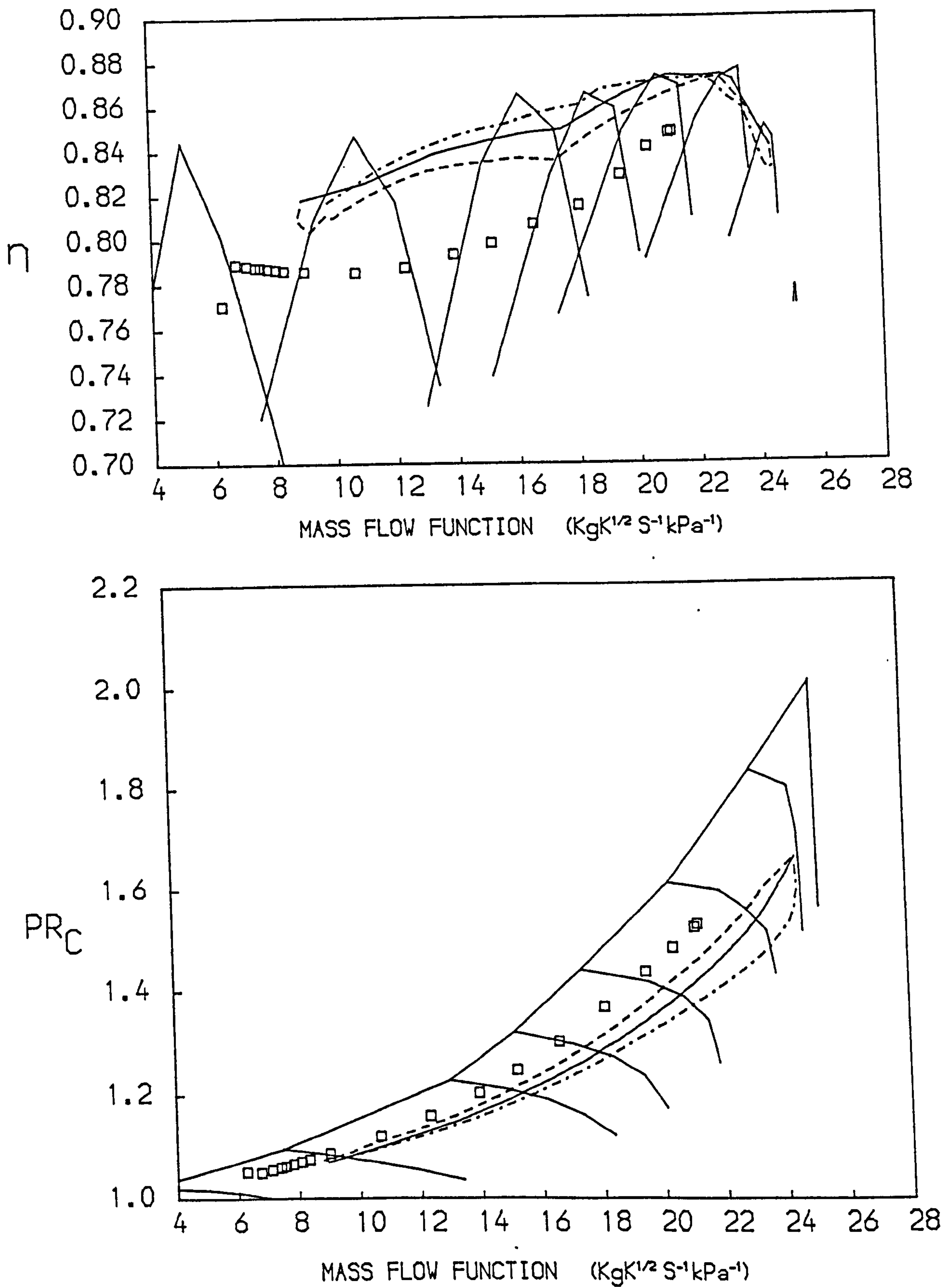


FIG. 39
 PATHS ON THE CHARACTERISTIC MAPS OF THE OUTER FAN OF A
 TWO SPOOL TURBOFAN WITH MIXED EXHAUSTS
 -- ACCELERATION — STEADY RUNNING --- DECELERATION
 □ STEADY RUNNING RESULTS FROM REF. 75 AT SEA LEVEL

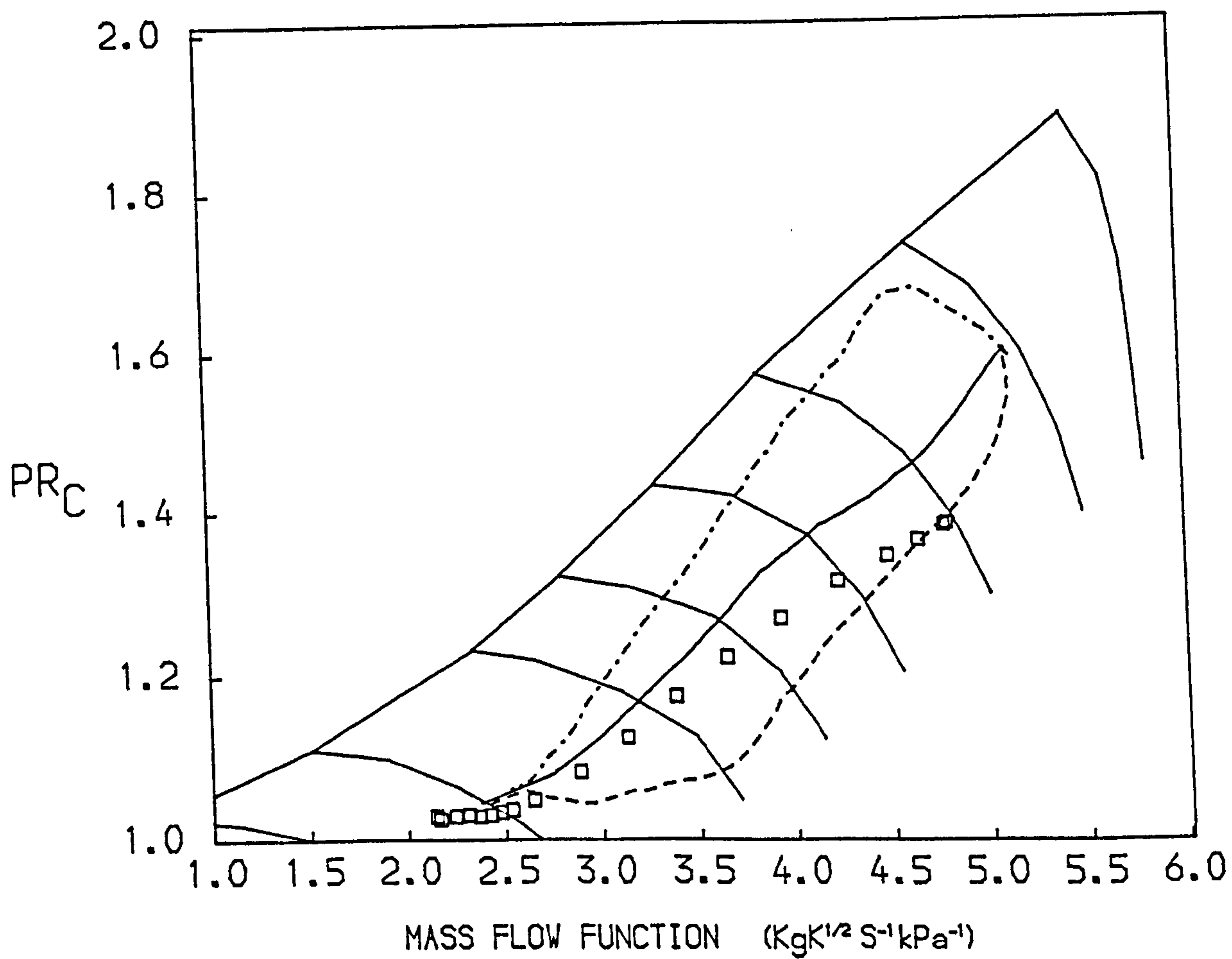
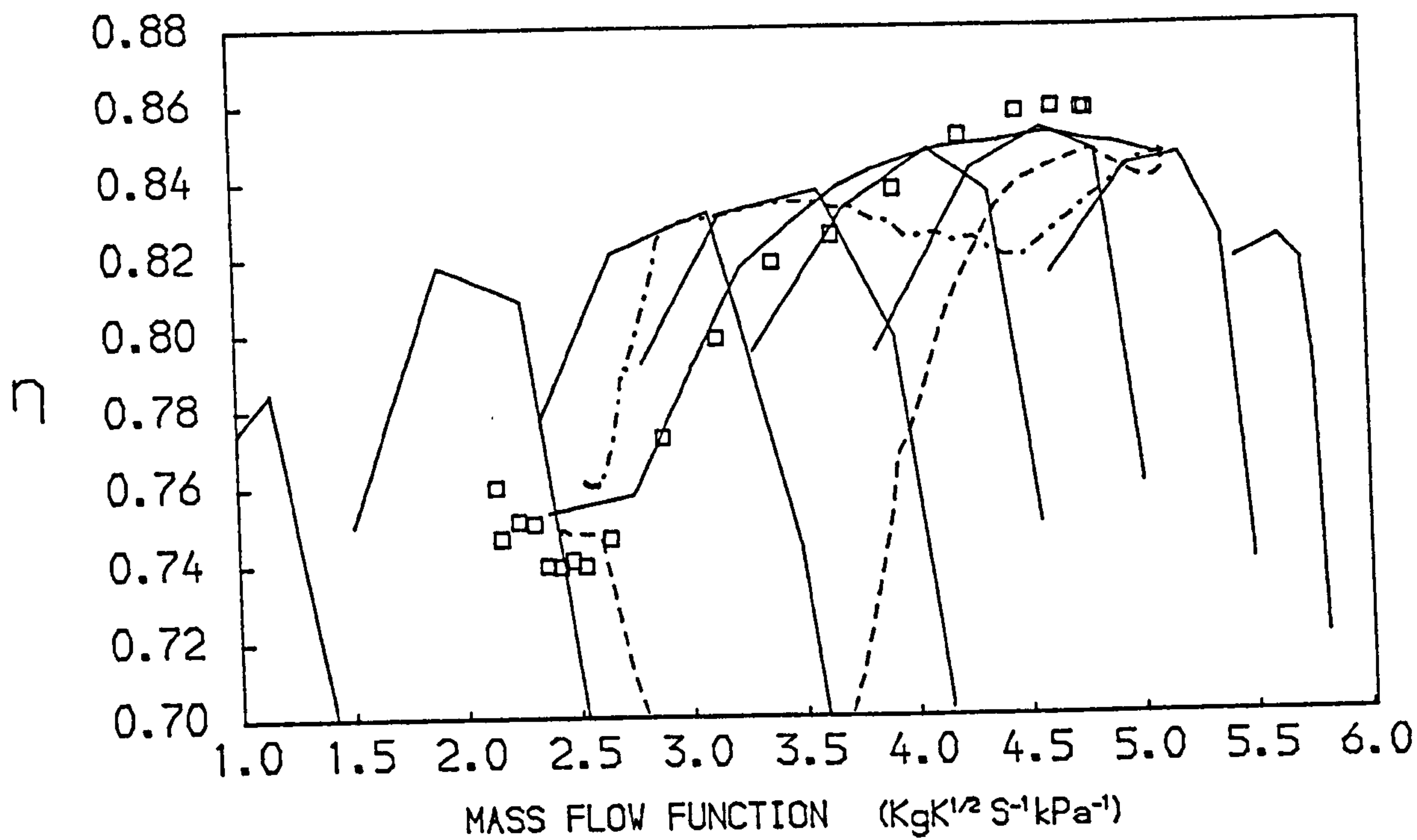


FIG. 40
 PATHS ON THE CHARACTERISTIC MAPS OF THE I.P. COMPRESSOR OF A
 TWO SPOOL TURBOFAN WITH MIXED EXHAUSTS
 -- ACCELERATION — STEADY RUNNING --- DECELERATION
 □ STEADY RUNNING RESULTS FROM REF. 75 AT SEA LEVEL

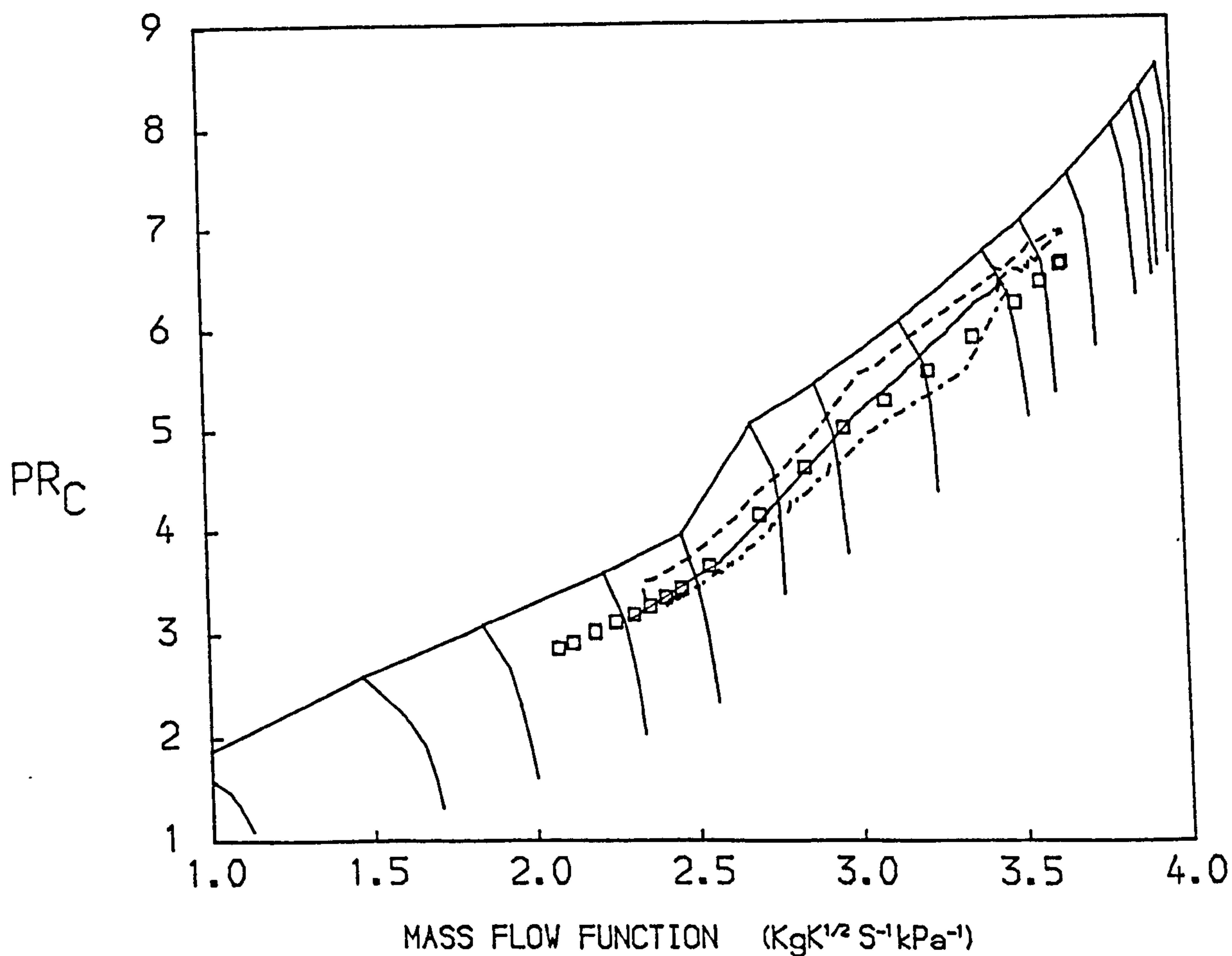
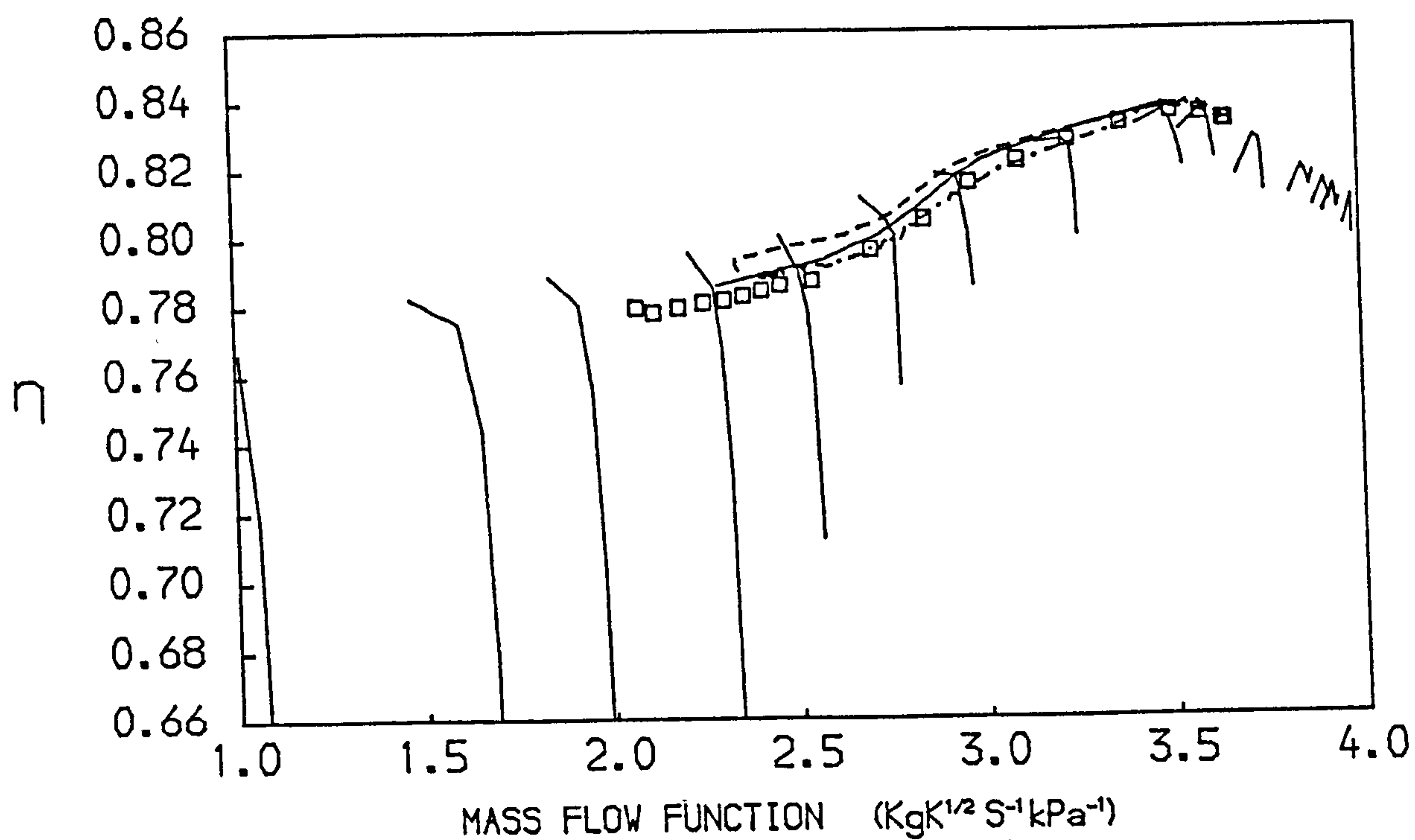


FIG. 41
 PATHS ON THE CHARACTERISTIC MAPS OF THE H.P. COMPRESSOR OF A
 TWO SPOOL TURBOFAN WITH MIXED EXHAUSTS
 -- ACCELERATION — STEADY RUNNING --- DECELERATION
 □ STEADY RUNNING RESULTS FROM REF. 75 AT SEA LEVEL

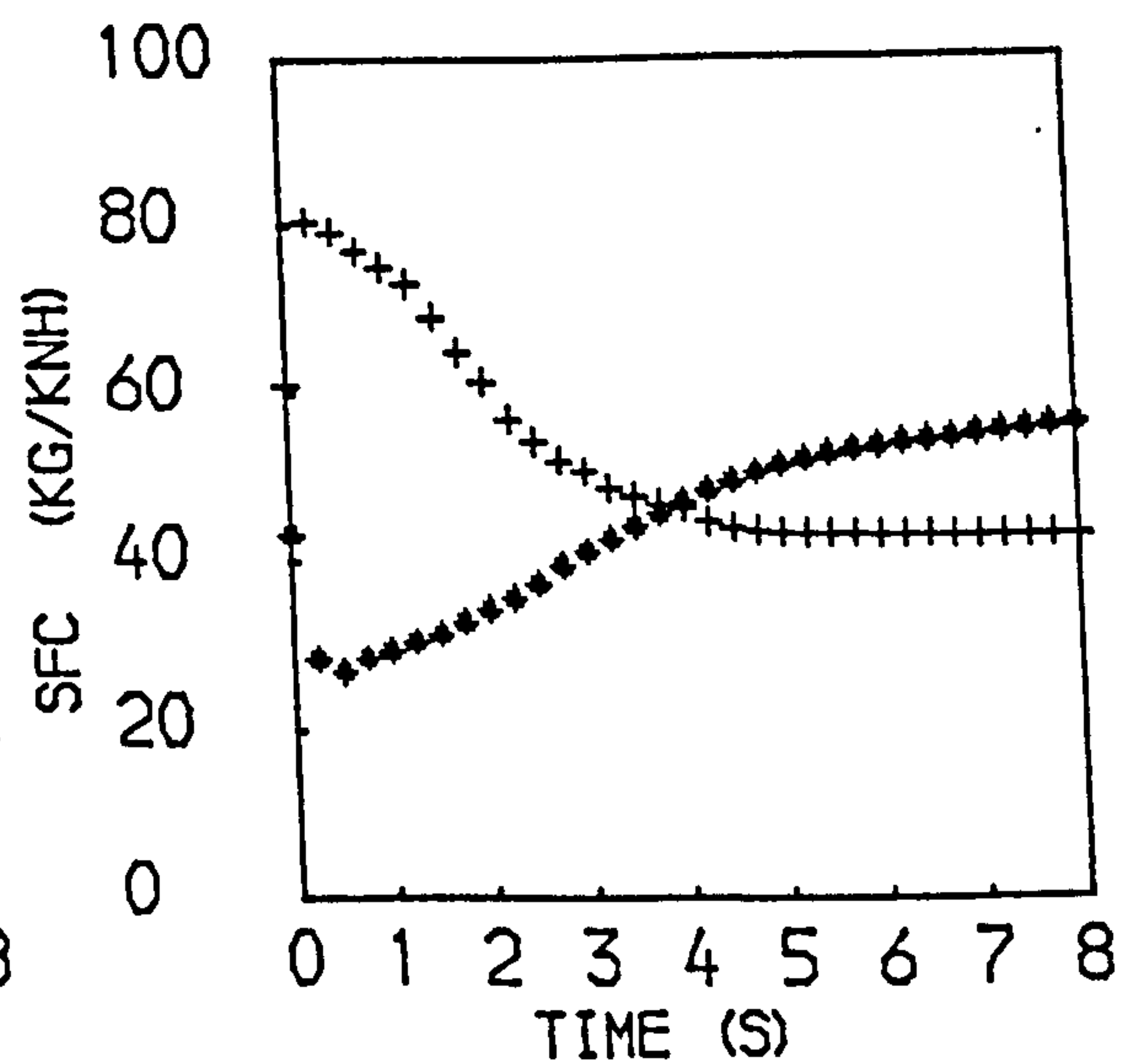
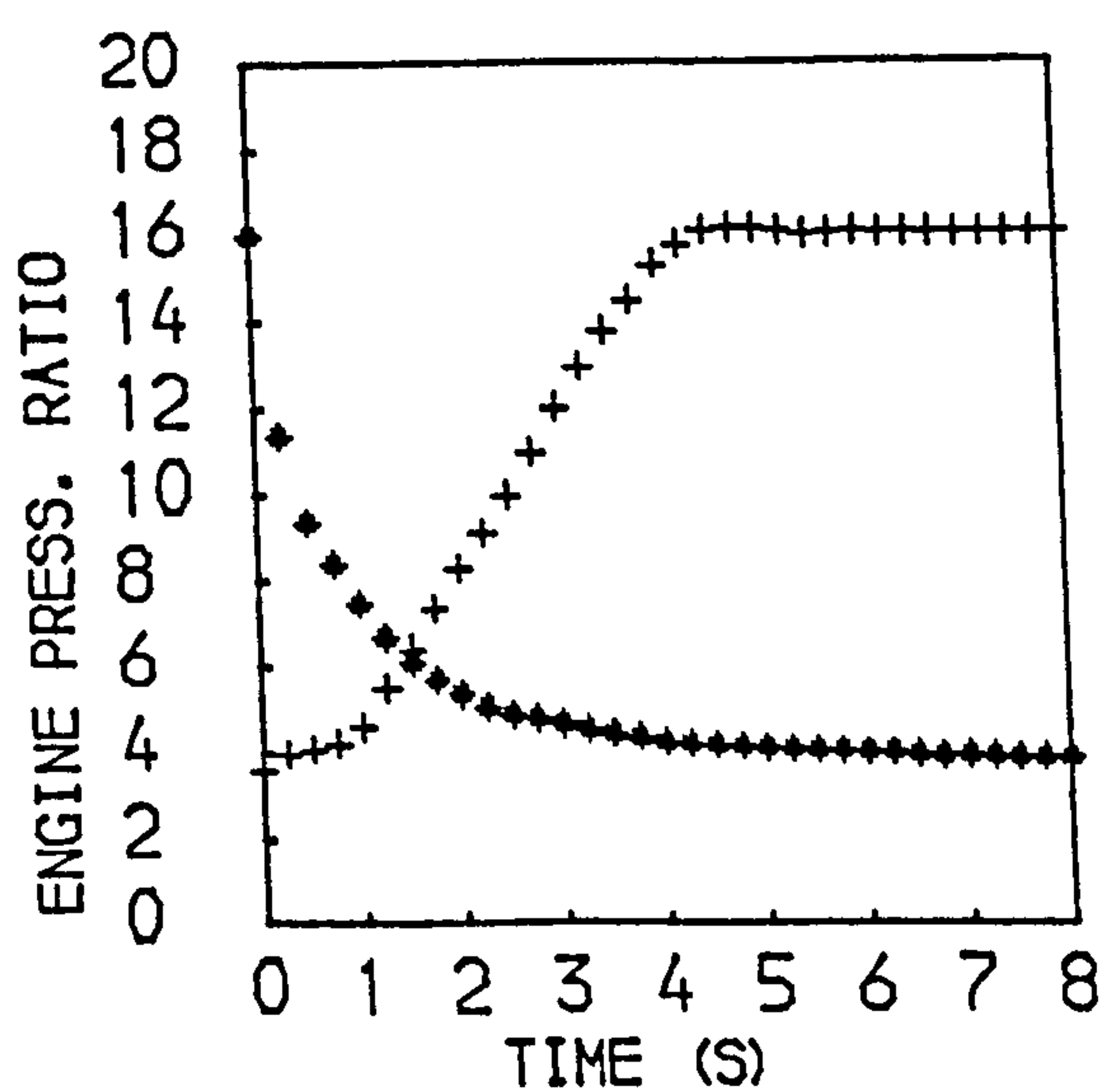
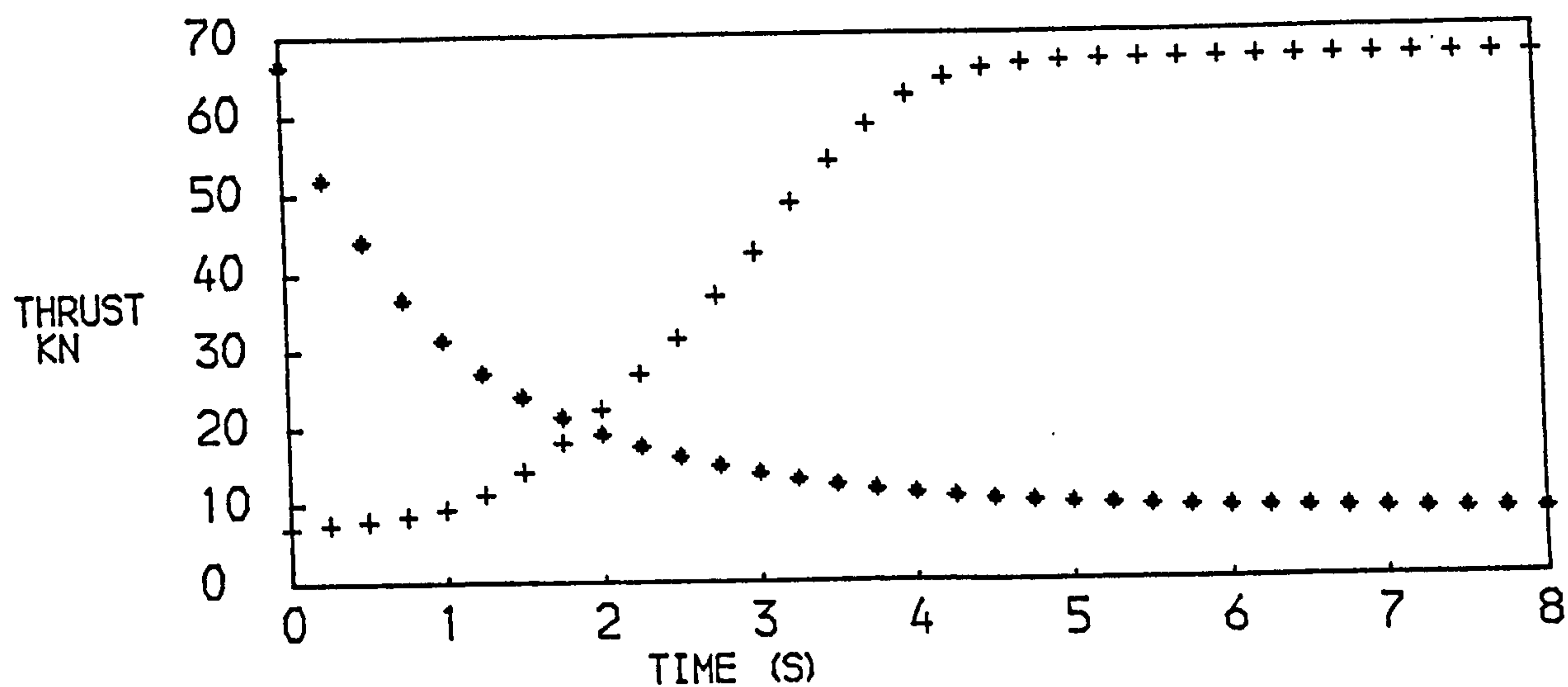
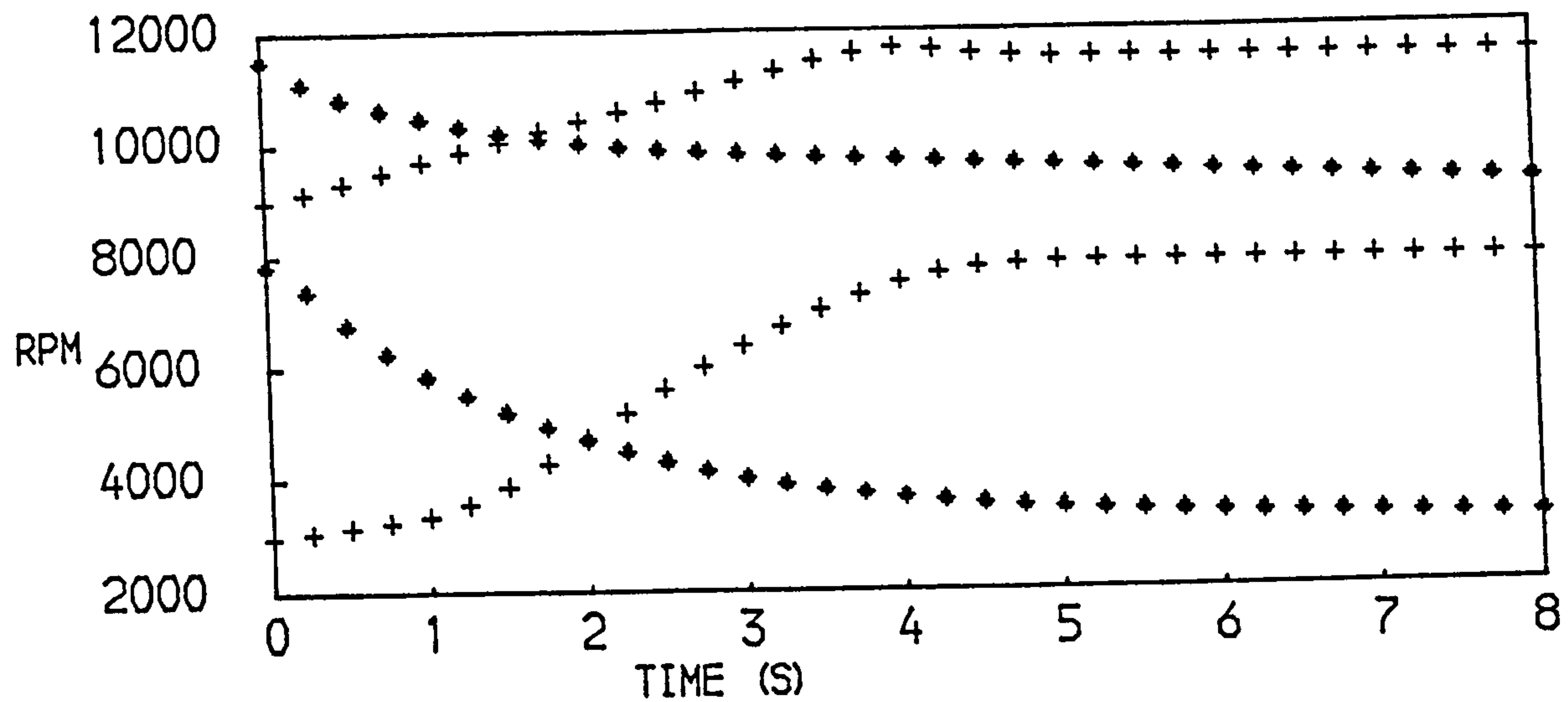


FIG. 42
PERFORMANCE OF A TWO SPOOL TURBOFAN WITH MIXED EXHAUSTS
+ACCELERATION ♦ DECELERATION

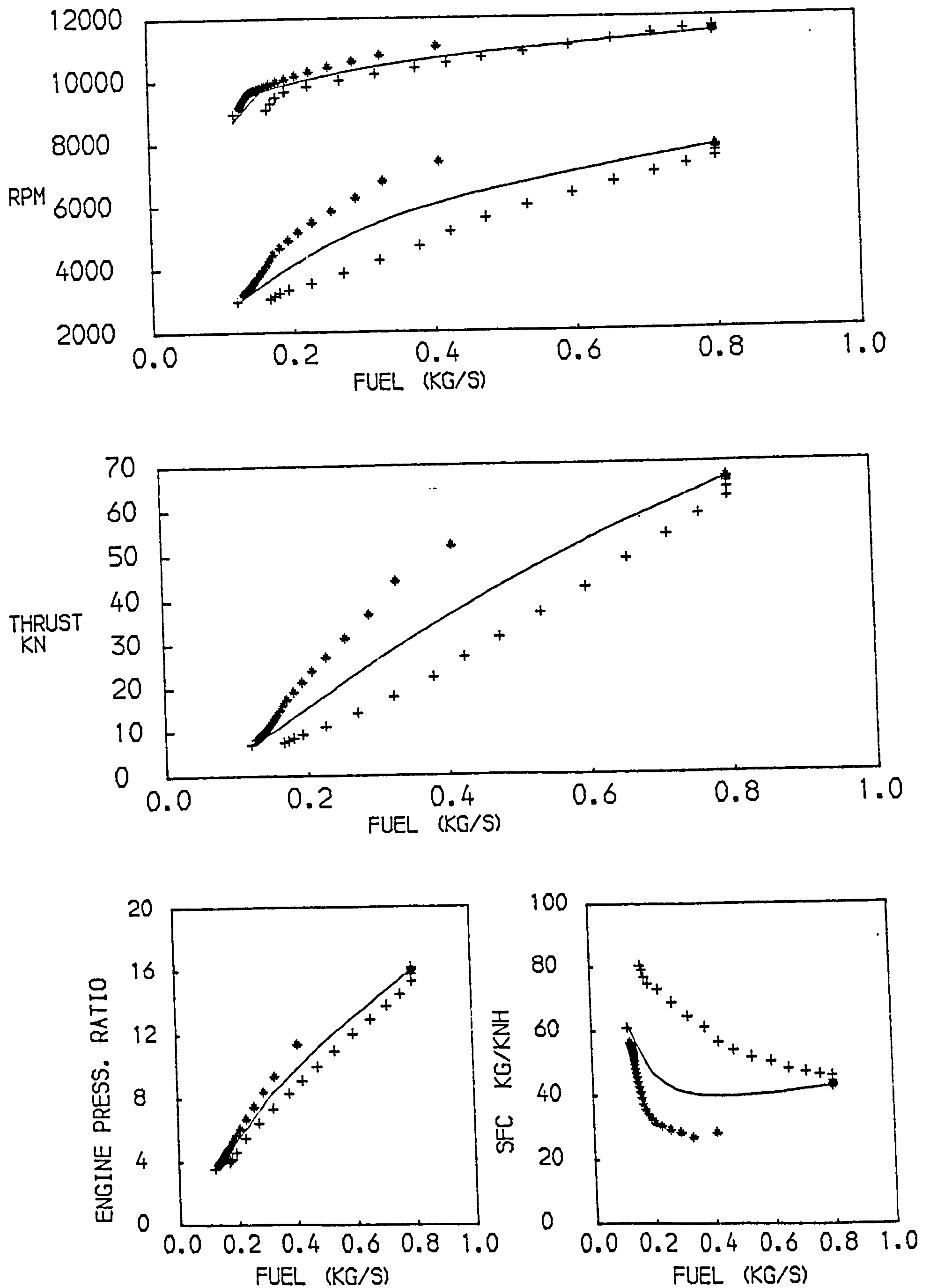


FIG. 43
 PERFORMANCE OF A TWO SPOOL TURBOFAN WITH MIXED EXHAUSTS
 +ACCELERATION * DECELERATION —STEADY RUNNING

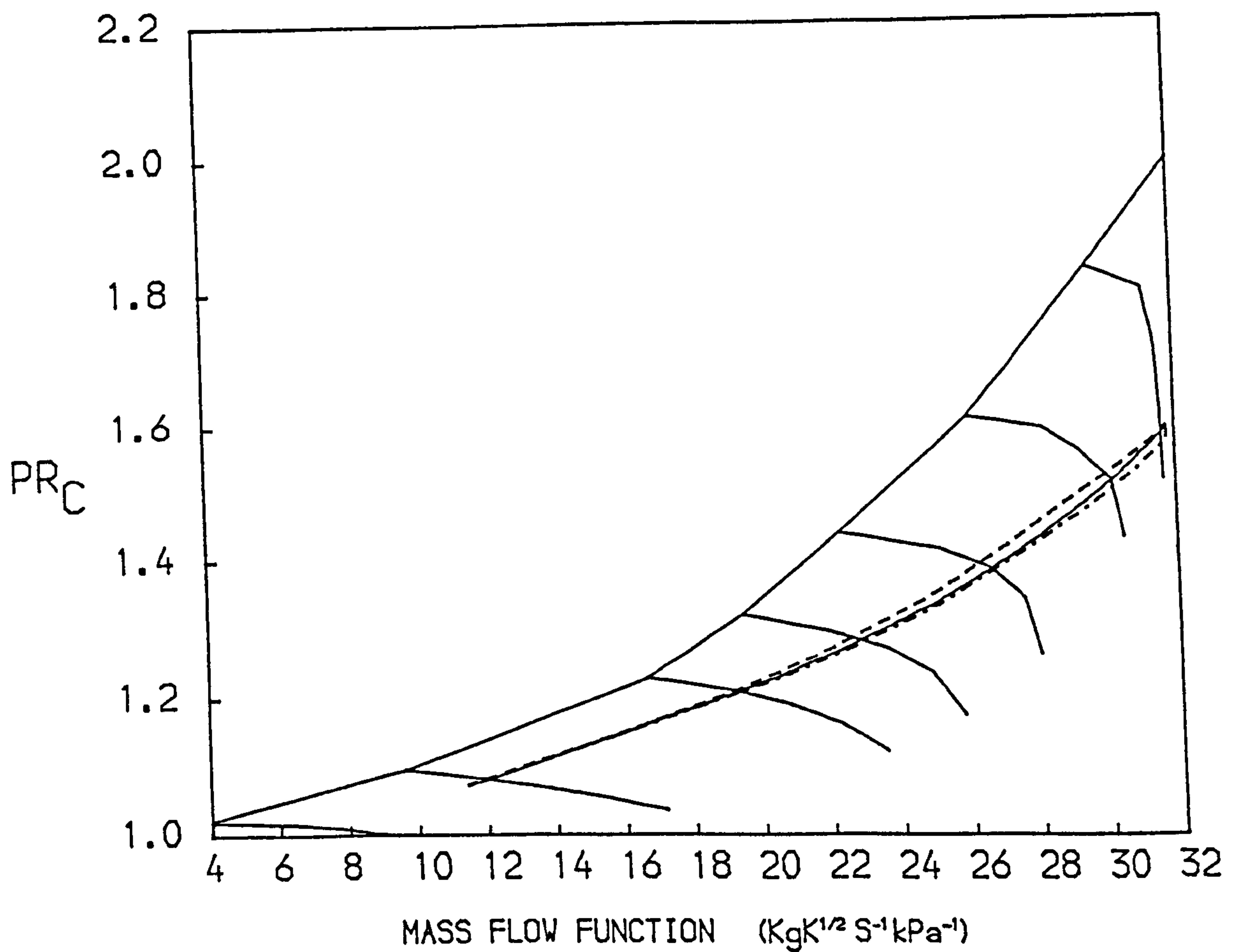
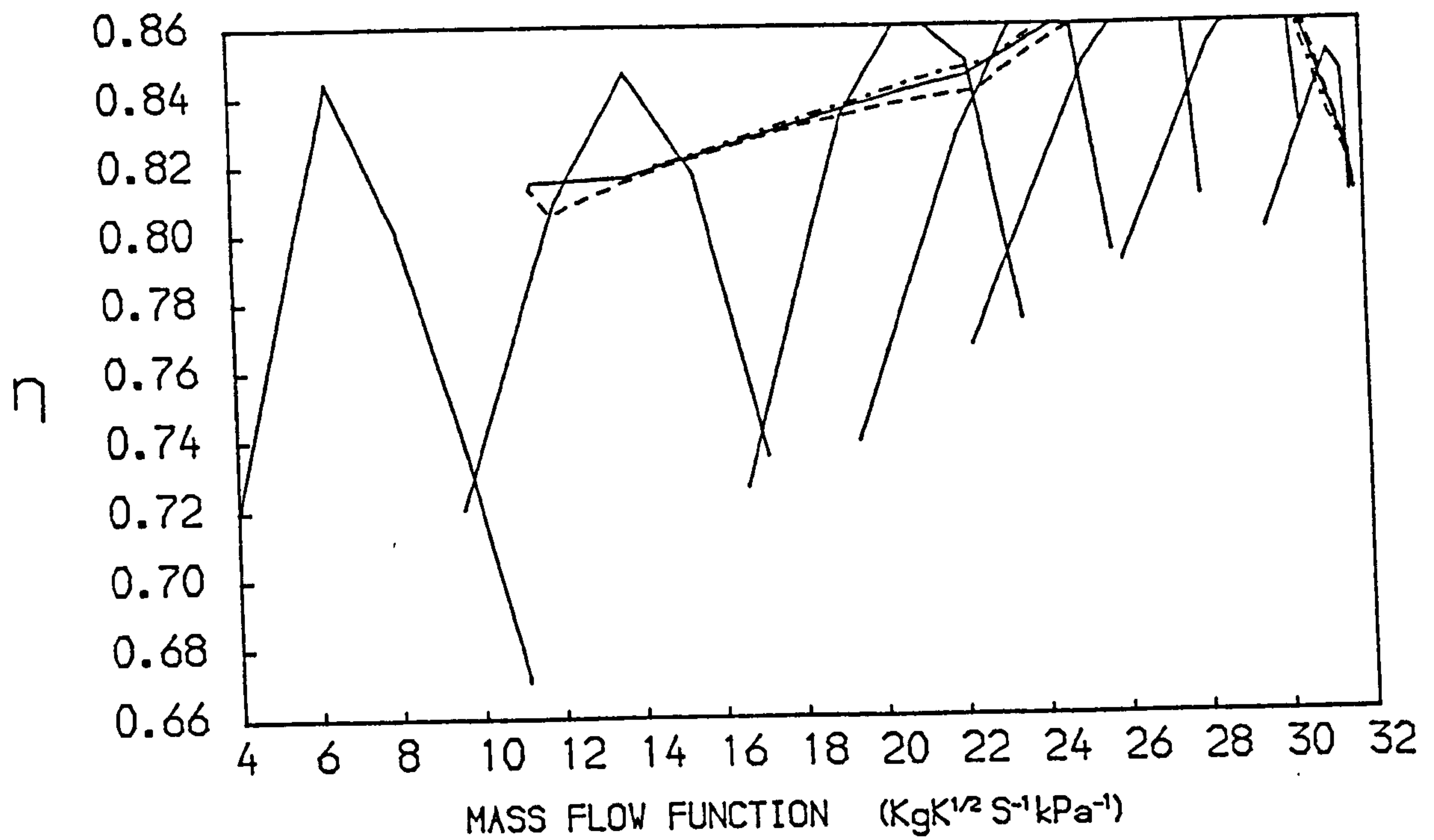


FIG. 44
 PATHS ON THE CHARACTERISTIC MAPS OF THE FAN OF A
 TWO SPOOL TURBOFAN WITH MIXED EXHAUSTS
 -- ACCELERATION — STEADY RUNNING --- DECELERATION

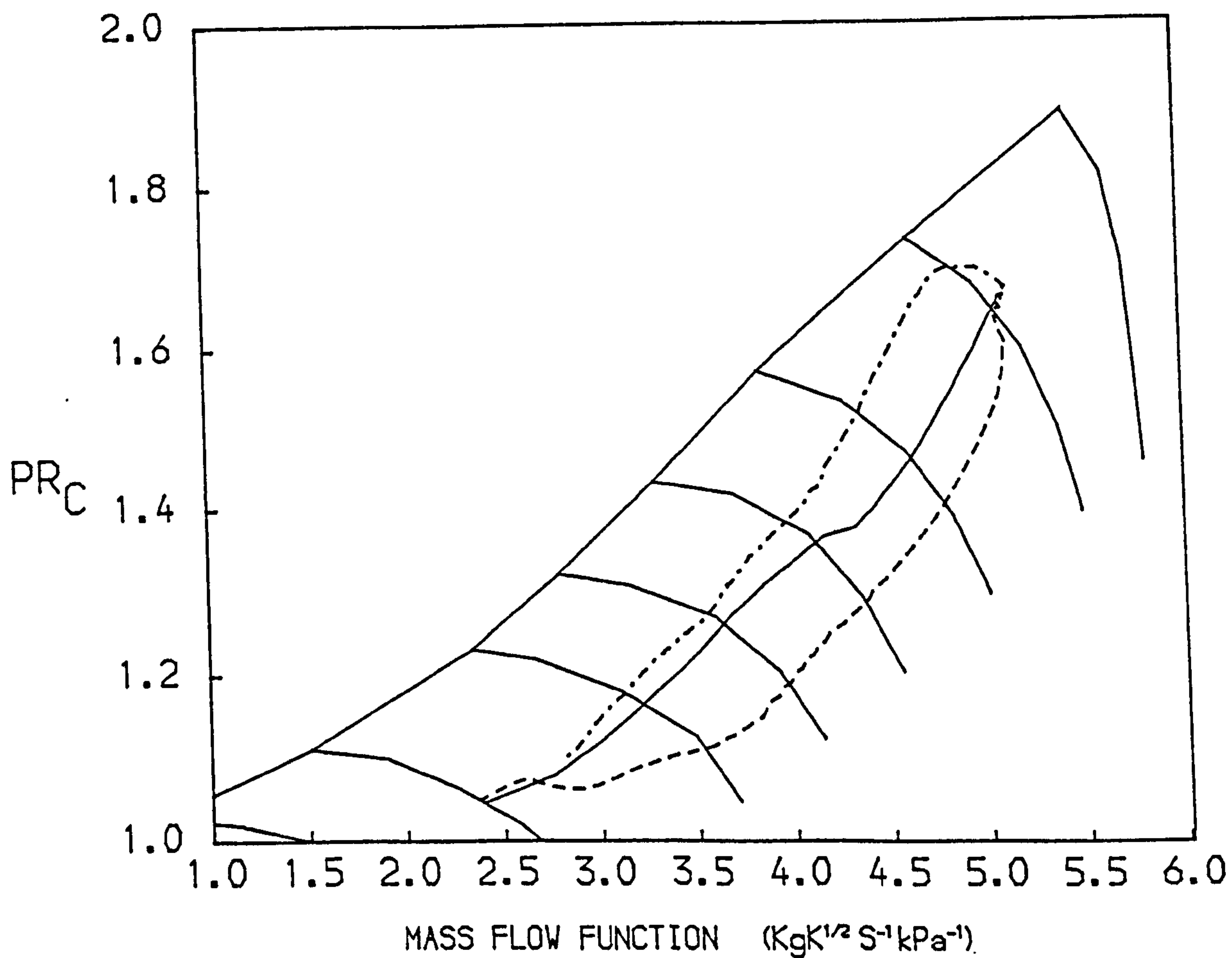
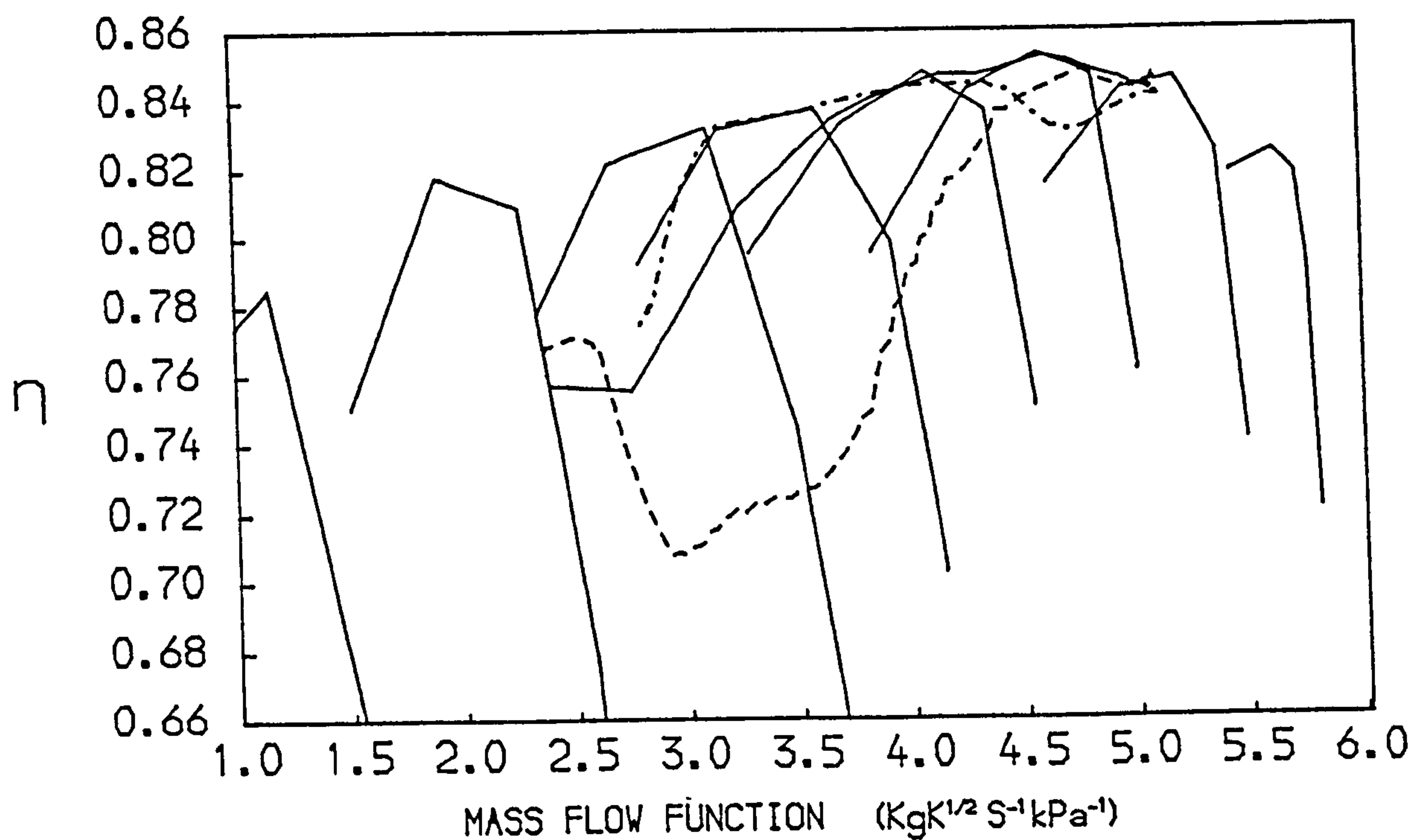


FIG. 45
 PATHS ON THE CHARACTERISTIC MAPS OF THE I.P. COMPRESSOR OF A
 TWO SPOOL TURBOFAN WITH MIXED EXHAUSTS
 -- ACCELERATION — STEADY RUNNING --- DECELERATION

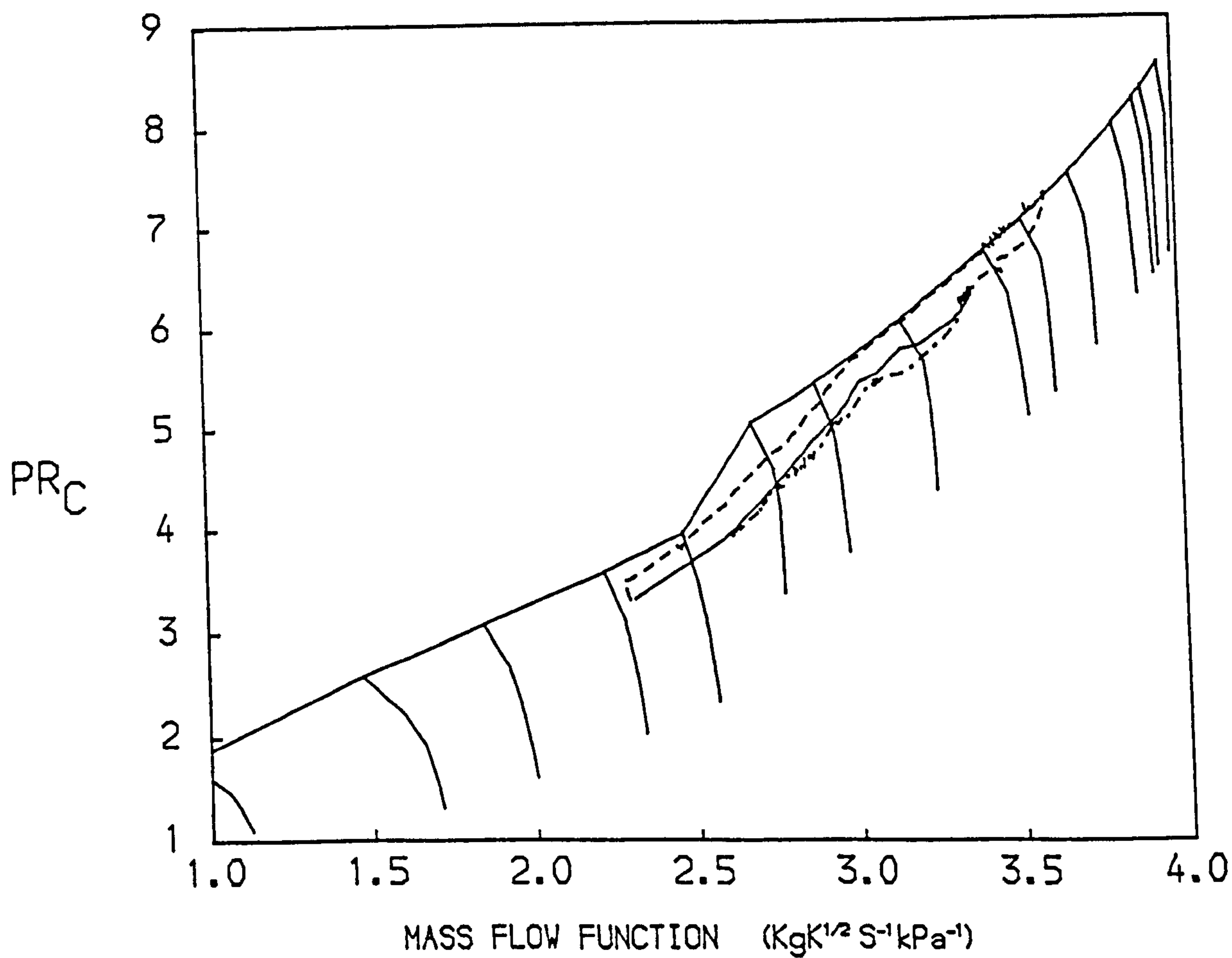
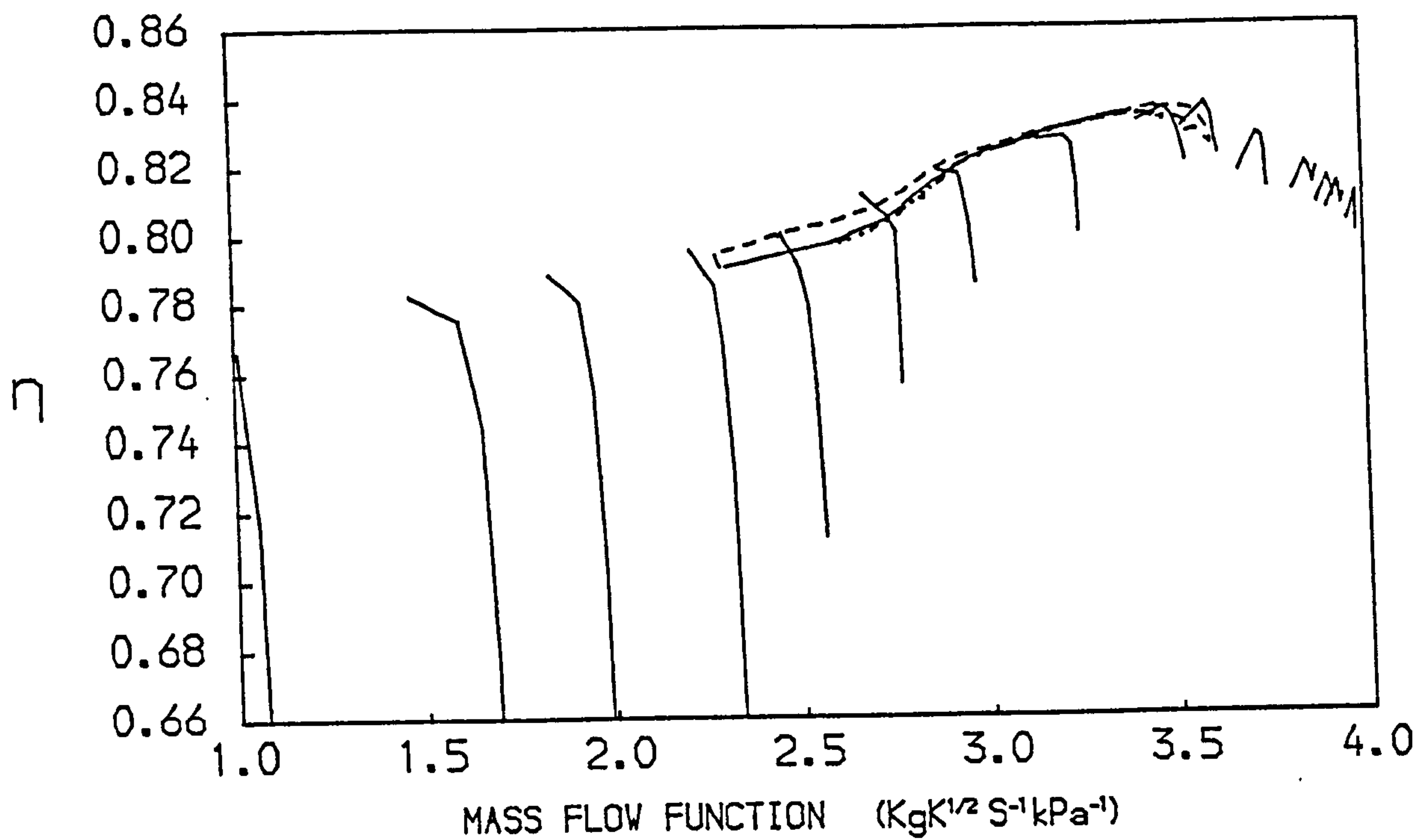


FIG. 46
 PATHS ON THE CHARACTERISTIC MAPS OF THE H.P. COMPRESSOR OF A
 TWO SPOOL TURBOFAN WITH MIXED EXHAUSTS
 -- ACCELERATION — STEADY RUNNING --- DECELERATION

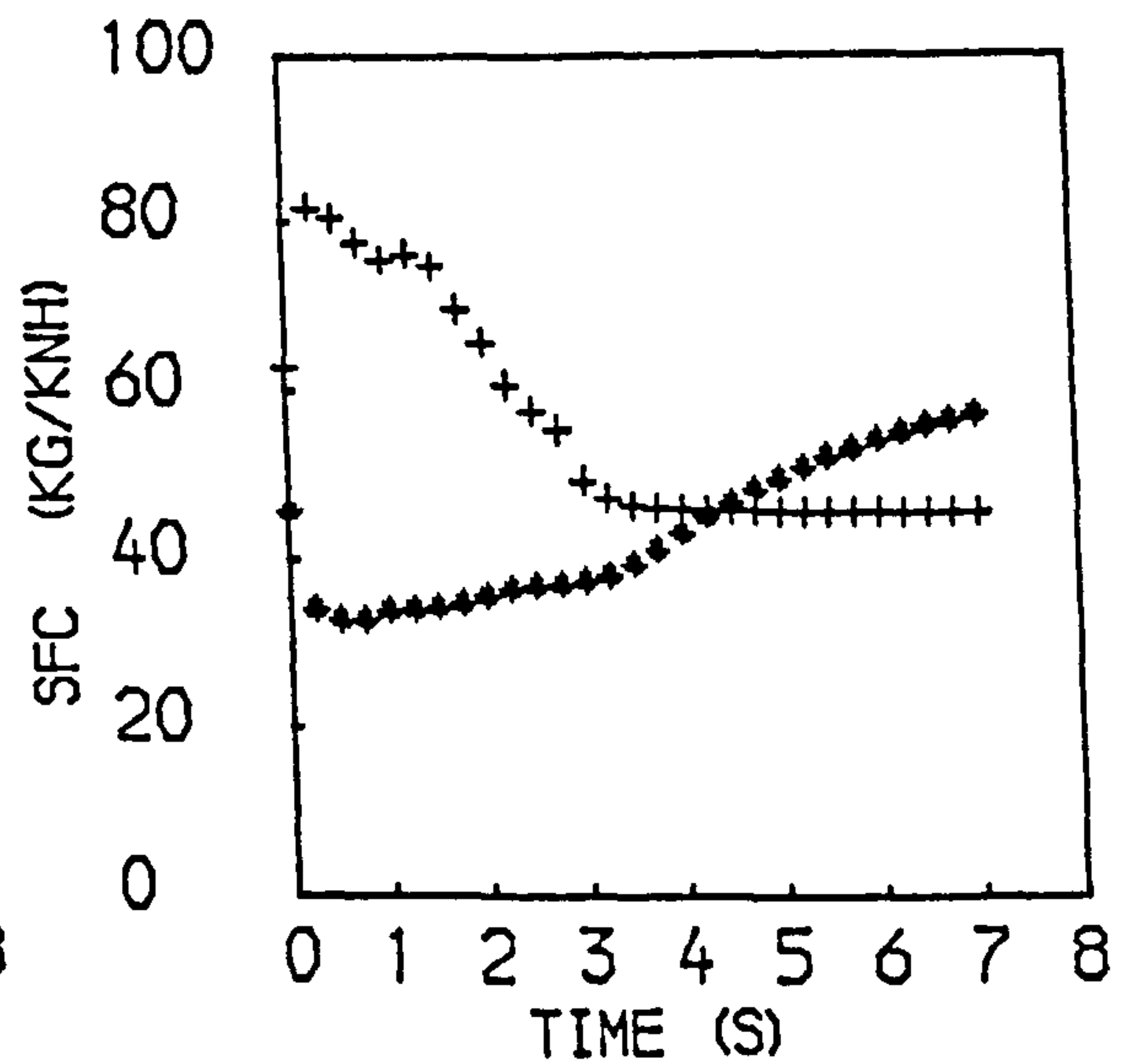
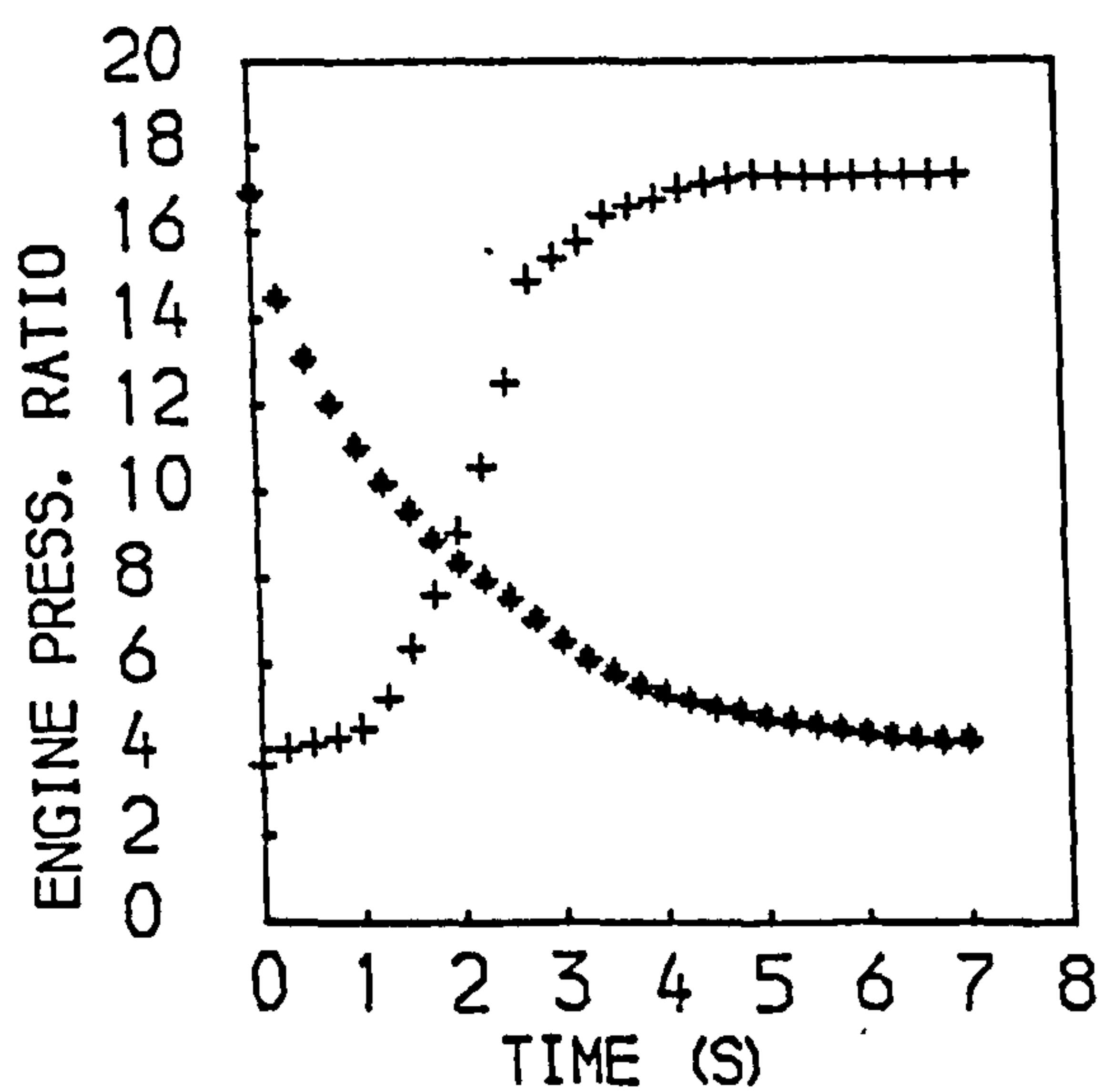
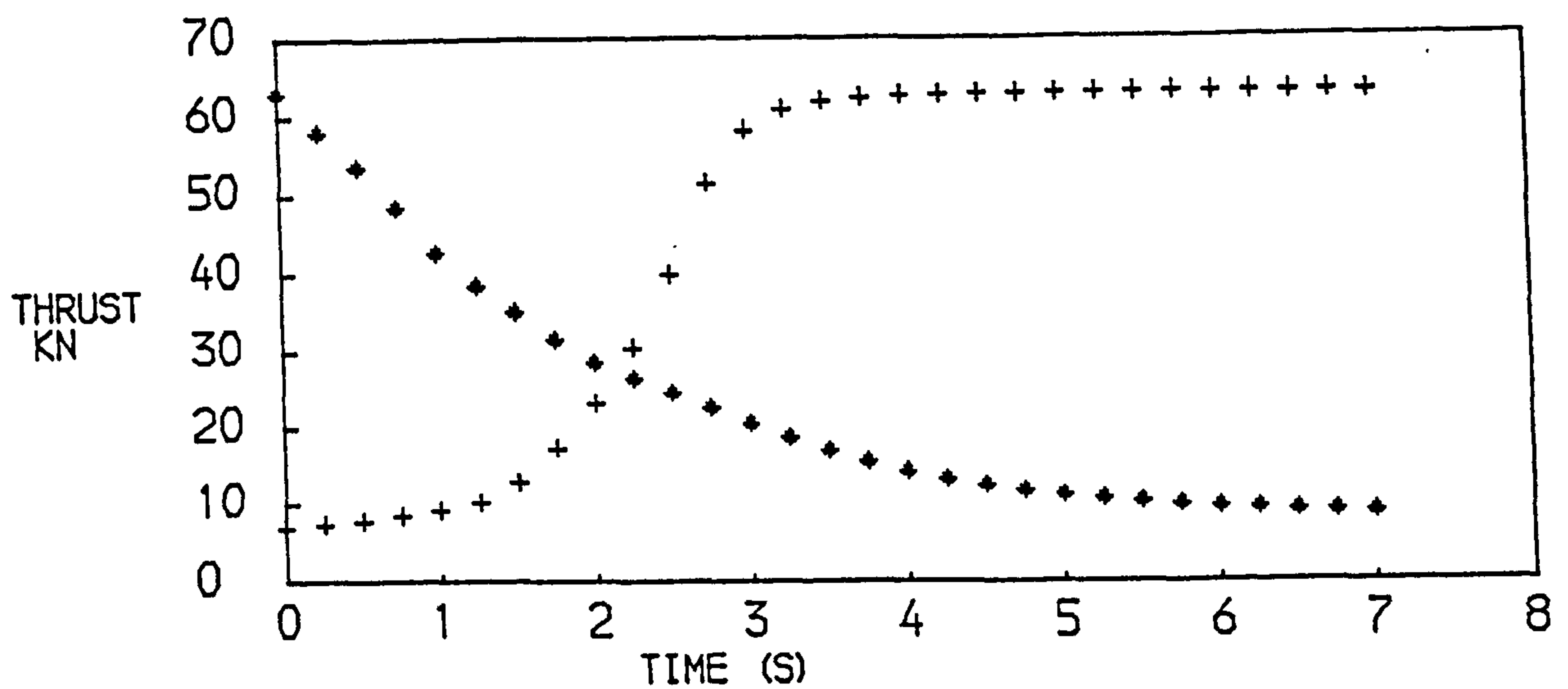
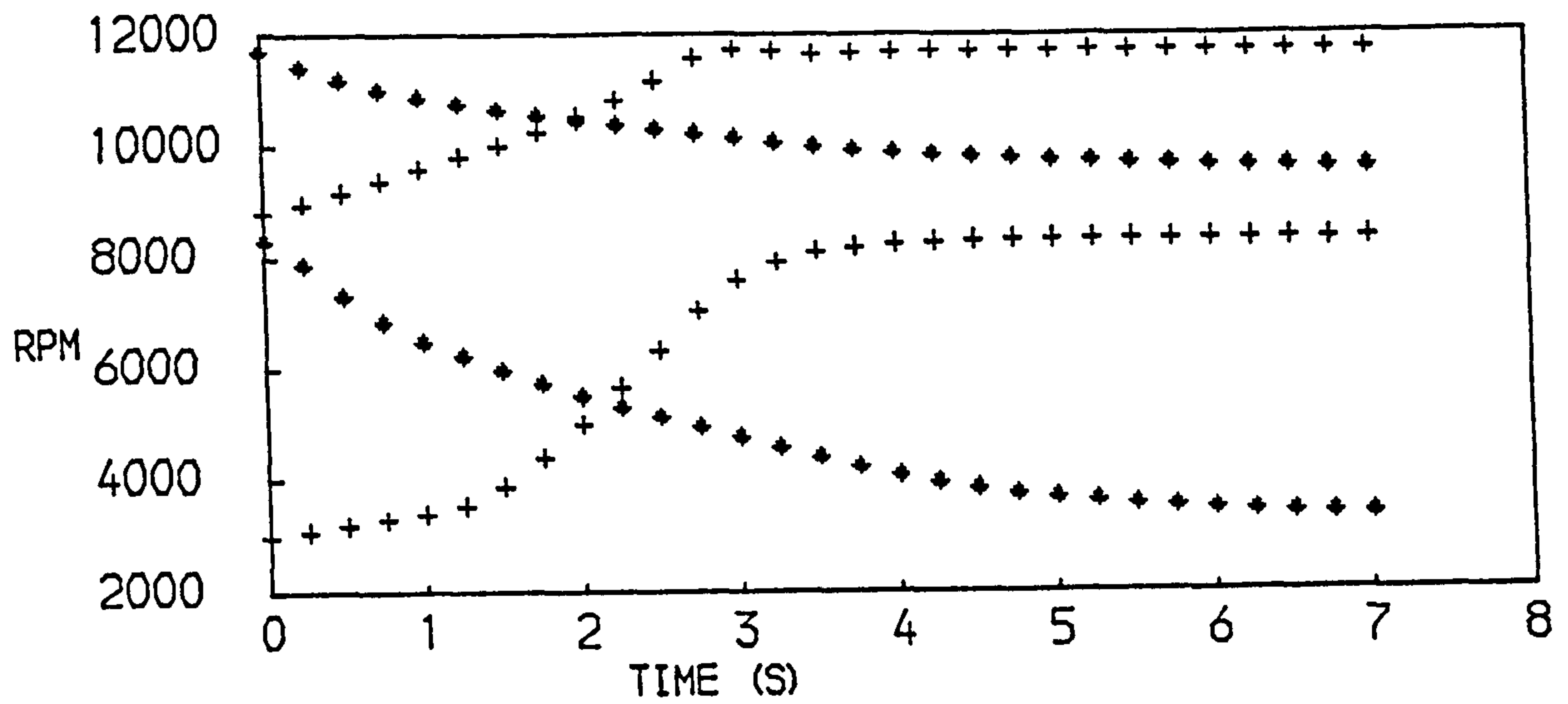


FIG. 47
PERFORMANCE OF A TWO SPOOL TURBOFAN WITH MIXED EXHAUSTS
+ACCELERATION ◆ DECELERATION

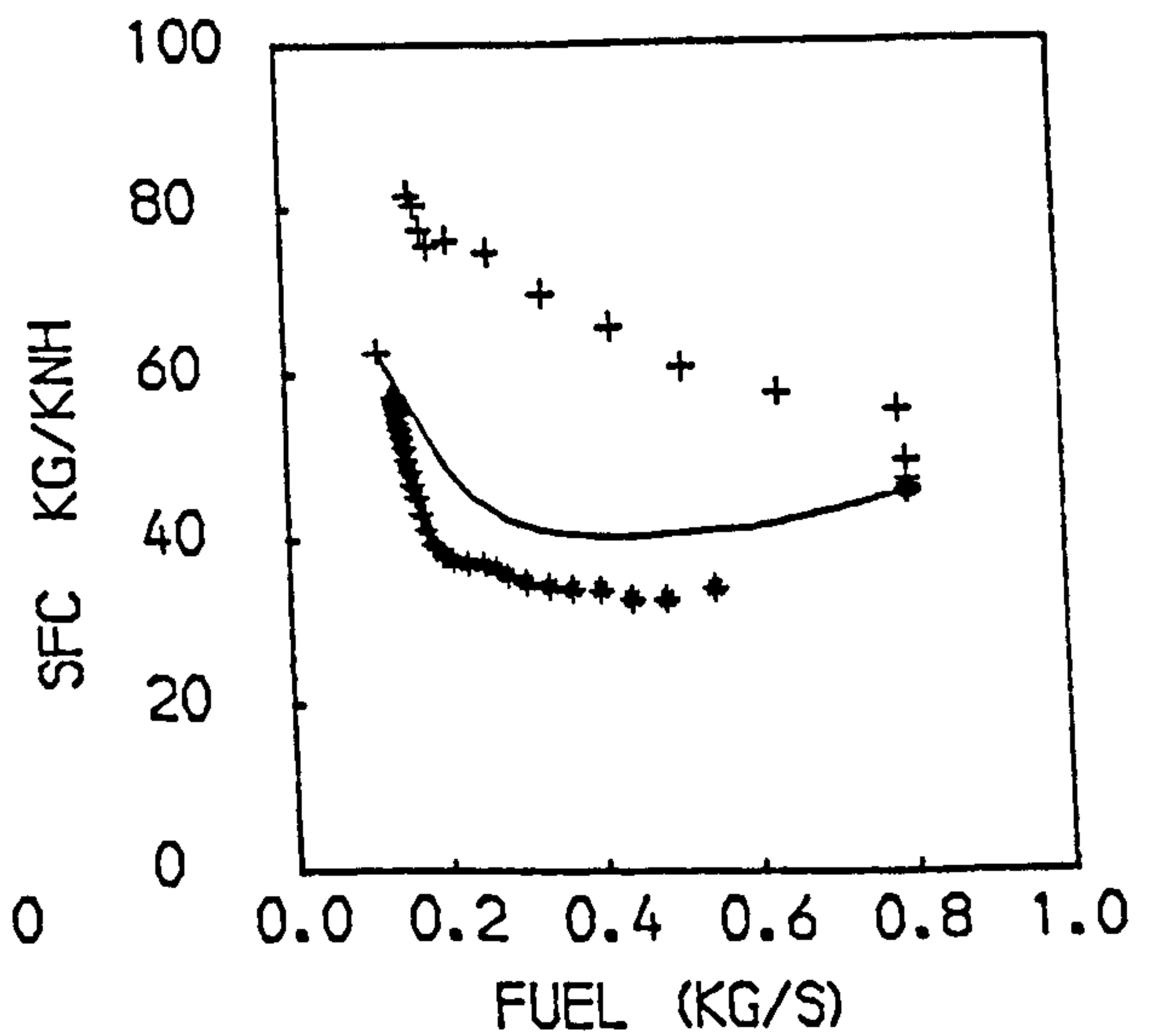
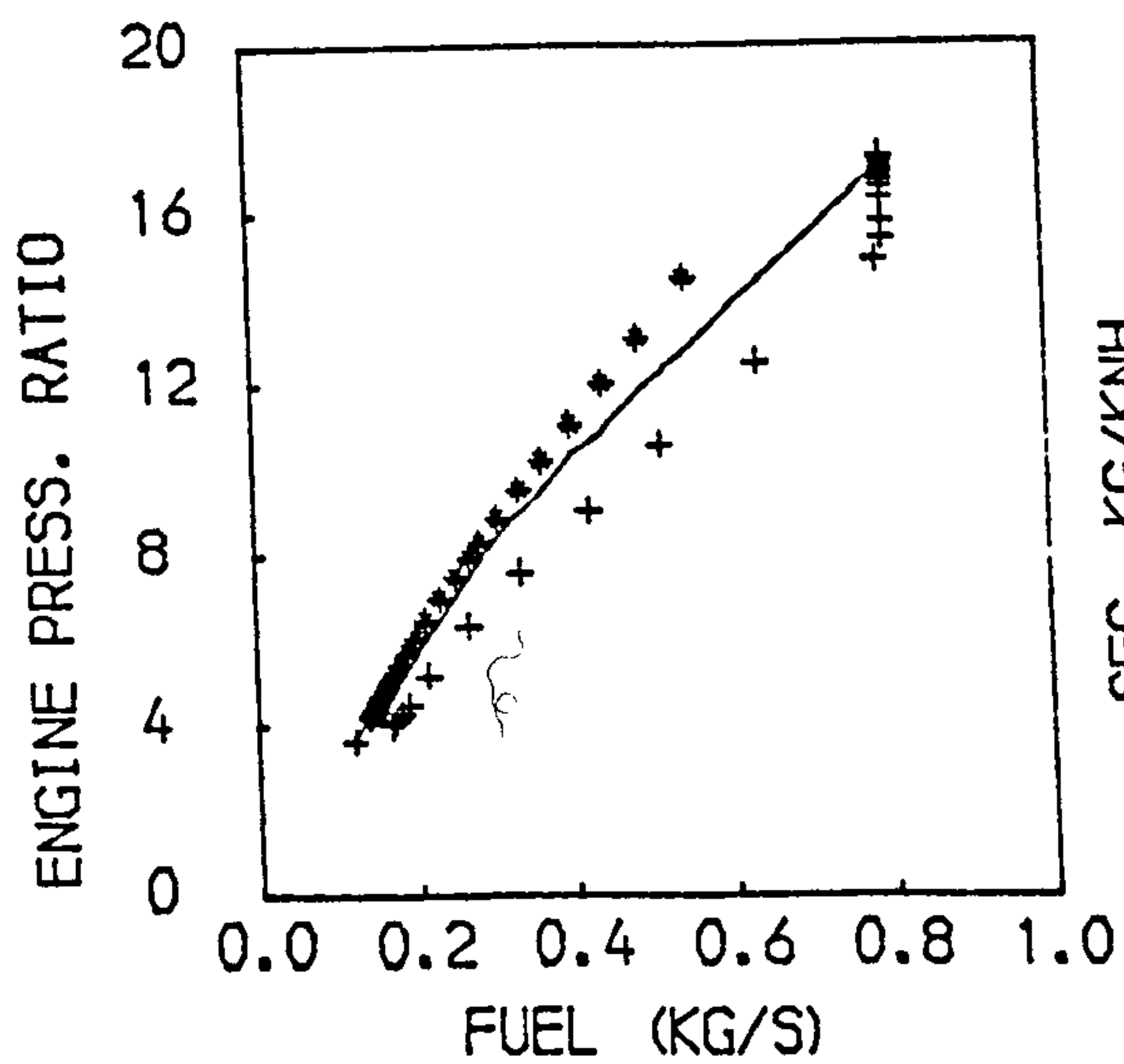
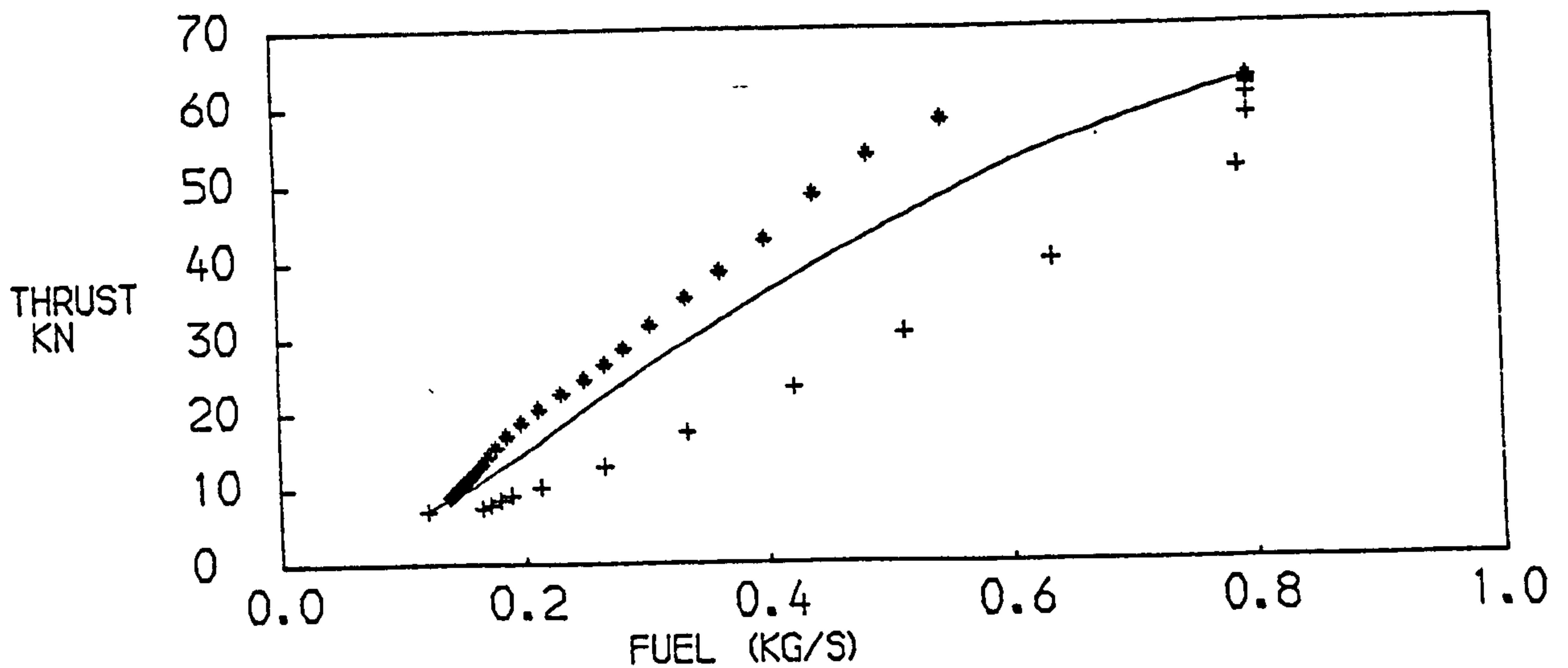
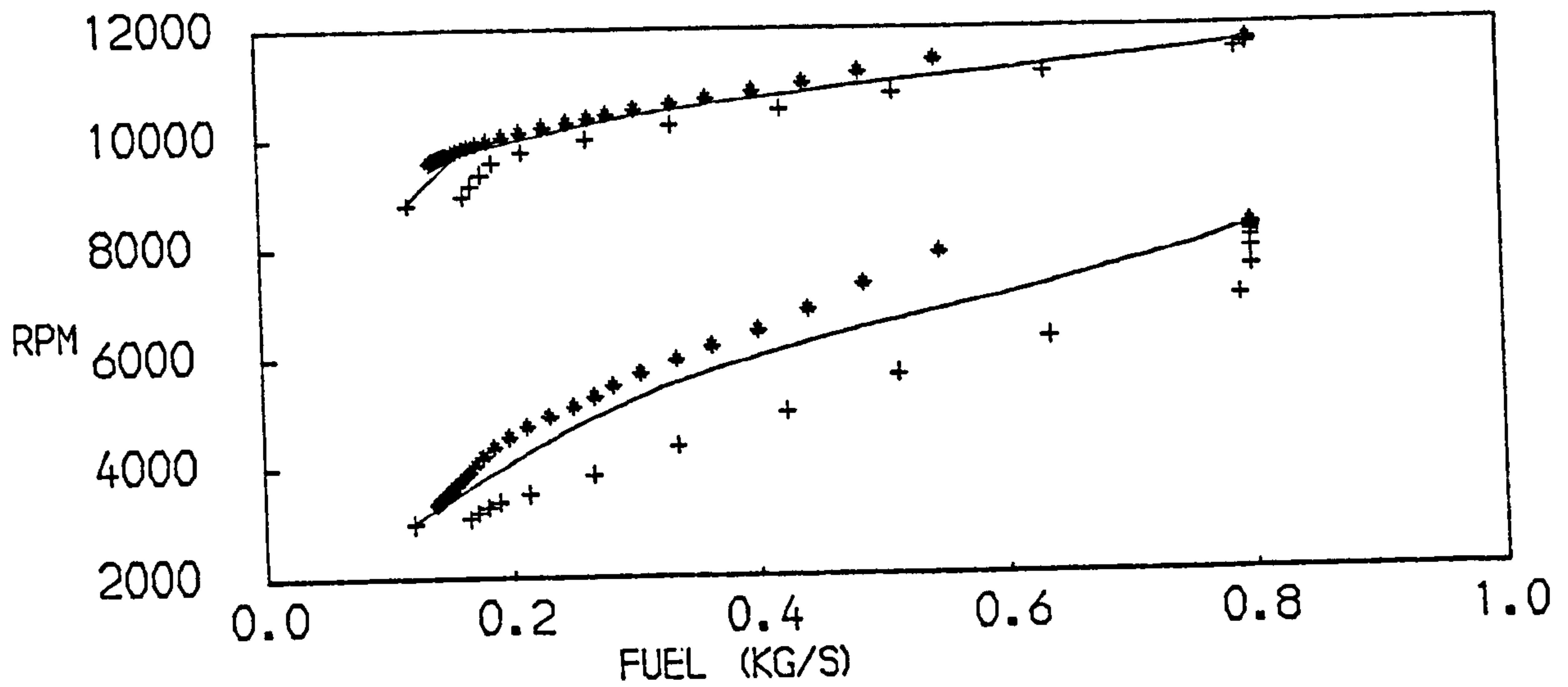


FIG. 48
PERFORMANCE OF A TWO SPOOL TURBOFAN WITH MIXED EXHAUSTS
+ACCELERATION * DECELERATION —STEADY RUNNING

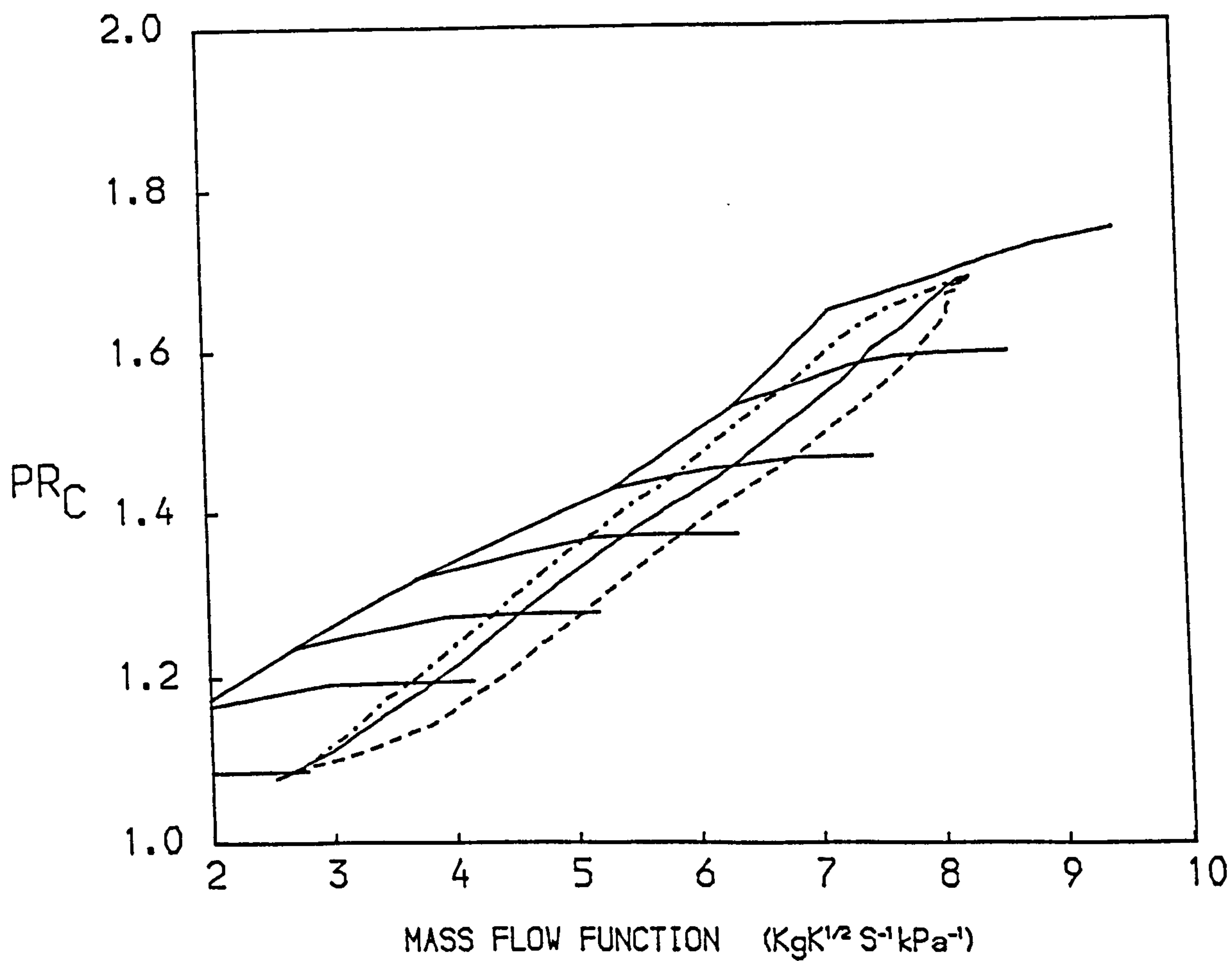
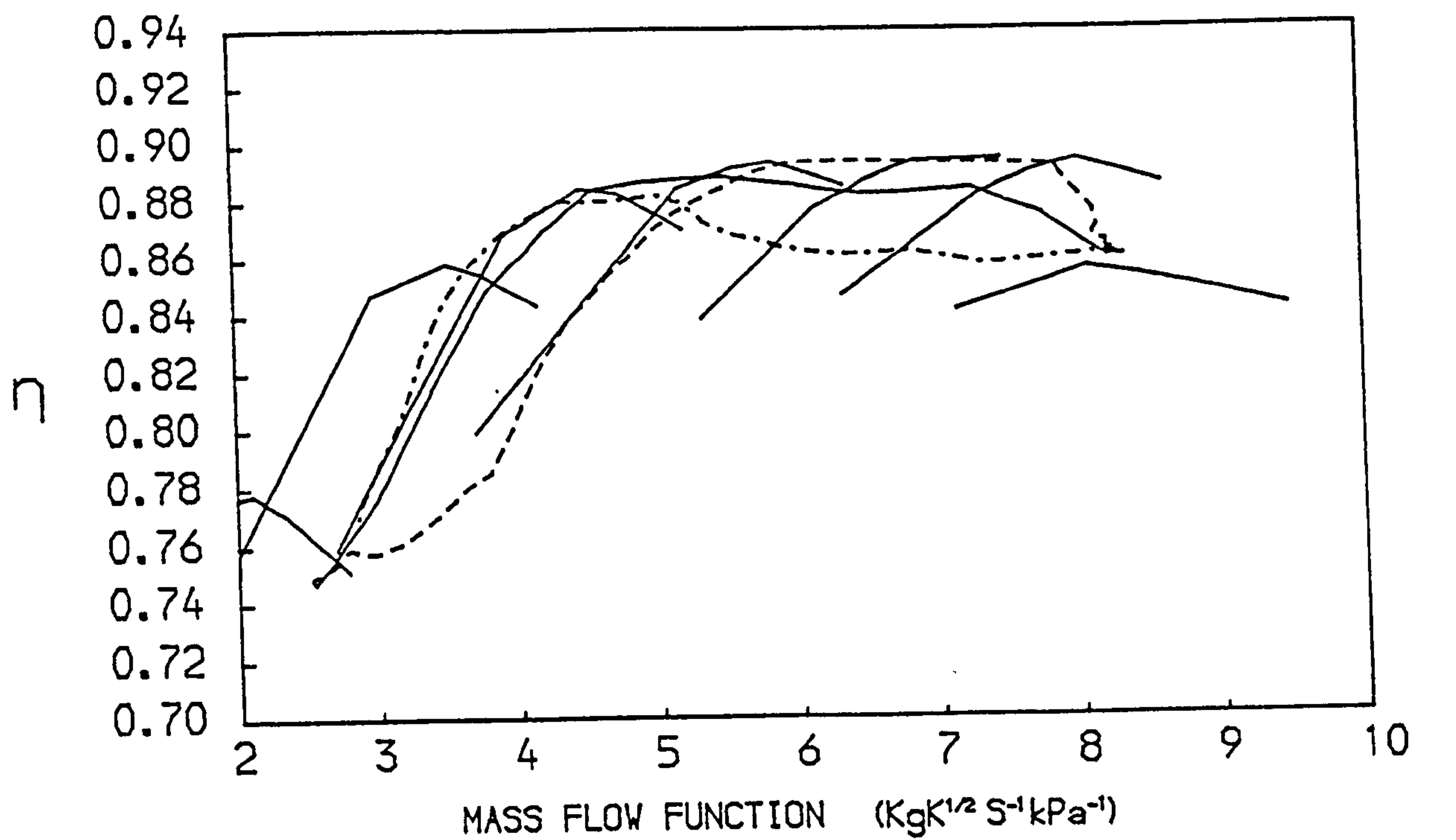


FIG. 49
 PATHS ON THE CHARACTERISTIC MAPS OF THE INNER FAN OF A
 TWO SPOOL TURBOFAN WITH SEPARATE EXHAUSTS
 -- ACCELERATION — STEADY RUNNING --- DECELERATION

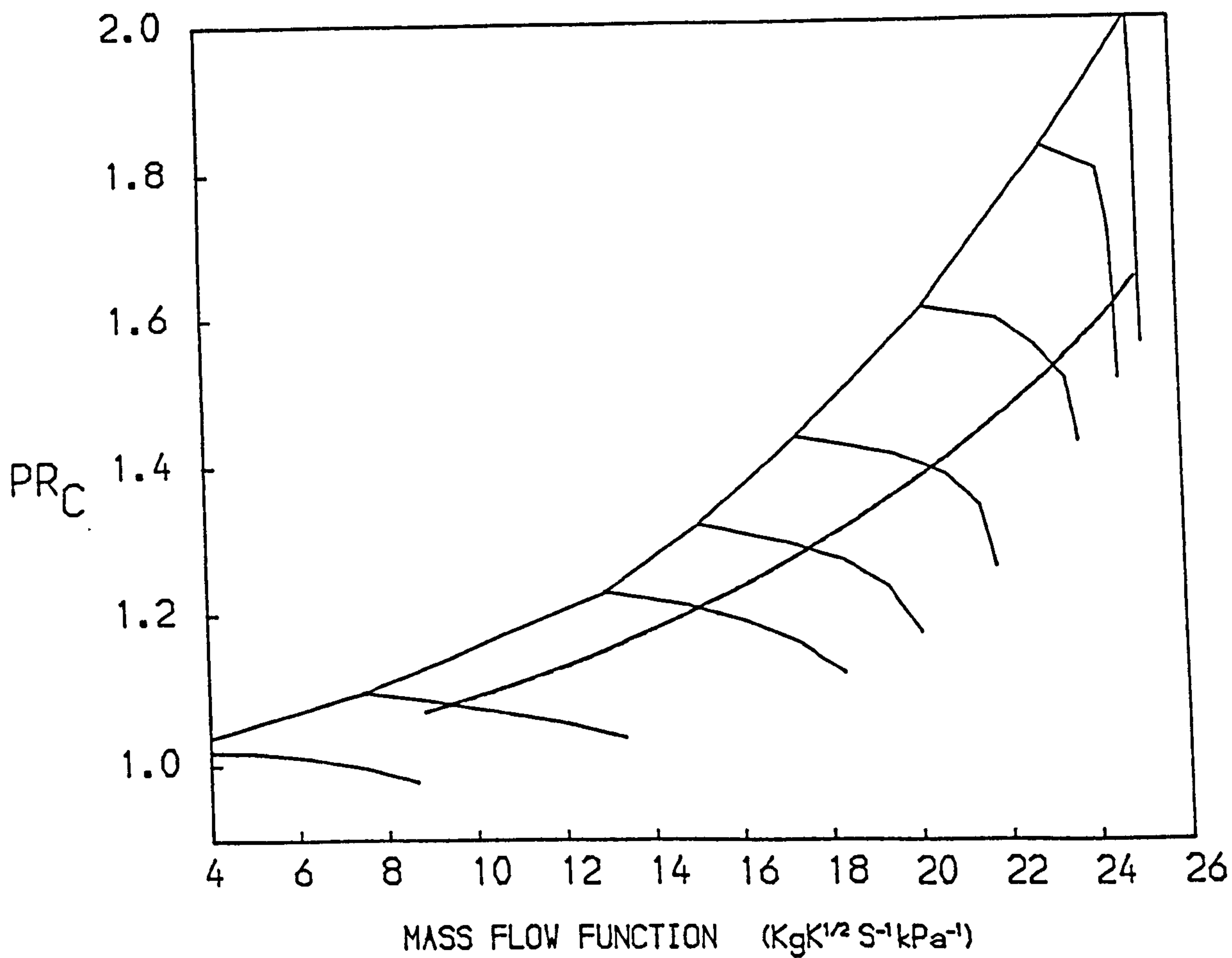
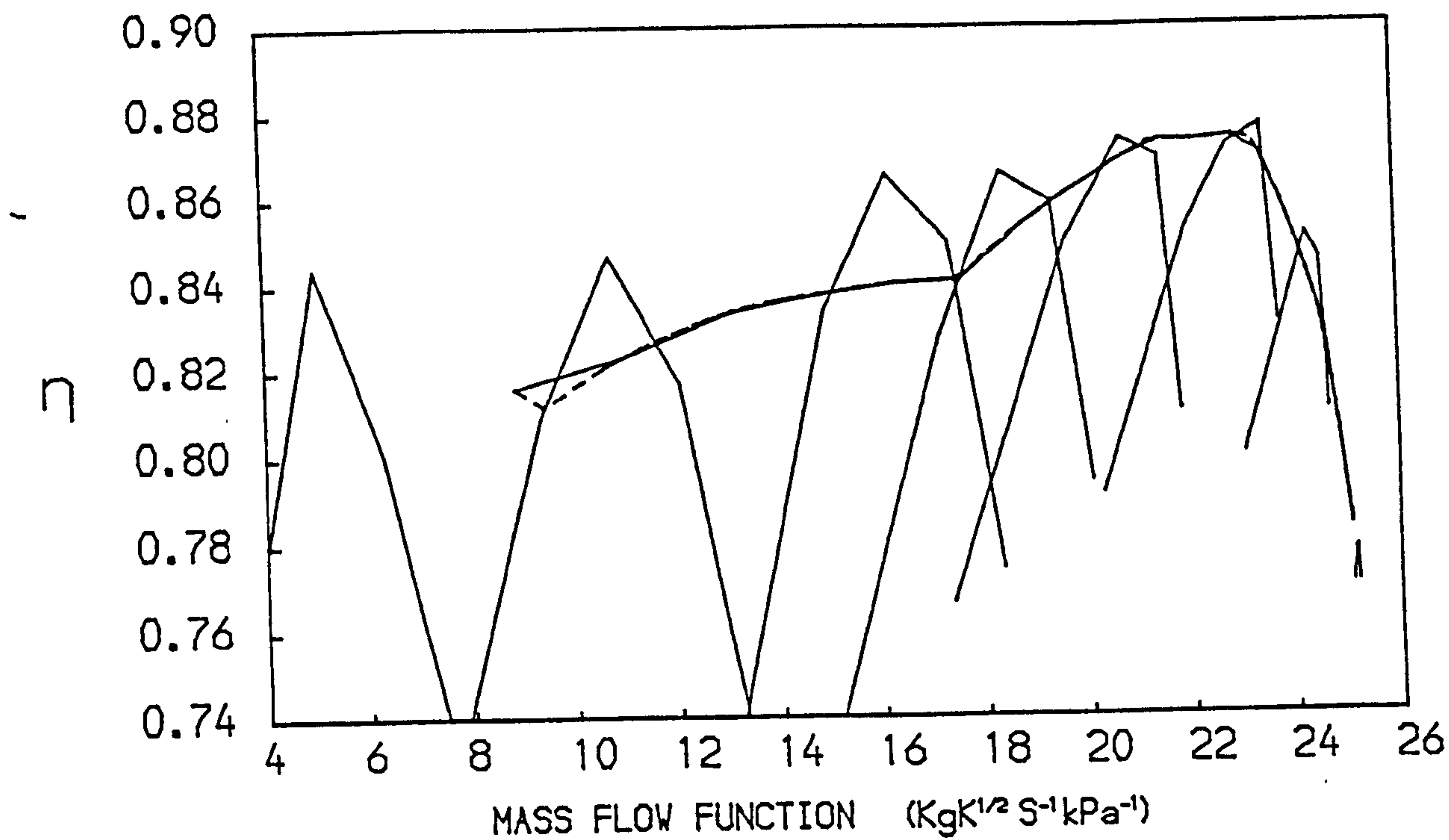


FIG. 50
 PATHS ON THE CHARACTERISTIC MAPS OF THE OUTER FAN OF A
 TWO SPOOL TURBOFAN WITH SEPARATE EXHAUSTS
 -- ACCELERATION — STEADY RUNNING --- DECELERATION

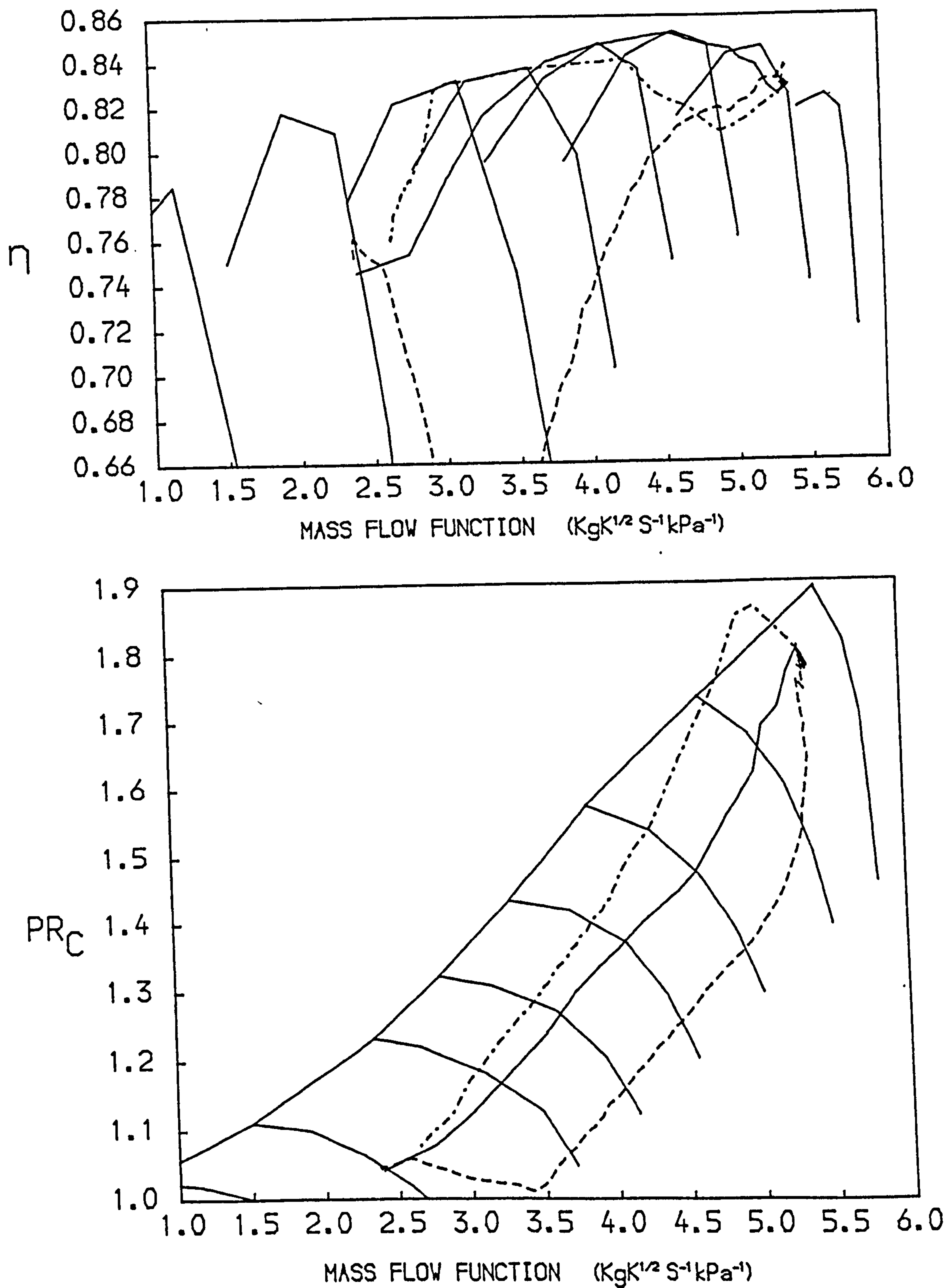


FIG. 51
 PATHS ON THE CHARACTERISTIC MAPS OF THE I.P. COMPRESSOR OF A
 TWO SPOOL TURBOFAN WITH SEPARATE EXHAUSTS
 -- ACCELERATION — STEADY RUNNING --- DECELERATION

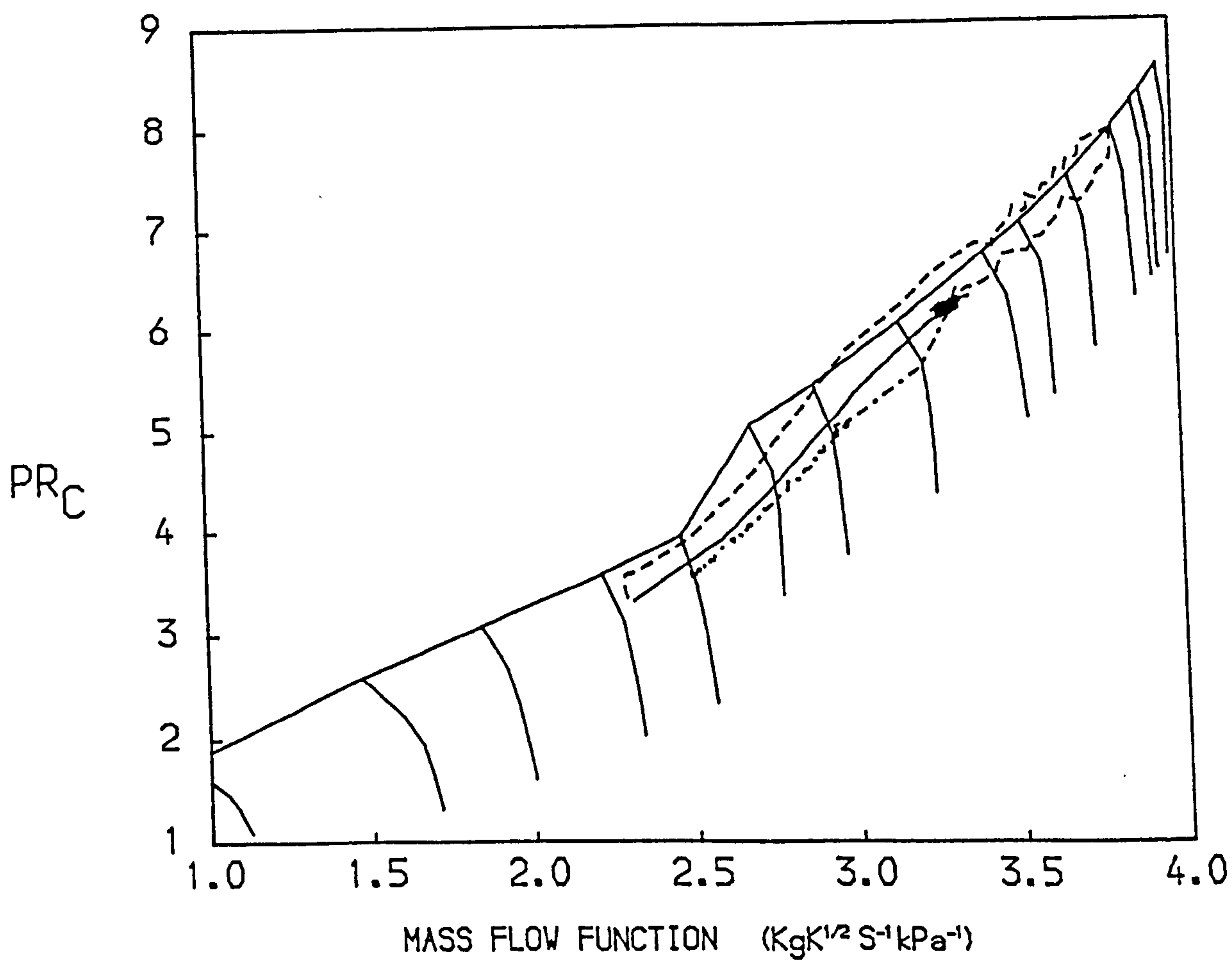
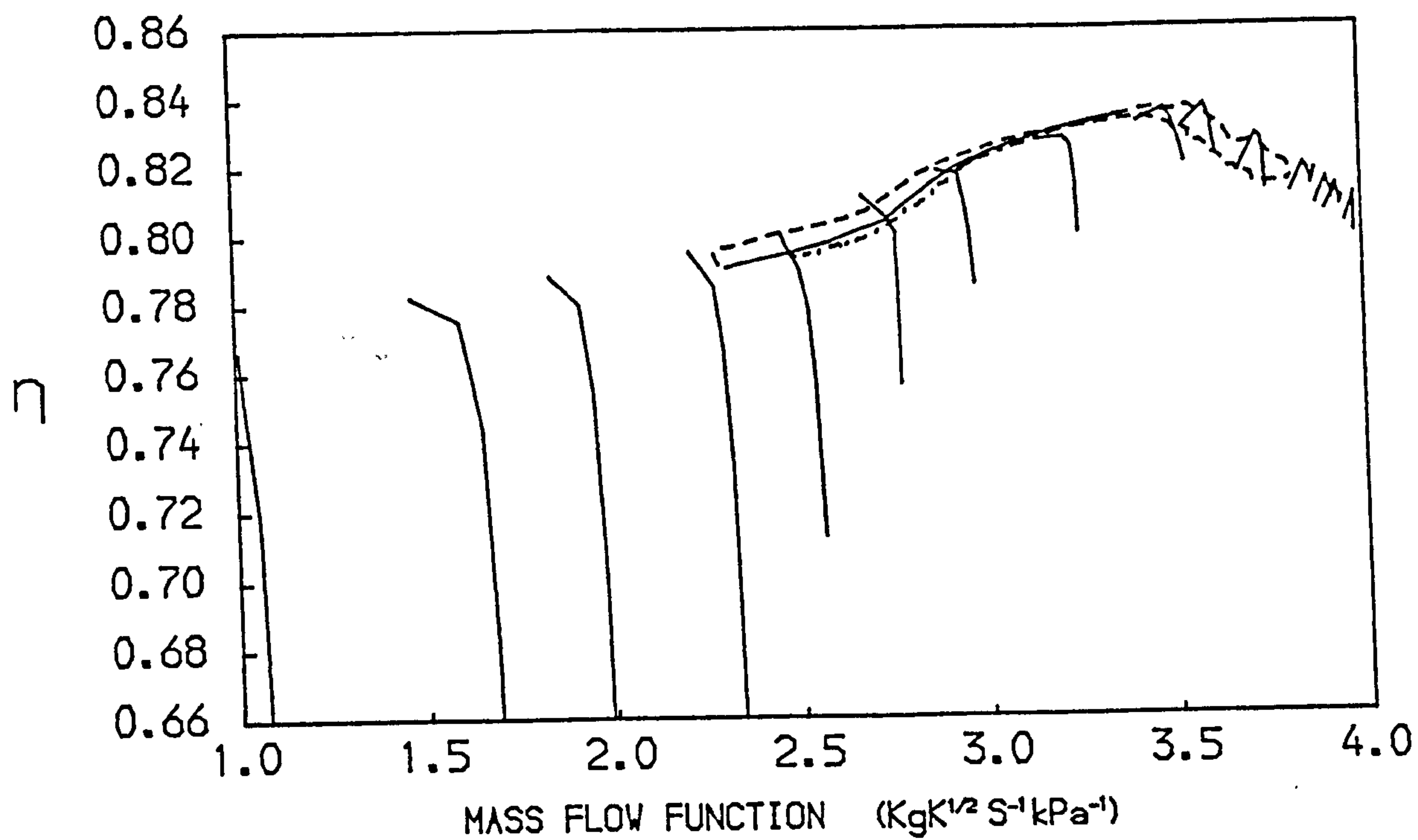


FIG. 52
 PATHS ON THE CHARACTERISTIC MAPS OF THE H.P. COMPRESSOR OF A
 TWO SPOOL TURBOFAN WITH SEPARATE EXHAUSTS
 -- ACCELERATION — STEADY RUNNING --- DECELERATION

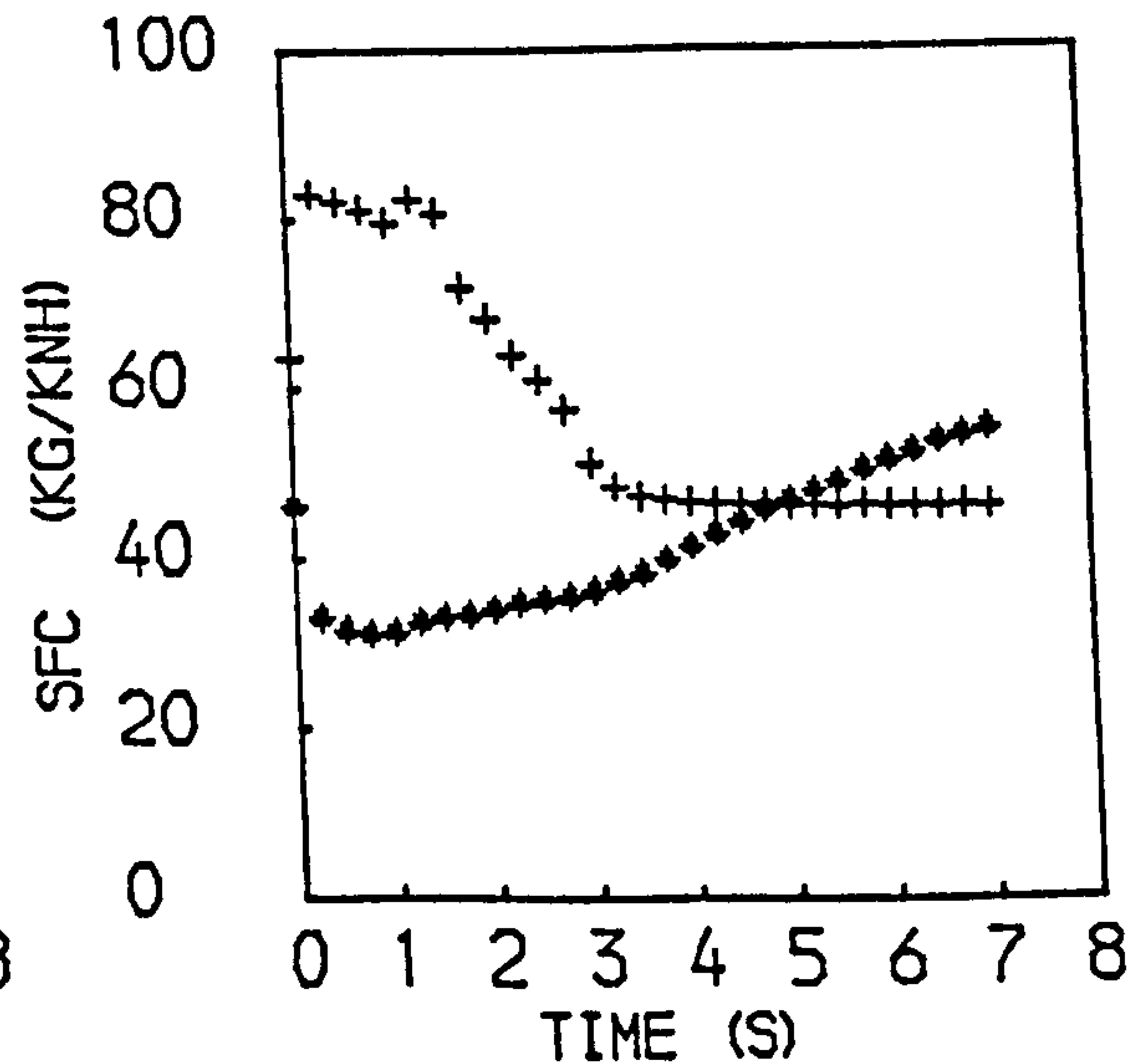
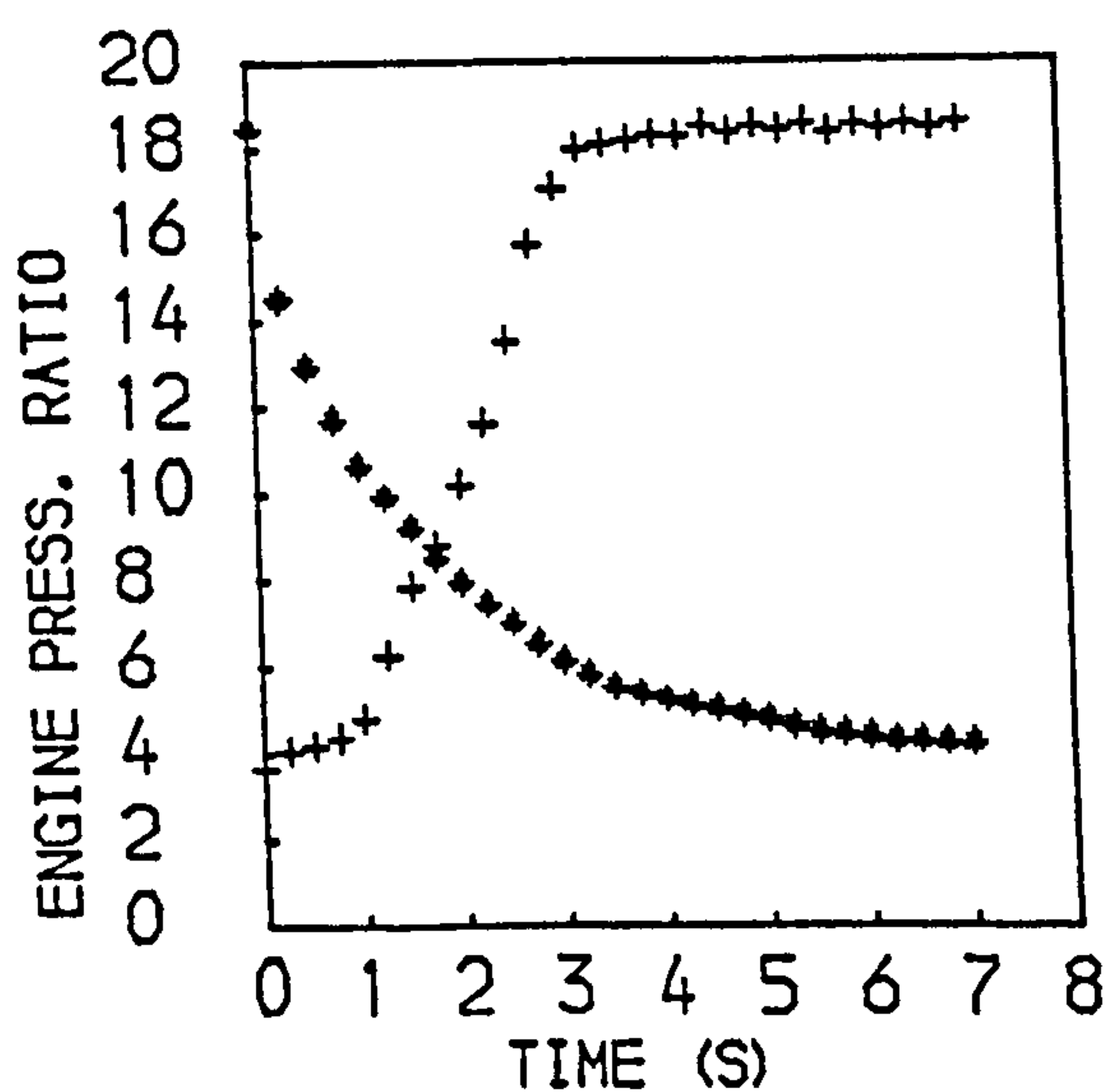
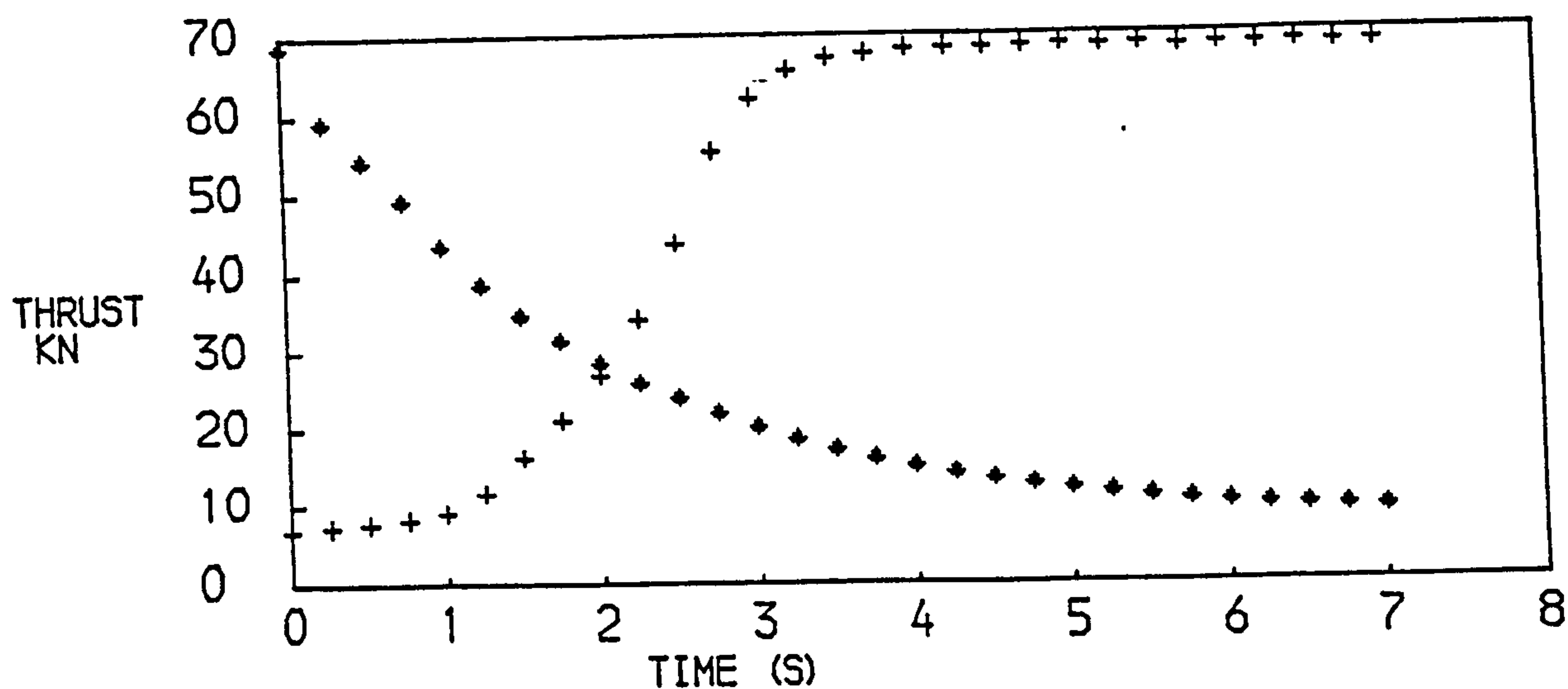
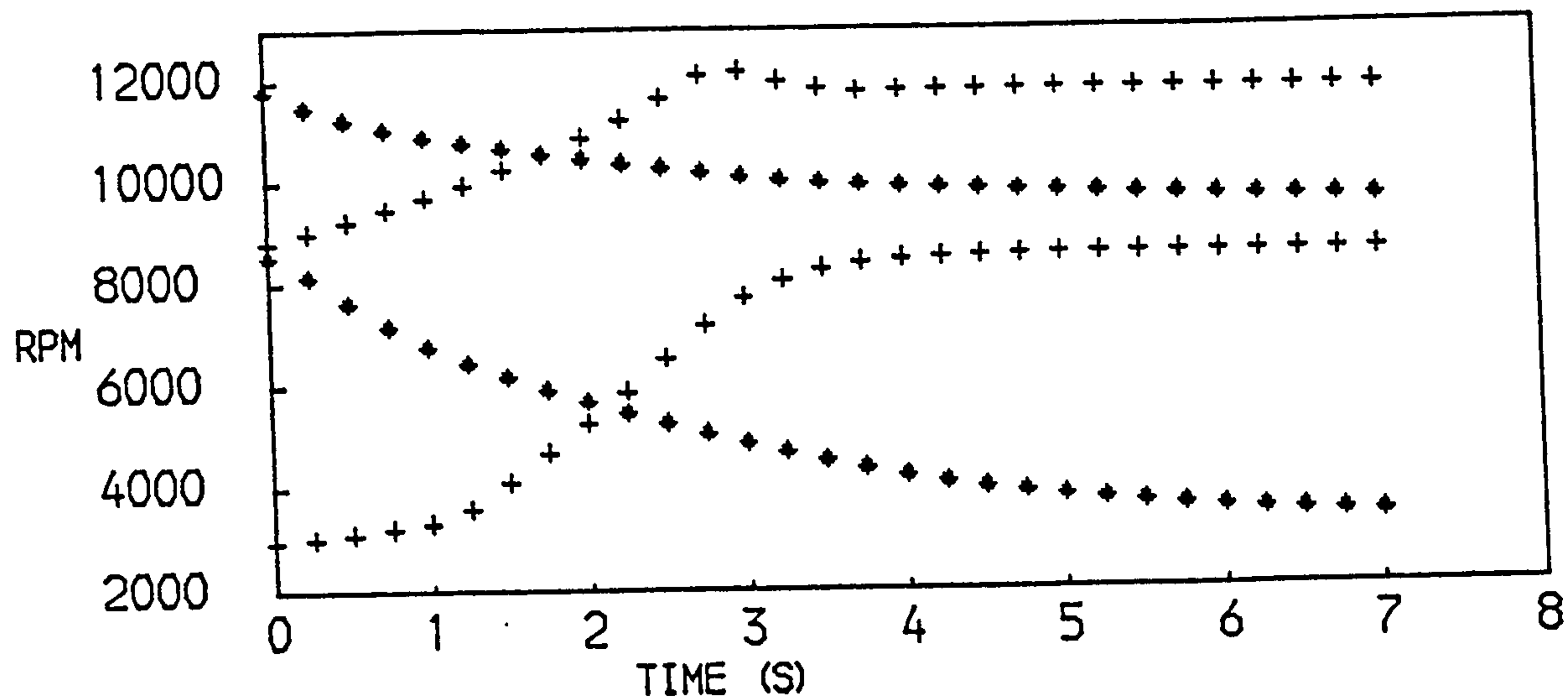


FIG. 53
PERFORMANCE OF A TWO SPOOL TURBOFAN WITH SEPARATE EXHAUSTS
+ACCELERATION ♦ DECELERATION

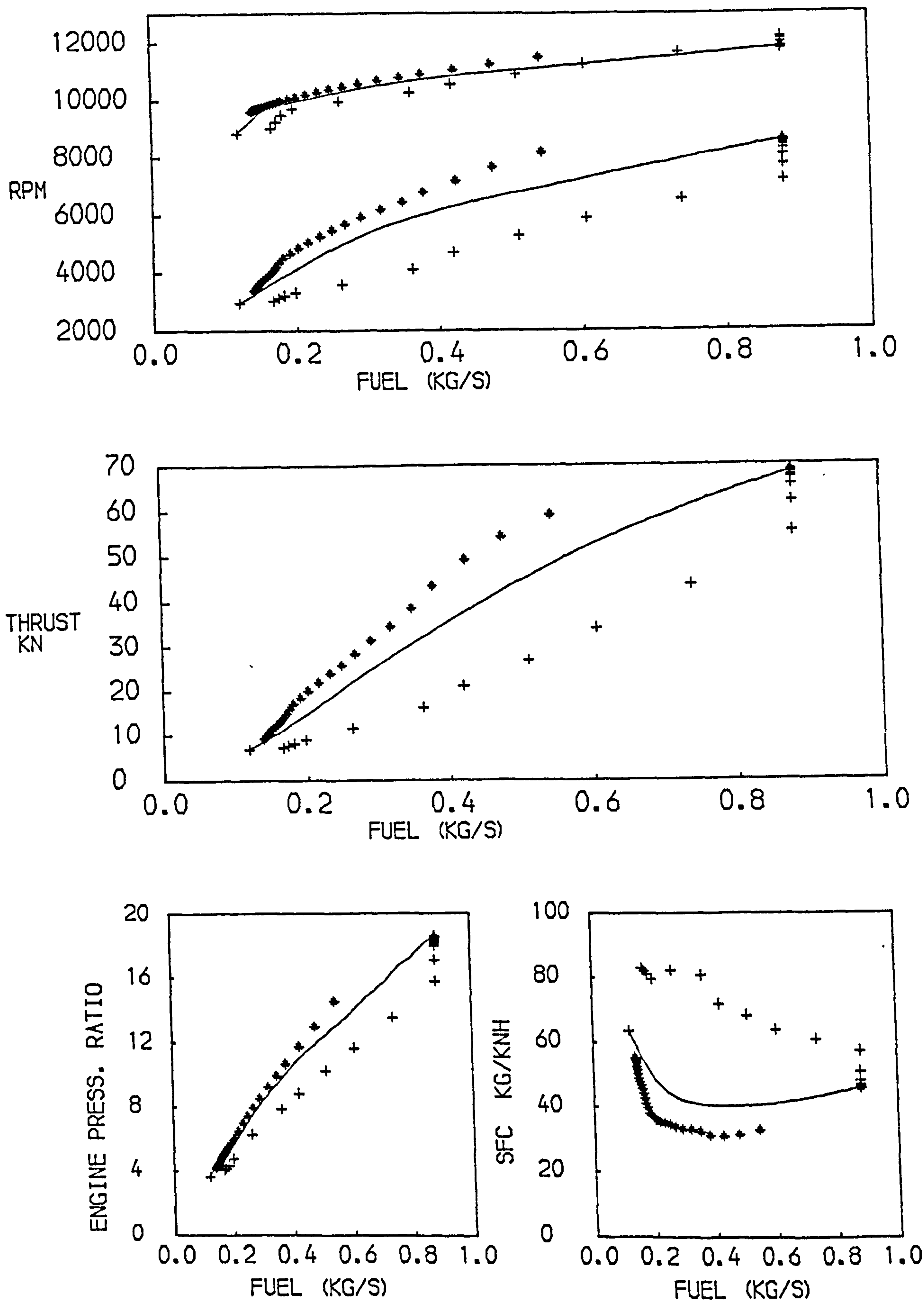


FIG. 54
 PERFORMANCE OF A TWO SPOOL TURBOFAN WITH SEPARATE EXHAUSTS
 +ACCELERATION * DECELERATION —STEADY RUNNING

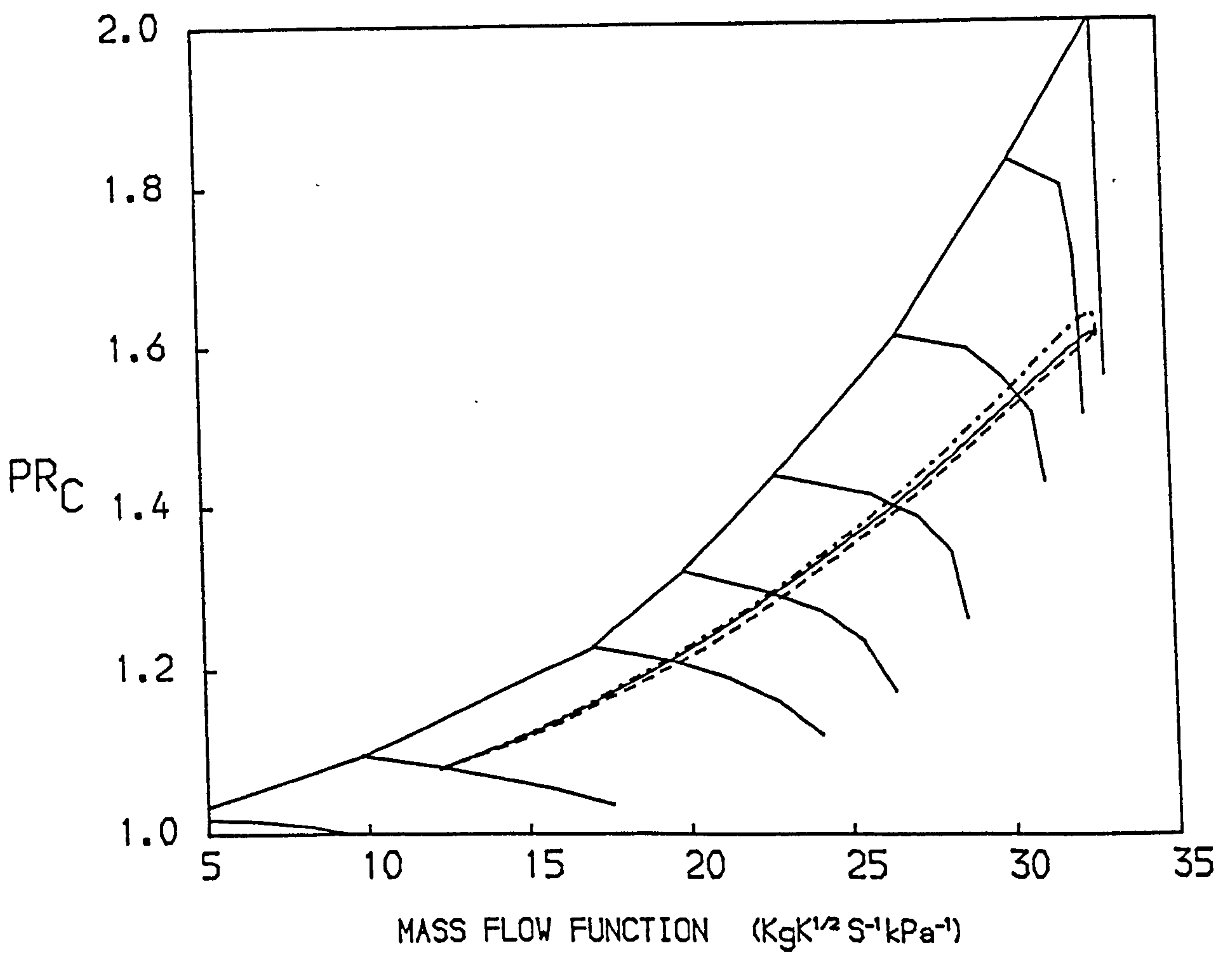
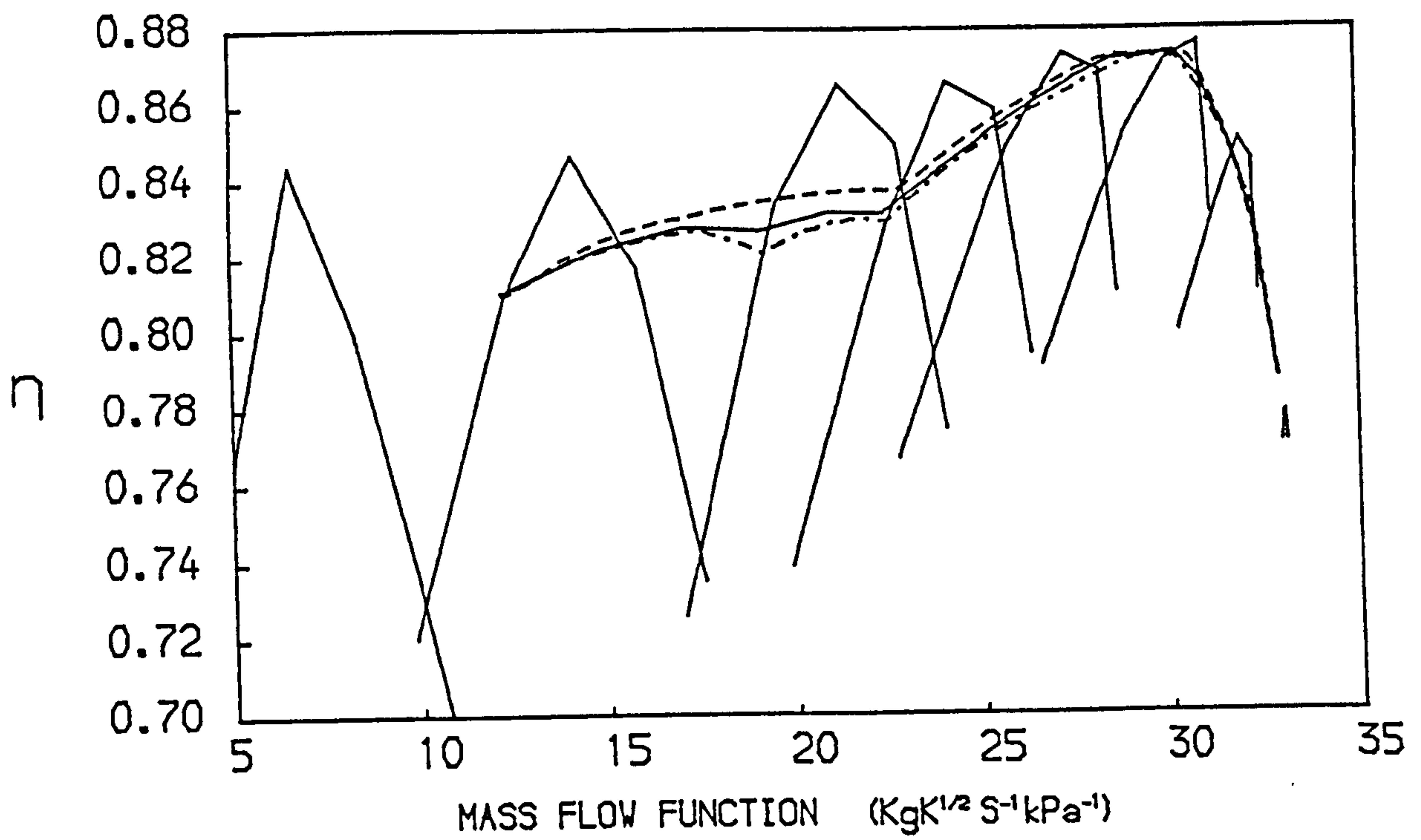


FIG. 55
 PATHS ON THE CHARACTERISTIC MAPS OF THE FAN OF A
 TWO SPOOL TURBOFAN WITH SEPARATE EXHAUSTS
 -- ACCELERATION — STEADY RUNNING --- DECELERATION

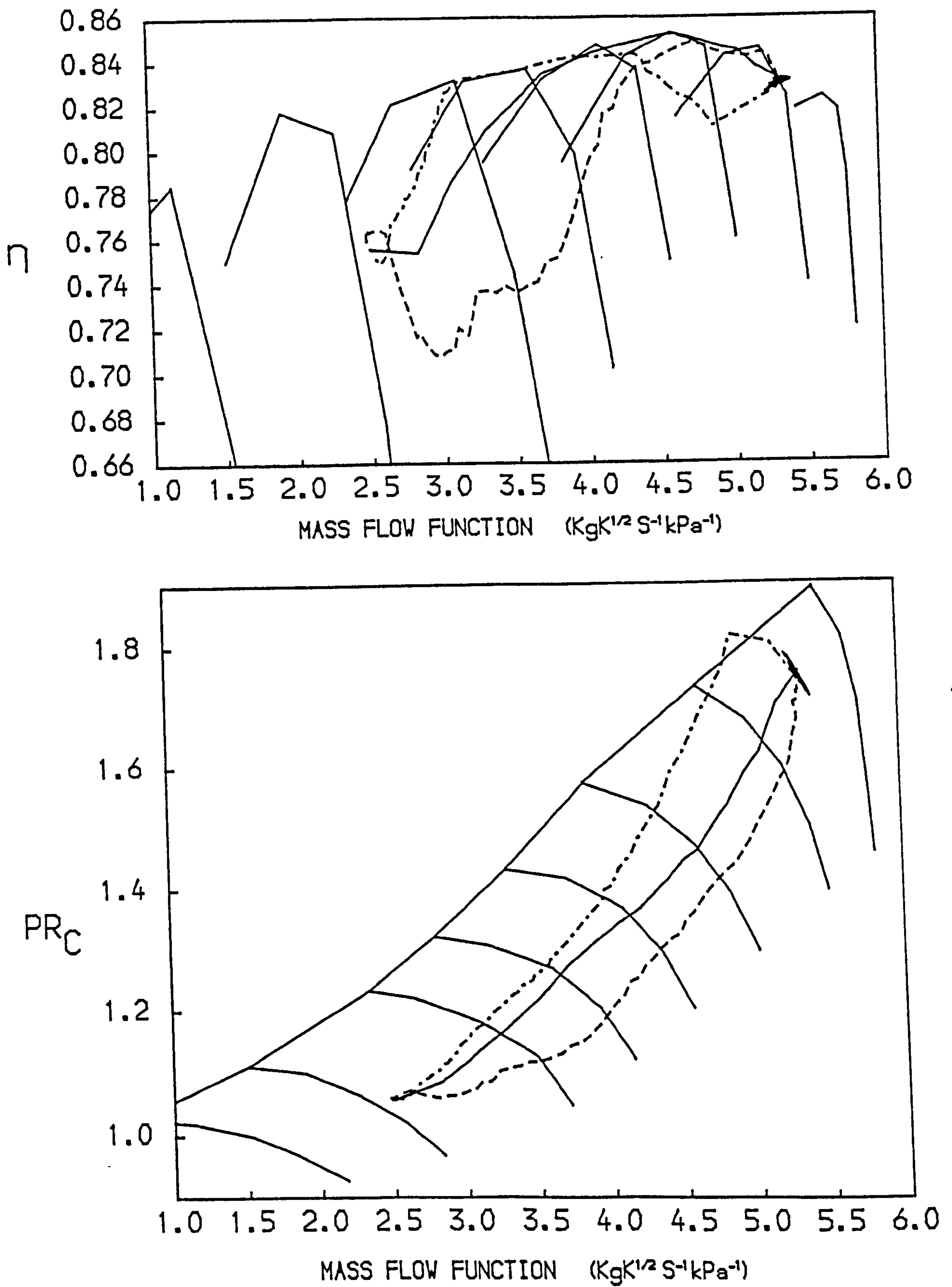


FIG. 56
 PATHS ON THE CHARACTERISTIC MAPS OF THE I.P. COMPRESSOR OF A
 TWO SPOOL TURBOFAN WITH SEPARATE EXHAUSTS
 -- ACCELERATION — STEADY RUNNING --- DECELERATION

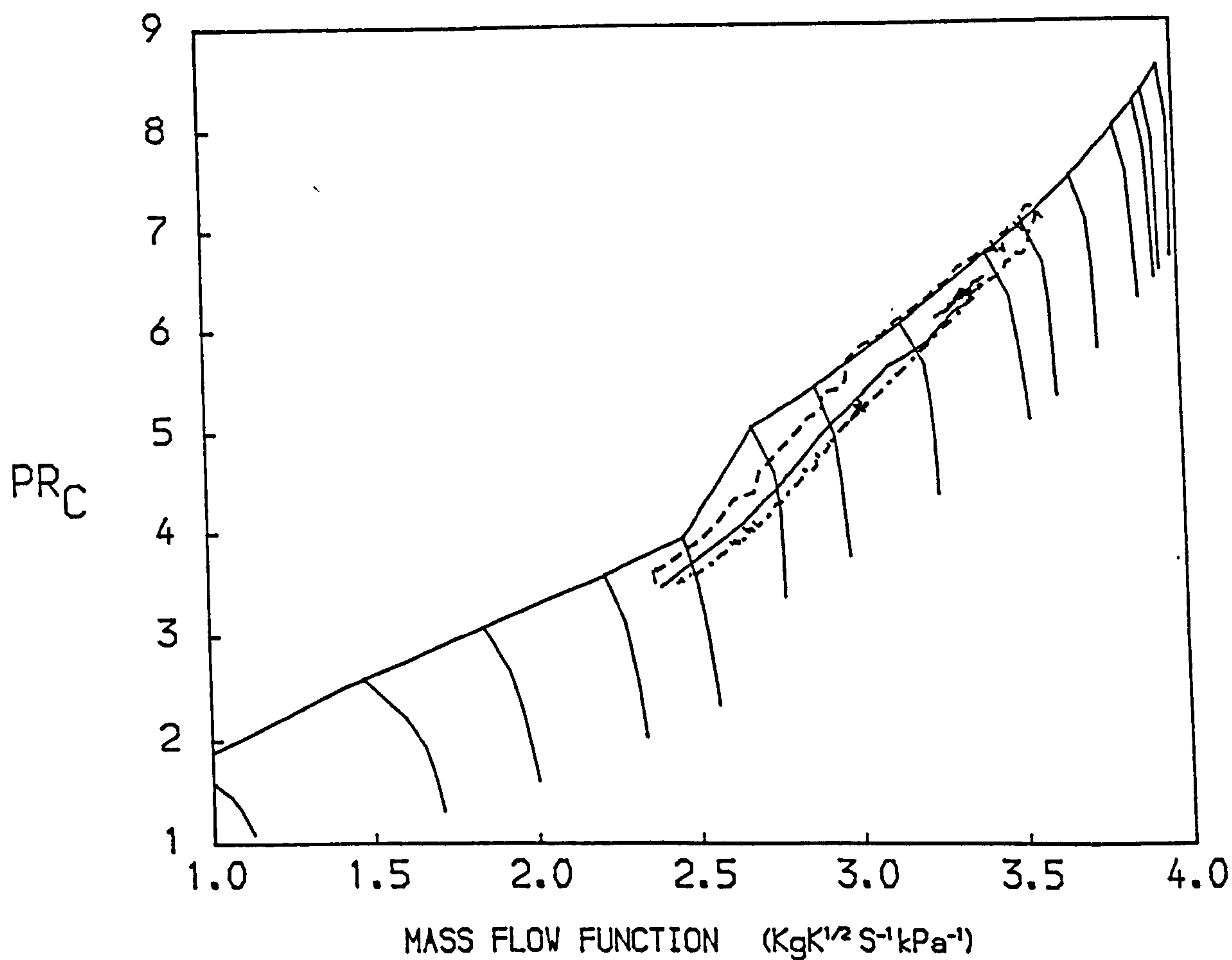
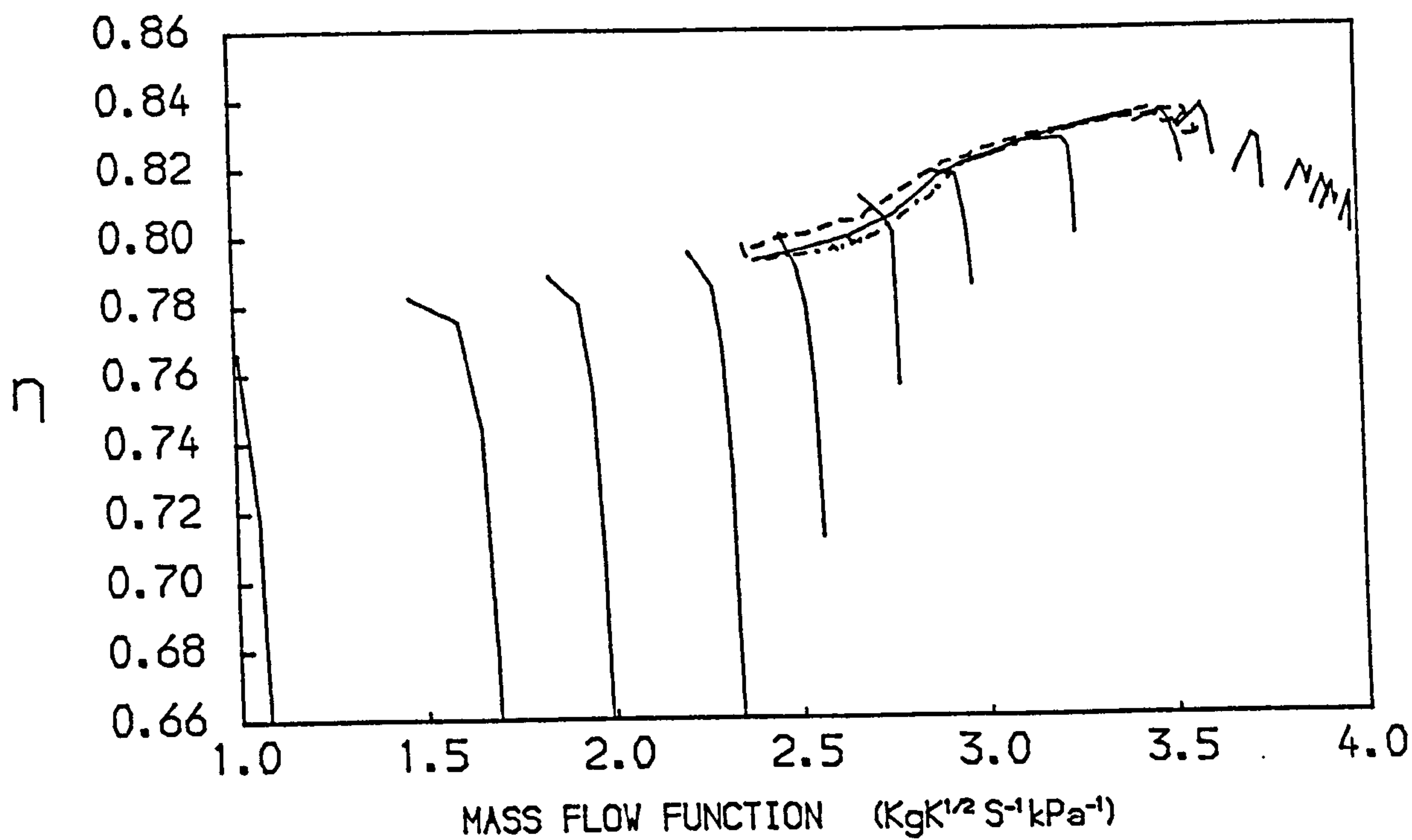


FIG. 57
 PATHS ON THE CHARACTERISTIC MAPS OF THE H.P. COMPRESSOR OF A
 TWO SPOOL TURBOFAN WITH SEPARATE EXHAUSTS
 -- ACCELERATION — STEADY RUNNING --- DECELERATION

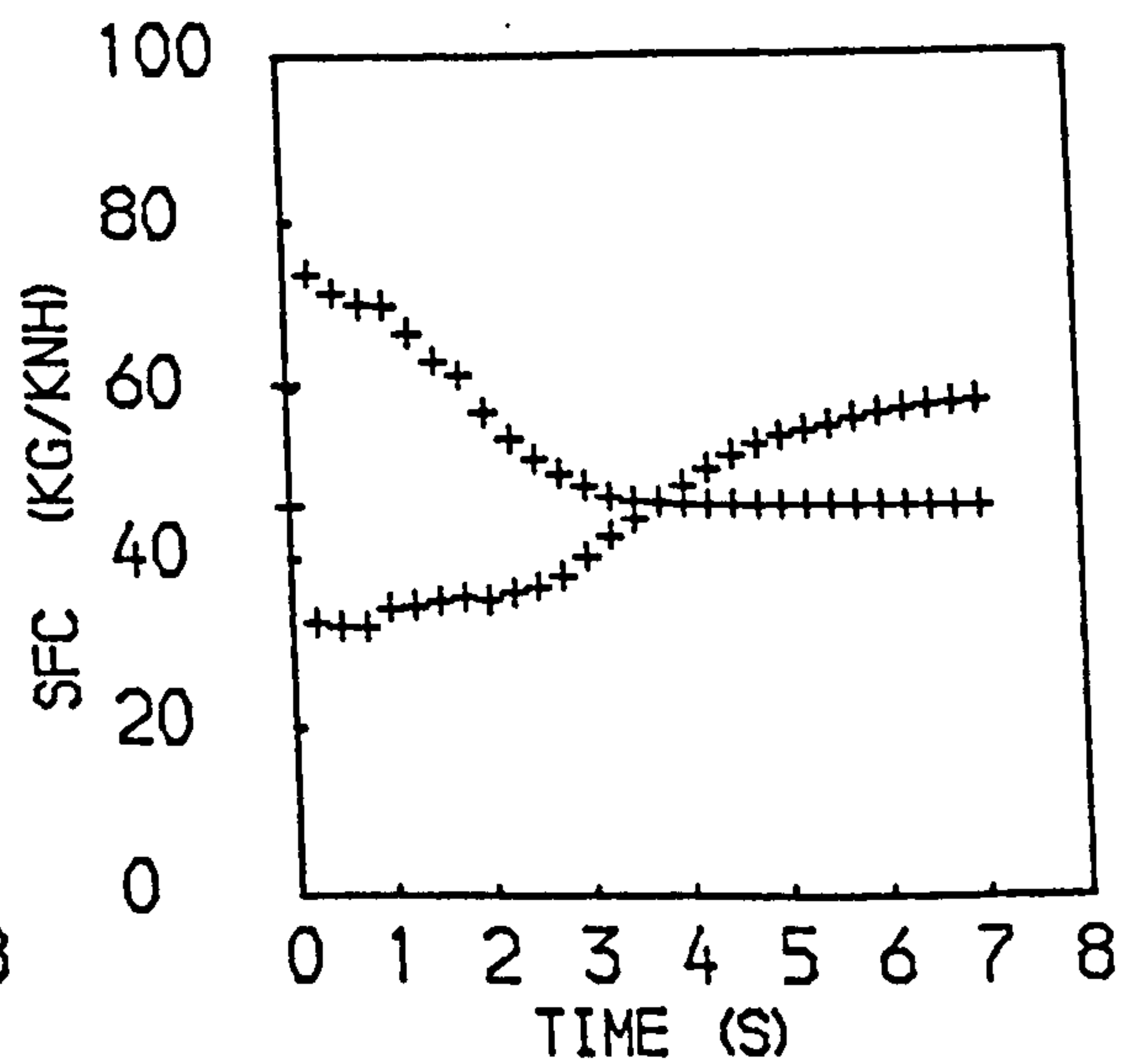
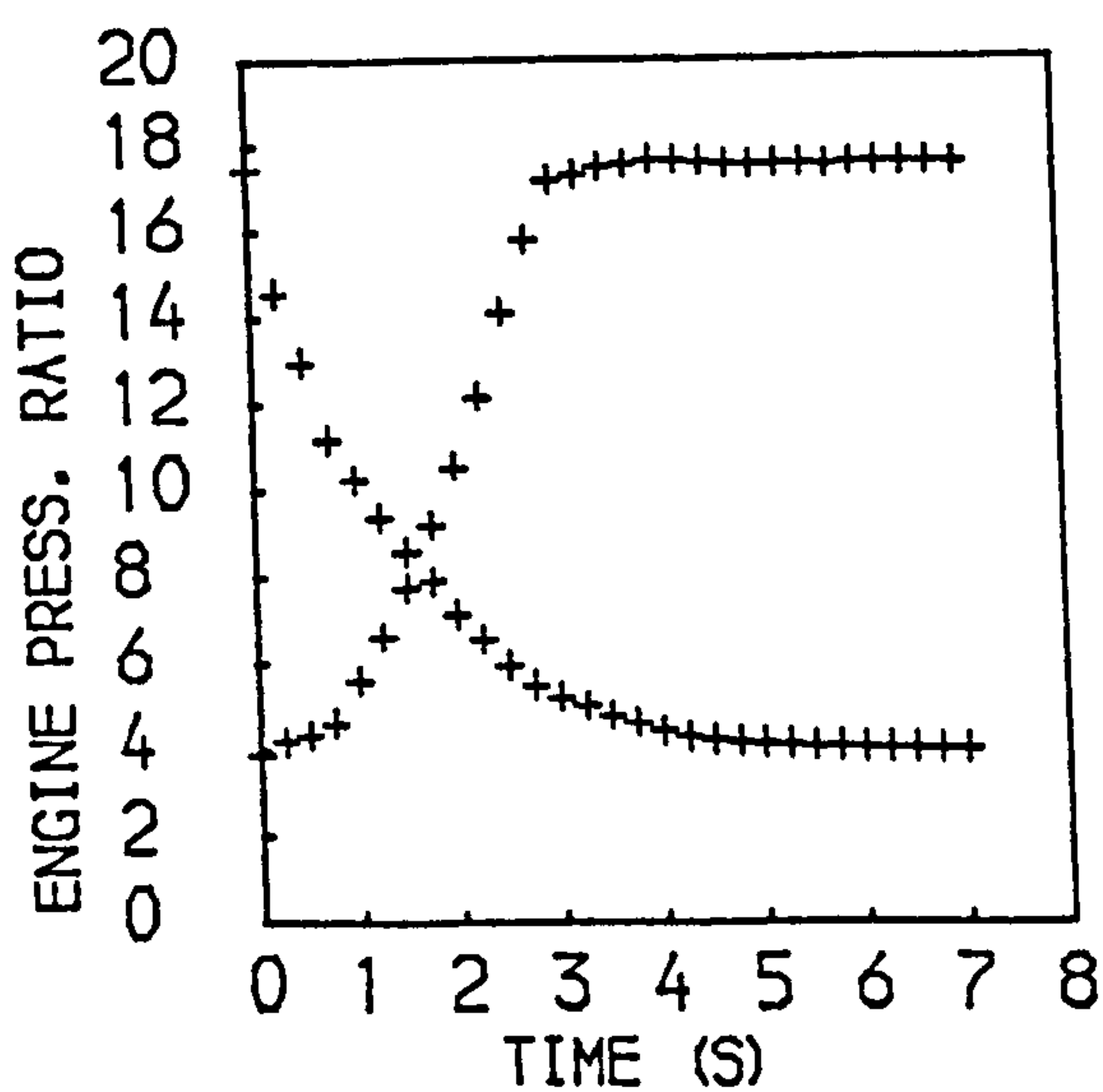
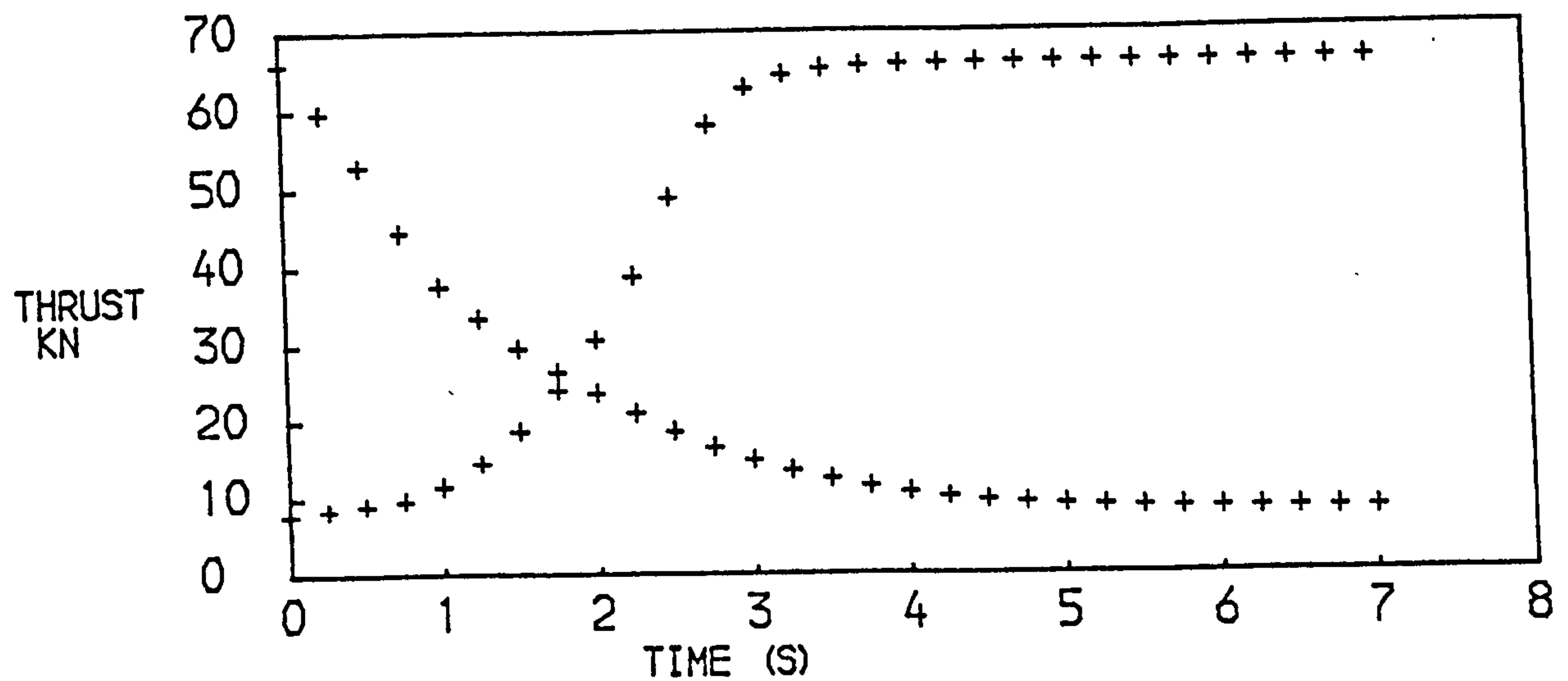
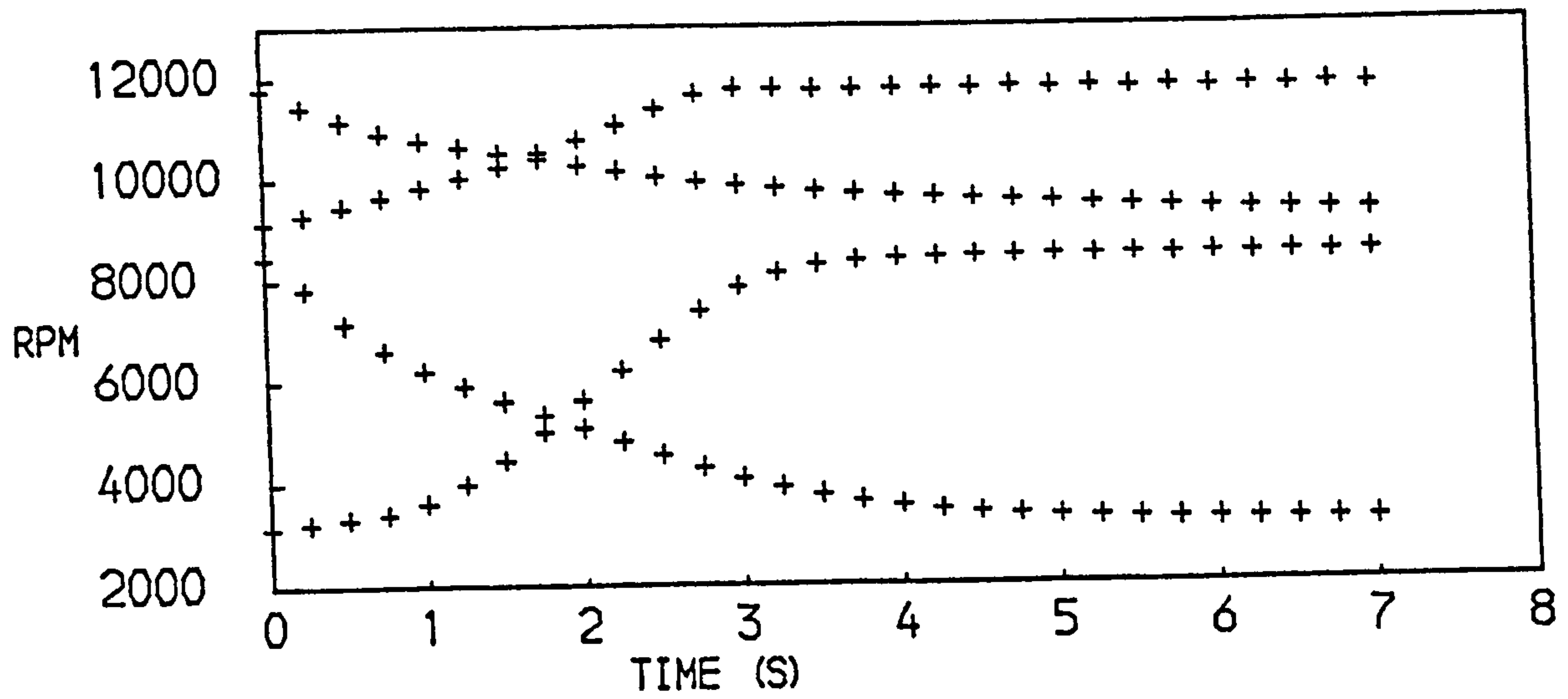


FIG. 58
PERFORMANCE OF A TWO SPOOL TURBOFAN WITH SEPARATE EXHAUSTS
+ACCELERATION * DECELERATION

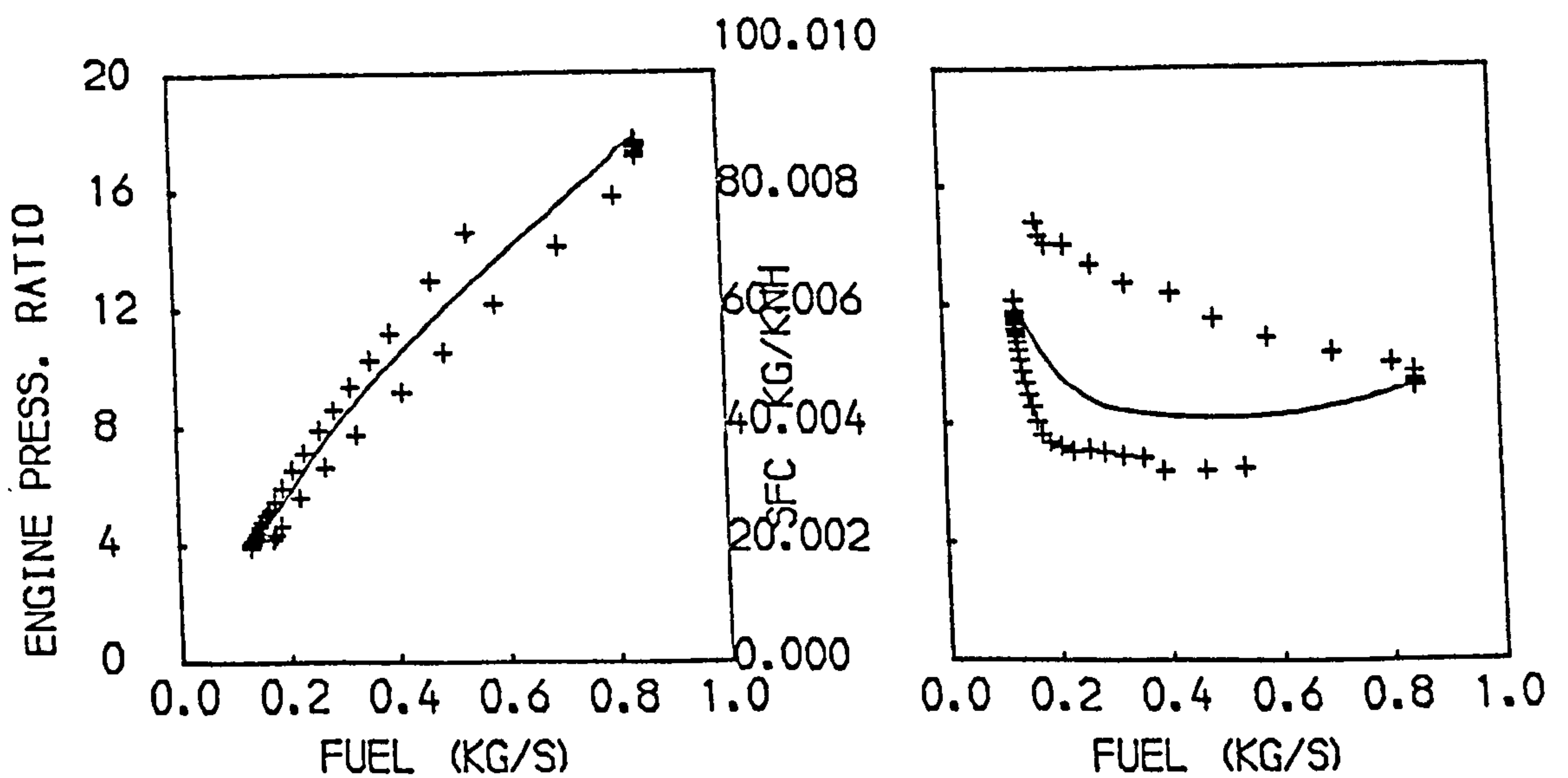
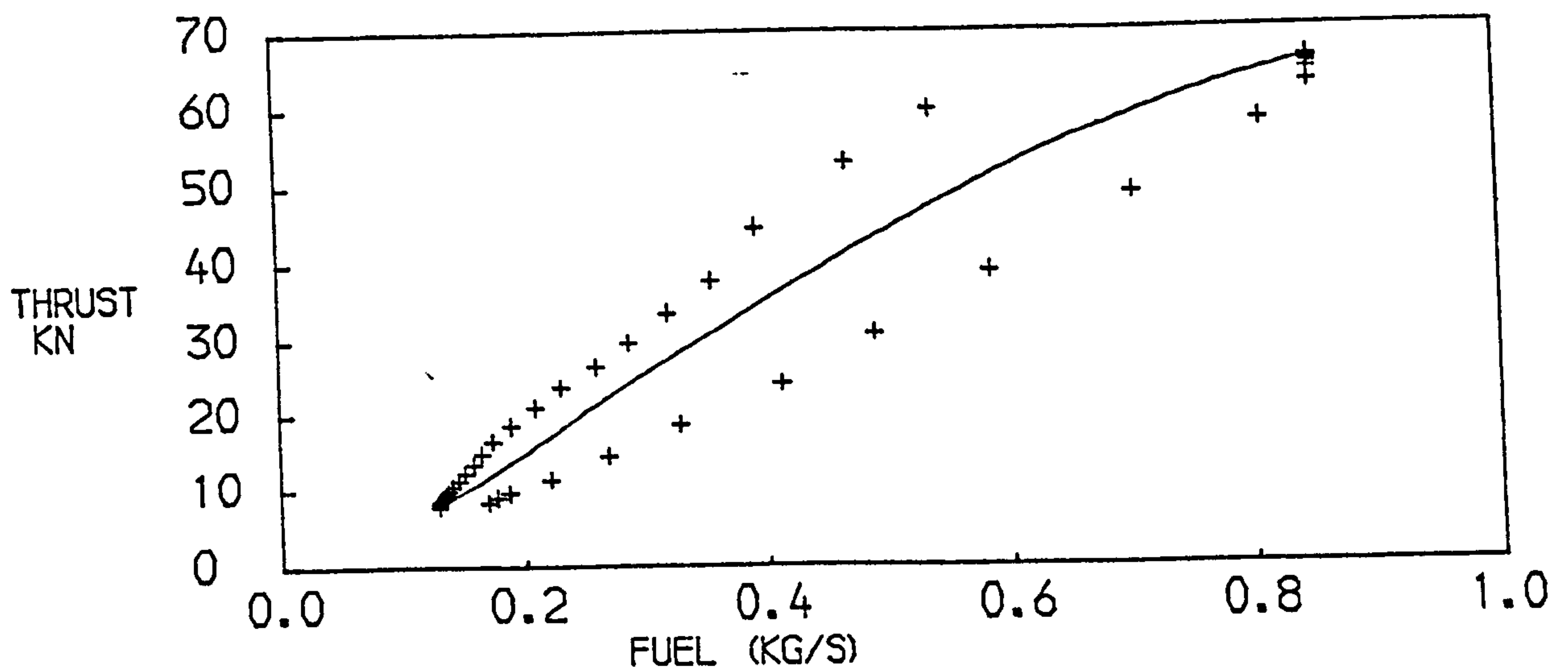
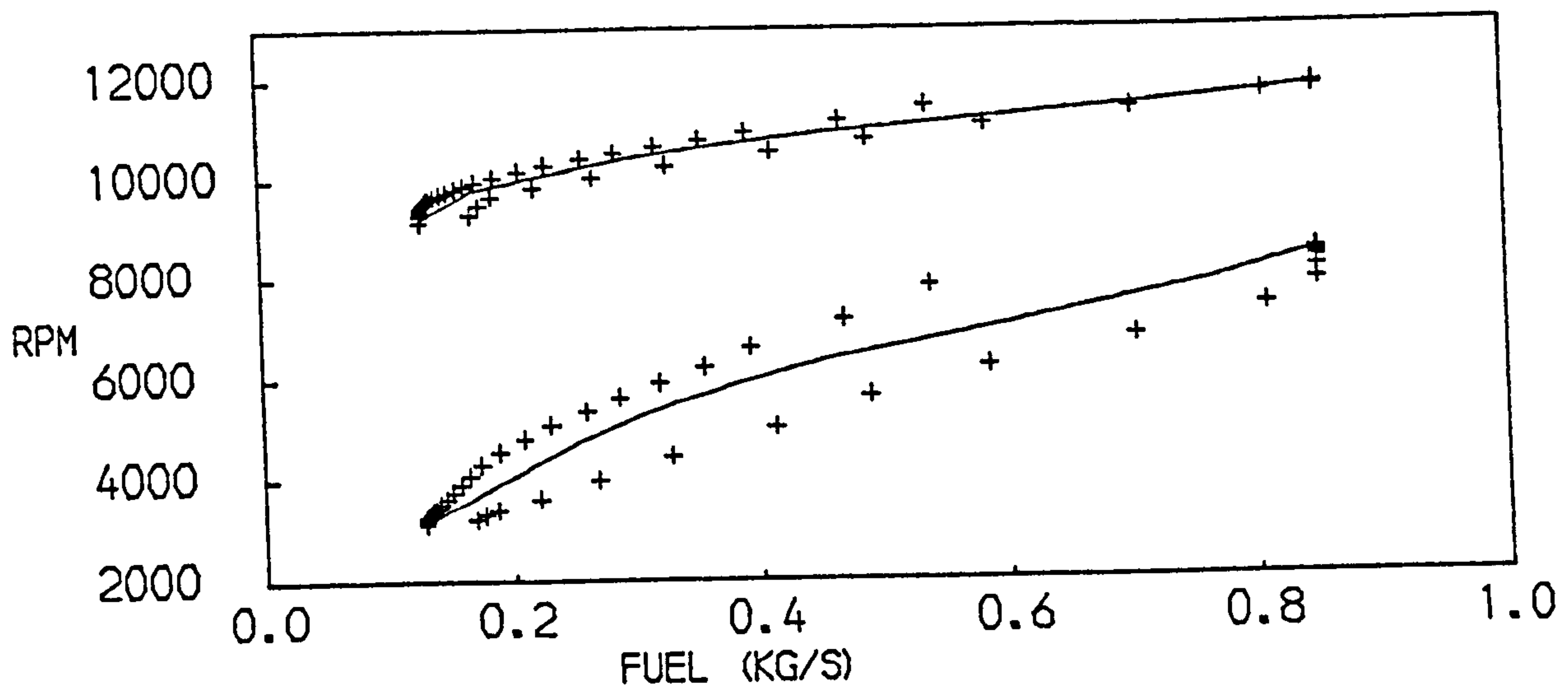


FIG. 59
PERFORMANCE OF A TWO SPOOL TURBOFAN WITH SEPARATE EXHAUSTS
+ACCELERATION + DECELERATION —STEADY RUNNING

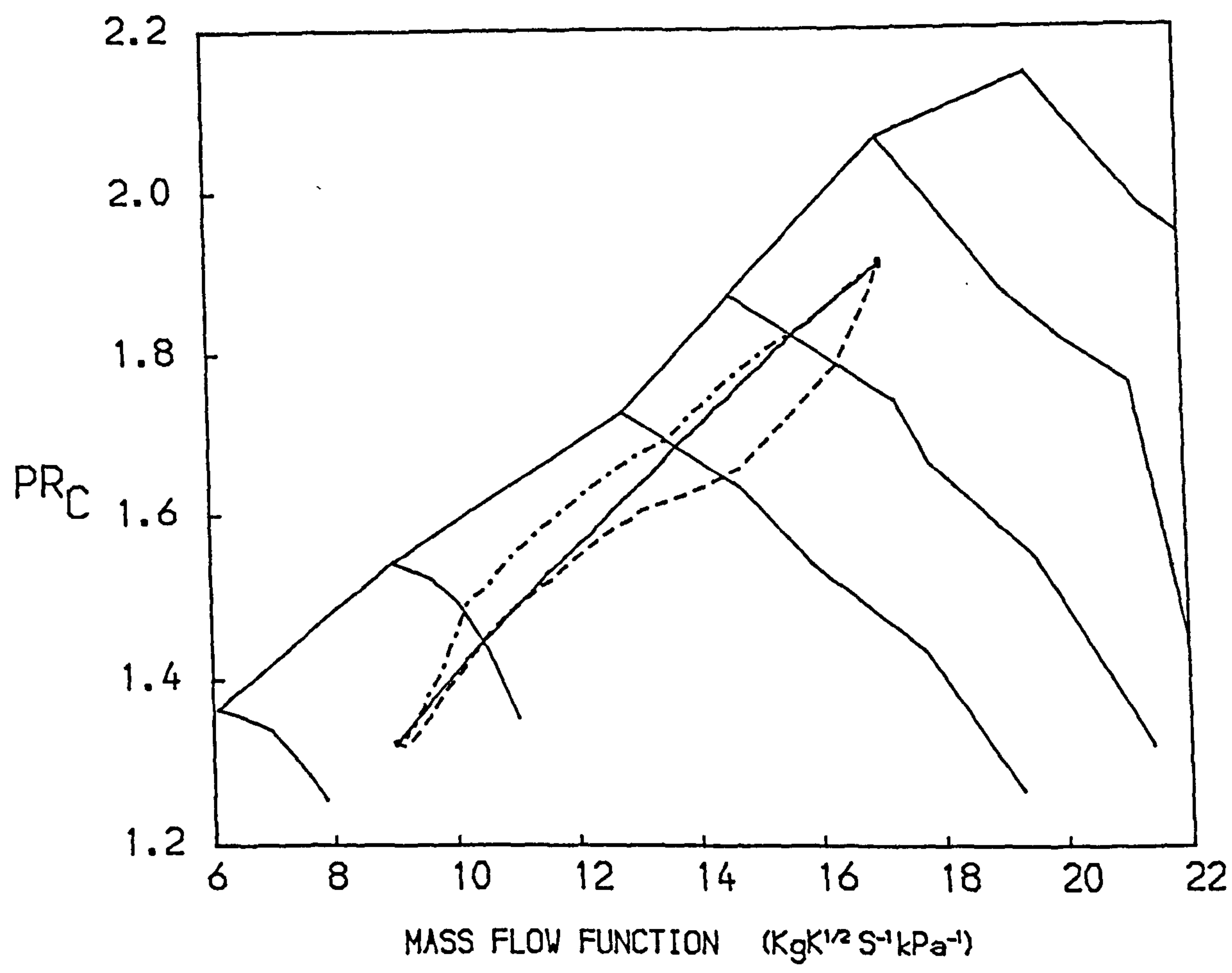
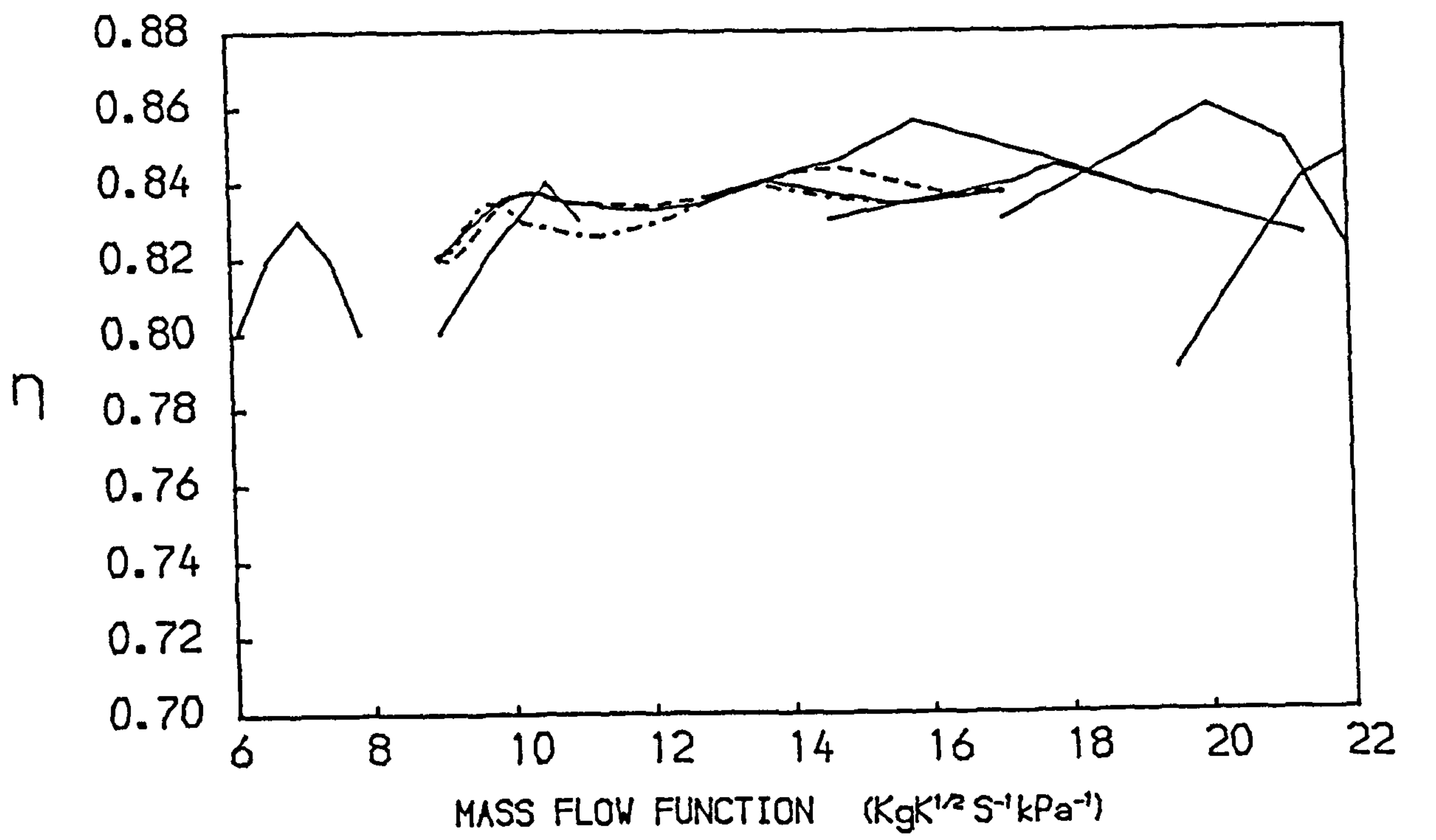


FIG. 60
 PATHS ON THE CHARACTERISTIC MAPS OF THE FAN OF A
 THREE SPOOL TURBOJET
 -- ACCELERATION — STEADY RUNNING --- DECELERATION

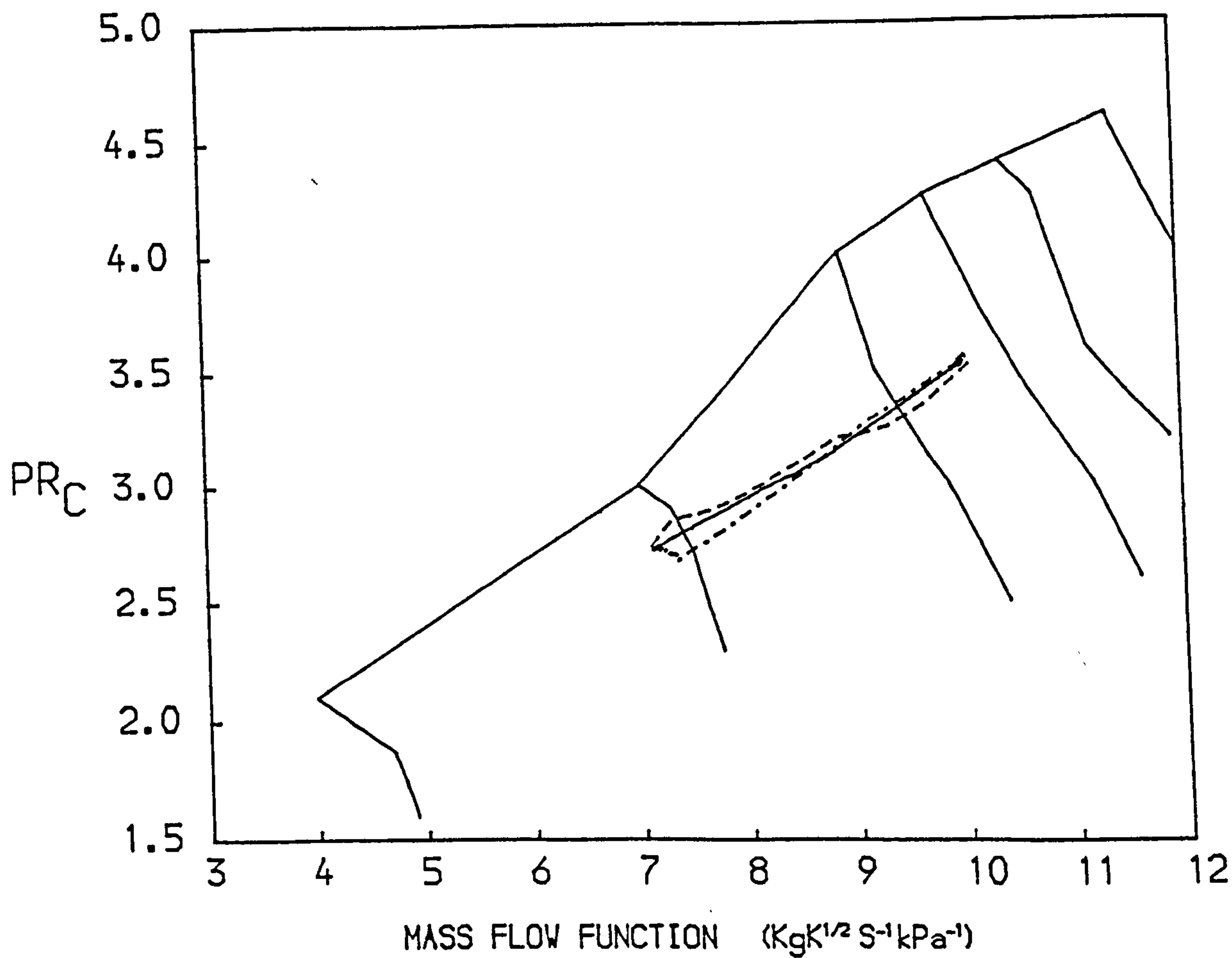
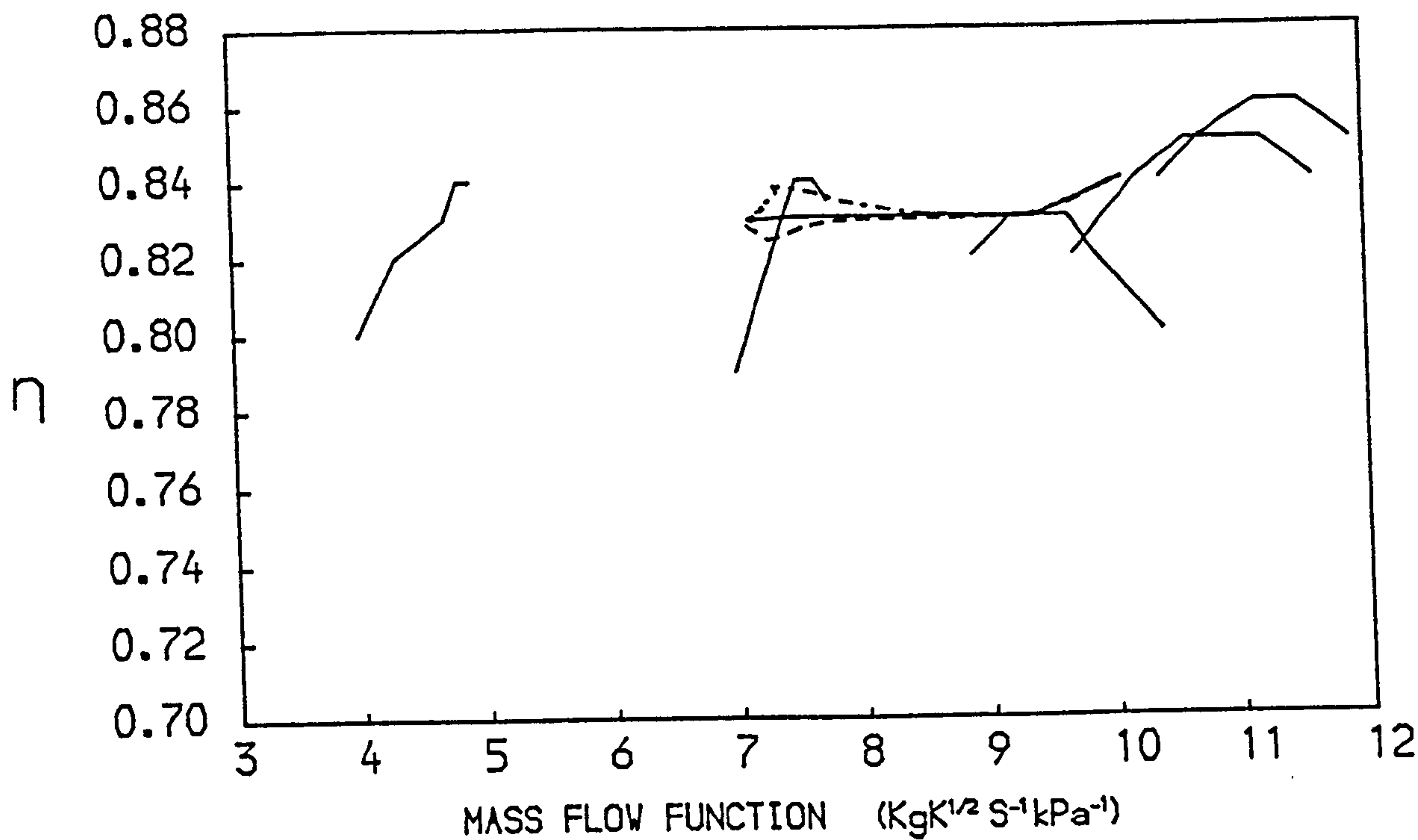


FIG. 61
 PATHS ON THE CHARACTERISTIC MAPS OF THE I.P. COMPRESSOR OF A
 THREE SPOOL TURBOJET
 -- ACCELERATION — STEADY RUNNING --- DECELERATION

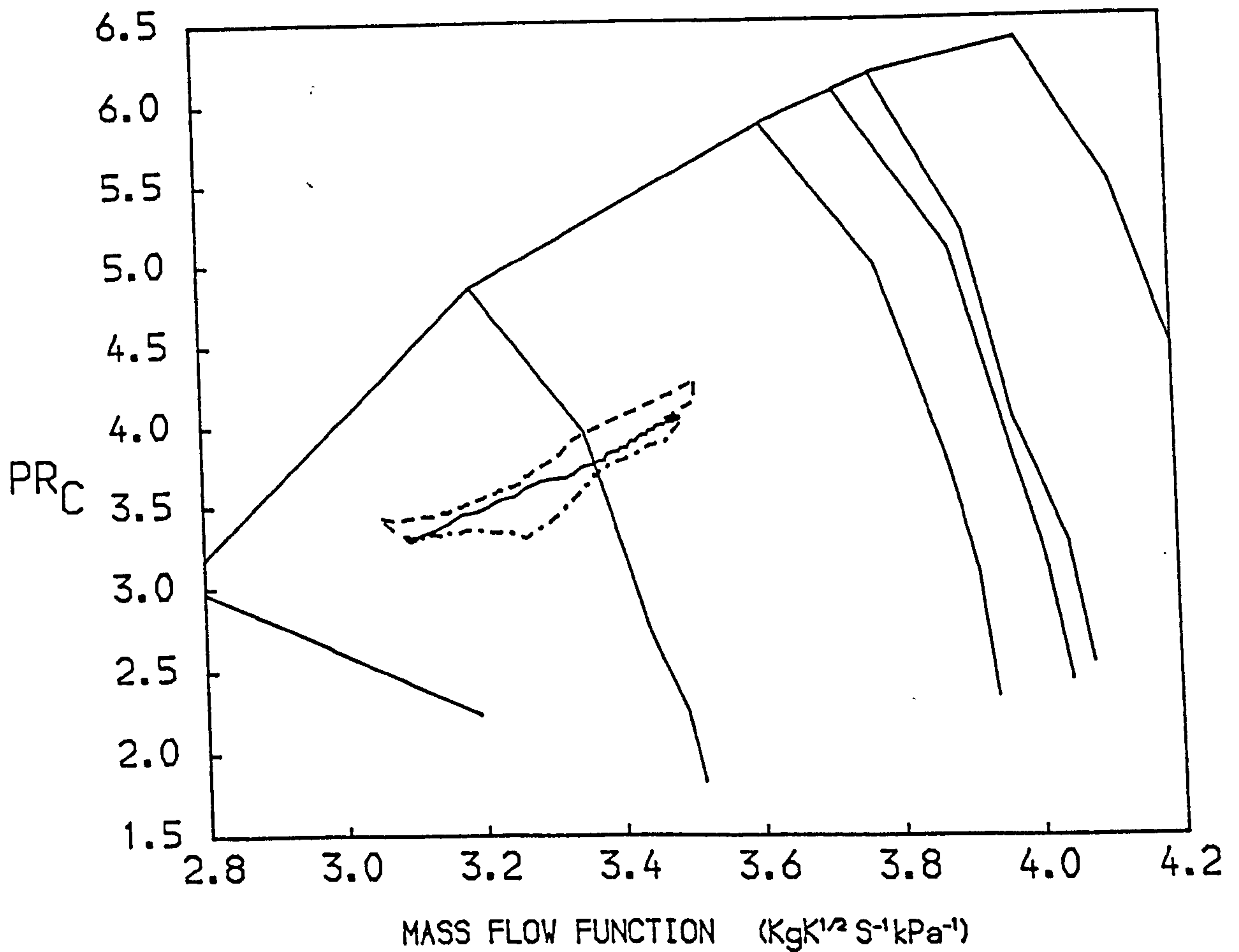
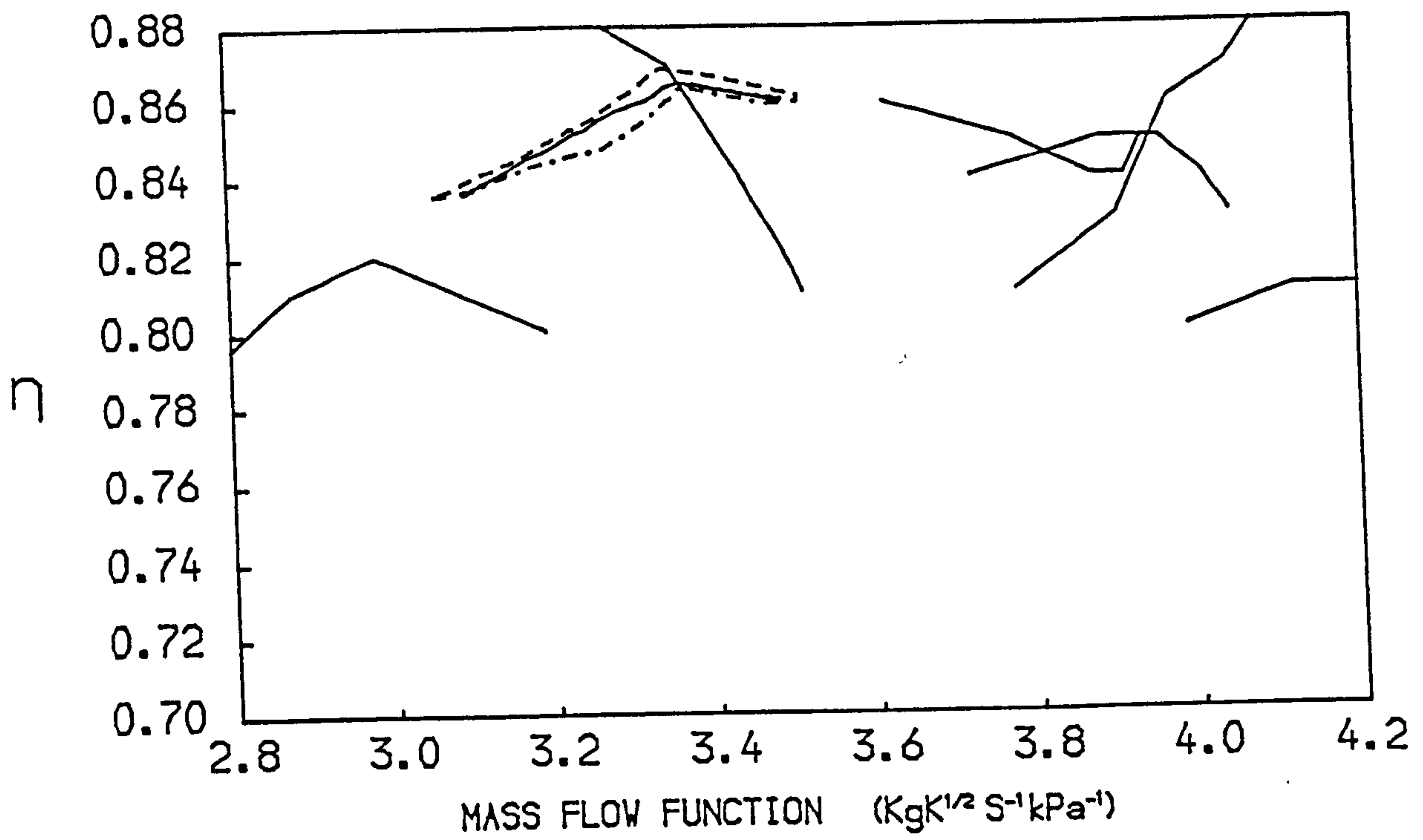


FIG. 62
 PATHS ON THE CHARACTERISTIC MAPS OF THE H.P. COMPRESSOR OF A
 THREE SPOOL TURBOJET
 -- ACCELERATION — STEADY RUNNING --- DECELERATION

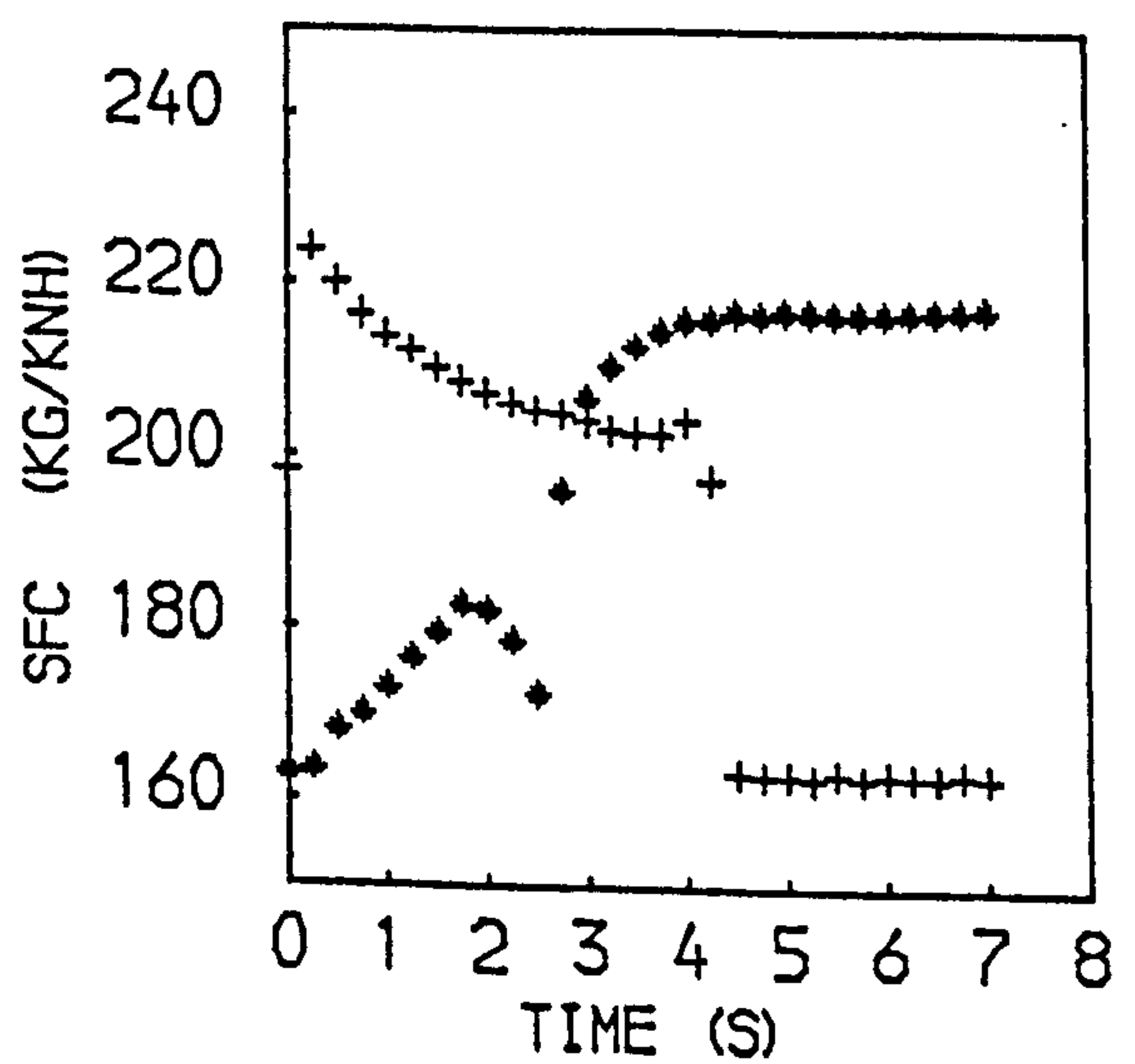
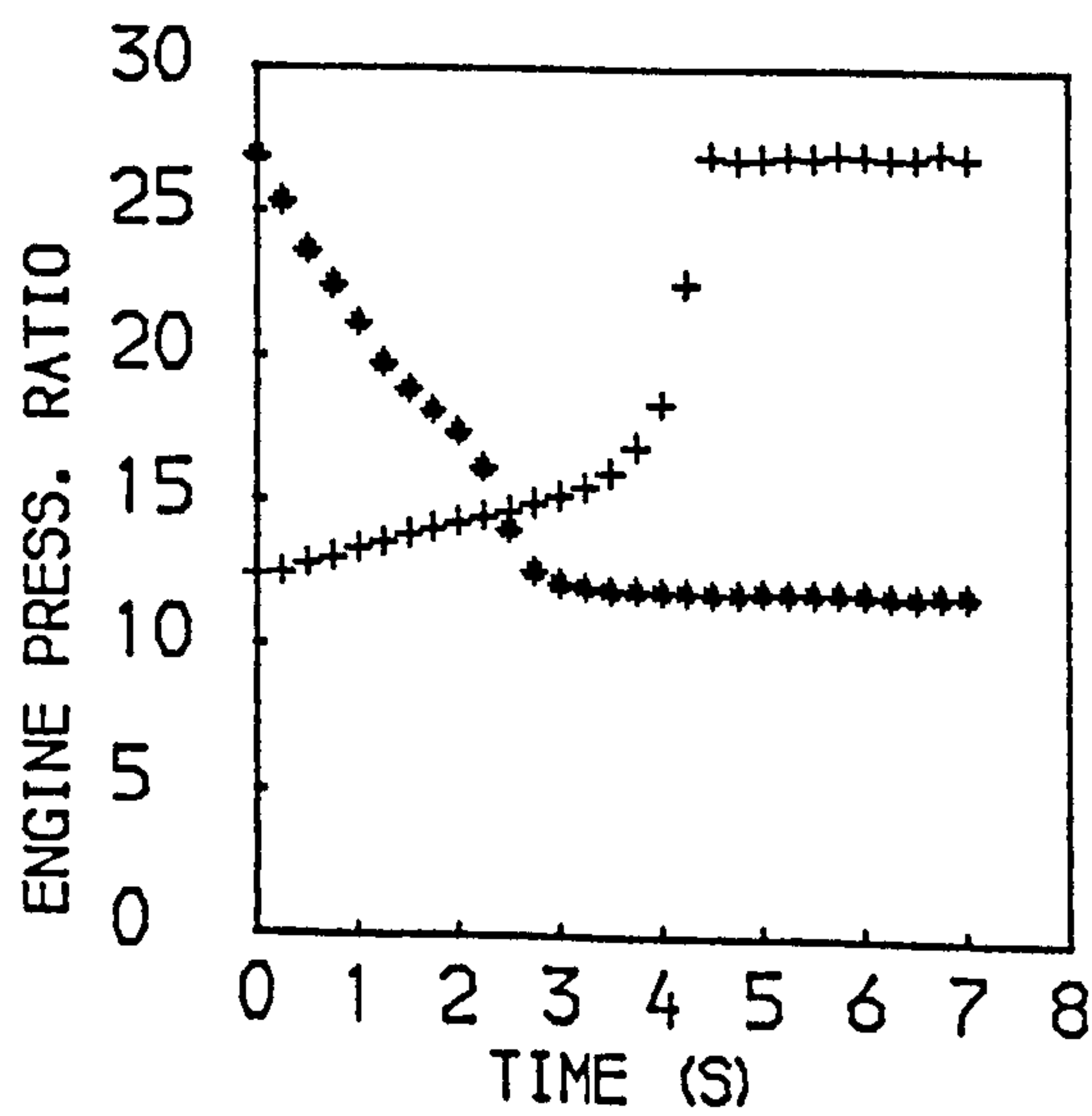
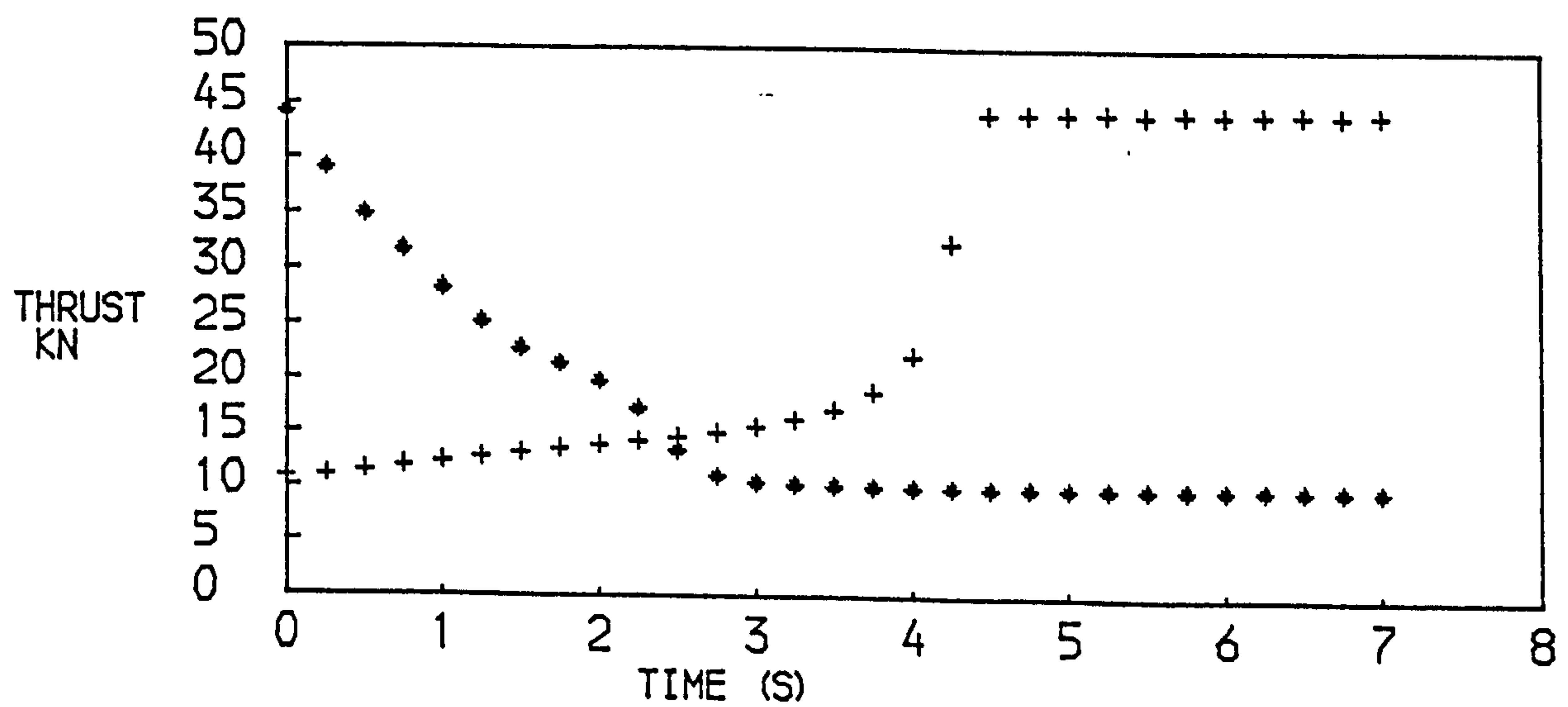
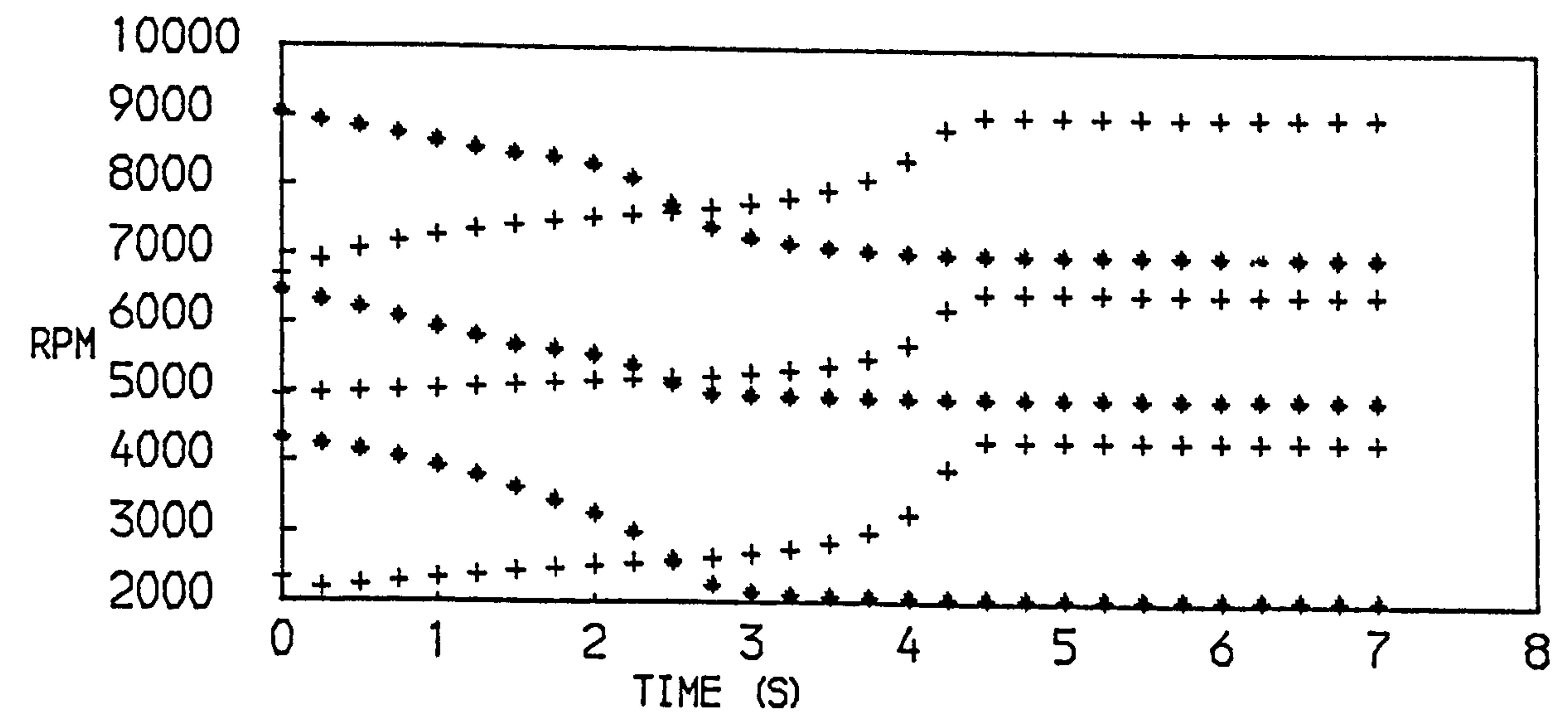


FIG. 63
PERFORMANCE OF A THREE SPOOL TURBOJET ENGINE
+ACCELERATION * DECELERATION

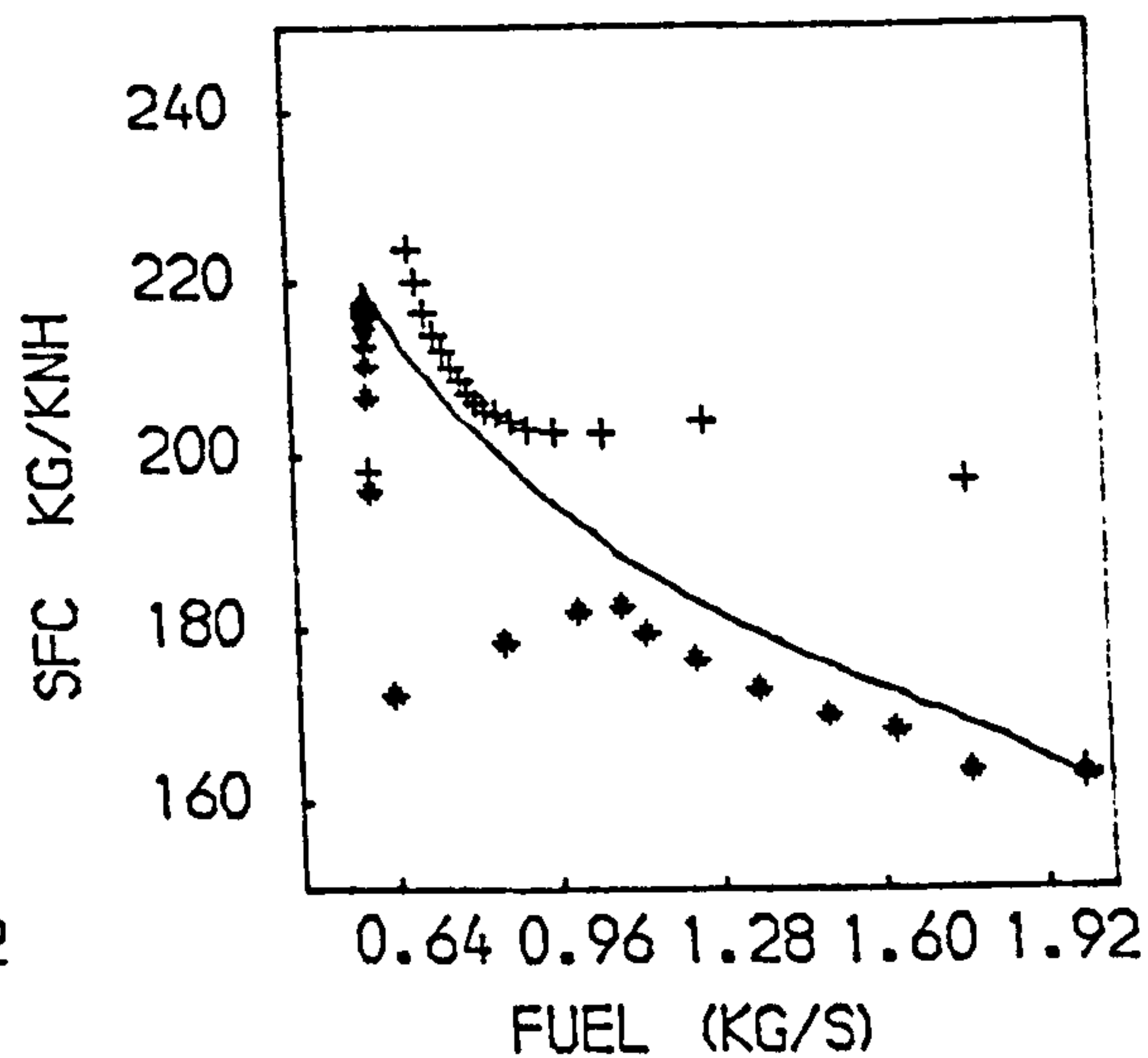
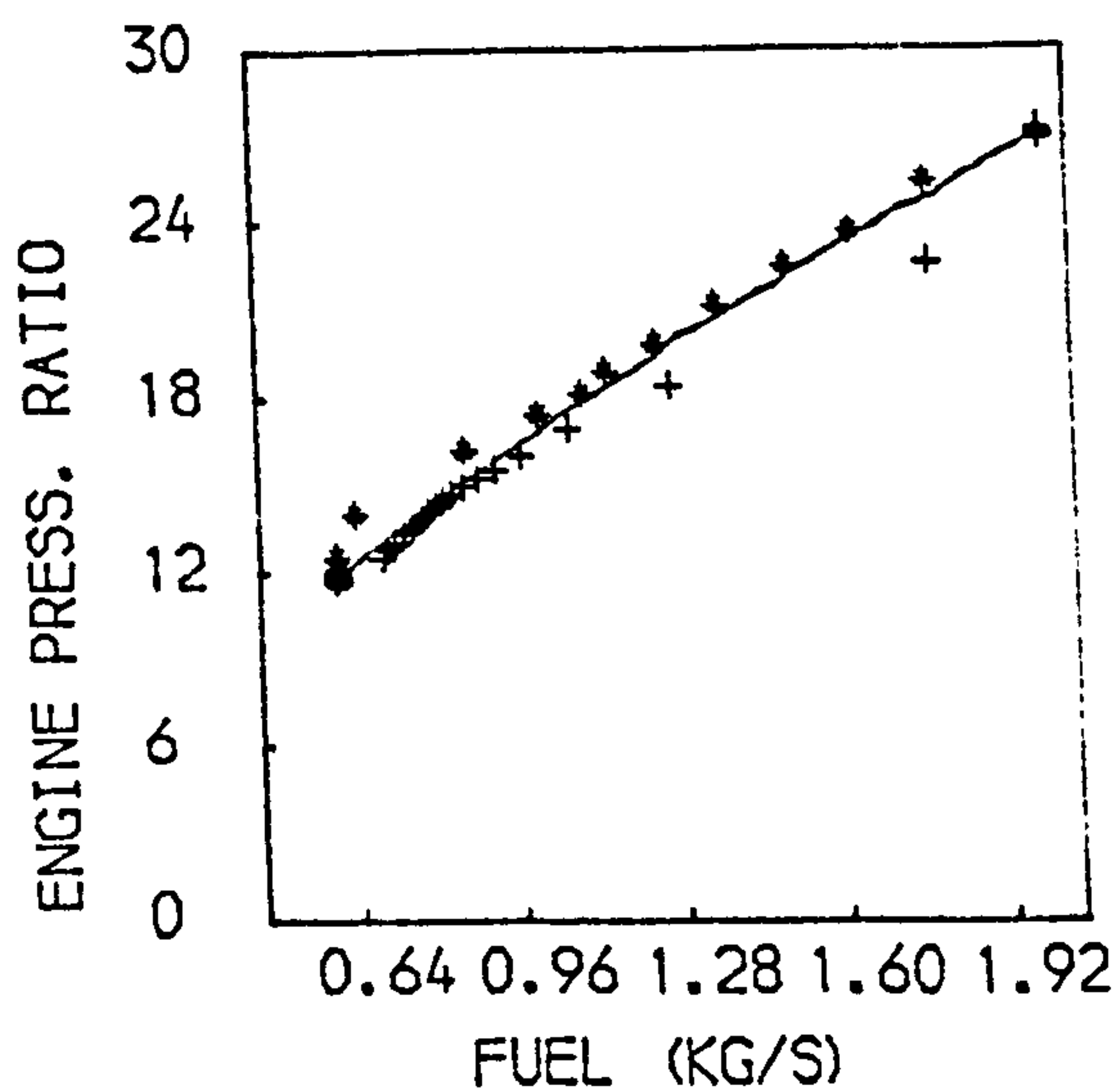
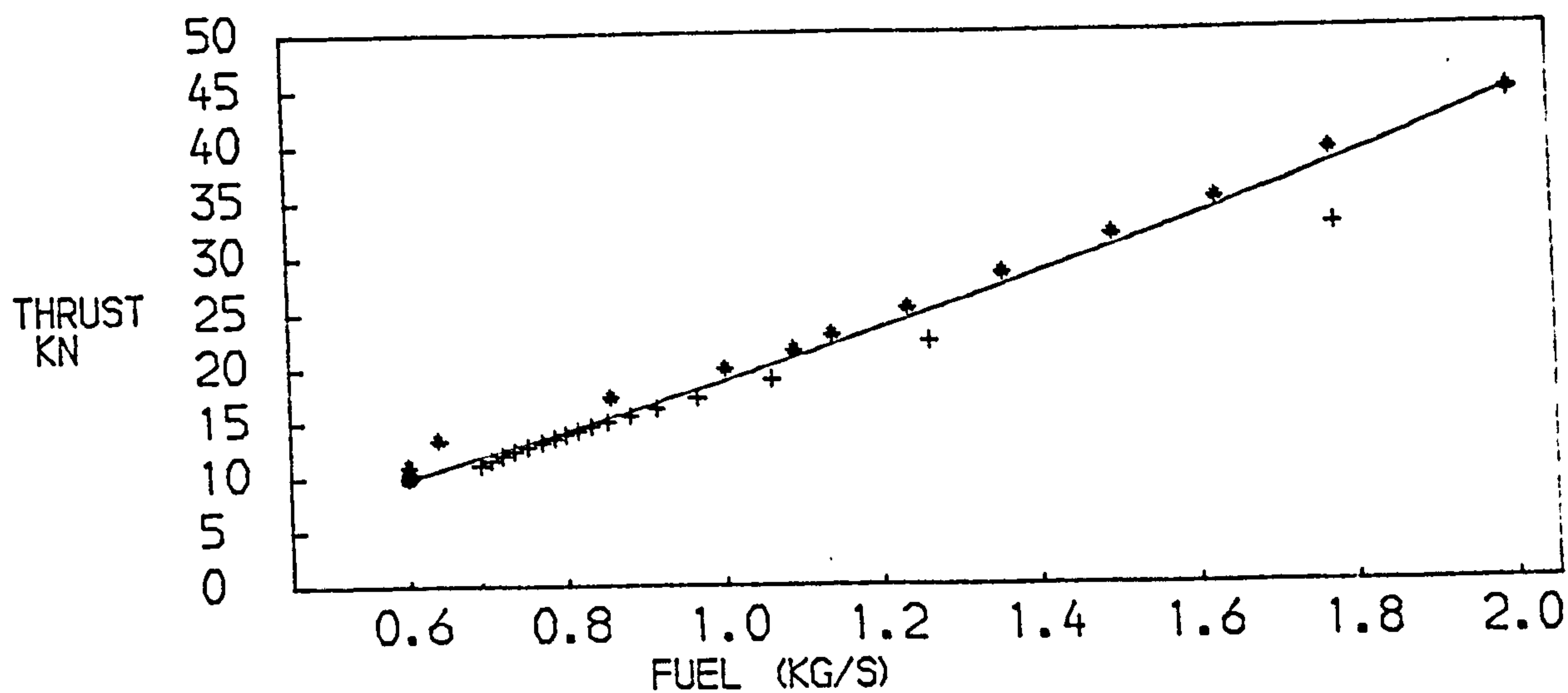
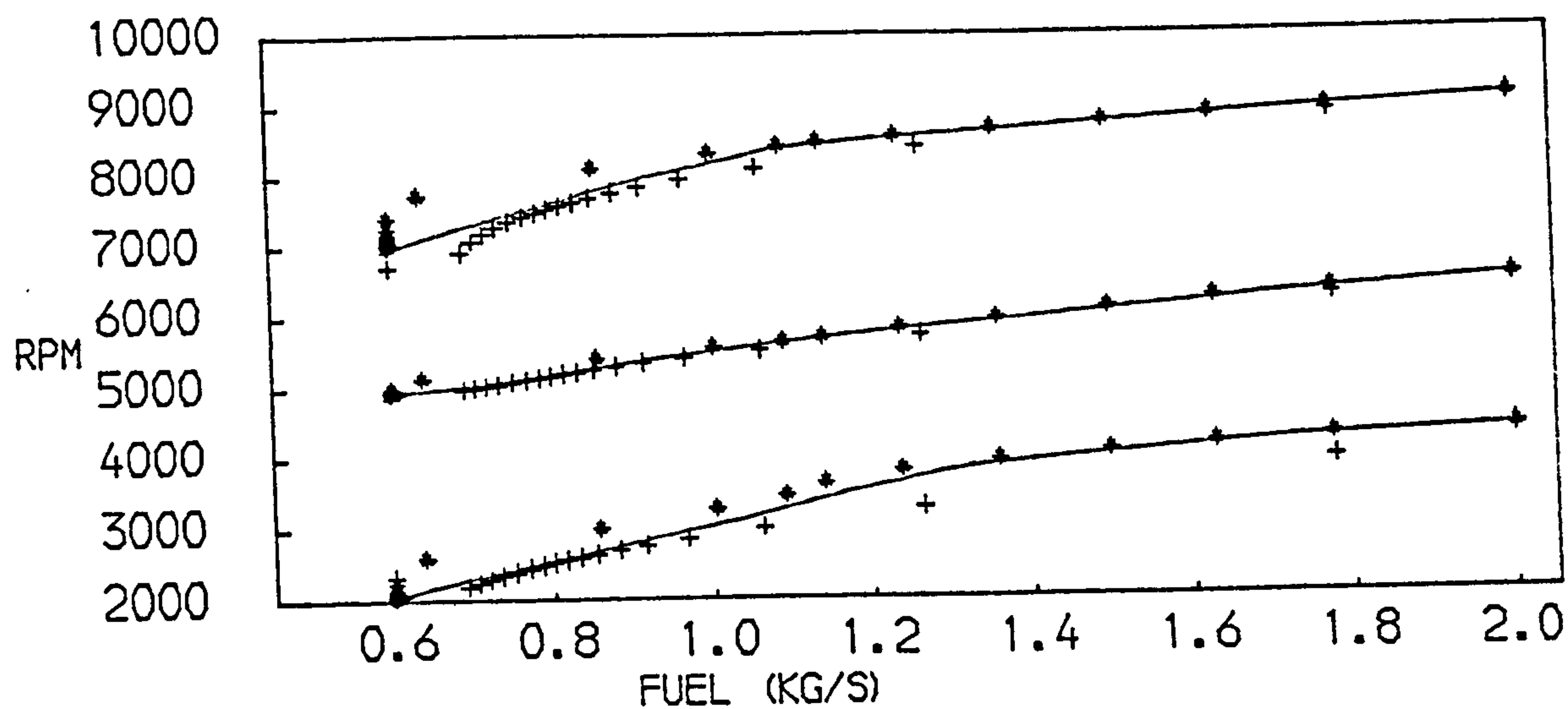


FIG. 64
PERFORMANCE OF A THREE SPOOL TURBOJET
+ACCELERATION * DECELERATION —STEADY RUNNING

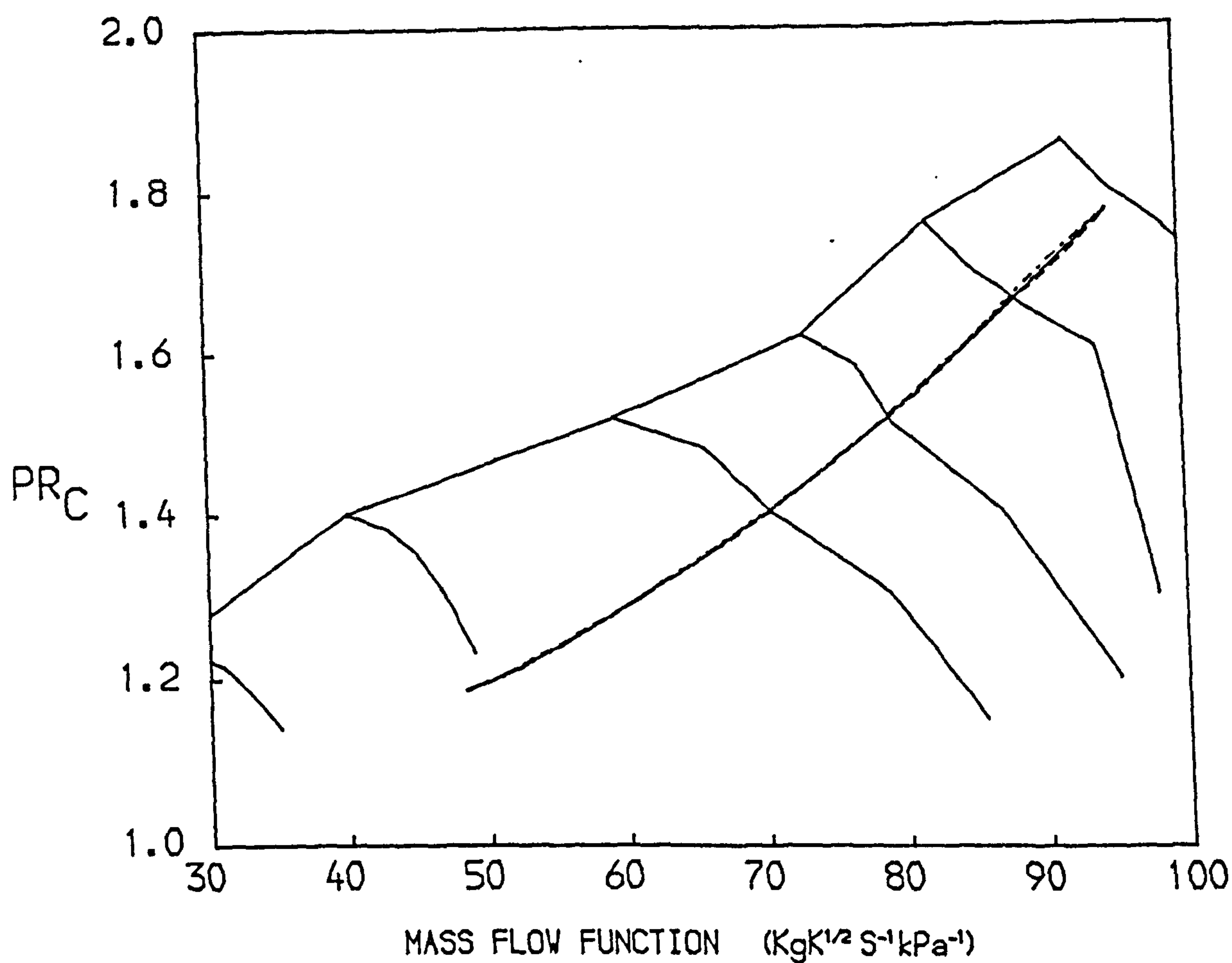
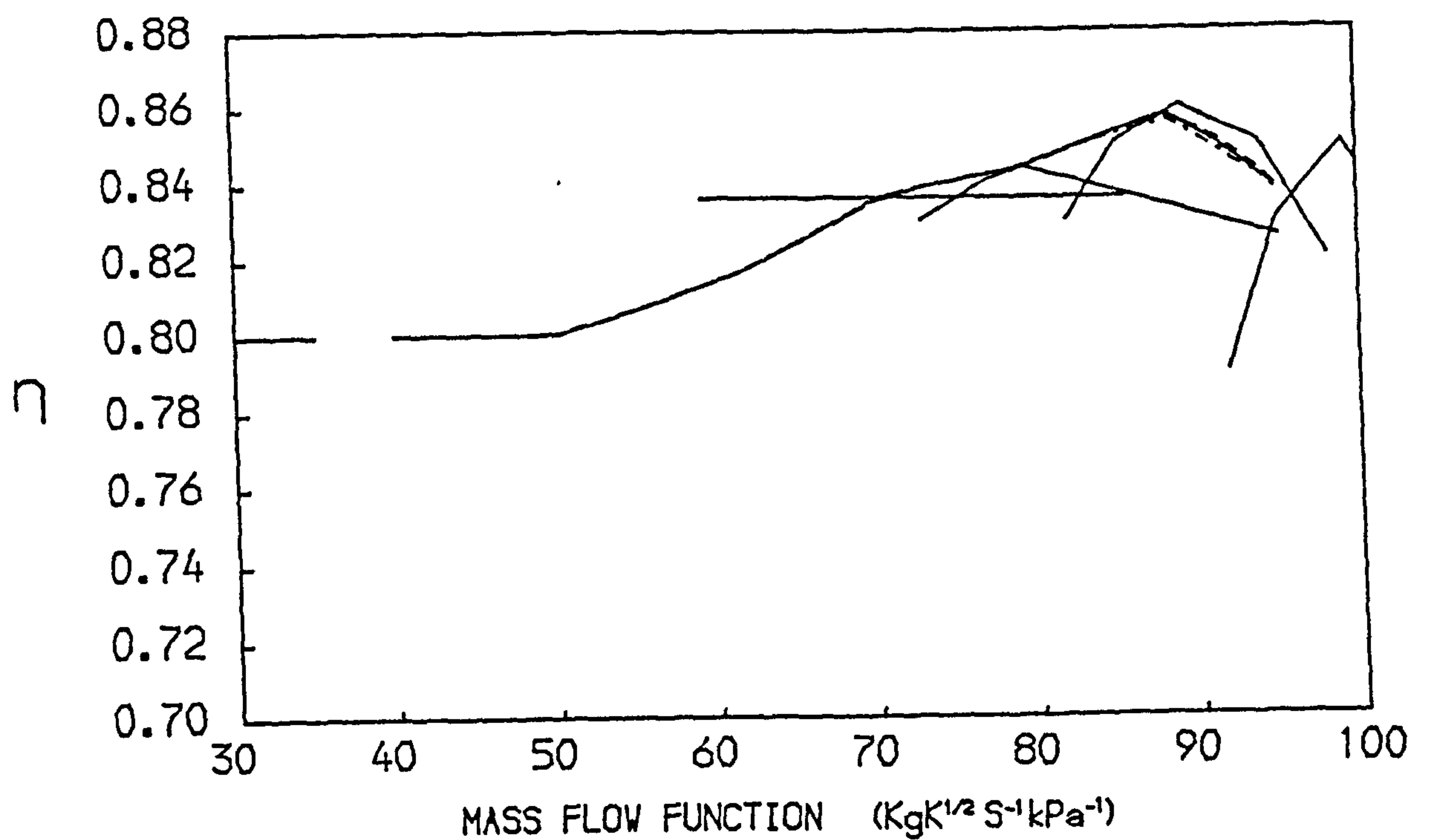


FIG. 65
 PATHS ON THE CHARACTERISTIC MAPS OF THE FAN OF A
 THREE SPOOL TURBOFAN WITH SEPARATE EXHAUSTS
 -- ACCELERATION — STEADY RUNNING --- DECELERATION

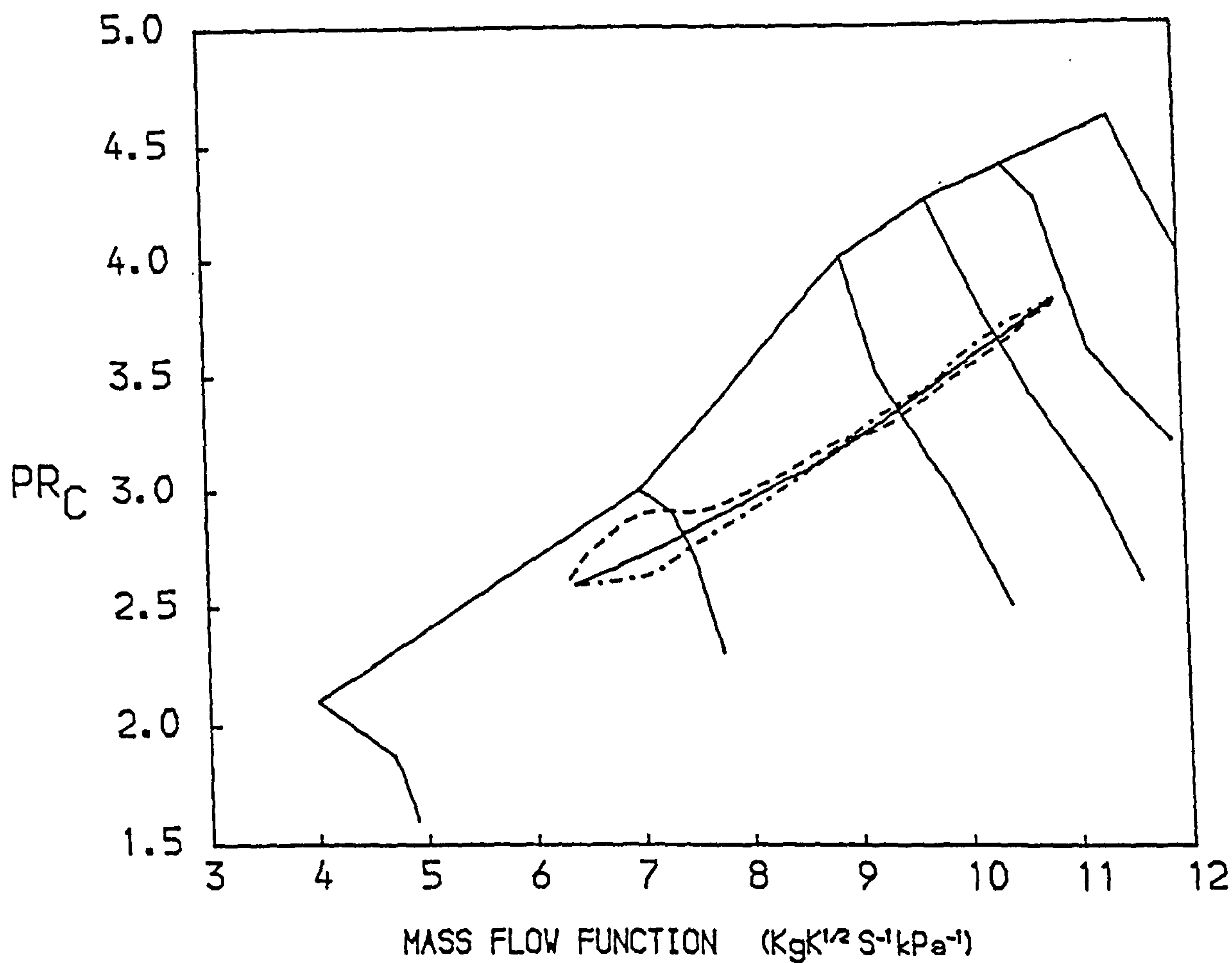
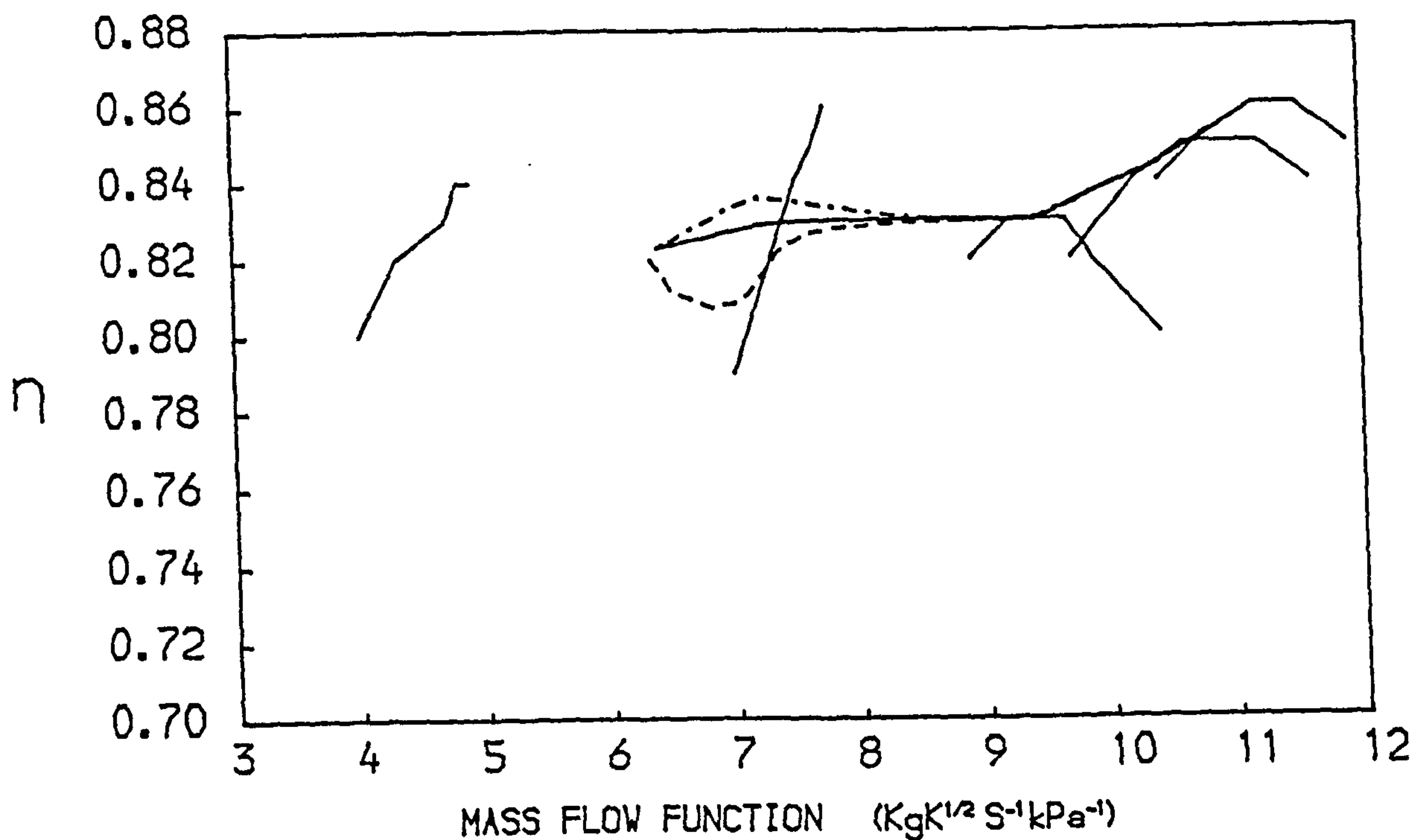


FIG. 66
 PATHS ON THE CHARACTERISTIC MAPS OF THE I.P. COMPRESSOR OF A
 THREE SPOOL TURBOFAN WITH SEPARATE EXHAUSTS
 -- ACCELERATION — STEADY RUNNING --- DECELERATION

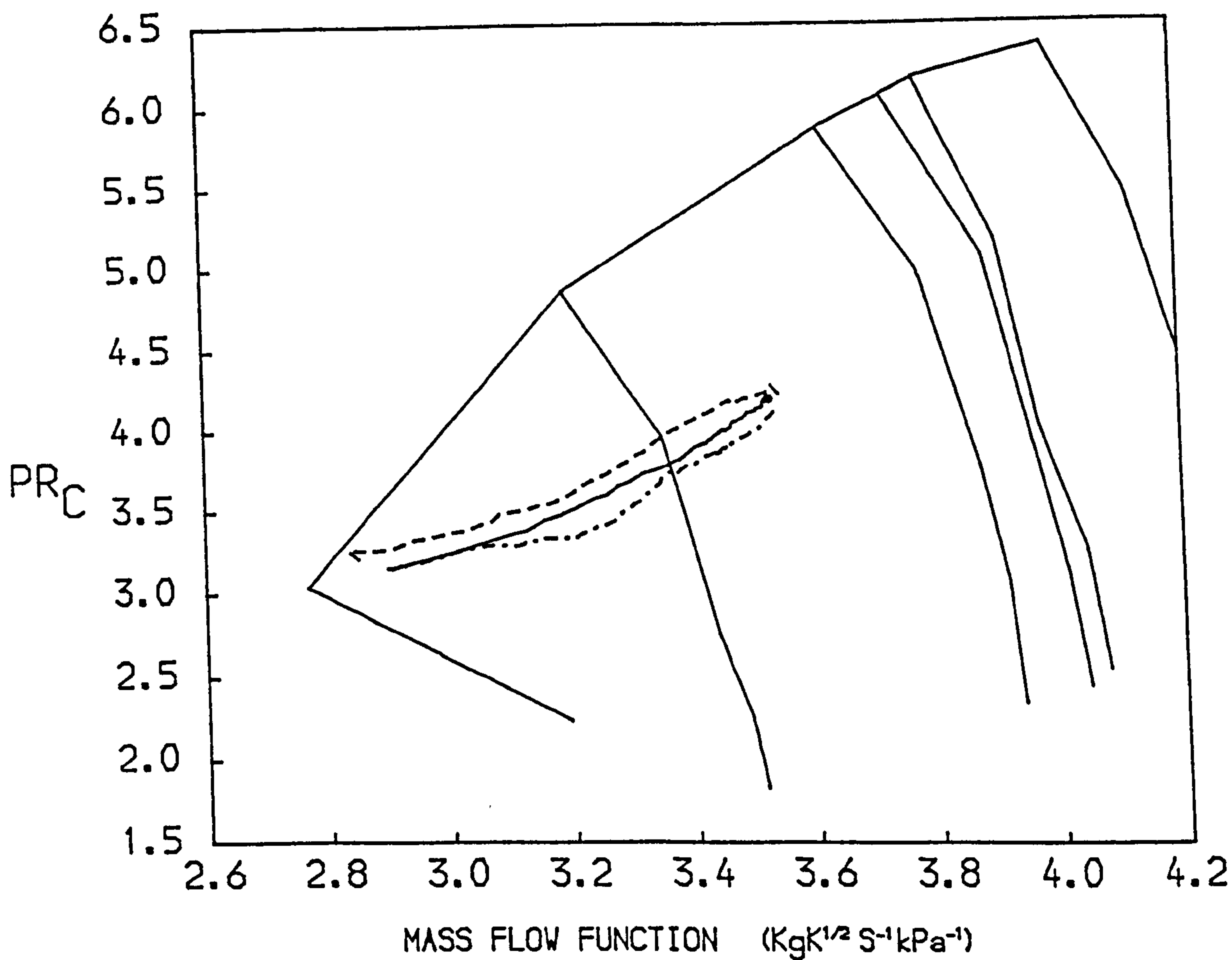
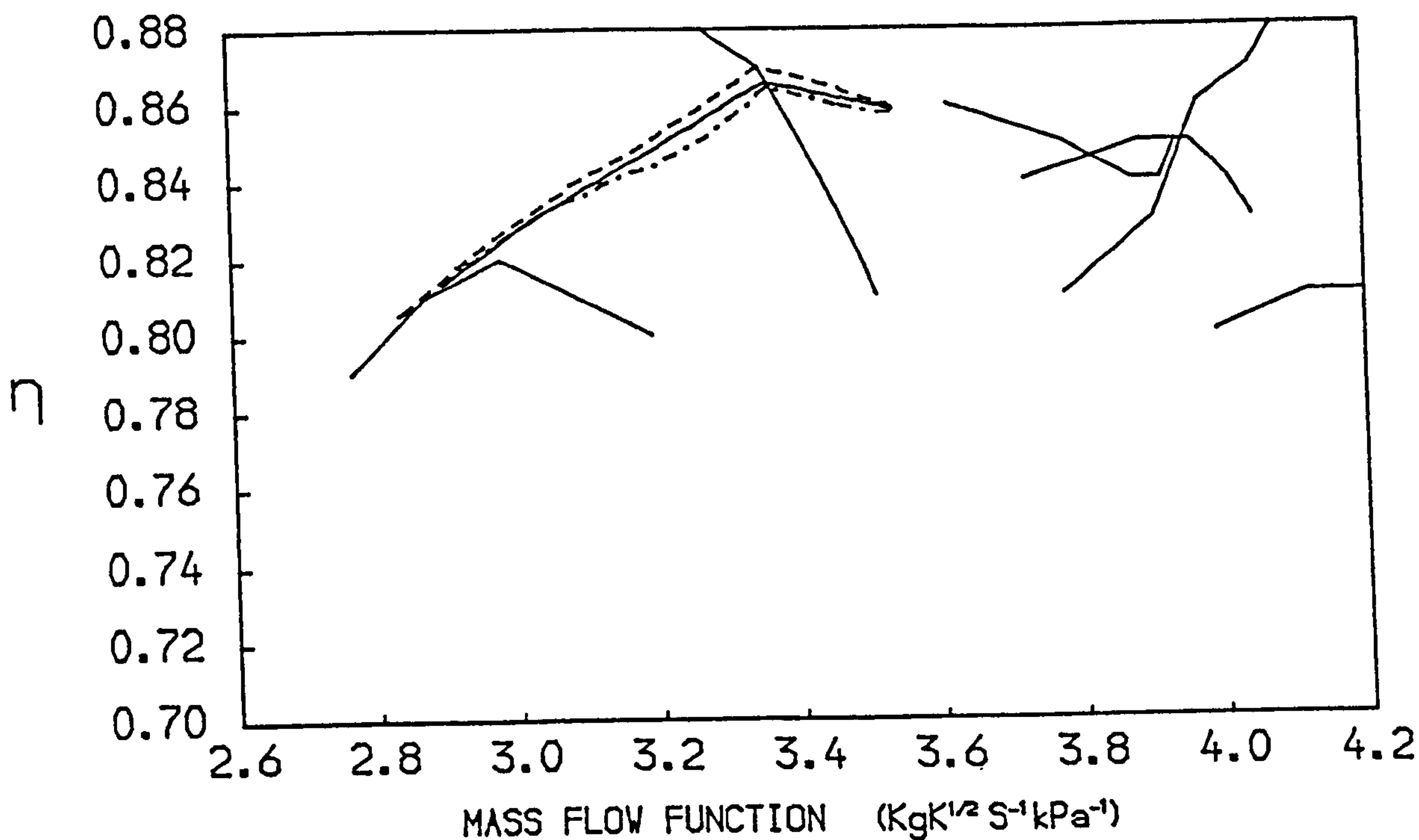


FIG. 67
 PATHS ON THE CHARACTERISTIC MAPS OF THE H.P. COMPRESSOR OF A
 THREE SPOOL TURBOFAN WITH SEPARATE EXHAUSTS
 -- ACCELERATION — STEADY RUNNING --- DECELERATION

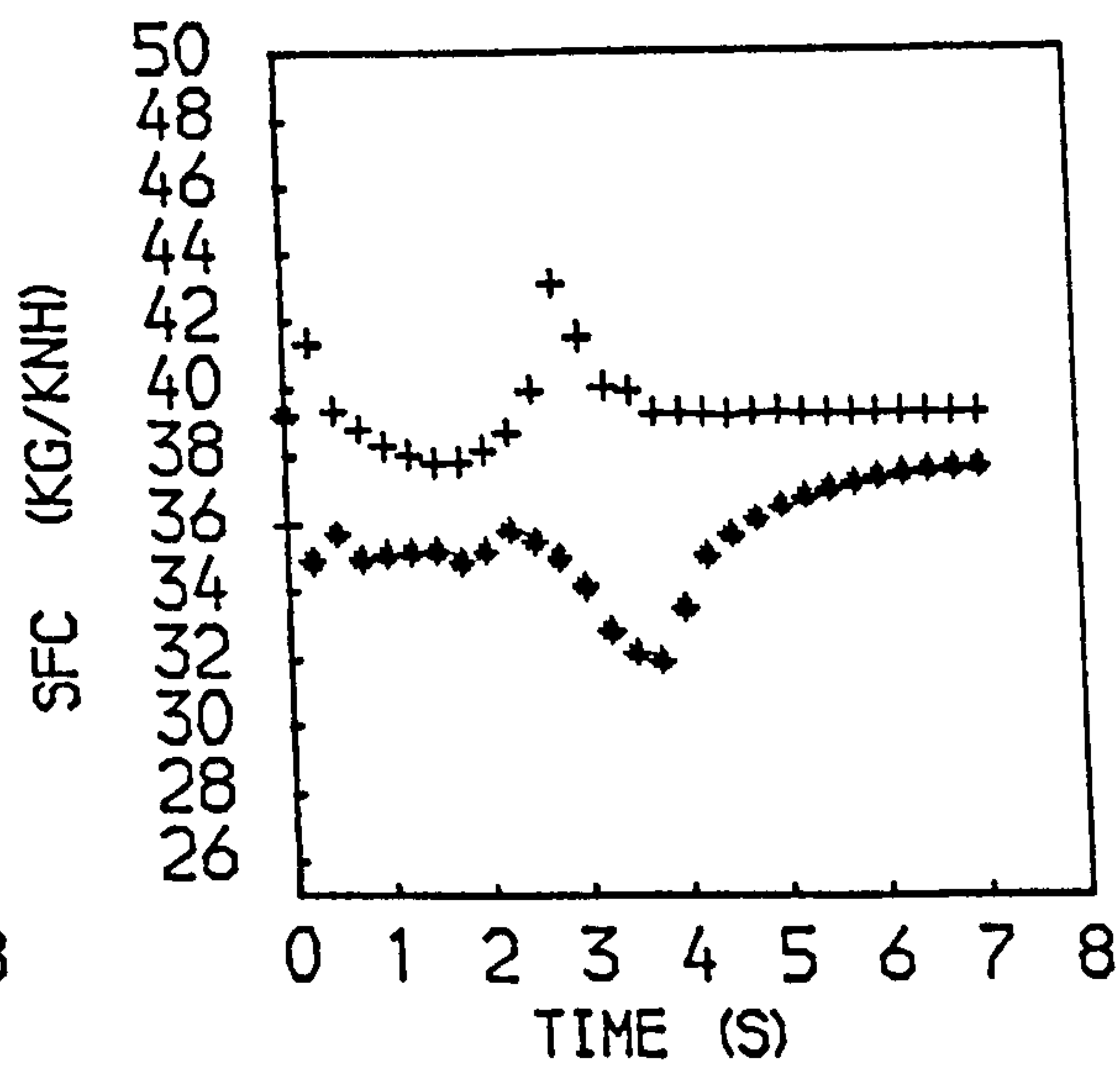
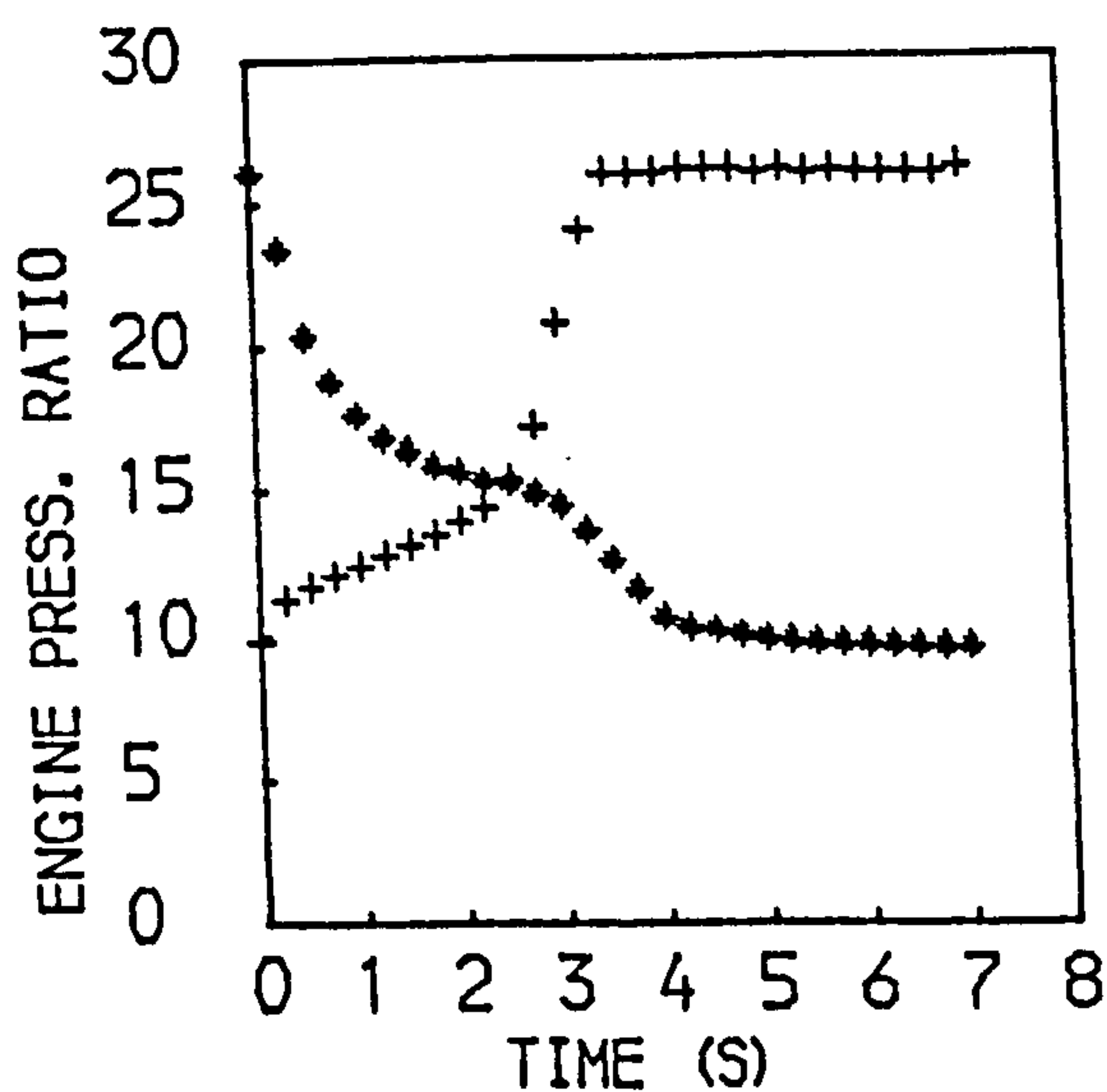
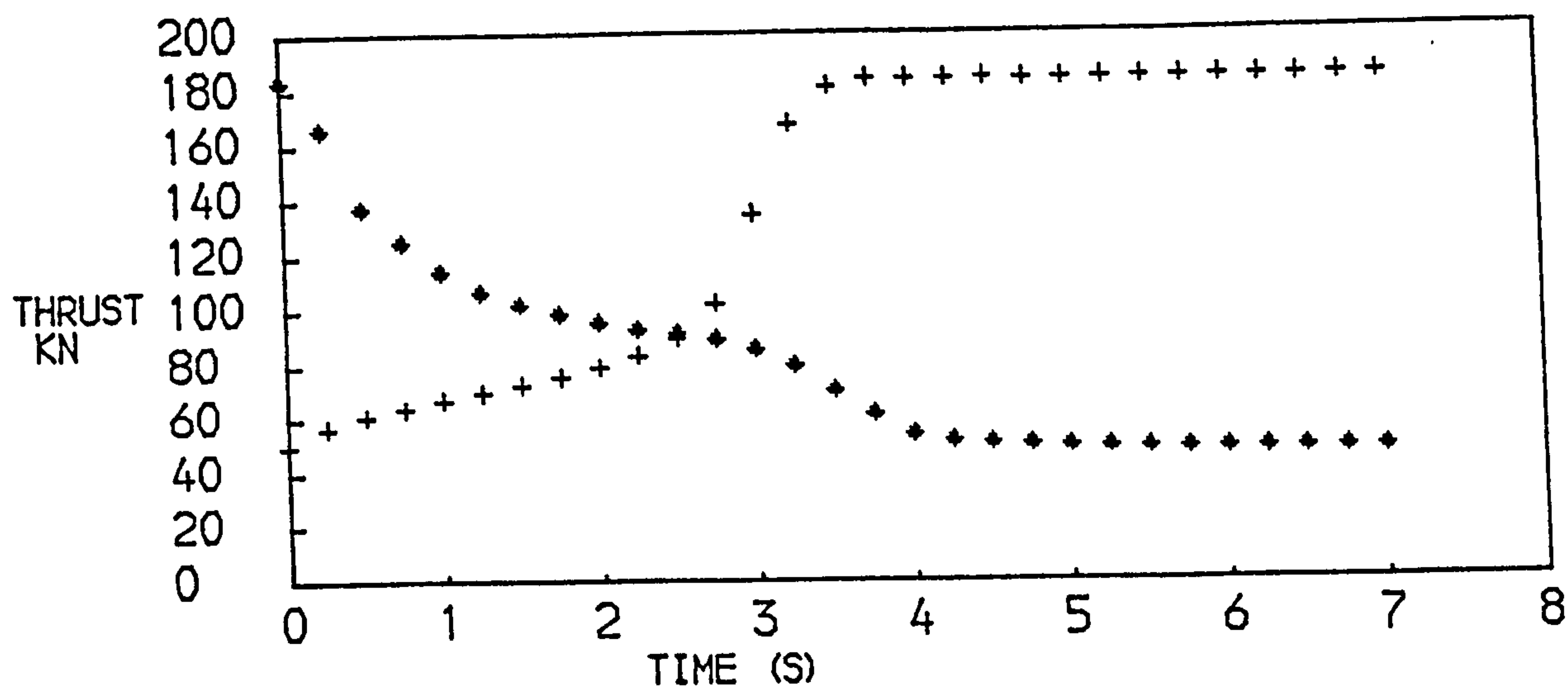
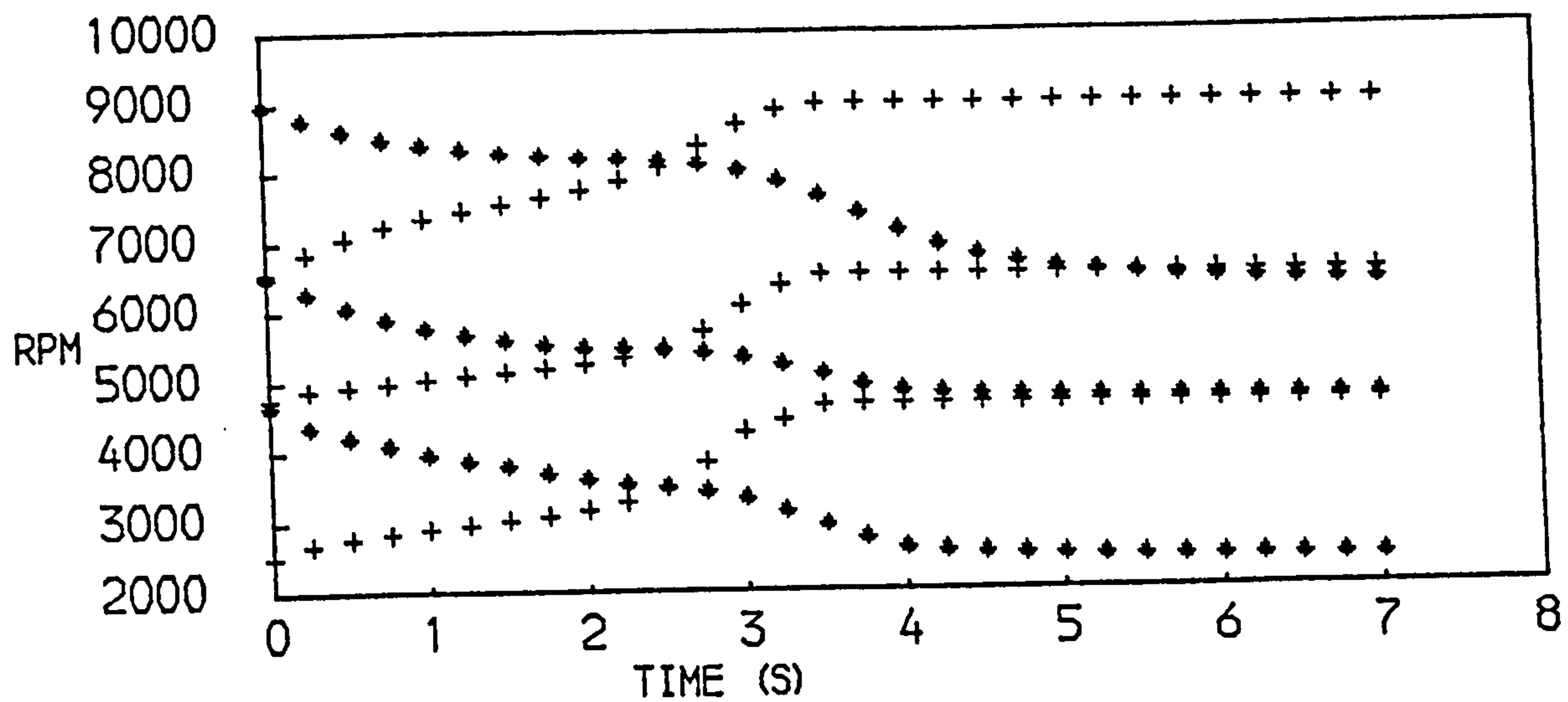


FIG. 68
PERFORMANCE OF A THREE SPOOL TURBOFAN WITH SEPARATE EXHAUSTS
+ACCELERATION * DECELERATION

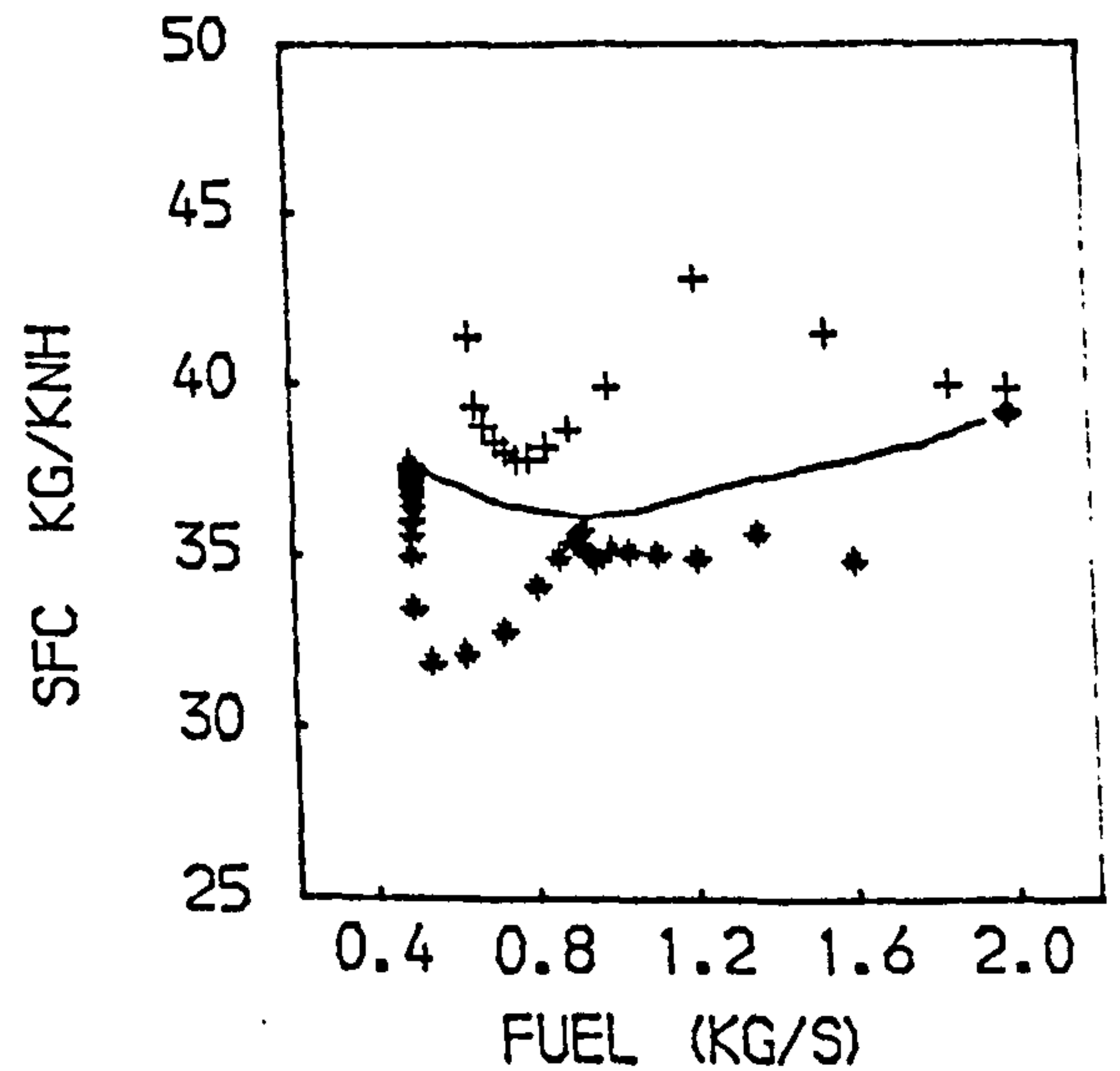
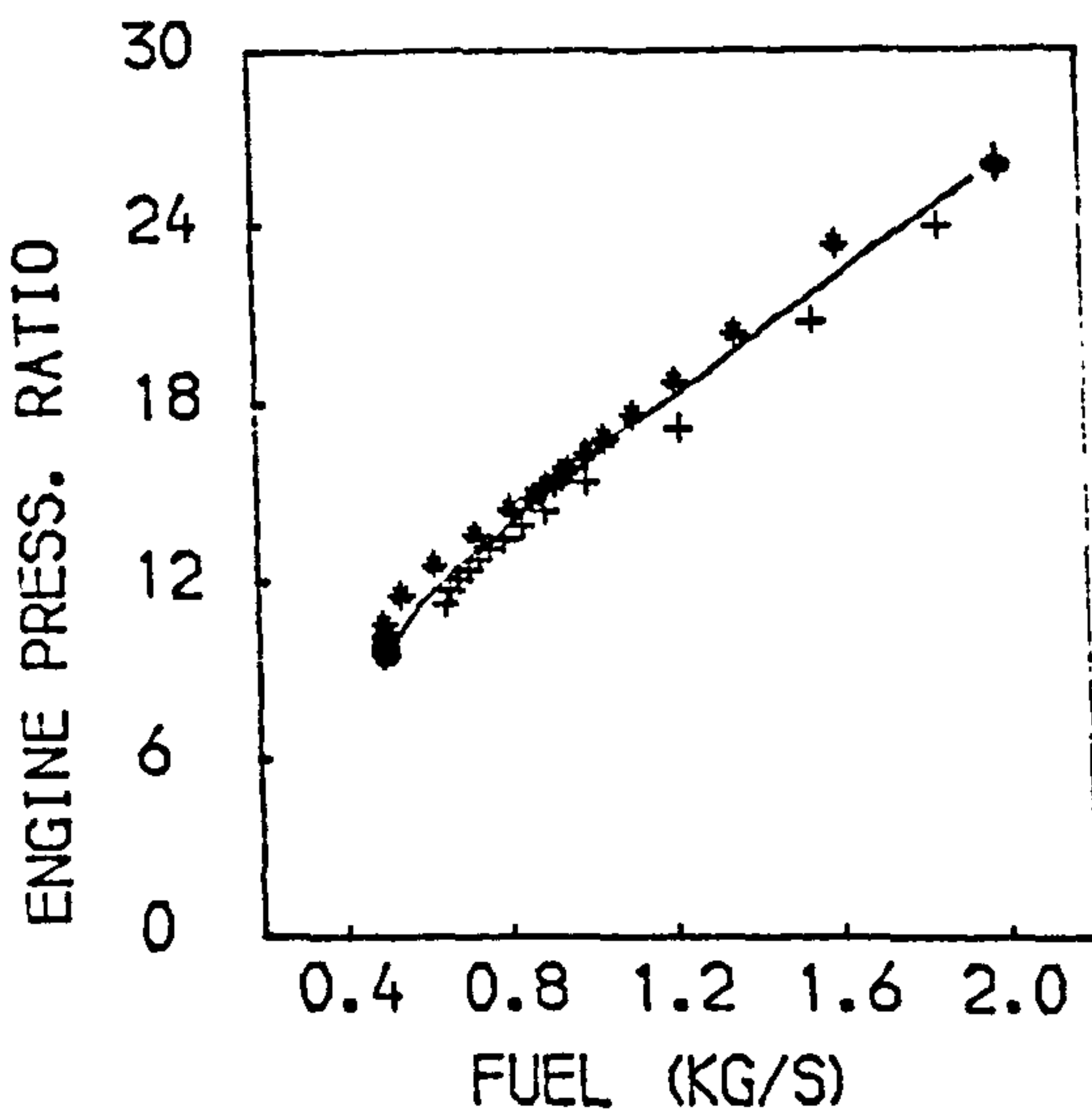
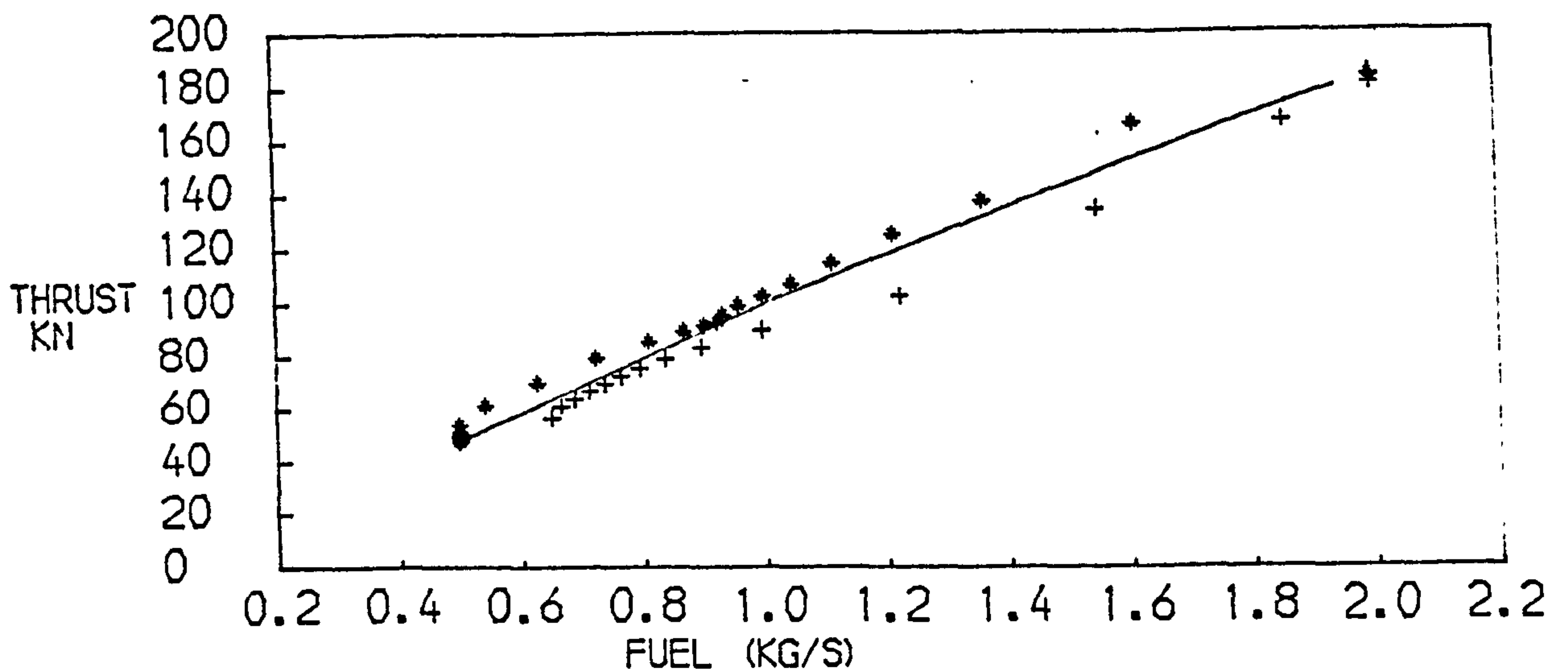
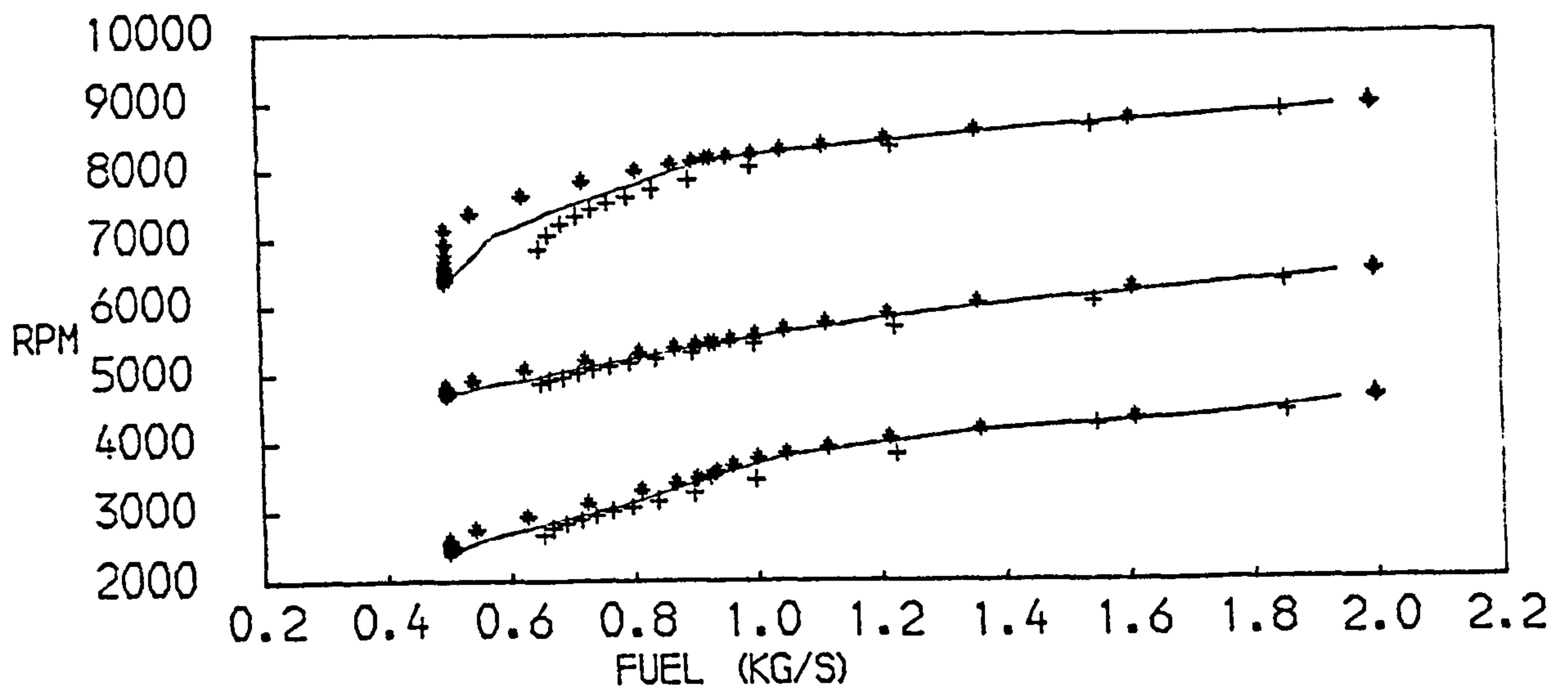


FIG. 69
PERFORMANCE OF A THREE SPOOL TURBOFAN WITH SEPARATE EXHAUSTS
+ ACCELERATION * DECELERATION — STEADY RUNNING

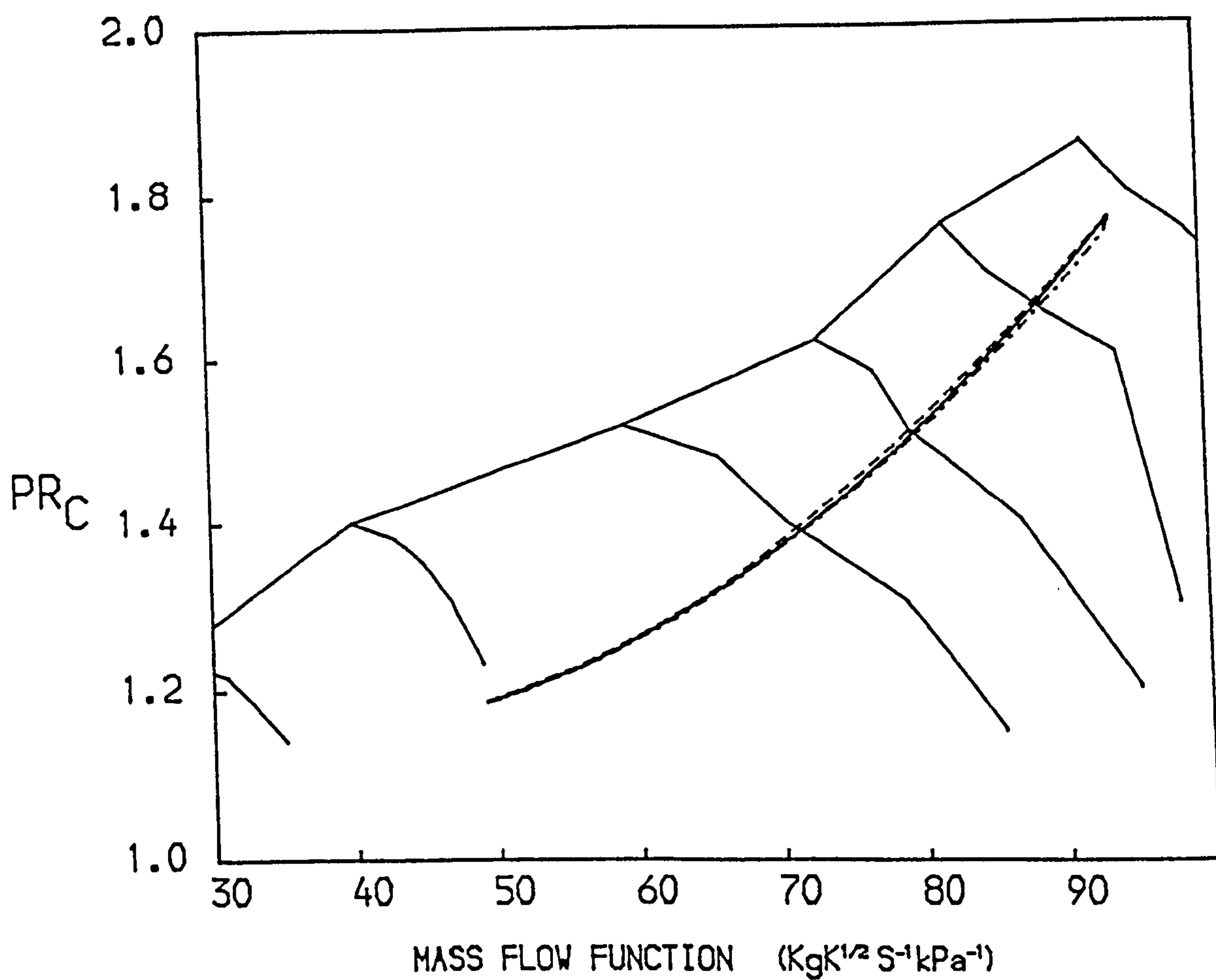
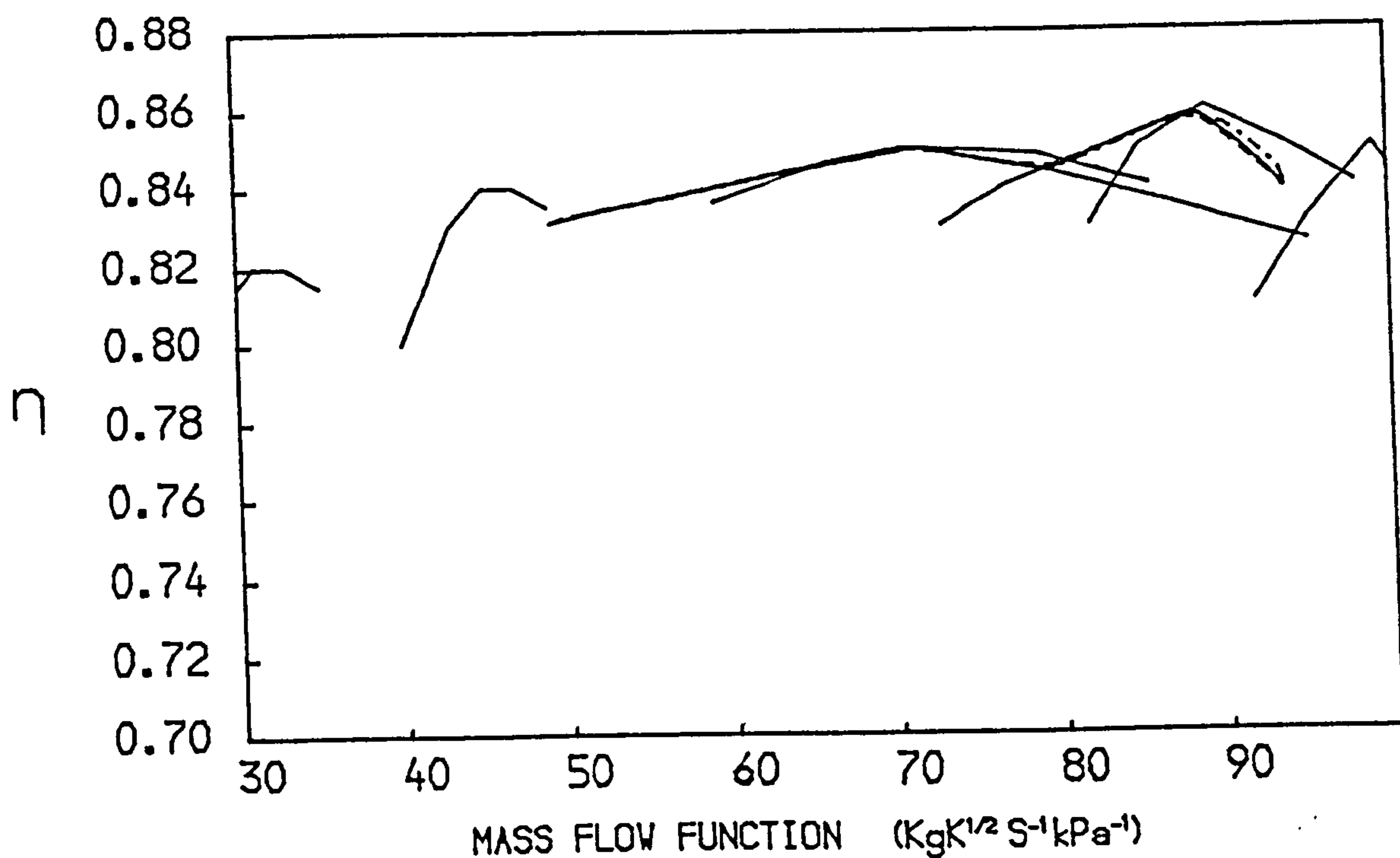


FIG. 70
 PATHS ON THE CHARACTERISTIC MAPS OF THE FAN OF A
 THREE SPOOL TURBOFAN WITH MIXED EXHAUSTS
 -- ACCELERATION — STEADY RUNNING --- DECELERATION

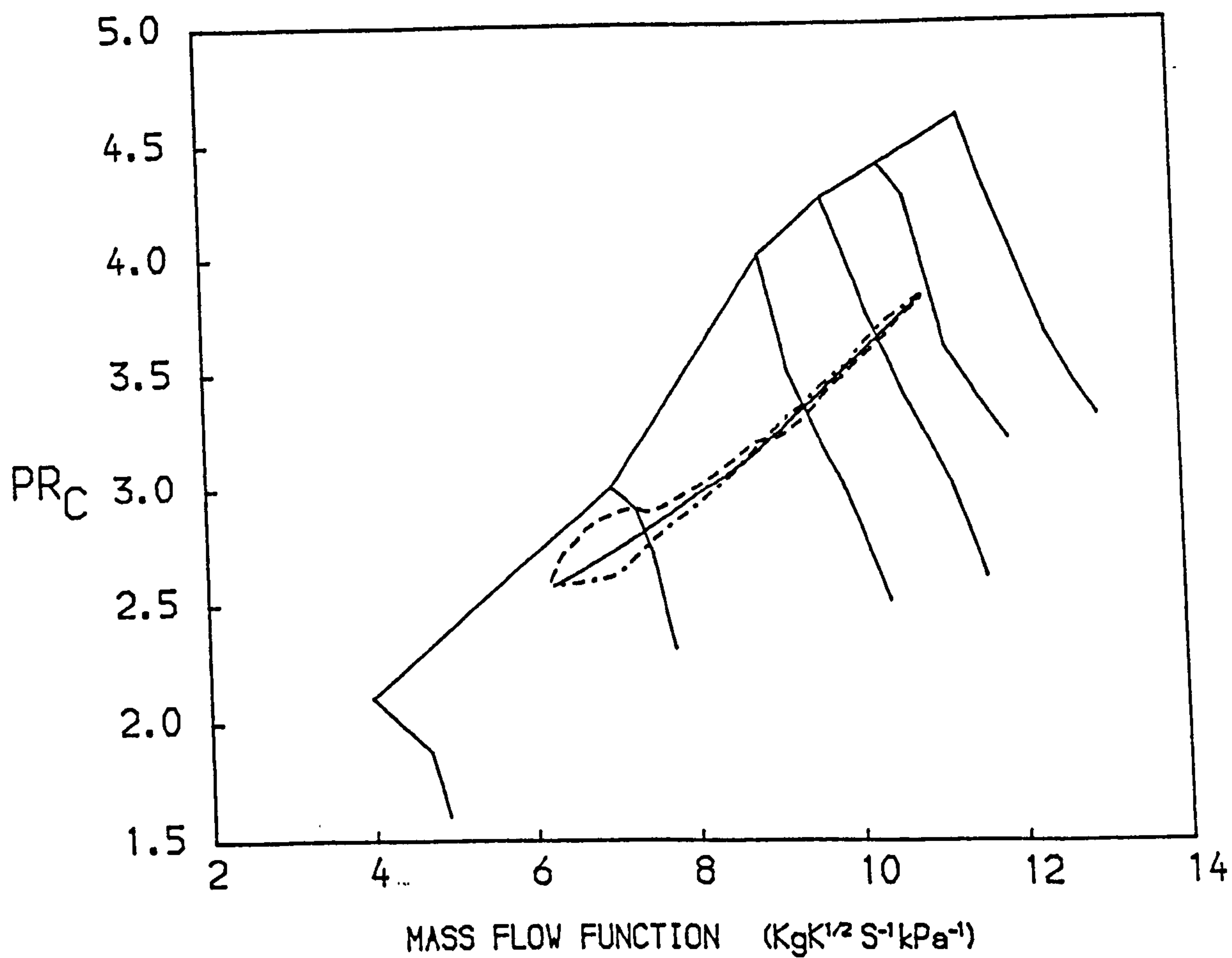
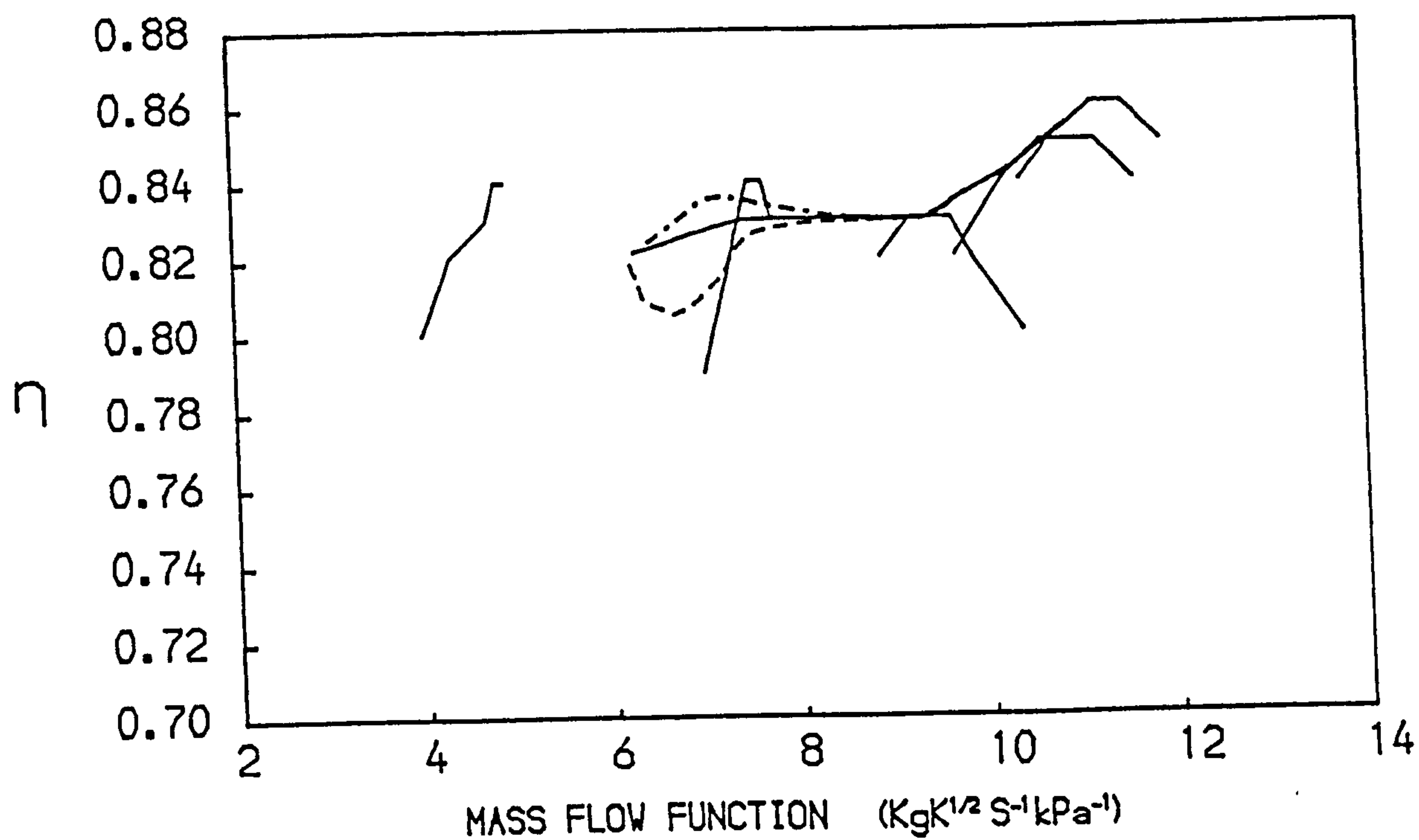


FIG. 71
 PATHS ON THE CHARACTERISTIC MAPS OF THE I.P. COMPRESSOR OF A
 THREE SPOOL TURBOFAN WITH MIXED EXHAUSTS
 -- ACCELERATION — STEADY RUNNING --- DECELERATION

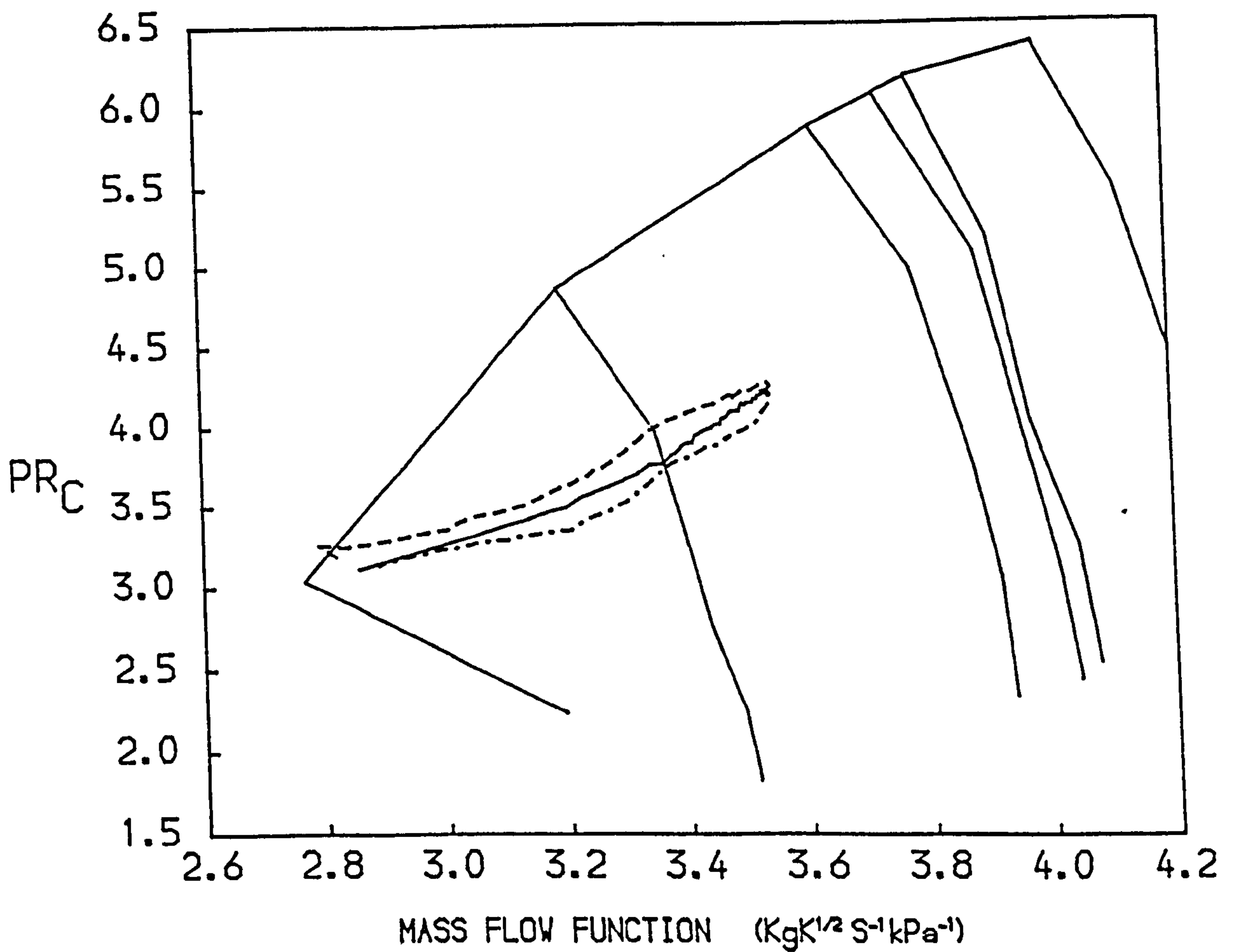
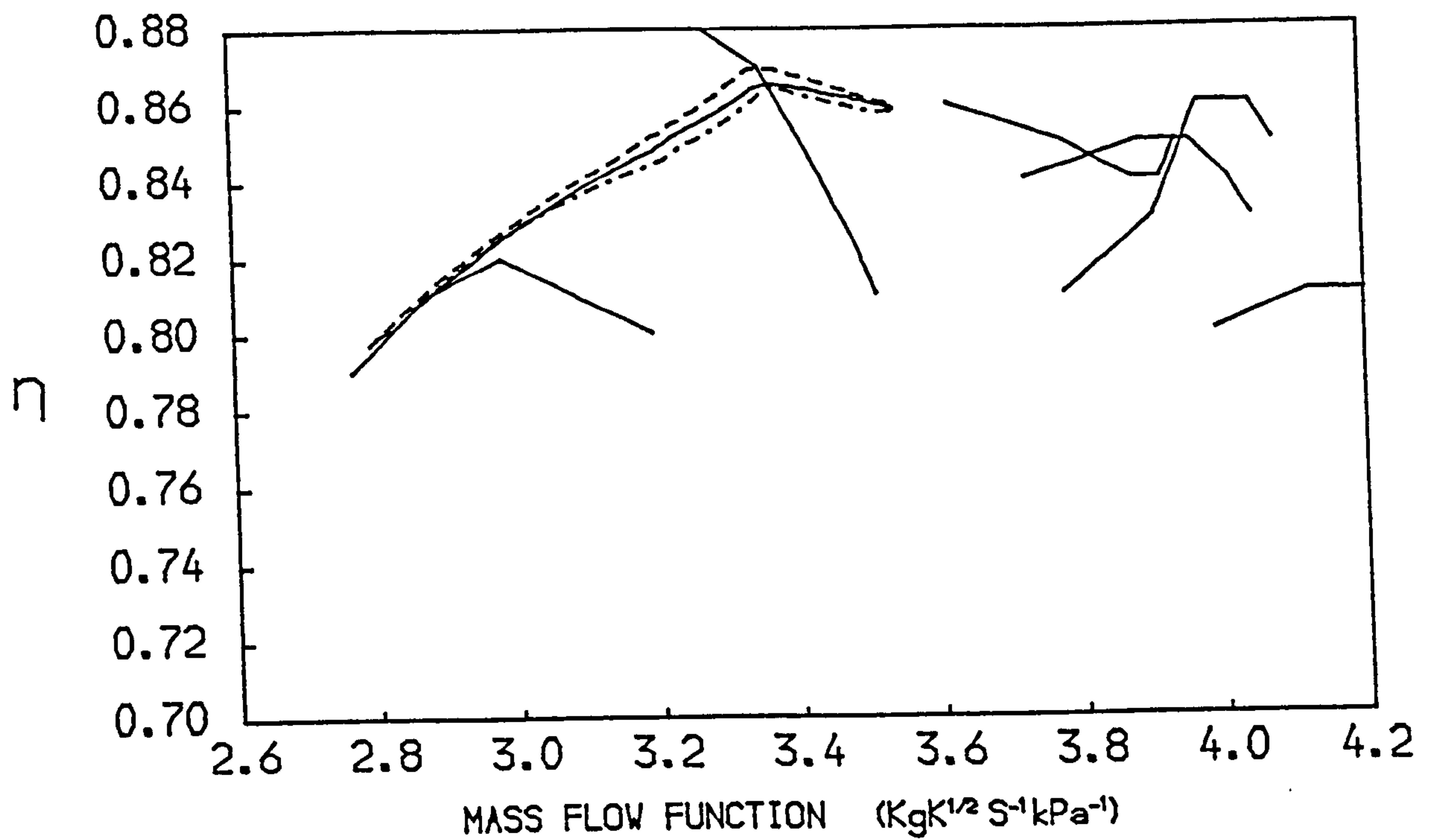


FIG. 72
 PATHS ON THE CHARACTERISTIC MAPS OF THE H.P. COMPRESSOR OF A
 THREE SPOOL TURBOFAN WITH MIXED EXHAUSTS
 -- ACCELERATION — STEADY RUNNING --- DECELERATION

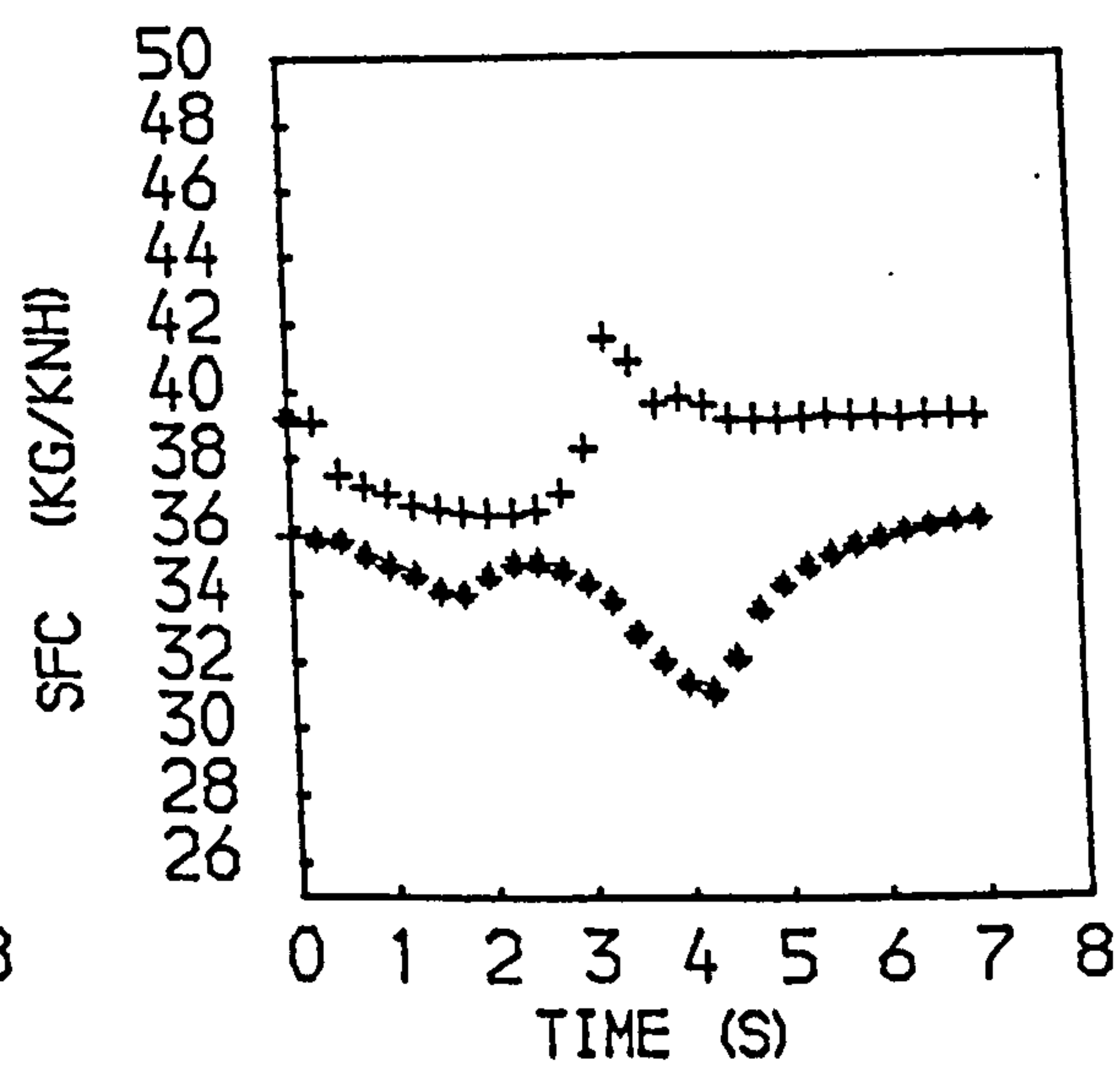
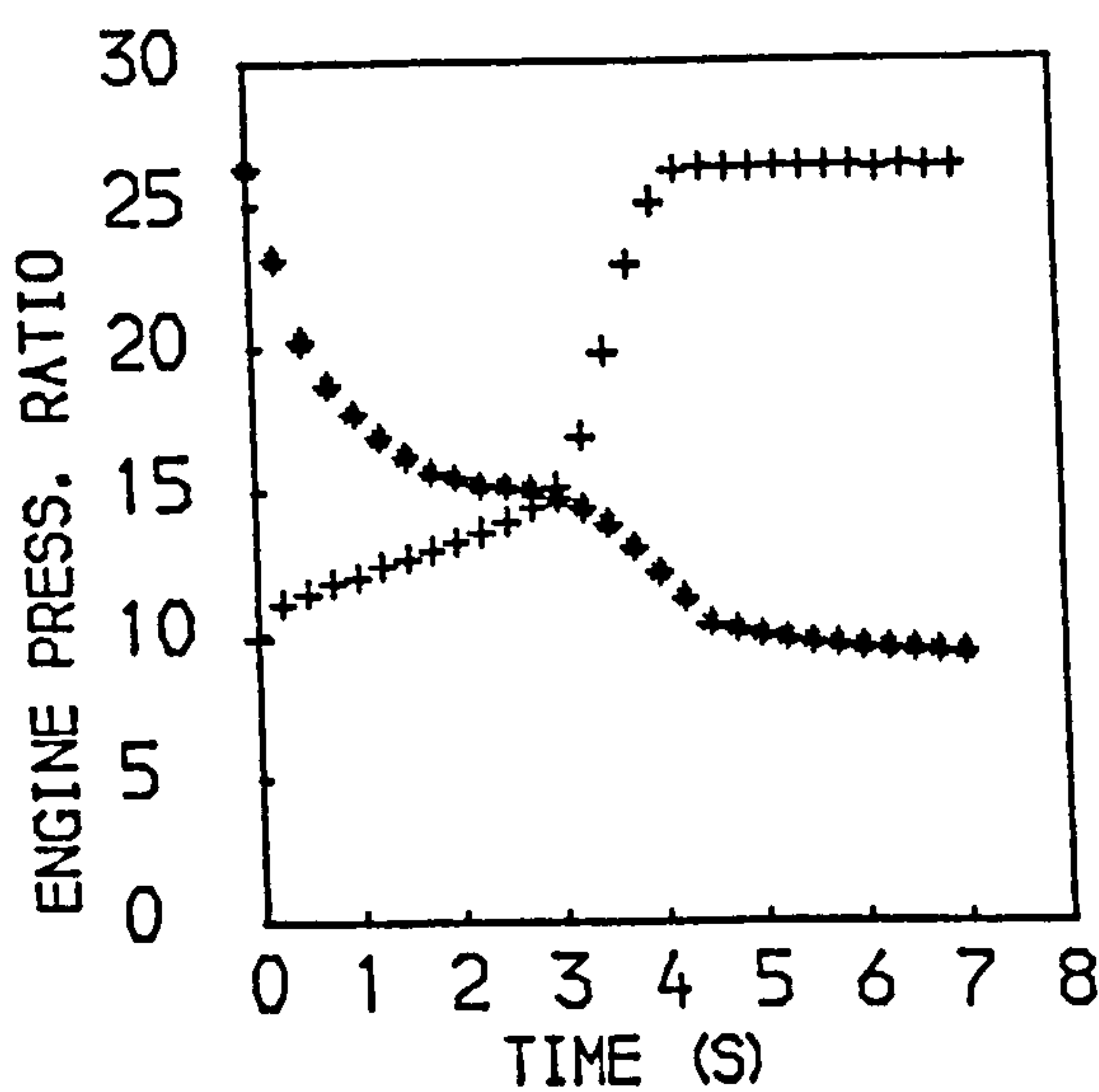
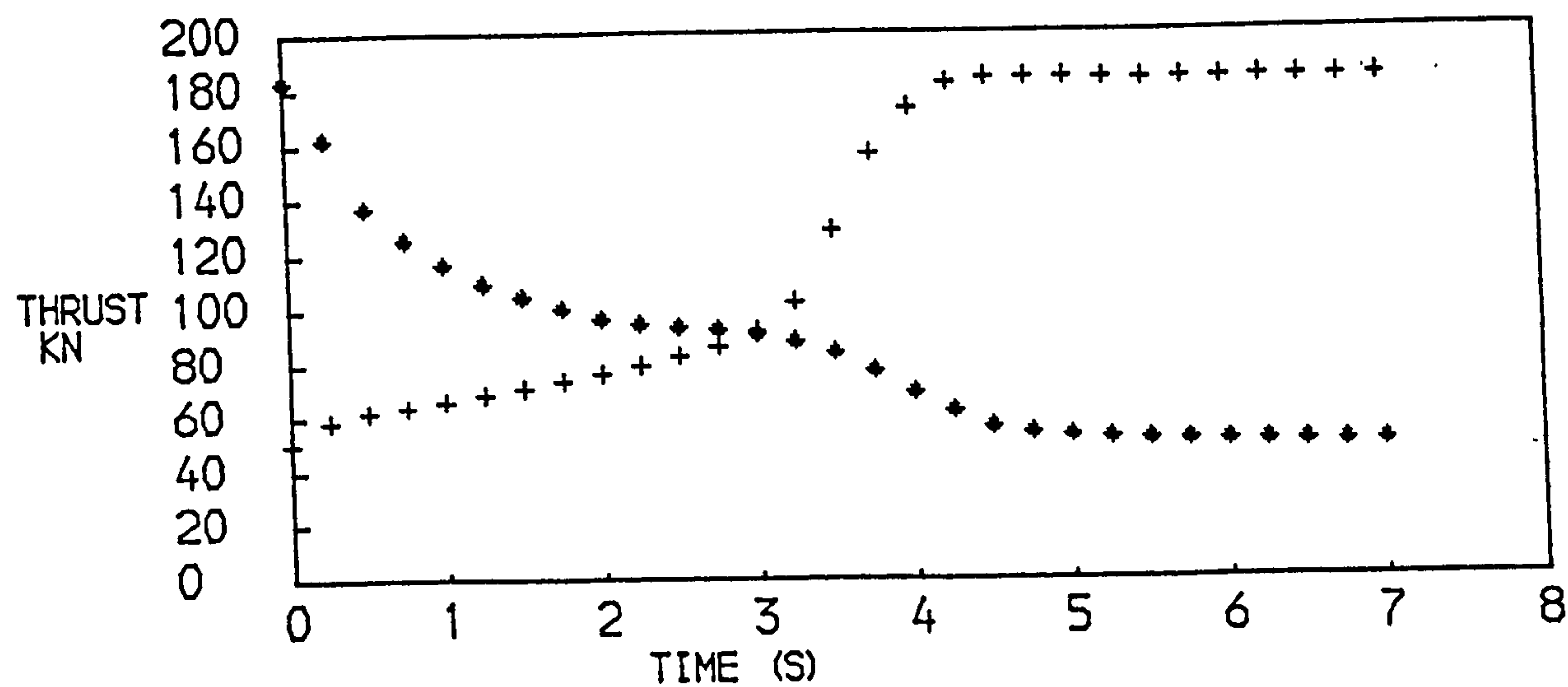
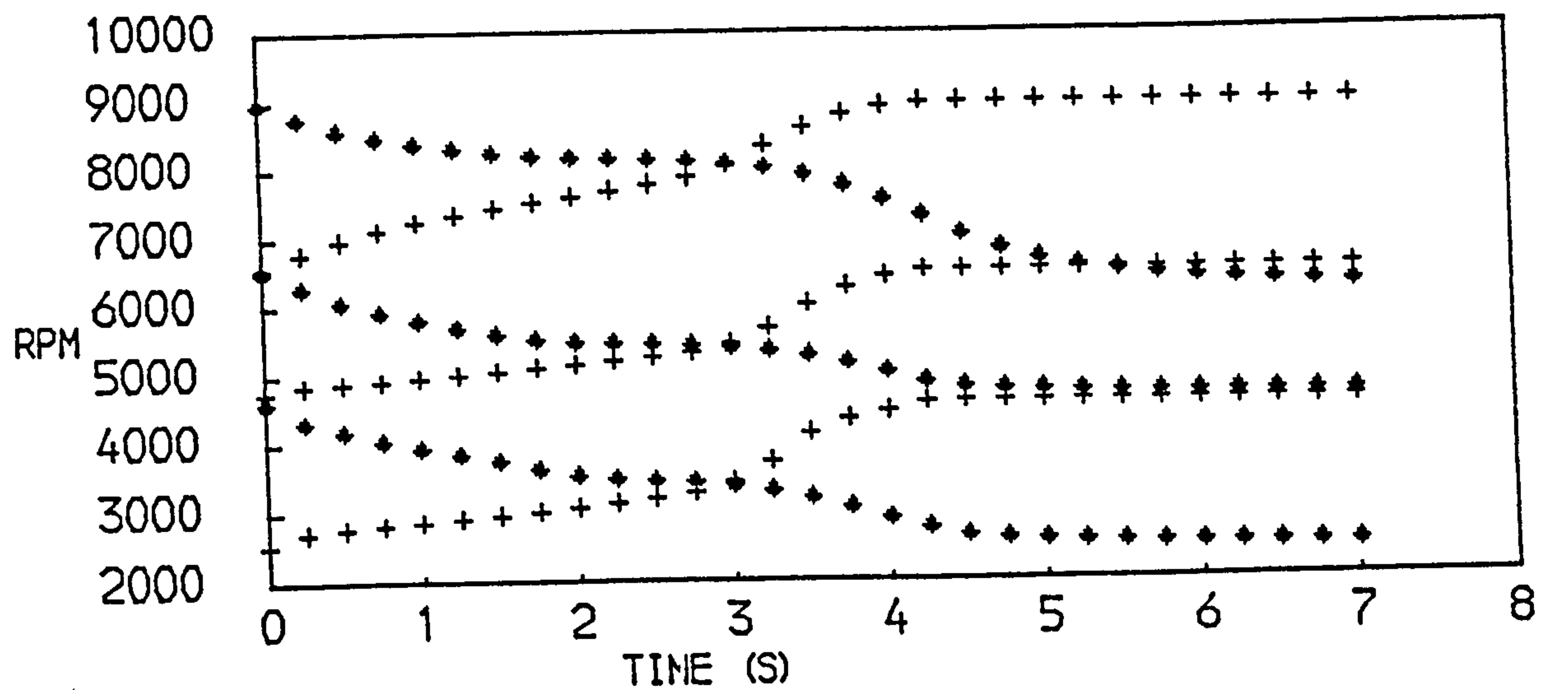


FIG. 73
PERFORMANCE OF A THREE SPOOL TURBOFAN WITH MIXED EXHAUSTS
+ACCELERATION * DECELERATION

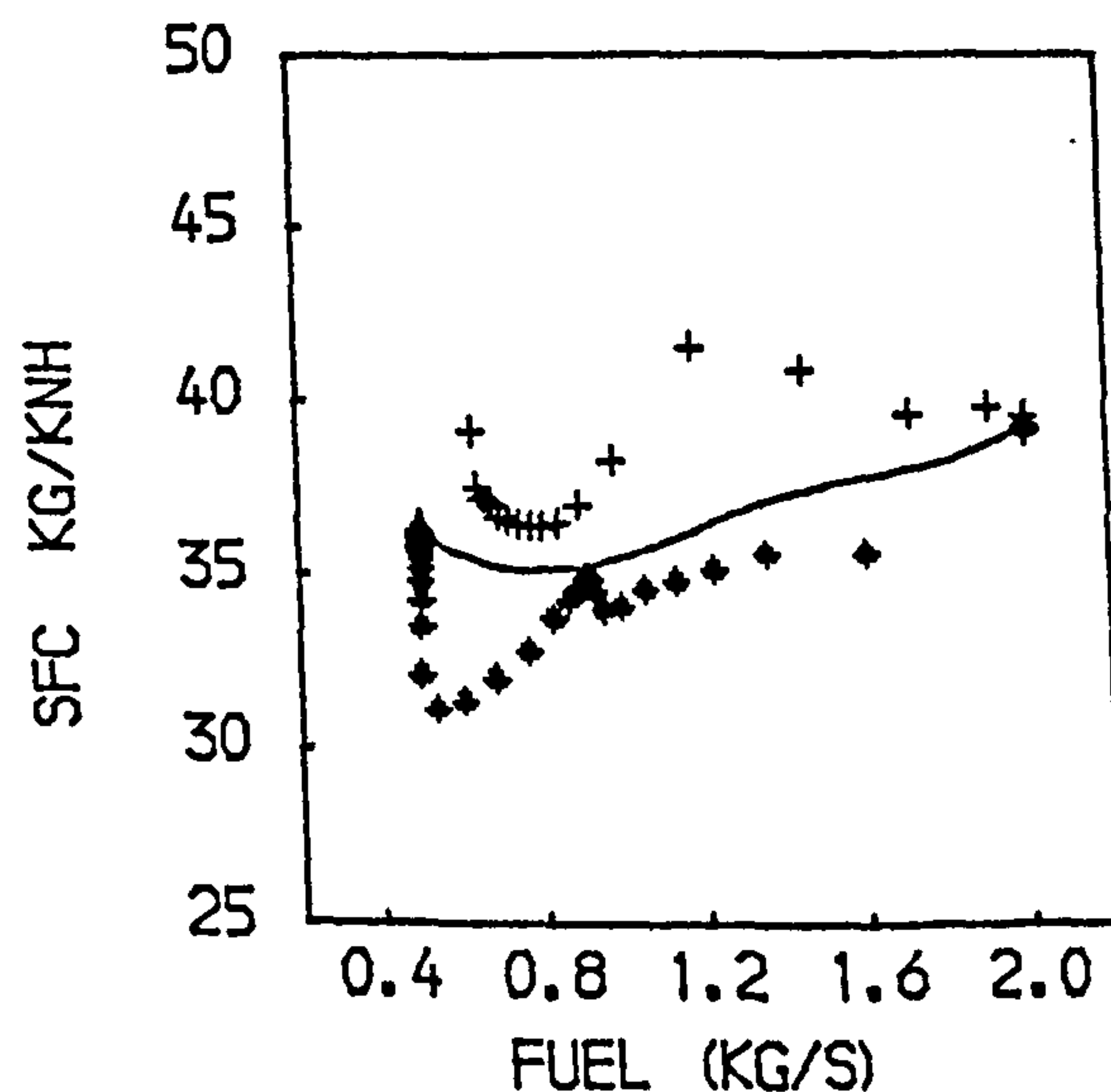
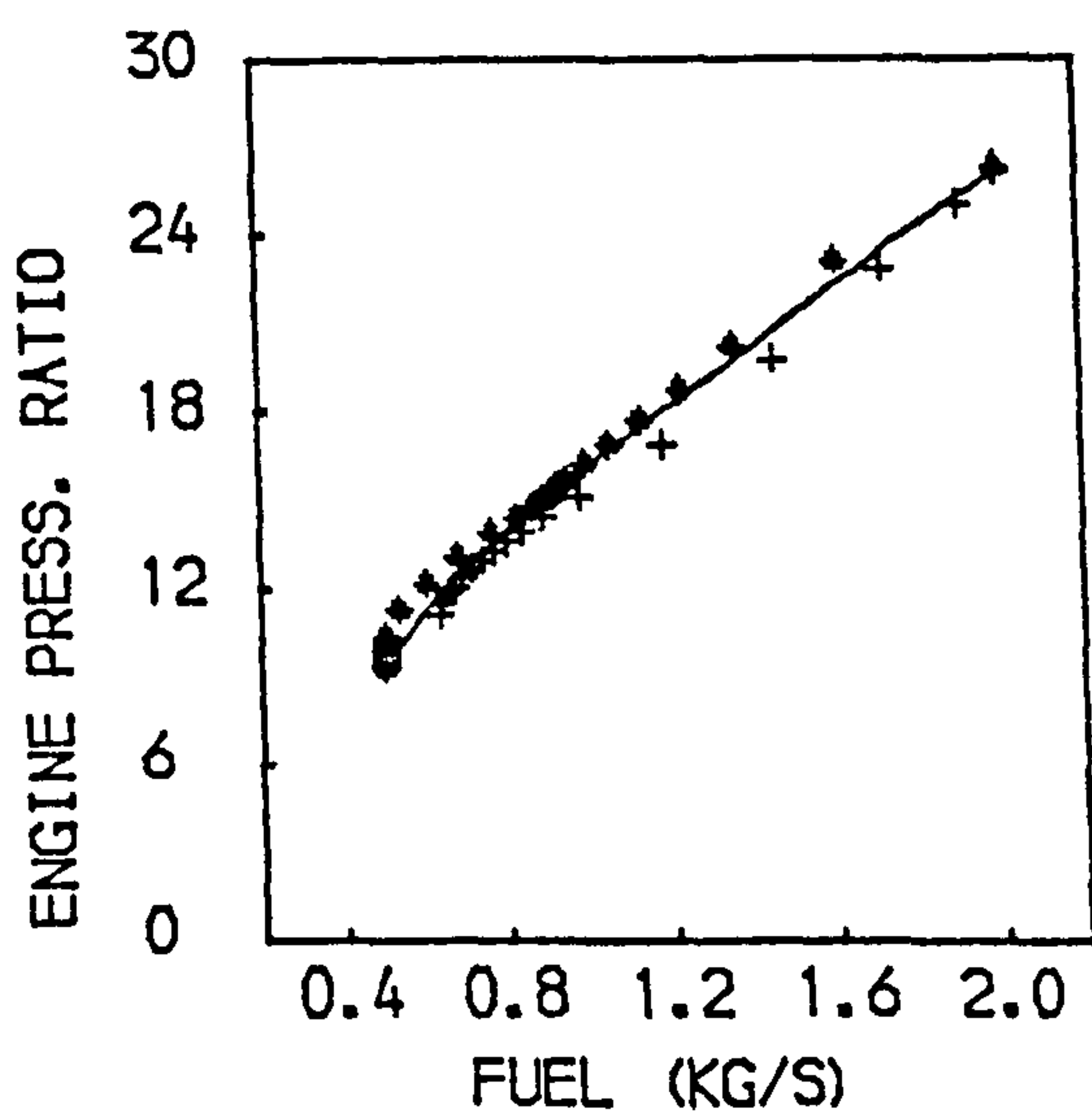
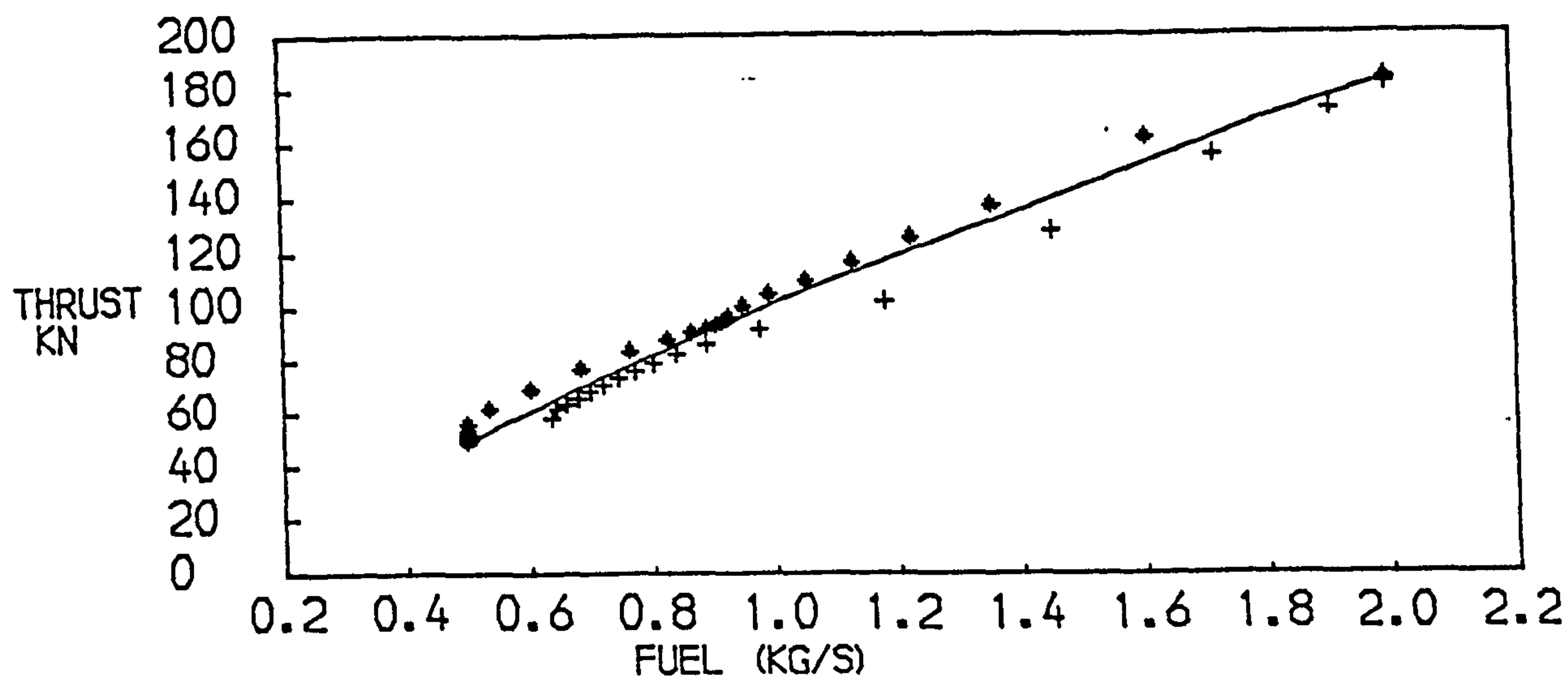
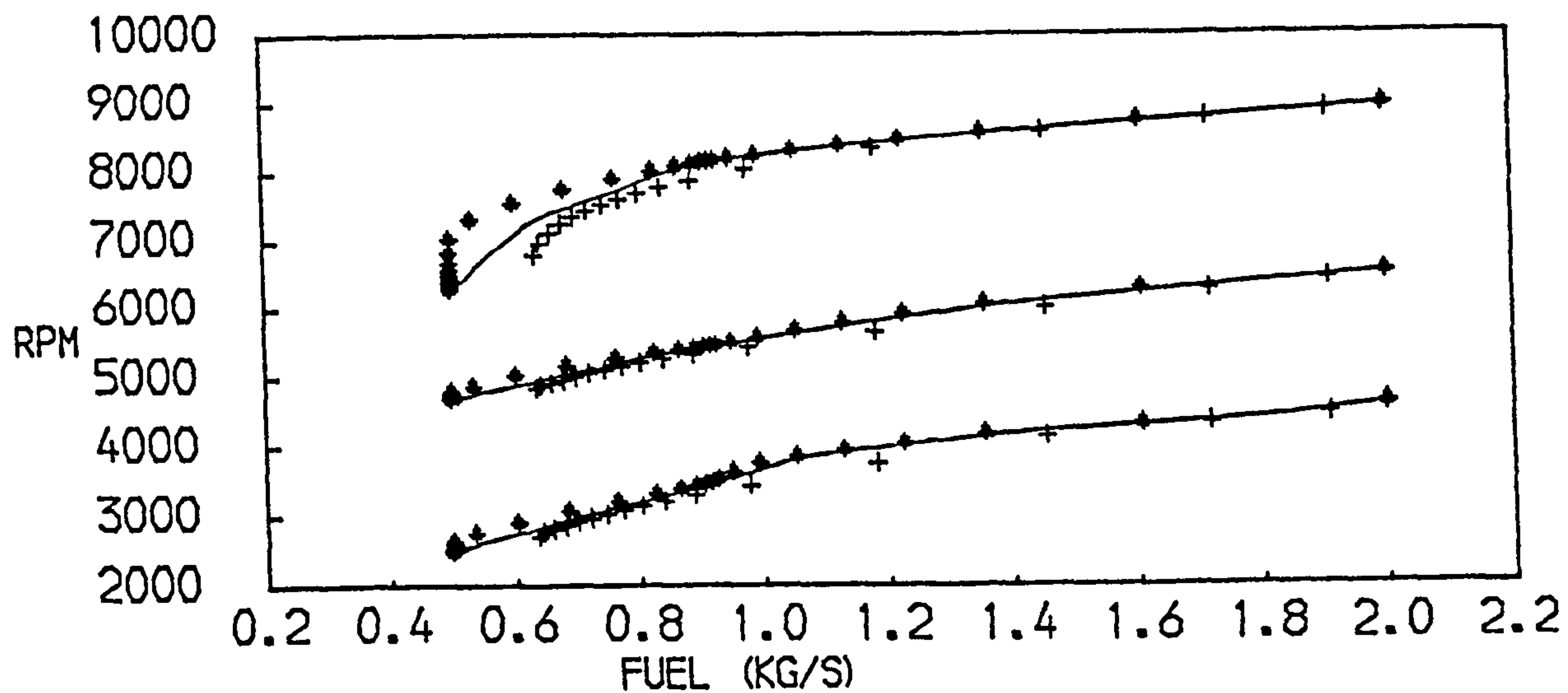


FIG. 74
PERFORMANCE OF A THREE SPOOL TURBOFAN WITH MIXED EXHAUSTS
+ACCELERATION * DECELERATION —STEADY RUNNING

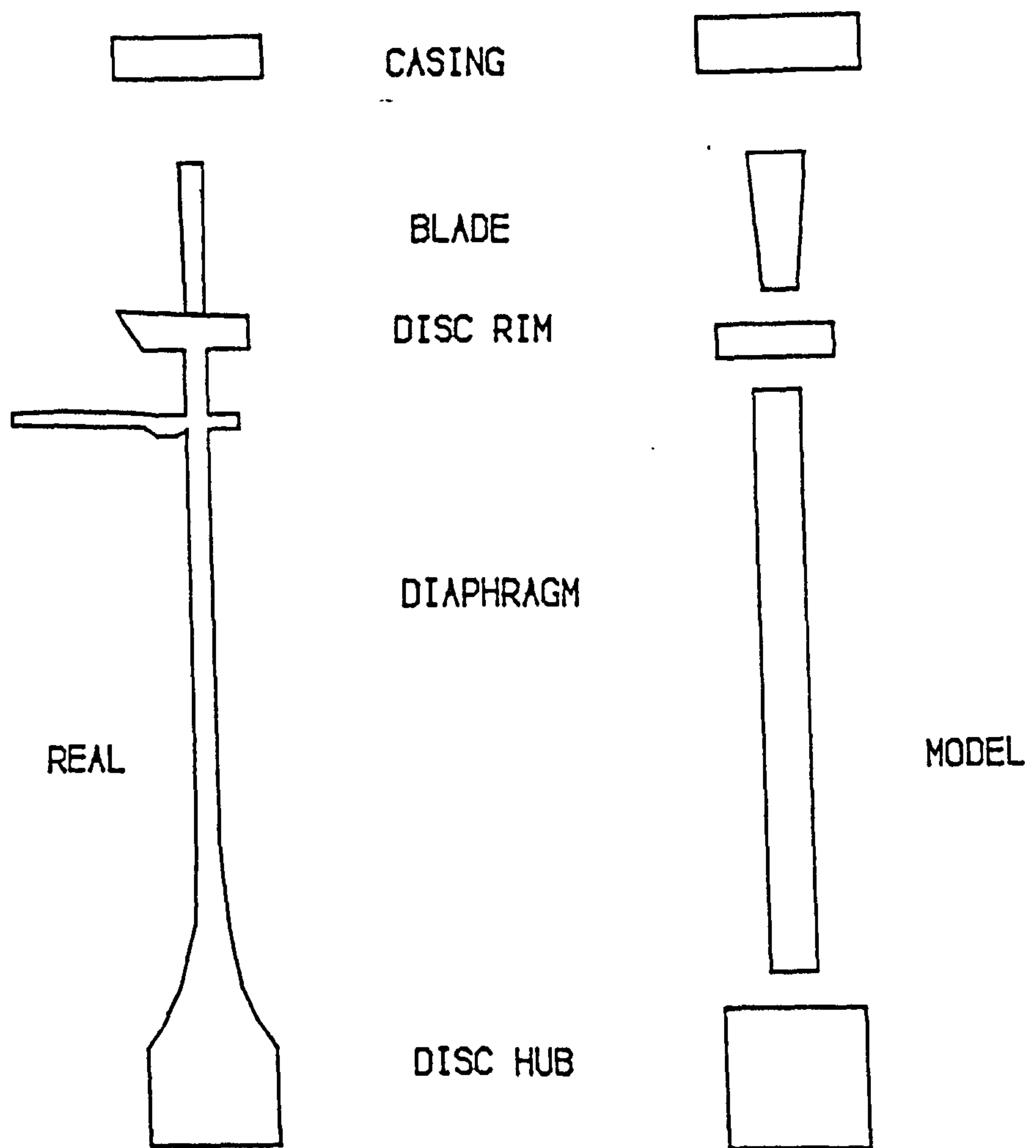


FIG. 75
REPRESENTATION OF A TYPICAL STAGE.

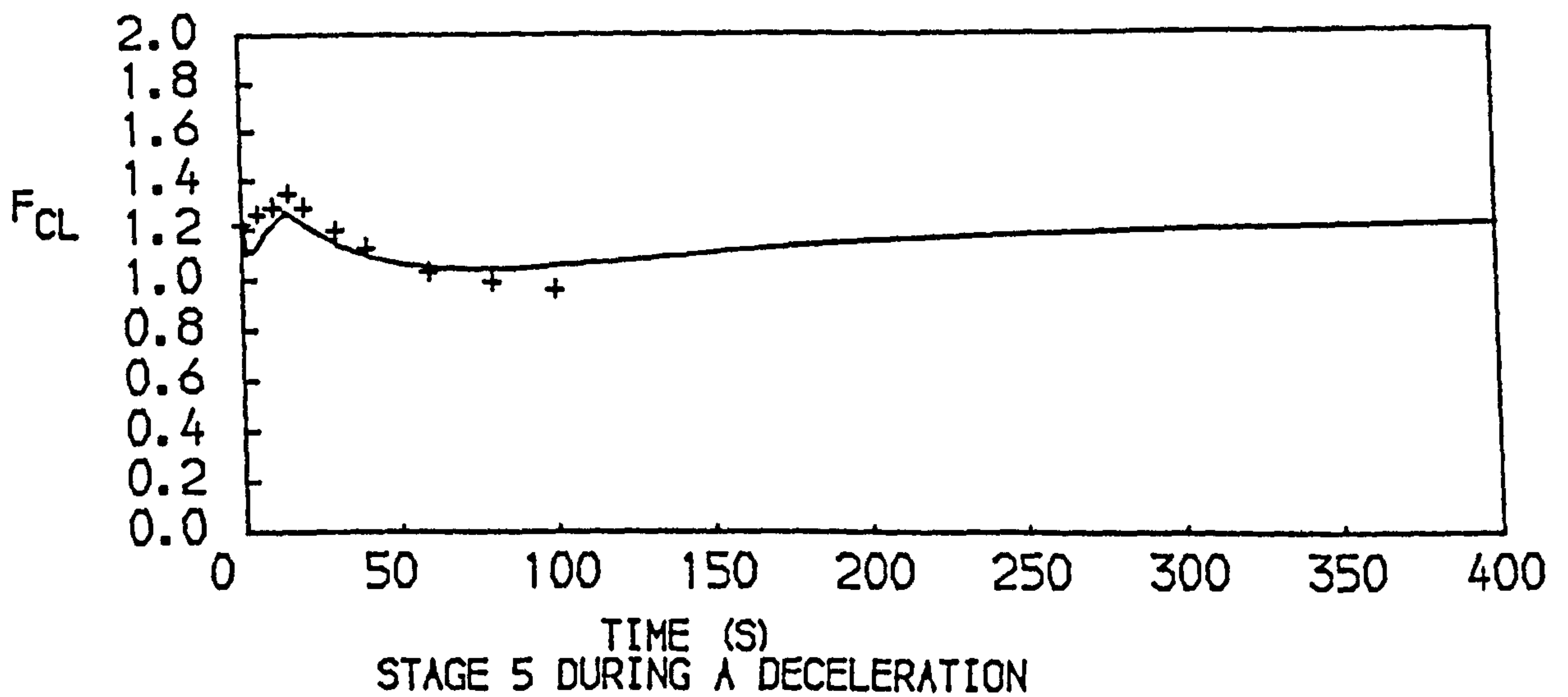
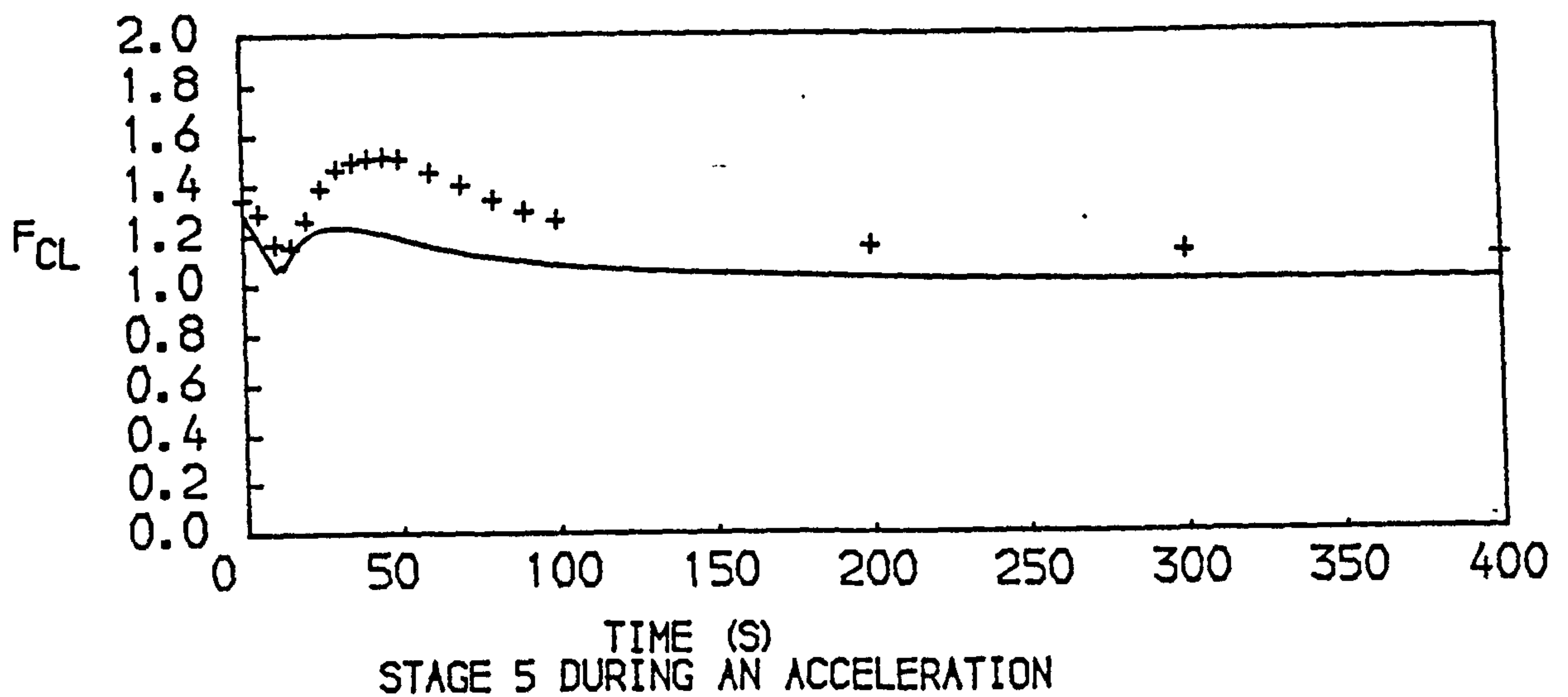
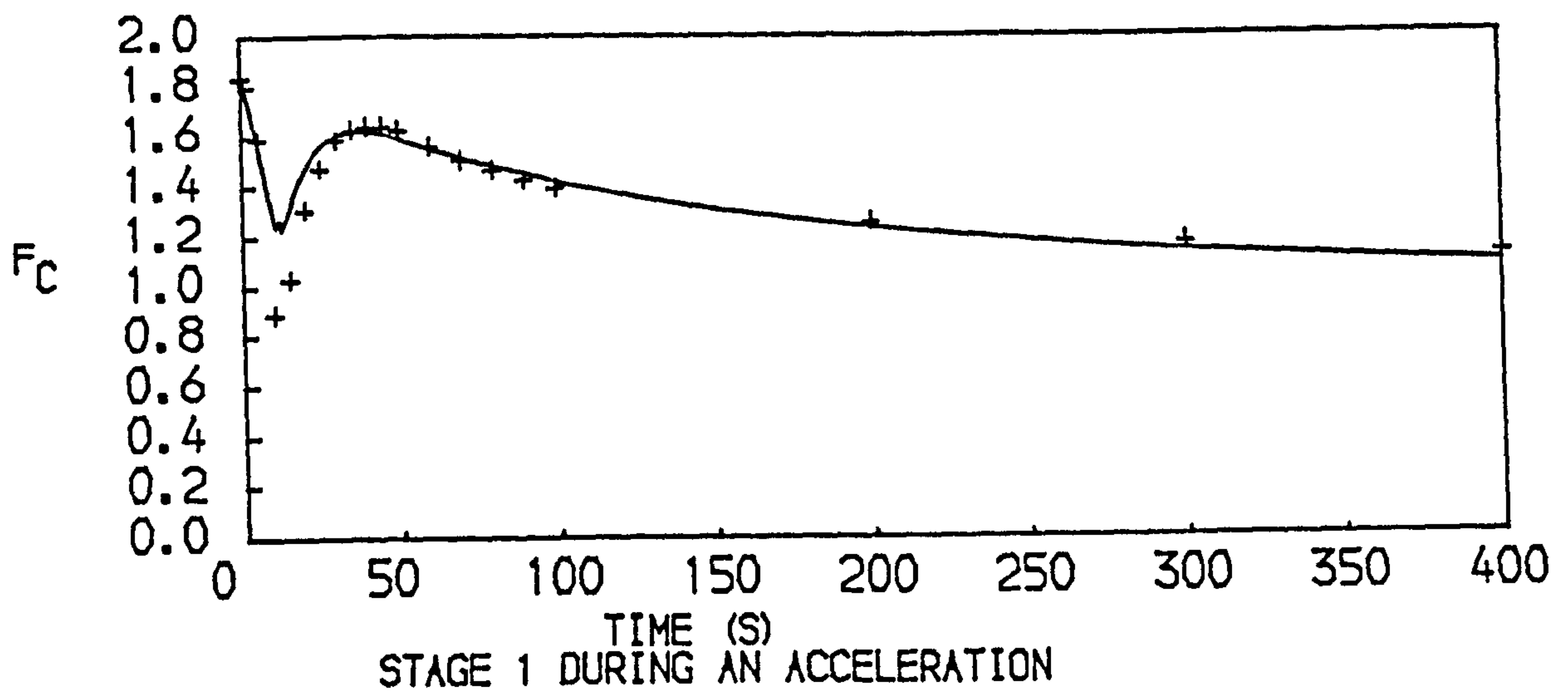


FIG. 76
 CLEARANCE MOVEMENTS OF THE H.P. COMPRESSOR OF A THREE SPOOL
 TURBOFAN ENGINE WITH SEPARATE EXHAUSTS
 $F_{CL} = (\text{TRANSIENT CLEARANCE}) / (\text{HOT STABILISED CLEARANCE})$
 -- FULL MODEL, + ANALYSIS OF REF. 75

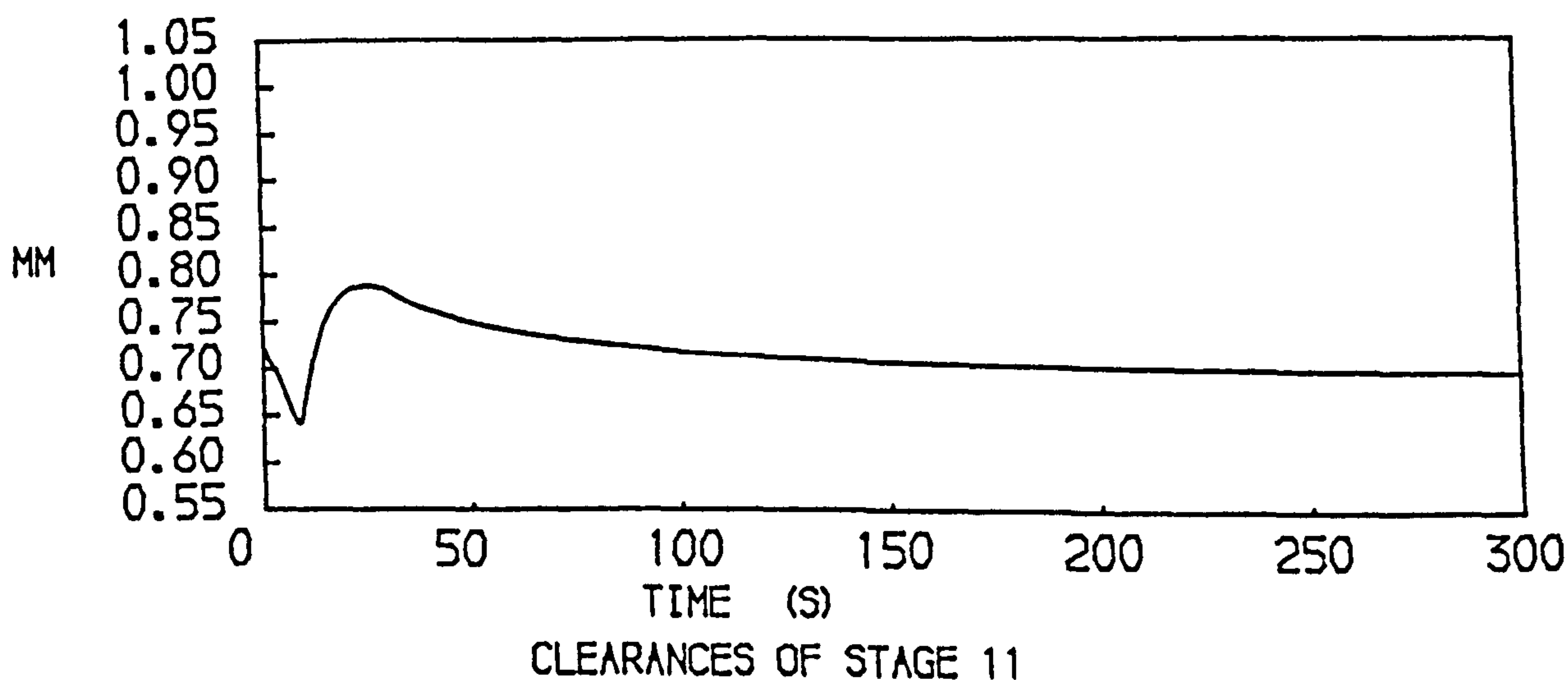
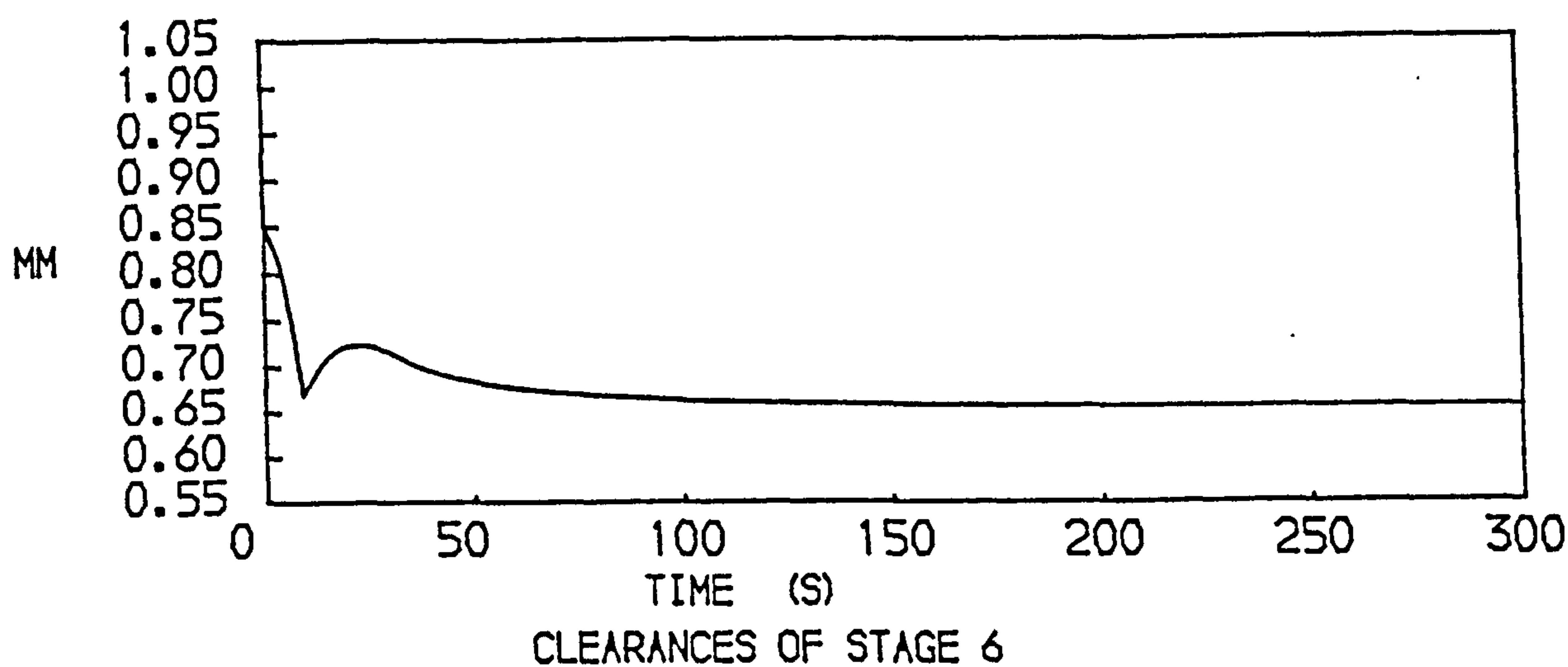
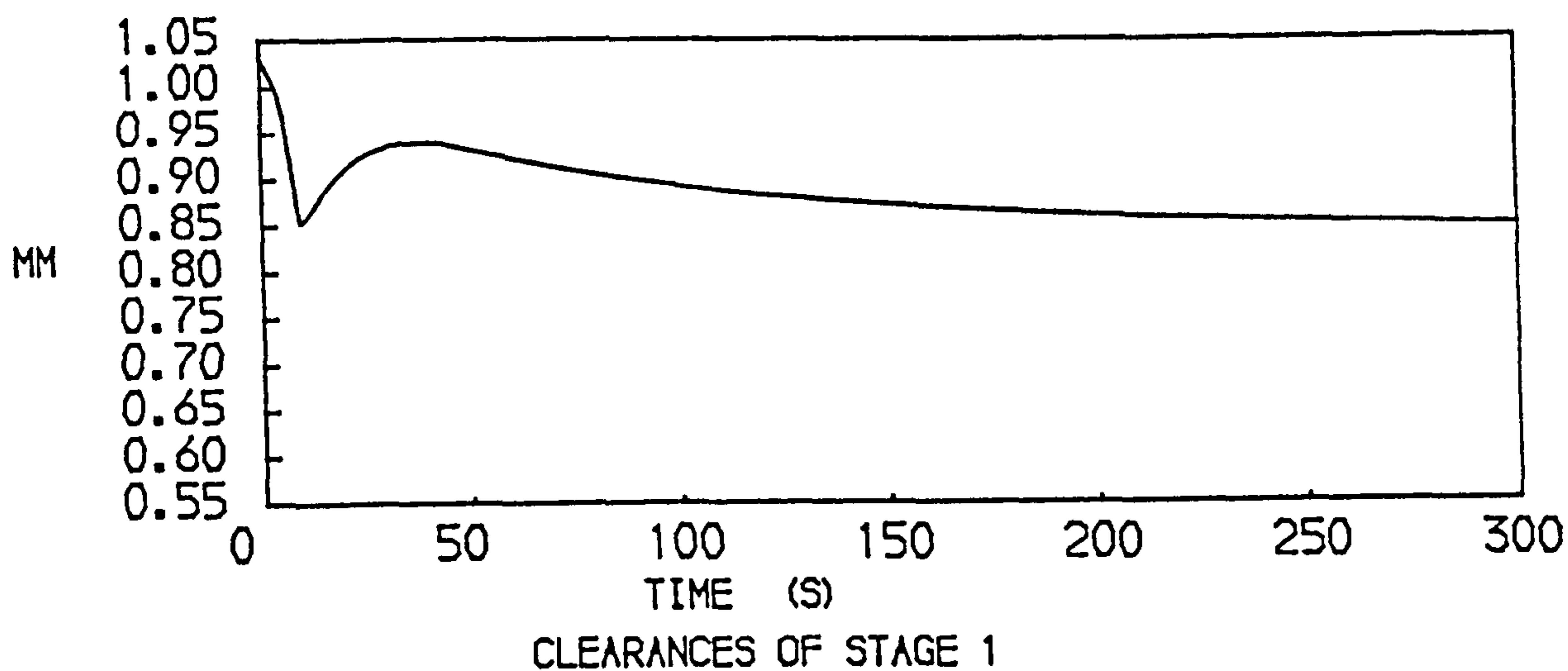


FIG. 77

PREDICTED BLADE TIP CLEARANCES OF THE TWO SPOOL ENGINE H.P. COMPRESSOR (STAGES 1, 6 AND 11) DURING AND FOLLOWING A SEA LEVEL ACCELERATION

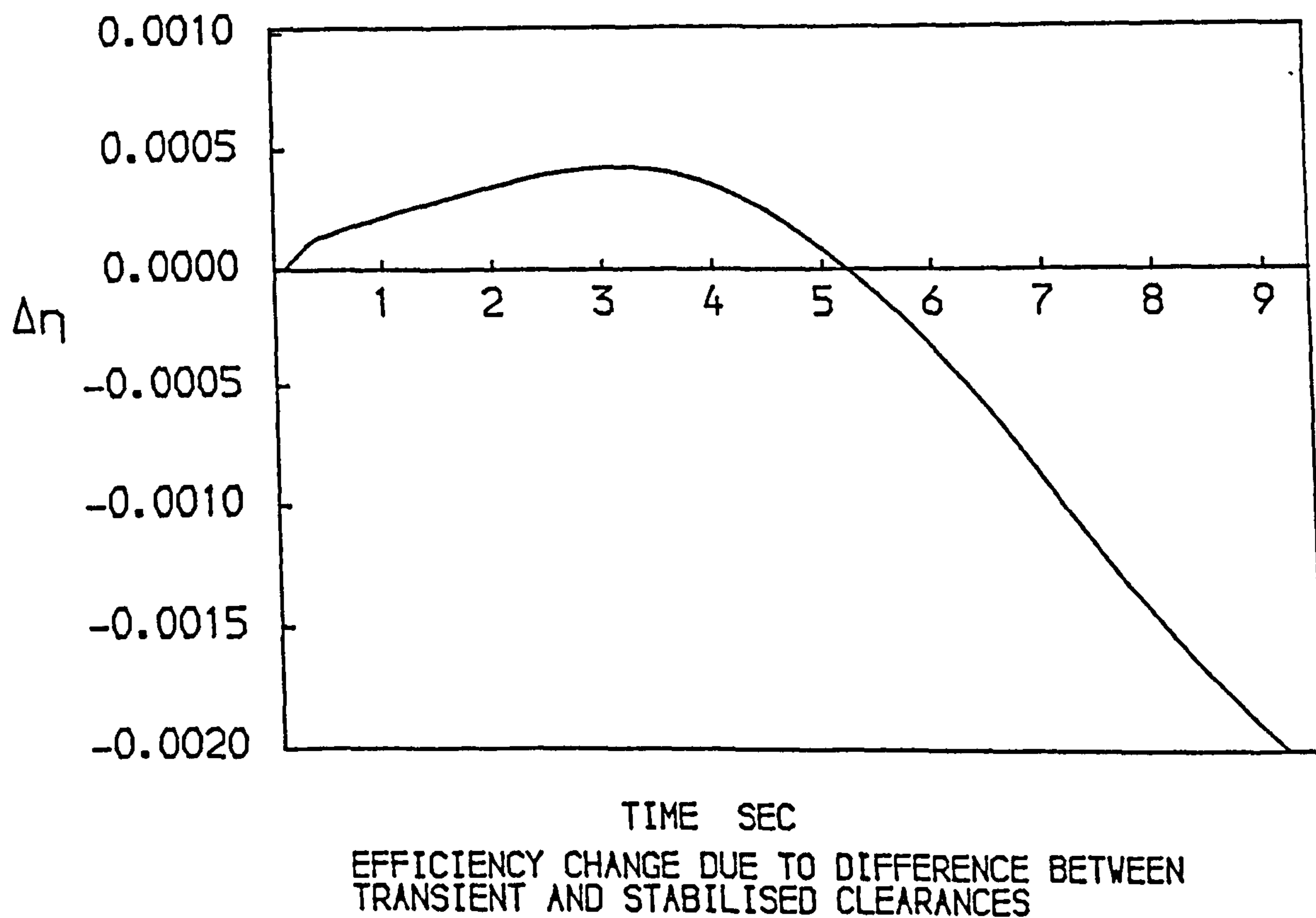
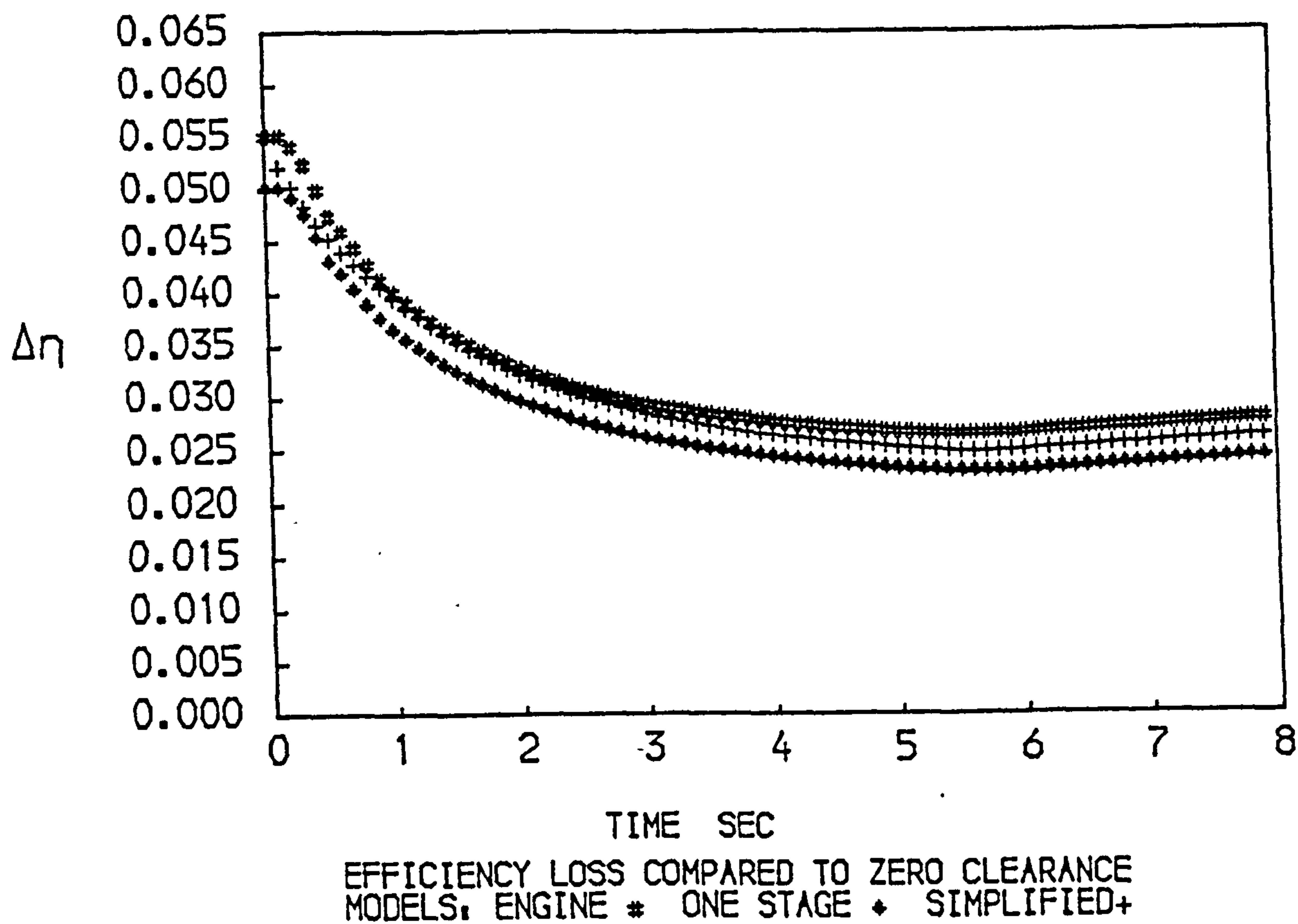


FIG. 78
EFFECTS OF CLEARANCE MOVEMENTS ON COMPRESSOR EFFICIENCY

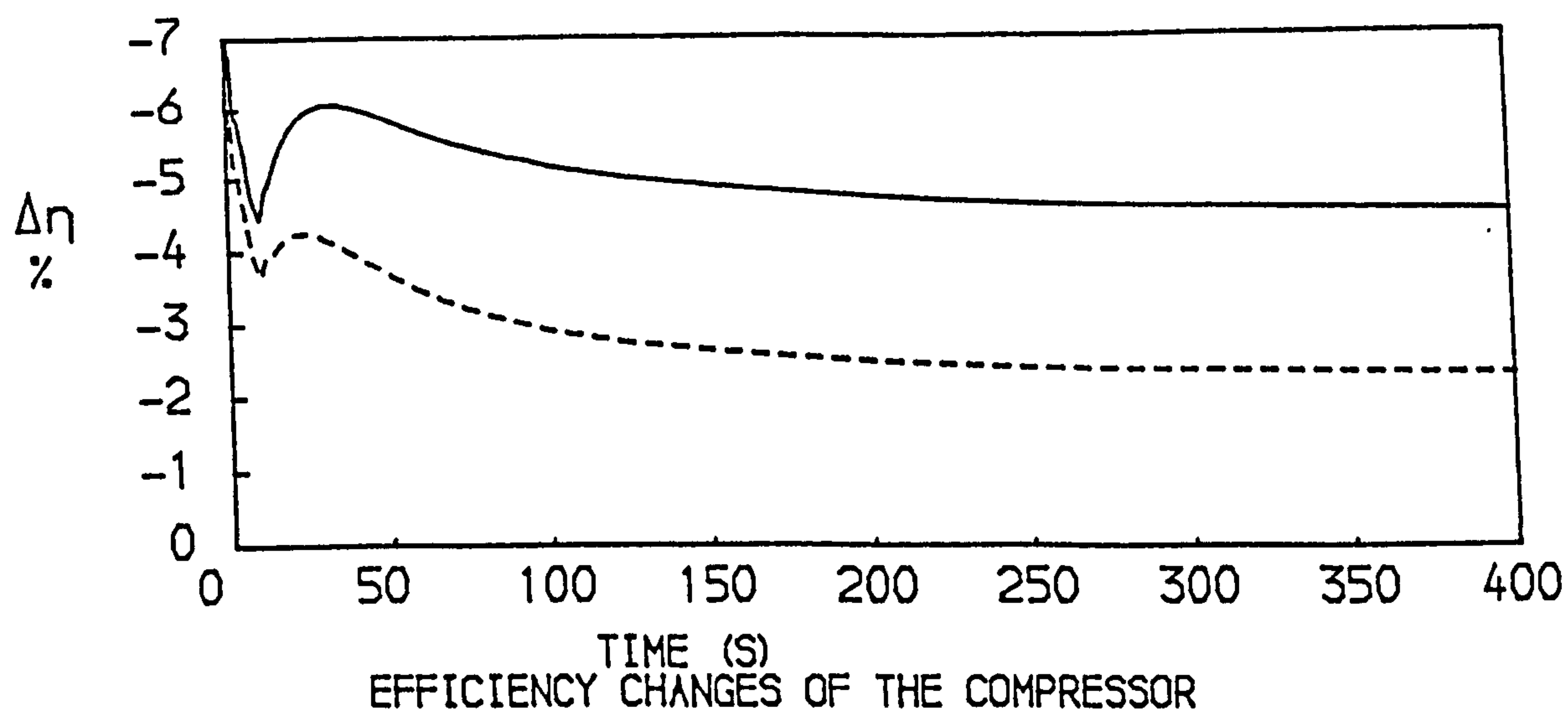
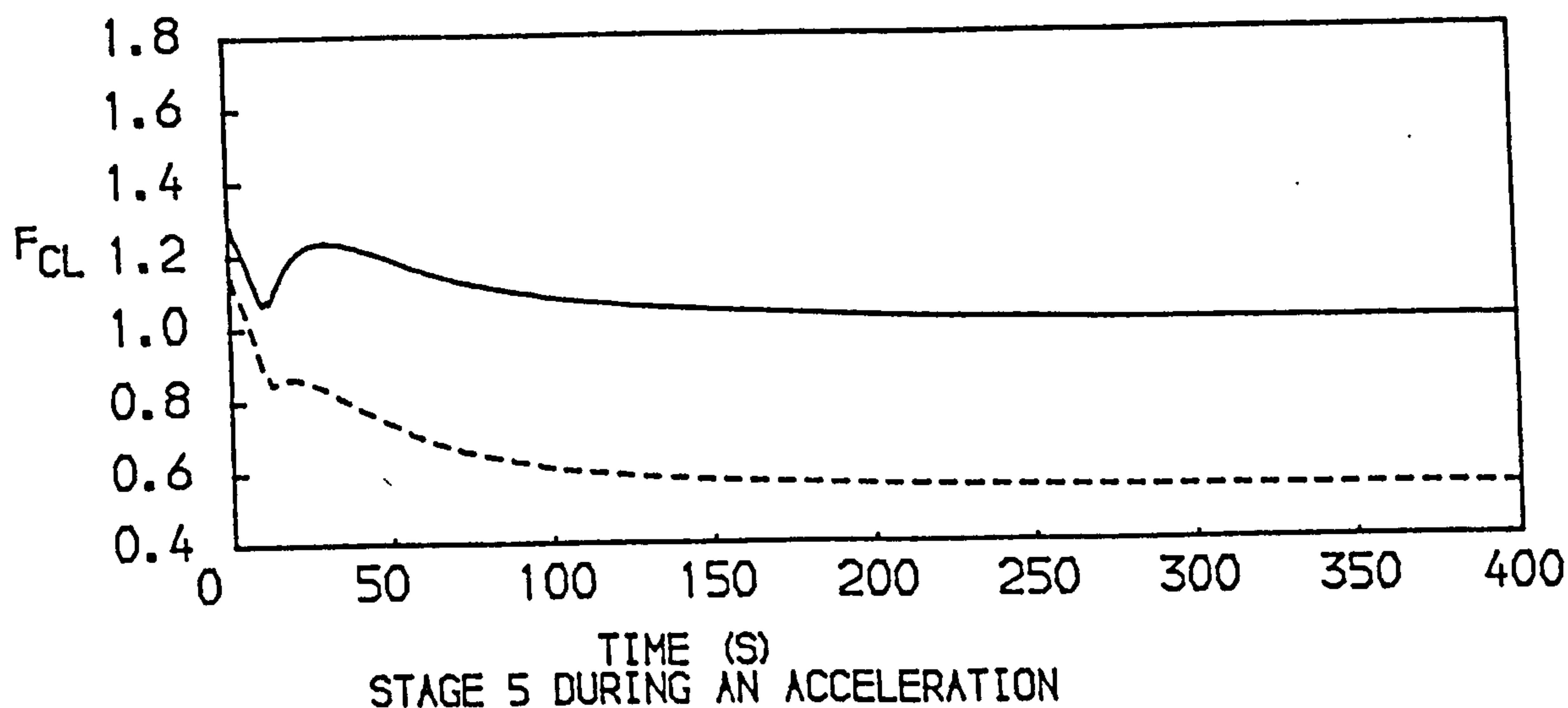
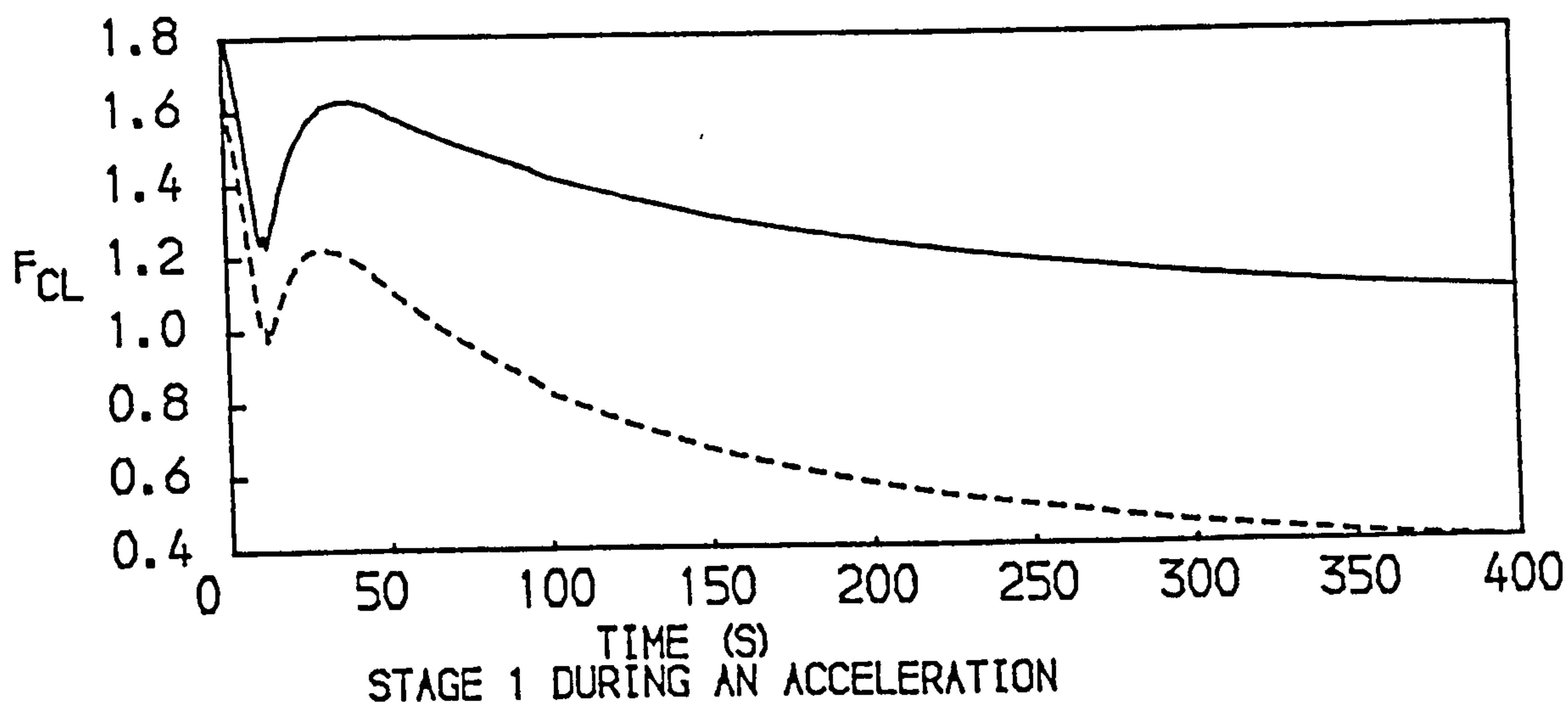


FIG. 79
EFFECT OF THE MODIFIED COOLING FLOWS OF THE H.P. COMPRESSOR
OF A THREE SPOOL TURBOFAN ENGINE WITH SEPARATE EXHAUSTS
 $F_{CL} = (\text{TRANSIENT CLEARANCE}) / (\text{HOT STABILISED CLEARANCE})$
— REAL ENGINE, - - MODIFIED

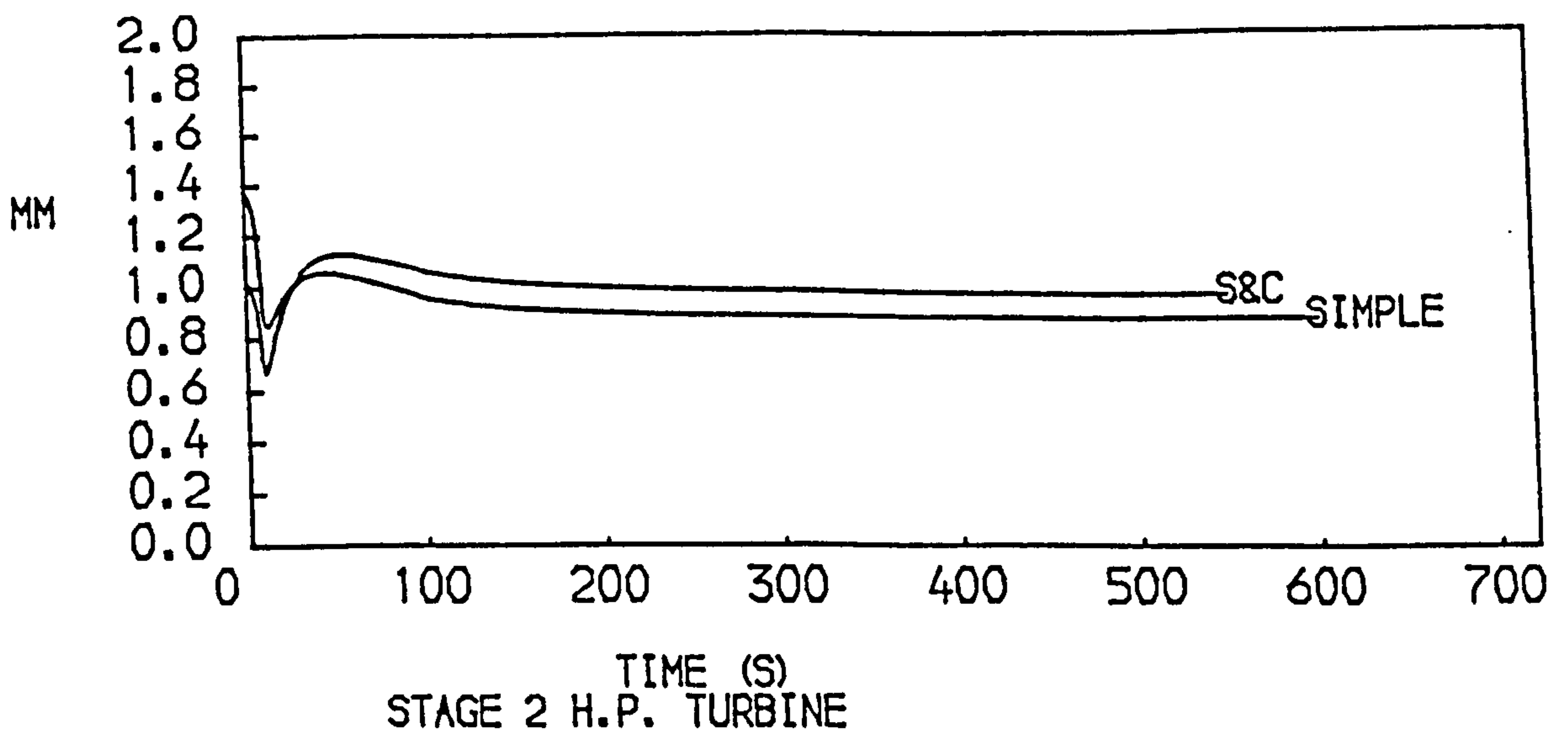
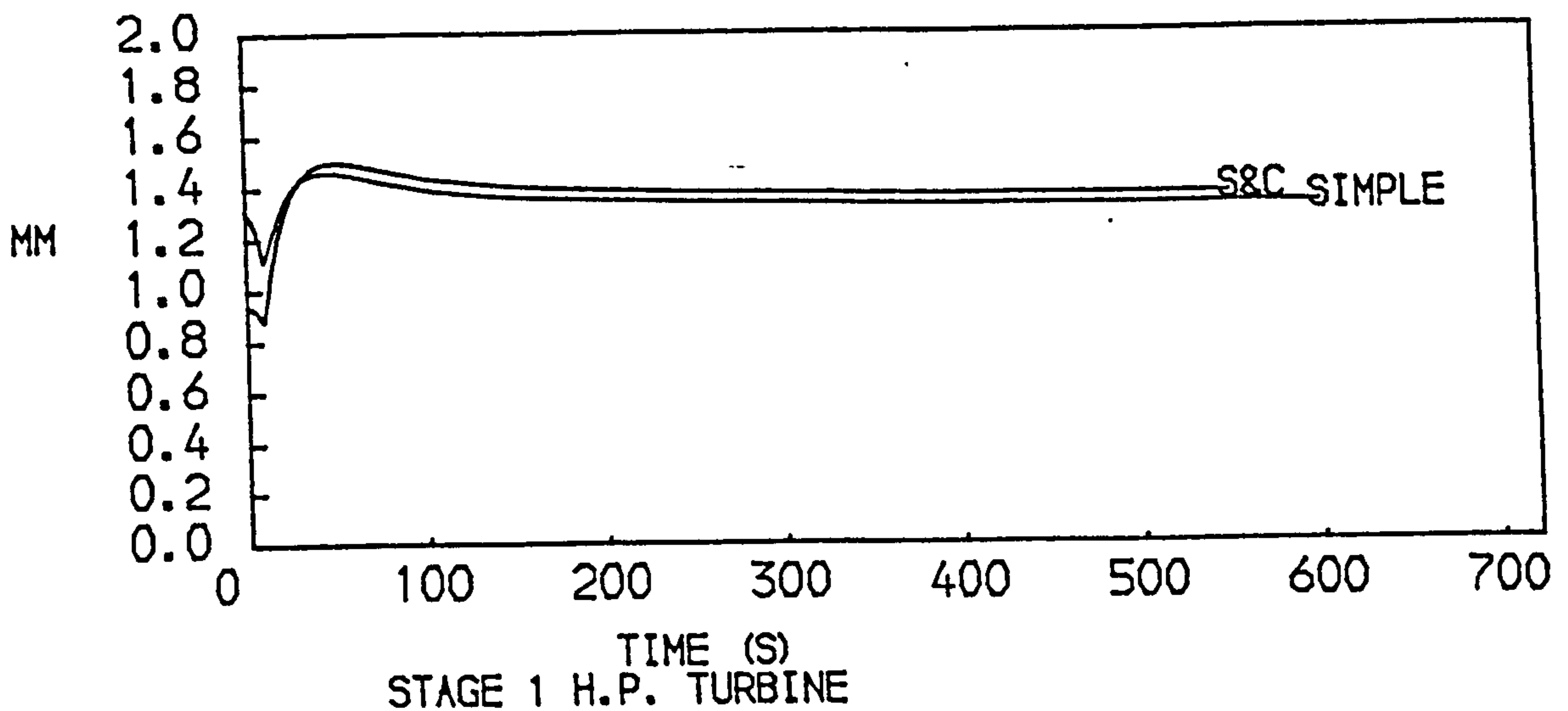
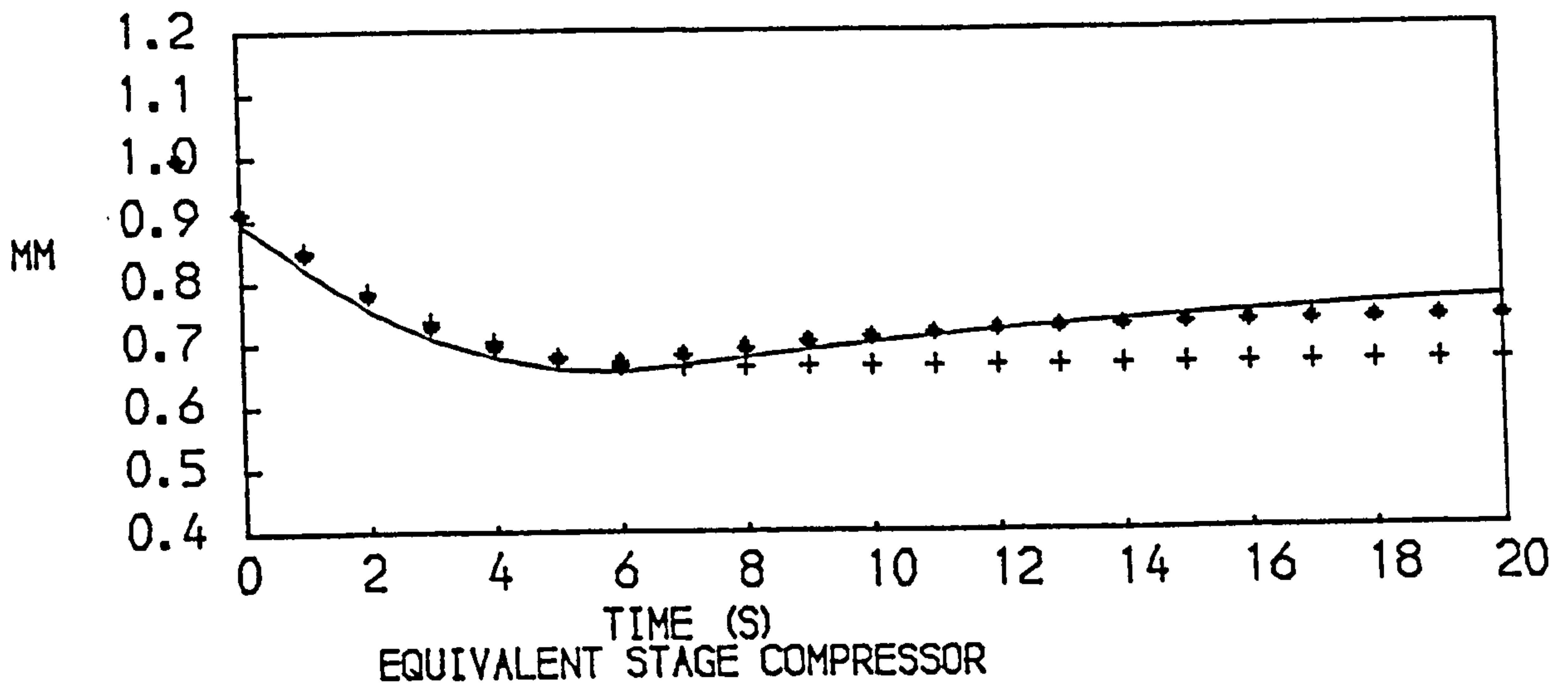


FIG. 80
 CLEARANCES OF TWO COMPONENTS OF A TWO SPOOL BYPASS
 ENGINE WITH MIXED EXHAUSTS DURING A TRANSIENT
 — FULL MODEL TRANSIENT CLEARANCES
 SIMPLE MODEL CLEARANCES, + STEADY RUNNING ♦ TRANSIENT
 SIMPLE, SIMPLE BLADE, S&C, SHROUDED AND COOLED BLADE

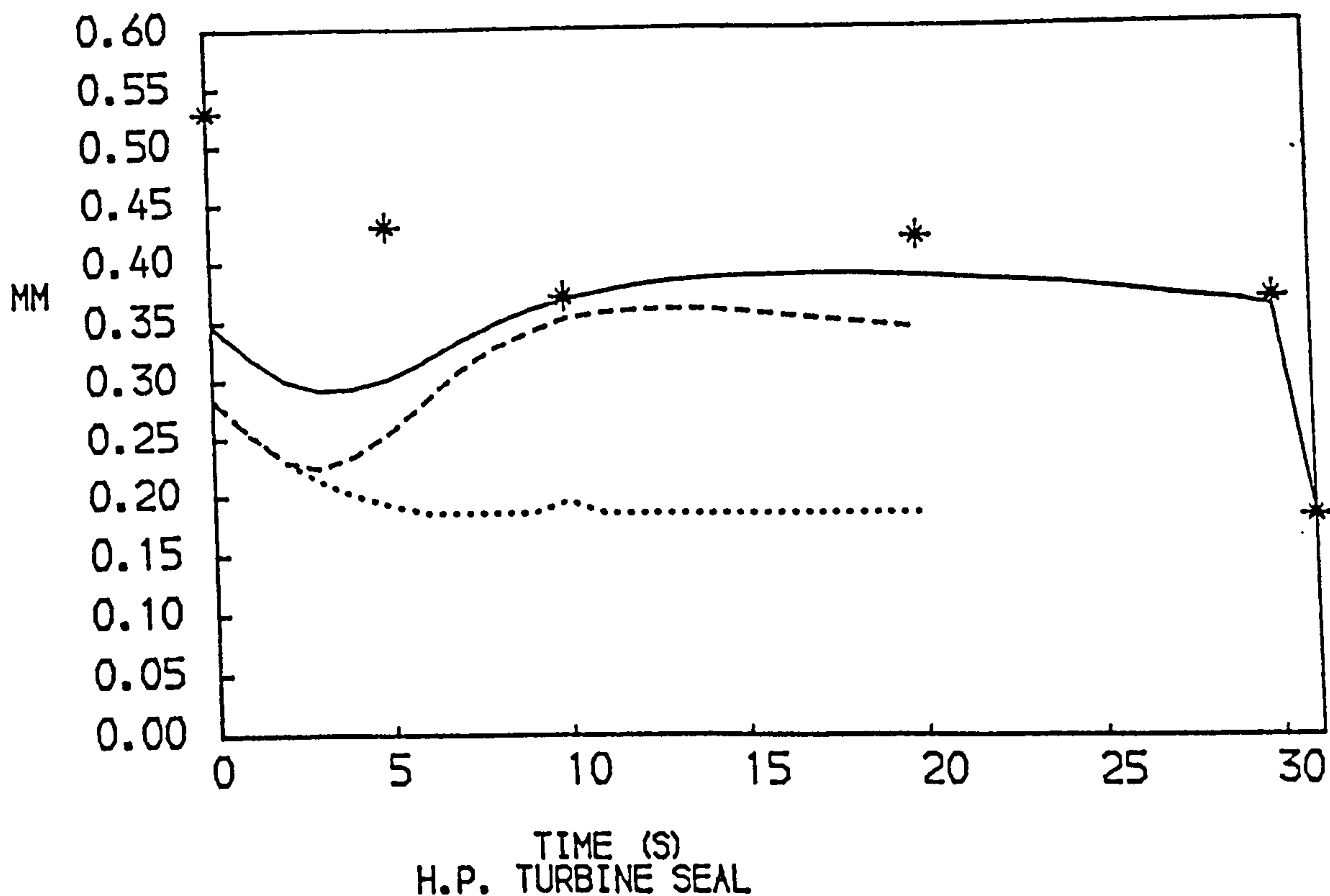
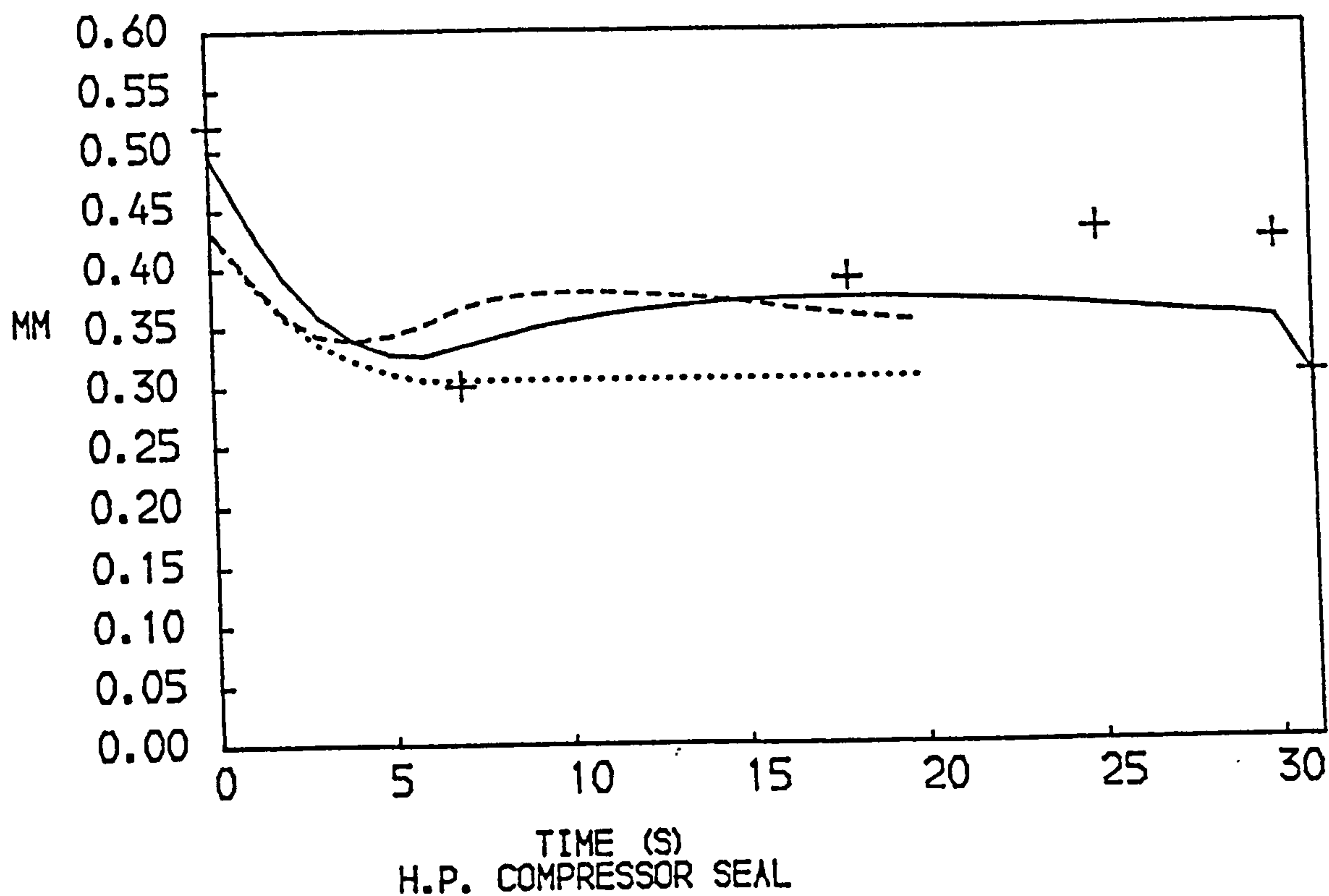


FIG. 81
 CLEARANCES OF TWO SEALS OF THE TWO SPOOL BYPASS ENGINE
 WITH MIXED EXHAUSTS DURING AN ACCELERATION
 — FULL MODEL TRANSIENT CLEARANCES
 SIMPLE MODEL CLEARANCES, TRANSIENT - -, STABILISED...
 ANALYSIS OF, REF. 49 +, REF. 52 *

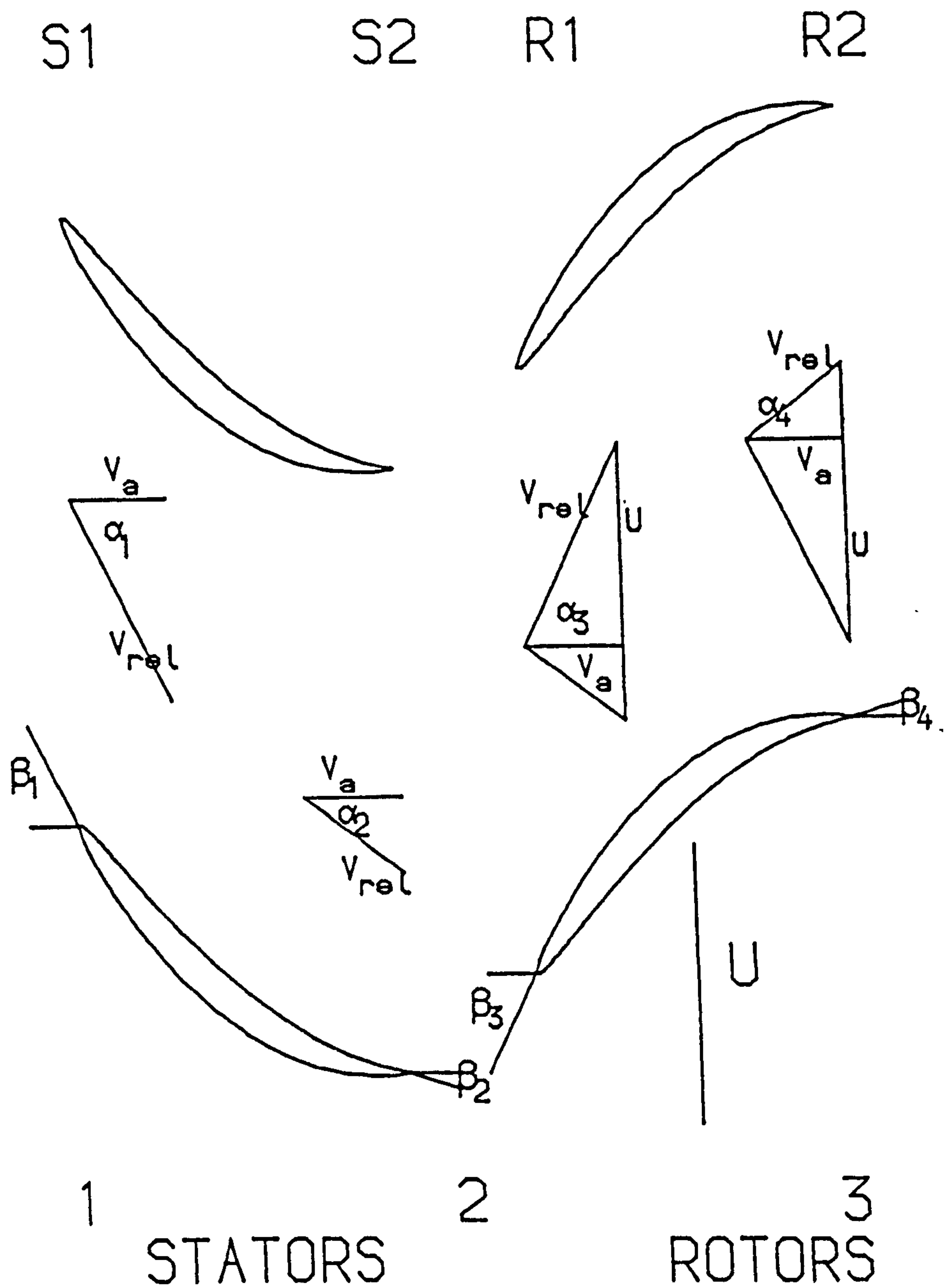
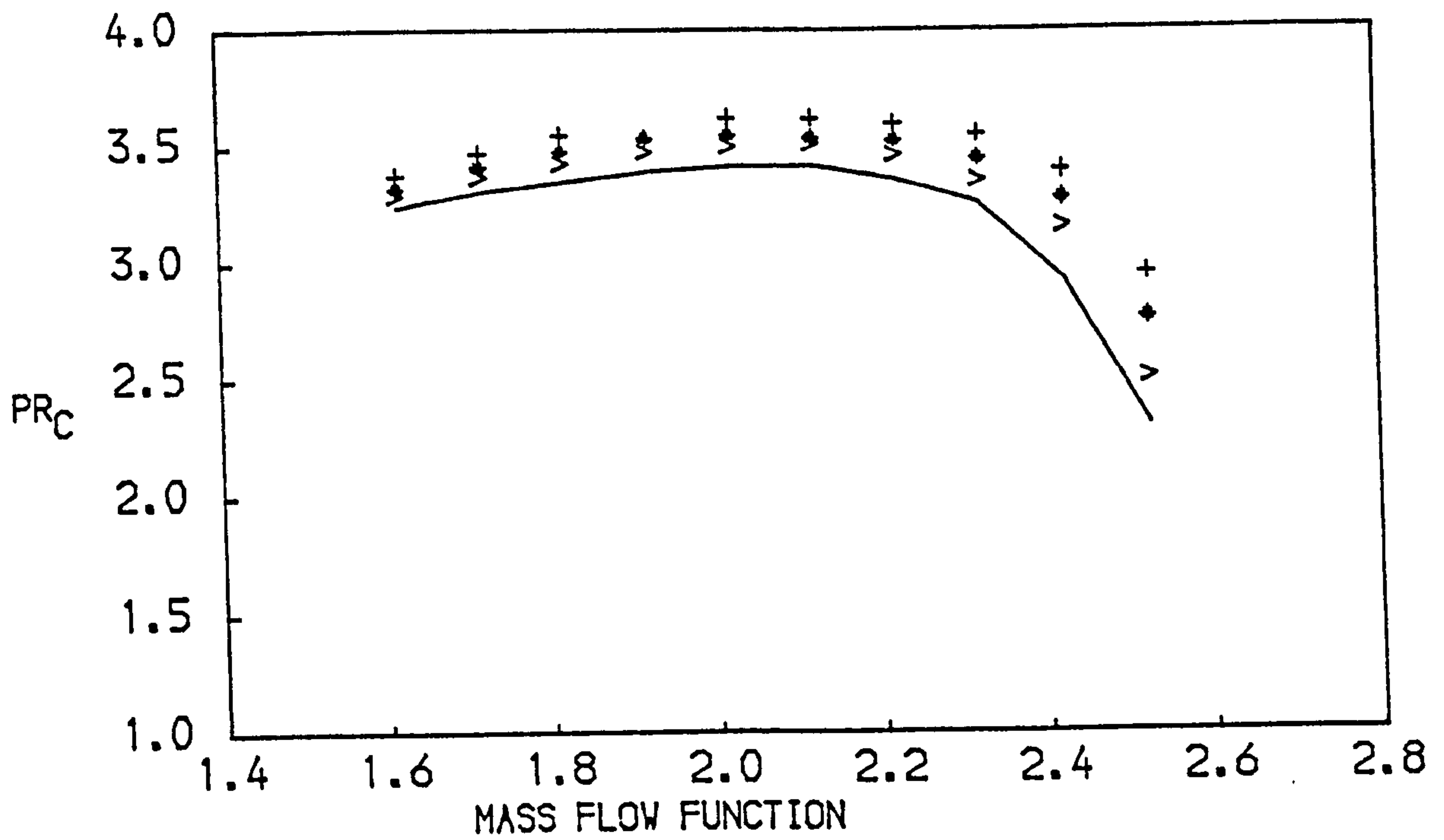
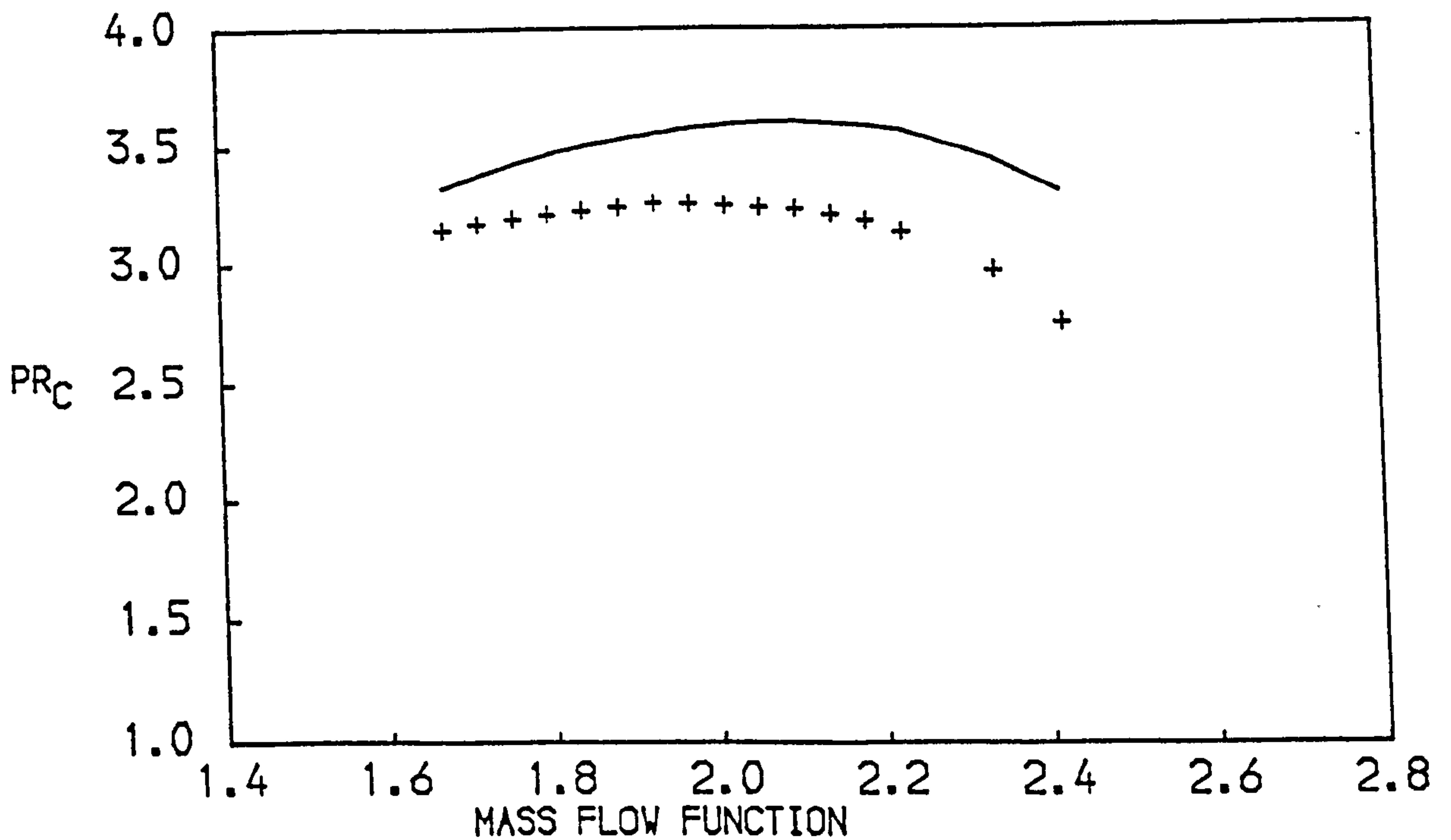


FIG. 82

BLADE AND AIR FLOW DIAGRAMS FOR THE
 PREDICTION OF COMPRESSOR PERFORMANCE
 U , PERIPHERAL VELOCITY V_a , AXIAL VELOCITY
 V_{rel} , RELATIVE VELOCITY OF AIR AND BLADES



ACCELERATION AT SEA LEVEL STATIC CONDITIONS
 — ADIABATIC, $F = 0.045$, $+$ $F = 0.060$, v $F = 0.090$



DECELERATION AT 9150 M, FLIGHT MACH NO = 0.6
 — ADIABATIC, $+$ $F = 0.25$

FIG. 83
 MOVEMENTS OF THE CHARACTERISTICS OF THE H.P. COMPRESSOR
 OF A TWO SPOOL BYPASS ENGINE DURING TRANSIENTS

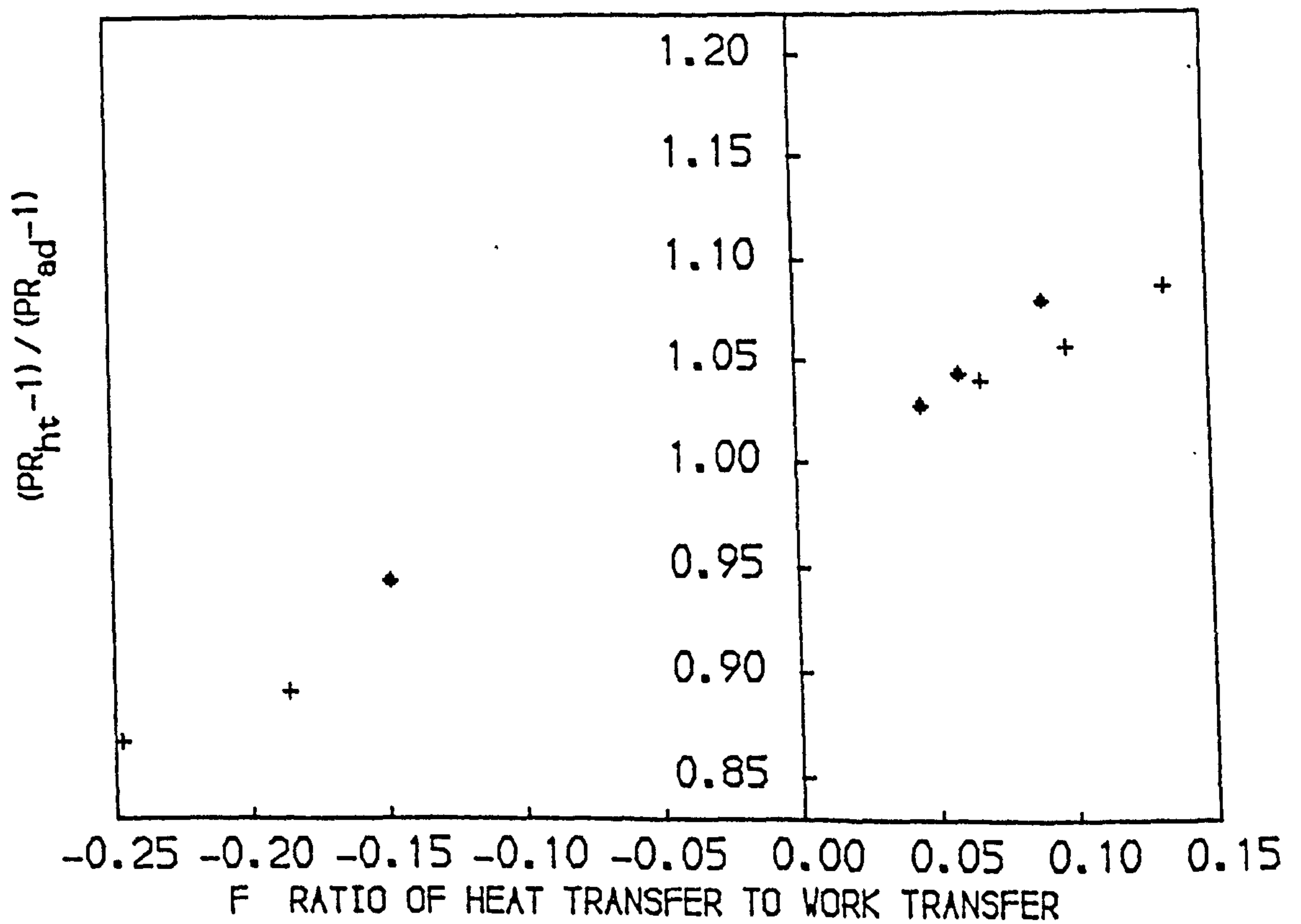
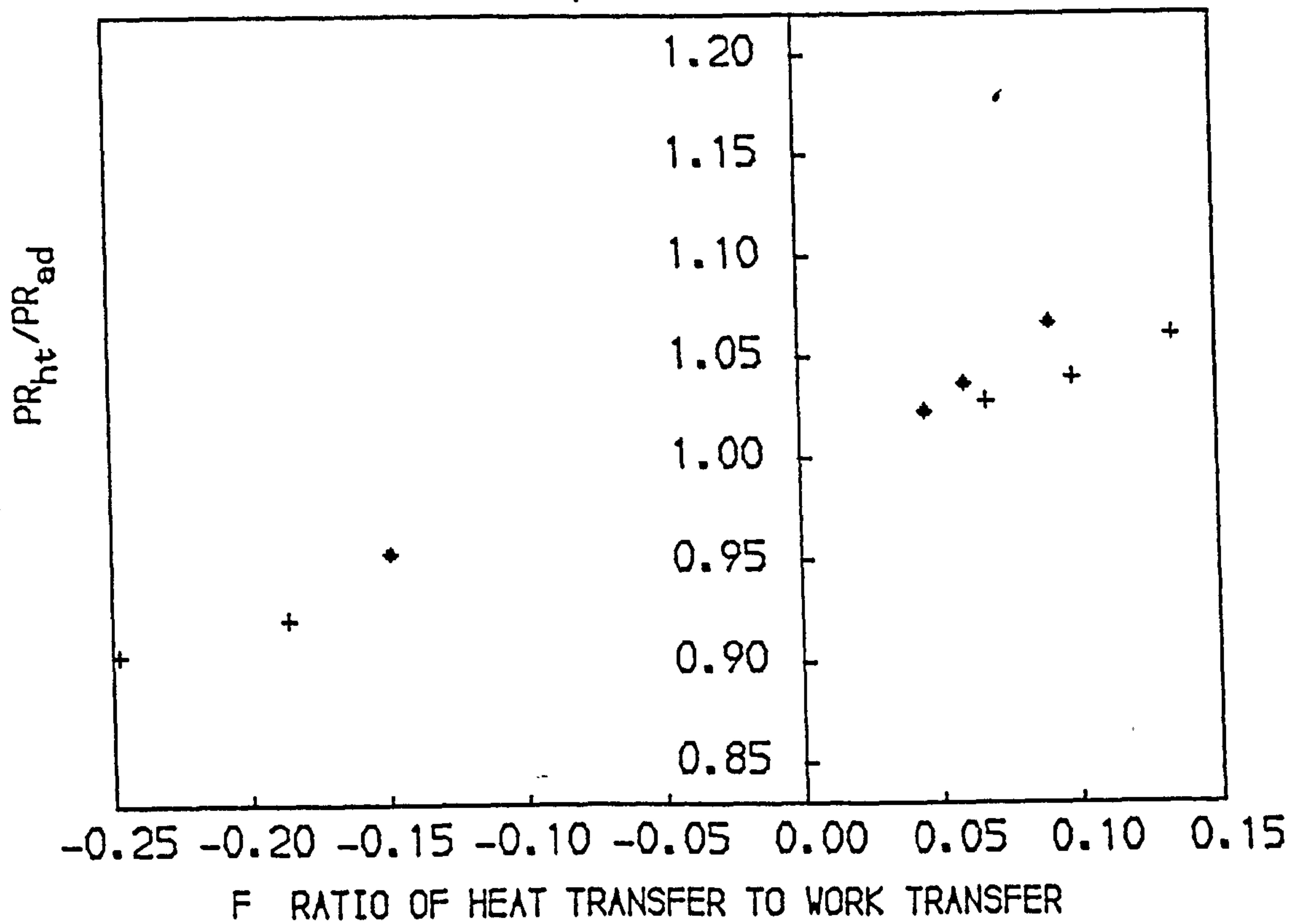


FIG. 84

MOVEMENTS OF THE SURGE LINES WITH HEAT TRANSFER
NON DIMENSIONAL SPEED LINES: + 495 • 578

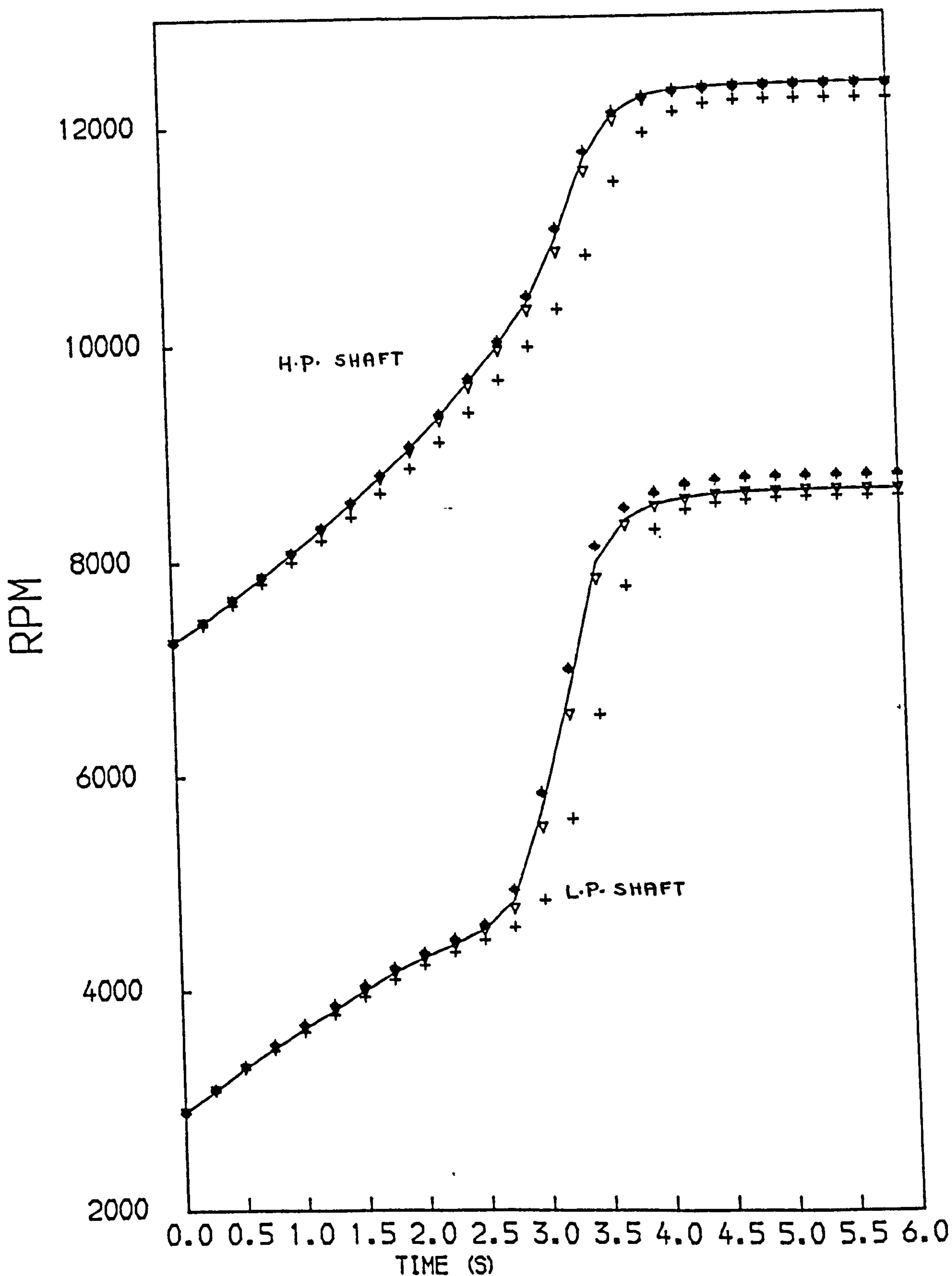


FIG. 85
 SENSITIVITY OF A TWO SPOOL BYPASS ENGINE WITH MIXED EXHAUSTS
 TO COMPONENT INEFFICIENCIES DURING A SEA LEVEL ACCELERATION
 -DATUM ENGINE
 +1% LOSS IN H.P. TURBINE EFFICIENCY
 ♦2% GAIN IN L.P. TURBINE OR L.P. COMPRESSOR EFFICIENCY
 ▽2% LOSS IN H.P. COMPRESSOR EFFICIENCY

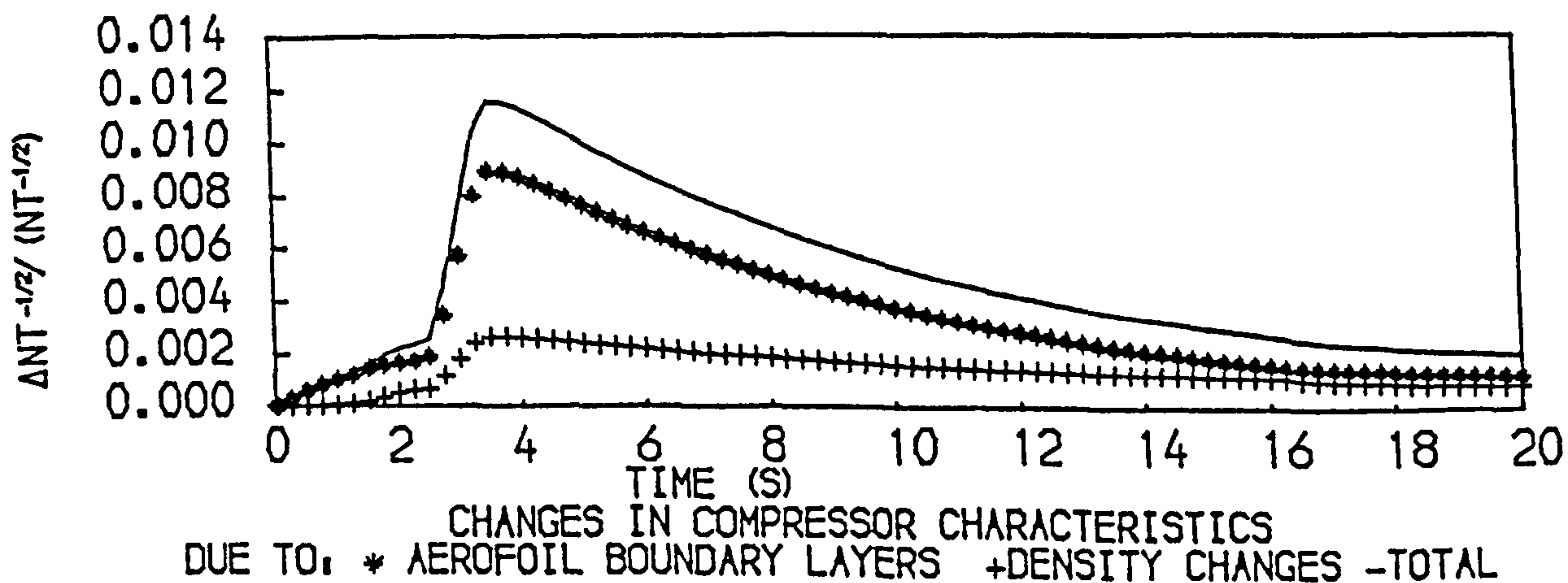
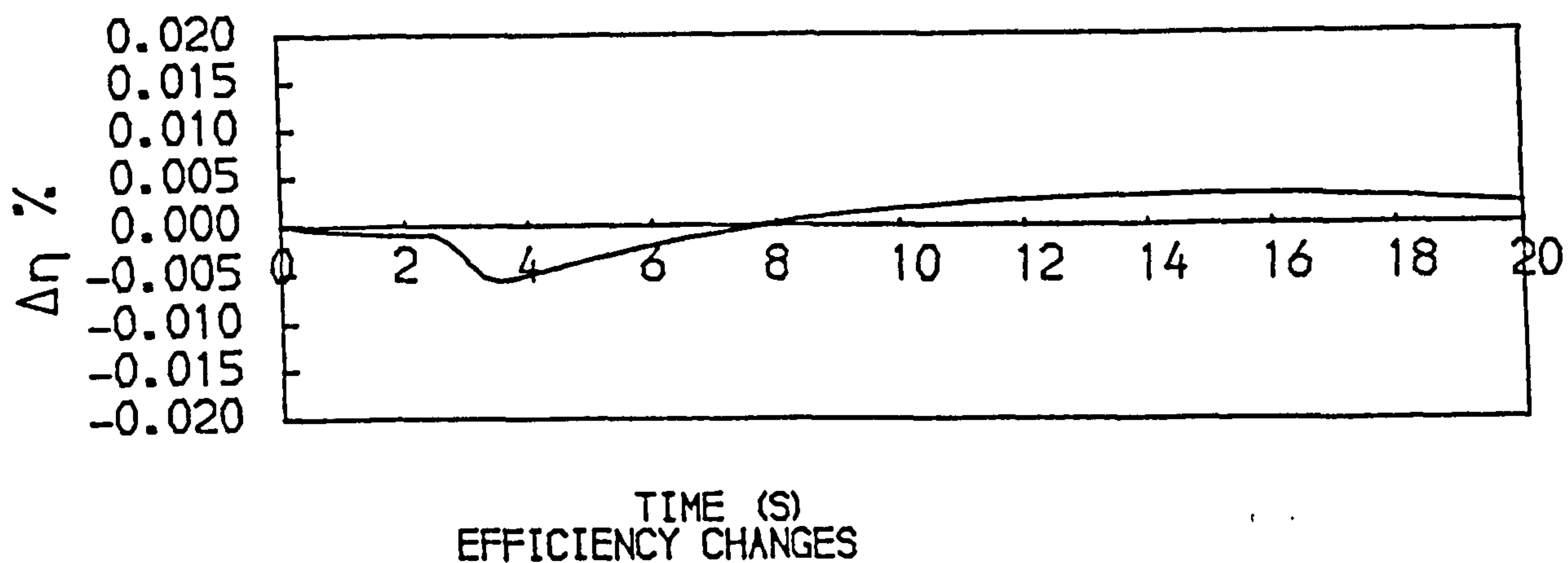
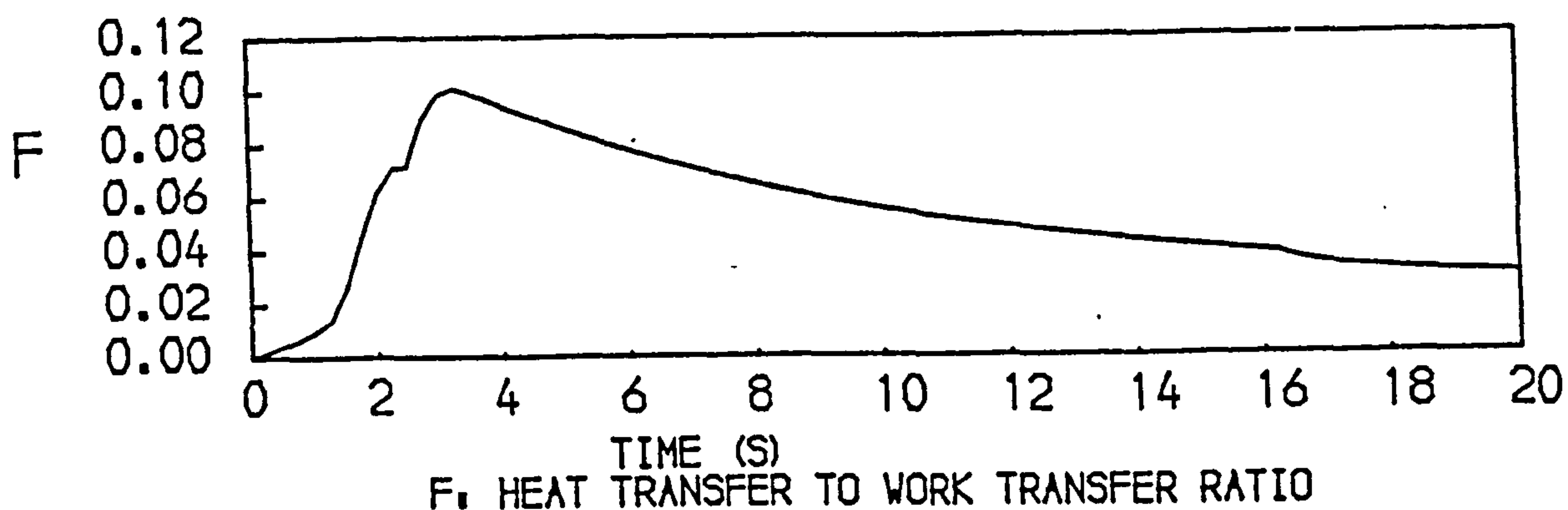
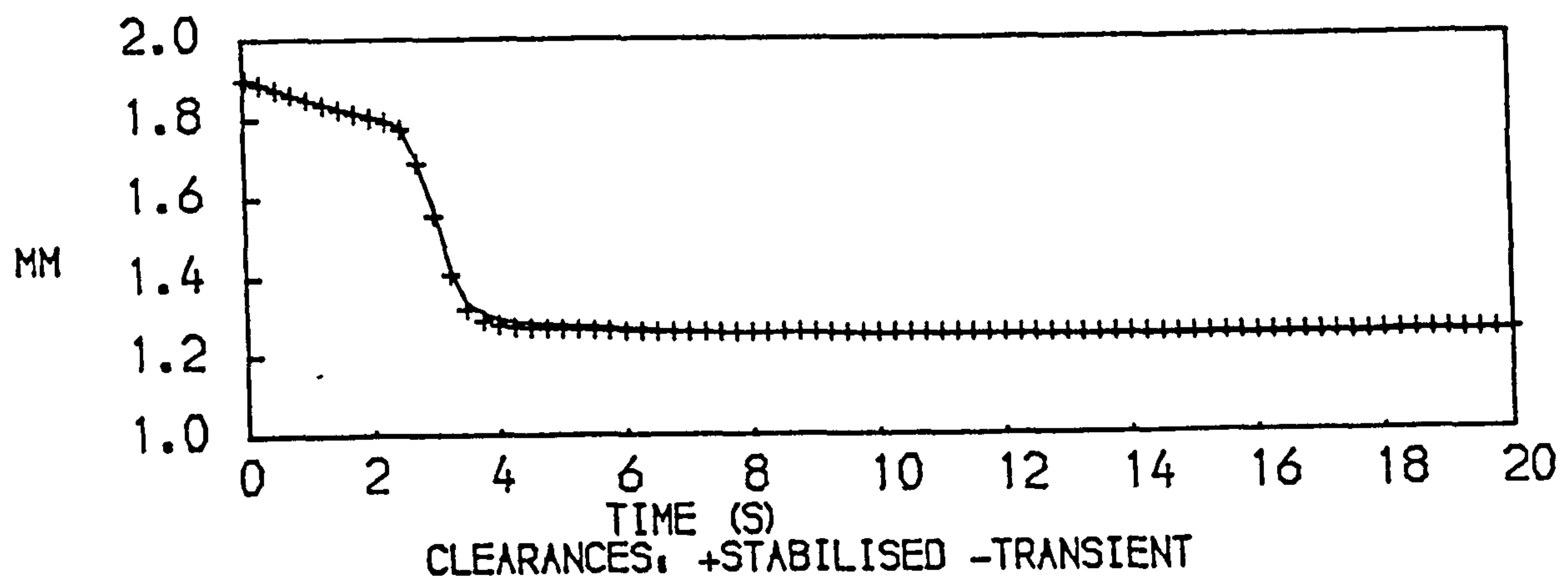


FIG. 86
PERFORMANCE OF THE LOW PRESSURE COMPRESSOR OF A TWO SPOOL BYPASS ENGINE WITH MIXED EXHAUSTS DURING AN ACCELERATION AT SEA LEVEL, STATIC CONDITIONS

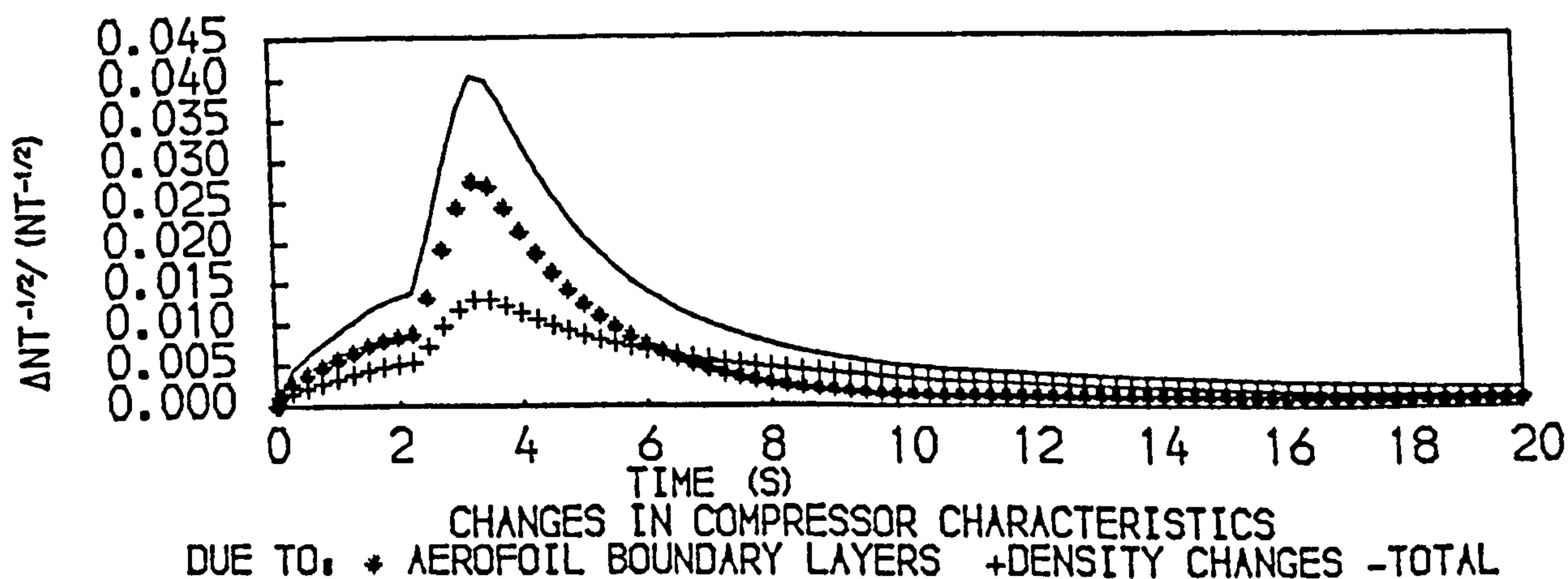
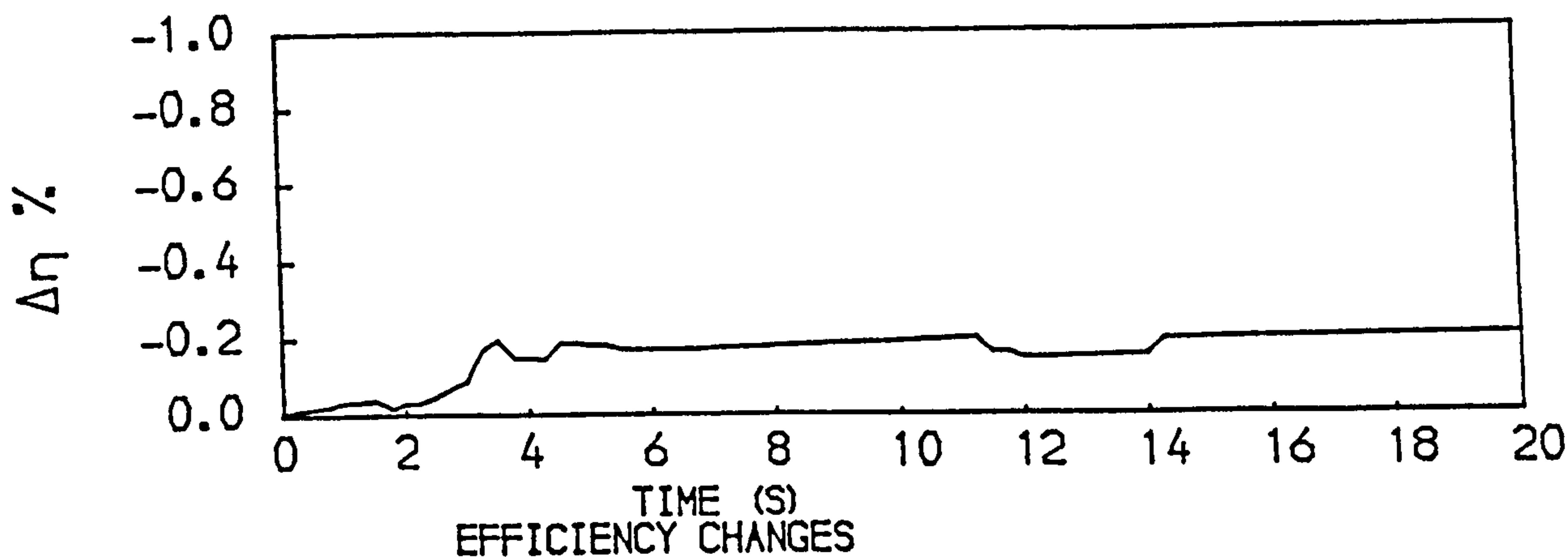
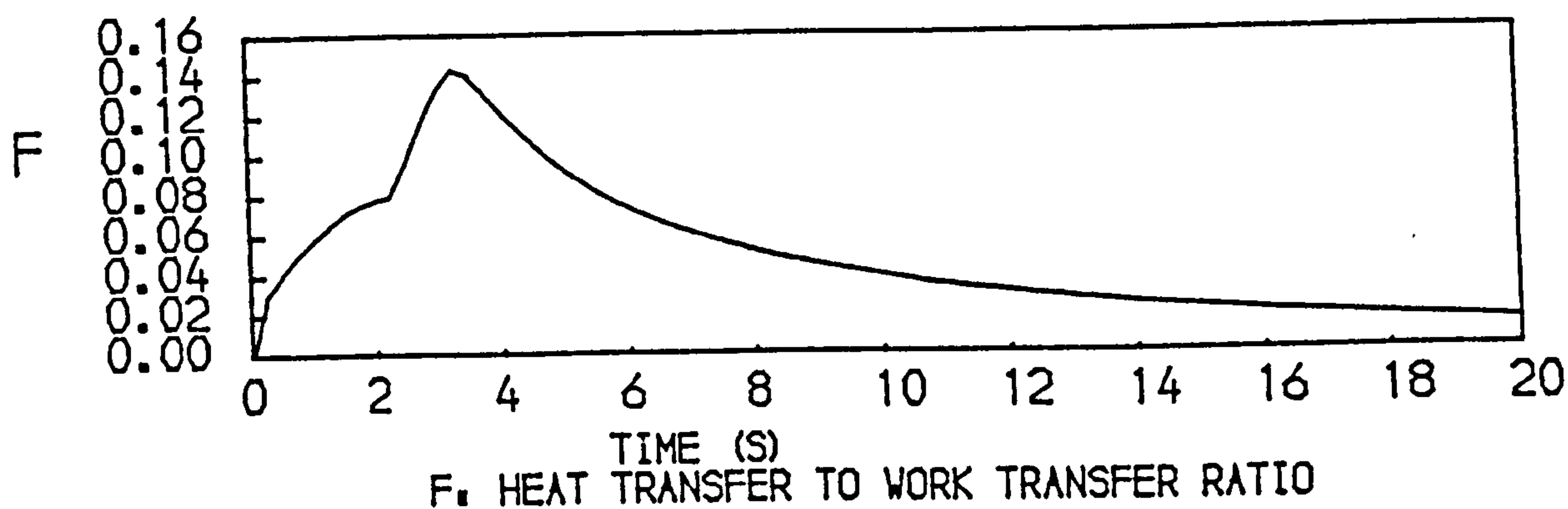
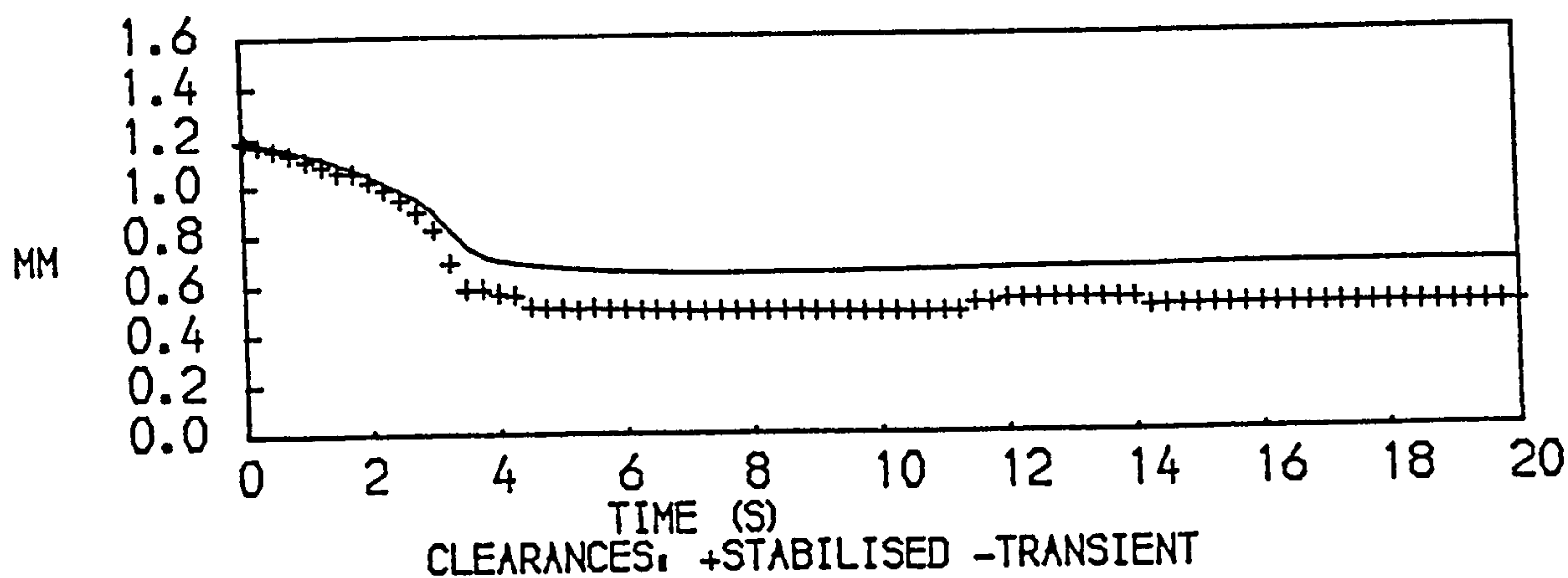


FIG. 87
PERFORMANCE OF THE HIGH PRESSURE COMPRESSOR OF A TWO SPOOL
BYPASS ENGINE WITH MIXED EXHAUSTS DURING AN ACCELERATION
AT SEA LEVEL, STATIC CONDITIONS

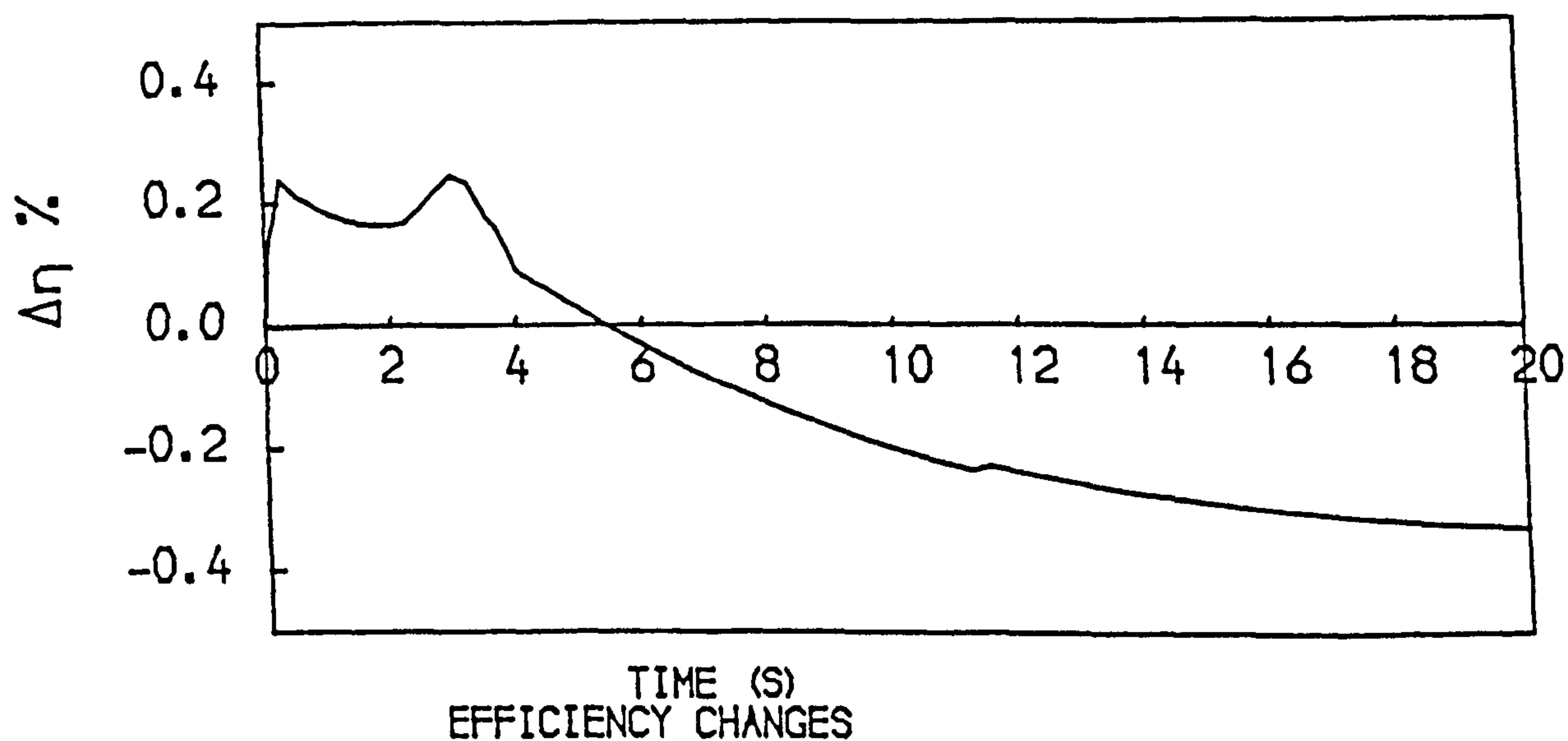
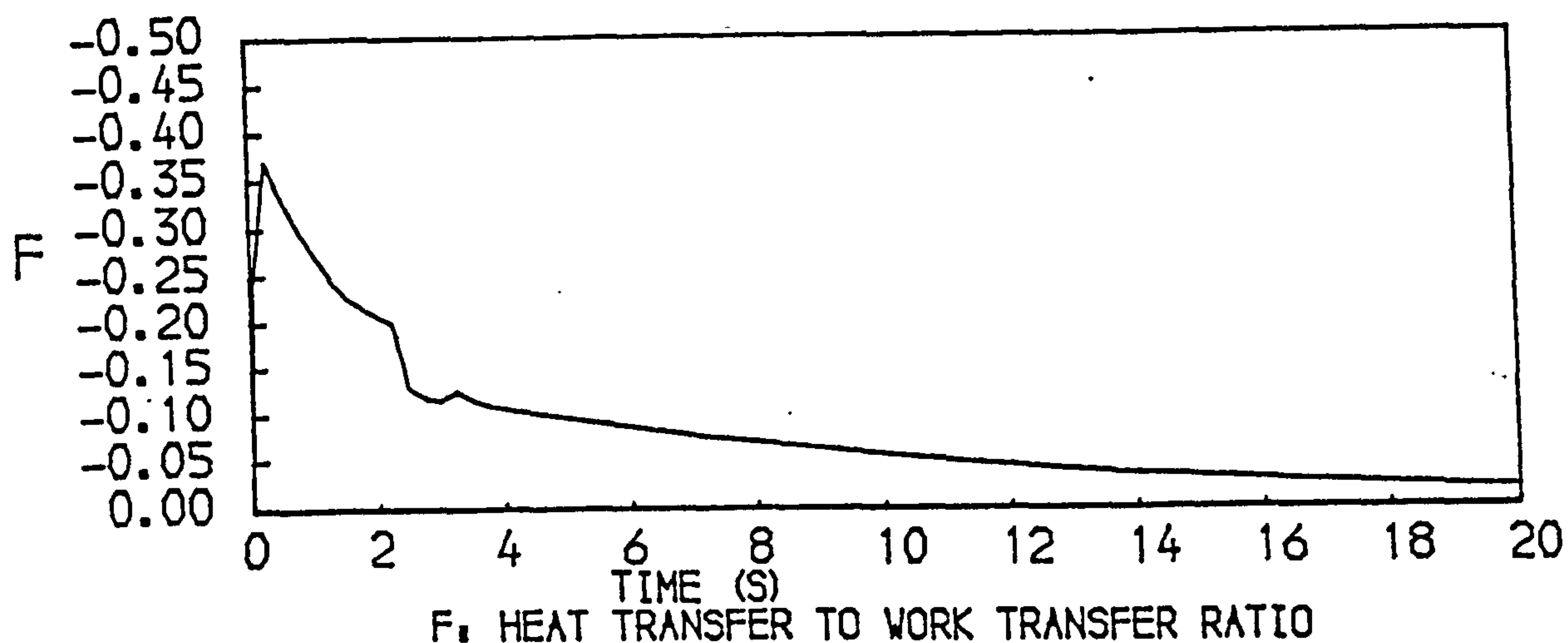
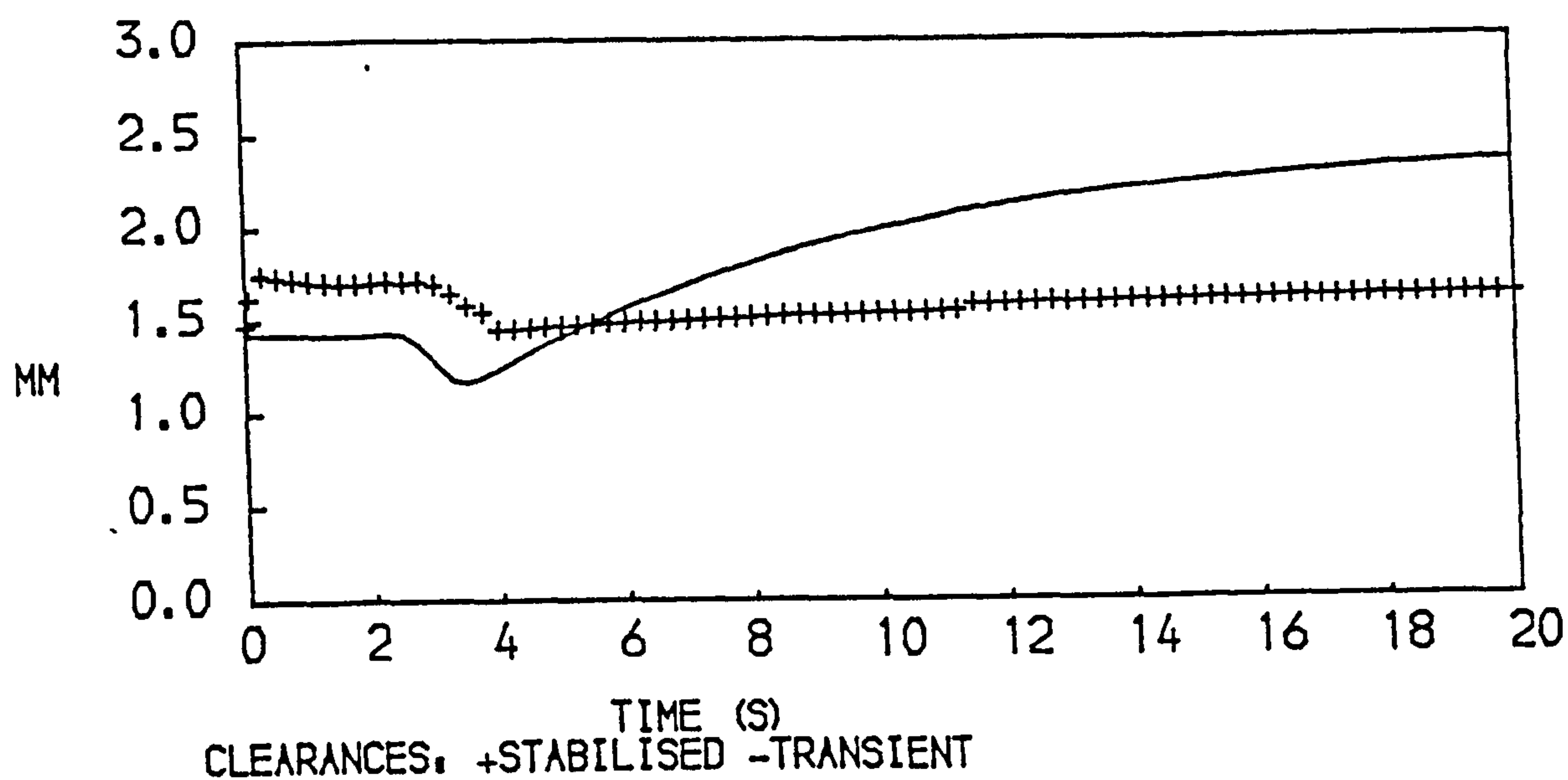


FIG. 88
PERFORMANCE OF THE LOW PRESSURE TURBINE OF A TWO SPOOL
BYPASS ENGINE WITH MIXED EXHAUSTS DURING AN ACCELERATION
AT SEA LEVEL, STATIC CONDITIONS

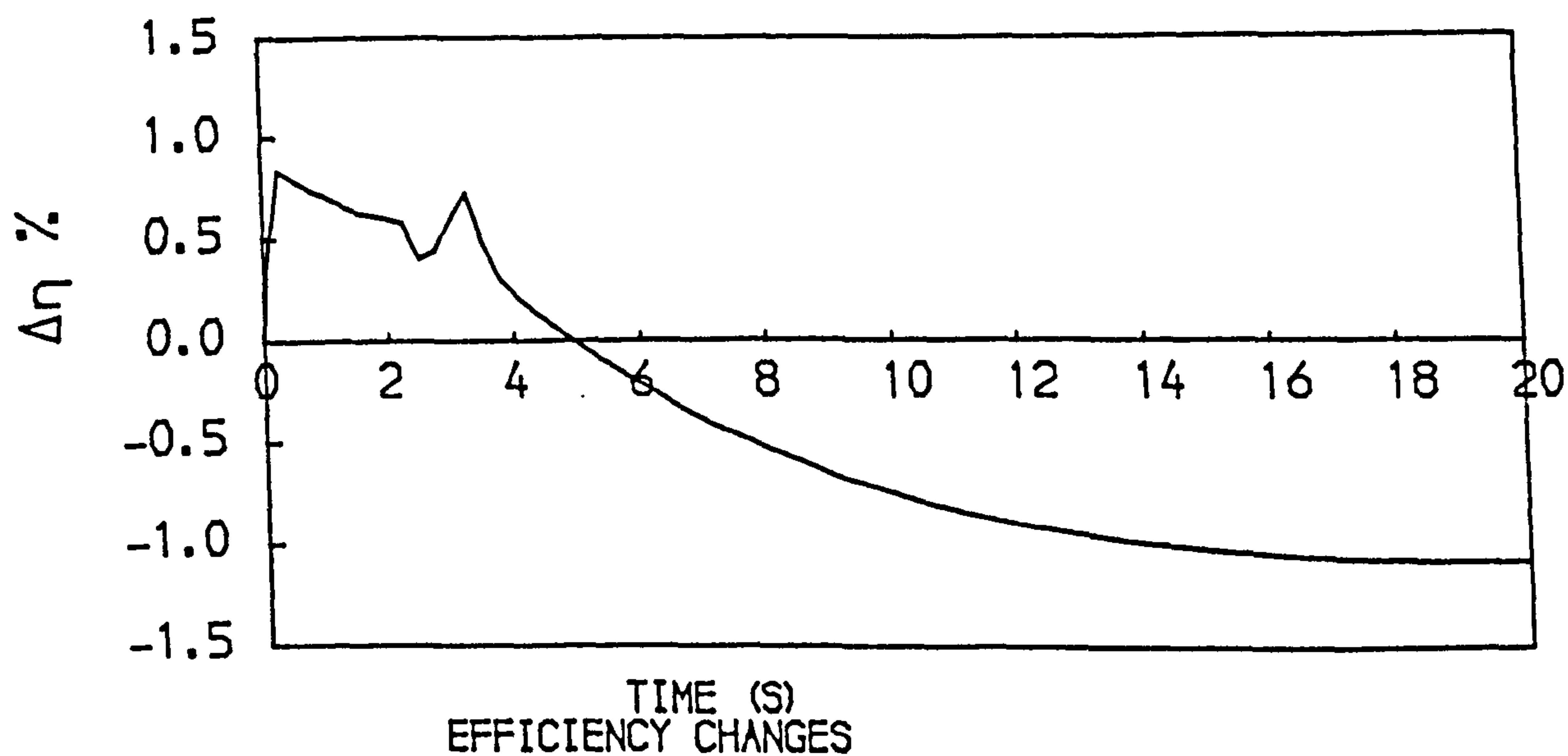
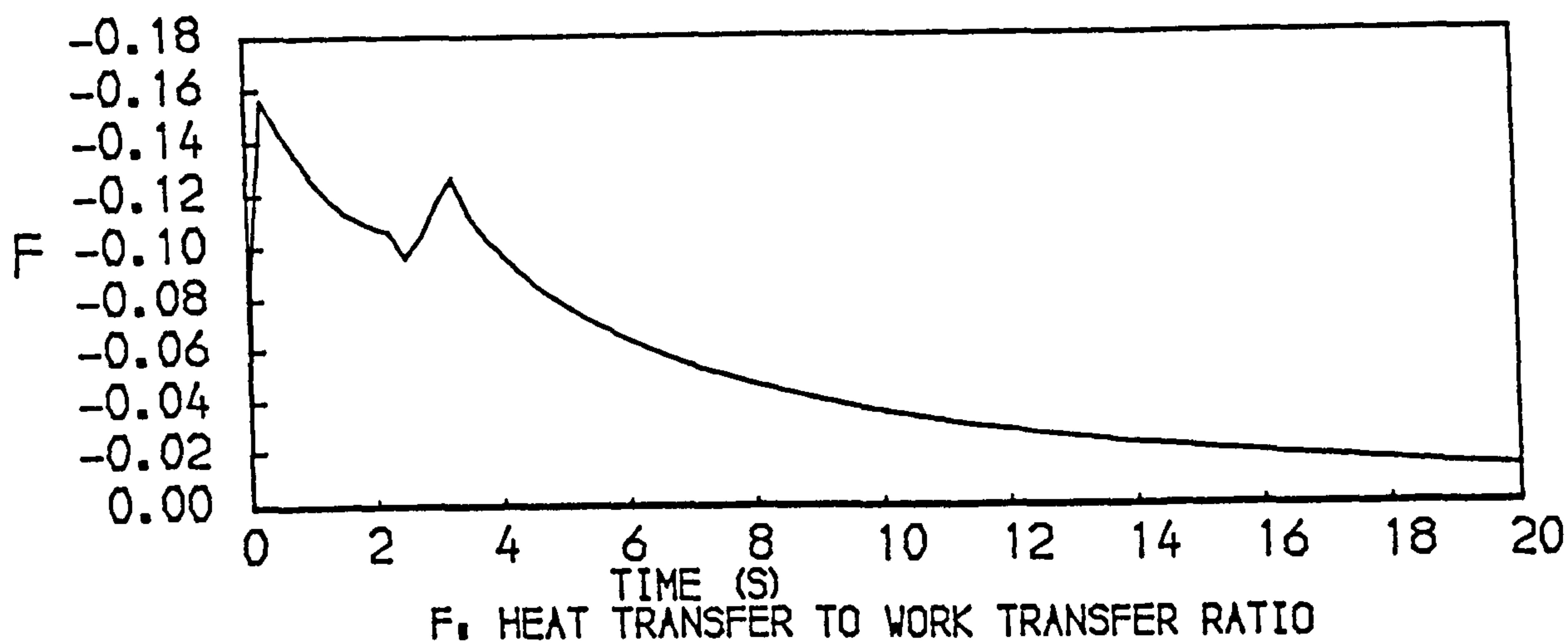
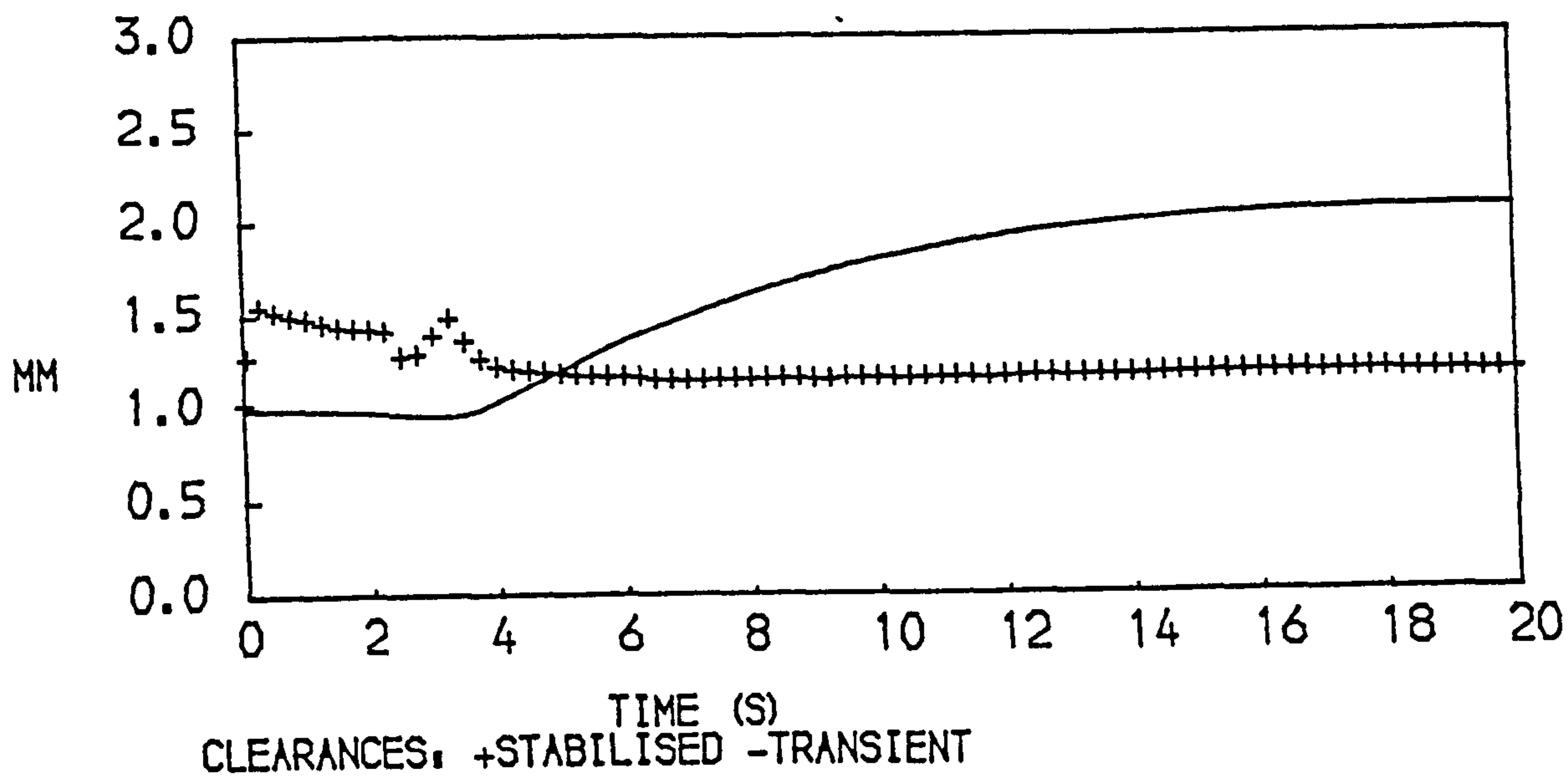


FIG. 89
PERFORMANCE OF THE HIGH PRESSURE TURBINE OF A TWO SPOOL
BYPASS ENGINE WITH MIXED EXHAUSTS DURING AN ACCELERATION
AT SEA LEVEL, STATIC CONDITIONS

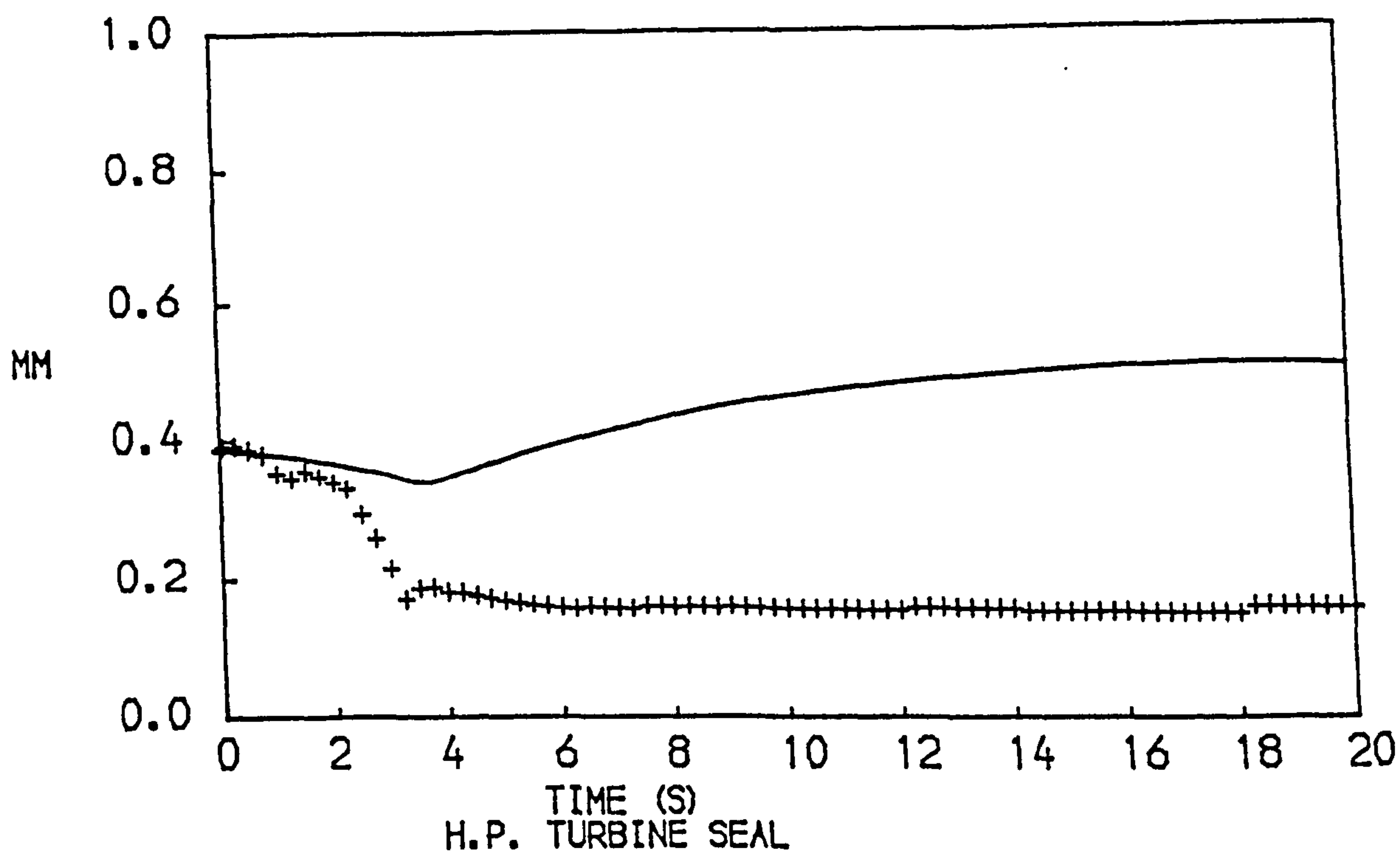
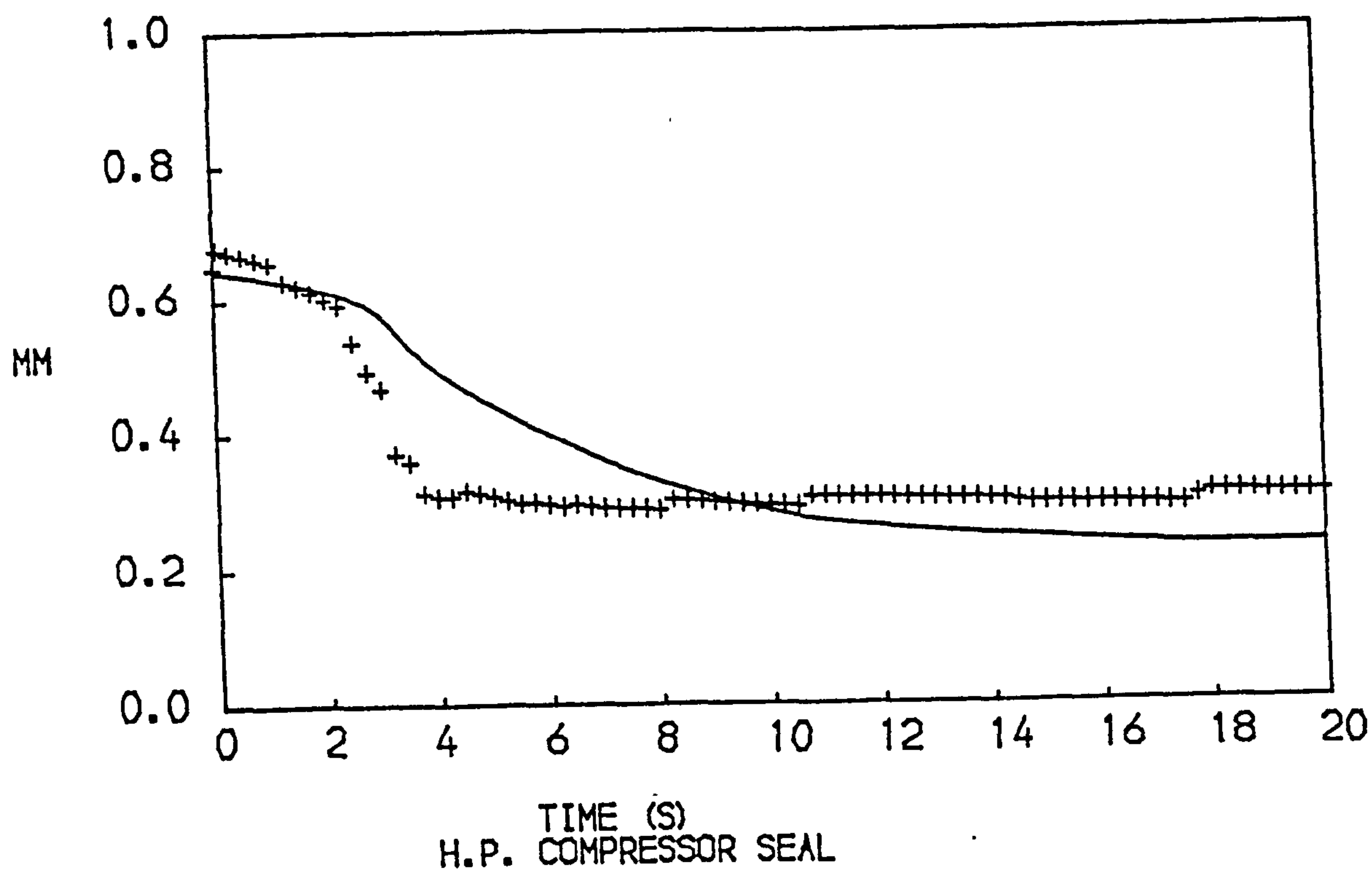


FIG. 90
 PERFORMANCE OF THE TWO COOLING FLOW SEALS OF A TWO SPOOL
 BYPASS ENGINE WITH MIXED EXHAUSTS DURING AN ACCELERATION
 AT SEA LEVEL, STATIC CONDITIONS
 CLEARANCES +STEADY RUNNING —TRANSIENT

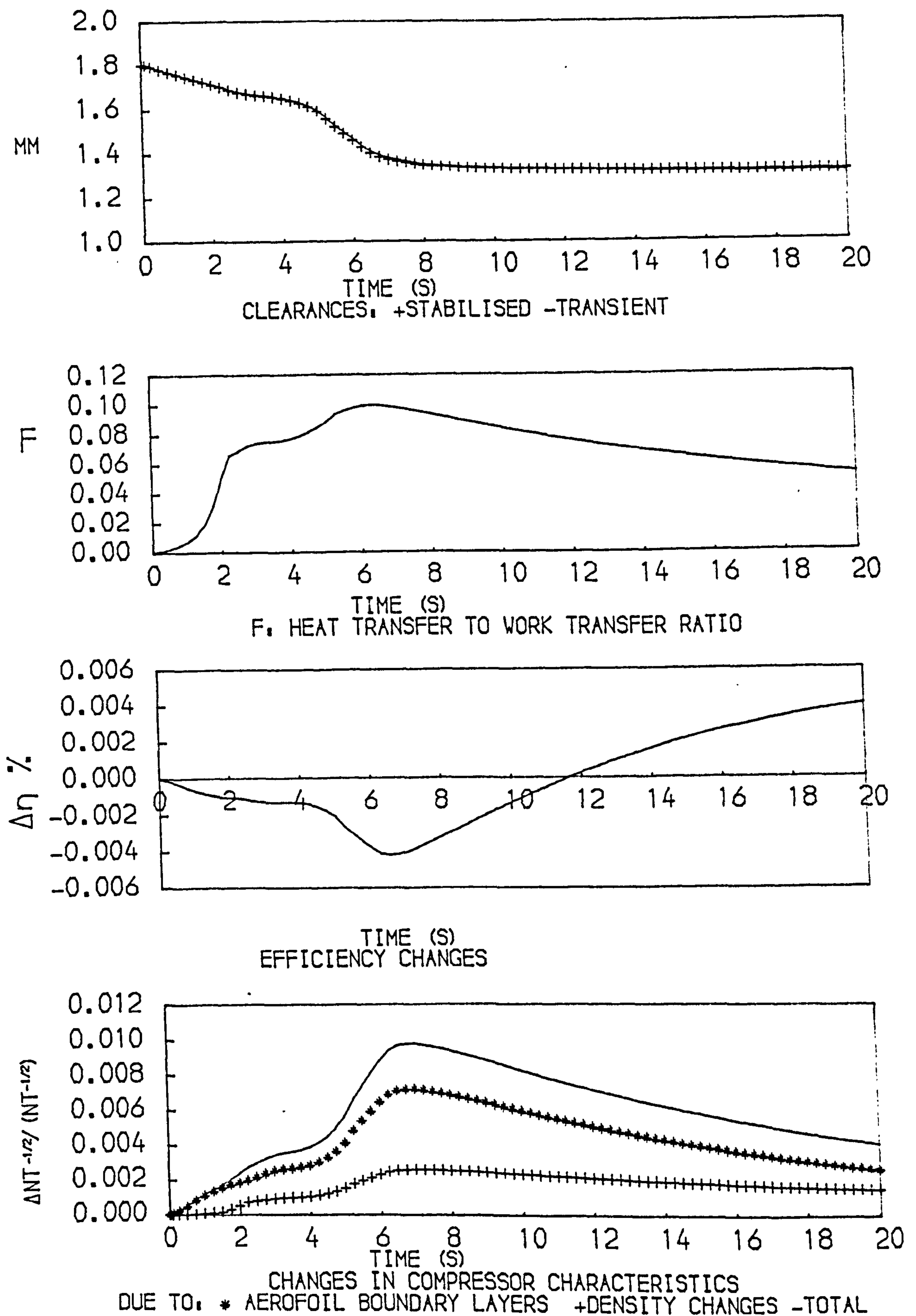


FIG. 91
PERFORMANCE OF THE LOW PRESSURE COMPRESSOR OF A TWO SPOOL
BYPASS ENGINE WITH MIXED EXHAUSTS DURING AN ACCELERATION
AT AN ALTITUDE OF 9150 M, FLIGHT MACH N 0.8

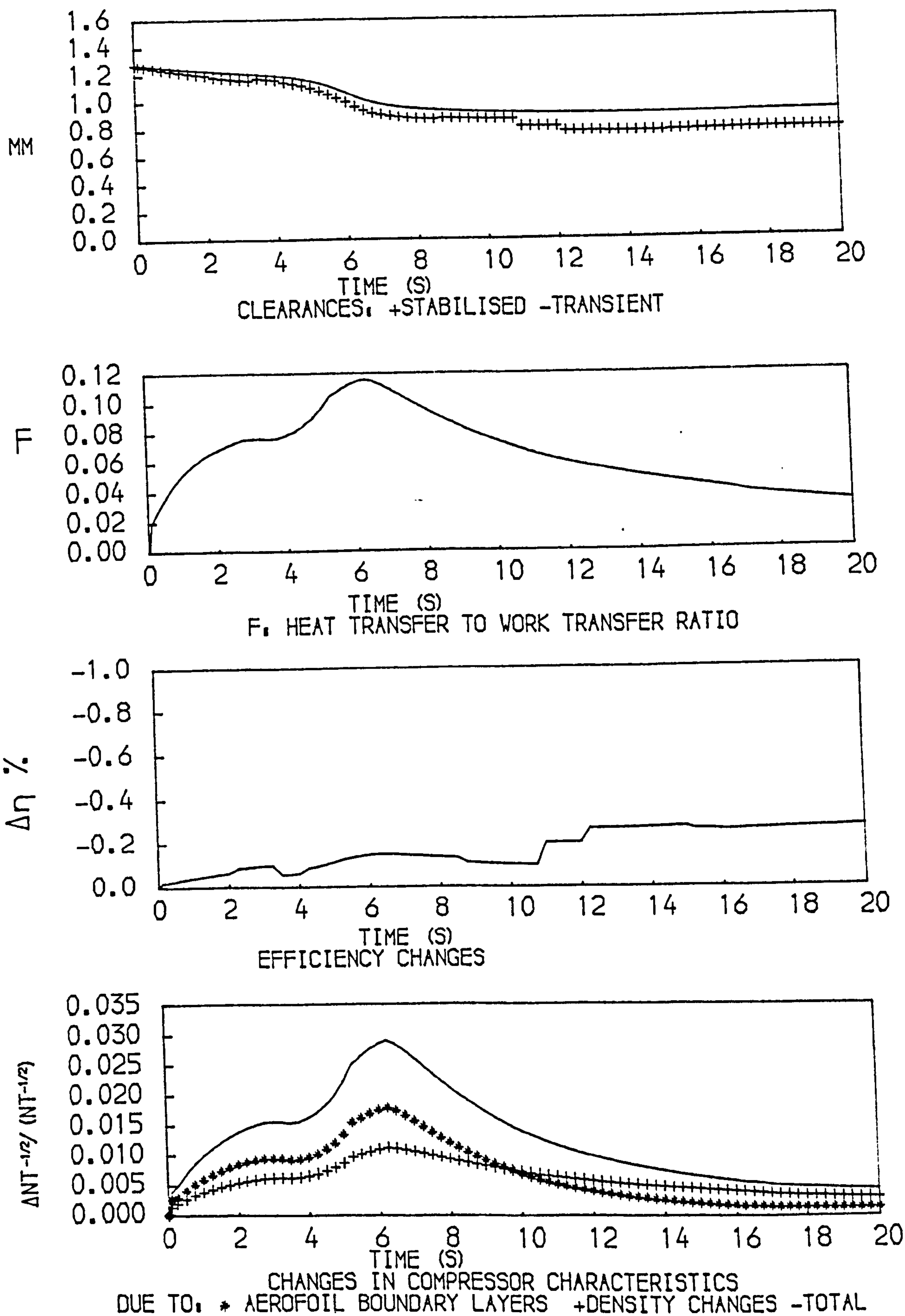


FIG. 92
PERFORMANCE OF THE HIGH PRESSURE COMPRESSOR OF A TWO SPOOL
BYPASS ENGINE WITH MIXED EXHAUSTS DURING AN ACCELERATION
AT AN ALTITUDE OF 9150 M, FLIGHT MACH N 0.8

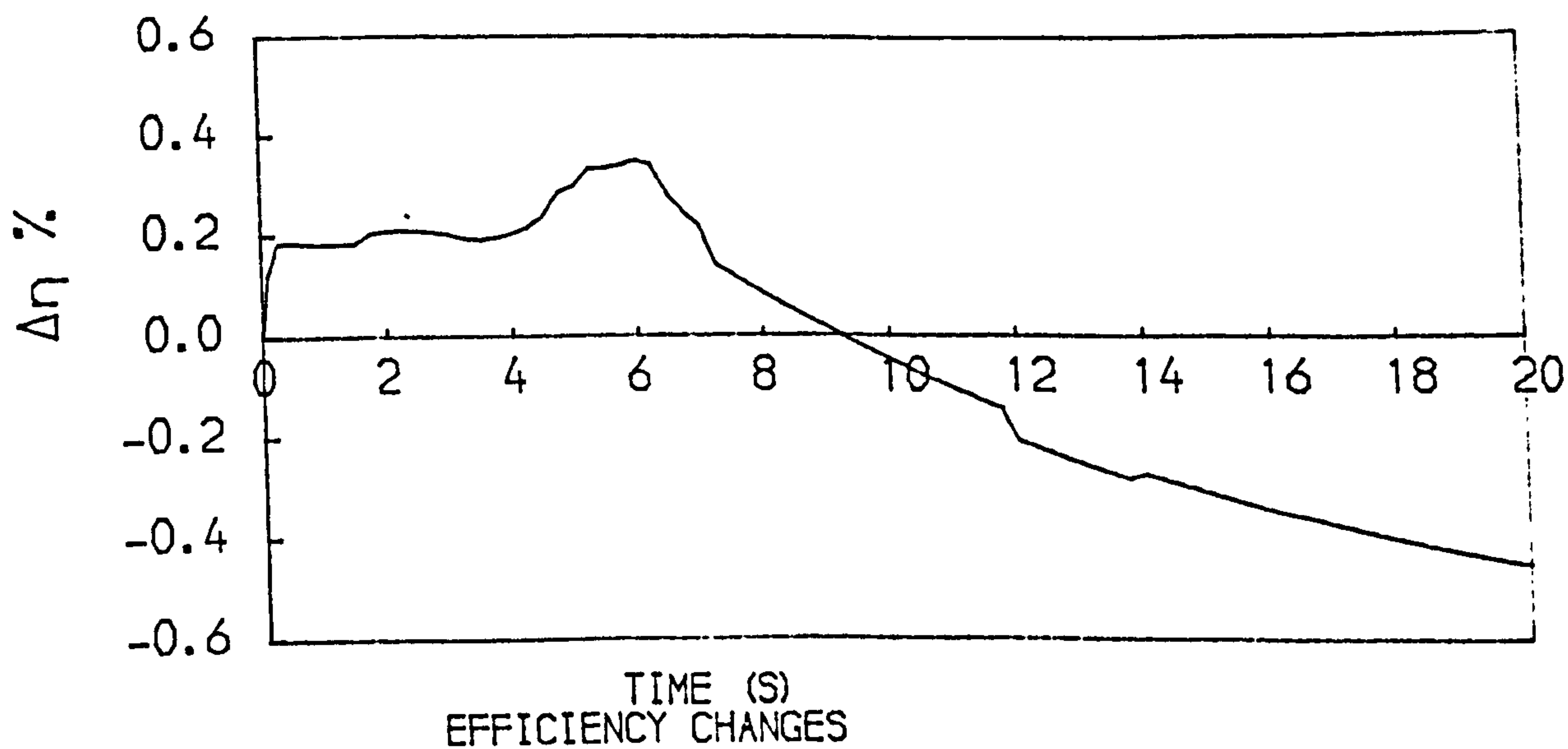
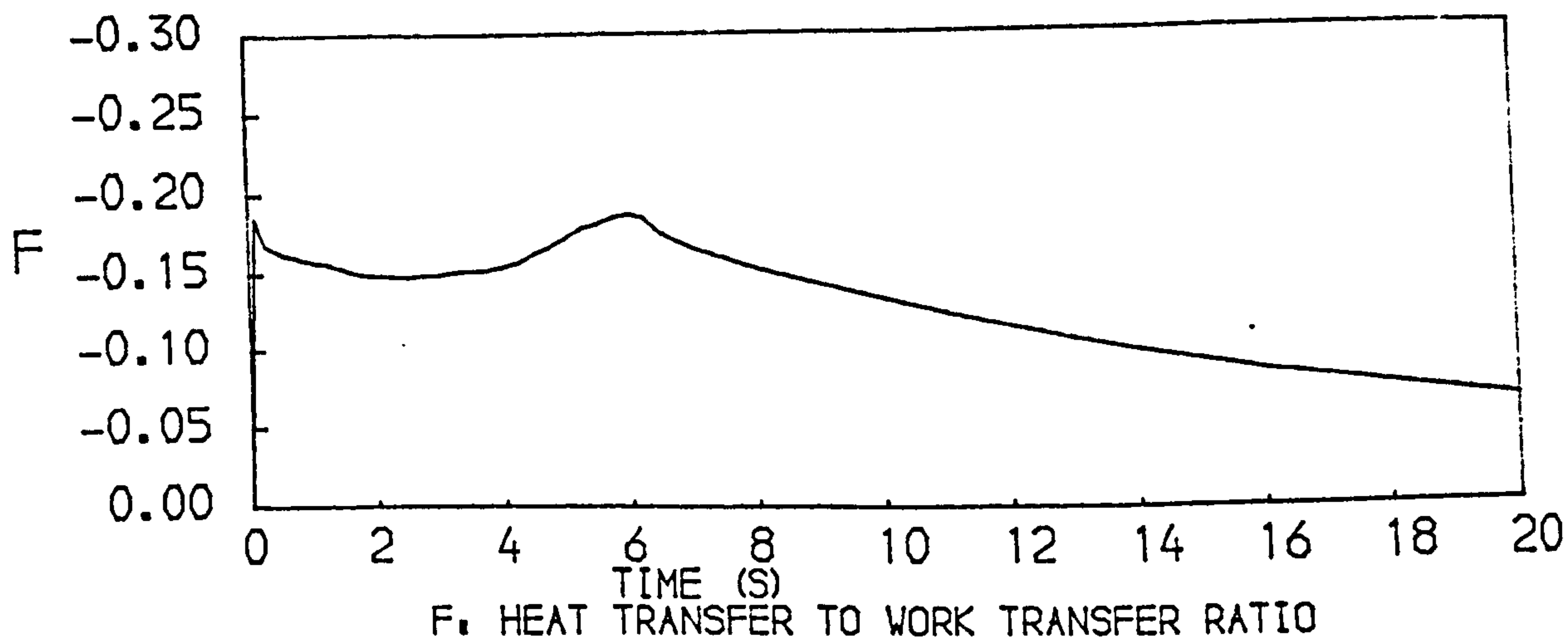
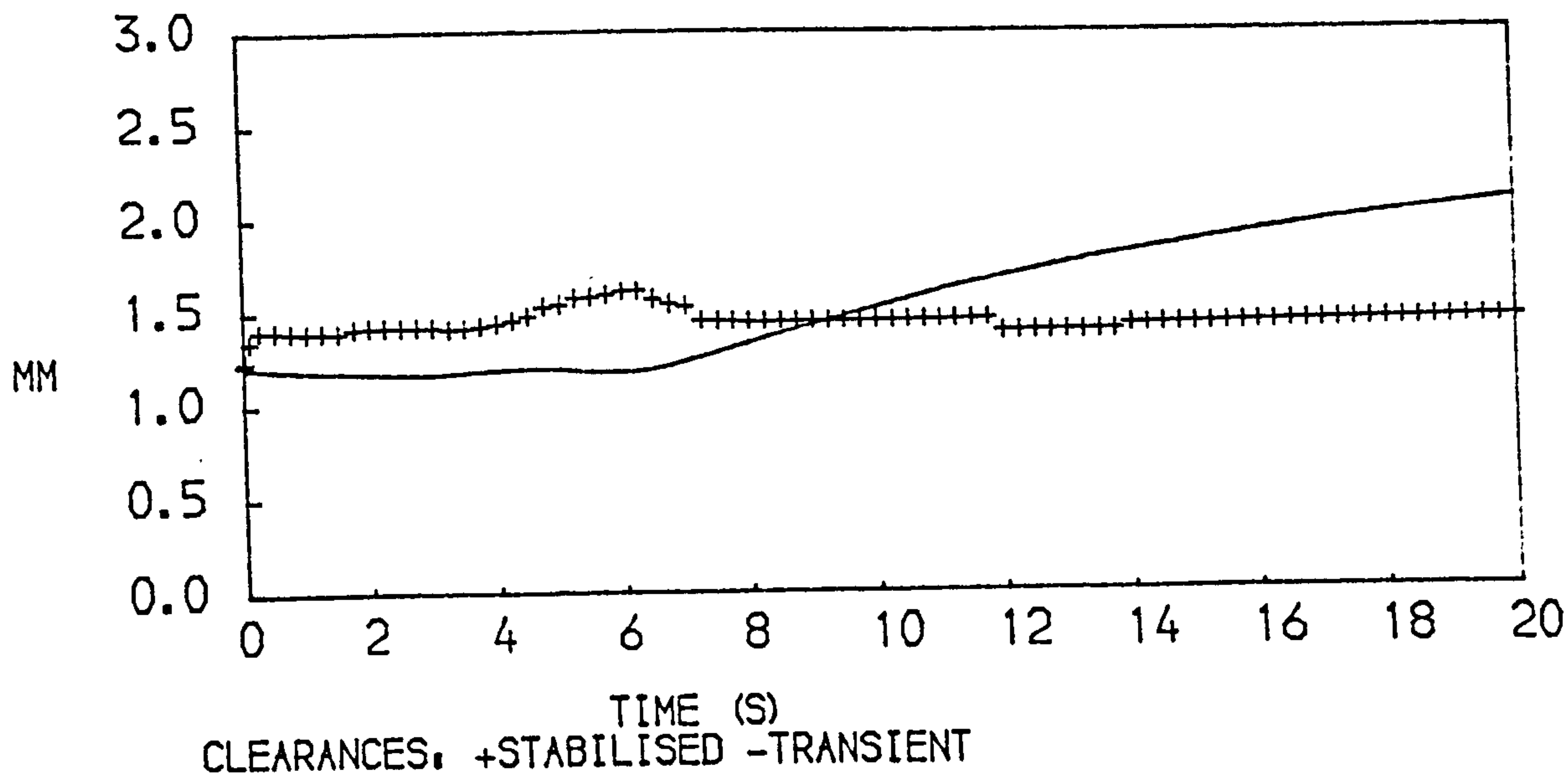


FIG. 93
PERFORMANCE OF THE LOW PRESSURE TURBINE OF A TWO SPOOL
BYPASS ENGINE WITH MIXED EXHAUSTS DURING AN ACCELERATION
AT AN ALTITUDE OF 9150 M, FLIGHT MACH N 0.8

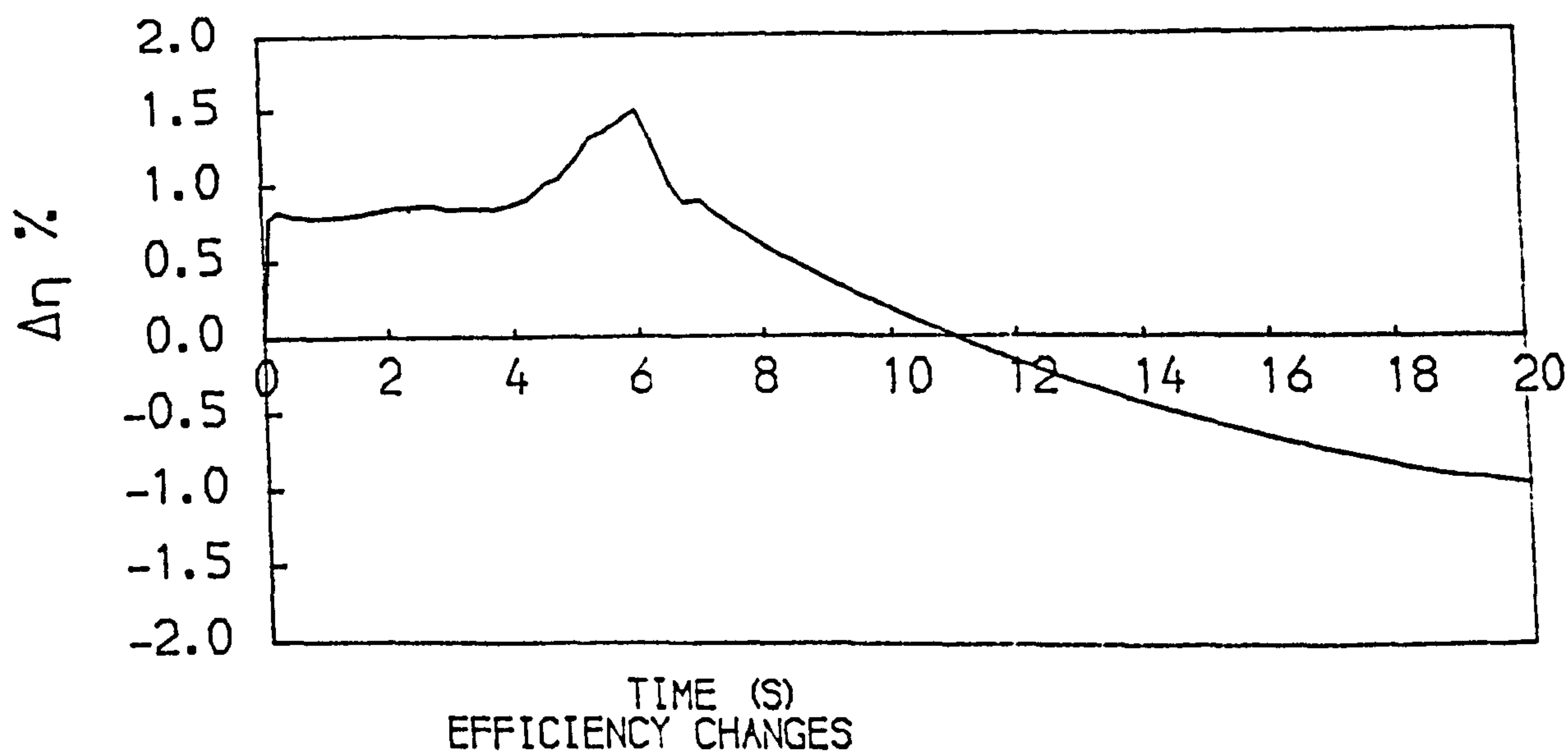
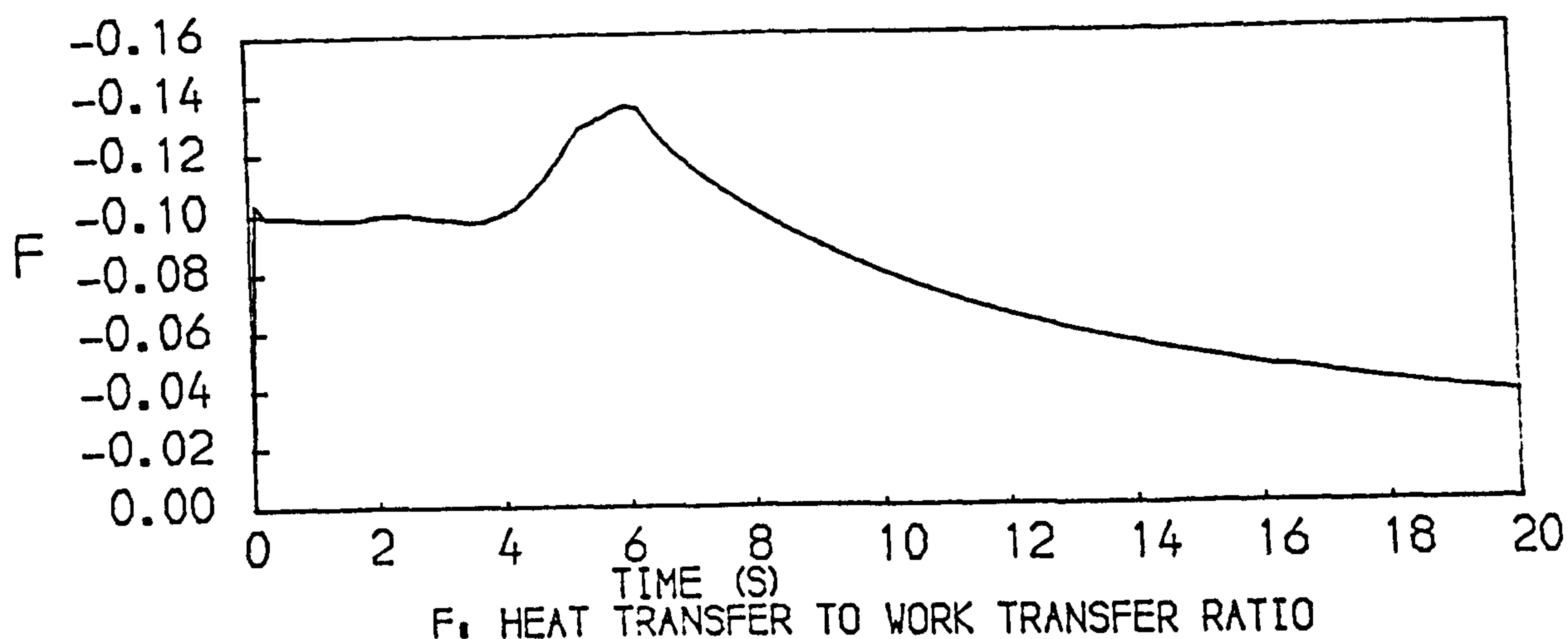
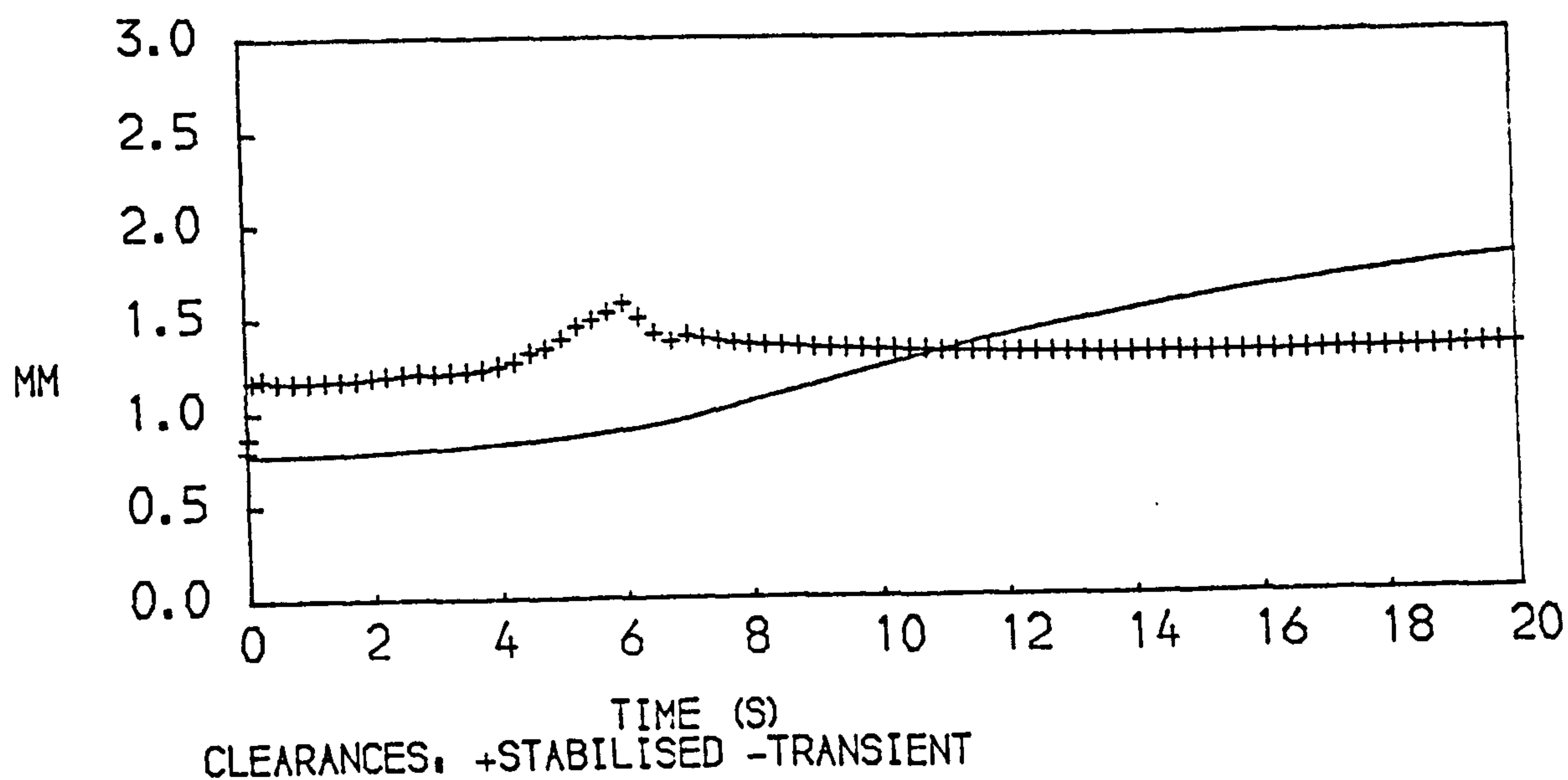


FIG. 94
PERFORMANCE OF THE HIGH PRESSURE TURBINE OF A TWO SPOOL
BYPASS ENGINE WITH MIXED EXHAUSTS DURING AN ACCELERATION
AT AN ALTITUDE OF 9150 M, FLIGHT MACH N 0.8

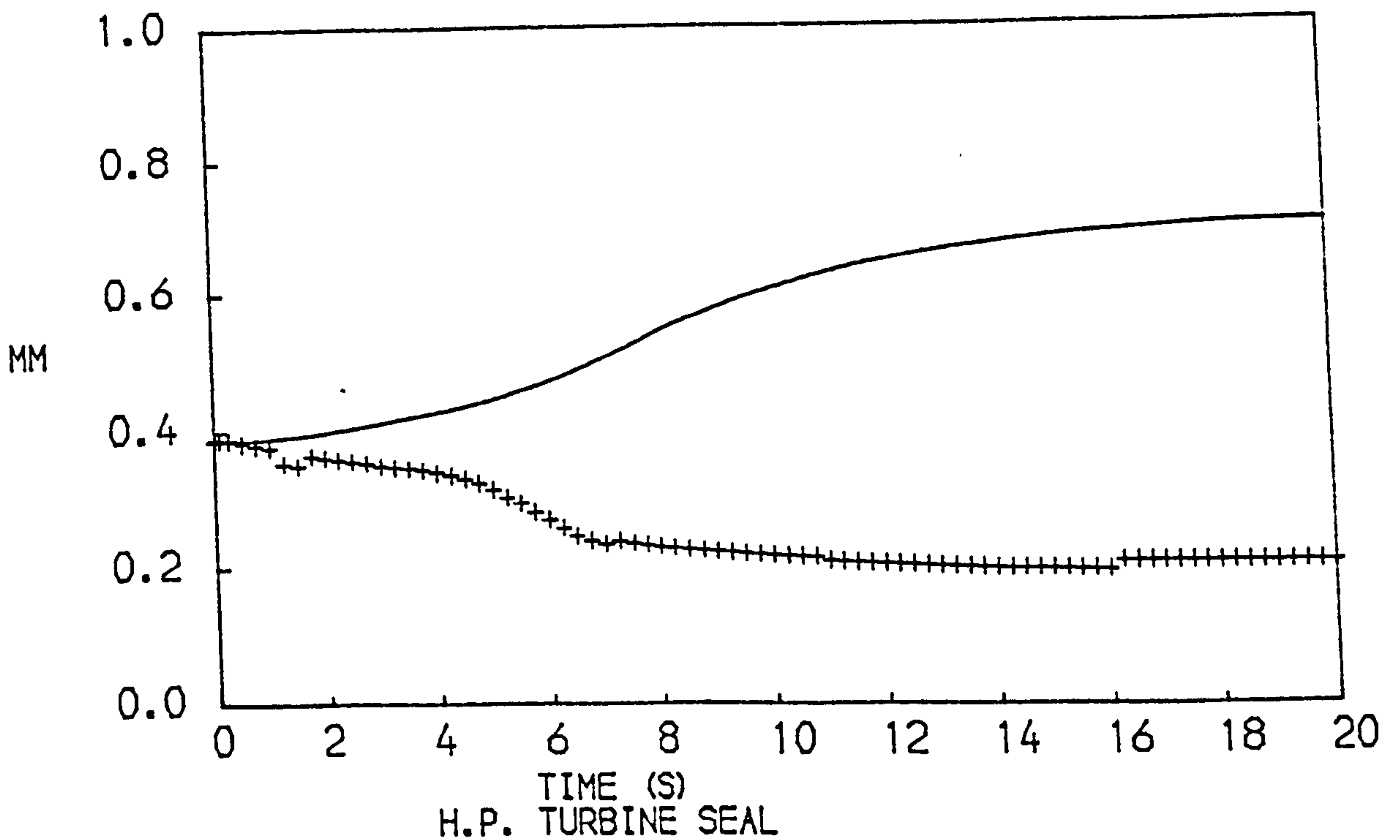
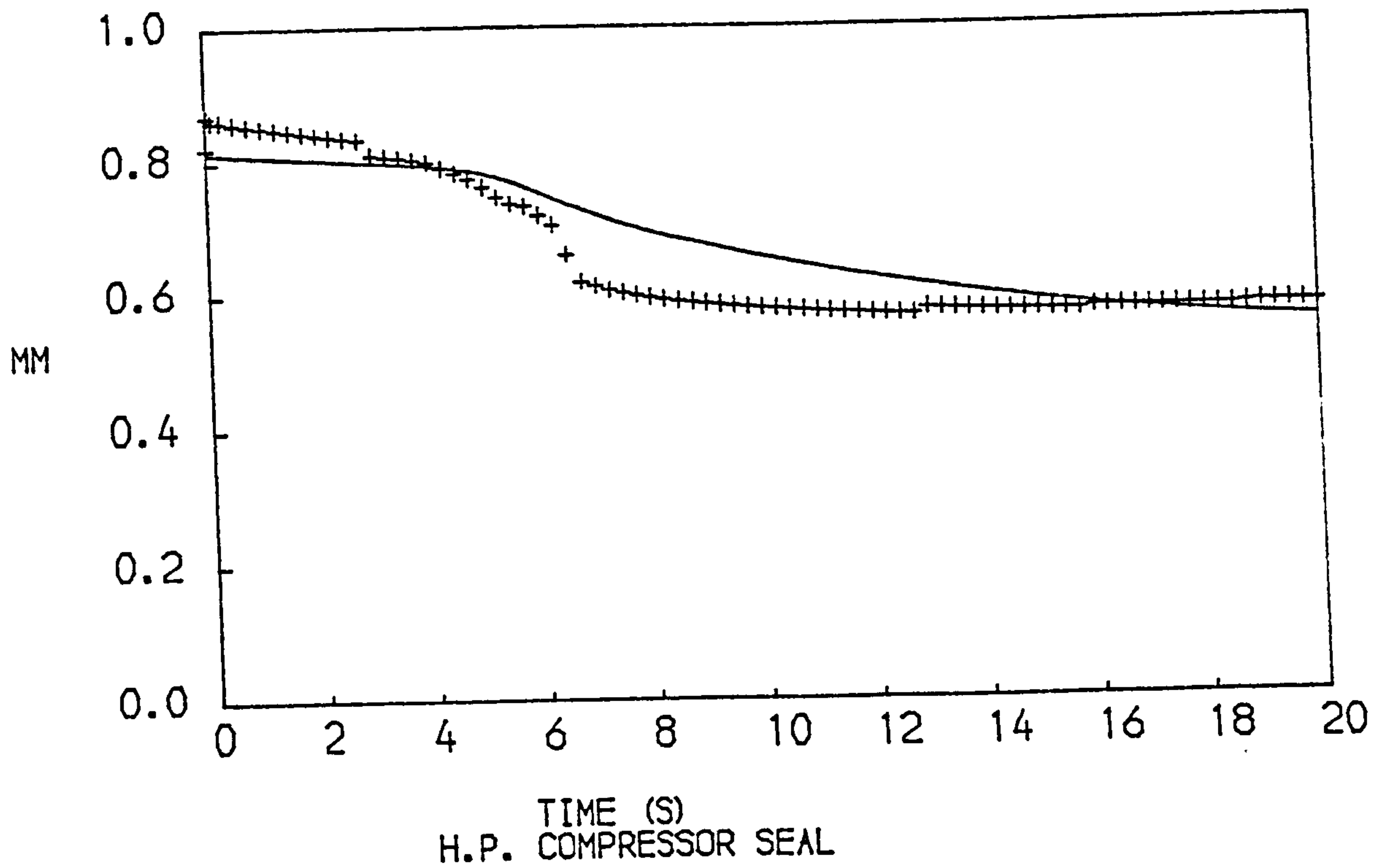


FIG. 95
 PERFORMANCE OF THE TWO COOLING FLOW SEALS OF A TWO SPOOL
 BYPASS ENGINE WITH MIXED EXHAUSTS DURING AN ACCELERATION
 AT AN ALTITUDE OF 9150 M, FLIGHT MACH N 0.8
 CLEARANCES +STEADY RUNNING —TRANSIENT

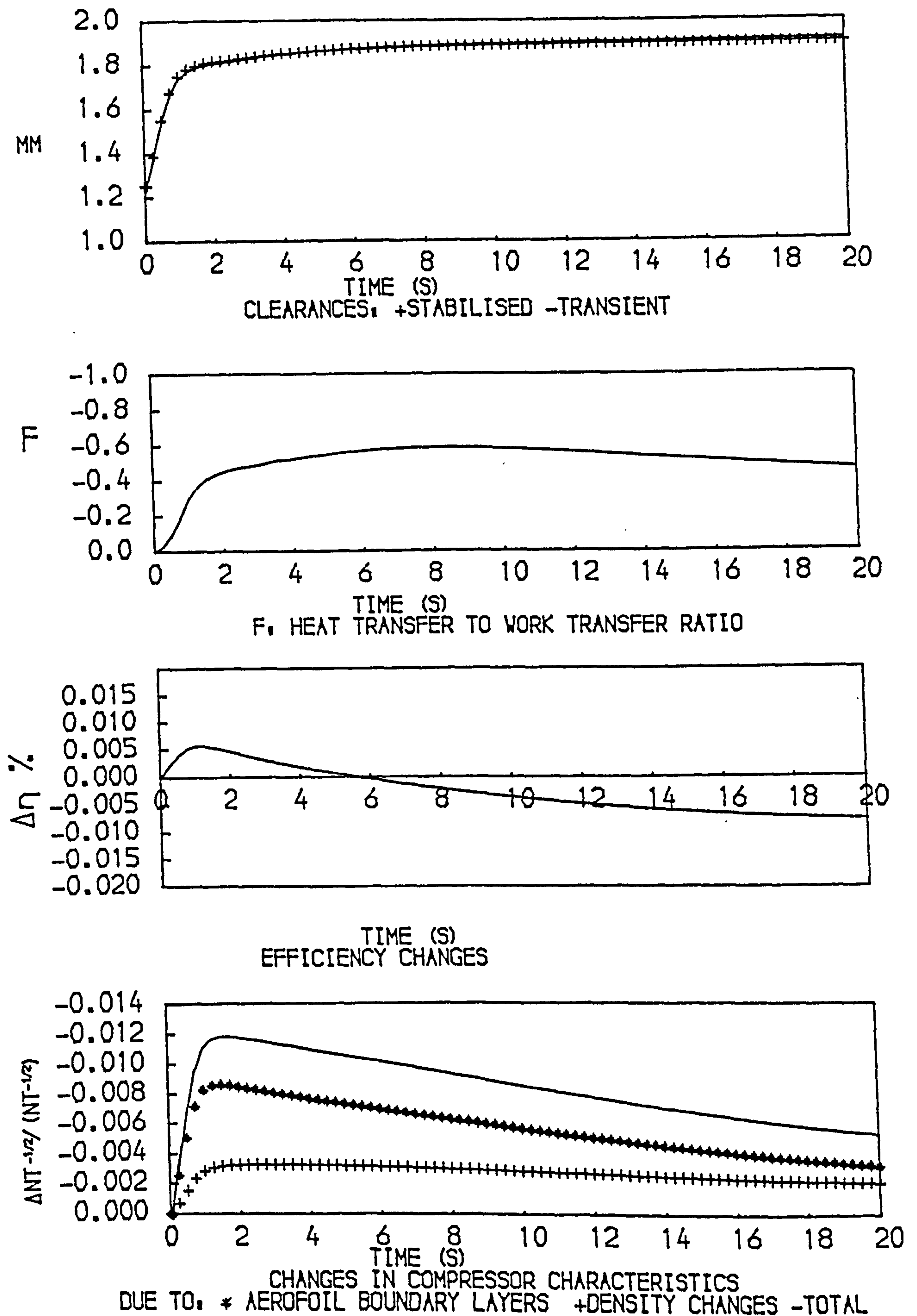


FIG. 96
PERFORMANCE OF THE LOW PRESSURE COMPRESSOR OF A TWO SPOOL
BYPASS ENGINE WITH MIXED EXHAUSTS DURING A DECELERATION
AT SEA LEVEL, STATIC CONDITIONS

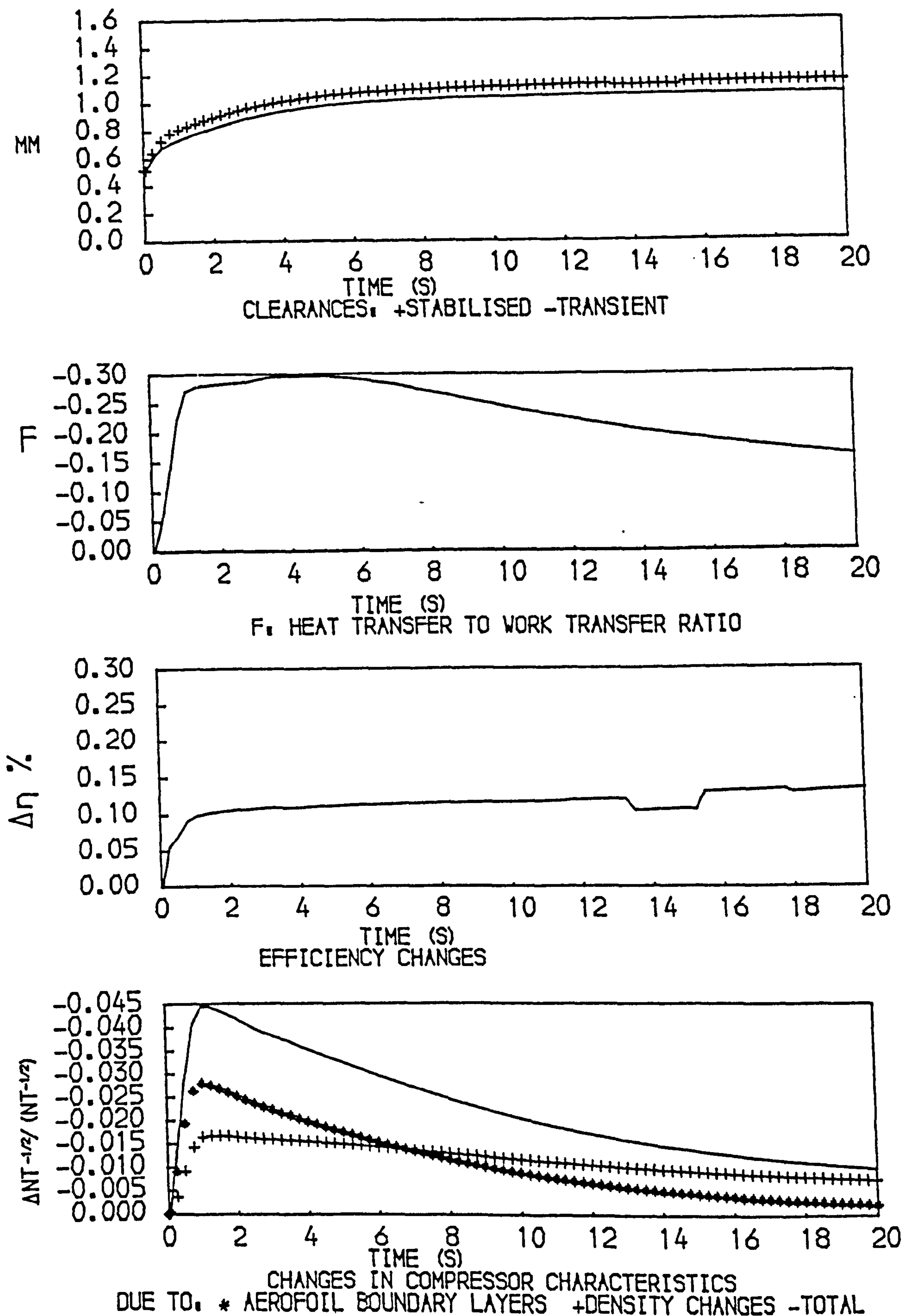


FIG. 97
 PERFORMANCE OF THE HIGH PRESSURE COMPRESSOR OF A TWO SPOOL
 BYPASS ENGINE WITH MIXED EXHAUSTS DURING A DECELERATION
 AT SEA LEVEL, STATIC CONDITIONS

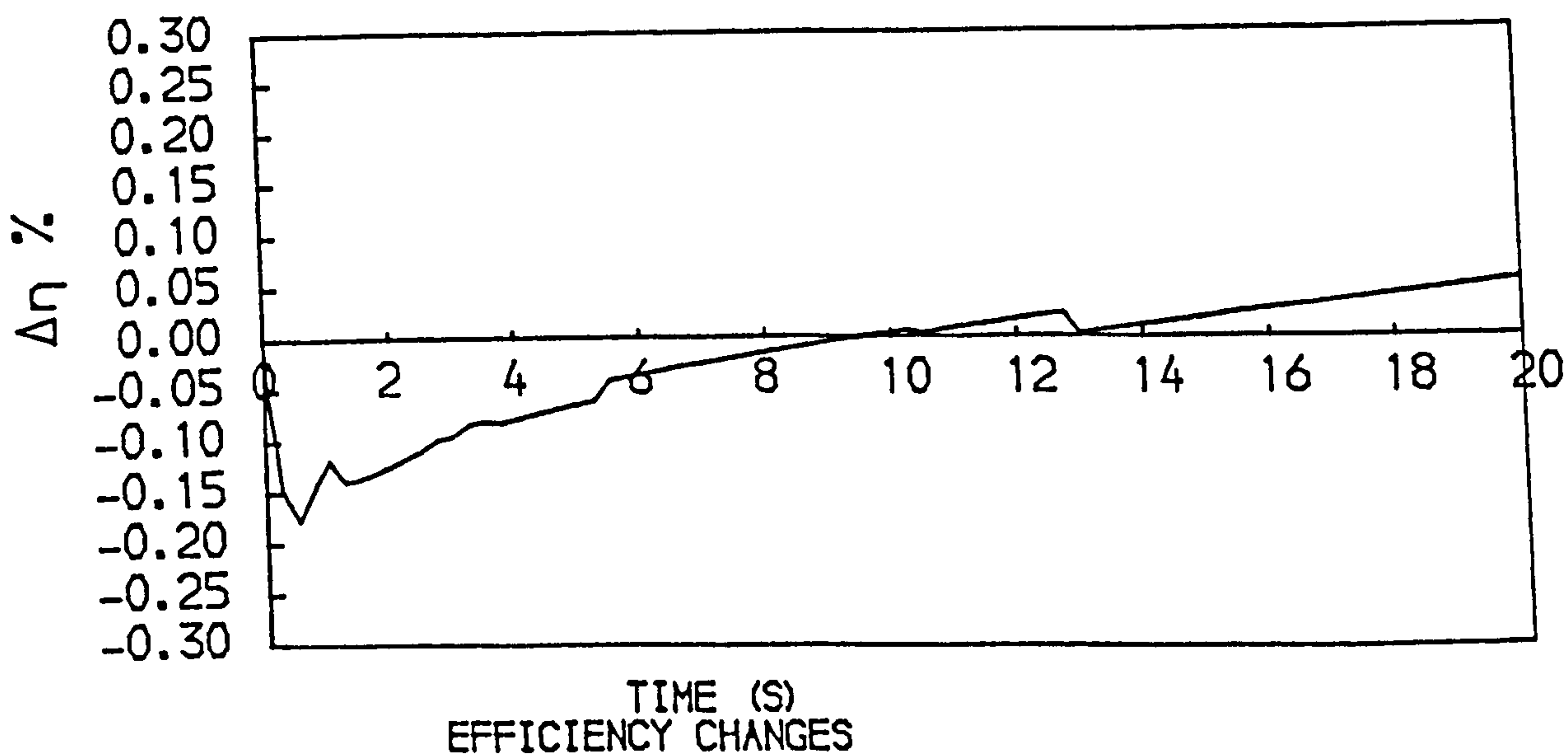
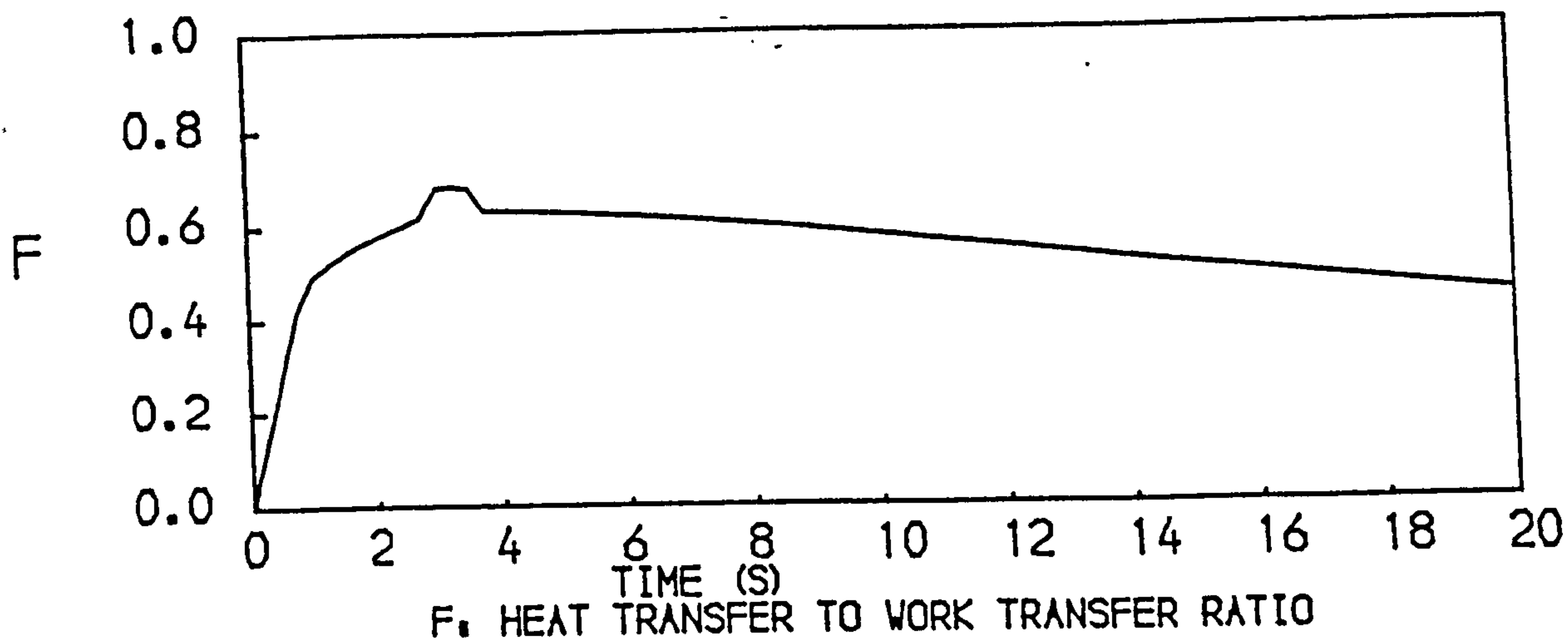
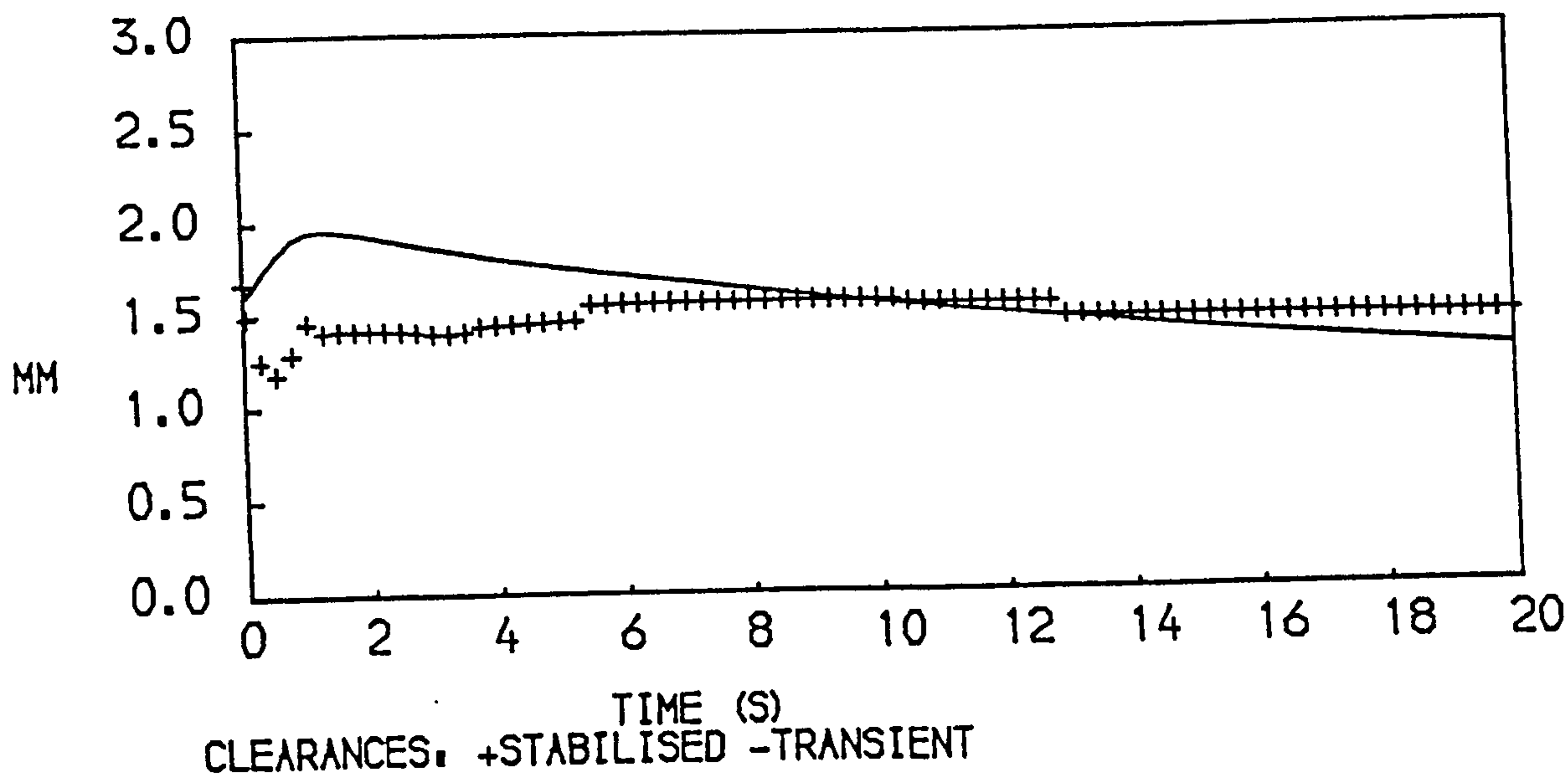


FIG. 98
PERFORMANCE OF THE LOW PRESSURE TURBINE OF A TWO SPOOL
BYPASS ENGINE WITH MIXED EXHAUSTS DURING A DECELERATION
AT SEA LEVEL, STATIC CONDITIONS

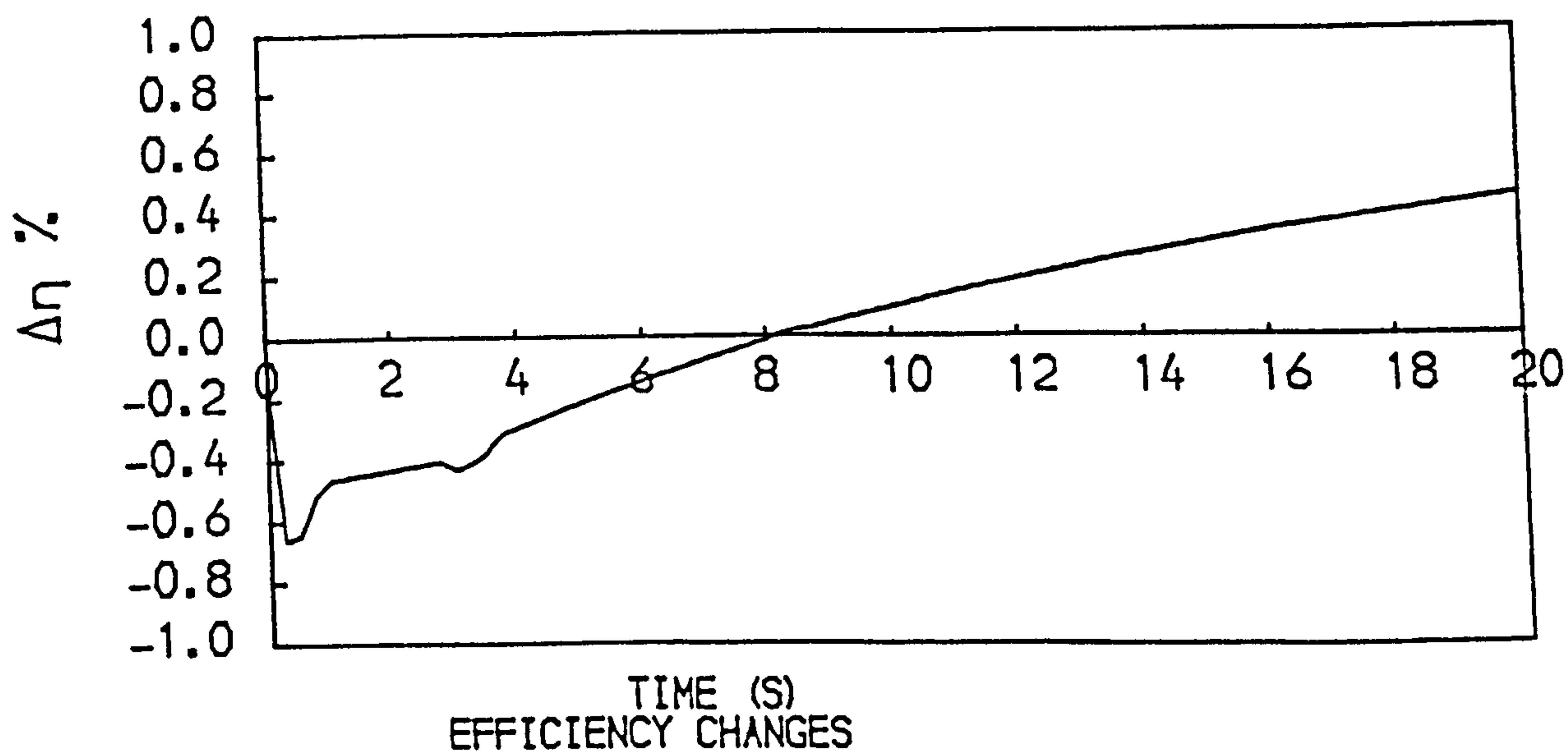
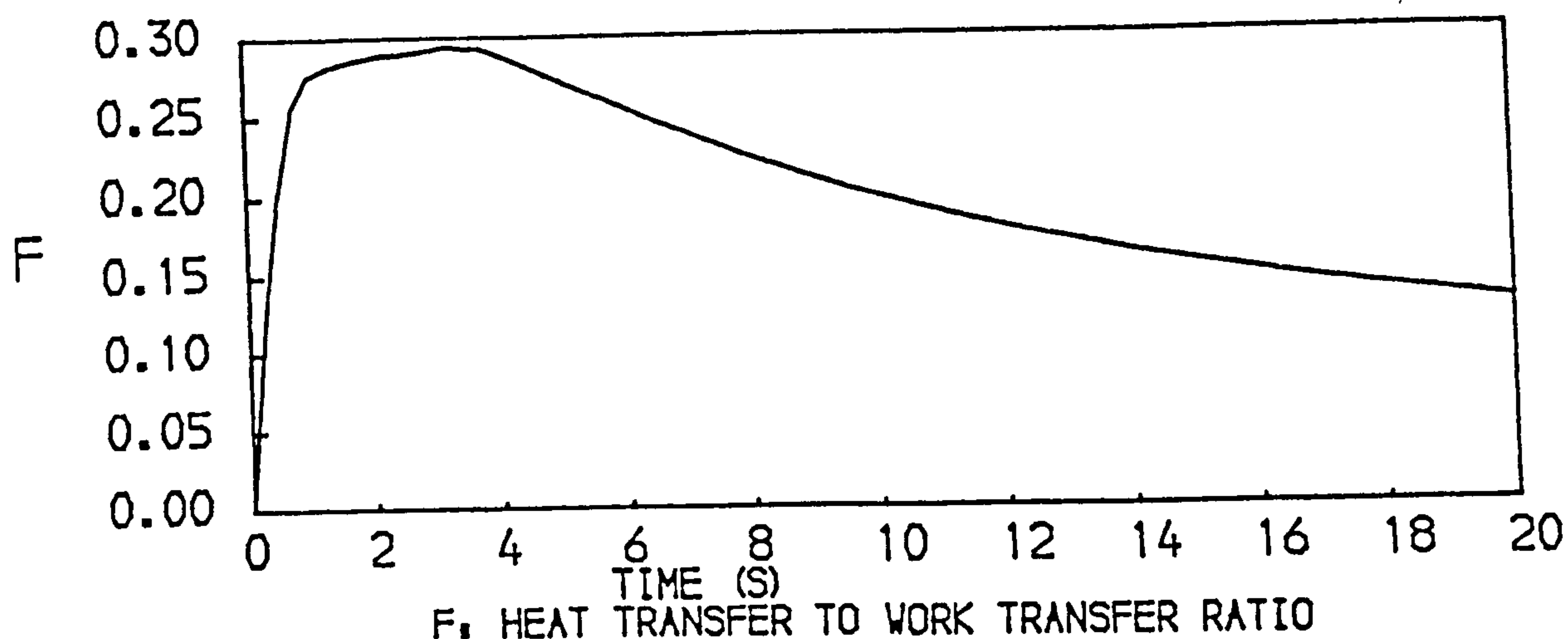
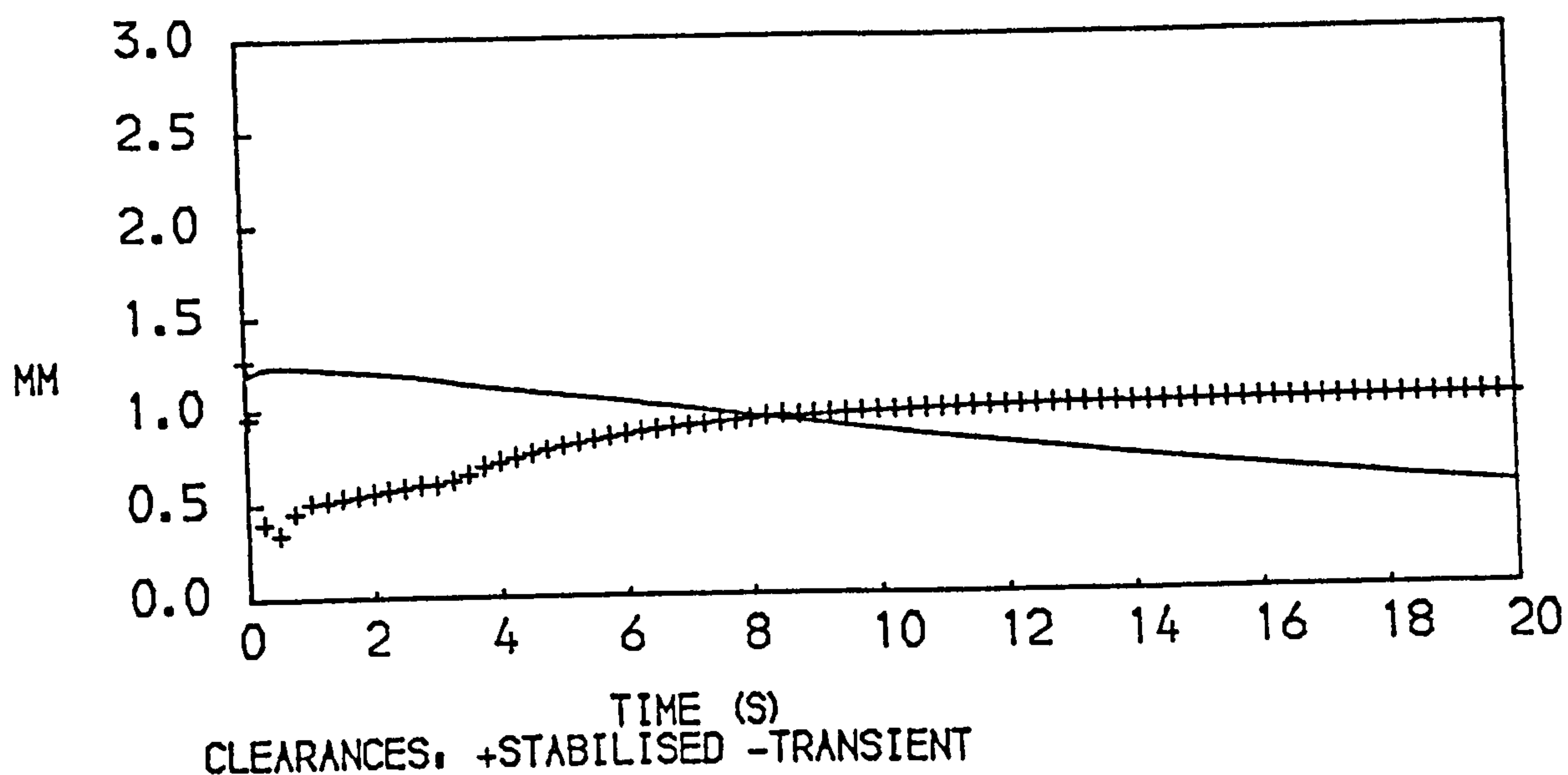


FIG. 99
PERFORMANCE OF THE HIGH PRESSURE TURBINE OF A TWO SPOOL
BYPASS ENGINE WITH MIXED EXHAUSTS DURING A DECELERATION
AT SEA LEVEL, STATIC CONDITIONS

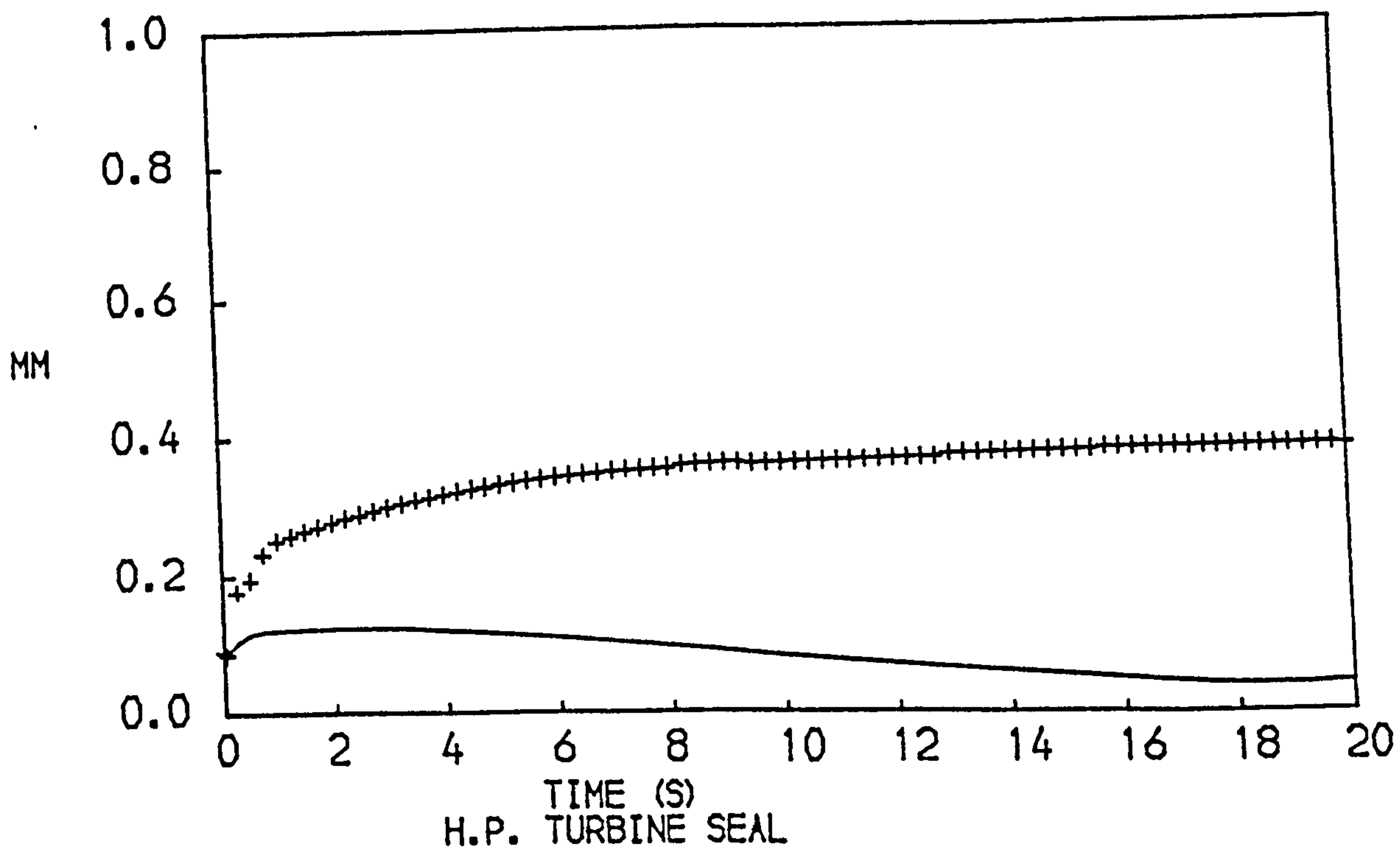
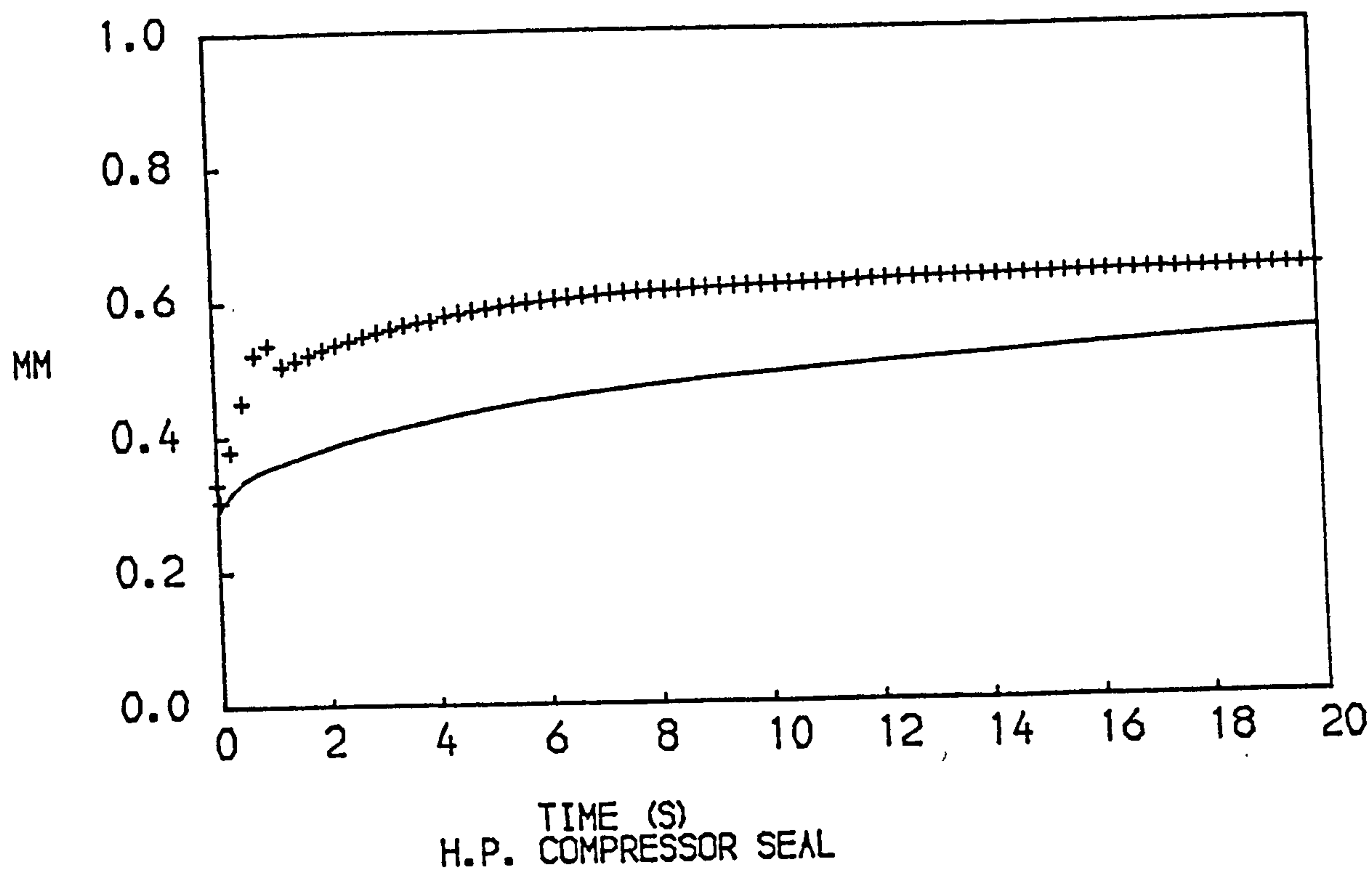


FIG. 100
 PERFORMANCE OF THE TWO COOLING FLOW SEALS OF A TWO SPOOL
 BYPASS ENGINE WITH MIXED EXHAUSTS DURING A DECELERATION
 AT SEA LEVEL, STATIC CONDITIONS
 CLEARANCES +STEADY RUNNING —TRANSIENT

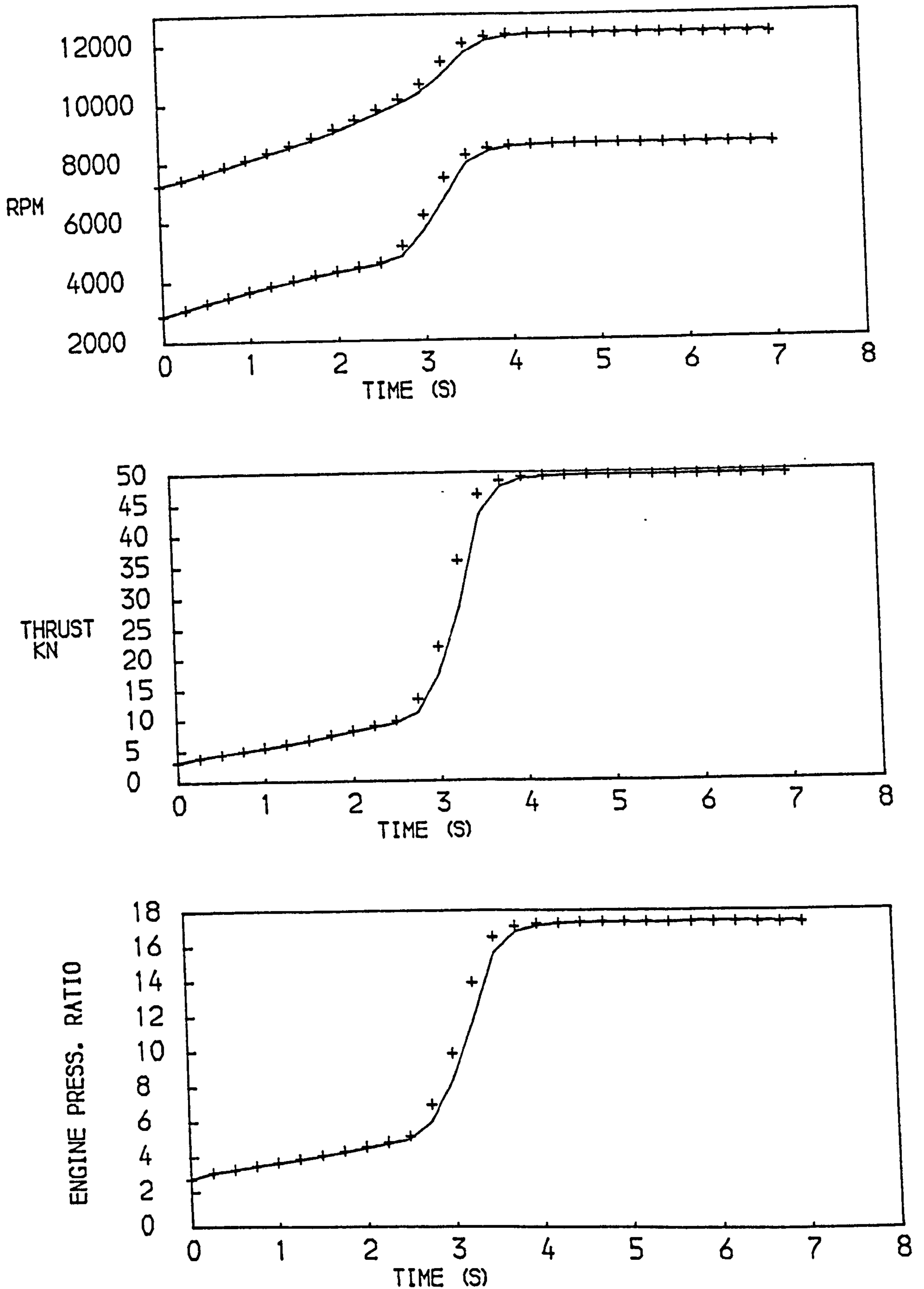


FIG. 101
EFFECT OF NON-DESIGN TRANSIENT BLADE TIP CLEARANCES ON THE PREDICTED PERFORMANCE OF A TWO SPOOL BYPASS ENGINE WITH MIXED EXHAUSTS DURING AN ACCELERATION AT SEA LEVEL, STATIC CONDITIONS
NON DIMENSIONAL FUEL FLOW SCHEDULED ON H.P. COMPRESSOR PRESSURE RATIO
—ADIABATIC +ALL COMPONENTS

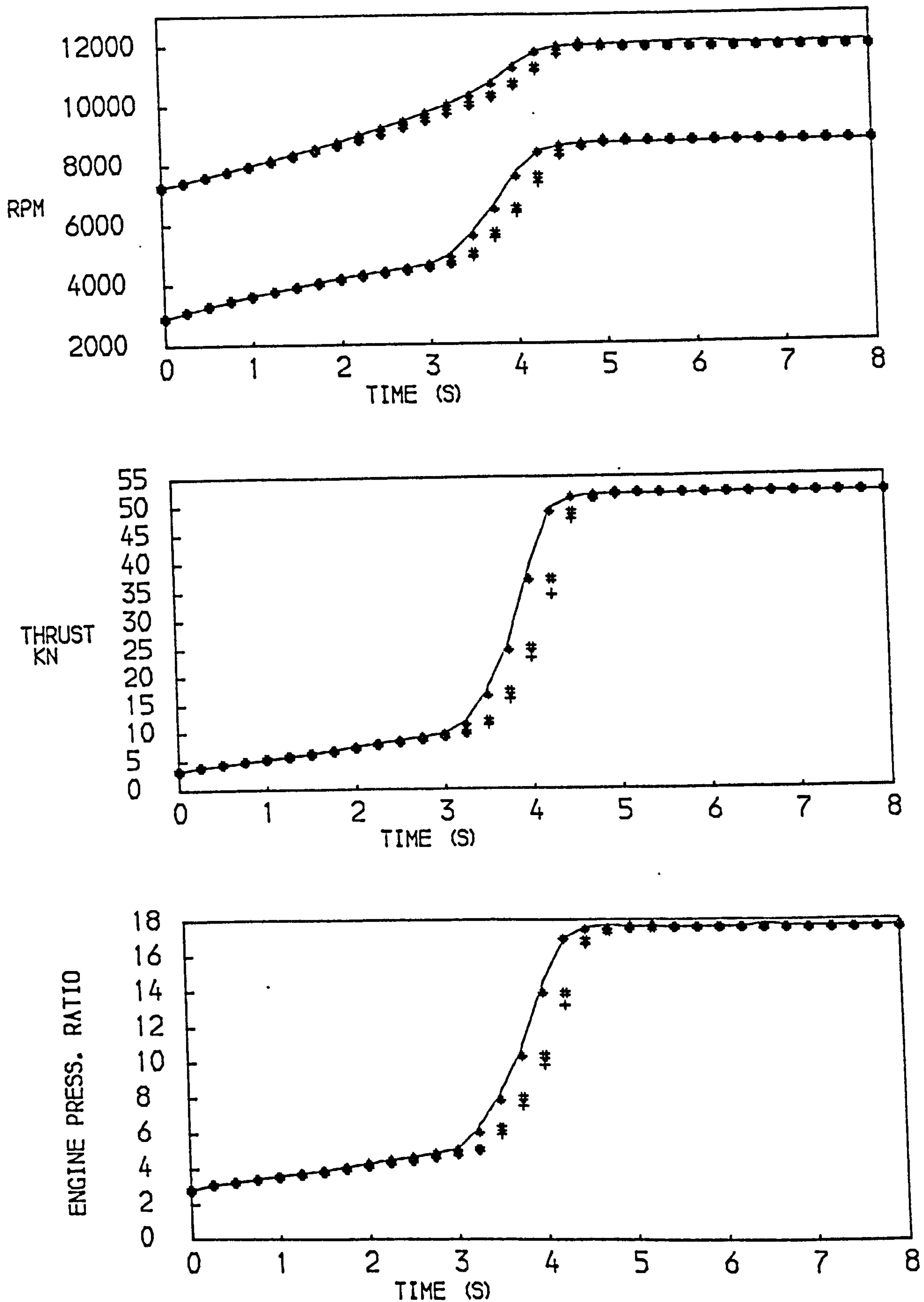


FIG. 102
EFFECTS OF NON-DESIGN TRANSIENT SEAL CLEARANCES ON THE PREDICTED
PERFORMANCE OF A TWO SPOOL BYPASS ENGINE WITH MIXED EXHAUSTS
DURING AN ACCELERATION AT SEA LEVEL, STATIC CONDITIONS
NON DIMENSIONAL FUEL FLOW SCHEDULED ON H.P. COMPRESSOR PRESSURE RATIO
—NO SEAL EFFECTS ♦H.P.C. SEAL *H.P.T. SEAL +TWO SEALS

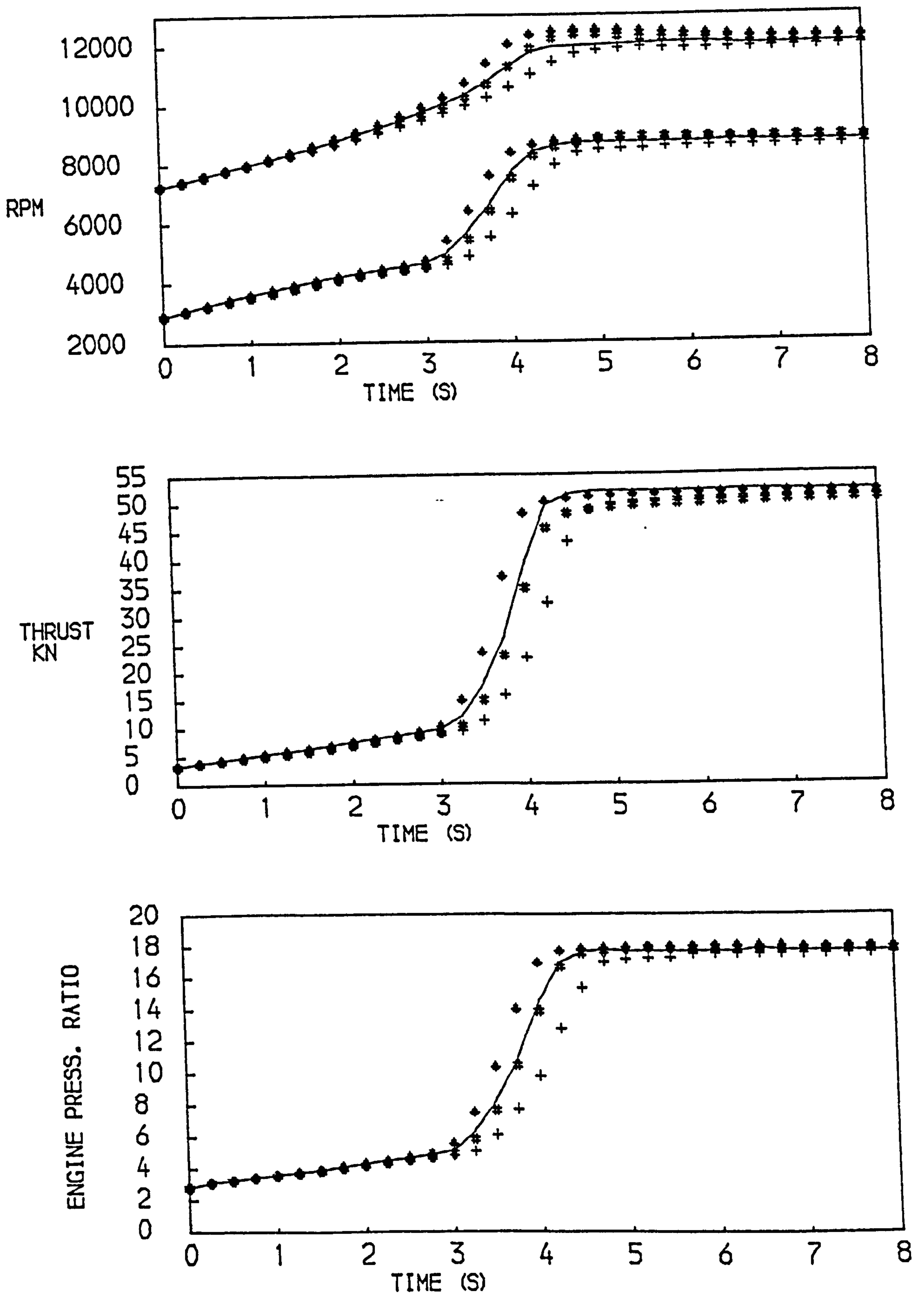


FIG. 103
 EFFECT OF THE HEAT CAPACITIES OF THE COMPONENTS ON THE PREDICTED
 PERFORMANCE OF A TWO SPOOL BYPASS ENGINE WITH MIXED EXHAUSTS
 DURING AN ACCELERATION AT SEA LEVEL, STATIC CONDITIONS
 NON DIMENSIONAL FUEL FLOW SCHEDULED ON H.P. COMPRESSOR PRESSURE RATIO
 —ADIABATIC ♦H.P.COMPRESSOR +H.P.TURBINE *ALL HEAT CAPACITIES

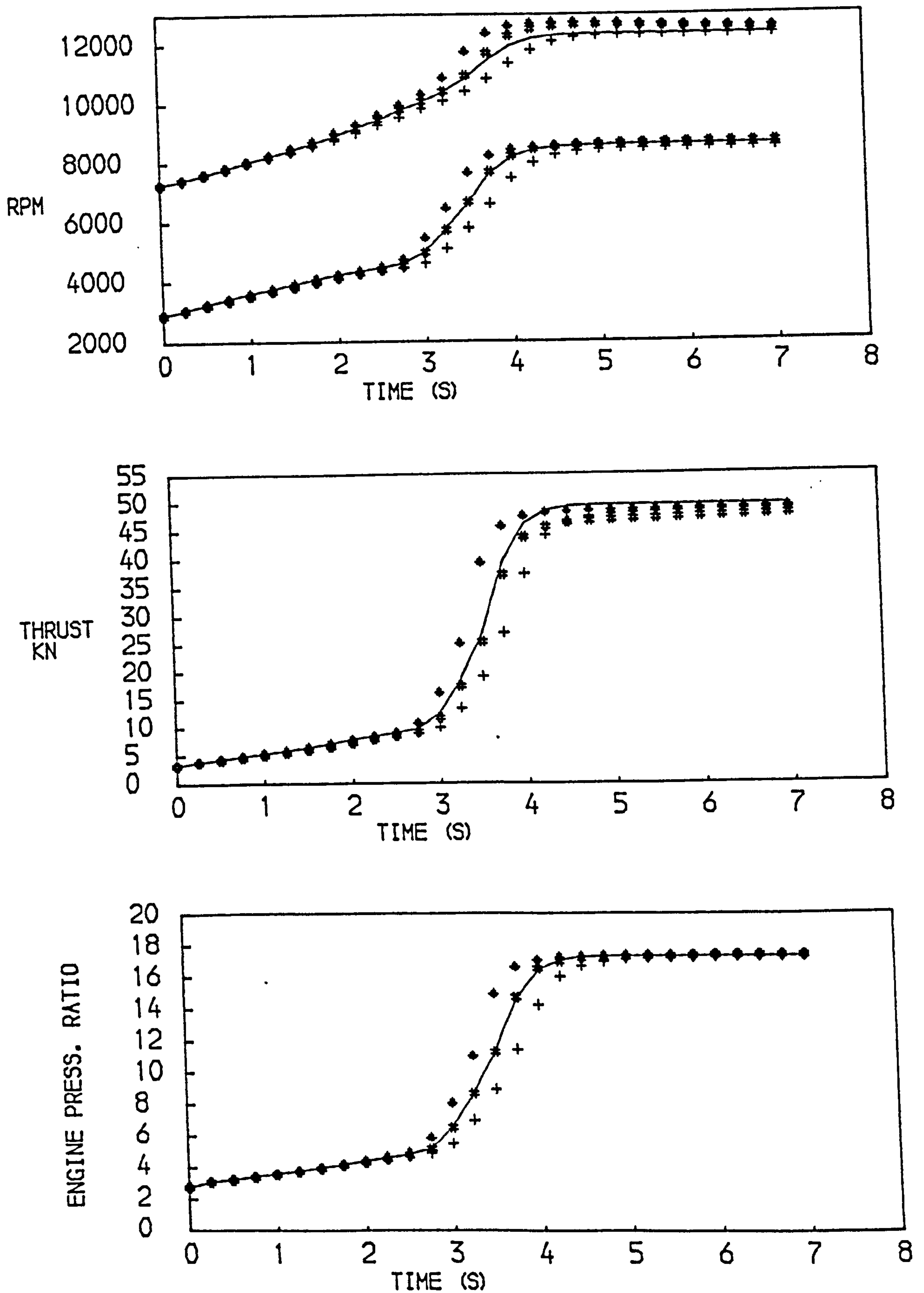


FIG. 104
 EFFECT OF THE HEAT CAPACITIES OF THE COMPONENTS ON THE PREDICTED
 PERFORMANCE OF A TWO SPOOL BYPASS ENGINE WITH MIXED EXHAUSTS
 DURING AN ACCELERATION AT SEA LEVEL, STATIC CONDITIONS
 FUEL FLOW SCHEDULED ON H.P. SPOOL ROTATIONAL SPEED
 —ADIABATIC ♦H.P.COMPRESSOR +H.P.TURBINE *ALL HEAT CAPACITIES

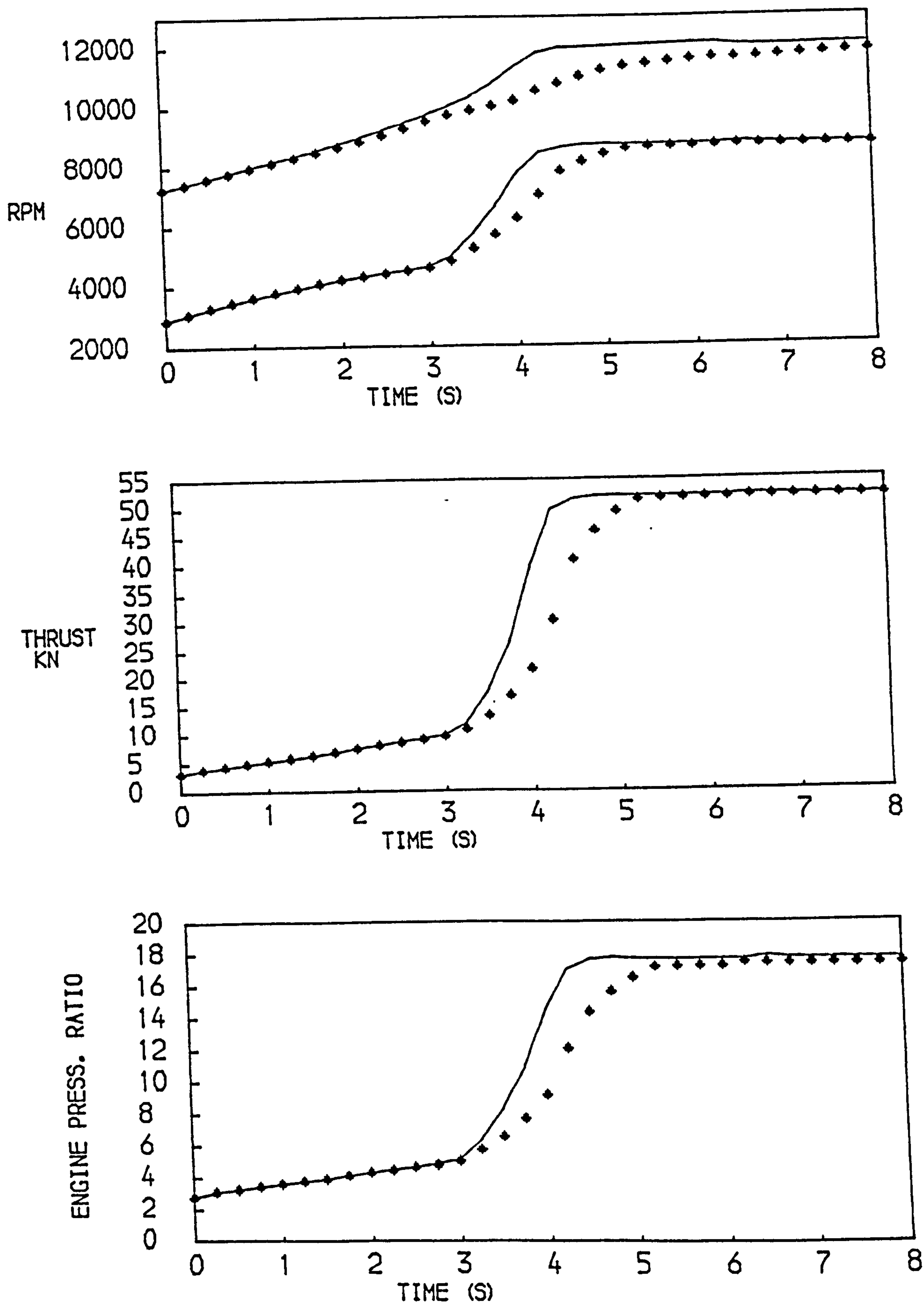


FIG. 105
 EFFECTS OF COMPRESSOR CHARACTERISTIC CHANGES ON THE PREDICTED
 PERFORMANCE OF A TWO SPOOL BYPASS ENGINE WITH MIXED EXHAUSTS
 DURING AN ACCELERATION AT SEA LEVEL, STATIC CONDITIONS
 NON DIMENSIONAL FUEL FLOW SCHEDULED ON H.P. COMPRESSOR PRESSURE RATIO
 —ADIABATIC +CHANGES IN H.P. COMPRESSOR CHARACTERISTICS

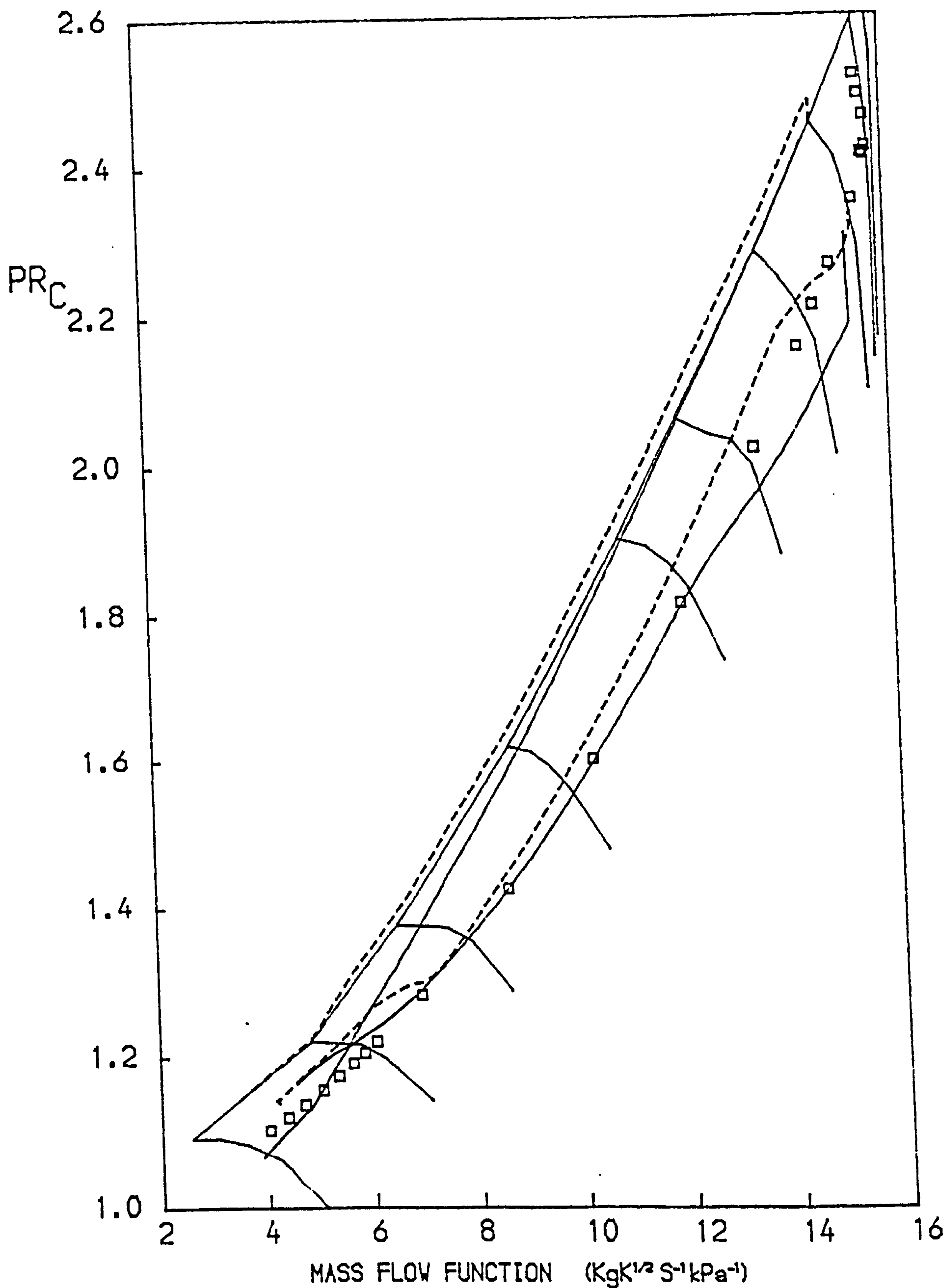


FIG. 106

PATHS ON THE CHARACTERISTIC MAPS OF THE L.P. COMPRESSOR OF A
TWO SPOOL BYPASS ENGINE WITH MIXED EXHAUSTS
MOVEMENTS OF THE SURGE LINE DURING TRANSIENTS
-- ACCELERATION — DECELERATION
□ STEADY RUNNING TEST BED DATA

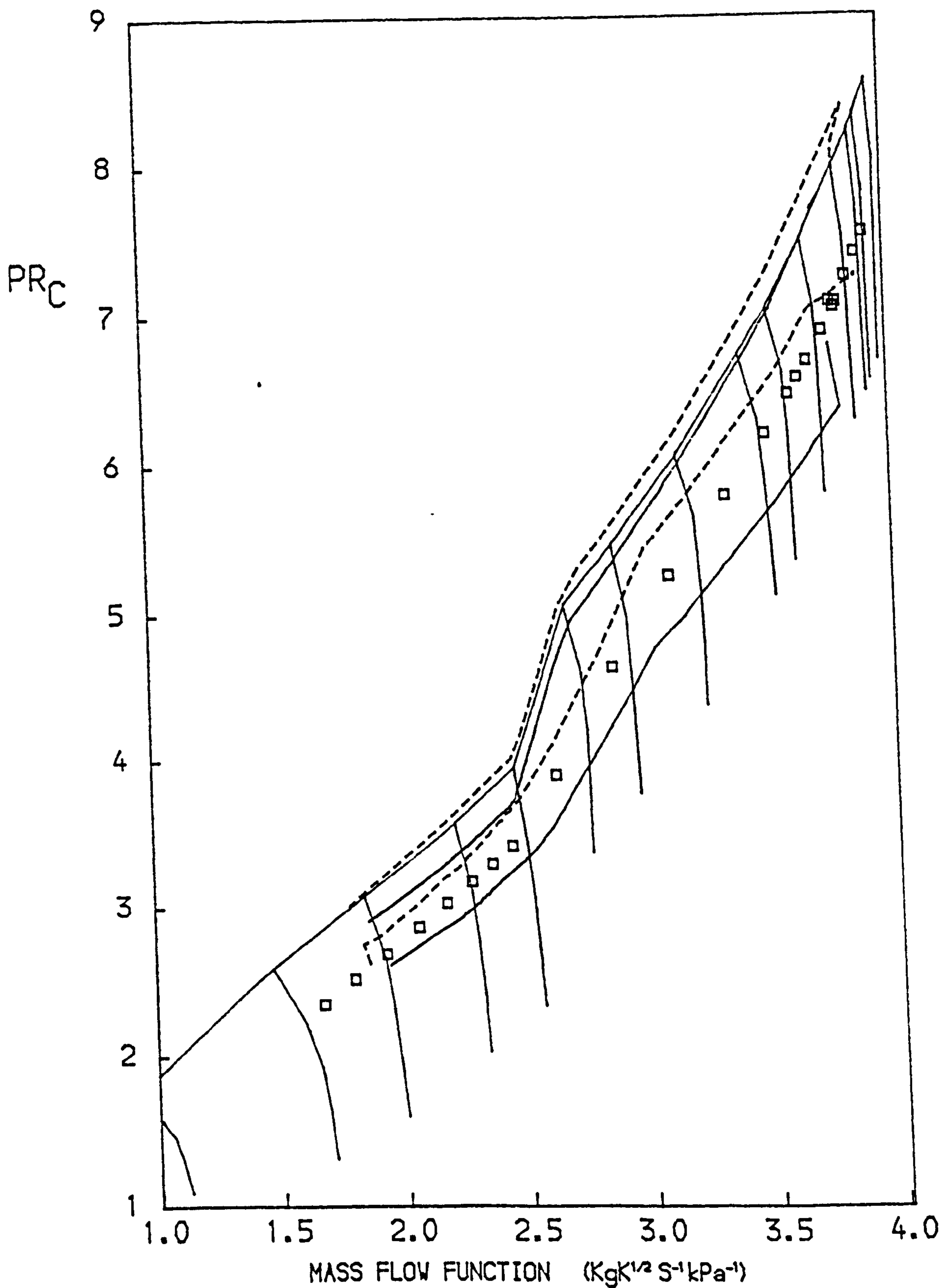


FIG. 107

PATHS ON THE CHARACTERISTIC MAPS OF THE H.P. COMPRESSOR OF A
TWO SPOOL BYPASS ENGINE WITH MIXED EXHAUSTS
MOVEMENTS OF THE SURGE LINE DURING TRANSIENTS
-- ACCELERATION — DECELERATION
□ STEADY RUNNING TEST BED DATA

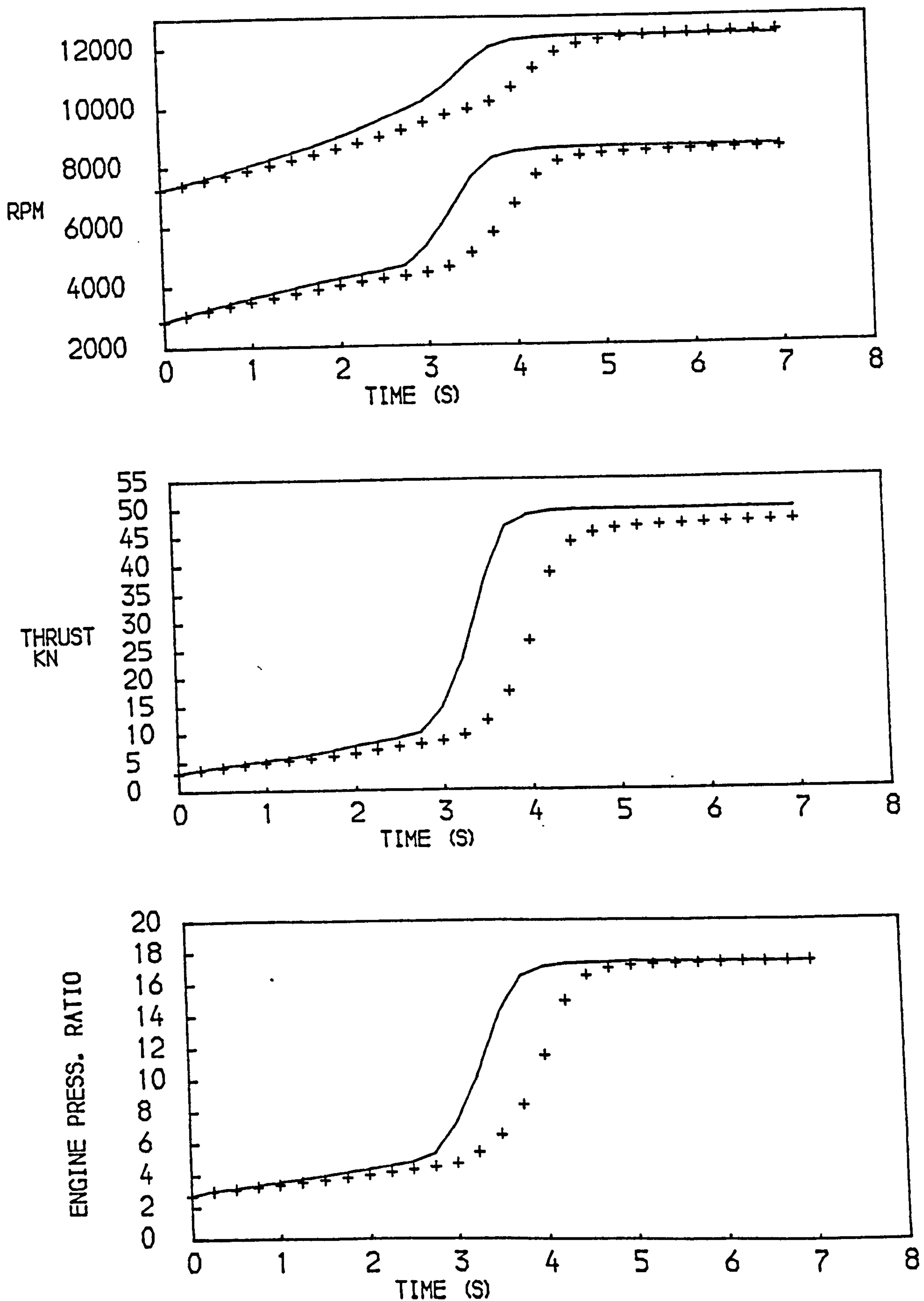


FIG. 108
 CLEARANCE MOVEMENTS AND HEAT TRANSFER AFFECTING THE PREDICTED
 PERFORMANCE OF A TWO SPOOL BYPASS ENGINE WITH MIXED EXHAUSTS
 DURING AN ACCELERATION AT SEA LEVEL, STATIC CONDITIONS
 NON DIMENSIONAL FUEL FLOW SCHEDULED ON H.P. COMPRESSOR PRESSURE RATIO
 —ADIABATIC +ALL HEAT TRANSFER EFFECTS

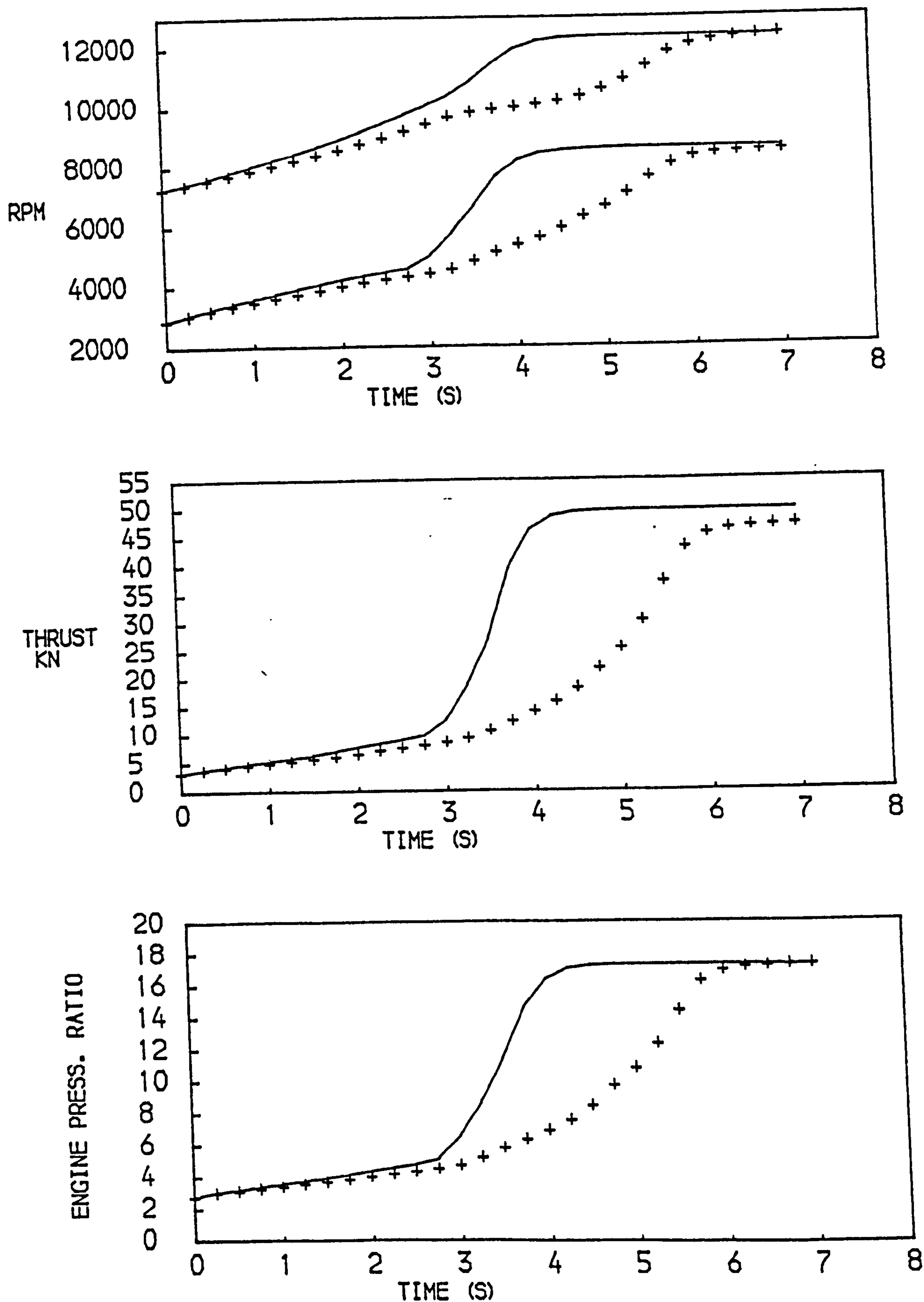


FIG. 109
 CLEARANCE MOVEMENTS AND HEAT TRANSFER AFFECTING THE PREDICTED
 PERFORMANCE OF A TWO SPOOL BYPASS ENGINE WITH MIXED EXHAUSTS
 DURING AN ACCELERATION AT SEA LEVEL, STATIC CONDITIONS
 FUEL FLOW SCHEDULED ON H.P. SPOOL ROTATIONAL SPEED
 —ADIABATIC +ALL HEAT TRANSFER EFFECTS

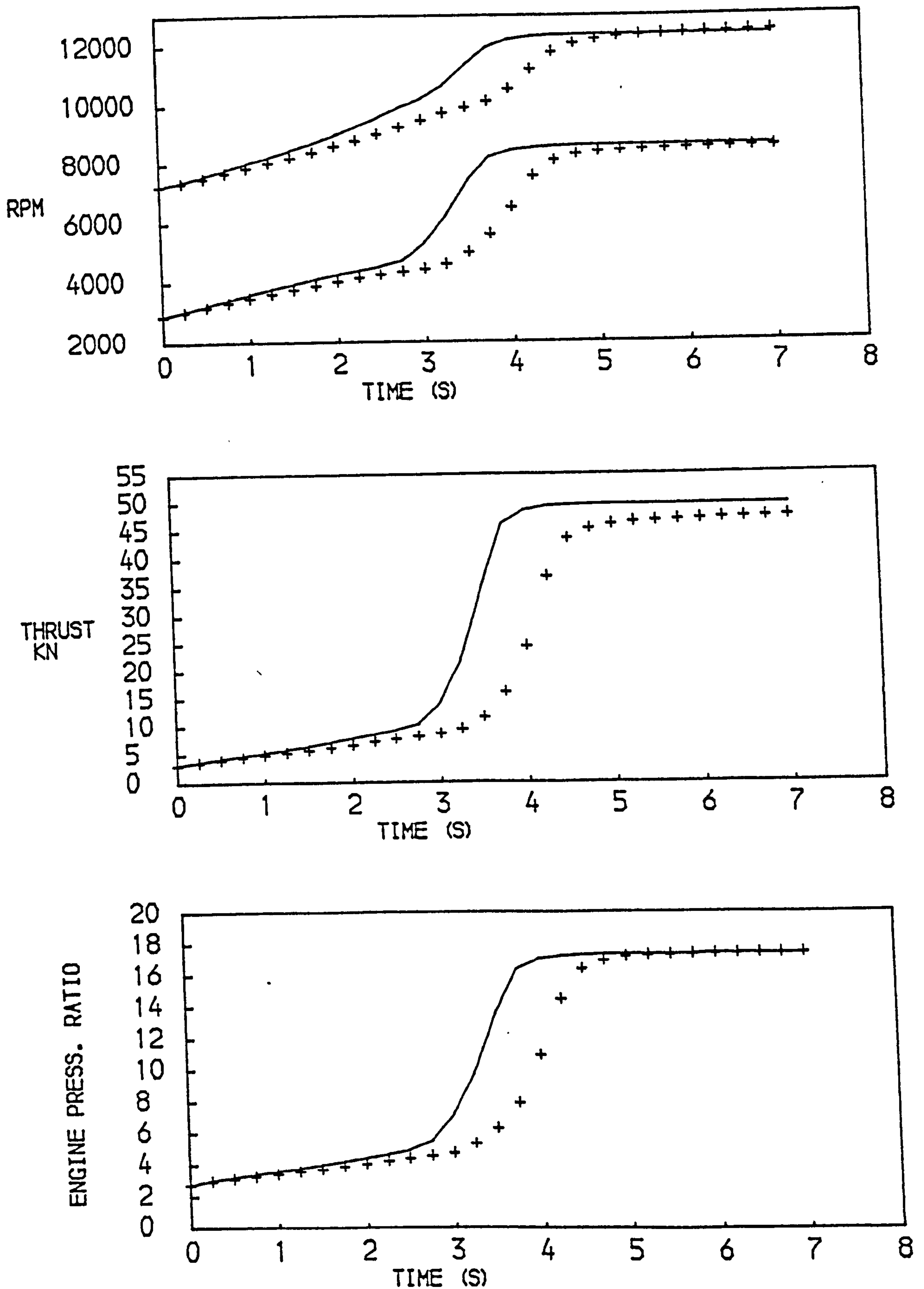


FIG. 110
 CLEARANCE MOVEMENTS AND HEAT TRANSFER AFFECTING THE PREDICTED
 PERFORMANCE OF A TWO SPOOL BYPASS ENGINE WITH MIXED EXHAUSTS
 DURING AN ACCELERATION AT SEA LEVEL, STATIC CONDITIONS
 FUEL FLOW SCHEDULED ON L.P. SPOOL ROTATIONAL SPEED
 —ADIABATIC +ALL HEAT TRANSFER EFFECTS

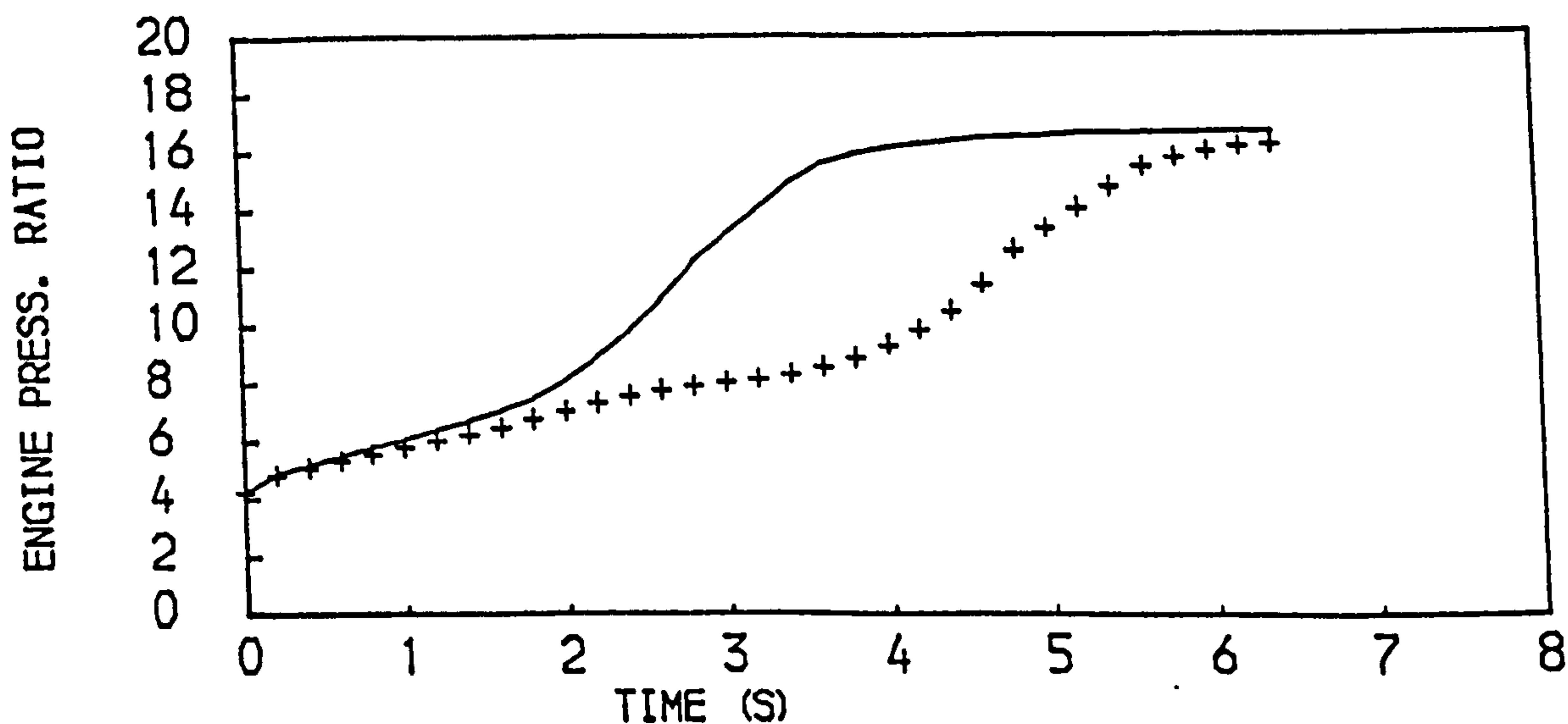
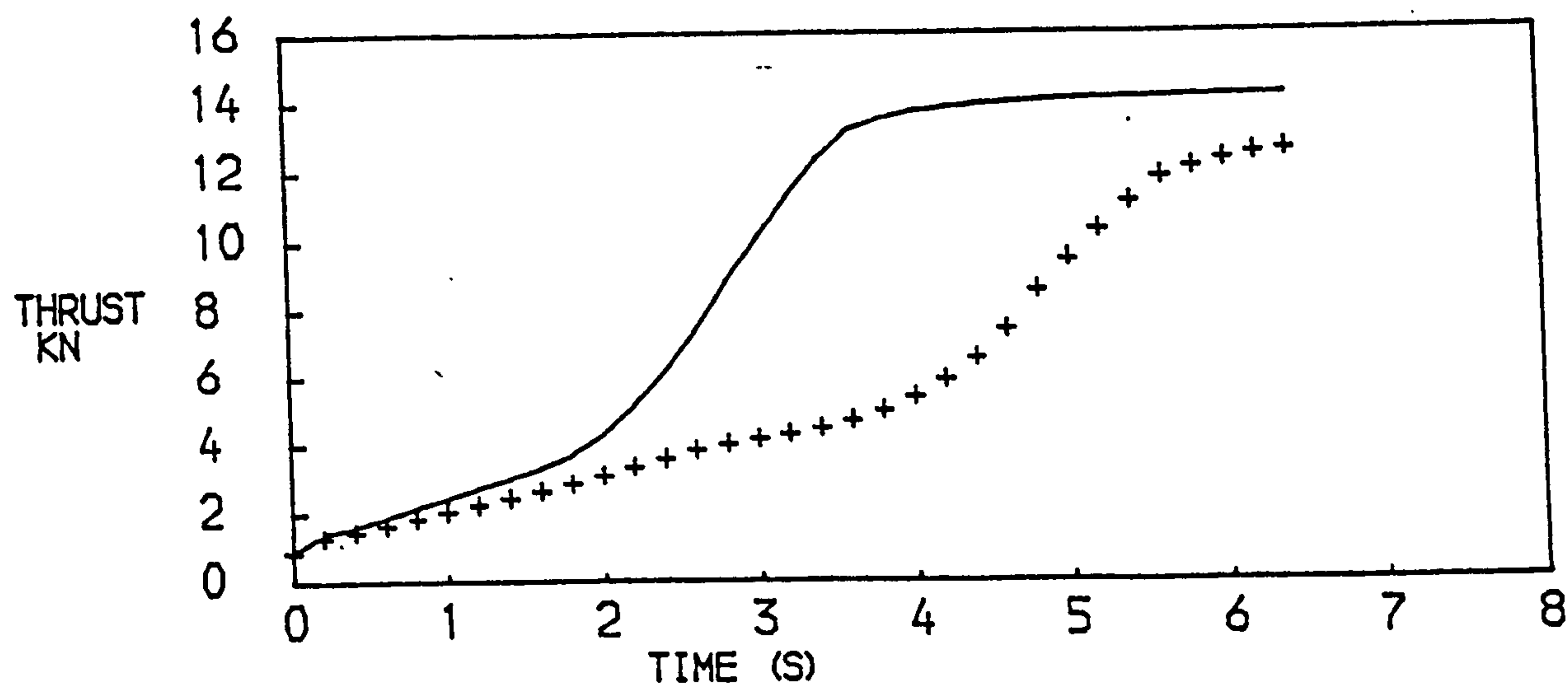
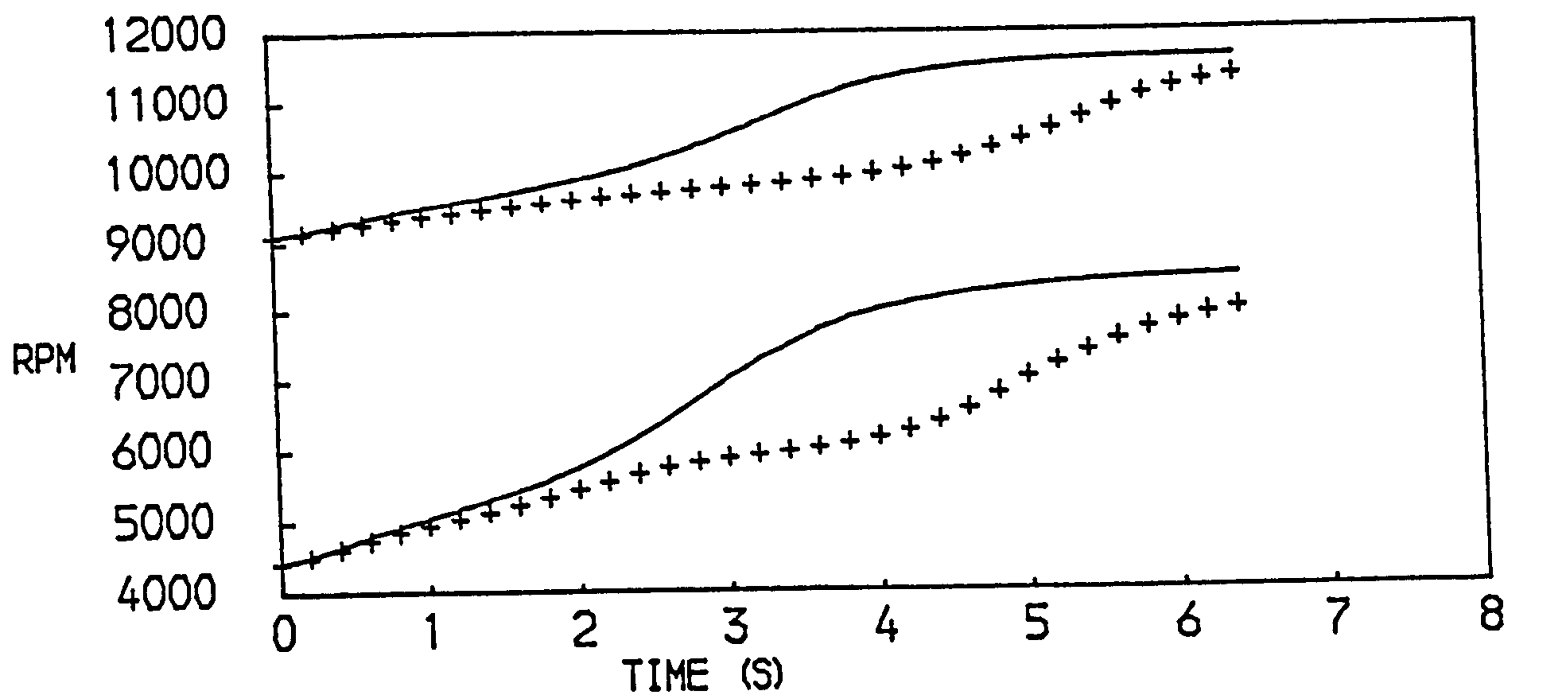


FIG. 111
 CLEARANCE MOVEMENTS AND HEAT TRANSFER AFFECTING THE PREDICTED
 PERFORMANCE OF A TWO SPOOL BYPASS ENGINE WITH MIXED EXHAUSTS
 DURING AN ACCELERATION AT AN ALTITUDE OF 9150 M, $M = 0.8$
 NON DIMENSIONAL FUEL FLOW SCHEDULED ON H.P. COMPRESSOR PRESSURE RATIO
 —ADIABATIC +ALL HEAT TRANSFER EFFECTS

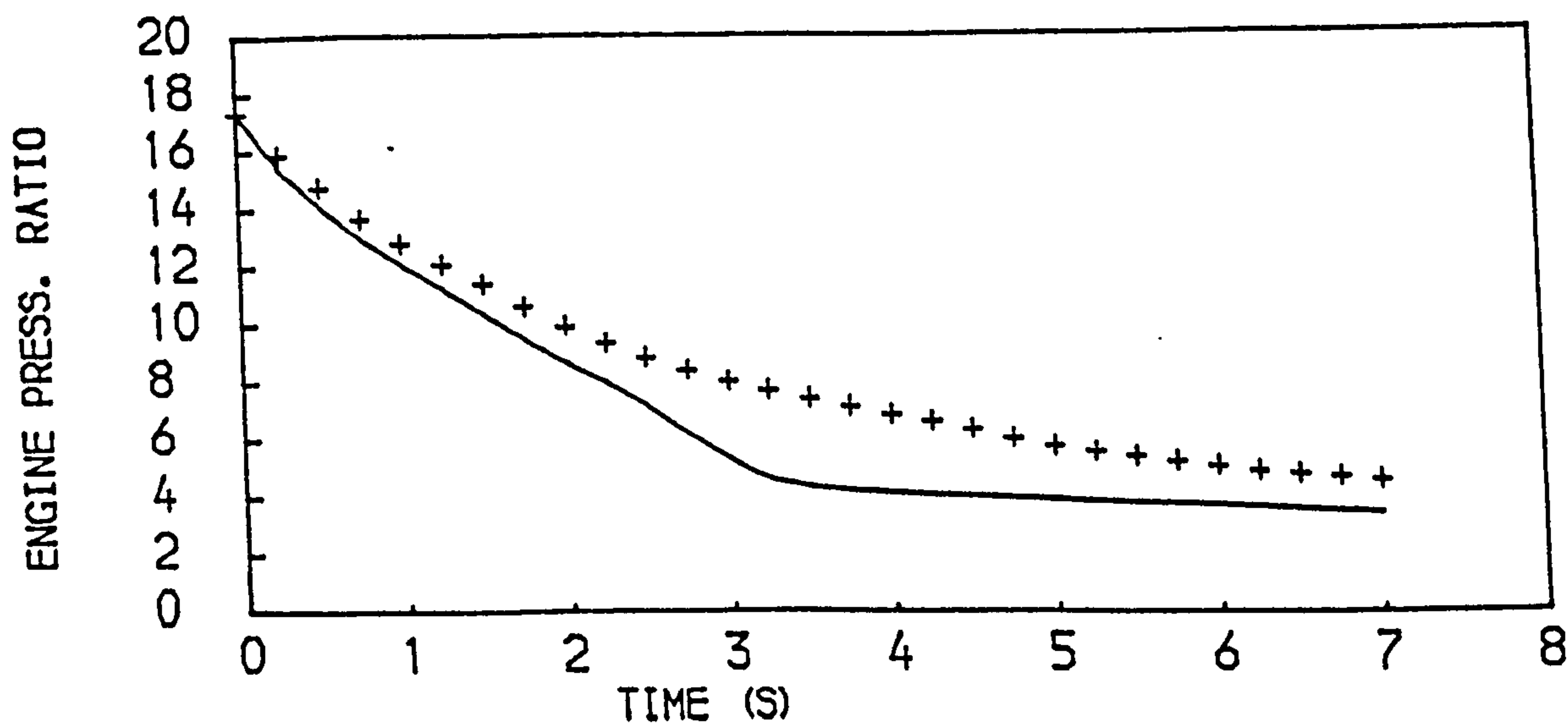
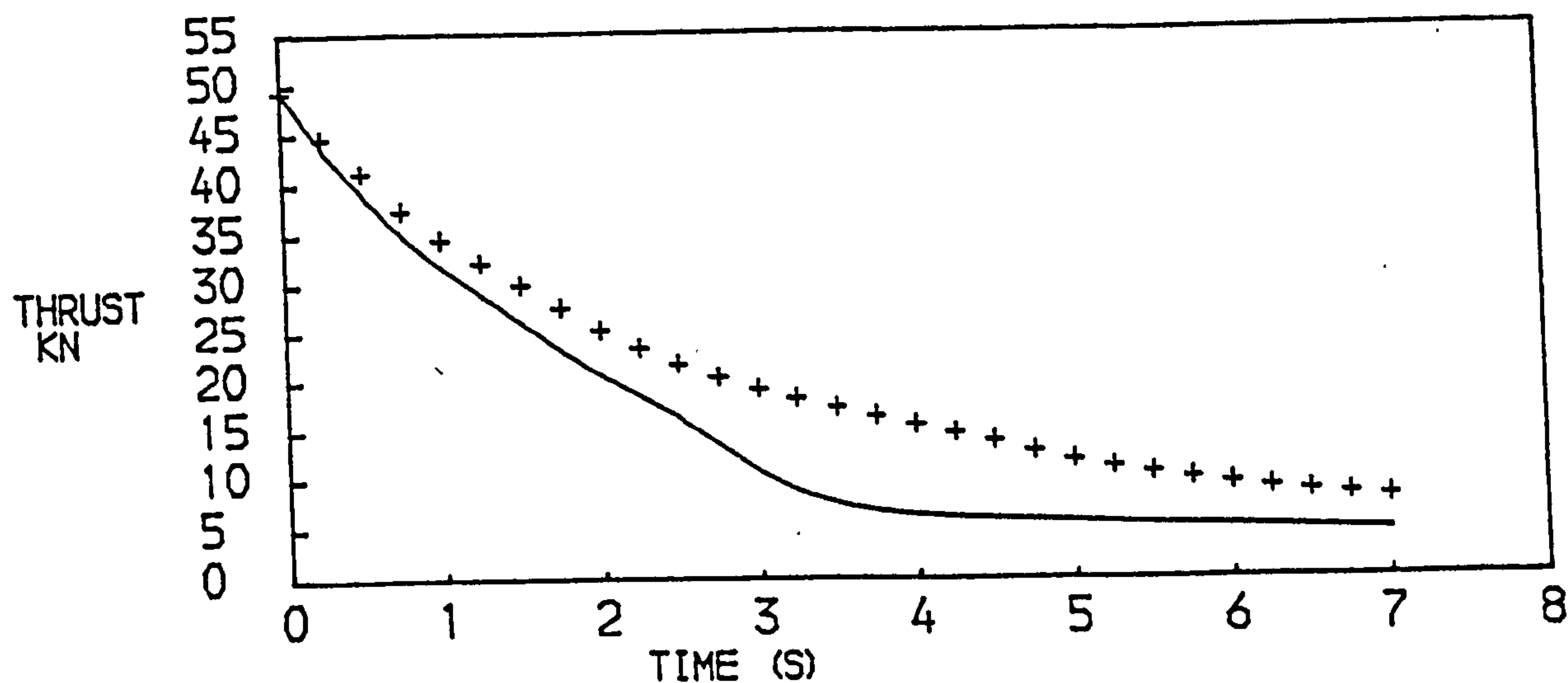
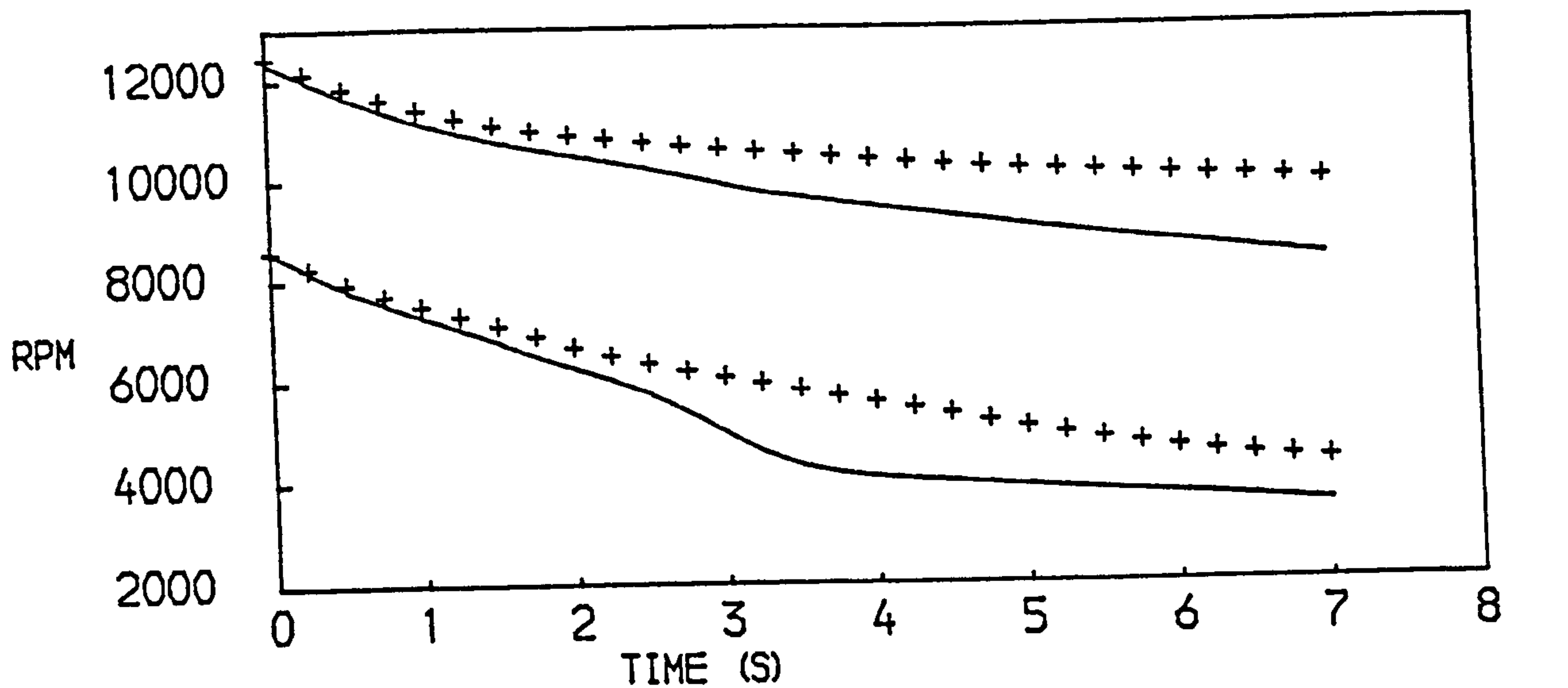


FIG. 112
 CLEARANCE MOVEMENTS AND HEAT TRANSFER AFFECTING THE PREDICTED
 PERFORMANCE OF A TWO SPOOL BYPASS ENGINE WITH MIXED EXHAUSTS
 DURING A DECELERATION AT SEA LEVEL, STATIC CONDITIONS
 NON DIMENSIONAL FUEL FLOW SCHEDULED ON H.P. COMPRESSOR PRESSURE RATIO
 —ADIABATIC +ALL HEAT TRANSFER EFFECTS

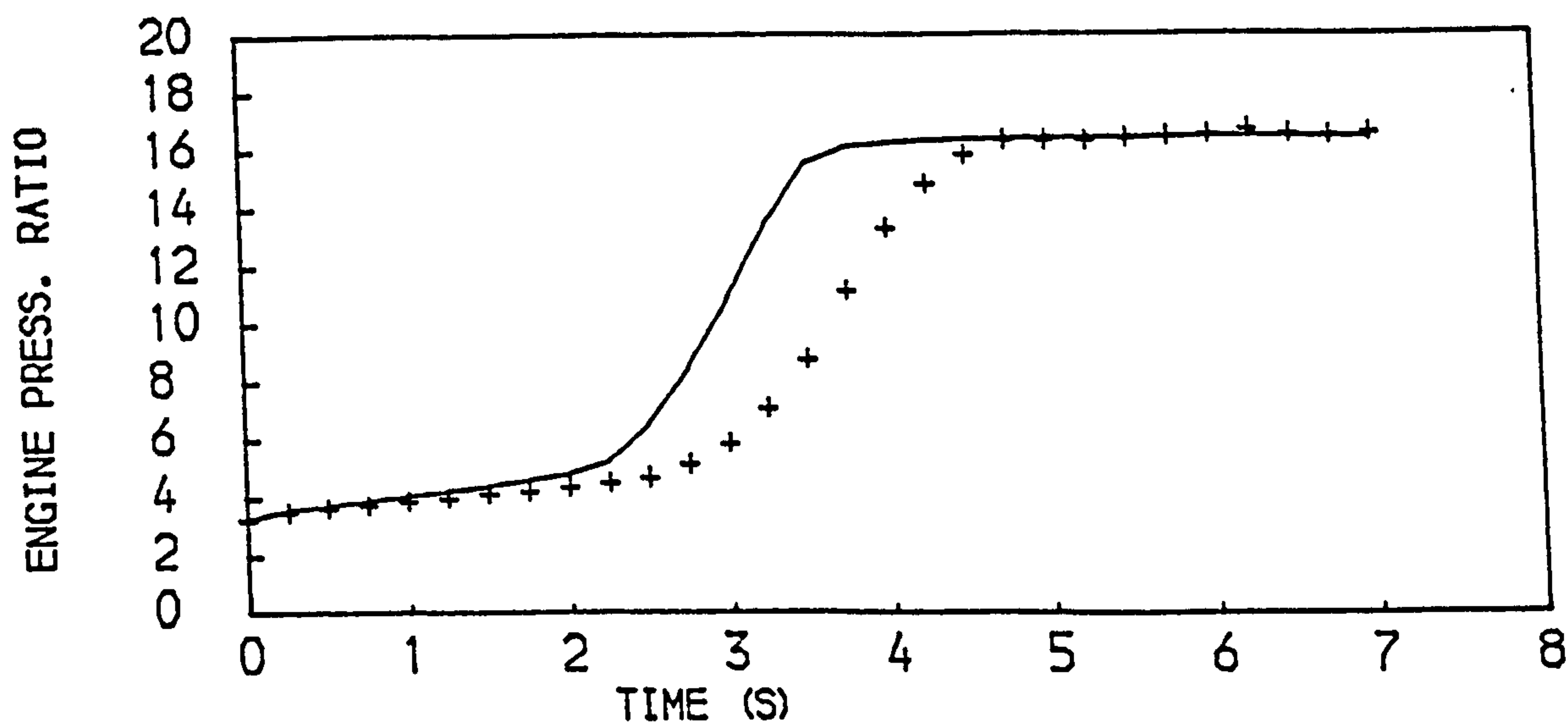
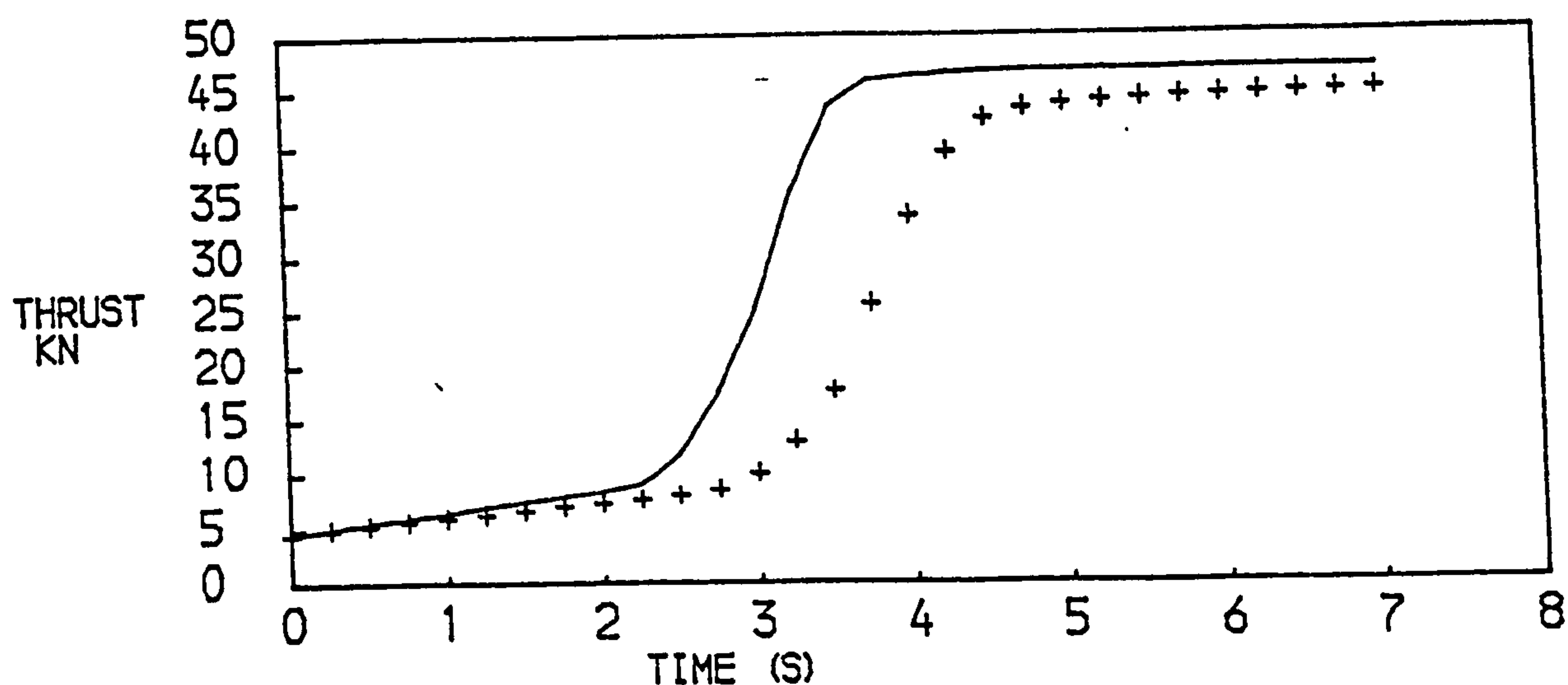
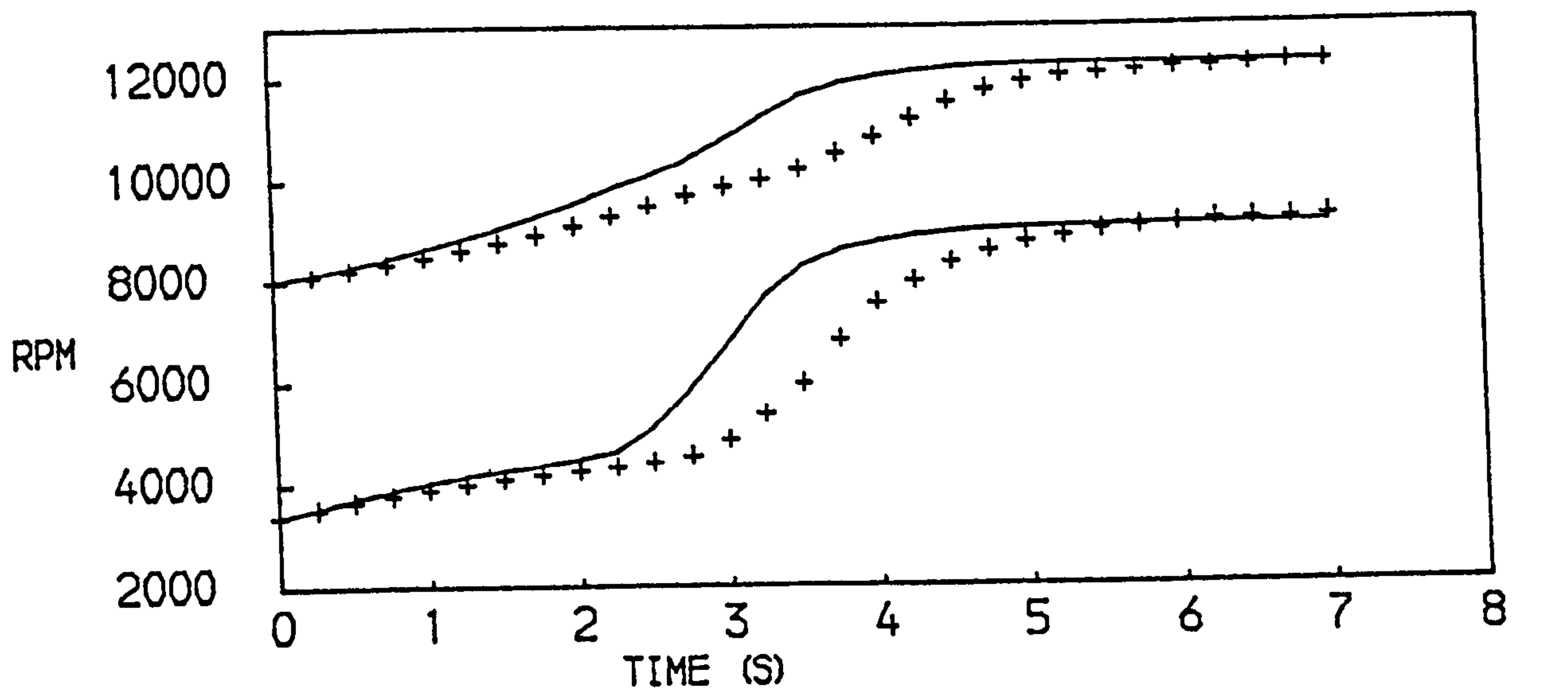


FIG. 113
 CLEARANCE MOVEMENTS AND HEAT TRANSFER AFFECTING THE PREDICTED
 PERFORMANCE OF A TWO SPOOL BYPASS ENGINE WITH SEPARATE EXHAUSTS
 DURING AN ACCELERATION AT SEA LEVEL, STATIC CONDITIONS
 NON DIMENSIONAL FUEL FLOW SCHEDULED ON H.P. COMPRESSOR PRESSURE RATIO
 —ADIABATIC +ALL HEAT TRANSFER EFFECTS

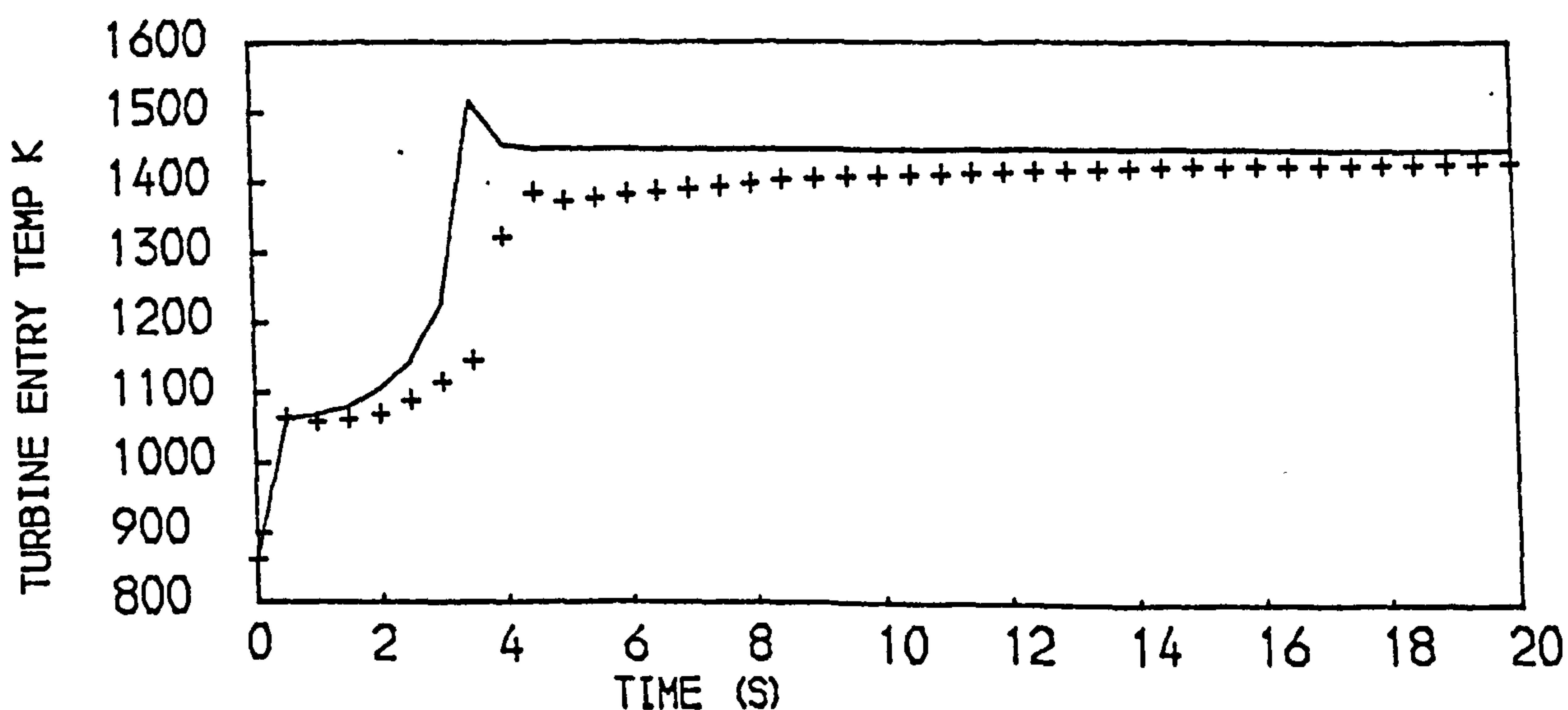
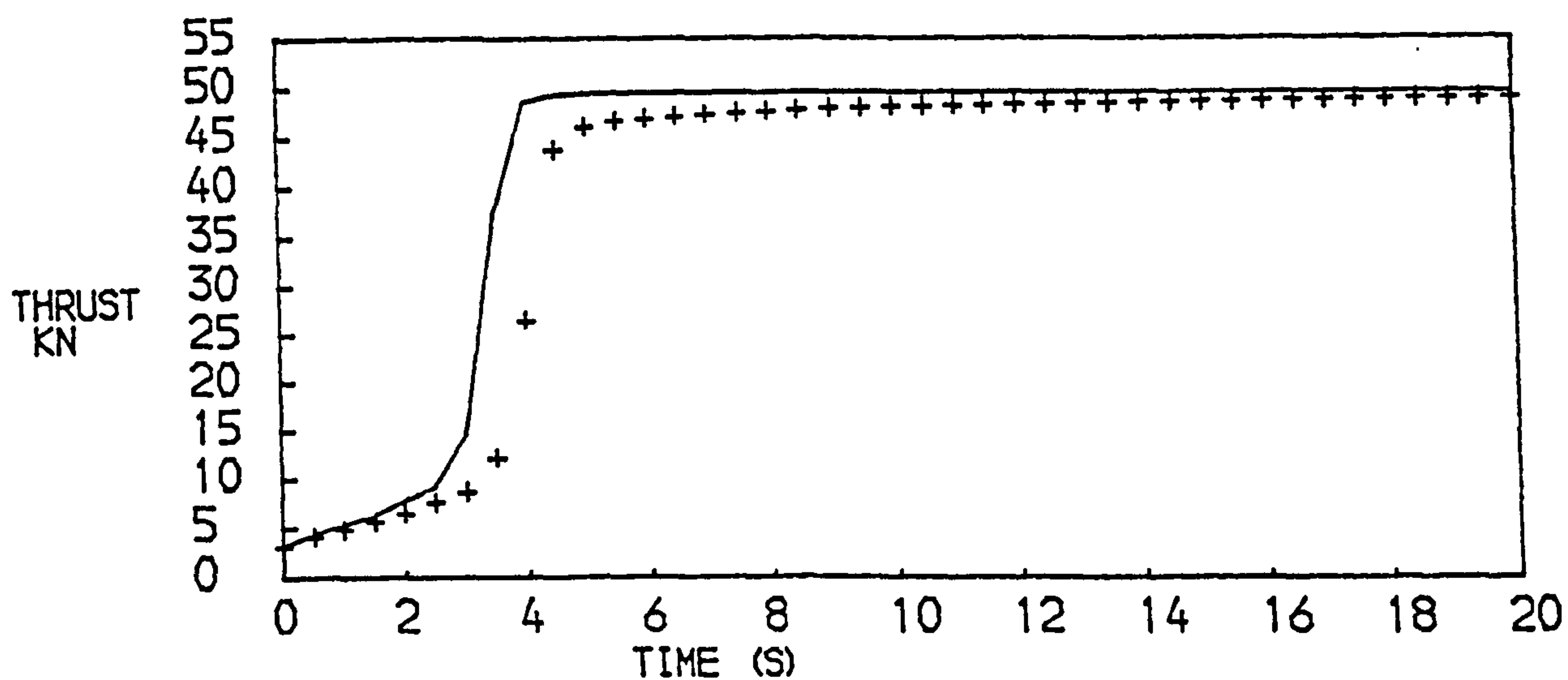
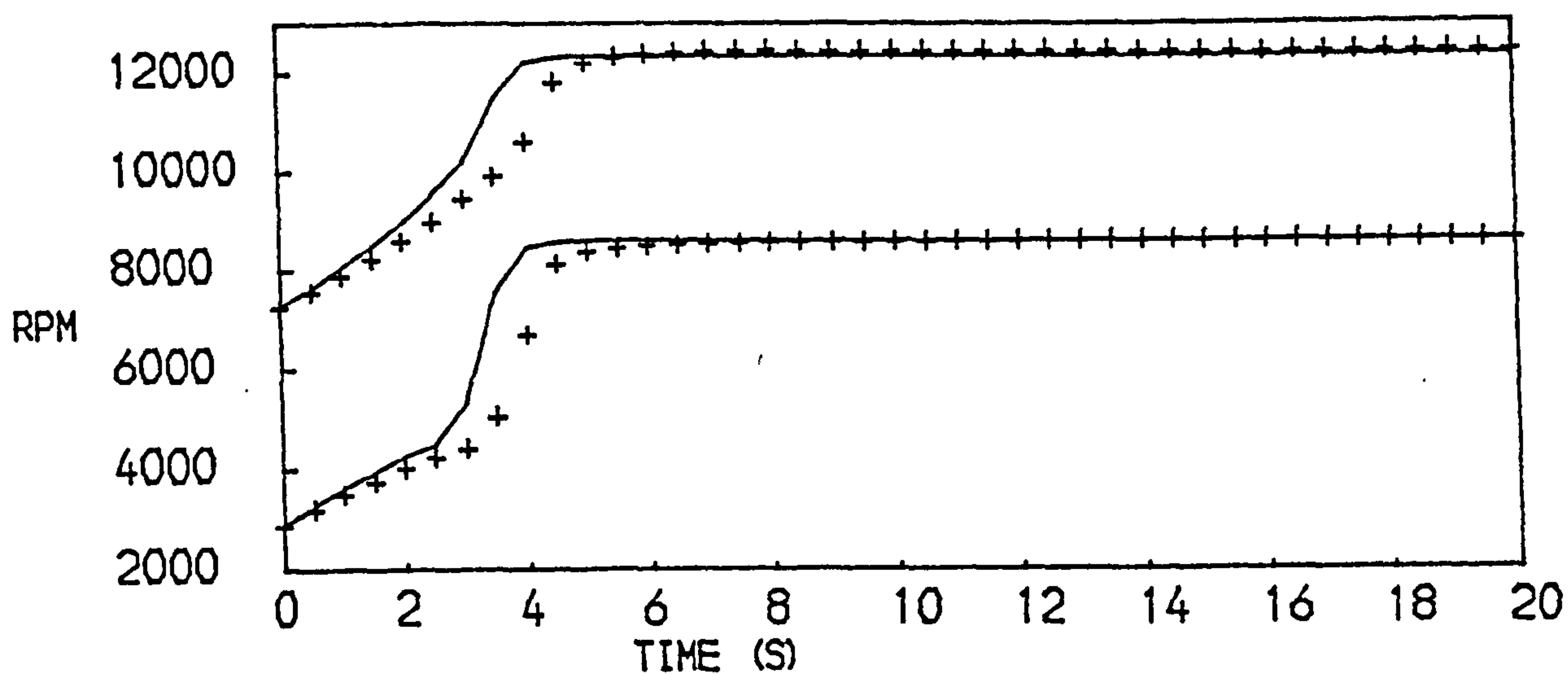


FIG. 114
EFFECTS OF HEAT TRANSFER ON A MEDIUM TERM TRANSIENT OF A
TWO SPOOL BYPASS ENGINE WITH MIXED EXHAUSTS
—ADIABATIC + HEAT TRANSFER EFFECTS

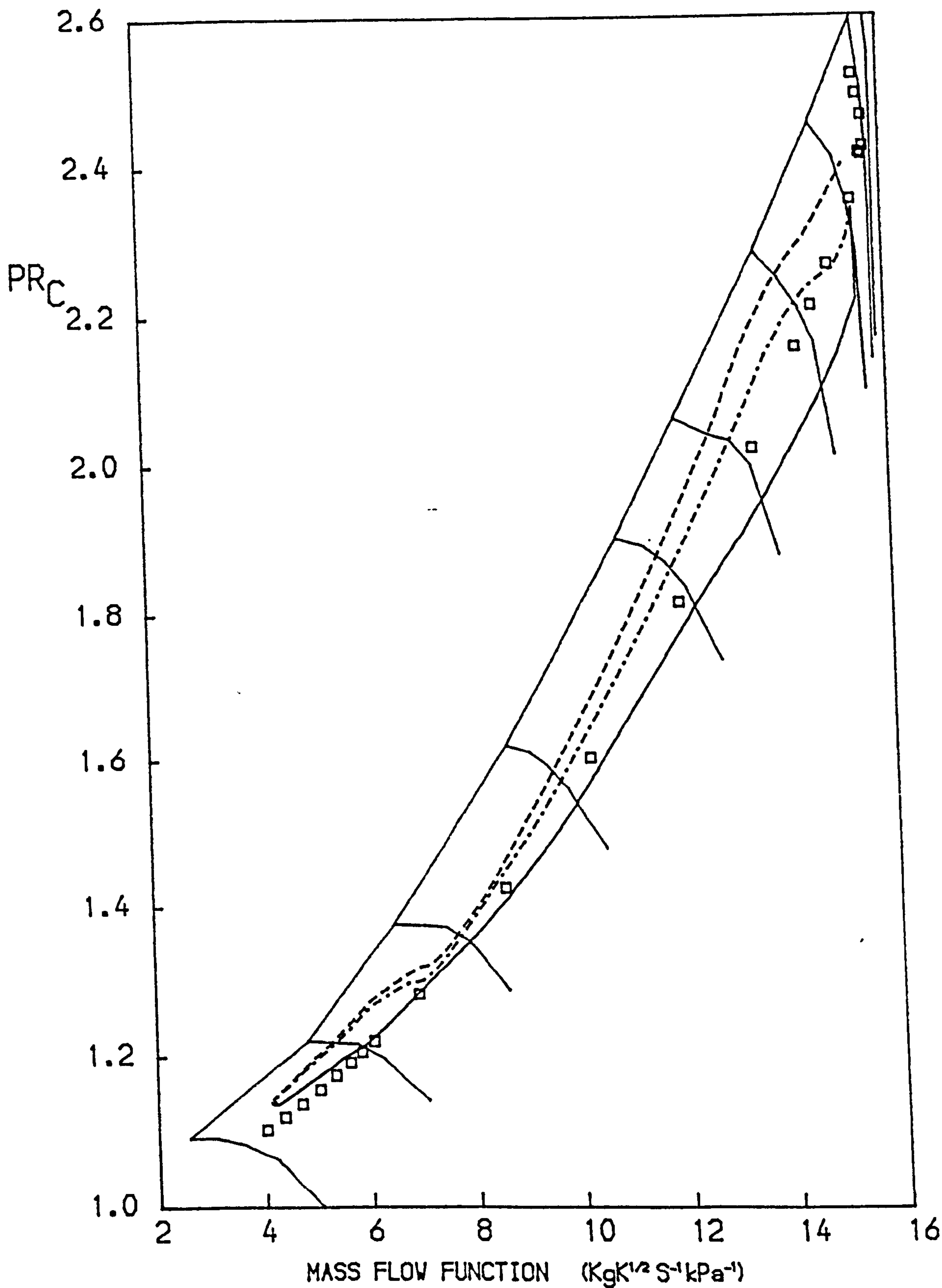


FIG. 115

PATHS ON THE CHARACTERISTIC MAPS OF THE L.P. COMPRESSOR OF A
TWO SPOOL BYPASS ENGINE WITH MIXED EXHAUSTS
MODIFICATION OF TRANSIENT PATH DUE TO HEAT TRANSFER EFFECTS
— ACCELERATION — DECELERATION --- ACCELERATION (HT)
□ STEADY RUNNING TEST BED DATA

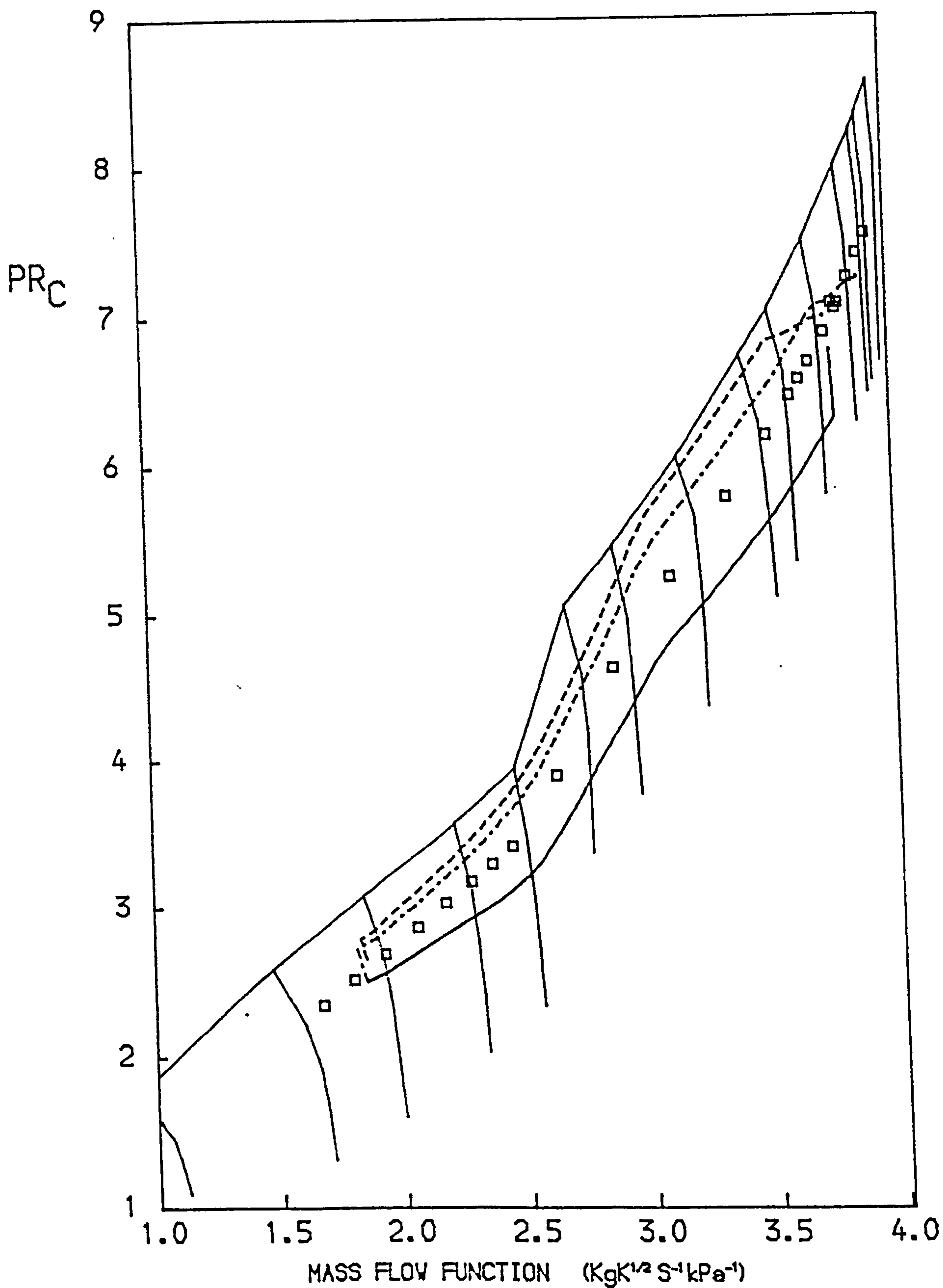


FIG. 116

PATHS ON THE CHARACTERISTIC MAPS OF THE H.P. COMPRESSOR OF A
TWO SPOOL BYPASS ENGINE WITH MIXED EXHAUSTS
MODIFICATION OF TRANSIENT PATH DUE TO HEAT TRANSFER EFFECTS
-- ACCELERATION — DECELERATION --- ACCELERATION (HT)
□ STEADY RUNNING TEST BED DATA

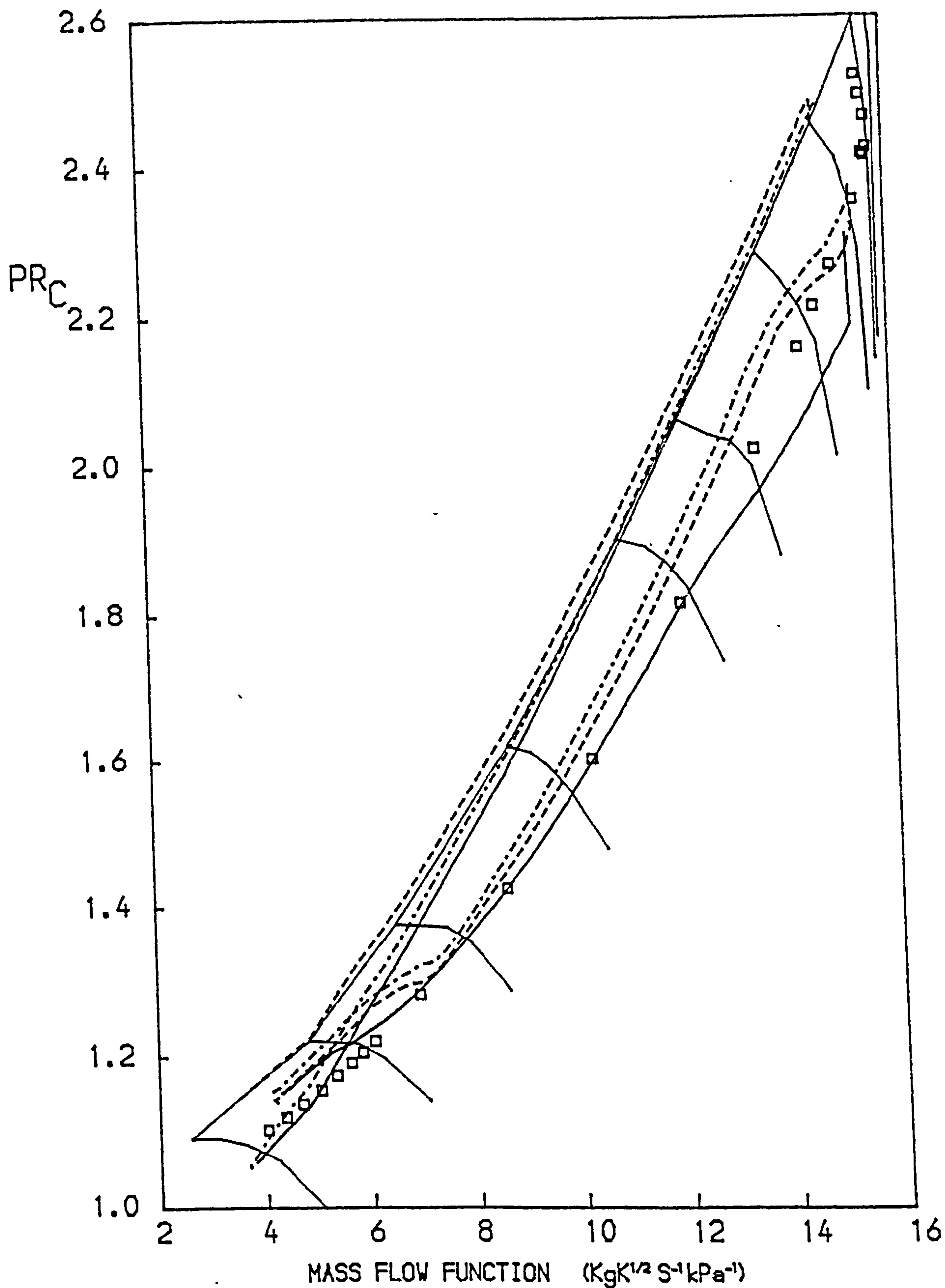


FIG. 117

PATHS ON THE CHARACTERISTIC MAPS OF THE L.P. COMPRESSOR OF A
TWO SPOOL BYPASS ENGINE WITH MIXED EXHAUSTS
PATHS AND SURGE LINE MOVEMENTS DURING A "BODIE" TRANSIENT
-- ACCELERATION — DECELERATION --- HOT ACCELERATION
□ STEADY RUNNING TEST BED DATA

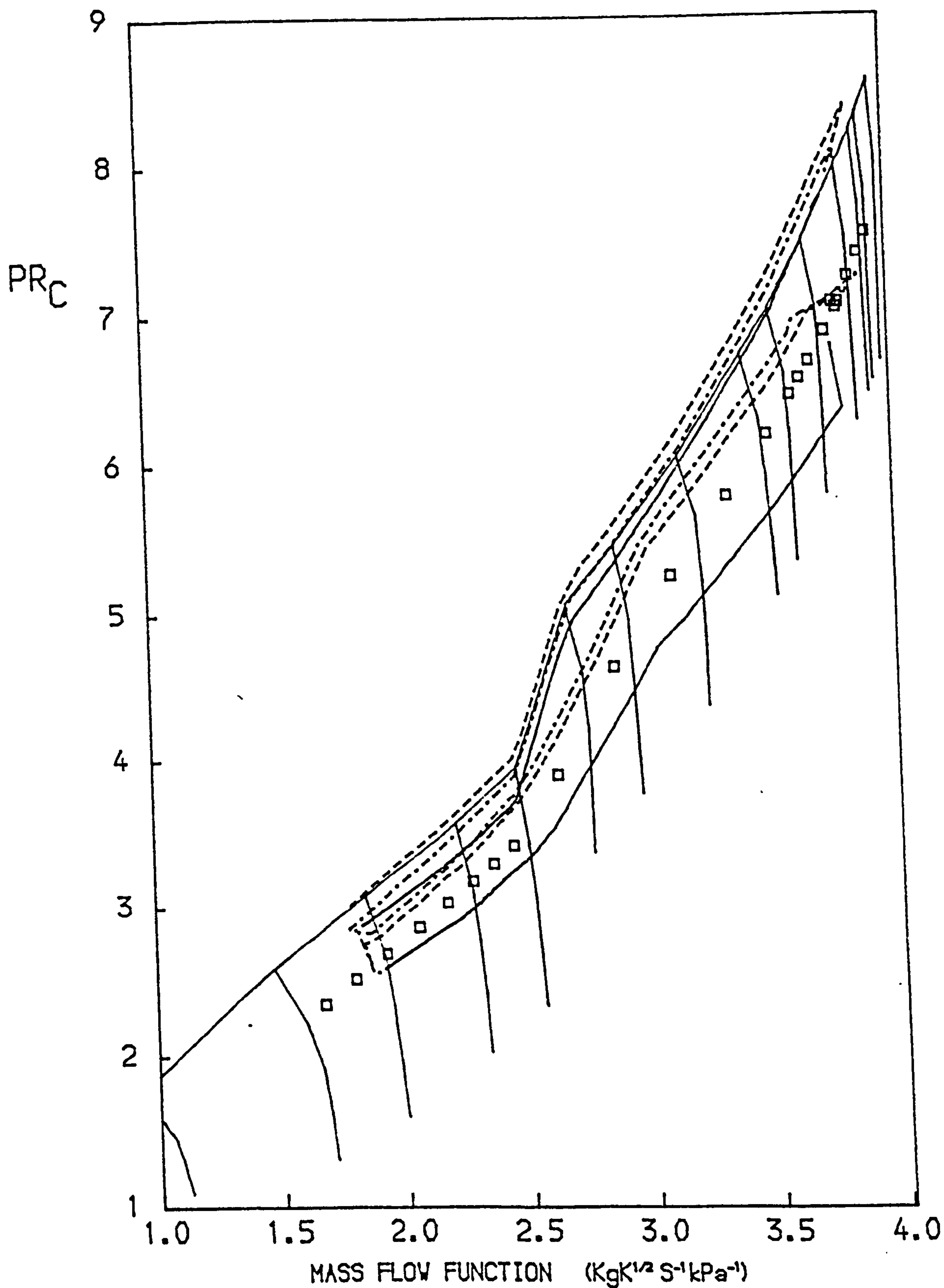


FIG. 118

PATHS ON THE CHARACTERISTIC MAPS OF THE H.P. COMPRESSOR OF A
TWO SPOOL BYPASS ENGINE WITH MIXED EXHAUSTS
PATHS AND SURGE LINE MOVEMENTS DURING A "BODIE" TRANSIENT
-- ACCELERATION — DECELERATION -.- HOT ACCELERATION
□ STEADY RUNNING TEST BED DATA

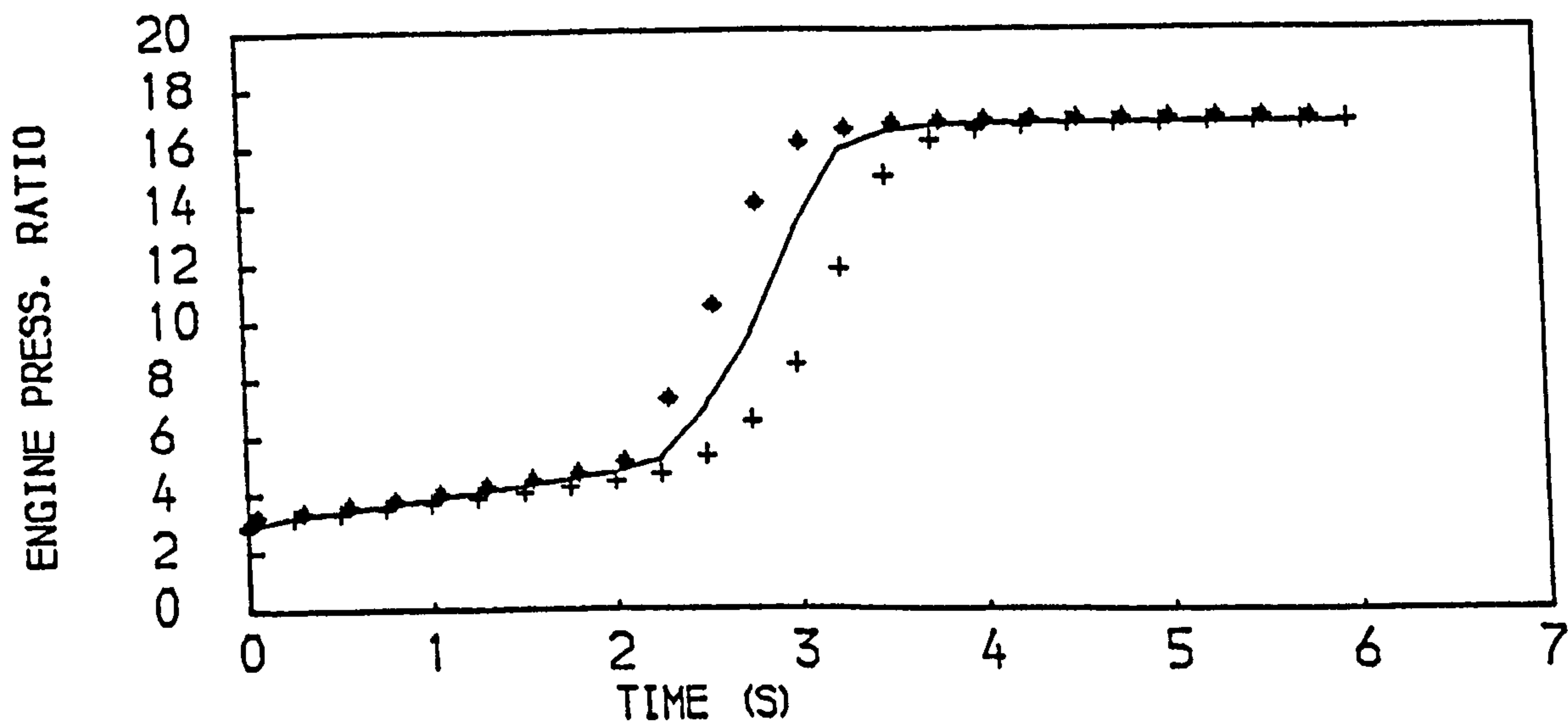
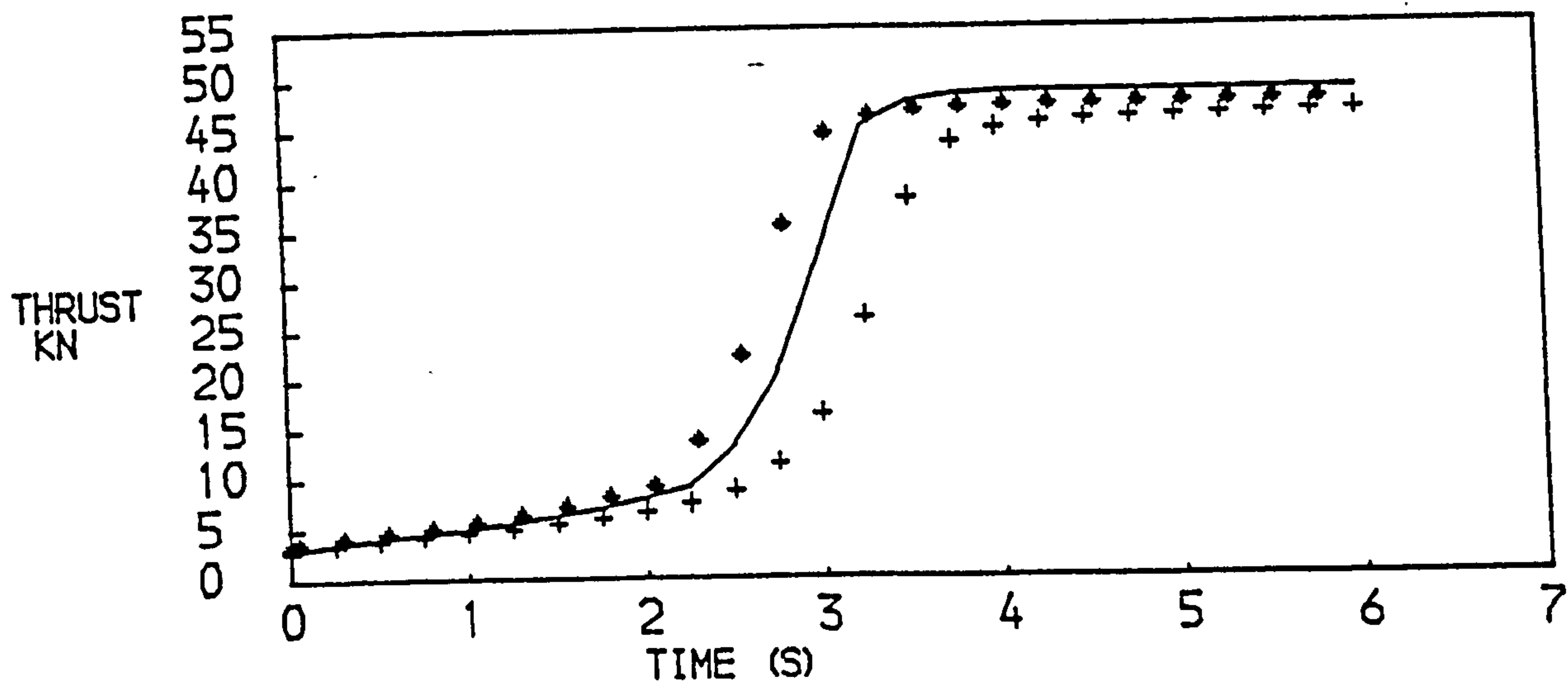
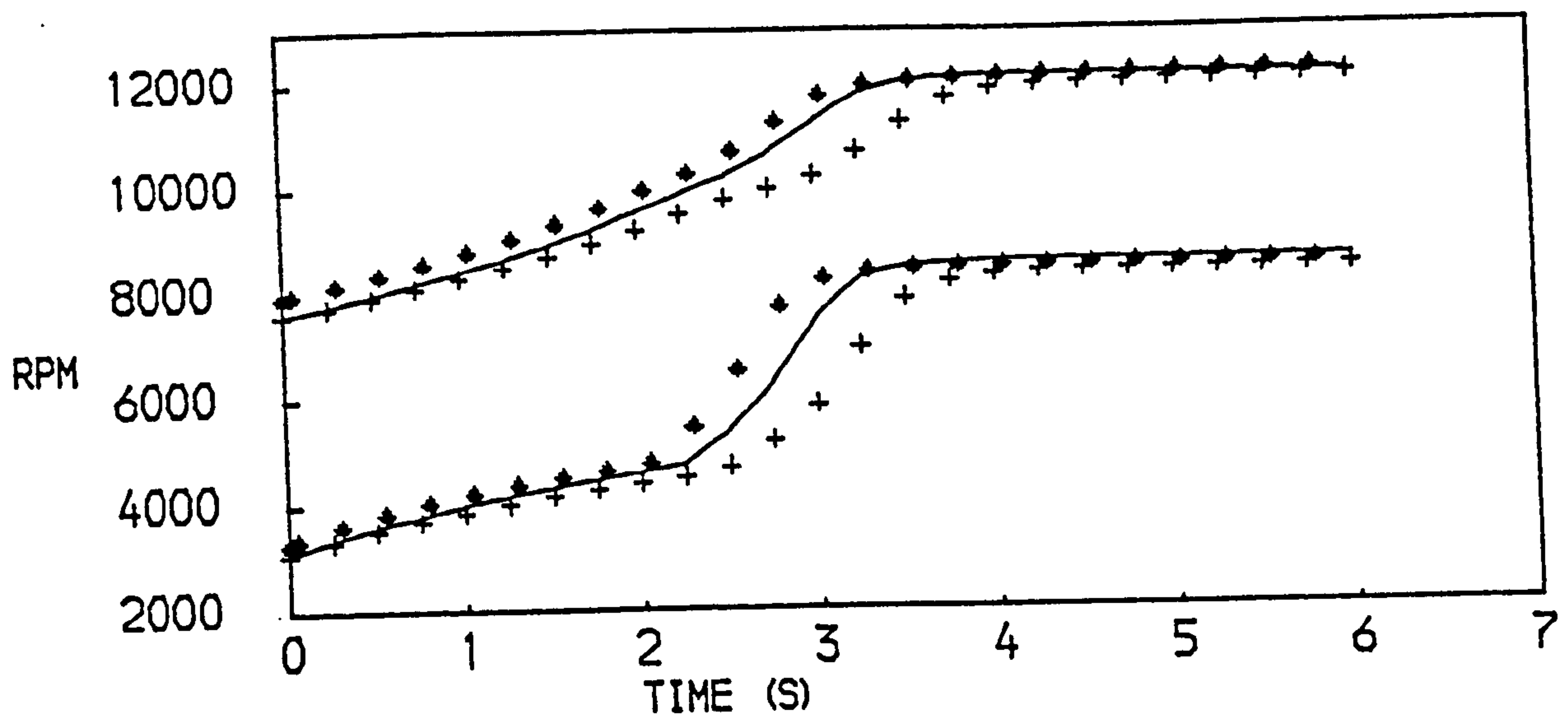


FIG. 119

PERFORMANCE OF A TWO SPOOL BYPASS ENGINE WITH MIXED EXHAUSTS
 DURING A "BODIE" TRANSIENT
 —ADIABATIC +COLD ACCELERATION ♦HOT ACCELERATION

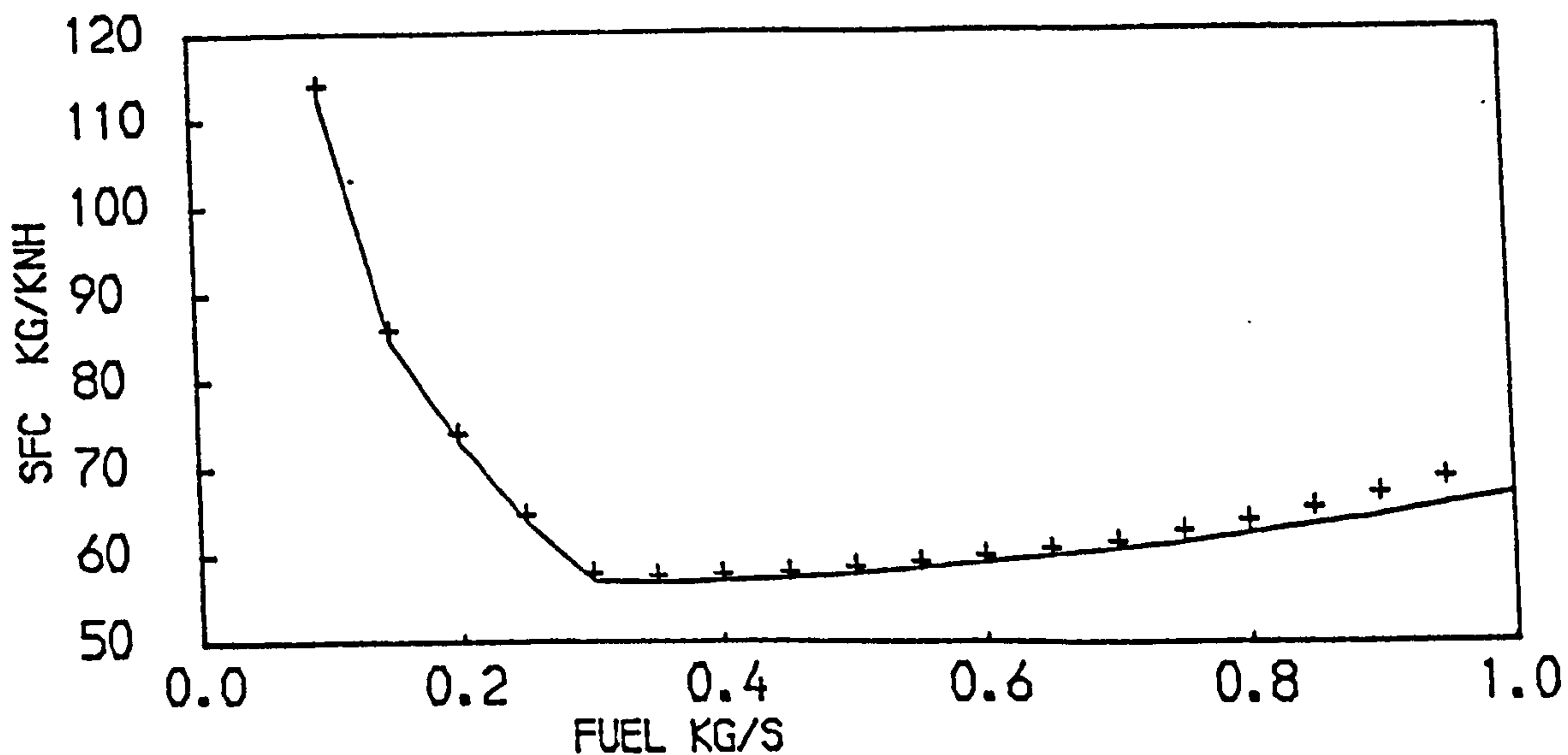
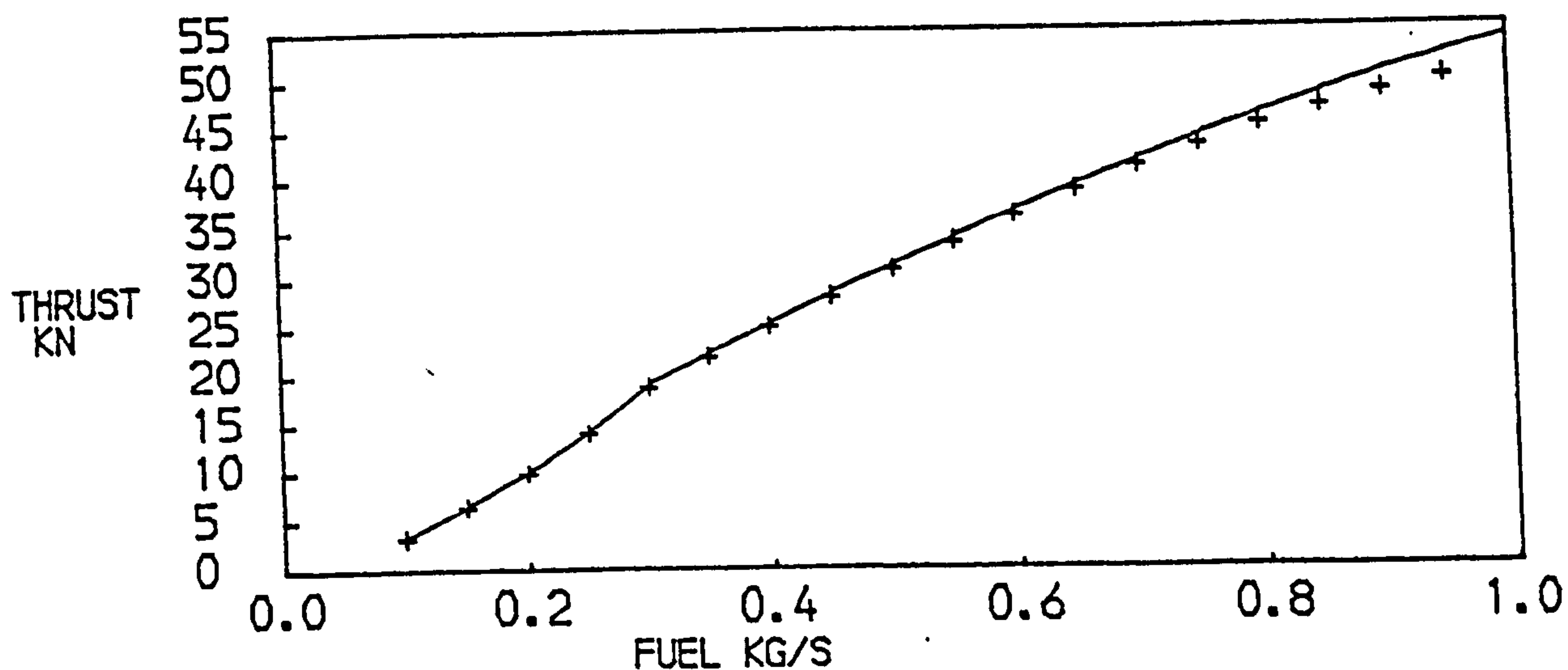
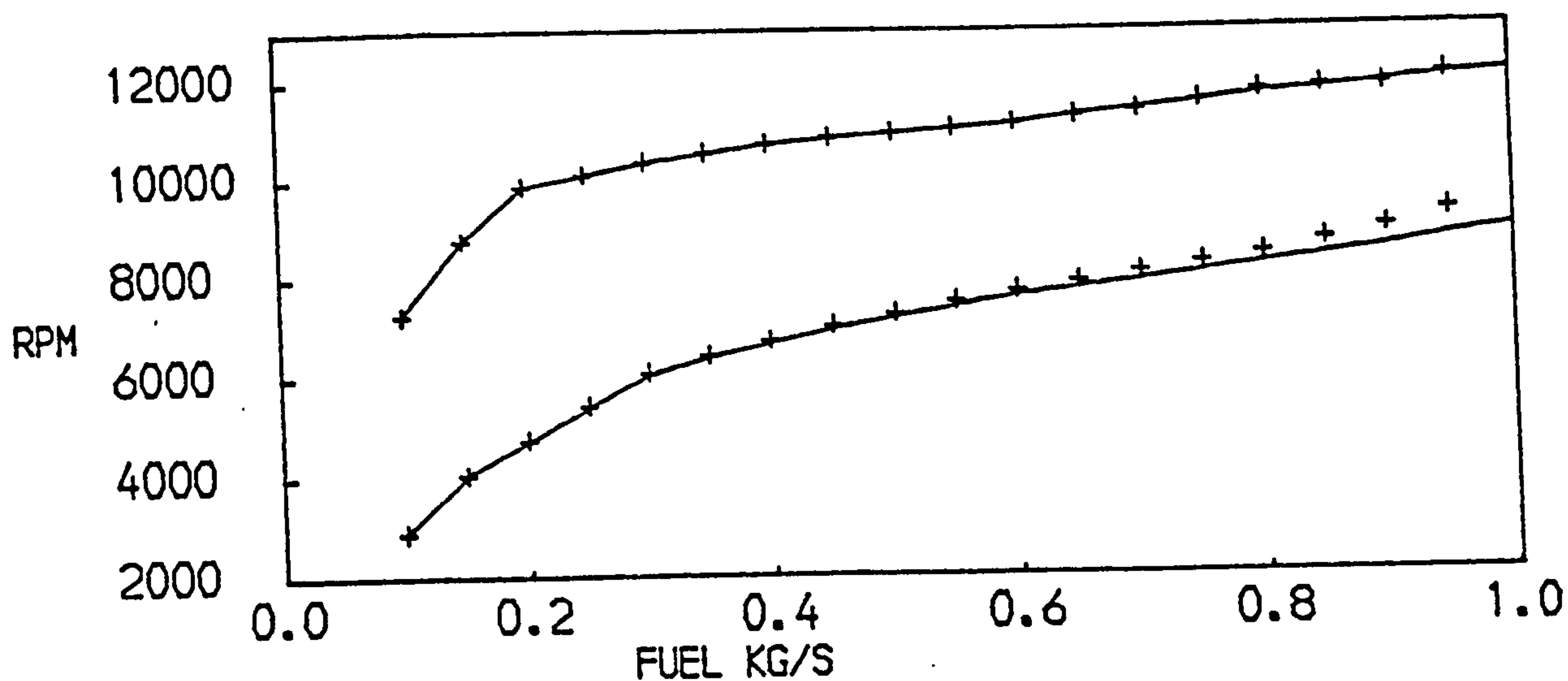


FIG. 120
EFFECT OF MIXING ON THE STEADY STATE PERFORMANCE
OF A TWO SPOOL BYPASS ENGINE WITH MIXED EXHAUSTS
AT SEA LEVEL STATIC CONDITIONS
+NO MIXING —COMPLETE MIXING

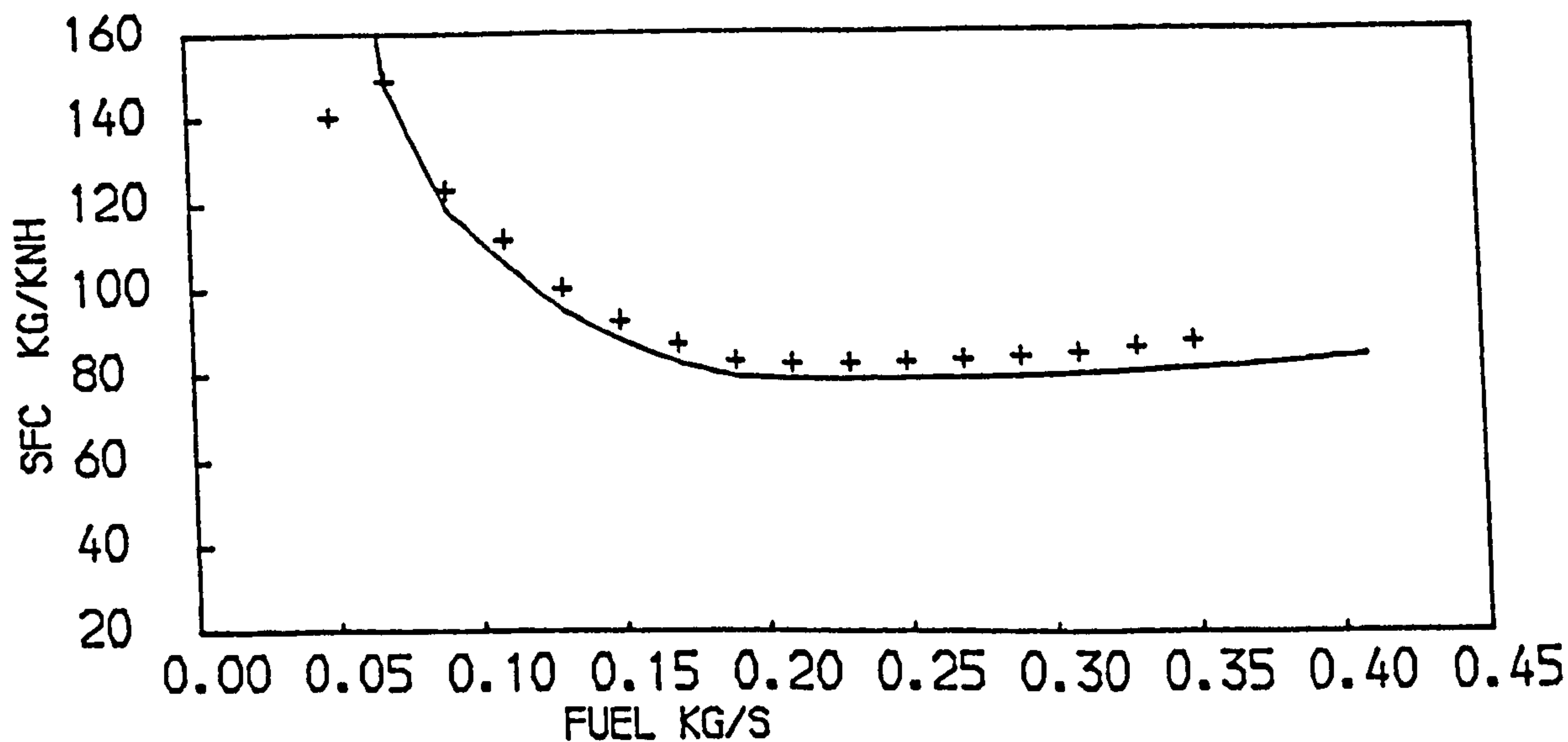
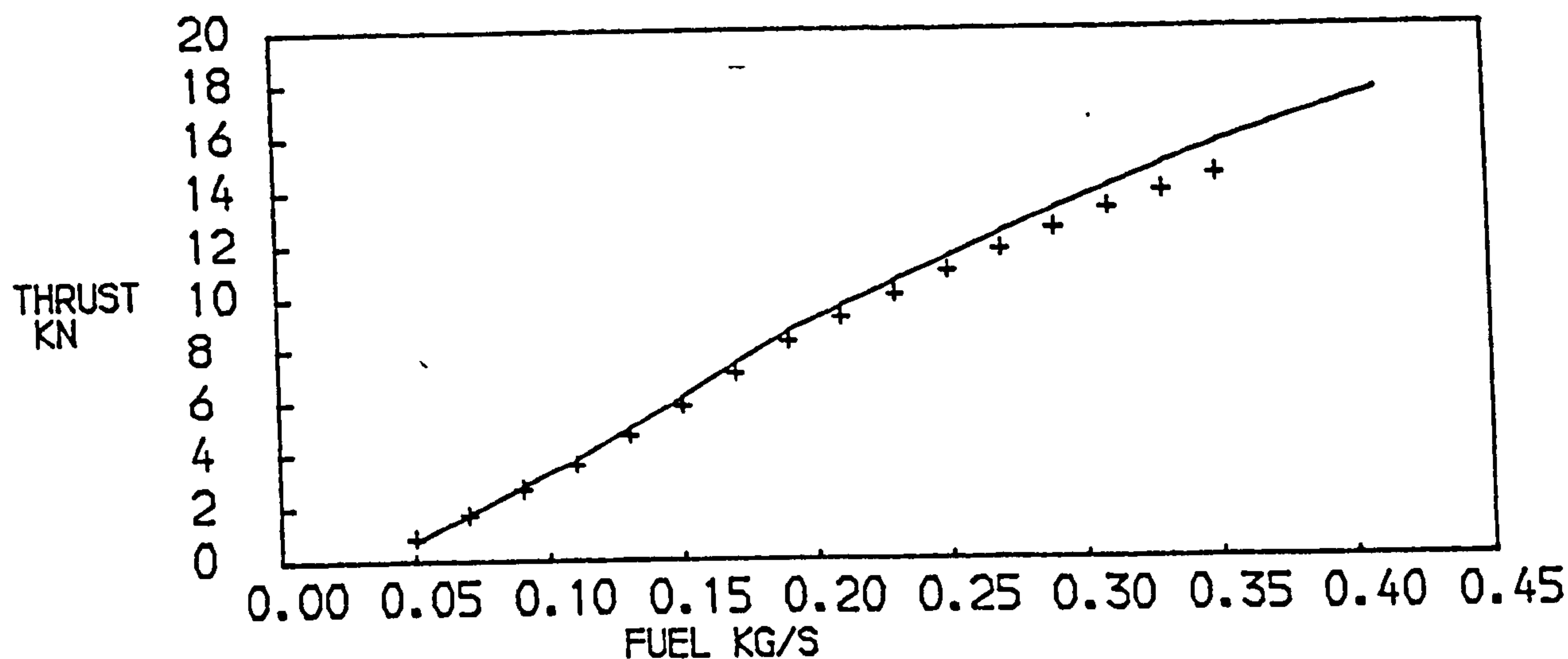
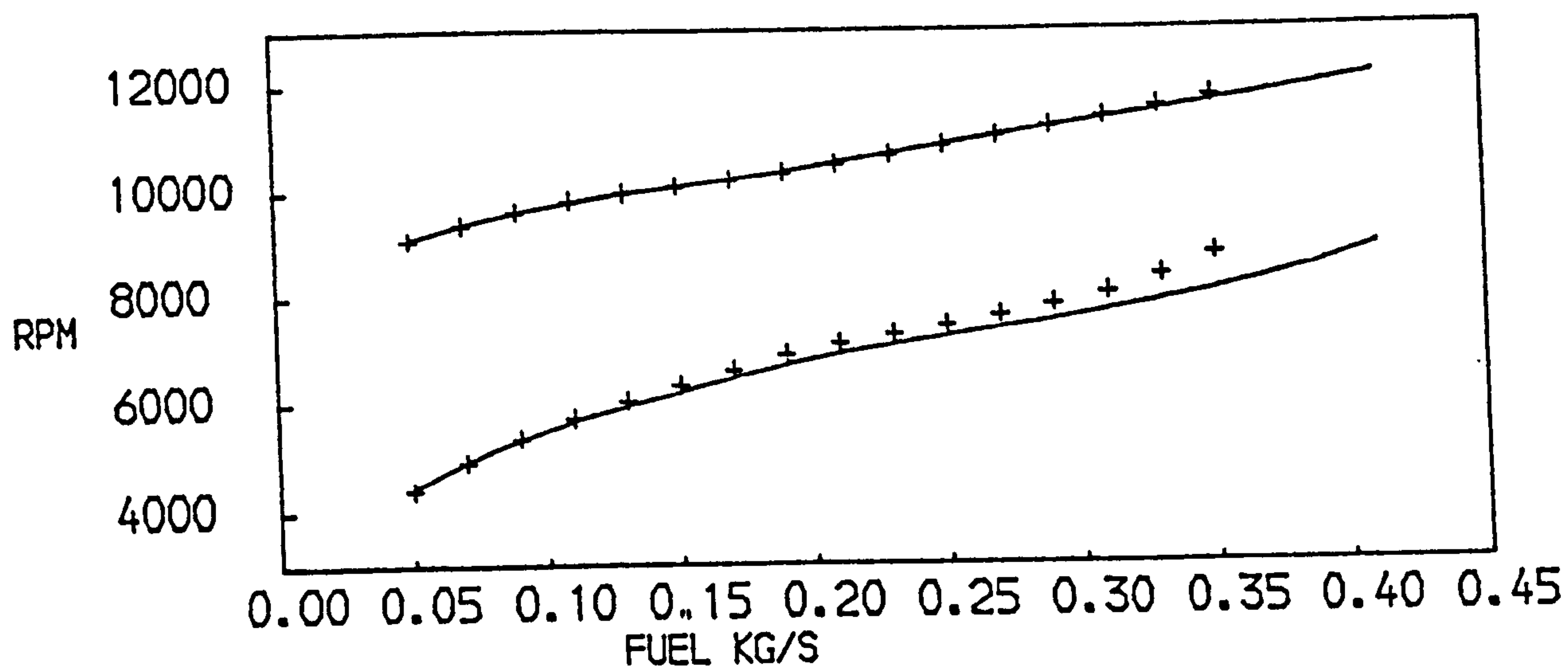


FIG. 121
EFFECT OF MIXING ON THE STEADY STATE PERFORMANCE
OF A TWO SPOOL BYPASS ENGINE WITH MIXED EXHAUSTS
AT AN ALTITUDE OF 9150 M, FLIGHT MACH NUMBER = 0.8
+NO MIXING —COMPLETE MIXING

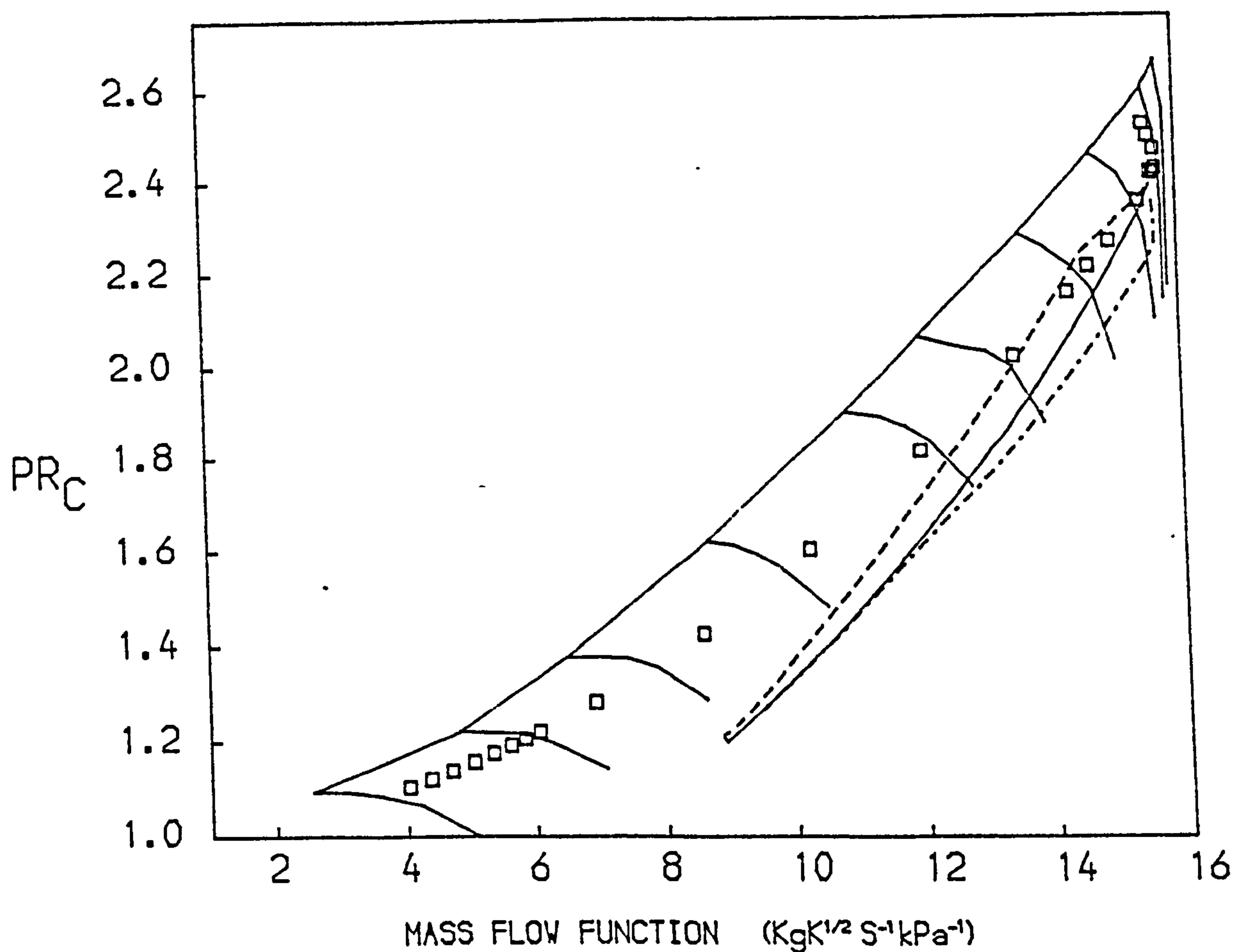
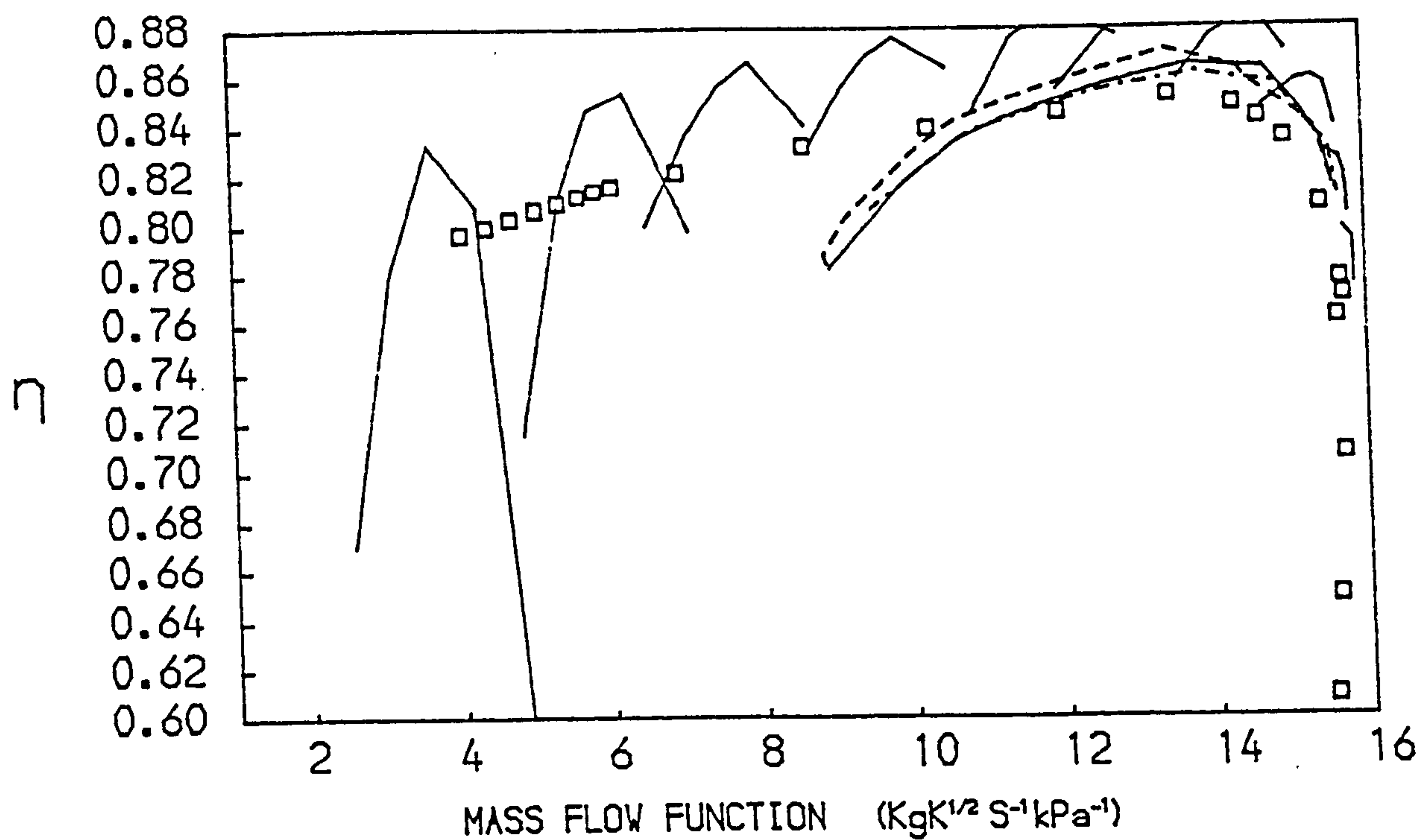


FIG. 122
 PATHS ON THE CHARACTERISTIC MAPS OF THE L.P. COMPRESSOR OF A
 TWO SPOOL BYPASS ENGINE WITH MIXED EXHAUSTS AT ALTITUDE
 -- ACCELERATION — STEADY RUNNING --- DECELERATION
 □ STEADY RUNNING TEST BED DATA AT SEA LEVEL

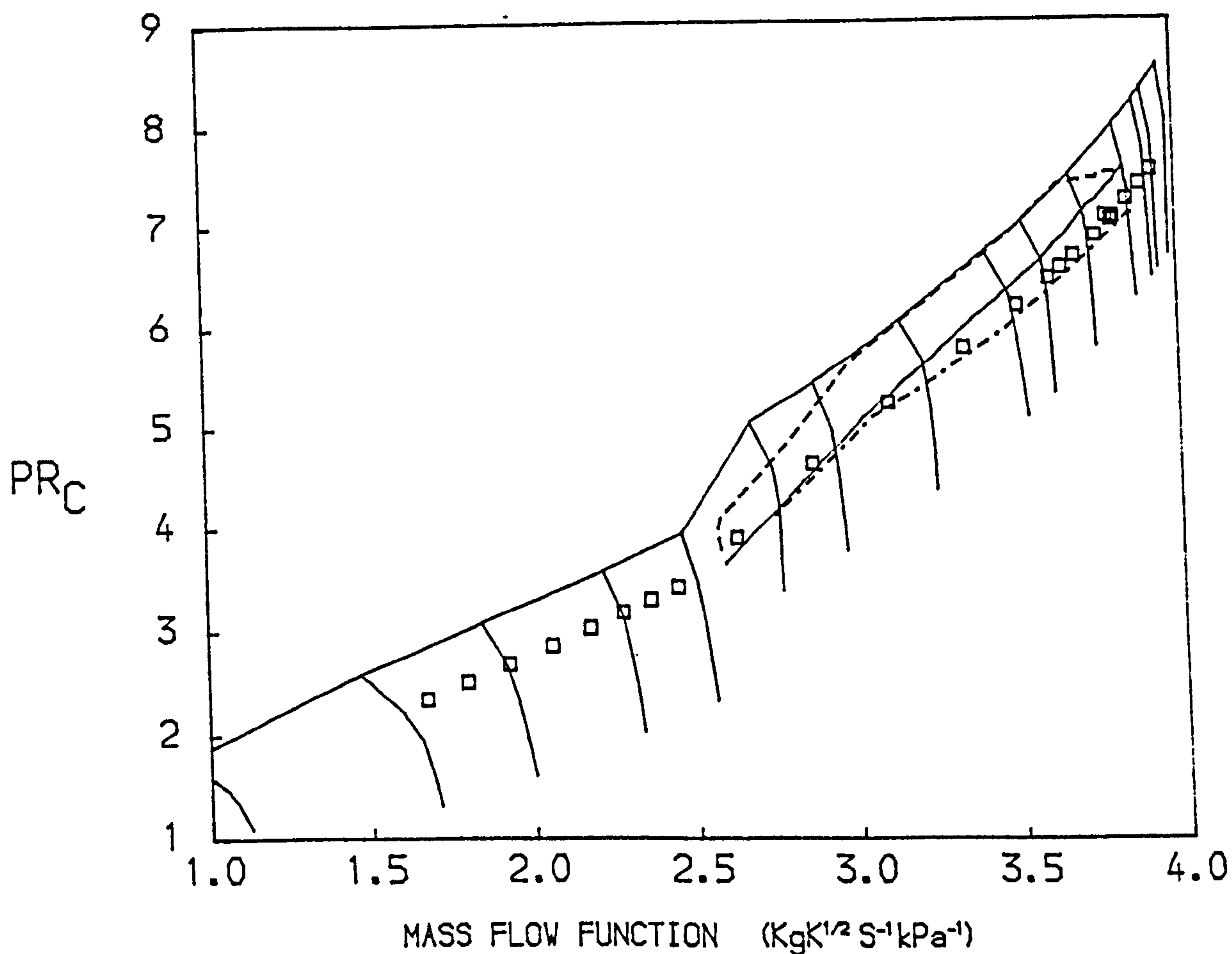
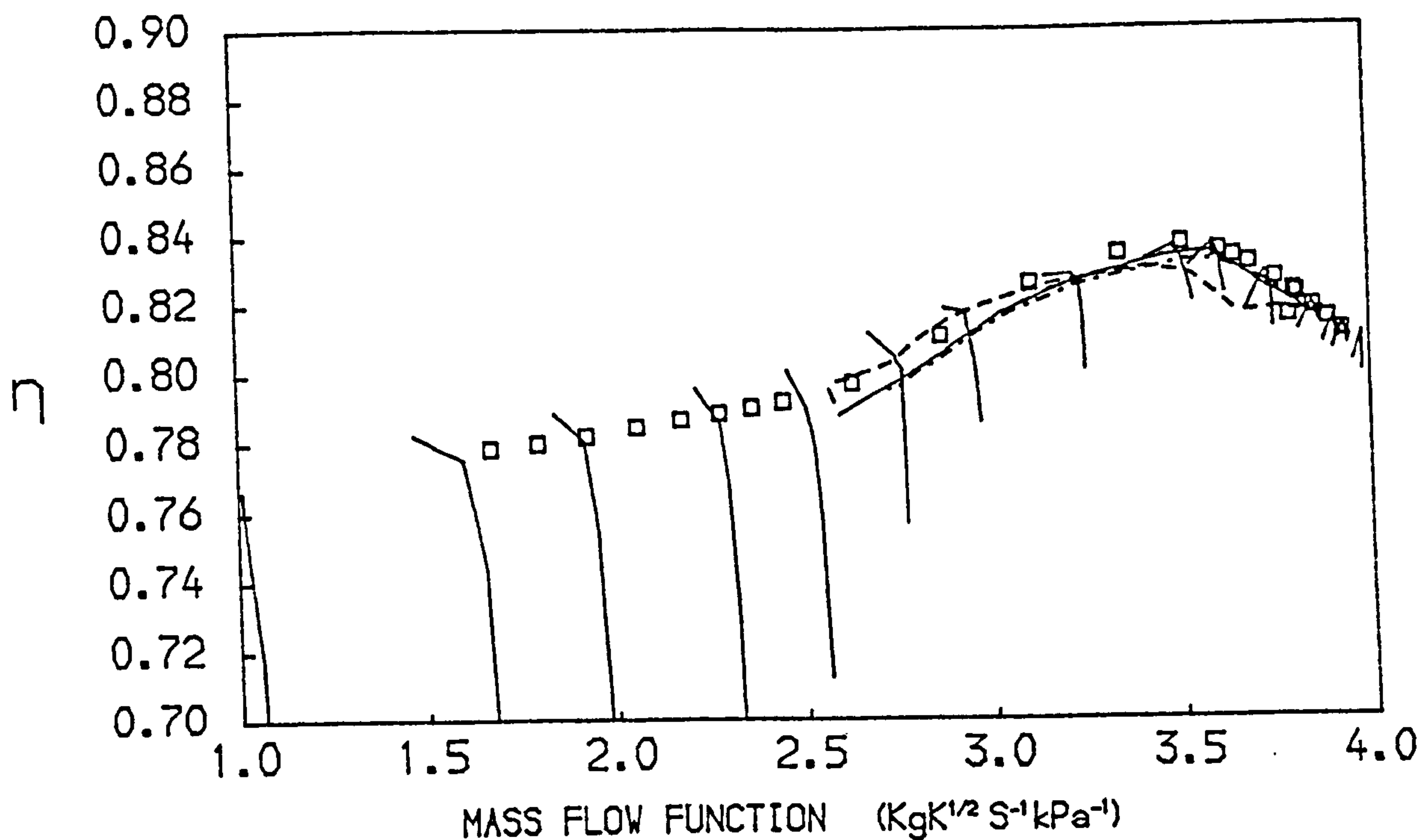


FIG. 123
 PATHS ON THE CHARACTERISTIC MAPS OF THE H.P. COMPRESSOR OF A
 TWO SPOOL BYPASS ENGINE WITH MIXED EXHAUSTS AT ALTITUDE
 -- ACCELERATION — STEADY RUNNING --- DECELERATION
 \square STEADY RUNNING TEST BED DATA AT SEA LEVEL

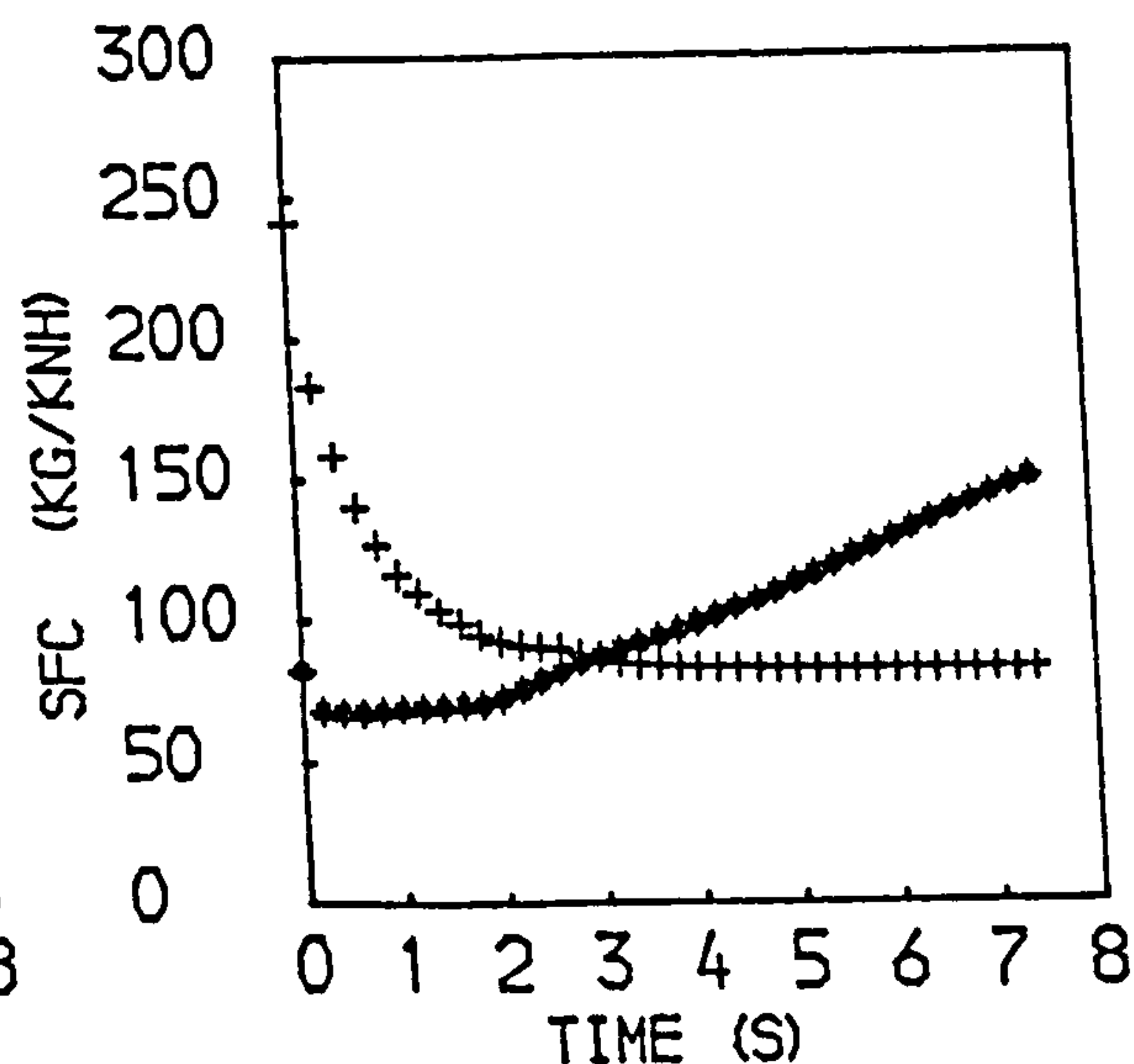
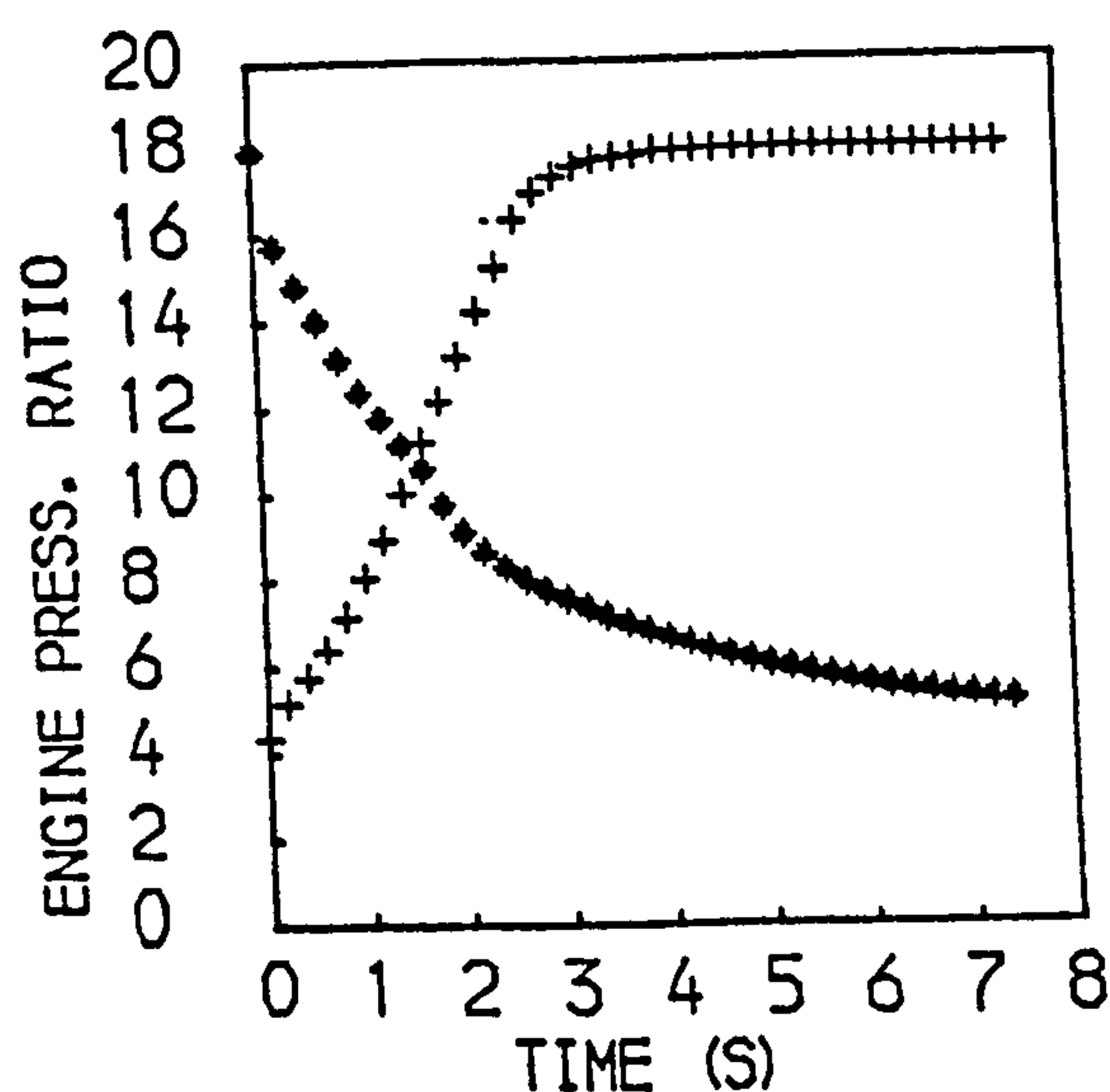
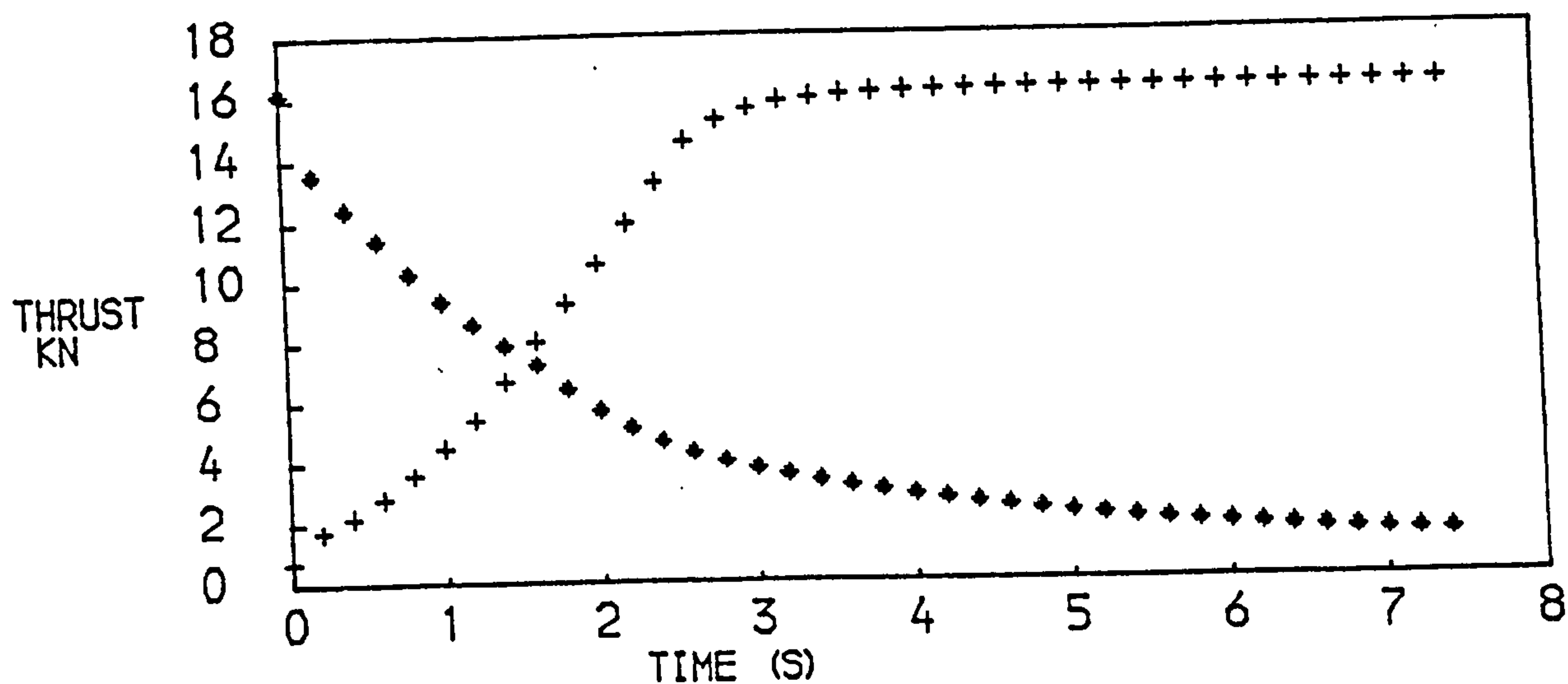
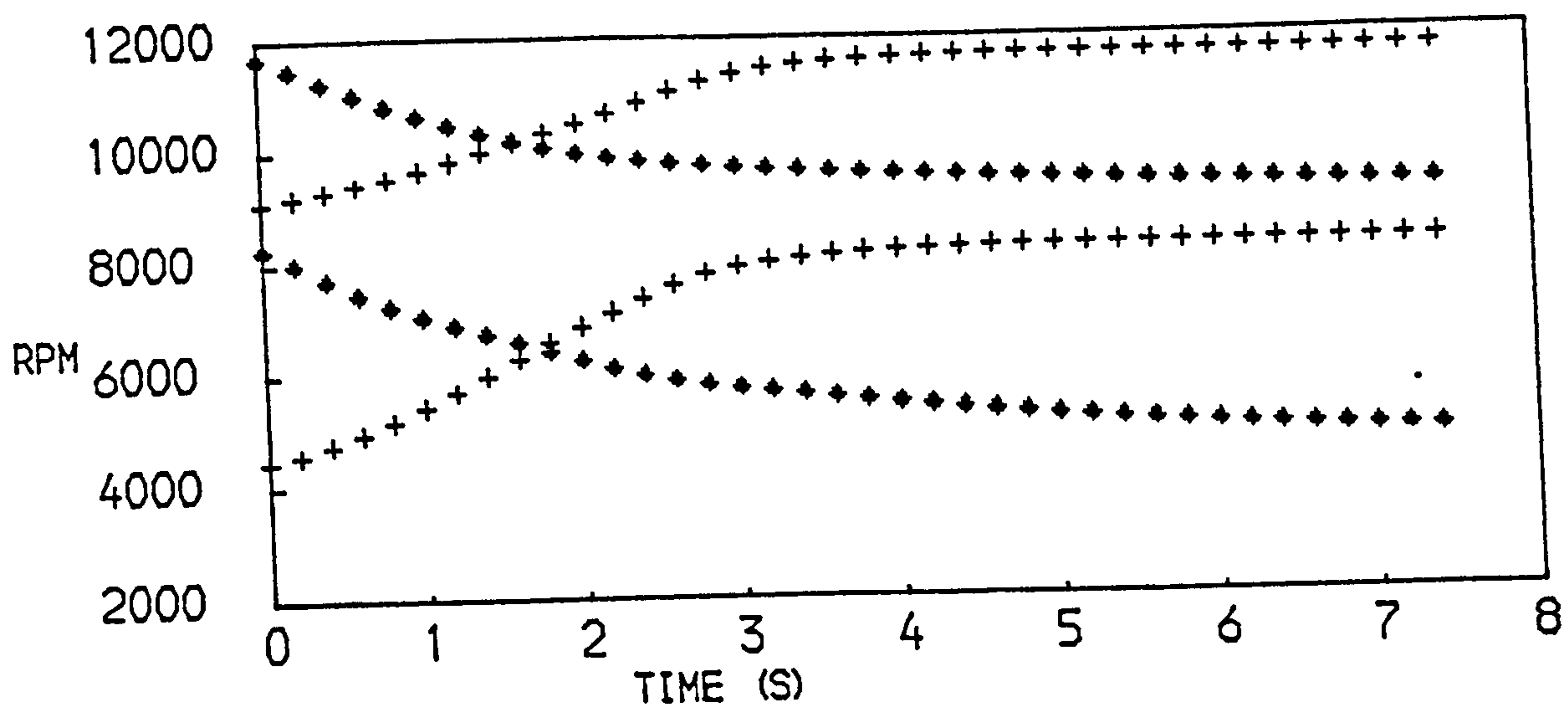


FIG. 124
PERFORMANCE OF A TWO SPOOL BYPASS ENGINE WITH MIXED EXHAUSTS
AT ALTITUDE. +ACCELERATION ♦ DECELERATION

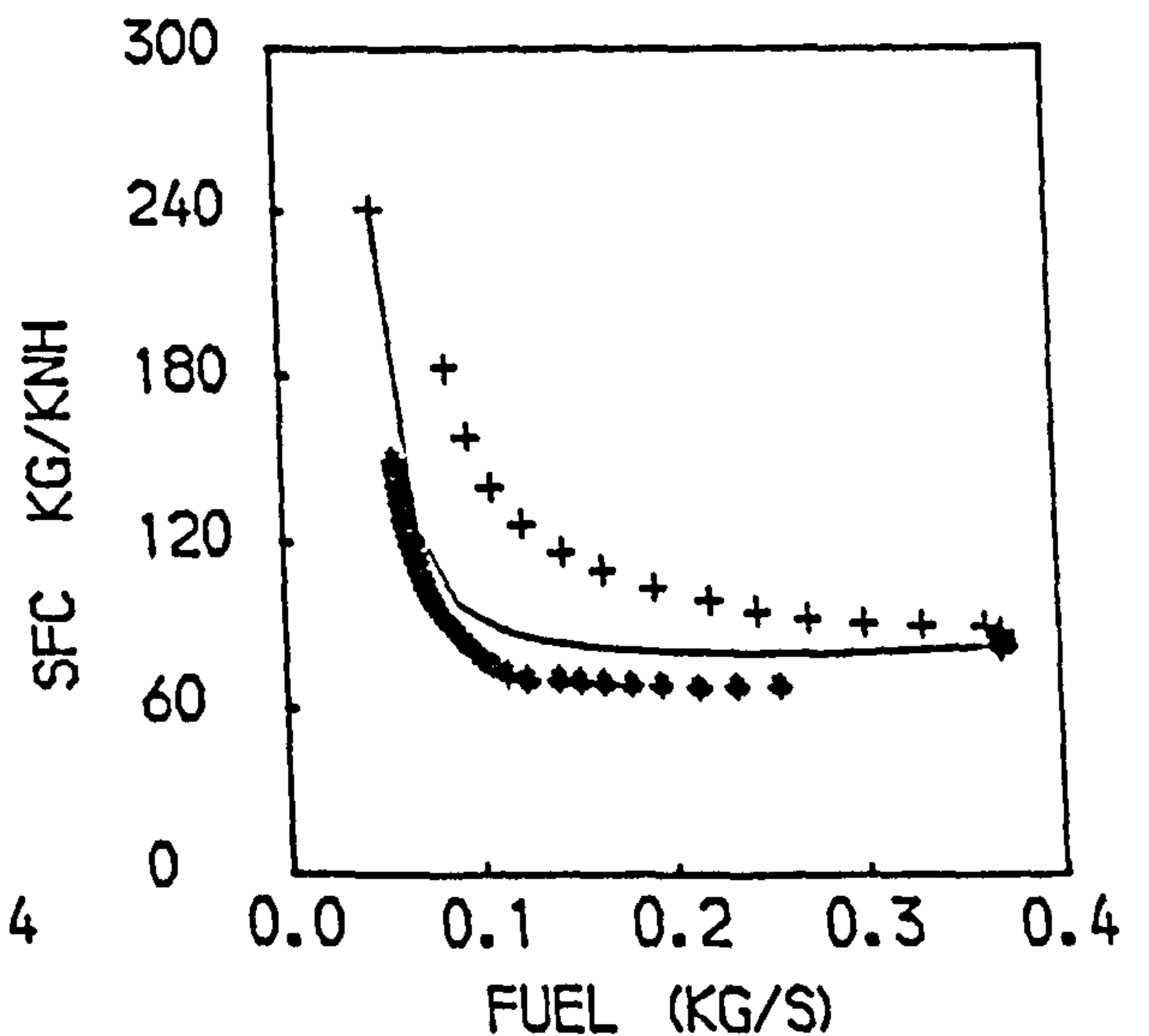
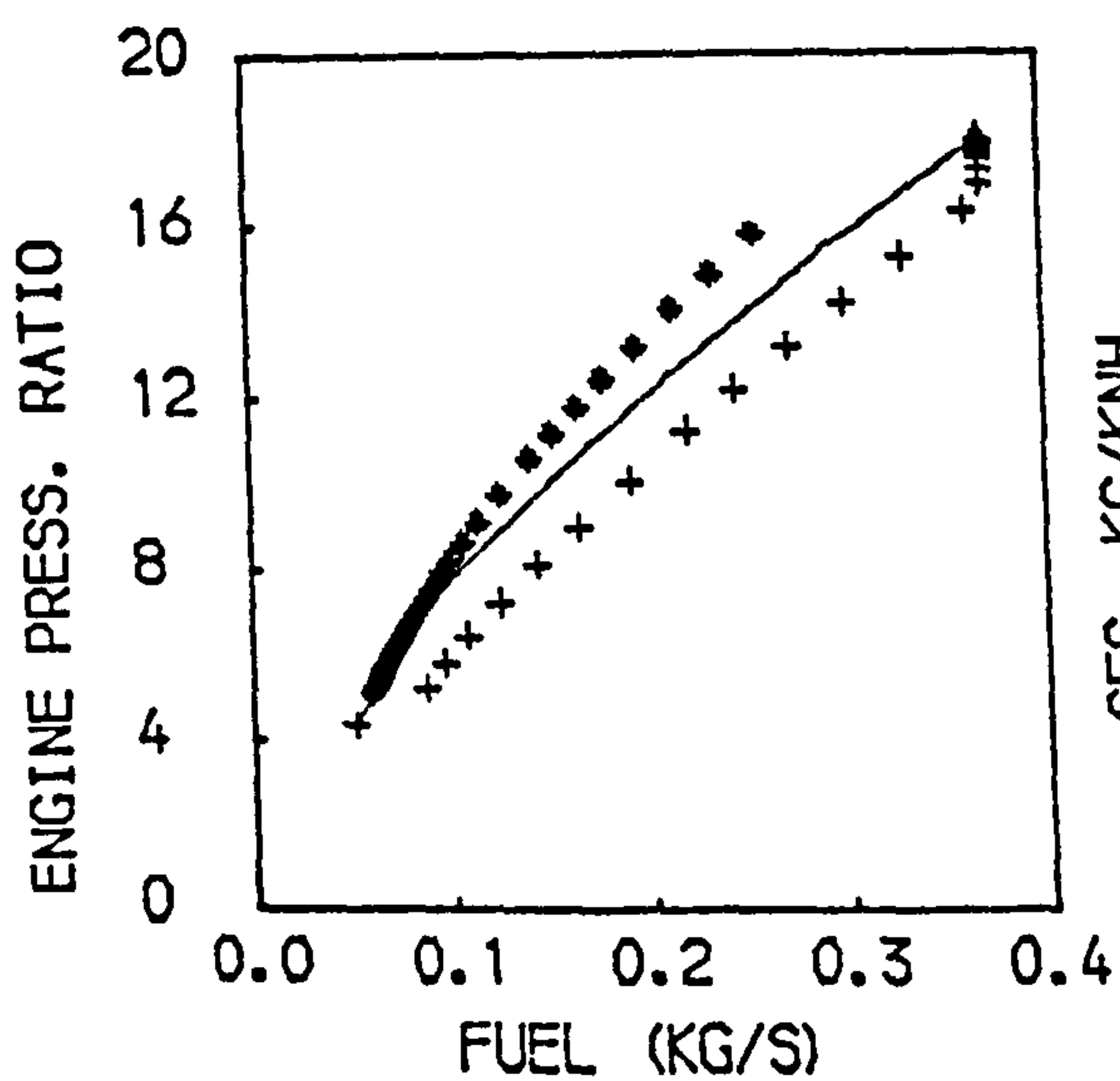
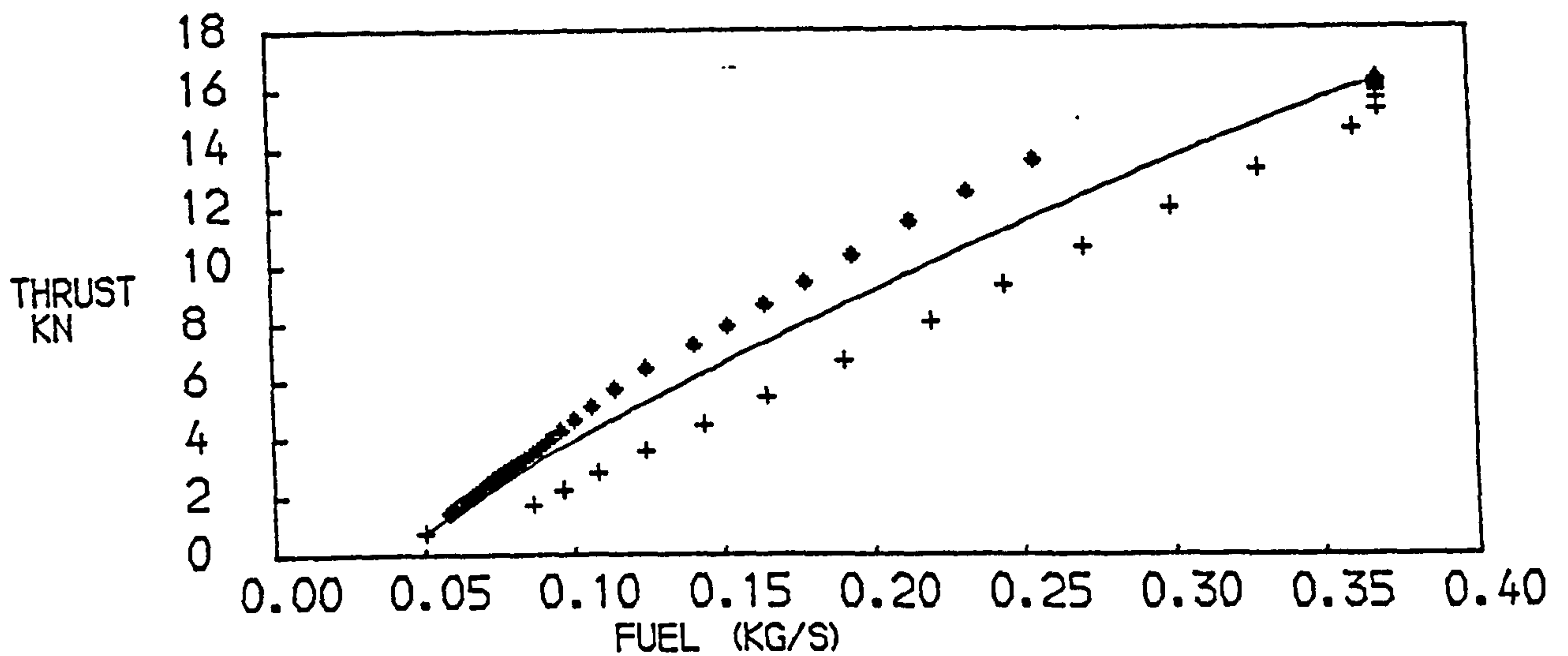
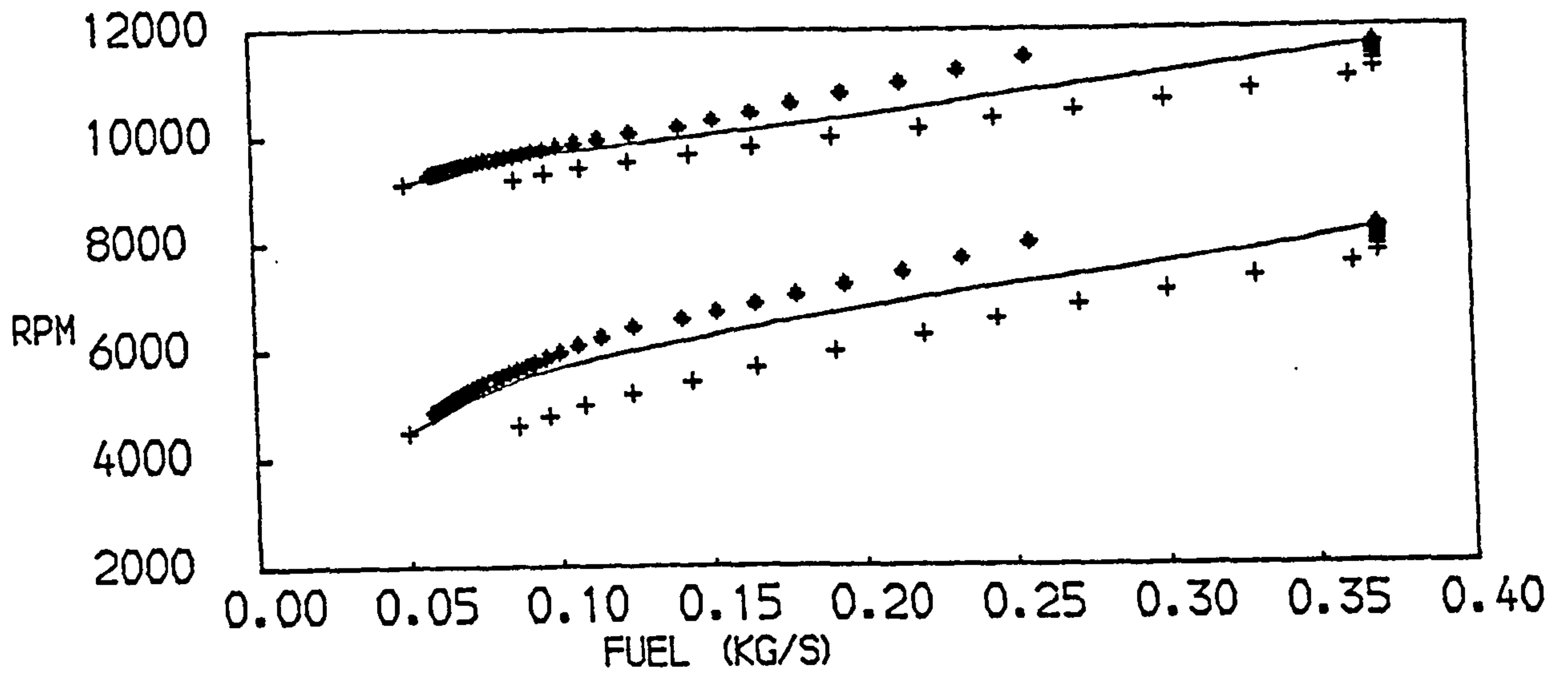


FIG. 125
PERFORMANCE OF A TWO SPOOL BYPASS ENGINE WITH MIXED EXHAUSTS
AT ALTITUDE. +ACCELERATION ♦ DECELERATION —STEADY RUNNING

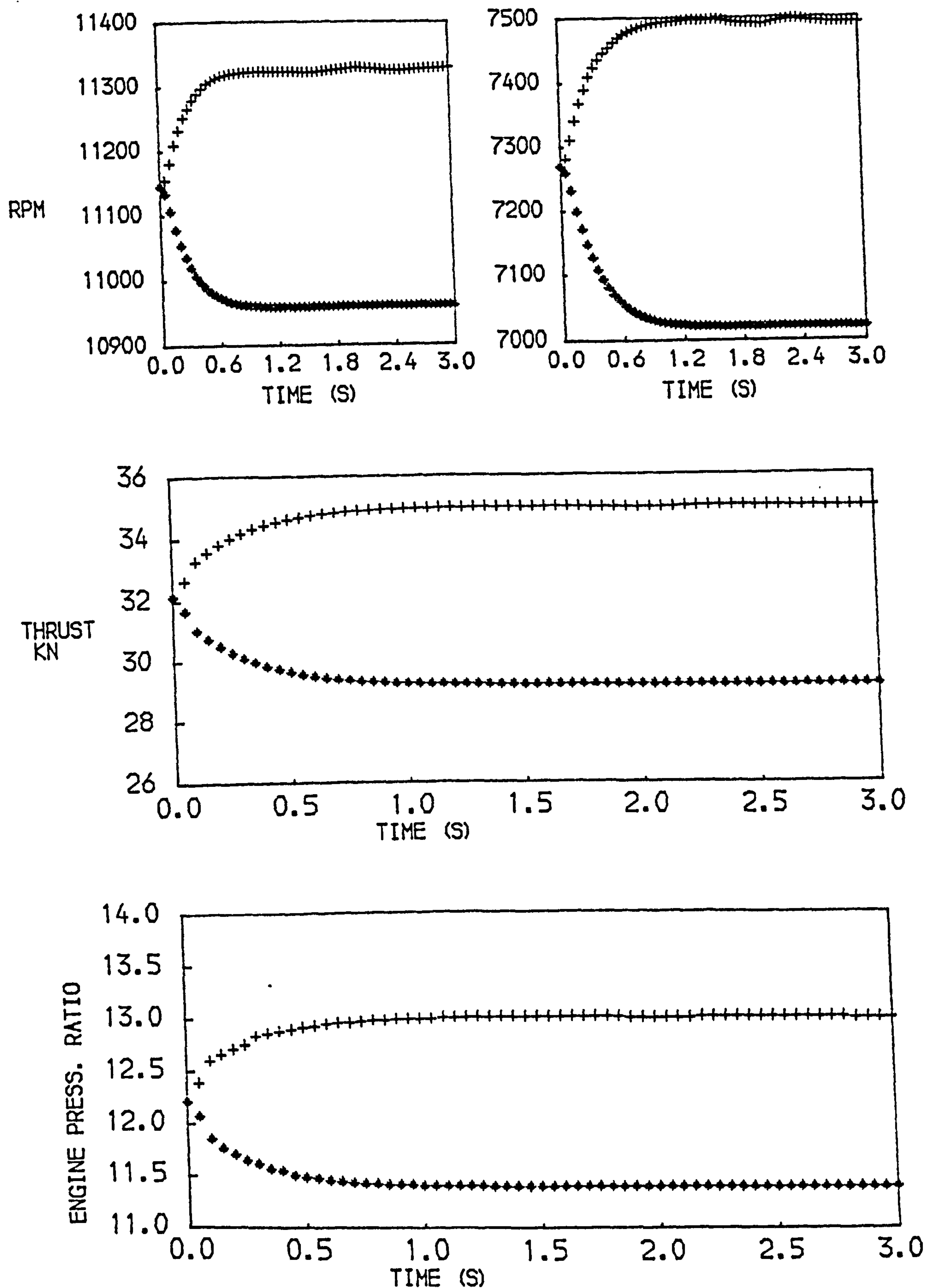


FIG. 126
EFFECT OF A STEP CHANGE IN FUEL FLOW ON THE PERFORMANCE OF A
TWO SPOOL BYPASS ENGINE WITH MIXED EXHAUSTS
AT SEA LEVEL STATIC CONDITIONS
+ACCELERATION • DECELERATION

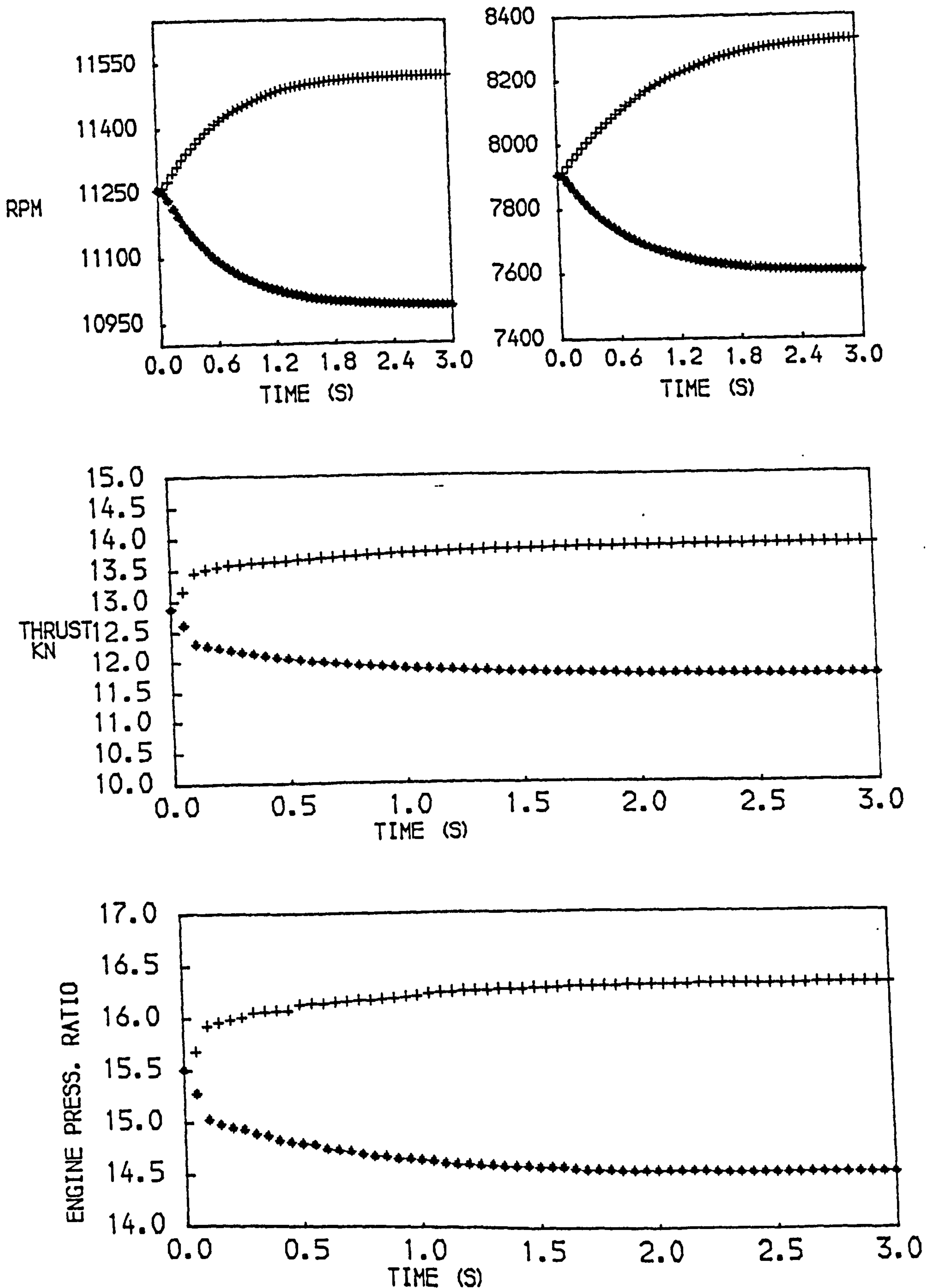


FIG. 127
EFFECT OF A STEP CHANGE IN FUEL FLOW ON THE PERFORMANCE OF A
TWO SPOOL BYPASS ENGINE WITH MIXED EXHAUSTS
AT AN ALTITUDE OF 9150 M, FLIGHT MACH NUMBER OF 0.8
+ACCELERATION • DECELERATION

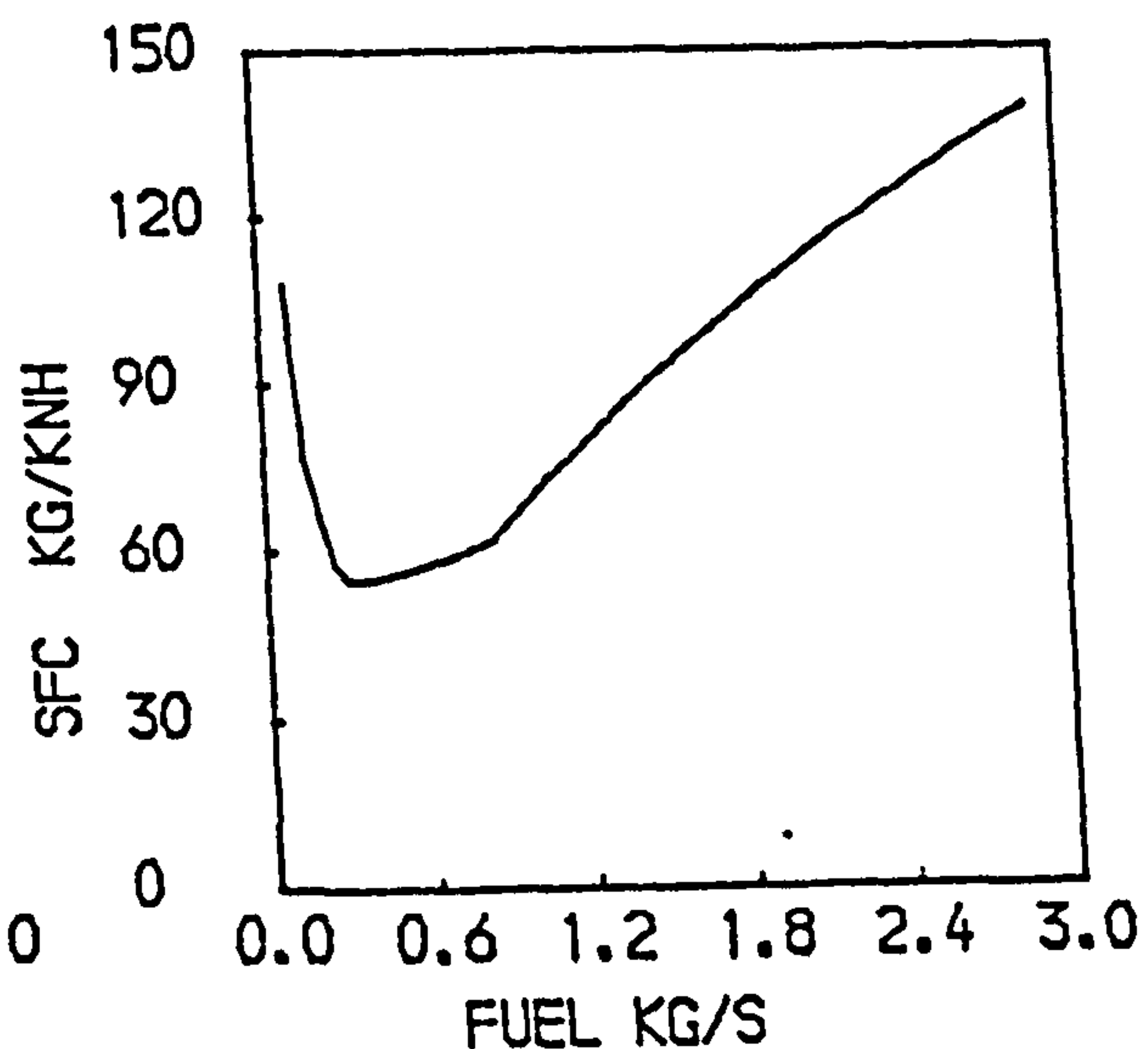
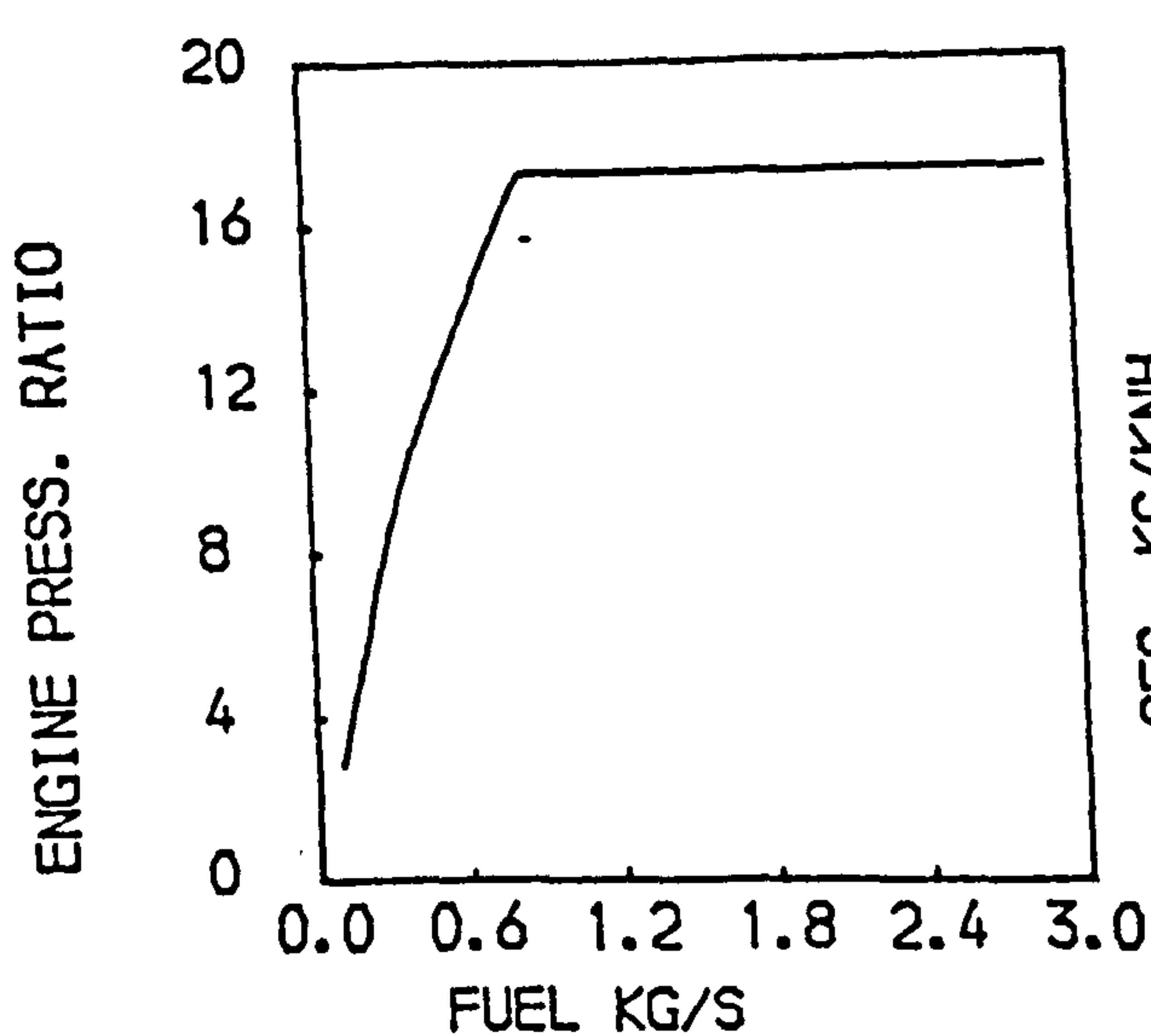
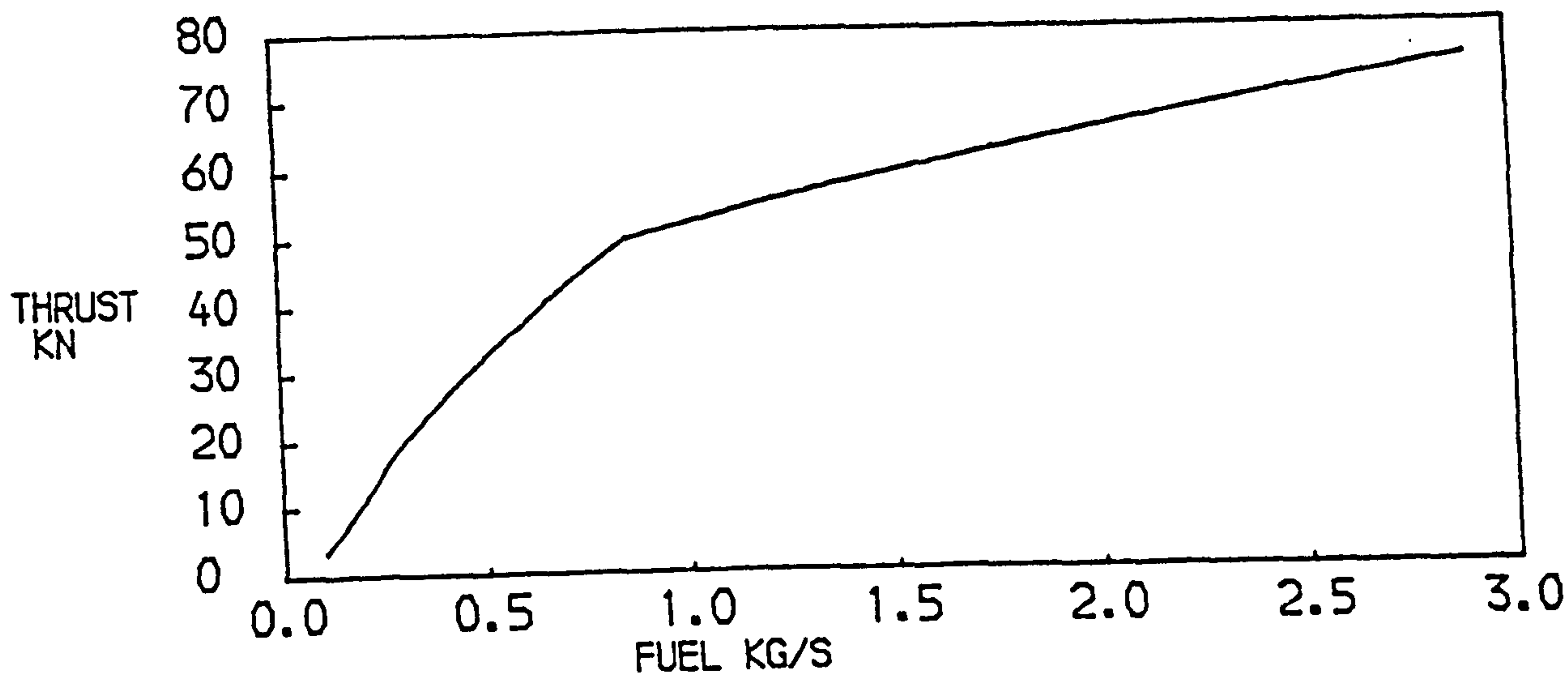
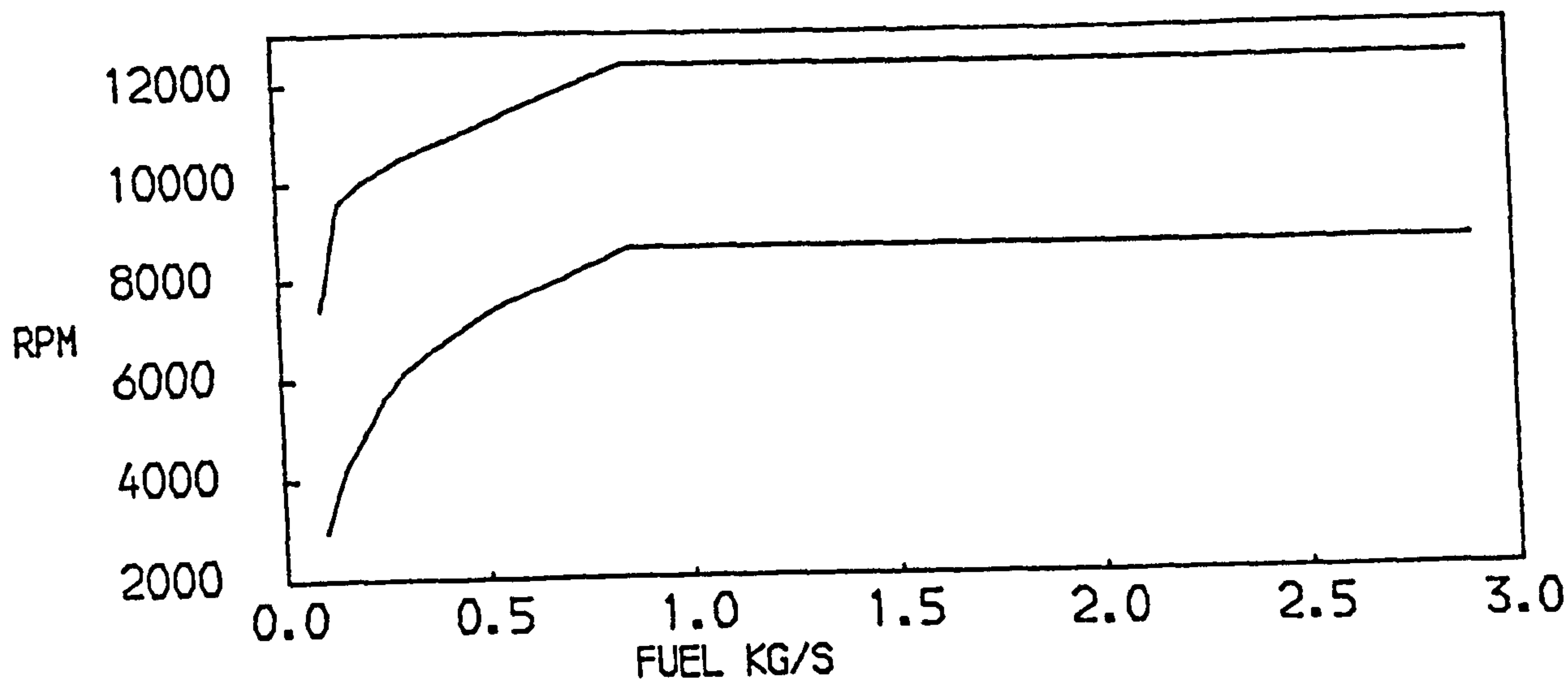


FIG. 128
STEADY STATE PERFORMANCE WITH REHEAT OF A
TWO SPOOL BYPASS ENGINE WITH MIXED EXHAUSTS
AT SEA LEVEL STATIC CONDITIONS
MAXIMUM FUEL FLOW IN DRY MODE = 0.85 KG/S

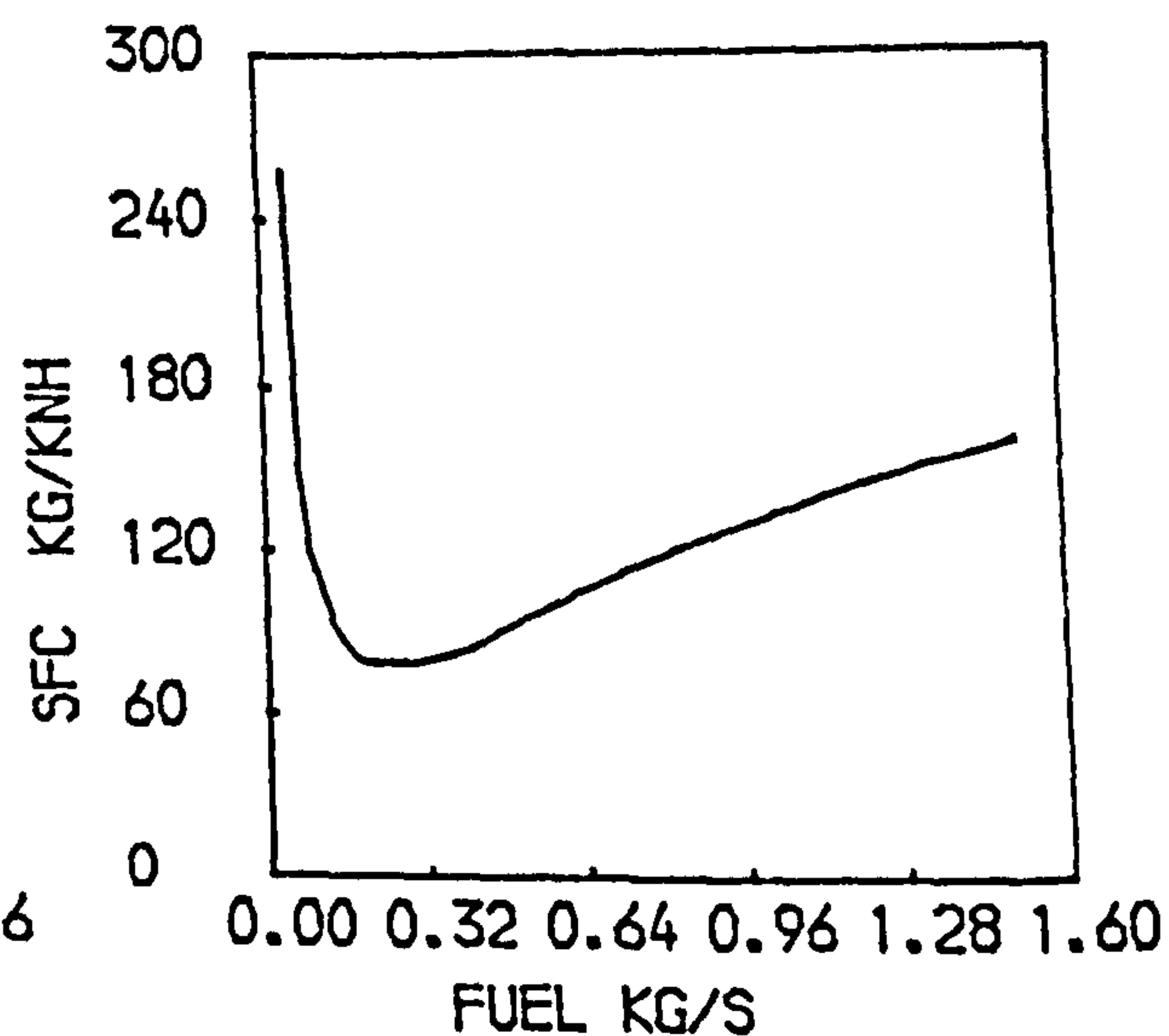
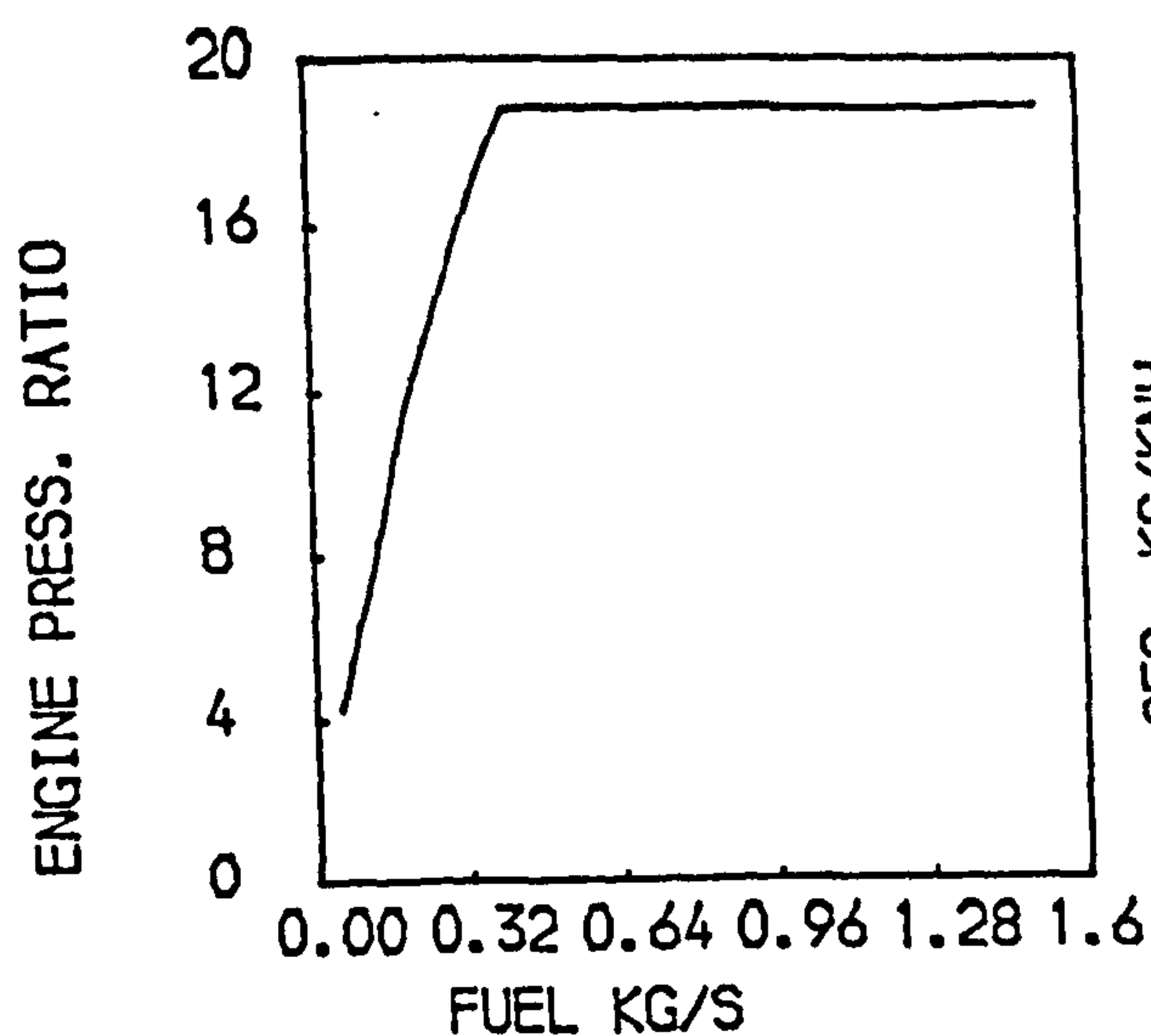
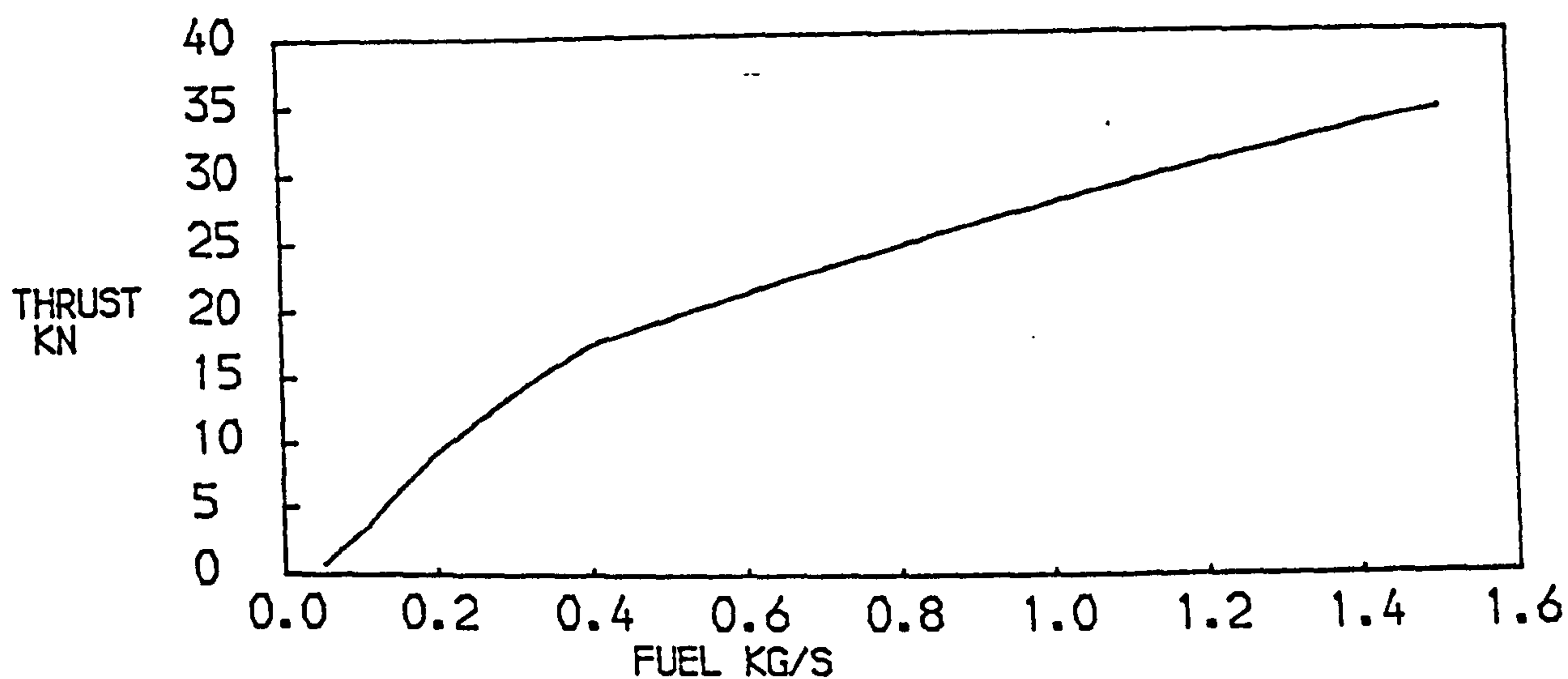
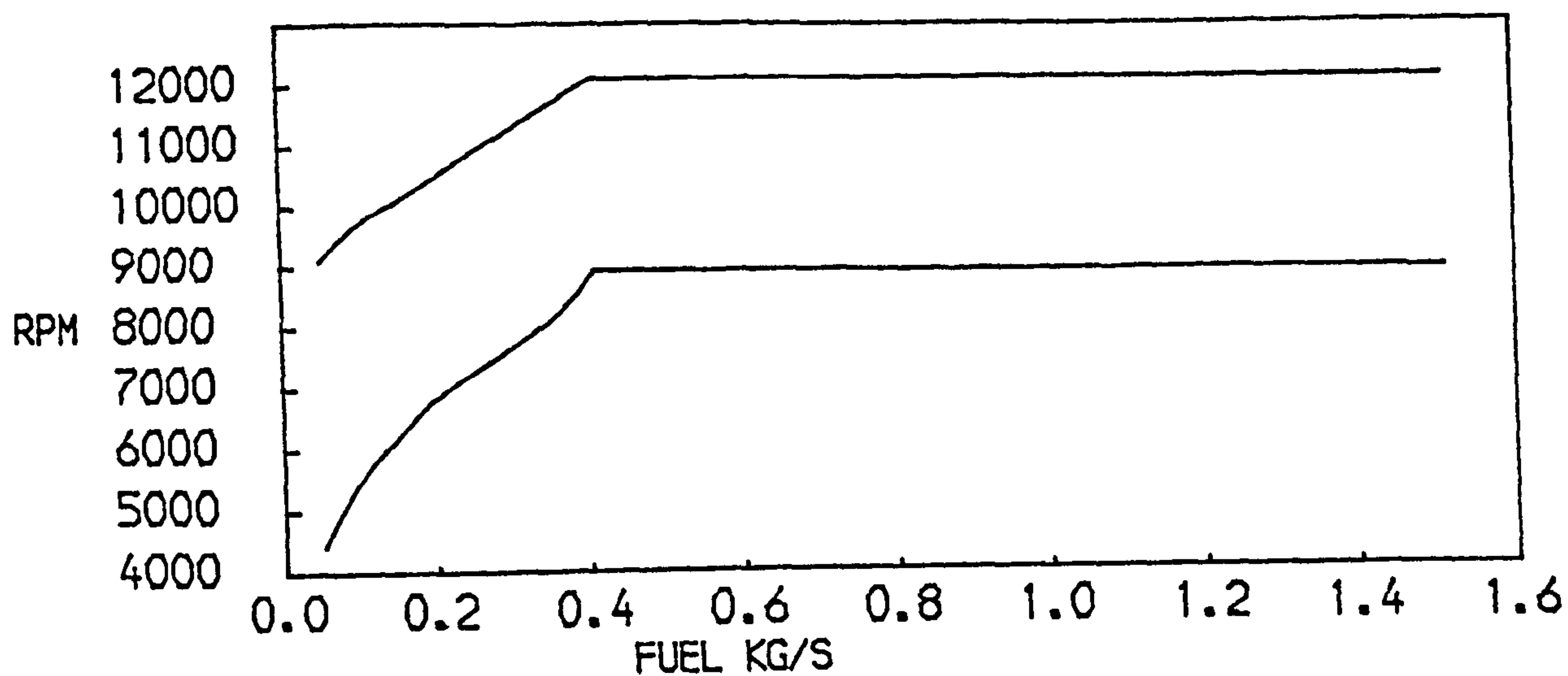


FIG. 129
STEADY STATE PERFORMANCE WITH REHEAT OF A
TWO SPOOL BYPASS ENGINE WITH MIXED EXHAUSTS
AT AN ALTITUDE OF 9140M, FLIGHT MACH NO = 0.8
MAXIMUM FUEL FLOW IN DRY MODE = 0.41 KG/S

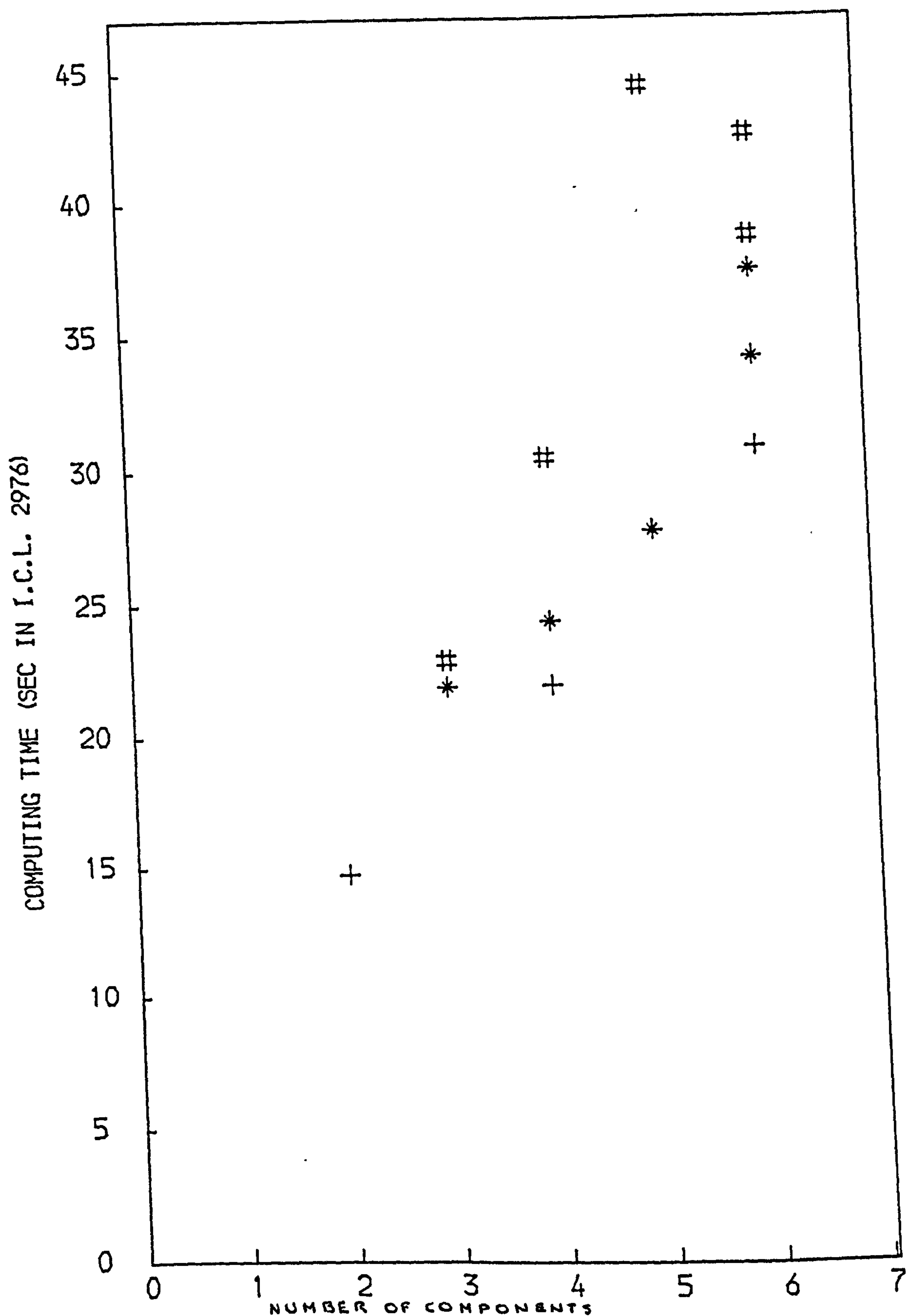


FIG. 130

COMPUTING EFFICIENCY OF THE PROGRAMME
 + TURBOJETS
 ♦ ENGINES WITH SEPARATE EXHAUSTS
 # ENGINES WITH MIXED EXHAUSTS